TARGETING CARDIAC PROTEOTOXICITY

EDITED BY: Xuejun Wang, Hui-Hua Li, Md. Shenuarin Bhuiyan and Mark J. Ranek
PUBLISHED IN: Frontiers in Physiology

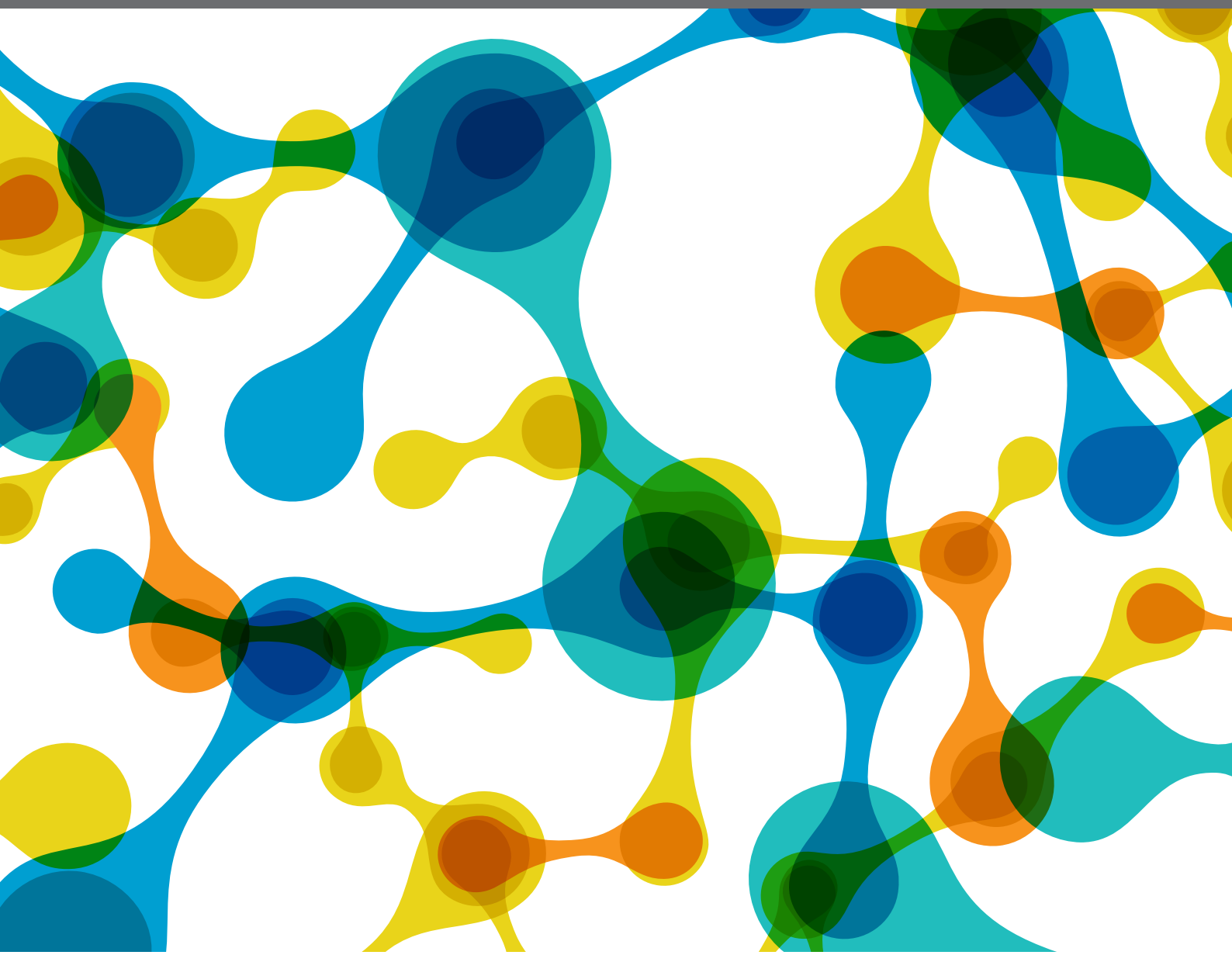

frontiers Research Topics

frontiers

ISSN 1664-8714
ISBN 978-2-88966-806-9
DOI 10.3389/978-2-88966-806-9

About Frontiers

Frontiers is more than just an open-access publisher of scholarly articles: it is a pioneering approach to the world of academia, radically improving the way scholarly research is managed. The grand vision of Frontiers is a world where all people have an equal opportunity to seek, share and generate knowledge. Frontiers provides immediate and permanent online open access to all its publications, but this alone is not enough to realize our grand goals.

Frontiers Journal Series

The Frontiers Journal Series is a multi-tier and interdisciplinary set of open-access, online journals, promising a paradigm shift from the current review, selection and dissemination processes in academic publishing. All Frontiers journals are driven by researchers for researchers; therefore, they constitute a service to the scholarly community. At the same time, the Frontiers Journal Series operates on a revolutionary invention, the tiered publishing system, initially addressing specific communities of scholars, and gradually climbing up to broader public understanding, thus serving the interests of the lay society, too.

Dedication to Quality

Each Frontiers article is a landmark of the highest quality, thanks to genuinely collaborative interactions between authors and review editors, who include some of the world's best academicians. Research must be certified by peers before entering a stream of knowledge that may eventually reach the public - and shape society; therefore, Frontiers only applies the most rigorous and unbiased reviews.
Frontiers revolutionizes research publishing by freely delivering the most outstanding research, evaluated with no bias from both the academic and social point of view. By applying the most advanced information technologies, Frontiers is catapulting scholarly publishing into a new generation.

What are Frontiers Research Topics?

Frontiers Research Topics are very popular trademarks of the Frontiers Journals Series: they are collections of at least ten articles, all centered on a particular subject. With their unique mix of varied contributions from Original Research to Review Articles, Frontiers Research Topics unify the most influential researchers, the latest key findings and historical advances in a hot research area! Find out more on how to host your own Frontiers Research Topic or contribute to one as an author by contacting the Frontiers Editorial Office: frontiersin.org/about/contact

TARGETING CARDIAC PROTEOTOXICITY

Topic Editors:
Xuejun Wang, University of South Dakota, United States
Hui-Hua Li, Capital Medical University, China
Md. Shenuarin Bhuiyan, Louisiana State University Health Shreveport, United States
Mark J. Ranek, Johns Hopkins University, United States

Citation: Wang, X., Li, H.-H., Bhuiyan, M. S., Ranek, M. J., eds. (2021). Targeting Cardiac Proteotoxicity. Lausanne: Frontiers Media SA. doi: 10.3389/978-2-88966-806-9

Table of Contents

frontiers in Physiology

EDITORIAL
published: 25 March 2021
doi: 10.3389/fphys.2021.669356

Editorial: Targeting Cardiac Proteotoxicity

Mark J. Ranek[1,2], *Md. Shenuarin Bhuiyan*[3,4] *and Xuejun Wang*[5]*

[1] Department of Medicine, Division of Cardiology, The Johns Hopkins Medical Institutions, Baltimore, MD, United States, [2] Department of Pharmacology and Molecular Sciences, The Johns Hopkins University School of Medicine, Baltimore, MD, United States, [3] Department of Pathology and Translational Pathobiology, Louisiana State University Health Sciences Center, Shreveport, LA, United States, [4] Department of Molecular and Cellular Physiology, Louisiana State University Health Sciences Center, Shreveport, LA, United States, [5] Division of Basic Biomedical Sciences, The University of South Dakota Sanford School of Medicine, Vermillion, SD, United States

Keywords: autophagy, proteasome, mitochondria, heart disease, chaperone, small heat shock protein, protein quality control, increased proteotoxic stress

Editorial on the Research Topic

Targeting Cardiac Proteotoxicity

Misfolded proteins not only lose their normal functions but also perturb other proteins, organelles, and cellular processes, causing cell malfunction and cell death (Wang et al., 2008). Proteotoxicity refers to all damaging effects exerted by misfolded proteins in the cell (Sandri and Robbins, 2014). To sense and minimize the level and toxicity of misfolded proteins, the cell has developed multi-layered protein quality control (PQC) mechanisms. PQC is performed by the intricate collaboration between molecular chaperones and targeted protein degradation; the latter involves primarily the ubiquitin-proteasome system (UPS) and autophagy (Wang et al., 2008). Both increased production of misfolded proteins and PQC impairment can lead to an increased proteotoxic stress state (IPTS), which can result from genetic mutations, environmental stressors, aging process, and even chemotherapies (Wang and Wang, 2020).

Over the last two decades, it is increasingly evident that IPTS contributes to the genesis of a large subset of heart failure (HF) (Willis and Patterson, 2013, Wang and Wang, 2020). During cardiac IPTS, the accumulation of misfolded proteins and resultant aberrant protein aggregation further impair PQC, compromise the integrity of contractile apparatus and organelles (e.g., mitochondria), and cause cardiomyocyte death, eventually leading to HF (Wang et al., 2008). Recent advances in the molecular mechanisms regulating proteasome- and lysosome-mediated protein degradation promise new strategies to prevent or more effectively treat HF via targeting cardiac proteotoxicity. This is exciting as there are no current HF therapies aimed at targeting cardiac proteotoxicity. The present Research Topic, *Targeting Cardiac Proteotoxicity*, not only reports new work of cardiac IPTS but also discusses the current understanding, knowledge gap, potential molecular mechanisms and targets, and the obstacles to broad clinical implementation.

Autophagy is pivotal to both PQC and organelle quality control. Hence, suppressing autophagy is generally detrimental and, conversely, enhancing autophagy protects against IPTS (Wang and Cui, 2017). This is well-reflected in this *Research Topic*. LMP10 (β2i) is a proteolytic subunit of the immunoproteasome, which is the primary form of proteasomes in immune cells and an inducible form in non-immune cells (Aki et al., 1994). Yan et al. reveal that LMP10 deficiency attenuates maladaptive cardiac remodeling induced by angiotensin-II infusion in mice, perhaps through enhanced autophagic degradation of insulin growth factor receptor 1 and glycoprotein 130. This study supports the notion that proteasome malfunction activates autophagy (Pan et al., 2020); however, a direct anti-inflammatory effect from inhibition of immunoproteasomes remains possible. Consistent with this possibility, Guo et al. show that shikonin, an anti-inflammatory

OPEN ACCESS

Edited and reviewed by:
Peter J. Reiser,
The Ohio State University,
United States

***Correspondence:**
Xuejun Wang
xuejun.wang@usd.edu

Specialty section:
This article was submitted to Striated Muscle Physiology, a section of the journal Frontiers in Physiology

Received: *18 February 2021*
Accepted: *04 March 2021*
Published: *25 March 2021*

Citation:
Ranek MJ, Bhuiyan MS and Wang X (2021) Editorial: Targeting Cardiac Proteotoxicity. Front. Physiol. 12:669356. doi: 10.3389/fphys.2021.669356

compound extracted from natural herbs, protects the heart from sepsis-induced injury. Notably, shikonin was shown by others to inhibit proteasome activities in macrophages (Lu et al., 2011). Occasionally a normally protective factor may become detrimental when autophagy becomes impaired or insufficient in the cell (Wang and Cui, 2017). This is exemplified by the perplexing effect of nuclear factor erythroid factor 2-related factor (Nrf2) in cardiac disease, as reviewed by Zang et al.

Since late 2019, all of humanity has been afflicted by the COVID-19 pandemic caused by the severe acute respiratory syndrome coronavirus 2 (SARS-CoV-2). A timely review by Gupta and colleague summarizes what we have learned during the 12 months following the first report of COVID-19, particularly the interaction between SARS-CoV-2 and autophagy. They describe that once SARS-CoV-2 enters the host cell, it can be degraded via autophagy or highjack the replication machinery. After evading degradation in the lysosome SARS-CoV-2 can replicate in an autophagosome, thereby reducing the influence of lysosomes on COVID-19 pathogenesis, which helps explain why autophagosome-lysosome fusion inhibitors (e.g., hydroxychloroquine) failed to meet the promises made early in the COVID-19 pandemic.

Mitophagy removes damaged mitochondria to limit reactive oxygen species production, crucial to maintaining mitochondrial, thus cardiomyocyte health (Tong et al., 2020). Impaired mitophagy contributes to doxorubicin-mediated cardiotoxicity, where the development of cardiomyopathy limits the clinical use of this powerful anti-neoplastic drug. Xu et al. report that Luteolin, a natural product extracted from plants alleviates doxorubicin-induced cardiotoxicity via enhancing mitophagy, effects that were abrogated with concomitant treatment with a Drp1 inhibitor, Mdivi-1. Kobayashi et al. explore the interplay of mitochondrial fission and mitophagy in a hyperglycemic model. Cultured cardiomyocytes subjected to high glucose displayed a marked reduction in mitophagy and mitochondrial health. Both genetic and pharmacological interrogations unveil that increasing mitophagy flux protects against high glucose induced cardiomyocyte injury. These studies add new evidence to the cardioprotective potential of enhancing mitophagy. The latter is comprehensively reviewed by Alam et al. which describes the potential role of mitochondrial proteostasis in cardiac IPTS, provides new insights into the mechanisms regulating mitophagy, and highlights potential targets for enhancing mitochondrial proteostasis to treat cardiac disease.

The contractile apparatus is central to the mechanical function of cardiomyocytes and is thereby under constant stress (Chung et al., 2016). Islam et al. review systematically small heat shock proteins that chaperone cytoskeletal integrity and the turnover of sarcomeres in cardiomyocytes. They propose a provocative "sarcostat" concept, a PQC mechanism located within the sarcomere that oversees sarcomere proteostasis. The authors also discuss potential targets for therapeutic intervention to enhance sarcomeric PQC. Further testing of the sarcostat model will be interesting. Mutations in genes encoding sarcomeric proteins cause cardiomyopathy, where pathogenesis likely involves IPTS as sarcomeric proteins are the most abundant proteins in cardiomyocytes (Willis and Patterson, 2013). McNamara et al. uncover an intronic variant of *TNNT2* that leads to the development of hypertrophic cardiomyopathy in felines. Distal arthrogryposis (DA) is another disorder that can be caused by genetic mutations affecting striated muscle, characterized by joint contractures, with the heart often affected. Desai et al. summarize the different forms of DA, their clinical features, and associated genetic mutations. It will be interesting to investigate how would the DA-linked mutations affect cardiac PQC.

Recent advances in the regulation of the protein degradation pathways have dramatically expanded our understanding of cardiac PQC. Li et al. review the role of a ubiquitin-like protein NEDD8. The covalent attachment of NEDD8 to substrate proteins is known as neddylation, critical to cardiac development and found to be dysregulated in vascular disease, liver disease, obesity, and HF. Oeing et al. highlight the newly identified roles of protein kinase G (PKG) in cardiac PQC that provide exciting new mechanism for PKG-mediated cardioprotection unveiled since early 2000s. Activation of PKG improves PQC via both priming the proteasome and increasing autophagy. The ability to activate PKG with drugs already in clinical use elevates the interest surrounding PKG as a therapeutic target for cardiac proteotoxicity.

Emerging evidence suggests inter-organ communication in proteotoxicity (Liu et al., 2021). To this end, Evangelisti et al. comprehensively contrast IPTS pathophysiology between the central nervous and the cardiovascular systems and nicely highlight the shared pathological features of IPTS diseases in the heart and brain, calling for studying IPTS in the two systems in parallel. Intriguingly, augmenting protein kinase A- or PKG-mediated proteasome activation reduces both cardiac and neural proteotoxicity in animal models (Zhang et al., 2019, Wang and Wang, 2020).

As illustrated by this series, the cardiac PQC field is bourgeoning and recently has made significant and exciting advances, providing new therapeutic targets that can be potentially translated into the clinic in the near future. Meanwhile, our understating of the molecular mechanisms underlying cardiac proteotoxicity remains quite limited. Continuing effort in defining pathways that regulate chaperones, the UPS, and autophagy is warranted for discovering new nodal points and methods for therapeutic intervention while we facilitate the translation of some of the most promising strategies to the clinic.

AUTHOR CONTRIBUTIONS

MR writing the first draft and grammatical polishing of the editorial. MB editing the draft of the editorial. XW planning, editing, and finalizing of the editorial, as well as response to editors' report. All authors contributed to the article and approved the submitted version.

FUNDING

This work was supported in part by National Institutes of Health (NIH) grants HL122354 and HL145753, LSUHSC-S CCDS

Finish Line Award, COVID-19 Research Award, and LARC Research Award (to MB), by American Heart Association (AHA) grants 18CDA34110140 and 20TPA35500008, an Amyloidosis Foundation Donald C. Brockman Memorial Research Grant (to MR), by NIH grants HL072166, HL085629, HL131667, and HL153614, and an AHA grant 20TPA35490091 (to XW).

REFERENCES

Aki, M., Shimbara, N., Takashina, M., Akiyama, K., Kagawa, S., Tamura, T., et al. (1994). Interferon-gamma induces different subunit organizations and functional diversity of proteasomes. *J. Biochem*. 115, 257–269. doi: 10.1093/oxfordjournals.jbchem.a124327

Chung, J. H., Biesiadecki, B. J., Ziolo, M. T., Davis, J. P., and Janssen, P. M. (2016). Myofilament calcium sensitivity: role in regulation of *in vivo* cardiac contraction and relaxation. *Front. Physiol*. 7:562. doi: 10.3389/fphys.2016.00562

Liu, Y., Subedi, K., Baride, A., Romanova, S., Callegari, E., Huber, C. C., et al. (2021). Peripherally misfolded proteins exacerbate ischemic stroke-induced neuroinflammation and brain injury. *J. Neuroinflammation* 18:29. doi: 10.1186/s12974-021-02081-7

Lu, L., Qin, A., Huang, H., Zhou, P., Zhang, C., Liu, N., et al. (2011). Shikonin extracted from medicinal Chinese herbs exerts anti-inflammatory effect via proteasome inhibition. *Eur. J. Pharmacol*. 658, 242–247. doi: 10.1016/j.ejphar.2011.02.043

Pan, B., Li, J., Parajuli, N., Tian, Z., Wu, P., Lewno, M. T., et al. (2020). The calcineurin-TFEB-p62 pathway mediates the activation of cardiac macroautophagy by proteasomal malfunction. *Circ. Res*. 127, 502–518. doi: 10.1161/CIRCRESAHA.119.316007

Sandri, M., and Robbins, J. (2014). Proteotoxicity: an underappreciated pathology in cardiac disease. *J. Mol. Cell. Cardiol*. 71, 3–10. doi: 10.1016/j.yjmcc.2013.12.015

Tong, M., Zablocki, D., and Sadoshima, J. (2020). The role of Drp1 in mitophagy and cell death in the heart. *J. Mol. Cell. Cardiol*. 142, 138–145. doi: 10.1016/j.yjmcc.2020.04.015

Wang, X., and Cui, T. (2017). Autophagy modulation: a potential therapeutic approach in cardiac hypertrophy. *Am. J. Physiol. Heart Circ. Physiol*. 313, H304–H319. doi: 10.1152/ajpheart.00145.2017

Wang, X., Su, H., and Ranek, M. J. (2008). Protein quality control and degradation in cardiomyocytes. *J. Mol. Cell. Cardiol*. 45, 11–27. doi: 10.1016/j.yjmcc.2008.03.025

Wang, X., and Wang, H. (2020). Priming the proteasome to protect against proteotoxicity. *Trends Mol. Med*. 26, 639–648. doi: 10.1016/j.molmed.2020.02.007

Willis, M. S., and Patterson, C. (2013). Proteotoxicity and cardiac dysfunction–Alzheimer's disease of the heart? *N. Engl. J. Med*. 368, 455–464. doi: 10.1056/NEJMra1106180

Zhang, H., Pan, B., Wu, P., Parajuli, N., Rekhter, M. D., Goldberg, A. L., et al. (2019). PDE1 inhibition facilitates proteasomal degradation of misfolded proteins and protects against cardiac proteinopathy. *Sci. Adv*. 5:eaaw5870. doi: 10.1126/sciadv.aaw5870

Conflict of Interest: The authors declare that the research was conducted in the absence of any commercial or financial relationships that could be construed as a potential conflict of interest.

frontiers in Physiology

ORIGINAL RESEARCH
published: 14 February 2020
doi: 10.3389/fphys.2020.00113

Luteolin Attenuates Doxorubicin-Induced Cardiotoxicity Through Promoting Mitochondrial Autophagy

Haixia Xu[1,2†], Wenjun Yu[1,2†], Shiqun Sun[1,2†], Congye Li[3], Yingmei Zhang[1,2] and Jun Ren[1,2*]*

[1] Department of Cardiology, Zhongshan Hospital, Fudan University, Shanghai, China, [2] Shanghai Institute of Cardiovascular Diseases, Shanghai, China, [3] Department of Cardiology, Xijing Hospital, Air Force Medical University, Xi'an, China

Doxorubicin is a valuable antineoplastic drug although its clinical use is greatly hindered by its severe cardiotoxicity with dismal target therapy available. Luteolin is a natural product extracted from vegetables and fruits with a wide range of biological efficacies including anti-oxidative, anti-tumorigenic, and anti-inflammatory properties. This study was designed to examine the possible effect of luteolin on doxorubicin-induced cardiotoxicity, if any, and the mechanism(s) involved with a focus on mitochondrial autophagy. Luteolin application (10 μM) in adult mouse cardiomyocytes overtly improved doxorubicin-induced cardiomyocyte contractile dysfunction including elevated peak shortening amplitude and maximal velocity of shortening/relengthening along with unchanged duration of shortening and relengthening. Luteolin alleviated doxorubicin-induced cardiotoxicity including apoptosis, accumulation of reactive oxygen species (ROS) and loss of mitochondrial membrane potential. Furthermore, luteolin attenuated doxorubicin-induced cardiotoxicity through promoting mitochondrial autophagy in association with facilitating phosphorylation of Drp1 at Ser^{616}, and upregulating TFEB expression. In addition, luteolin treatment partially attenuated low dose doxorubicin-induced elongation of mitochondria. Treatment of Mdivi-1, a Drp1 GTPase inhibitor, negated the protective effect of luteolin on levels of TFEB, LAMP1, and LC3B, as well as loss of mitochondrial membrane potential and cardiomyocyte contractile dysfunction in the face of doxorubicin challenge. Taken together, these findings provide novel insights for the therapeutic efficacy of luteolin against doxorubicin-induced cardiotoxicity possibly through improved mitochondrial autophagy.

Keywords: luteolin, doxorubicin, cardiotoxicity, mitochondria, autophagy

OPEN ACCESS

Edited by:
Md. Shenuarin Bhuiyan, Louisiana State University, United States

Reviewed by:
Huabo Su, Augusta University, United States
Taixing Cui, University of South Carolina, United States

***Correspondence:**
Yingmei Zhang
zhangym197951@126.com
Jun Ren
jrenuwyo@126.com

† These authors have contributed equally to this work

Specialty section:
This article was submitted to Striated Muscle Physiology, a section of the journal Frontiers in Physiology

Received: *19 November 2019*
Accepted: *30 January 2020*
Published: *14 February 2020*

Citation:
Xu H, Yu W, Sun S, Li C, Zhang Y and Ren J (2020) Luteolin Attenuates Doxorubicin-Induced Cardiotoxicity Through Promoting Mitochondrial Autophagy. Front. Physiol. 11:113. doi: 10.3389/fphys.2020.00113

INTRODUCTION

Doxorubicin is an effective anti-neoplastic chemotherapeutic agent although its clinical application has been greatly hindered by its severe and pronounced cardiotoxicity. Ample clinical and experimental evidence has depicted that doxorubicin triggers cardiac anomalies including tachycardia, myocardial injury and heart failure (Sun et al., 2014; Ge et al., 2016;

Wenningmann et al., 2019). Over the past decades, extensive efforts have been made toward exploring the mechanisms behind doxorubicin-induced cardiotoxicity including accumulation of reactive oxygen species (ROS), compromised lysosomal function, reduction of ATP production, mitochondrial membrane potential collapse and apoptosis (Octavia et al., 2012; Ma et al., 2017; Guo et al., 2018). Nonetheless, effective target therapy for doxorubicin-induced cardiotoxicity is still lacking.

Luteolin (3′,4′,5′,7′-tetrahydroxyflavone, LUT), as a natural flavone rich in vegetables, fruits and herbs, has shown beneficial properties in multiple biological processes including anti-carcinogenic, anti-apoptotic activities and anti-oxidative stress properties (Rao et al., 2012; Xu et al., 2019). The average consumption of luteolin is approximately 0.01–0.20 mg from our daily diet (Wang et al., 2009). Luteolin is one of the major metabolites upon oral administration of luteolin-7-O-glucoside and generally absorbed by intestinal mucosa into the systemic circulation after oral administration. It was demonstrated that oral bioavailability of luteolin was approximately 26% following administration (Lin et al., 2015). Ample evidence has indicated that luteolin offers cardiovascular protection including ischemia/reperfusion and heart failure through alleviating ROS and apoptosis, as well as intracellular Ca^{2+} dysregulation (Galati et al., 2001; He et al., 2012; Rao et al., 2012; Zhu et al., 2017). Several theories have been proposed for the underlying mechanisms of doxorubicin-induced cardiotoxicity including mitochondrial damage (Marechal et al., 2011; Octavia et al., 2012; Ichikawa et al., 2014), although whether luteolin affects doxorubicin-induced cardiotoxicity remains elusive.

Mitochondria play a pivotal role in energy production, maintaining homeostatic control of ROS production in cardiomyocytes. Clearance of damaged mitochondria exerts a critical role in the mitochondrial quality control. There is emerging evidence for defective mitochondrial autophagy or mitophagy in mitochondrial damage from doxorubicin-induced cardiotoxicity (Abdullah et al., 2019). Mitochondrial autophagy is a conserved cellular process to degrade and recycle damaged mitochondria through formation of autophagosomes and fusion with lysosomes. Autophagy has been shown to play a rather complex role in doxorubicin-induced cardiotoxicity due to excessive or defective autophagy (Li et al., 2016; Koleini and Kardami, 2017; Wang et al., 2019a). It appears that the onset and development of doxorubicin-induced cardiotoxicity is dependent upon drug dosage and duration (Wenningmann et al., 2019). More recent finding has depicted a likely role for interrupted autophagy in low dose doxorubicin (5 mg/kg/week for 4 weeks)-elicited cardiomyopathy (Li et al., 2016). In addition, it was reported that luteolin alleviated post-infarction cardiac dysfunction through upregulation of autophagy (Hu et al., 2016). Given the established property of luteolin on regulation of mitochondrial function and autophagy, this study was designed to examine the impact of luteolin on cardiac contractile function, apoptosis, and mitochondrial autophagy in doxorubicin-induced cardiotoxicity and the underlying mechanisms involved in adult mouse cardiomyocytes (AMCMs).

MATERIALS AND METHODS

Isolation of Adult Murine Cardiomyocytes (AMCMs)

All animal procedures were approved by our institutional Animal Care and Use Committee at the Zhongshan Hospital Fudan University (Shanghai, China). In brief, adult male C57/BL6J mice aged 8 weeks were anesthetized, and chest was opened to fully expose the heart. Inferior vena cava and descending aorta were cut, and EDTA buffer was immediately injected into the right ventricle. Then ascending aorta was tightly clamped and the heart was removed. EDTA buffer and perfusion buffer were injected into left ventricles prior to perfusion of a collagenase buffer (type II and IV collagenase). Left ventricle was then separated and gently pulled into 1 mm^3 pieces using forceps and was dissociated by gentle pipetting. Cell suspension underwent four sequential rounds of gravity settling, using three intermediate Ca^{2+} reintroduction buffers to gradually restore extracellular Ca^{2+} concentration to 1.2 mM. A yield of at least 80% rod-shaped CMs were deemed successful (Ackers-Johnson et al., 2016; Wang et al., 2018).

Cell Culture and Treatment

Cardiomyocytes were re-suspended in pre-warmed plating media and plated onto laminin (5 μg/mL) pre-coated culture plastics or glass coverslips in an incubator (37°C, 95% O2, and 5% CO2). Media was changed to replaced 1 h later. After 1 h, AMCMs were treated with DMSO (control), doxorubicin (DOX, 1 μM), luteolin (LUT, at different concentrations of 1, 10, and 50 μM) and the concurrent treatment of doxorubicin and luteolin for 24 h. Mdivi-1 (1 μM) was added in order to confirm the role of Drp1 in luteolin-offered response against doxorubicin-induced cardiotoxicity.

Measurement of Cell Shortening and Relengthening

Mechanical properties of single cardiomyocytes were measured with an IonOptix Myocam system (IonOptix Inc., Milton, MA, United States). Cells were placed on the stage of an inverted microscope (×400 objective). The cells were stimulated with an electrical field at a frequency of 0.5 Hz. Cell shortening and re-lengthening were assessed according to the previous study with parameters as follows: resting cell length, peak shortening amplitude (PS), time-to-peak shortening (TPS), and maximum velocity of shortening and relengthening (±dL/dt) (Zhang et al., 2014a).

Assessment of LDH and CK Release

Release of lactate dehydrogenase (LDH) and creatine kinase (CK) was evaluated in culture medium using ELISA assays with the Lactate dehydrogenase assay and Creatine kinase assay kits (Nanjing Jiancheng Bioengineering Institute, Nanjing, China).

Assessment of TUNEL Staining

Cardiomyocyte apoptosis was analyzed by TUNEL staining using *In Situ* Cell Death Detection Kit (Roche Diagnostics

GmbH, Mannheim, Germany). Briefly, after fixed with 4% paraformaldehyde, CMs were incubated with permeabilizing solution for 30 min and were then treated in TUNEL reaction mixture for 1 h at 37°C. Morphological assessment was performed by fluorescence microscopy (20 × objective) (Zhou et al., 2018b). Nine microscopic fields were randomly selected to observe at least 100 cells to assess apoptosis.

Detection of Reactive Oxygen Species (ROS)

Mitochondrial superoxide level was detected using 2′,7′-dichlorofuorescein-diacetate (DCFH-DA, Beyotime Institute of Biotechnology, Shanghai, China), which can be oxidized by superoxide to emit green fluorescence. Briefly, cells were treated in a ROS working solution for 20 min at 37°C. Thereafter, cells were washed with DMEM three times to remove the dye. A laser confocal microscope microscopy (LECIA) was used to evaluate the fluorescence of ROS production with the Image J software (Zhou et al., 2018a).

Detection of Mitochondrial Membrane Potential ($\Delta\psi m$)

$\Delta\psi m$ was measured using a JC-1 kit (Beyotime Institute of Biotechnology, Shanghai, China) (Zhou et al., 2019). JC-1 forms J-aggregates at high $\Delta\psi m$ and emits red fluorescence. However, JC-1 remains in monomer form at low $\Delta\psi m$ and emits green fluorescence. AMCMs were stained with a JC-1 solution for 20 min at 37°C according to the manufacturer's instructions. The ratio of red-to-green fluorescence was calculated using the Image J software to reflect $\Delta\psi m$.

Immunofluorescence Assay

Immunofluorescence for LC3B and COXIV were performed per the established protocols. Briefly, AMCMs were fixed and permeabilized at room temperature. After blocking for 1 h, AMCMs were incubated with rabbit anti-LC3B antibody (1:50) and mouse anti-COXIV antibody (1:50) overnight at 4°C. Afterward, AMCMs were incubated with anti-rabbit Alexa Fluor 488 (1:800) and anti-mouse Alexa Fluor 546 (1:800 dilution) secondary antibodies for 1 h in the dark (Zhou et al., 2018a). Immunofluorescence was assessed on a laser confocal microscope with a ×630 oil objective (Laser Scanning Confocal Microscopy, Leica, Germany).

Mitochondrial Isolation and Purification

Mitochondria were isolated from AMCMs using a Mitochondria Isolation Kit (Abcam, ab110170) according to the manufacturer's instruction. In brief, cells were collected and were homogenized with 30 strokes using pestle B. After centrifuging at 1,000 × g for 10 min at 4°C, supernatants were saved. Pellets were resuspended and homogenized. Then, supernatants were combined and were centrifuged at 12,000 × g for 15 min at 4°C and were resuspend with a RIPA buffer. Protein concentration was determined using a BCA Protein Assay Kit (Beyotime Institute of Biotechnology, Shanghai, China).

Western Blot Analysis

Western blot was performed based on our previous report (Zhang et al., 2014b). Cell lysates were extracted in a RIPA buffer supplemented with protease inhibitors. After 20 min, CMs were centrifuged at 12,000 × rpm for 20 min at 4°C,

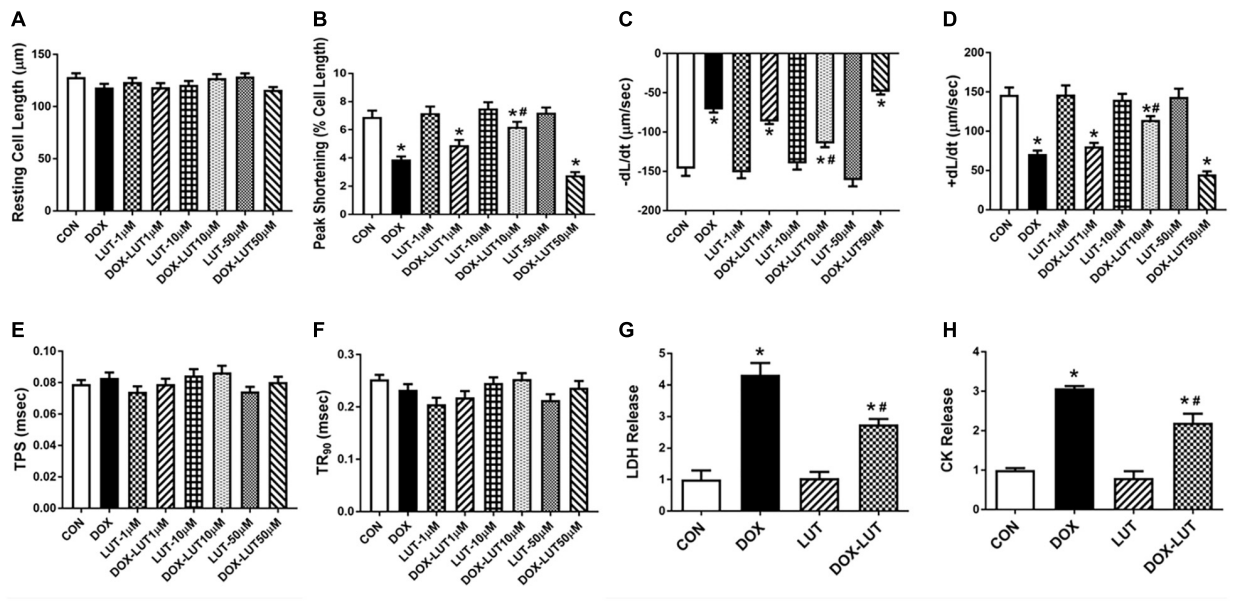

FIGURE 1 | Cardiomyocyte contractile function and cell injury following doxorubicin and luteolin (at various concentrations) exposure for 24 h. **(A)** Resting cell length; **(B)** Peak shortening (PS); **(C)** Maximal velocity of shortening (–dL/dt); **(D)** Maximal velocity of relengthening (+dL/dt); **(E)** Time-to -peak shortening (TPS); **(F)** Time-to-90% relengthening (TR_{90}); **(G)** LDH; and **(H)** CK. Mean ± SEM, n = 30 cells each group from three independent experiment. * $p < 0.05$ vs. CON group, # $p < 0.05$ vs. DOX group.

and protein level was determined using a BCA Protein Assay Kit (Beyotime Institute of Biotechnology, Shanghai, China). Samples (25 μg) were analyzed using 10–12% SDS-PAGE, and was then transferred to PVDF membranes. After blocking with 5% non-fat milk, membranes were incubated with primary antibodies overnight at 4°C. Blots were washed three times

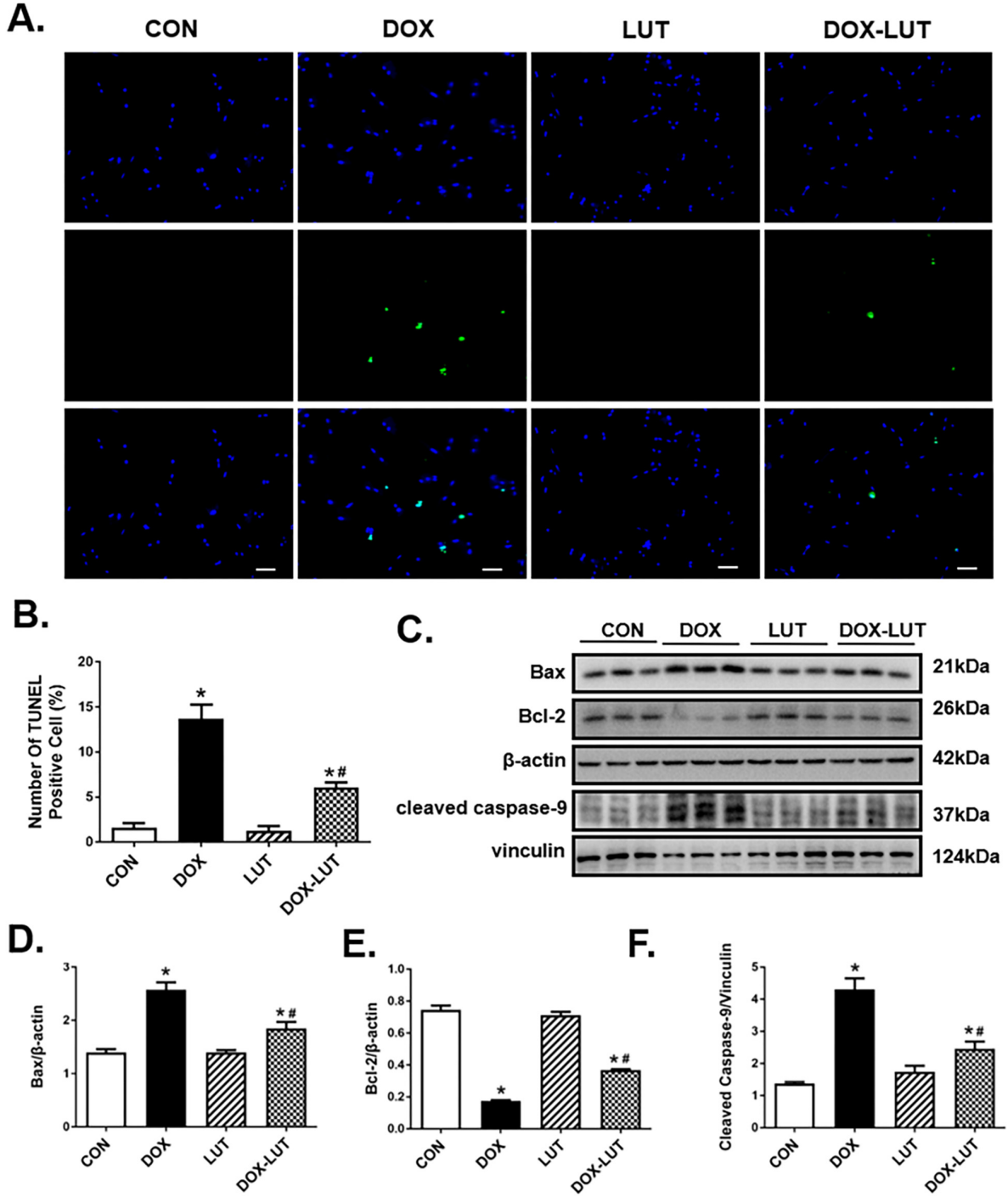

FIGURE 2 | Effect luteolin treatment on doxorubicin-induced cardiomyocyte apoptosis. **(A)** Representative TUNEL staining depicting AMCM apoptosis after doxorubicin and luteolin treatment. All nuclei were stained with DAPI (blue), whereas TUNEL-positive nuclei were visualized using green fluorescence. Original magnification = 200×. **(B)** Quantified TUNEL apoptosis manifested as percentage of TUNEL-positive cells from nine fields per group. **(C)** Representative western blot images of AMCM apoptosis using Bax, Bcl-2 and cleaved caspase-9. **(D–F)** Quantitative analysis of cardiomyocyte apoptosis using Bax, Bcl-2 and cleaved caspase-9. Scale bars = 50 μm. Mean ± SEM, $n = 3$ independent experiment. * $p < 0.05$ vs. CON group, # $p < 0.05$ vs. DOX group.

for 10 min in TBST and were incubated with the HRP-conjugated secondary antibody for 2 h at room temperature. Bands were detected using enhanced chemiluminescence luminal reagents (Bio-Rad Laboratories, United States). Gray value was measured using an Image Lab 3.0 (National Institutes of Health, Bethesda, United States).

Regents and Antibodies

Doxorubicin (Beyotime Institute of Biotechnology, Shanghai, China), luteolin (≥98%, Santa Cruz Biotechnology, sc-203119), mdivi-1 (≥98%, Sigma Aldrich, M0199). Bax (1:1,000, Cell Signaling Technology, #5023S), Bcl-2 (1:1,000, Cell Signaling Technology, #15071S), Bnip3 (1:1,000, Cell Signaling Technology, #44060), cleaved caspase-9 (1:1,000, Cell Signaling Technology, #9509S), Drp1 (1:1,000, Cell Signaling Technology, #8570), p-Drp1 (Ser^{616}) (1:1,000, Cell Signaling Technology, #3455S), LAMP1 (1:500, Abcam, ab208943), LC3B (1:1,000, Abcam, ab48394), mTOR (1:1,000, Cell Signaling Technology, #2983S), p-mTOR (Ser^{2448}) (1:1,000, Cell Signaling Technology, #5536S), P62 (1:1,000, Cell Signaling Technology, #5114S), parkin (1:1,000, Cell Signaling Technology, #4211), Pink1 (1:1,000, Abcam, ab216144), TFEB (1:500, Cell Signaling Technology, #32361S), vinculin (1:1,000, Abcam, ab129002);anti-mouse Alexa Fluor (1:1000, Cell Signaling Technology, #4408), anti-rabbit Alexa Fluor (1:1,000, Cell Signaling Technology, #8890);β-actin (1:5,000, KangChen Bio-tech, Shanghai, China).

Statistical Analysis

Data were reported as mean ± SEM. Statistical analysis was performed using Prism 6.0 software (GraphPad, San Diego, CA, United States). One-way ANOVA followed by Tukey's test was used to analyze the statistical significance of difference ($P < 0.05$).

RESULTS

Luteolin Improved Cardiomyocyte Shortening and Relengthening in the Face of Doxorubicin Challenge

To evaluate the effect of luteolin on doxorubicin-induced cardiotoxicity, cell shortening was evaluated in doxorubicin (1 μM, 24 h)-challenged AMCMs in the absence or presence of various concentrations of luteolin (1, 10, and 50 μM). As depicted in **Figures 1A–F**, doxorubicin treatment overtly decreased peak shortening and ±dL/dt, the effect of which was mitigated by luteolin at the concentration of 10 but not 1 or 50 μM. Luteolin did not exhibit any notable effect itself at these concentrations. Thus, 10 μM was chosen as the concentration for luteolin for the rest of our study, consistent with previous reports (Yao et al., 2016, 2017; Bustos et al., 2018; Park et al., 2018; Zhou et al., 2018b). Neither doxorubicin nor luteolin (at various concentrations), or both, overtly affected resting cell length, TPS and TR_{90} ($P > 0.05$). LDH and CK release were employed to assess cell injuries of cultured AMCMs. Our data shown in **Figures 1G,H** indicated that doxorubicin overtly promoted release of LDH and CK in cardiomyocytes, the effect of which was significantly attenuated by luteolin at the level of 10 μM.

Luteolin Attenuated Doxorubicin-Induced Cardiomyocyte Apoptosis

TUNEL assay was performed to assess cell damage following doxorubicin treatment. In comparison with control group, doxorubicin challenge significantly increased apoptosis as evidenced by the elevated number of TUNEL-positive cardiomyocytes ($P < 0.01$), the effect of which was significantly attenuated by luteolin treatment. Along the same line, Western blot analysis revealed upregulated levels of cleaved caspase-9 and Bax in conjunction with the downregulated Bcl2 levels in doxorubicin-treated AMCMs, the effect of which was partially attenuated by luteolin treatment (**Figure 2**).

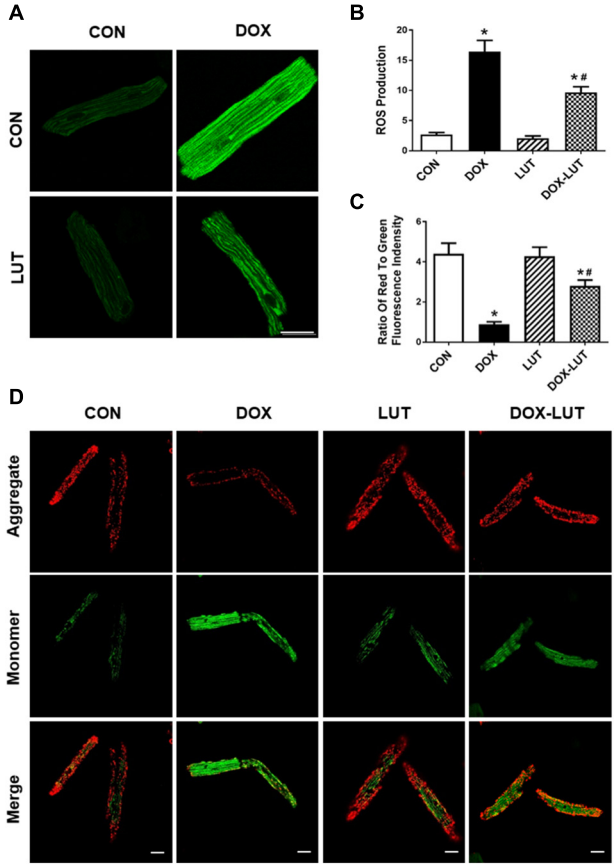

FIGURE 3 | Effect of luteolin on doxorubicin-induced cardiomyocyte mitochondrial injury. **(A)** Representative fluorescence images of AMCMs (original magnification = 630×) showing ROS production in cardiomyocytes after exposure of doxorubicin and luteolin. **(B)** Pooled data of ROS production from nine fields per group. **(C,D)** Representative fluorescence images and quantitative analysis of cardiomyocyte $\Delta\psi m$ using JC-1 fluorescence from nine fields (original magnification = 400×). Scale bars = 25 μm. Mean ± SEM, $n = 3$ independent experiments in duplicates per group, * $p < 0.05$ vs. CON group, # $p < 0.05$ vs. DOX group.

Luteolin Suppressed Doxorubicin-Induced Mitochondrial Injuries in Cardiomyocytes

Mitochondrial membrane potential and ROS levels were assessed using JC-1 staining and DCF staining, respectively. As shown in **Figure 3**, doxorubicin treatment overtly decreased $\Delta\Psi m$ and promoted intracellular ROS generation, the effects of which were markedly attenuated by luteolin. Luteolin exerted little effect on $\Delta\Psi m$ and ROS production itself.

Luteolin Attenuated Doxorubicin-Induced Cardiotoxicity Through Promoting Mitochondrial Autophagy

To discern the possible role of mitochondrial autophagy following doxorubicin challenge, changes in mitochondrial autophagy protein markers were evaluated. Data in **Figures 4A–D** indicated that doxorubicin suppressed levels of LC3B, P62 and mitochondrial LC3BII, the effects of which (with the exception of p62) was partially reversed by luteolin. In addition, to further discern the effect of doxorubicin and luteolin on mitochondrial autophagy, we used immunofluorescence technique to evaluate co-localization between LC3B and mitochondria. Mitochondria were labeled with COX-IV (green fluorescence) and LC3B was labeled with red fluorescence, co-localization of mitochondria and LC3B was verified using the merged yellow fluorescence. Our results indicated that doxorubicin overtly decreased the number of LC3 dots co-localized with mitochondria, the effects of which were reversed by luteolin, indicative of improved LC3B abundance in mitochondria in response to luteolin treatment (**Figures 4E,F**). Moreover, luteolin significantly reversed the inhibition of pink1, parkin and Bnip3 in the face of doxorubicin treatment without eliciting any effect itself (**Figures 4G–J**).

Luteolin Promoted Mitochondrial Autophagy Possibly via a Drp1/mTOR/TFEB-Dependent Mechanism

To explore the possible mechanism of action behind luteolin-promoted autophagy, transcription factor EB (TFEB), a master

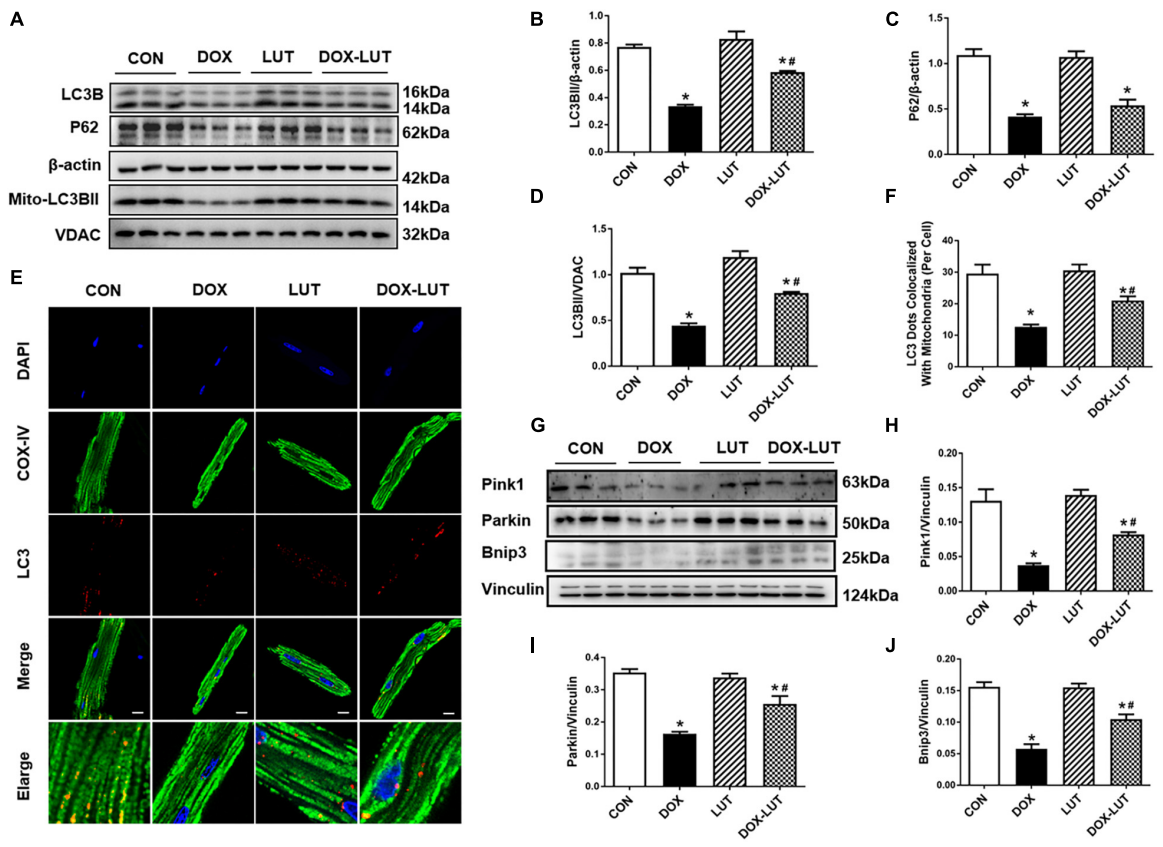

FIGURE 4 | Effect of luteolin treatment on doxorubicin-induced change in cardiomyocyte mitochondrial autophagy. **(A)** Representative Western gel blots depicting protein levels of mitochondrial autophagy, including LC3B and P62 in cardiomyocytes after doxorubicin and luteolin treatment. **(B)** LC3B; **(C)** P62; **(D)** mitochondrial LC3B; **(E)** Representative fluorescence images of LC3B co-localized with mitochondria (COXIV) from 9 to 10 fields per group. **(F)** Quantitative analysis of LC3 dots co-localized with mitochondria. **(G)** Representative Western gel blots of pink1, parkin and Bnip3; **(H)** pink1; **(I)** parkin; **(J)** Bnip3. Scale bars = 25 μm. Mean ± SEM, $n = 3$ independent experiment. * $p < 0.05$ vs. CON group, # $p < 0.05$ vs. DOX group.

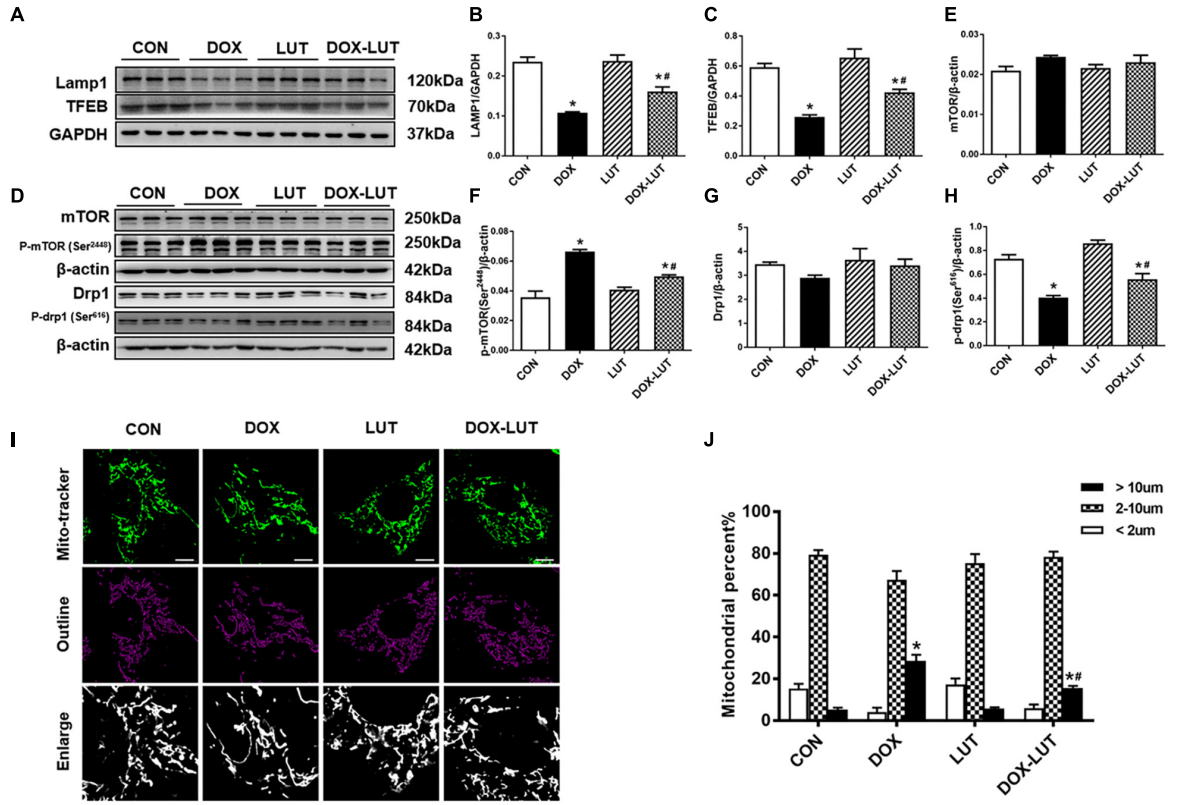

FIGURE 5 | Effect of luteolin treatment on lysosomal Drp1/mTOR/TFEB signaling cascade. **(A)** Representative Western blot of lysosomal generation and number including TFEB and LAMP1. **(B,C)** Quantitative data for TFEB and LAMP1. **(D)** Representative Western blot of mTOR, pSer^{2448}-mTOR, Drp1, pSer^{616}-Drp1. **(E)** mTOR; **(F)** p-mTOR (Ser^{2448}); **(G)** Drp1; **(H)** p-Drp1 (Ser^{616}). **(I,J)** Representative fluorescence images and quantitative analysis of morphology of mitochondria in neonatal mouse cardiomyocytes (NMCMs) from 6 fields (original magnification = 630×). Mean ± SEM, $n = 3$ independent experiments in duplicates per group. Scale bars = 10 μm. * $p < 0.05$ vs. CON group, # $p < 0.05$ vs. DOX group.

regulator of autophagy and lysosomal biogenesis (Settembre et al., 2011), were evaluated. As shown in **Figures 5A,B**, doxorubicin treatment overtly downregulated levels of TFEB, the effect of which was mitigated by luteolin. Given that TFEB is known to regulate lysosomal generation (Settembre et al., 2011), levels of LAMP1 were examined. Our result suggested that doxorubicin downregulated the level of LAMP1, the effect of which was significantly attenuated by luteolin without any notable effect from luteolin itself (**Figure 5C**).

Since TFEB is negatively regulated through phosphorylation of TFEB by way of mTOR, level of phosphorylated mTOR (Ser^{2448}) (Settembre et al., 2012) was examined. Our results indicated that doxorubicin significantly promoted mTOR phosphorylation (Ser^{2448}) and inhibited Drp1 phosphorylation (Ser^{616}) without affecting pan protein expression of mTOR and Drp1 in AMCMs, the effect of which was overtly attenuated by luteolin (**Figures 5D–H**). In addition, morphology of mitochondria was scrutinized in neonatal mouse cardiomyocytes (NMCMs). As shown in **Figures 5I,J**, doxorubicin resulted in elongation of mitochondria, the effect of which was partially attenuated by luteolin treatment.

To explore the role of Drp1 in the regulation of mTOR and TFEB in doxorubicin-induced cardiotoxicity, cardiomyocytes were pretreated with mdivi-1, a Drp1 GTPase inhibitor (1 μM for 1 h, prior to exposure of doxorubicin and luteolin for 24 h (**Figures 6A–F**). Treatment of mdivi-1 obliterated luteolin-offered protective action on levels of LC3B and LAMP1, as well as phosphorylation of mTOR (Ser^{2448}) and TFEB. To discern the role of phosphorylated Drp1 (Ser^{616}), mitochondrial membrane potential was evaluated using JC-1. Our data shown in **Figures 6G,H** revealed that treatment of mdivi-1 prevented the protective effect of luteolin on doxorubicin challenge-induced $\Delta\psi m$ loss. Moreover, cell shortening was evaluated in AMCMs following mdivi-1 treatment. As shown in **Figure 7**, mdivi-1 canceled off the beneficial effect of luteolin on doxorubicin-induced decrease in peak shortening and ±dl/dt without eliciting any effect itself in AMCMs.

DISCUSSION

The salient findings from our study noted that luteolin protected against doxorubicin-induced contractile dysfunction and apoptosis in cardiomyocytes. Our data also revealed that

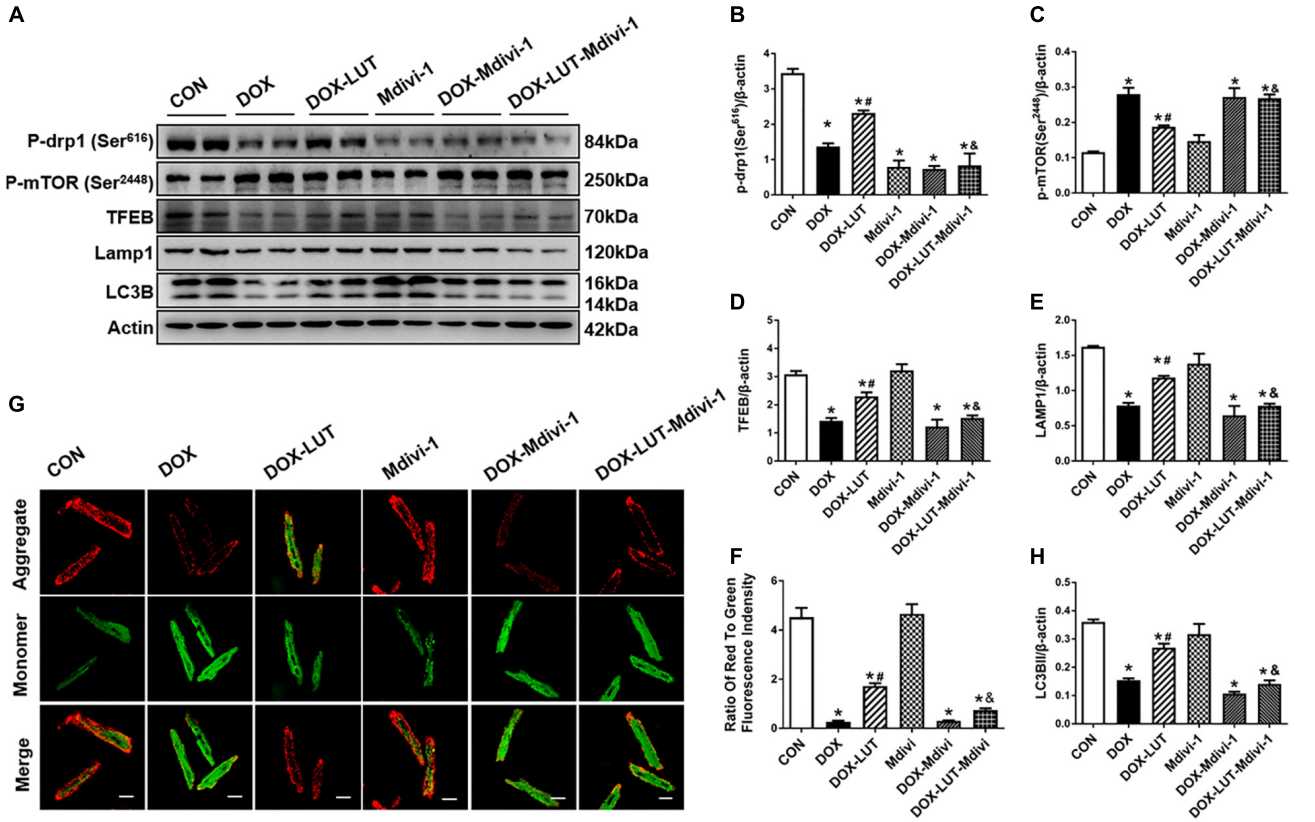

FIGURE 6 | Treatment of Mdivi-1, a Drp1 GTPase inhibitor, on luteolin-offered benefit against doxorubicin-induced cardiotoxicity. **(A)** Representative Western blot of p-Drp1 (Ser^{616}), p-mTOR (Ser^{2448}), TFEB, LAMP1, and LC3B. **(B)** Quantitative data of p-Drp1 (Ser^{616}); **(C)** p-mTOR (Ser^{2448}); **(D)** LAMP1; **(E)** TFEB; **(F)** LC3B; and **(G,H)**: Representative fluorescence images and quantitative analysis of cardiomyocyte $\Delta\psi m$ using JC-1 fluorescence following mdivi-1 treatment from nine fields. Mean ± SEM, $n = 3$ independent experiments in duplicates per group. Scale bars = 25 μm. * $p < 0.05$ vs. CON group, # $p < 0.05$ vs. DOX group, & $p < 0.05$ vs. DOX-LUT group.

luteolin attenuated cardiomyocyte mitochondrial injury through regulation of autophagy via Drp1/mTOR/TFEB pathway (**Figure 8**). Mitochondria-mediated apoptosis plays a pivotal role in programmed cell death (Green, 1998). In this study, doxorubicin decreased the expression of the anti-apoptotic protein Bcl-2, while upregulating levels of pro-apoptotic protein Bax and cleaved caspase-9. These findings were in accordance with previous studies highlighting the pro-apoptotic property of doxorubicin from both *in vivo* and *in vitro* settings (Dimitrakis et al., 2012; Octavia et al., 2012; Bartlett et al., 2016; Li et al., 2016; Wenningmann et al., 2019). An elevated Bax-to-Bcl-2 ratio would disrupt $\Delta\psi m$ and activate caspase-9, an apoptotic initiator caspase (Cohen, 1997). In addition, doxorubicin provoked mitochondrial injury including decreased $\Delta\psi$m and increased ROS production, in line with mitochondrial injury noted in doxorubicin-induced cardiotoxicity (Marechal et al., 2011; Octavia et al., 2012; Ichikawa et al., 2014). Treatment of luteolin effectively alleviated doxorubicin-induced mitochondrial apoptosis. Taken together, these findings should help offering novel insights for the therapeutic efficacy of luteolin against doxorubicin-induced cardiomyocyte contractile and mitochondrial defects possibly related to regulation of apoptosis.

Moreover, our finding in AMCMs revealed that doxorubicin treatment interrupted the initiation and completion of mitochondrial autophagy with downregulated levels of TFEB, LC3B, p62, LAMP1, pink1, parkin, and BNIP3. Furthermore, data from our study revealed suppressed TFEB in conjunction with elevated mTOR phosphorylation (Ser^{2448}) in doxorubicin-induced cardiotoxicity, in line with previous reports (Settembre et al., 2012; Bartlett et al., 2017; Koleini and Kardami, 2017). It remains debatable whether activating or inhibiting autophagy is beneficial for doxorubicin-induced cardiotoxicity (Sishi et al., 2013; Bartlett et al., 2017; Koleini and Kardami, 2017). It is conceived that low dose doxorubicin disrupts cardiac autophagy by inhibiting lysosomal biogenesis and function due to the abnormalities of TFEB function (Kawaguchi et al., 2012; Bartlett et al., 2016; Wang et al., 2019b). Disruption in cardiac autophagic processes leads to ROS overproduction, and $\Delta\psi m$ dissociation, contributing to mitochondria-mediated apoptosis and death, consistent with the previous finding (Bartlett et al., 2016).

Previous Ingenuity Pathway Analysis (IPA) showed that mTOR was one of the proteins which could interact with

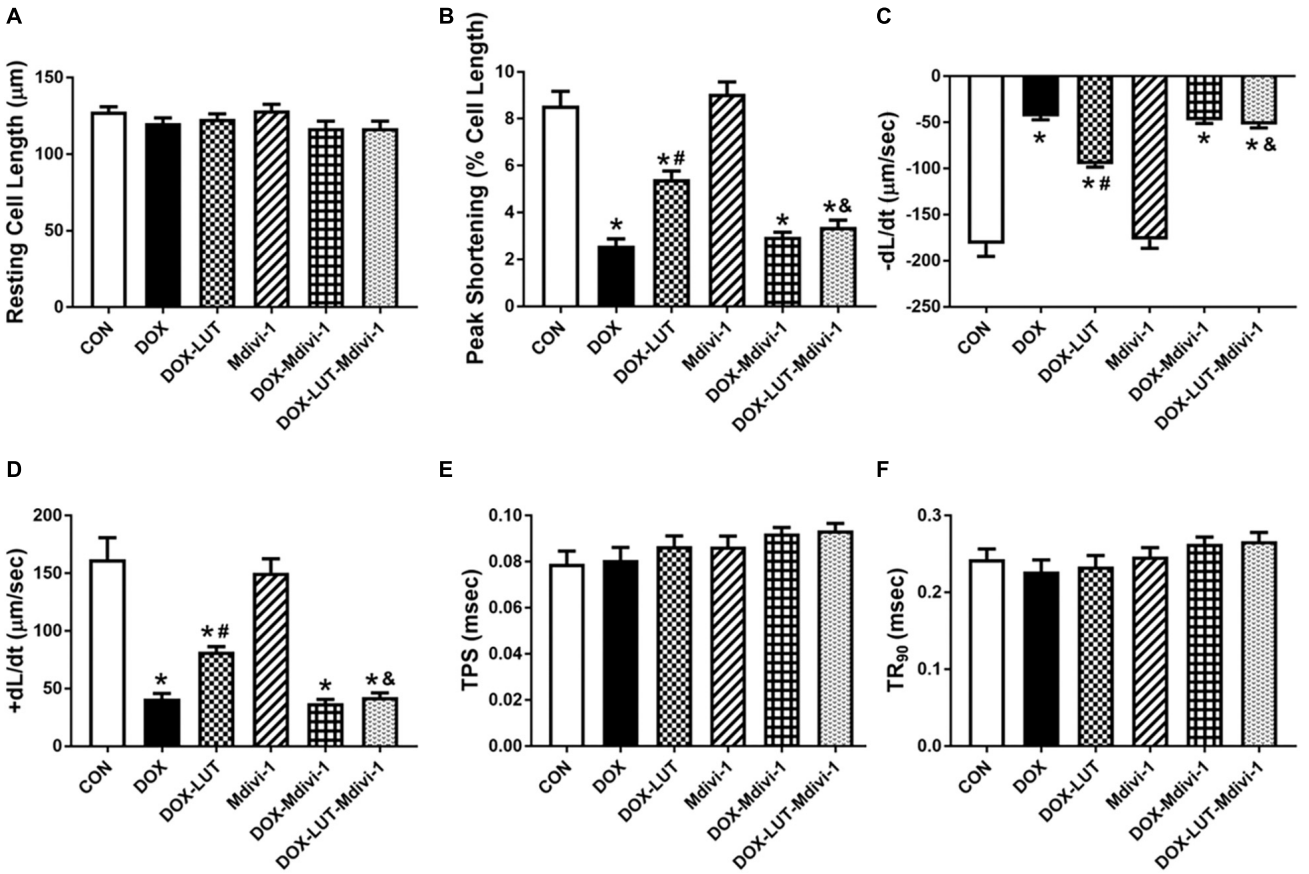

FIGURE 7 | The effect of Mdivi-1 on cardiomyocyte contractile function following doxorubicin and luteolin treatment. **(A)** Resting cell length; **(B)** Peak shortening (PS); **(C)** Maximal velocity of shortening (–dL/dt); **(D)** Maximal velocity of relengthening (+dL/dt); **(E)** Time-to -peak shortening (TPS); **(F)** Time-to-90% relengthening (TR_{90}). Mean ± SEM, n = 30 cells each group from three independent experiment. * $p < 0.05$ vs. CON group, # $p < 0.05$ vs. DOX group, & $p < 0.05$ vs. DOX-LUT group.

Drp1 (Chen et al., 2018). In this work, further analysis suggested that Drp1 phosphorylation induced mitochondrial fragmentation, phosphorylation of mTOR and inhibition of autophagic degradation through a Drp1/mTOR/TFEB-dependent pathway (Chen et al., 2018). Up-to-date, few studies have reported the interplay between Drp1 phosphorylation and TFEB. In our study, doxorubicin-induced cardiotoxicity was associated with inhibited phosphorylation of Drp1 at Ser^{616}, elevated phosphorylation of mTOR at Ser^{2448} and dampened TFEB expression. In low-dose doxorubicin treated AMCMs, the Drp1 selective inhibitor Mdivi-1 greatly increased phosphorylation of mTOR and decreased TFEB expression. Moreover, it was revealed that low dose of doxorubicin induced elongation of mitochondria in NMCMs. Recent evidence also reported that endogenous Drp1-mediated-mitochondrial autophagy may protect cardiac function in glucose deprivation and pressure overload induced heart failure (Ikeda et al., 2015; Shirakabe et al., 2016). It was indicated that the deletion of Drp1 resulting in mitochondrial elongation and mitochondrial autophagy suppression played a critical role in various cardiac disorders.

Previous analysis showed little changes in Drp1 and more mitochondrial elongation in doxorubicin-treated hearts (Abdullah et al., 2019). It was also suggested that levels of Drp1 and Drp1 Ser^{616} phosphorylation were increased following doxorubicin challenge (Xia et al., 2017; Catanzaro et al., 2019). Indeed, these authors went on to reveal elevated mitochondrial autophagy, contributing to mitochondrial dysfunction and doxorubicin toxicity. Conflicting findings have been noted with either increased or decreased autophagy with either hyperfused or fragmented mitochondria in doxorubicin-induced cardiotoxicity (Lu et al., 2009; Kobayashi et al., 2010; Dimitrakis et al., 2012; Kawaguchi et al., 2012; Sishi et al., 2013). Ample evidence suggested the low-dose doxorubicin was connected with interrupted cardiac autophagy while high-dose doxorubicin was tied with increased autophagy and cardiac dysfunction (Bartlett et al., 2017; Koleini and Kardami, 2017). Clinically, the risk of doxorubicin cardiotoxicity was increased corresponding to the accumulative dose of 400–700 mg/m^2 and the onset of

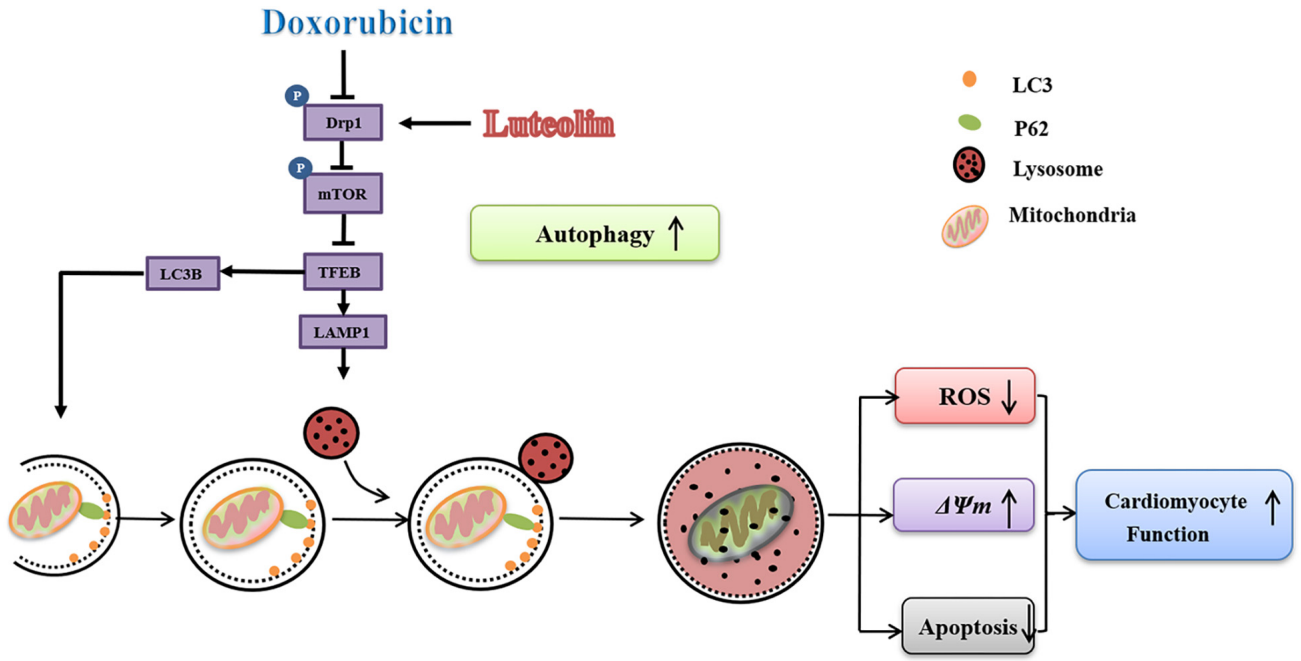

FIGURE 8 | Scheme illustrating proposed possible mechanism of action for luteolin. Doxorubicin challenge inhibits autophagy through disrupting formation of autophagosome and suppressing lysosomal generation in association with changes in Drp1/mTOR/TFEB signaling cascade. Luteolin treatment effectively facilitates autophagosome formation, and improves lysosomal function possibly through a Drp1/mTOR/TFEB-dependent mechanism, resulting in alleviation of ROS accumulation, $\Delta\Psi m$ collapse and apoptosis upon doxorubicin challenge.

delayed cardiomyopathy may occur years after initial usage (Koleini and Kardami, 2017). In this report, in order to mimic clinical application of doxorubicin in patients, the observation of experiments was conducted based on a low dose doxorubicin treatment in adult mouse cardiomyocytes which resulted in modest and progressive cardiac injury, and is consistent with conserved study (Minotti et al., 2004; Li et al., 2016). Our data revealed that decreased phosphorylation of Drp1 at Ser^{616} and autophagy upon doxorubicin challenge, which may be due to the low dose doxorubicin induced toxicity in AMCMs.

In this report, our data indicated that luteolin promoted autophagy initiation process and at the same time it promoted the lysosome generation via phosphorylation of Drp1 at Ser^{616} and TFEB, which may become a new therapeutic target of doxorubicin-induced cardiotoxicity due to the restoration of autophagy. It is perceived that a low concentration of luteolin offers cardiac protective effects, including phospholamban phosphorylation, enhance sarcoplasmic reticulum SERCA activity, MAPK signaling pathway and PI3K/Akt-mediated regulations (Wu et al., 2013; Yao et al., 2016; Xia et al., 2017; Wei et al., 2018). Furthermore, pretreatment of luteolin enhances autophagy while 3-methyladenine may block the protective effects of luteolin against myocardial injury induced by starvation (Kawaguchi et al., 2012; Sishi et al., 2013; Yao et al., 2016). In addition, previous work has reported that luteolin significantly attenuated doxorubicin-induced cardiotoxicity by inhibiting ROS accumulation and apoptosis in H9C2 cells (Wang et al., 2010; Yao et al., 2016). This finding suggested potential beneficial effect of luteolin in enhancing cardiac contractility to benefit pathological conditions with compromised heart function including doxorubicin-induced cardiotoxicity. Our present work confirmed protective property of luteolin against doxorubicin-induced cardiotoxicity, possibly related to the capacity of promoting mitochondrial autophagy and improving mitochondrial function.

A number of experimental limitations existed in this study. First and foremost, our study was a cell-based *in vitro* study lacking the *in vivo* proof-of-concept. It would be ideal to use a chronic doxorubicin-induced cardiotoxicity model with intermittent injection of doxorubicin for at least 4 weeks. In addition, it remains elusive with regards to the regulation of luteolin on Drp1 phosphorylation. Possible site of phosphorylation or phosphatase behind luteolin on Drp1 warrants further examination. Meanwhile, the molecular mechanism of Drp1-dependent mitochondrial autophagy remains unclear. In our hands, inhibition of Drp1 phosphorylation might contribute to the activation of mTORC1, the inhibition of TFEB and mitochondrial autophagy in the face of low dose doxorubicin challenge. Further work should focus on the relationship between Drp1 and mTOR, the mechanism of which may partially mediate Drp1-dependent mitochondrial autophagy. Moreover, it still remains uncertain how mTOR phosphorylation contributes to the regulation of mitochondrial autophagy and function. Although our present data seem to favor a role for TFEB-mediated mitochondrial regulation, more

in-depth work is needed for the precise mechanism behind mTOR-governed mitophagy response.

In summary, our findings reported that doxorubicin-induced cardiotoxicity is associated with defective mitochondrial autophagy, which leads to mitochondrial dysfunction and cardiomyocyte injury including apoptosis. Luteolin protects cardiomyocytes to some extent via promoting the autophagosome formation and improving lysosomal generation through a Drp1/mTOR/TFEB-dependent mechanism. These findings should provide a new avenue for the treatment of cardiotoxicity in the clinical applications of doxorubicin.

DATA AVAILABILITY STATEMENT

The datasets generated for this study are available on request to the corresponding author.

ETHICS STATEMENT

The animal study was reviewed and approved by the Zhongshan Hospital Fudan University IACUC.

AUTHOR CONTRIBUTIONS

HX, WY, SS, and CL contributed to data collection and data analysis. HX drafted the manuscript. YZ and JR contributed to conception of study, and provided funding and manuscript editing.

FUNDING

This work was supported by the National Natural Science Foundation of China 81900233 and 81770261.

REFERENCES

Abdullah, C. S., Alam, S., Aishwarya, R., Miriyala, S., Bhuiyan, M. A. N., Panchatcharam, M., et al. (2019). Doxorubicin-induced cardiomyopathy associated with inhibition of autophagic degradation process and defects in mitochondrial respiration. *Sci. Rep.* 9:2002. doi: 10.1038/s41598-018-37862-3

Ackers-Johnson, M., Li, P. Y., Holmes, A. P., O'brien, S. M., Pavlovic, D., and Foo, R. S. (2016). A simplified, langendorff-free method for concomitant isolation of viable cardiac myocytes and nonmyocytes from the adult mouse heart. *Circ. Res.* 119, 909–920. doi: 10.1161/CIRCRESAHA.116.309202

Bartlett, J. J., Trivedi, P. C., and Pulinilkunnil, T. (2017). Autophagic dysregulation in doxorubicin cardiomyopathy. *J. Mol. Cell Cardiol.* 104, 1–8. doi: 10.1016/j.yjmcc.2017.01.007

Bartlett, J. J., Trivedi, P. C., Yeung, P., Kienesberger, P. C., and Pulinilkunnil, T. (2016). Doxorubicin impairs cardiomyocyte viability by suppressing transcription factor EB expression and disrupting autophagy. *Biochem. J.* 473, 3769–3789. doi: 10.1042/bcj20160385

Bustos, P. S., Deza-Ponzio, R., Paez, P. L., Cabrera, J. L., Virgolini, M. B., and Ortega, M. G. (2018). Flavonoids as protective agents against oxidative stress induced by gentamicin in systemic circulation. Potent protective activity and microbial synergism of luteolin. *Food Chem. Toxicol.* 118, 294–302. doi: 10.1016/j.fct.2018.05.030

Catanzaro, M. P., Weiner, A., Kaminaris, A., Li, C., Cai, F., Zhao, F., et al. (2019). Doxorubicin-induced cardiomyocyte death is mediated by unchecked mitochondrial fission and mitophagy. *FASEB J.* 33, 11096–11108. doi: 10.1096/fj.201802663R

Chen, Z., Li, Y., Wang, Y., Qian, J., Ma, H., Wang, X., et al. (2018). Cardiomyocyte-restricted low density lipoprotein receptor-related protein 6 (LRP6) deletion leads to lethal dilated cardiomyopathy partly through Drp1 signaling. *Theranostics* 8, 627–643. doi: 10.7150/thno.22177

Cohen, G. M. (1997). Caspases: the executioners of apoptosis. *Biochem. J.* 326 (Pt 1), 1–16. doi: 10.1042/bj3260001

Dimitrakis, P., Romay-Ogando, M. I., Timolati, F., Suter, T. M., and Zuppinger, C. (2012). Effects of doxorubicin cancer therapy on autophagy and the ubiquitin-proteasome system in long-term cultured adult rat cardiomyocytes. *Cell Tissue Res.* 350, 361–372. doi: 10.1007/s00441-012-1475-8

Galati, G., Moridani, M. Y., Chan, T. S., and O'brien, P. J. (2001). Peroxidative metabolism of apigenin and naringenin versus luteolin and quercetin: glutathione oxidation and conjugation. *Free Radic. Biol. Med.* 30, 370–382. doi: 10.1016/s0891-5849(00)00481-0

Ge, W., Yuan, M., Ceylan, A. F., Wang, X., and Ren, J. (2016). Mitochondrial aldehyde dehydrogenase protects against doxorubicin cardiotoxicity through a transient receptor potential channel vanilloid 1-mediated mechanism. *Biochim. Biophys. Acta* 1862, 622–634. doi: 10.1016/j.bbadis.2015.12.014

Green, D. R. (1998). Apoptotic pathways: the roads to ruin. *Cell* 94, 695–698.

Guo, R., Hua, Y., Ren, J., Bornfeldt, K. E., and Nair, S. (2018). Cardiomyocyte-specific disruption of Cathepsin K protects against doxorubicin-induced cardiotoxicity. *Cell Death Dis.* 9:692. doi: 10.1038/s41419-018-0727-2

He, D., Ma, X., Chen, Y., Cai, Y., Ru, X., Bruce, I. C., et al. (2012). Luteolin inhibits pyrogallol-induced apoptosis through the extracellular signal-regulated kinase signaling pathway. *FEBS J.* 279, 1834–1843. doi: 10.1111/j.1742-4658.2012.08558.x

Hu, J., Man, W., Shen, M., Zhang, M., Lin, J., Wang, T., et al. (2016). Luteolin alleviates post-infarction cardiac dysfunction by up-regulating autophagy through Mst1 inhibition. *J. Cell Mol. Med.* 20, 147–156. doi: 10.1111/jcmm.12714

Ichikawa, Y., Ghanefar, M., Bayeva, M., Wu, R., Khechaduri, A., Naga Prasad, S. V., et al. (2014). Cardiotoxicity of doxorubicin is mediated through mitochondrial iron accumulation. *J. Clin. Invest.* 124, 617–630. doi: 10.1172/JCI72931

Ikeda, Y., Shirakabe, A., Maejima, Y., Zhai, P., Sciarretta, S., Toli, J., et al. (2015). Endogenous Drp1 mediates mitochondrial autophagy and protects the heart against energy stress. *Circ. Res.* 116, 264–278. doi: 10.1161/CIRCRESAHA.116.303356

Kawaguchi, T., Takemura, G., Kanamori, H., Takeyama, T., Watanabe, T., Morishita, K., et al. (2012). Prior starvation mitigates acute doxorubicin cardiotoxicity through restoration of autophagy in affected cardiomyocytes. *Cardiovasc. Res.* 96, 456–465. doi: 10.1093/cvr/cvs282

Kobayashi, S., Volden, P., Timm, D., Mao, K., Xu, X., and Liang, Q. (2010). Transcription factor GATA4 inhibits doxorubicin-induced autophagy and cardiomyocyte death. *J. Biol. Chem.* 285, 793–804. doi: 10.1074/jbc.M109.070037

Koleini, N., and Kardami, E. (2017). Autophagy and mitophagy in the context of doxorubicin-induced cardiotoxicity. *Oncotarget* 8, 46663–46680. doi: 10.18632/oncotarget.16944

Li, D. L., Wang, Z. V., Ding, G., Tan, W., Luo, X., Criollo, A., et al. (2016). Doxorubicin blocks cardiomyocyte autophagic flux by inhibiting lysosome acidification. *Circulation* 133, 1668–1687. doi: 10.1161/CIRCULATIONAHA.115.017443

Lin, L. C., Pai, Y. F., and Tsai, T. H. (2015). Isolation of luteolin and luteolin-7-O-glucoside from dendranthema morifolium ramat tzvel and their pharmacokinetics in rats. *J. Agric. Food Chem.* 63, 7700–7706. doi: 10.1021/jf505848z

Lu, L., Wu, W., Yan, J., Li, X., Yu, H., and Yu, X. (2009). Adriamycin-induced autophagic cardiomyocyte death plays a pathogenic role in a rat model of heart failure. *Int. J. Cardiol.* 134, 82–90. doi: 10.1016/j.ijcard.2008.01.043

Ma, Y., Yang, L., Ma, J., Lu, L., Wang, X., Ren, J., et al. (2017). Rutin attenuates doxorubicin-induced cardiotoxicity via regulating autophagy and apoptosis. *Biochim. Biophys. Acta Mol. Basis Dis.* 1863, 1904–1911. doi: 10.1016/j.bbadis.2016.12.021

Marechal, X., Montaigne, D., Marciniak, C., Marchetti, P., Hassoun, S. M., Beauvillain, J. C., et al. (2011). Doxorubicin-induced cardiac dysfunction is attenuated by ciclosporin treatment in mice through improvements in mitochondrial bioenergetics. *Clin. Sci.* 121, 405–413. doi: 10.1042/CS20110069

Minotti, G., Menna, P., Salvatorelli, E., Cairo, G., and Gianni, L. (2004). Anthracyclines: molecular advances and pharmacologic developments in antitumor activity and cardiotoxicity. *Pharmacol. Rev.* 56, 185–229. doi: 10.1124/pr.56.2.6

Octavia, Y., Tocchetti, C. G., Gabrielson, K. L., Janssens, S., Crijns, H. J., and Moens, A. L. (2012). Doxorubicin-induced cardiomyopathy: from molecular mechanisms to therapeutic strategies. *J. Mol. Cell Cardiol.* 52, 1213–1225. doi: 10.1016/j.yjmcc.2012.03.006

Park, E. J., Kim, Y. M., Kim, H. J., and Chang, K. C. (2018). Luteolin activates ERK1/2- and Ca(2+)-dependent HO-1 induction that reduces LPS-induced HMGB1, iNOS/NO, and COX-2 expression in RAW264.7 cells and mitigates acute lung injury of endotoxin mice. *Inflamm. Res.* 67, 445–453. doi: 10.1007/s00011-018-1137-8

Rao, P. S., Satelli, A., Moridani, M., Jenkins, M., and Rao, U. S. (2012). Luteolin induces apoptosis in multidrug resistant cancer cells without affecting the drug transporter function: involvement of cell line-specific apoptotic mechanisms. *Int. J. Cancer* 130, 2703–2714. doi: 10.1002/ijc.26308

Settembre, C., Di Malta, C., Polito, V. A., Garcia Arencibia, M., Vetrini, F., Erdin, S., et al. (2011). TFEB links autophagy to lysosomal biogenesis. *Science* 332, 1429–1433. doi: 10.1126/science.1204592

Settembre, C., Zoncu, R., Medina, D. L., Vetrini, F., Erdin, S., Erdin, S., et al. (2012). A lysosome-to-nucleus signalling mechanism senses and regulates the lysosome via mTOR and TFEB. *EMBO J.* 31, 1095–1108. doi: 10.1038/emboj.2012.32

Shirakabe, A., Zhai, P., Ikeda, Y., Saito, T., Maejima, Y., Hsu, C. P., et al. (2016). Drp1-dependent mitochondrial autophagy plays a protective role against pressure overload-induced mitochondrial dysfunction and heart failure. *Circulation* 133, 1249–1263. doi: 10.1161/circulationaha.115.020502

Sishi, B. J., Loos, B., Van Rooyen, J., and Engelbrecht, A. M. (2013). Autophagy upregulation promotes survival and attenuates doxorubicin-induced cardiotoxicity. *Biochem. Pharmacol.* 85, 124–134. doi: 10.1016/j.bcp.2012.10.005

Sun, A., Cheng, Y., Zhang, Y., Zhang, Q., Wang, S., Tian, S., et al. (2014). Aldehyde dehydrogenase 2 ameliorates doxorubicin-induced myocardial dysfunction through detoxification of 4-HNE and suppression of autophagy. *J. Mol. Cell Cardiol.* 71, 92–104. doi: 10.1016/j.yjmcc.2014.01.002

Wang, L., Lee, I. M., Zhang, S. M., Blumberg, J. B., Buring, J. E., and Sesso, H. D. (2009). Dietary intake of selected flavonols, flavones, and flavonoid-rich foods and risk of cancer in middle-aged and older women. *Am. J. Clin. Nutr.* 89, 905–912. doi: 10.3945/ajcn.2008.26913

Wang, P., Wang, L., Lu, J., Hu, Y., Wang, Q., Li, Z., et al. (2019a). SESN2 protects against doxorubicin-induced cardiomyopathy via rescuing mitophagy and improving mitochondrial function. *J. Mol. Cell Cardiol.* 133, 125–137. doi: 10.1016/j.yjmcc.2019.06.005

Wang, S., Ge, W., Harns, C., Meng, X., Zhang, Y., and Ren, J. (2018). Ablation of toll-like receptor 4 attenuates aging-induced myocardial remodeling and contractile dysfunction through NCoRI-HDAC1-mediated regulation of autophagy. *J. Mol. Cell Cardiol.* 119, 40–50. doi: 10.1016/j.yjmcc.2018.04.009

Wang, S. Q., Han, X. Z., Li, X., Ren, D. M., Wang, X. N., and Lou, H. X. (2010). Flavonoids from Dracocephalum tanguticum and their cardioprotective effects against doxorubicin-induced toxicity in H9c2 cells. *Bioorg. Med. Chem. Lett.* 20, 6411–6415. doi: 10.1016/j.bmcl.2010.09.086

Wang, X., Li, C., Wang, Q., Li, W., Guo, D., Zhang, X., et al. (2019b). Tanshinone IIA restores dynamic balance of autophagosome/autolysosome in doxorubicin-induced cardiotoxicity via targeting Beclin1/LAMP1. *Cancers* 11:910. doi: 10.3390/cancers11070910

Wei, B., Lin, Q., Ji, Y. G., Zhao, Y. C., Ding, L. N., Zhou, W. J., et al. (2018). Luteolin ameliorates rat myocardial ischaemia-reperfusion injury through activation of peroxiredoxin II. *Br. J. Pharmacol.* 175, 3315–3332. doi: 10.1111/bph.14367 doi: 10.1111/bph.14367

Wenningmann, N., Knapp, M., Ande, A., Vaidya, T. R., and Ait-Oudhia, S. (2019). Insights into doxorubicin-induced cardiotoxicity: molecular mechanisms, preventive strategies, and early monitoring. *Mol. Pharmacol.* 96, 219–232. doi: 10.1124/mol.119.115725

Wu, X., Xu, T., Li, D., Zhu, S., Chen, Q., Hu, W., et al. (2013). ERK/PP1a/PLB/SERCA2a and JNK pathways are involved in luteolin-mediated protection of rat hearts and cardiomyocytes following ischemia/reperfusion. *PLoS One* 8:e82957. doi: 10.1371/journal.pone.0082957

Xia, Y., Chen, Z., Chen, A., Fu, M., Dong, Z., Hu, K., et al. (2017). LCZ696 improves cardiac function via alleviating Drp1-mediated mitochondrial dysfunction in mice with doxorubicin-induced dilated cardiomyopathy. *J. Mol. Cell Cardiol.* 108, 138–148. doi: 10.1016/j.yjmcc.2017.06.003

Xu, H., Linn, B. S., Zhang, Y., and Ren, J. (2019). A review on the antioxidative and prooxidative properties of luteolin. *React. Oxyg. Species* 7, 136–147.

Yao, H., Shang, Z., Wang, P., Li, S., Zhang, Q., Tian, H., et al. (2016). Protection of Luteolin-7-O-Glucoside Against Doxorubicin-Induced Injury Through PTEN/Akt and ERK Pathway in H9c2 Cells. *Cardiovasc. Toxicol.* 16, 101–110. doi: 10.1007/s12012-015-9317-z

Yao, H., Zhou, L., Tang, L., Guan, Y., Chen, S., Zhang, Y., et al. (2017). Protective effects of luteolin-7-O-glucoside against starvation-induced injury through upregulation of autophagy in H9c2 Cells. *Biosci. Trends* 11, 557–564. doi: 10.5582/bst.2017.01111

Zhang, Y., Han, X., Hu, N., Huff, A. F., Gao, F., and Ren, J. (2014a). Akt2 knockout alleviates prolonged caloric restriction-induced change in cardiac contractile function through regulation of autophagy. *J. Mol. Cell Cardiol.* 71, 81–91. doi: 10.1016/j.yjmcc.2013.12.010

Zhang, Y., Mi, S. L., Hu, N., Doser, T. A., Sun, A., Ge, J., et al. (2014b). Mitochondrial aldehyde dehydrogenase 2 accentuates aging-induced cardiac remodeling and contractile dysfunction: role of AMPK, Sirt1, and mitochondrial function. *Free Radic. Biol. Med.* 71, 208–220. doi: 10.1016/j.freeradbiomed.2014.03.018

Zhou, H., Wang, J., Hu, S., Zhu, H., Toanc, S., and Ren, J. (2019). BI1 alleviates cardiac microvascular ischemia-reperfusion injury via modifying mitochondrial fission and inhibiting XO/ROS/F-actin pathways. *J. Cell Physiol.* 234, 5056–5069. doi: 10.1002/jcp.27308

Zhou, H., Wang, J., Zhu, P., Hu, S., and Ren, J. (2018a). Ripk3 regulates cardiac microvascular reperfusion injury: the role of IP3R-dependent calcium overload, XO-mediated oxidative stress and F-action/filopodia-based cellular migration. *Cell Signal* 45, 12–22. doi: 10.1016/j.cellsig.2018.01.020

Zhou, H., Wang, J., Zhu, P., Zhu, H., Toan, S., Hu, S., et al. (2018b). NR4A1 aggravates the cardiac microvascular ischemia reperfusion injury through suppressing FUNDC1-mediated mitophagy and promoting Mff-required mitochondrial fission by CK2alpha. *Basic. Res. Cardiol.* 113:23. doi: 10.1007/s00395-018-0682-1

Zhu, S., Xu, T., Luo, Y., Zhang, Y., Xuan, H., Ma, Y., et al. (2017). Luteolin enhances sarcoplasmic reticulum Ca2+-ATPase activity through p38 MAPK signaling thus improving rat cardiac function after ischemia/reperfusion. *Cell Physiol. Biochem.* 41, 999–1010. doi: 10.1159/000460837

Conflict of Interest: The authors declare that the research was conducted in the absence of any commercial or financial relationships that could be construed as a potential conflict of interest.

frontiers in Physiology

REVIEW
published: 04 June 2020
doi: 10.3389/fphys.2020.00586

Come Together: Protein Assemblies, Aggregates and the Sarcostat at the Heart of Cardiac Myocyte Homeostasis

Moydul Islam[1,2,3], *Abhinav Diwan*[1,2,4]* *and Kartik Mani*[1,2,4]*

[1] Division of Cardiology, Washington University School of Medicine, St. Louis, MO, United States, [2] Center for Cardiovascular Research, Washington University School of Medicine, St. Louis, MO, United States, [3] Department of Chemistry, Washington University in St. Louis, St. Louis, MO, United States, [4] John Cochran Veterans Affairs Medical Center, St. Louis, MO, United States

OPEN ACCESS

Edited by:
Xuejun Wang,
University of South Dakota,
United States

Reviewed by:
Sonia R. Singh,
University Medical Center
Hamburg-Eppendorf, Germany
Federica del Monte,
Medical University of South Carolina,
United States

***Correspondence:**
Abhinav Diwan
adiwan@wustl.edu;
adiwan@dom.wustl.edu
Kartik Mani
kmani@wustl.edu

Specialty section:
This article was submitted to
Striated Muscle Physiology,
a section of the journal
Frontiers in Physiology

Received: 21 February 2020
Accepted: 11 May 2020
Published: 04 June 2020

Citation:
Islam M, Diwan A and Mani K
(2020) Come Together: Protein
Assemblies, Aggregates
and the Sarcostat at the Heart
of Cardiac Myocyte Homeostasis.
Front. Physiol. 11:586.
doi: 10.3389/fphys.2020.00586

Homeostasis in vertebrate systems is contingent on normal cardiac function. This, in turn, depends on intricate protein-based cellular machinery, both for contractile function, as well as, durability of cardiac myocytes. The cardiac small heat shock protein (csHsp) chaperone system, highlighted by αB-crystallin (CRYAB), a small heat shock protein (sHsp) that forms ∼3–5% of total cardiac mass, plays critical roles in maintaining proteostatic function via formation of self-assembled multimeric chaperones. In this work, we review these ancient proteins, from the evolutionarily preserved role of homologs in protists, fungi and invertebrate systems, as well as, the role of sHsps and chaperones in maintaining cardiac myocyte structure and function. We propose the concept of the "sarcostat" as a protein quality control mechanism in the sarcomere. The roles of the proteasomal and lysosomal proteostatic network, as well as, the roles of the aggresome, self-assembling protein complexes and protein aggregation are discussed in the context of cardiac myocyte homeostasis. Finally, we will review the potential for targeting the csHsp system as a novel therapeutic approach to prevent and treat cardiomyopathy and heart failure.

Keywords: aggregates, autophagy, ubiquitin 26S-proteasome system, lysosome, heat shock proteins

INTRODUCTION

Evolving over the previous 600 million years (Poelmann and Gittenberger-de Groot, 2019), the metazoan circulatory system is at the center of the explosion of multicellular functionality, culminating in the human era. From primordial heart tubes in early protostomes to the four-chambered hearts of mammals, each of these circulations have ensured nutrient and oxygen supply, maintenance of temperature, as well as waste removal. In each instance, the circulatory system is driven by contractile cells, from the endo-symbiotic contractile elements in ancient protists a billion years ago, to the cardiac myocytes of chordates. The highlight of all these cells is a complex network of protein assemblies that form organized contractile machines. Cardiac myocytes are

unique in lifespan, size, structure, function, durability, and metabolism. Each of these features is essential in ensuring continuous uninterrupted cardiac function, from early embryo, through the entire duration of post-natal life. Morphologically, the cardiac syncytium is similar to that observed in many protists and yeasts. In addition to the unusually large energetic apparatus, essential for powering the contractile machinery, cardiac myocytes, like yeast, require a complex proteostatic system. Unlike the dominant role of the proteasome in other cell types, cardiac myocyte lysosome function, like the vacuole in bacteria, plants and yeast, plays a major role in integrating metabolism (Mani et al., 2018) with both synthetic and degradation machinery for the contractile proteins. Thus, lysosome dysfunction results in metabolic derangement, as well as, proteotoxicity. This ultimately presents as cardiomyopathy and heart failure (Platt et al., 2012). Given the enormous and dynamic proteostatic load, in both long-lived monads as well as cardiac myocytes, evolutionarily preserved chaperones, like the small heat shock protein, αB-crystallin (CRYAB), play a critical role in maintaining cardiac homeostasis. sHsp mutations as well as those in proteostatic machinery components, such as BAG3, have been implicated as mediators of cardiomyopathy. In this review, we highlight the role of these proteostatic systems that constitute the underpinnings on normal cardiac function, as well as their roles, both, as arbiters of heart failure and, as potential novel therapeutic targets.

PROTEOSTATIC FAILURE IN HEART DISEASE: *THE DEVIL IN THE HEART*

Given the primacy of their contractile function in homeostasis, diseases affecting cardiac myocytes result in impairment of, either or both, systolic (contractile) and diastolic (relaxation) properties of the heart. This ultimately presents as cardiomyopathy and heart failure leading to death. From a public health point of view, unlike advances in infectious diseases and cancer, epidemiologic indices have lagged with regards to the societal impact of cardiovascular disease, especially heart failure (Virani et al., 2020). This is despite considerable advances in neuro-hormonally targeted approaches in pharmacotherapy, as well as hemodynamically focused and perfusion-directed invasive procedures and devices. A critical lacuna remains in development of strategies specifically directed toward the cardiac contractile system. Notably, with the limited efforts to augment or replace cardiac contractility, current approaches in the form of mechanical assist devices, stem cell therapy and, select pharmacological therapies, have minimal overall lasting benefits. Furthermore, recent epidemiologic trends show a worrisome reversal of hard-fought prior gains with improvements in cardiovascular mortality and mortality (Virani et al., 2020), dictating a sense of urgency. Optimal cardiac function depends on both optimal function of the cardiac myocytes as well as preservation of the tissue architecture. Thus, targeting the protein quality control systems in rebuilding, and possibly enhancing, the unique cardiac contractile protein network, *in situ*, is a very attractive strategy.

Cardiomyopathies are traditionally classified by etiology, either as sequelae of ischemic heart disease (due to occlusion of coronary arteries) [ischemic cardiomyopathy (ICM], or those without ischemic insults [non-ischemic cardiomyopathy (NICM)] (McKenna et al., 2017). Despite this differentiation, the transition from incipient to overt heart failure in both forms of cardiomyopathy shares many common mechanisms such as incremental hemodynamic stresses, metabolic alterations, abnormal tissue perfusion and inflammatory changes. Abnormalities in protein quality control also appear to play roles in both ischemic and non-ischemic dilated cardiomyopathy (reviewed in Henning and Brundel, 2017). Similar to the "second hit" hypothesis in malignant transformation, it has been suggested that genetic predisposition in the form of abnormal protein quality control may provoke changes in the sarcomere that result in cardiomyopathy and heart failure (Predmore et al., 2010; Herrmann et al., 2013; Rainer et al., 2018). Indeed, while mutations in candidate protein quality control machinery proteins like αB-crystallin, BAG3, HspB7, Vps34, p97 appear to play mechanistic roles in inducing dilated cardiomyopathy in genetic myofibrillar myopathies (Vicart et al., 1998; Bova et al., 1999; Fang et al., 2017; Judge et al., 2017; Kimura et al., 2017; Dominguez et al., 2018; Brody et al., 2019); variants in many of these, such as BAG3 and KLHL3 are also associated with cardiomyopathy in population-based genomic analyses (Aragam et al., 2018; Myers et al., 2018; Shah et al., 2020). Conversely, mutations in sarcomeric components like desmin, titin, actin, myosin, myosin binding protein C (cMyBP-C) are associated with features of abnormal proteostasis and are similarly reflected in population genomic studies as well (Goldfarb and Dalakas, 2009; Herman et al., 2012; Schlossarek et al., 2012; Esslinger et al., 2017; Hoorntje et al., 2017; McNally and Mestroni, 2017; Glazier et al., 2018). Interestingly, in humans, autosomal recessive deletion-mutant of αB-crystallin at *M1* (Ma K. et al., 2019) as well as missense mutations in this protein at *D109A* (Fichna et al., 2017), *D109H* (Sacconi et al., 2012), *R120G* (Vicart et al., 1998), and *R157H* (Inagaki et al., 2006) result in early fatality. In contrast, a murine model of αB-crystallin ablation (which is accompanied with unintended ablation of Hspb2; Brady et al., 2001) results primarily in skeletal myopathy which manifests with aging; and forced overexpression of αB-crystallin mutants (such as R120G) has been required to replicate human cardiomyopathy phenotype in a much more insidious and delayed fashion (Wang et al., 2001; Rajasekaran et al., 2007). This highlights differences in protein quality control mechanisms between species, whereby caution is warranted in interpreting findings from murine experiments as models of human disease.

A key feature of protein quality control pathways is the efficient functioning of systems to degrade misfolded, damaged and potentially superfluous proteins. Tagging of proteins to target them for degradation is typically achieved by ubiquitination, which involves a covalent attachment of the protein to a 76 amino acid protein ubiquitin moiety to a lysine residue; which may further expand via a variety of branching mechanisms to achieve poly-ubiquitination (Kwon and Ciechanover, 2017). In the process of poly-ubiquitination, a ubiquitin moiety can be conjugated to another one via one of its seven lysine

residues or its methionine residue to confer specificity in further processing of the host protein that is ubiquitinated. Ubiquitination of proteins can confer signaling roles, or result in degradation of the protein. Studies have demonstrated that linkages via lysine 48 (K48) and lysine 11 (K11) target proteins for degradation via the proteasome, whereas lysine 63 (K63) linkages confer signaling roles or are targeted for degradation via the autophagy-lysosome pathway (Kwon and Ciechanover, 2017). The proteasome is a specialized organelle in the cell comprised of a complex of proteolytic enzymes organized in two subunits, a catalytic 20S subunit; and a regulatory 19S subunit, which together form a cylindrical structure that de-ubiquitinates, unfolds and cleaves peptide bonds in proteins to generate amino acids (Bard et al., 2018). Ubiquitin tagging of aggregate-prone proteins is essential for their efficient removal (Galves et al., 2019). However, studies have documented impairment in the ubiquitin proteasome pathways by mutant αB-crystallin (R120G) (Chen et al., 2005; Zhang et al., 2010, 2019; Gupta et al., 2014) and desmin mutants (Liu et al., 2006a,b) that are linked to cardiomyopathy in humans; suggesting that worsening protein aggregate pathology is linked at least in part to progressive impairment in this arm of the protein quality control machinery. Moreover, recent studies conclusively demonstrate rapid development of fulminant cardiomyopathy and death in mice lacking *Psmc1* (that encodes for an essential component of the 19S proteasome subunit) (Pan et al., 2020); with concomitant upregulation of the autophagy-lysosome machinery as an adaptive response to remove accumulated protein aggregates.

Autophagy, a lysosomal degradative pathway that sequesters proteins, organelles and other cellular constituents is another mechanism for degradation of long-lived proteins and damaged proteins, and acts as a back-up in the setting of proteasome dysfunction (Pohl and Dikic, 2019). Autophagy or "self-eating" occurs via multiple pathways that involve sequestration of cargo within double membrane bound autophagosomes (termed as macroautophagy), direct uptake of proteins with a specific KFERQ motif into the lysosome via chaperone-mediated autophagy, or lysosomal membrane invagination and sequestration of proteins via microautophagy (reviewed in Dikic and Elazar, 2018). Studies from our lab as well as others have demonstrated that the autophagy-lysosome pathway also becomes progressively impaired with expression of aggregate-prone proteins in cardiac myocytes, such as R120G mutant of αB-crystallin (Ma X. et al., 2019; Pan et al., 2019); which is mechanistically secondary to suppression of the lysosome biogenesis program. Conversely, many lysosomal disorders including Danon' disease, Pompe's disease and Fabry's disease result in a cardiomyopathy with evidence of failed proteostasis (reviewed in Sciarretta et al., 2018a). Failure of the ubiquitin-proteasome system and autophagy-lysosome pathways has also been implicated in more common forms of cardiomyopathy and heart failure resulting from ischemia-reperfusion injury and pressure overload stress (reviewed in Wang et al., 2011). Specifically, we have uncovered evidence for lysosome impairment in cardiac myocytes (Ma et al., 2012a,b) and macrophages (Javaheri et al., 2019) in the setting of myocardial ischemia-reperfusion injury, at least in part due to suppression of the lysosome biogenesis program (Godar et al., 2015; Ma et al., 2015). This impairment of autophagy-lysosome pathway is associated with accumulation of poly-ubiquitinated proteins (Godar et al., 2015), pointing to a critical role for this pathway in protein quality control in the setting of ischemia-reperfusion injury. Moreover, autophagy suppression is also observed in the chronic phase after myocardial infarction and contributes to development of ischemic cardiomyopathy (Maejima et al., 2013). This is associated with formation of "aggresomes" which are p62-containing protein aggregates formed as a cellular response to sequester mis-folded and damaged proteins when their removal is impeded (Johnston et al., 1998). In this study (Maejima et al., 2013), the autophagy suppression was mechanistically driven by activation of Mst1 (mammalian Ste20-like kinase 1), a serine-threonine kinase component of the Hippo signaling pathway, which is sufficient to phosphorylate Beclin-1 to promote its sequestration by Bcl-2 and inhibit autophagosome formation. Indeed, work from this group subsequently demonstrated that stimulation of autophagy-lysosome pathway with trehalose was effective in clearing p62 and rescuing post-myocardial infarction ventricular dilation and dysfunction (Sciarretta et al., 2018b). p62 has also been described to play a critical role in aggresome formation in the setting of R120G αB-crystallin mutant or desmin mutant expression, which protects cardiac myocytes from cell death (Zheng et al., 2011). Other components of the aggresome have been uncovered in studies with laser microdissection of intracytoplasmic inclusions identified in muscle biopsies from patients with reducing body myopathy (RBM) which led to the identification of mutations in Xq26.3-encoded four and a half LIM domain 1 (FHL1) protein as a cause for cardiomyopathy (Schessl et al., 2008).

Impairment of the autophagy-lysosome pathway has also been described with progression of pressure-overload induced hypertrophy and cardiac failure (reviewed in Sciarretta et al., 2018a), which accompanies failure of ubiquitin proteasome system and impaired protein quality control (Wang et al., 2011). Recent also studies demonstrate that coupling of poly-ubiquitinated proteins to extra-proteasomal receptors, specifically Ubiquilin 1, plays an important role in removal of K48-linked poly-ubiquitinated substrates in cardiac myocytes to maintain homeostasis in response to ischemia-reperfusion stress (Hu et al., 2018). Conversely, activation of the ubiquitin-proteasome system or the SUMOylation pathways (with UBC9 overexpression) were sufficient to rescue many features of cardiomyopathy induced by expression of the R120G αB-crystallin mutant (Gupta et al., 2016). Taken together, these observations suggest an intricate relationship in the delicate balance between the sarcomere and proteostatic systems that are key to the otherwise robust, durable and reliable functioning of the sarcomere and the cardiac myocyte. Conceivably, while inciting event may differ based upon the individual pathology, failed proteostasis machinery and increased abundance of aggregate-prone protein may be part of a vicious cycle where either impairments trigger a feed forward loop to drive the pathology.

SARCOMERES: *SOMETHING IN THE WAY THEY MOVE*

In order to understand the key function of cardiac myocytes, it is imperative to focus on the complex protein architecture that define the essential contractile unit of the heart, namely the sarcomeres (see **Figure 1**). Consisting of repeating units of a near-identical arrangement of contractile, non-contractile proteins as well as a complex of regulatory proteins, up to 300 of these 2.2 μm-long sarcomeres are joined end-to-end to form the myofibrils that power cardiac contractility (Clark et al., 2002; van der Velden and Stienen, 2019; see **Figure 1**). Thus, each myofibril consists of repeating sarcomeres. Similar to the arrangement of proteins in the lens, a crystalline arrangement of large proteins in the sarcomeres results in the formation of the contractile system, which is key to the essential function of cardiac myocytes. This system of contractile proteins is held in place, attached to the sarcolemma and the extracellular matrix via integrins in a non-contractile protein assembly known as costameres. Unlike simpler myofibrils in other cell types, striated muscle cells (cardiac and skeletal myocytes) have organized bundles of myofibrils associated with a reticulum of both modified smooth endoplasmic reticulum [sarcoplasmic reticulum (SR)] and mitochondria. While the former coordinate the excitation-contraction coupling from the sarcoplasmic depolarization via local release of calcium, the latter are responsible for production of high-energy phosphates to power the contraction. As myocytes are attached to each other with an intercalated disk consisting of proteins like actinin and vinculin, contraction of individual myocytes in series results in shortening of myofibrils; and simultaneous shortening of myofibrils in parallel drives myocyte contraction. Therefore, the sum of individual sarcomere shortening, both in series across individual myofibrils, as well as in parallel across myofibrils in the same bundle and across bundles in an individual myocyte, results in contraction of the entire myocyte and consequently the muscle.

Each sarcomere is bound by sarcomeric a-actinin-rich and electron-dense Z-lines on either side that form the essential platform as well as a central M-line that forms the two ends of the platform on which sarcomeric shortening occurs (**Figure 1**). Contractile proteins arranged as isotropic thin filaments attached to the Z-lines on either side are pulled inwards by the movement of anisotropic thick filaments attached to the central M-line, resulting in sarcomeric shortening. Simultaneous activation of the entire myofibril driven by coordinated calcium fluxes in the SR results in a summed contraction across the entire myofibril as well as myofibril bundles, and consequently contraction of the entire cell. While the arrangement of the motor proteins, actin and myosin in the thin and thick filaments respectively, results in contraction, it is the creation of a platform for these elements as well the anchors to the myofibril and cell architecture that are key to successful generation of a force from a functional sarcomere. Of these platform proteins, the giant proteins, titin, obscurin and nebulette, form the underlying structure on which the cardiac sarcomere is constructed. The largest protein in mammals, titin (MW 3.7 Md) (Tskhovrebova and Trinick, 2003), consists of both elastic and inelastic elements that are key to both structural and mechano-transductive functions. In addition, the titin skeleton provides a platform for both regulatory and degradative elements for repair of sarcomere elements and adaptation to stress.

As touched on previously, anchor proteins such as desmin, are essential to anchor the filaments to the Z-line as well as to costameres linking the myofibrils to the sarcolemma, the extracellular matrix as well as other myocytes via the intercalated (I) disk. In addition, desmin appears to be key in binding the mitochondria, the endoplasmic reticulum and the lysosomes to the myofibrils. Unlike mitochondria in other tissues, the reticular arrangement of these sarcomere-associated mitochondria is facilitated by desmin and result in enhanced functioning of these mitochondria (Milner et al., 2000). Thus, loss of desmin, during stress states results in both disruption of the sarcomere as well as mitochondrial dysfunction reflected in abnormal giant mitochondrial with swelling of the cristae and membrane depolarization (Milner et al., 1999; Maloyan et al., 2005; Diokmetzidou et al., 2016). Loss of desmin function, either due to mutation (Dalakas et al., 2000) or stress related post-translational modifications (Rainer et al., 2018; Tsikitis et al., 2018) result in destabilization of the sarcomere characterized by widening and loss of definition of the otherwise sharp electron dense actinin rich Z-lines and I-disks. Contractile dysfunction in this setting results from the disarray of the elements of the sarcomere as well as disruption of the attachment of the myofibrils to the cell membrane and ECM, as well as from the interaction with the nuclear lamina resulting in loss of nuclear homeostasis (Heffler et al., 2020). While initially identified in desmin-related genetic cardiomyopathies (Goldfarb and Dalakas, 2009), these features of desmin mis-localization, as well as sarcomeric disarray, are increasingly identified as features of cardiomyopathy in general (Coats et al., 2018; Tsikitis et al., 2018; Nakano et al., 2019).

While the contraction of an individual sarcomere is a remarkable marvel of electromechanical and metabolic coordination, the real achievement is the scaling of this in a coordinated syncytial pattern to the level of the myofibril, myocyte, and, ultimately, the cardiac muscle resulting in a functional heartbeat. Furthermore, this repeats, without fail, from the embryonic contraction of cardiac precursors through to the adult heart for many decades. In fact, until recently, the cessation of heartbeat was the *sine qua non* of death, in general, prior to recognition of "brain death." With the exception of tonic contractility (albeit at lower frequencies) of the skeletal musculature powering respiration, cardiac myocyte function as well as the incredibly complex electromechanical cardiac syncytium is characterized by the amazing mechanical advantage generated by this unique morphology of the heart. This manifests with translating a 5–10% myofibril shortening into a 50–70% reduction in cardiac volume with each heartbeat. Thus, small disruptions in the contractility of individual sarcomeres result in equally dramatic and, potentially lethal, consequences to the organism. The close relationship of the sarcoplasmic reticulum, as well as sarcomere-associated mitochondria and lysosomes result in the ability to maintain unique metabolic signatures as well as a remarkable ability of the heart to endure during states of duress to the organism. Furthermore, the presence of direct

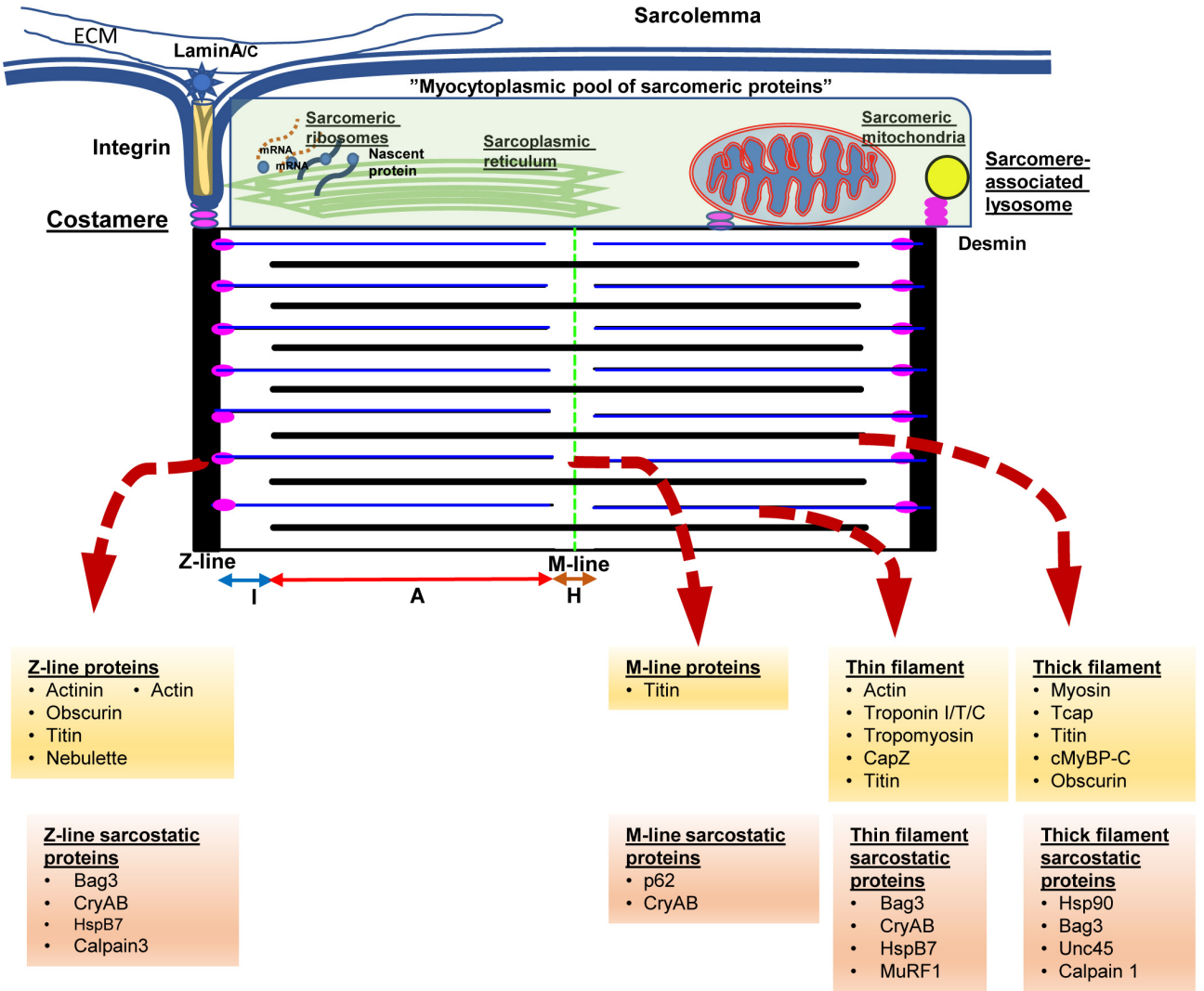

FIGURE 1 | The sarcomere from the protein quality control perspective. Cardiac myocytes contain multiple myofilament bundles running through the length of the cell and are attached on either end to the intercalated disk between adjacent cells. Each myofilament, in turn, consists of a series of repeating units of contractile assemblies, known as sarcomeres. Each sarcomere is 2.2 microns in length and extends between two electron dense lines, the Z-lines with alternating areas of isotropic (I band) and anisotropic (A band) with a slender electron dense central M-line. The A band consists of an overlap zone with both thick and thin filaments, while the I band extends from the Z-line consisting of only thin filaments. Around the M-line, there is a relatively isotropic area consisting of only thick filaments known as the H-zone. The thin filaments are attached to the Z-lines via the anchor protein desmin, which also results in anchoring sarcomeric mitochondria and lysosomes to the sarcomere. Each sarcomere is also attached via integrins and laminins to the extracellular matrix via costameres that also anchor the sarcomere to the sarcolemma as well as to the intercalated disk. Disruption of desmin results in disruption of the sarcomere, mitochondrial dysfunction, and cardiac myocyte dysfunction, ultimately presenting with fatal cardiomyopathy. The Z-lines are formed via assemblies of actinin, actin, as well as a host of Z-line associated proteins. The underlying skeleton of the entire sarcomere is created via the giant proteins, titn, obscurin, and nebulette. The titin sarcomeric skeleton extends from the Z-line to the M-line. Over the titin skeleton, thick, and thin filaments are assembled. High energy phosphate driven movement of the myosin (thick filaments) against the actin filaments, triggered by calcium fluxes from sarcolemmal depolarization, results in shortening of the sarcomere. Summation of sarcomere contraction results in cardiac myocyte and ultimately, the heartbeat. Cognate chaperones (e.g., unc-45) as well as multifunctional chaperones [CRYAB (αB-crystallin)/Bag3] play roles in maintaining the sarcomere and are listed above. The proteins at the above noted structures and associated chaperones are listed underneath in yellow and orange background.

points of communication (via integrins to the cell membrane and the extracellular matrix as well the between the myofibrils and the nucleus), allow the cardiac myocyte to maintain morphologic stability while dynamically adapting to continually variable hemodynamic, electromechanical, metabolic, and energetic changes (Henderson et al., 2017).

SARCOSTAT: *A PROPOSED FRAMEWORK TO UNDERSTAND SARCOMERIC PQC*

As maintenance of this assembly of large, otherwise insoluble, proteins is the key to homeostasis in chordates who depend on

the continuous contractile function of the cardiac system, it is necessary to understand how these sarcomeres assemble, endure stress, remodel and how these proteins are degraded. Unlike the cardiac myocytes that have a remarkably long life and low (if any) replacement potential in post-natal life, myofibrils, costameres, and organelles have a comparatively short existence. Half-lives of sarcomeric proteins vary but most proteins are replaced within a matter of days and weeks (Martin, 1981; Rudolph et al., 2019). While hemodynamic stress results in increased protein synthesis (Schreiber et al., 1981), this is often accompanied by accelerated degradation, consistent with stable stoichiometry and steady state half-lives. Furthermore, it was recently demonstrated that both overexpression experiments with troponin I as well as with photobleaching experiments in a titin-GFP transgenic mouse line, that the overall stoichiometry suggests dynamic movement between the sarcomere and a reserve pool in the cytosol exists (Feng et al., 2009; da et al., 2011). This is remarkable given the fact that these proteins are regarded as highly insoluble and in the case of titin, remarkably large. Despite data showing that mRNA localizes to the sarcomere with local ribosomal synthesis of protein (Lewis et al., 2018), the question remains as to how cardiac myocytes are able to efficiently maintain the structure and function of the sarcomeres with accurate replacement of both damaged components and reintegrate "repaired" proteins, particularly in the setting of ischemic stress. To understand the dynamic nature of these processes, we propose the concept of a "sarcostat" (see **Figure 2**).

In addition to contractile and cytoskeletal elements, each sarcomere has a variety of proteins which function to maintain optimal contractility of the sarcomere. These include association of calpain 3 and 4 with the M-line; and of the autophagic adaptors, p62 and NBR1, on the titin kinase domain on the thin filament. Also, a host of specific ring finger proteins (MuRFs) are associated with the sarcomere, which function both as E3 ligases to facilitate protein degradation via K48 ubiquitination of sarcomeric proteins (Kedar et al., 2004) and for lysosomal targeting (or activation of signaling) via K63 ubiquitination (as occurs via CHiP) (Ulbricht et al., 2013). In contrast to their expected function, the sarcomeric calpains do not degrade proteins but merely facilitate removal of individual proteins from the sarcomere by making single cuts (Williams et al., 1999). In this proposed model (see **Figure 2**), the released proteins are then directed to the sarcostat (*infra vide*) and either recycled or degraded, via either the ubiquitin-protesomal system or the autophagy-lysosomal pathway. As many of the sarcomeric proteins are large complex structures, they need to be chaperoned to prevent misfolding and aggregation. For instance, the anchor protein desmin, which is essential for maintaining sarcomere integrity as well as cardiac sarcomeric mitochondria, is characterized by a large intrinsically disordered (low complexity) domain with a predisposition to form stable misfolded oligomers in the absence of its cognate chaperone αB-crystallin (Wang et al., 2001; Sharma et al., 2017; Kedia et al., 2019). This phenomenon is also seen in the case of filamin C, actin and myosin (Wojtowicz et al., 2015; Szikora et al., 2020). The discovery of variants of the giant protein titin in genomic studies of cardiomyopathy (Tharp et al., 2019), has also had a major impact in our understanding of how sarcomeric proteins are chaperoned in homeostasis and under stress. αB-crystallin appears to interact with the n2b region of titin in cardiac muscle and this binding plays a role in the stiffness of the sarcomere (Bullard et al., 2004). Similar to the effect of preventing aggregation of desmin, the binding of CRYAB to titin prevents aggregation of the disordered aggregation prone PEVK domain in titin. This facilitates optimal titin folding and maintains sarcomere elasticity (Kotter et al., 2014).

Studies have demonstrated that all sarcomeric proteins are produced far in excess of the actual observed protein content in the sarcomere (Lewis et al., 2018), and a significant fraction of sarcomeric proteins is actively in flux to and from a presumed "pool" to the sarcomere. Most of these proteins are large (if not giant), intrinsically insoluble and thus, aggregate prone. Although protein aggregation has been demonstrated during stress states (i.e., hemodynamic and metabolic stress), microscopy of normally functioning sarcomeres do not show where this "lost" protein pool of insoluble proteins exists or even why this stoichiometric excess production and flux exists. The concept of a myocytoplasmic "sarcostat" helps explain these apparent inconsistencies (see **Figure 2**). The sarcostat consists of a complex of chaperone proteins (Bag3, Unc-45, Hsp90 as well as the sHsps [HspB1 and HspB5-8 (including CryAB)], adapter proteins (p62, nBR1, and atg8), and "sensor" protein kinases and phosphatases (PKA, PKC isoforms, mTORC1, p38 MAPK, calcineurin and the titin kinase domain of titin). These are also complexed with anchor proteins (e.g., desmin), structural proteins (e.g., titin and obscurin), RNA binding proteins, sarcomeric ribosomes, adjacent sarcoplasmic reticulum, intra-sarcomeric calpain proteases, proteasome-directed (MuRFs) and autophagy-lysosome (CHIP/STUB) directed ubiquitin ligases, protein aggregates, stress granules, sarcomeric mitochondria and last, but not least, the sarcomere-associated lysosomes. In this model, the sarcostat is critical in continuously building, repairing, remodeling and degrading the sarcomere, thus reinforcing the notion of a dynamic sarcomere that actively and rapidly responds to changes in loading and environmental cues, rather than the prior static model of a singular contractile apparatus. Evidence for this model, albeit fragmented, already exists. In addition to the stoichiometric argument, the energetic argument to be able to draw on a local pool of protein, rather than solely relying on newly synthesized protein adds tremendous flexibility during states of metabolic stress when transcription and translation may be affected. Furthermore, augmentation of the protein quality control machinery (both proteasomal as well as the autophagy-lysosomal pathway) is associated with benefits and sarcomere recovery in a variety of heart failure models associated with sarcomere dysfunction even in the absence of correction of the primary genetic abnormality (such as mutations in MYH7, desmin, and CryAB) (Li et al., 2011; Pattison et al., 2011; Ranek et al., 2013; Gupta et al., 2014; McLendon et al., 2014; Cabet et al., 2015; Su et al., 2015; Dahl-Halvarsson et al., 2018; Ma X. et al., 2019). Thus, various elements of the "sarcostat" are in dynamic equilibrium, whereby perturbations in one element (either genetic or environmental) induce structural and functional abnormalities, and therapeutic targeting of this inciting stimulus or another balancing node can restore homeostasis.

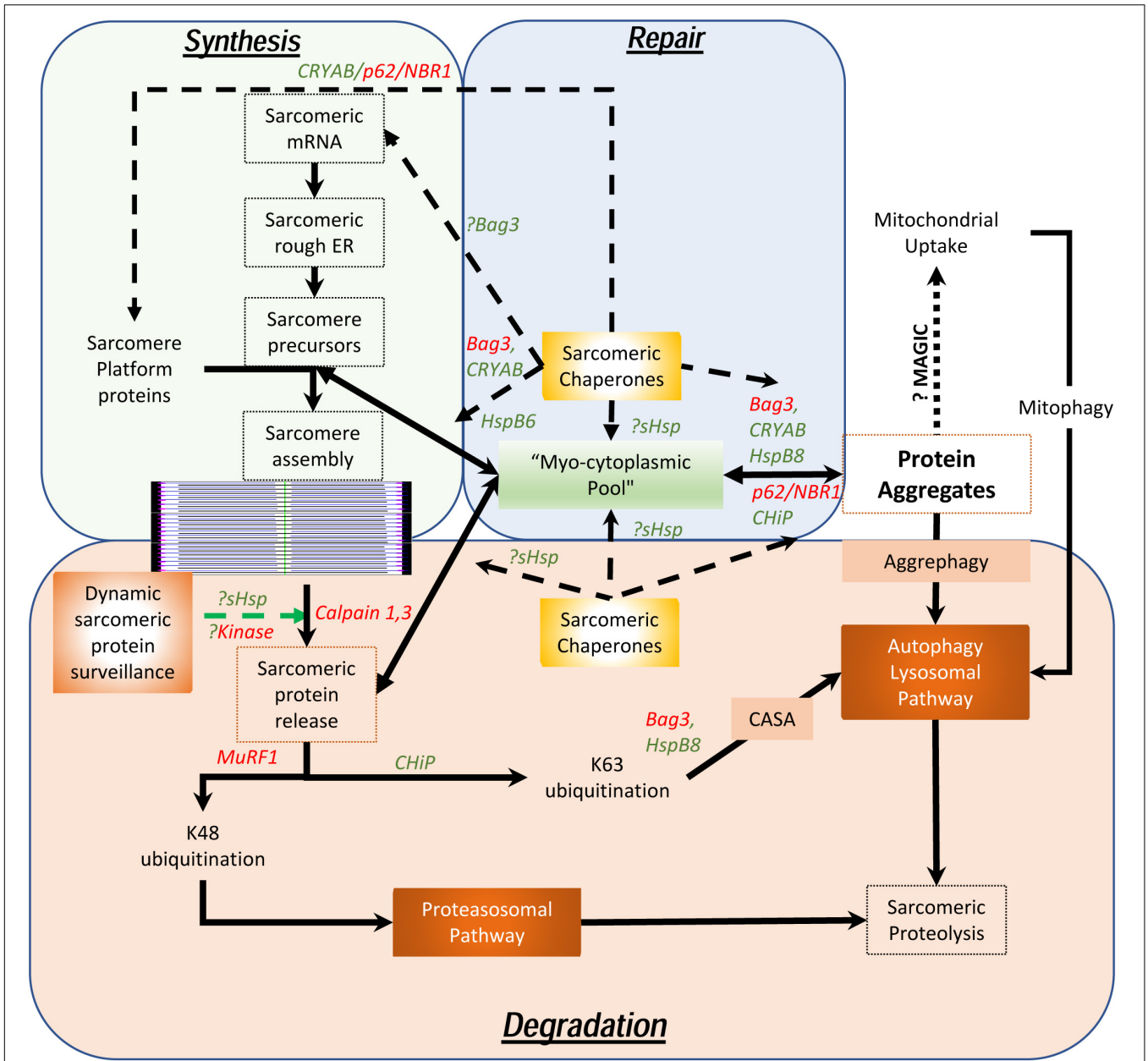

FIGURE 2 | Proposed model of the cardiac sarcostat. In this model, mRNA and proteins are located in stoichiometric excess, in vicinity of the sarcomere, as a myocytoplasmic pool. As most sarcomeric proteins are highly insoluble and aggregate prone, concerted action of a variety of sarcomeric chaperones (in green letters) and chaperone associated sarcomeric proteins (in red letters) is required to ensure normal sarcomere structure and function. These chaperones also appear to be integral to sarcomere assembly as well as repair and maintenance of sarcomeric proteins, *in situ*. When the damaged proteins are detected (often due to exposure of kinase sites) by the "sarcostat damage sensing mechanism," the proteins are removed from the sarcomere (via sarcomeric calpains) and returned to the myocytoplasmic reserve pool. When sarcomeric proteins acquire unfolded states due to nascent status, or are misfolded as a result of synthetic errors or due to damage, sarcostat chaperones assist in their refolding and in enabling dynamic equilibrium between the sarcomere-associated and the reserve pools. The proteins that are beyond the capacity of the refolding mechanism or require to be stored in the anticipation of continued stress, undergo aggregation under the action of Bag3, CryAB, and p62. As a result of liquid-liquid phase transition, these proteins and their cognate chaperones remain outside the osmotic load of the cell, stacked in a compact arrangement due to their intrinsic disordered domains (IDRs). These aggregates can be a source to release protein back in to the myocytoplasmic pool and, thus, the sarcomere. Normal lysosomal function and, possibly mitochondrial aggregate uptake (via a pathway termed as "MAGIC," see text), result in continuous flux of these aggregates. In addition, normal proteolysis of isolated proteins occurs via the ubiquitin proteasome system and the autophagy-lysosomal pathway. During states when the ubiquitin proteasome pathway is inhibited, proteins are diverted into storage as protein aggregates or for degradation via the autophagy-lysosomal pathway. As many disease states also result in lysosomal dysfunction, the accumulation of the protein aggregates accompanies failure of the sarcostat. In these states, upregulation of the sarcostat protein degradation machinery (both UPS and ALP), results in improved sarcomeric protein quality, while concurrently increasing aggregate removal.

PROTEIN AGGREGATION IN CARDIAC MYOCYTES: *FRIEND OR FOE?*

A fundamental question in protein aggregate pathologies across multiple organ systems is whether protein aggregates are "good" or "bad" (Cox et al., 2018). When viewed as part of the static sarcomere model, protein aggregates have always been regarded as a pathologic, potentially toxic entity (Henning and Brundel, 2017). Indeed, akin to the pathology observed in neurodegenerative diseases, both pre-amyloid oligomers (Del Monte and Agnetti, 2014) and protein aggregates, consisting of a combination of normal sarcomeric proteins with or without mutated proteins, have been ascribed toxic roles. This notion is reinforced by studies that show that intracytoplasmic accumulation of these pre-amyloid oligomers, aggregates or their "toxic" constituents, recapitulates cardiotoxicity (Sanbe et al., 2004; Pattison et al., 2008, 2011); akin to a toxic role for pre-amyloid Aβ oligomers postulated as a pathogenic mechanism in Alzheimer's disease (Demuro et al., 2011). Yet, the appearance of cardiac myocyte protein aggregates following hemodynamic stress in the pressure-overloaded left ventricle (Tannous et al., 2008) may be akin to the transient non-toxic Aβ plaques seen in traumatic brain injury (Scott et al., 2016) or reversible hyaline change in hepatic injury models (Kucukoglu et al., 2014); and may represent an adaptive state, to park large insoluble (and often ubiquitinated), proteins in a transitional state.

Understanding the dichotomous roles ascribed to such protein aggregates and assemblies will require experimental interrogation of their physico-chemical state using state of the art tools. A key feature of many protein aggregates is the presence of β-pleated sheets, which allow for efficient stacking of proteins as well as the concept of the liquid-liquid phase separation. Rather than conceptualizing these as precipitated solids in an otherwise liquid cytosol, protein aggregates can be considered as membrane-less organelles, similar to nucleoli, ribosomes, stress granules and P-bodies (Mitrea and Kriwacki, 2016; Uversky, 2017). As discussed in the subsequent section, protein aggregates in lower species are understood to play clearly adaptive roles as well as have potential toxic effects. The difference between the two functional states appears to be driven by the constituents of the aggregates rather than the aggregates themselves. Based on their currently understood role in protein aggregate formation in a variety of systems and species, the co-chaperone Bag3 (Meriin et al., 2018), the adaptor protein p62 (Komatsu et al., 2007; Sun et al., 2020) and small heat shock proteins (Ungelenk et al., 2016; Mogk and Bukau, 2017) (including the remarkably cardiac myocyte enriched chaperone αB-crystallin; Rajasekaran et al., 2007) appear to be critical in facilitating cardiac myocyte proteostasis. Of these, αB-crystallin (and its homologs) appears to be a universal component of these aggregates from bacteria to man (reviewed below). The presence of intrinsically disordered domains in all three of these proteins (Rauch et al., 2017; Wang et al., 2018; Haslbeck et al., 2019) as well as the potential for prion-like effects of proteins such as αB-crystallin that can exported via exosomes (D'Agostino et al., 2019) may result in both paracrine as well as potential endocrine effects.

In lower organisms, p62-enriched aggregates are believed to protect cells by sequestering toxic proteins [e.g., Keap1 (Pan et al., 2016) and mutant αB-crystallin (Zheng et al., 2011)]. In mammals, the preponderance of evidence points to protein aggregates being associated with cardiac pathology, suggesting that aggregates may be pathogenic (*vide infra*). Contrary to this assertion, the appearance of protein aggregates in cardiac myocytes after hemodynamic stress (pressure overload) in the myocardium (Tannous et al., 2008) may be adaptive as suggested by studies targeting TRIM21, a RING finger domain-containing ubiquitin E3 ligase that ubiquitylates p62 on lysine 7 to prevent is ability to aggregate (Pan et al., 2016). Mice lacking TRIM21 demonstrated near complete protection against pressure overload-induced left ventricular dilation and dysfunction, associated with marked aggregation of p62 and ubiquitylated proteins, suggesting that the inability to form protein aggregates worsens cardiomyopathy in this setting. This suggests that there is a "cinderella-zone" with respect to protein aggregate formation, akin to models seen in lower species (as discussed below). In this context, we speculate that the poorly understood "semi-crystalline" sarcomere assembly mechanism may share considerable similarity to the assembly of amyloid and protein aggregates; as mutations of key chaperones and components of the proposed cardiac sarcostat [i.e., Bag3 (Hishiya et al., 2010) and HspB7 (Mercer et al., 2018)] result in defects in sarcomere assembly, sarcomere maintenance and repair (see **Figure 2**).

A striking example of the physiologic role for such protein assemblies and aggregates was uncovered in studies focused on differentiation of neural stem and progenitor cells, wherein both ATP-dependent (TRiC/CCT) and ATP-independent sHsps (specifically CRYAB/HSPB5) promoted sequestration of mis-folded proteins into protective aggregates termed the "proteostat" to confer stress resilience (Vonk et al., 2020). Furthermore, the ability to form these protective aggregates declines with aging which may predispose to accelerated neurodegeneration with aging (Vonk et al., 2020); a premise that will require experimental testing in future studies. Another example of this phenomenon where heat shock proteins play a role in a "crystalline" structure is the role of HspA1 and HspB5 (αA- and αB-crystallin) in the lens (Horwitz, 2000). These findings support the notion that protein aggregates may not only be associated with pathology; but also play a protective role or trigger pathology in a context-dependent fashion.

While much evidence has been uncovered to understand the mechanisms for toxicity of aggregate prone proteins, such as the R120G mutant of αB-crystallin, potential mechanisms whereby protein aggregates confer cytotoxicity have largely remained unclear. In recent studies, we have uncovered a potential mechanism whereby protein aggregates induce toxicity in cardiac myocytes (Ma X. et al., 2019). Toxic mutations in aggregate-prone proteins (such as R120G αB-crystallin mutant) result in sticky aggregates that remove useful proteins (such as desmin) beyond the ability of the cardiac myocyte to compensate and result in sarcomere disruption and mitochondrial dysfunction as seen with expression of the R120G mutation in αB-crystallin that results in a desmin-deficient state (Ma X. et al., 2019).

Moreover, some mutant proteins such as the R120G mutant of αB-crystallin result in very large and sticky amorphous hydrophobic aggregates (unlike those resulting from stacking of β-sheets) that not only remove useful proteins beyond the ability of the cardiac myocyte to compensate but also cause formation of mechanical intracellular barriers (Hipp et al., 2014; Mogk et al., 2018), and result in sarcomere disruption, and mitochondrial dysfunction. While cardiac myocytes attempt to correct this by upregulating other chaperones, as well as increasing activation of protein quality control pathways, namely the ubiquitin-proteasome system and autophagy; emerging evidence points to dysfunction in the ubiquitin-proteasome pathway at an earlier stage of the disease (Chen et al., 2005) and for autophagy-lysosome pathway dysfunction at late stages as a mechanism for disease progression (Ma X. et al., 2019). Indeed, serial assessment of the autophagy-lysosome pathway in a mouse model of R120G αB-crystallin-induced cardiomyopathy demonstrates early induction of autophagic flux with development of cardiac hypertrophy, followed by subsequent impairment with disease progression predating cardiomyopathic dysfunction (Pan et al., 2019). Mechanistically, this appears to secondary to mTOR activation likely secondary to long standing lysosomal amino acid release due to accelerated protein breakdown, which results in phosphorylation of TFEB (transcription factor EB, a master regulator of autophagy and lysosome biogenesis) and its inactivation with sequestration away from the nucleus on lysosomes and in the cytosol (Ma X. et al., 2019; Pan et al., 2019). Activation of the autophagy-lysosome pathway by intermittent fasting or targeted activation of transcription factor EB (Settembre et al., 2011) even at an advanced stage of disease pathogenesis was sufficient to restore normal function and rescue cardiomyopathy by restoring normal desmin localization (Ma X. et al., 2019; Mukai et al., 2019).

These observations suggest that a strategy targeting removal of aggregate-prone proteins may be effective in preventing or delaying cardiac pathology. Indeed, driving removal of aggregates via stimulation of the ubiquitin-proteasome pathway (Ranek et al., 2013; Gupta et al., 2014; Zhang et al., 2019) or of the autophagy-lysosome pathway (with activation of ATG7-stimulated autophagy or exercise; Bhuiyan et al., 2013) prevents toxicity of the R120G αB-crystallin mutant protein (Pattison et al., 2011; Pan et al., 2017) to attenuate cardiomyopathy development in this model. Another example of toxic protein aggregates and aggregate-prone desmin was uncovered in studies with modeling the cardiomyopathy-causing mutation H222P in the lamin A/C gene (Galata et al., 2018). Both a strategy of overexpressing αB-crystallin that resulted in chaperoning desmin to its physiologic location, or inducing haplo-insufficiency of desmin rescued cardiomyopathy by preventing desmin-induced sequestration of sarcomeric proteins from their physiologic location.

Taken together, there data suggest that aggregate-prone proteins, rather than protein aggregates are the initial drivers of pathology and their sticky nature makes protein aggregates "pathogenic" by hijacking and sequestering normal proteins at advanced stage of disease pathogenesis. Moreover, it is critical to recognize that all instances of proteostatic dysfunction do not manifest with aggregate pathology. Indeed, mutations in BAG3, a critical proteostatic mediator in cardiac myocytes induce cardiomyopathy without formation of protein aggregates, likely because BAG3 is required for aggregate formation (Fang et al., 2019). For example, studies modeling cardiomyopathy-associated mutations in BAG3 in iPSC-derived cardiac myocyte demonstrate myofibrillar disarray and marked proteostatic dysfunction without appearance of protein aggregates (Judge et al., 2017; McDermott-Roe et al., 2019). And, targeted ablation of BAG3 in the murine heart or expression of cardiomyopathy-associated BAG3 mutants induces myofibrillar degeneration (Hishiya et al., 2010) with increased portioning of proteins to detergent insoluble fraction (revealing their aggregate prone state) without formation of protein aggregates in the context of fulminant cardiomyopathic manifestations (Fang et al., 2017). While BAG3 plays a critical role in chaperone-assisted selective autophagy of proteins whereby its loss-of-function affects proteostasis (Ulbricht et al., 2013), BAG3 mutations are also associated with dysfunction of the macro-autophagy-lysosome pathway (Schanzer et al., 2018), which further impairs protein quality control mechanisms. Indeed, in instances where BAG3 mutations do induce protein aggregates and provoke cardiomyopathy, the mutant BAG3 protein acquires a gain-of-function aggregate-prone state, which forms protein aggregates with Hsp70, its natural binding partner and Hsp70 clients (Meister-Broekema et al., 2018). These data points to a critical need for mechanisms to efficiently remove damaged and dysfunctional proteins as an effective countermeasure against development of pathology.

These data suggest that the sarcomere functions in a semiautonomous state of proteostasis with independent components for protein synthesis (peri-sarcomeric ribosomal complexes and sarcomeric mRNA), and sarcomere-linked chaperone proteins (sHsps and Hsp90 analogs as well as p62 and Bag3) that facilitate folding of key sarcomeric proteins (see **Figure 2**). These components also appear to play a role in stabilizing and maintaining the "reserve" sarcomeric protein to provide a ready source of replacement parts to ensure continuous function. Furthermore, sarcomere damage due to stretch and load, ischemia, and heat stress result in misfolding of components. These "damaged" components are released from the sarcomere by calpains and enter the "reserve" pool where the cognate chaperones assess the integrity of the protein and either assign these for removal via the uniquitin-proteasome system, or via the autophagy lysosomal pathway. In the latter, this takes the form of either chaperone-assisted selective autophagy (Tan and Wong, 2017) mediated by Bag3, p62, CHIP, and sHsps (HspB8 and CryAB) or via aggrephagy of protein aggregates directly. Each of these elements is proposed to contribute to the proposed cardiac sarcostat (**Figure 2**). Thus, failure of the sarcostat is predicted to engender sarcomere disruption and contractile dysfunction, culminating in cardiomyopathy, heart failure and death.

HEAT SHOCK PROTEINS: *WITH A LITTLE HELP FROM MY CHAPERONES*

As discussed in the prior sections, cardiac myocytes are unusually large cells that are dependent on complex quaternary structures of protein complexes to maintain homeostasis (**Figure 1**). Thus, it is critical to understand the biology of the chaperones that helps maintain an appropriate folded state of these proteins from synthesis, through deployment, and finally, to removal and degradation. Initially seen in *Archaea* as small moieties conferring resistance against heat denaturing insults (Macario et al., 1991), the so-called heat-shock proteins have evolved into a multitude of classes and, remarkably, have retained their underlying structure and function through the course of evolution.

Heat shock proteins can be broadly classified as large and small heat shock proteins. Large heat shock proteins (70–90 kDa) are known to have ATPase function and use energy dependent mechanisms to fold (foldase) proteins (Moran Luengo et al., 2019). By contrast, small heat shock proteins (15–30 kDa) have traditionally been thought to be energy-independent chaperones that sequester proteins and prevent misfolding (i.e., holdase) (Janowska et al., 2019). Newer data (as discussed subsequently) indicate that their function, both in isolation as well as in concert with large Hsps and other co-chaperones may be more complex, and sHsps may function in both BAG3-dependent and independent manner (reviewed in Fang et al., 2019).

Another class of heat shock proteins exist in bacterial, fungal and plant systems, i.e., the Hsp110 AAA + ATPase disaggregases that can disassemble amyloid and protein aggregates (Torrente and Shorter, 2013). Recent studies indicate that proteins with disaggregase function (some with Hsp homology) exist in the animal kingdom but their role appears to be unclear (Baker et al., 2017; Taguchi et al., 2019; Avellaneda et al., 2020). In this context, it is notable that physiologic or reversible protein aggregates are observed in yeast as a reserve pool of proteins to respond to stress (Saad et al., 2017). These amyloid proteins are disrupted by a yeast protein disaggregase, hsp104, which has been lost in metazoans and can drive rapid ATP and Hsp70/40-dependent disaggregation of amyloid protein in both yeast and metazoan cell types (Yokom et al., 2016; Gates et al., 2017; Shorter, 2017). Indeed, Hsp104, when exogenously introduced into models of neurodegenerative diseases, namely Parkinson's disease and frontotemporal dementia has demonstrated efficacy in disaggregating TDP-43, FUS, and α-synuclein with resulting attenuation of cellular pathology (DeSantis et al., 2012; Jackrel et al., 2014). Whether these protein systems are functional in mammalian cardiac myocytes or can be harnessed for therapeutic potential, remains to be explored.

Another exciting recent discovery has been the observation that mitochondria participate in taking up cytosolic misfolded proteins to facilitate their aggregation on the mitochondrial surface via a mitochondria-mediated proteostasis mechanism, termed MAGIC (mitochondria as guardian in cytosol; see **Figure 2**; Ruan et al., 2017). These aggregates are subsequently removed by mitochondrial fission and subsequent mitophagy to remove the fissioned-off mitochondria (Li et al., 2019). Hsp104 can forcibly disaggregate these mitochondrial protein aggregates and target their import into the mitochondrial matrix for degradation by Pim1 (LON protease). Whether mitochondrial handling of cytosolic protein aggregates participates in cardiac myocytes homeostasis and stress response, remains unknown.

A unifying factor across all heat shock proteins is HSF-1, the master regulator of the heat shock response in eukaryotes (Gomez-Pastor et al., 2018); which was demonstrated to be essential for thermos-tolerance in mammalian systems using a targeted genetic approach (McMillan et al., 1998). The HSF family of transcription factors (HSF1-6 in humans) appears to not only drive the various heat shock proteins but also induce a concerted array of stress response genes that respond to a variety of stimuli, including heat, oxidative stress, metals and proteotoxicity (Murshid et al., 2018). In response to stress, inactive monomeric HSF-1 is activated resulting in formation of a DNA-binding homotrimer via leucine-zipper domains. This multimerization results in activation of the bipartite NLS and nuclear translocation where the DNA binding N-terminal helix-turn-helix domain binds to the nGAAn consensus sequence on promoters. A bevy of heat-shock proteins (as well as 14-3-3, VCP, and TRiC proteins) are able to hold the HSFs in a monomeric state and are part of a feedback loop to prevent continued activation of the HSF target gene activation (Gomez-Pastor et al., 2018).

In mammals, Hsp70 and Hsp90 are the most prominent class of the large Hsp family of proteins. Both of these are notable for the presence of a nucleotide-binding domains, peptide-binding domains and variable C-terminal regions (reviewed in Moran Luengo et al., 2019). The Hsp90 proteins have greater substrate specificity as compared with the Hsp70 family. By and large, Hsp70 proteins play a role in protein folding from the nascent polypeptide chains at the ribosomes, through complex quaternary structures prior to protein deployment. In contrast, Hsp90 proteins collaborate with C-terminal Hsp-Interacting Protein (CHIP) and BAG3, directing their actions to specific targets (Ranek et al., 2018). Both of these proteins are key elements of the intracellular "sarcostat" in cardiac myocytes (**Figure 2**), and have been observed to play important roles in the pathogenesis of heart failure. Interestingly, in the setting of αB-crystallin R120G mutation, while overexpression of the foldase Hsp70 is unable to rescue the phenotype resulting from misfolded unchaperoned desmin, while overexpression of the holdase sHsps (HspB5, 6, and 8) was sufficient to confer rescue (Hussein et al., 2015). This suggests that many of the properties of the individual classes of proteins are more nuanced *in vivo* as compared to *in vitro* predictions.

Working hand-in-hand with these energy-dependent chaperones, small Hsps consist of a relatively diverse family of proteins with molecular weights mostly ranging from 15 kDa through 40 kDa. Unlike the large ATP-dependent Hsps that are conserved through fungi and eukaryotes, mammalian sHsps are also conserved with those in prokaryotes, *Archae* as well as viruses. Previously believed to be mere "holdases" that are critical in holding proteins in stable conformations in the cytosol, new evidence indicates far more diverse and complex roles (Fang et al., 2019; Haslbeck et al., 2019; Janowska et al., 2019). The

sHsps (HspB1-10 in humans) are present in many tissues, and observed to play roles in nearly every disease from infections through degenerative diseases. Of these, HspB-1, 2, 3, 5, 6, 7, and 8 have been shown to be present at relatively high levels in the heart with significant functional roles noted in both mouse models as well as human disease. With the exception of HspB7, which has a significant monomeric function, all of these appear to function as chaperones in an oligomeric state. This varies from dimers and trimers in the case of Hspb6 and HspB8 (Bukach et al., 2004; Shatov et al., 2018) to the 30–40-mers seen with CryAB (HspB5) (Aquilina et al., 2003; Janowska et al., 2019). Nonetheless, each of these sHsps and all of their evolutionary forebearers, are characterized by the presence of a β-sheet enriched "α-crystallin" domain (ACD) (Horwitz, 1992; Janowska et al., 2019) consisting of 6–8 β-sheets. Flanking this are relatively disordered N- and C-terminal (NTR and CTR) regions. While the CTR is rich in polar amino acids and may play a role in solubility (Janowska et al., 2019), the NTR is hydrophobic and may play a role predominantly in substrate specificity. Despite the overall structural similarities, the sHsps vary in presence of I/VXI/V motifs in either the CTR or the NTR that result in interaction of either regions with the hydrophobic cleft of the ACD. Notably, the CTR interacts with the hydrophobic groove in ACD between (β4 and β8) (Janowska et al., 2019). These folding events in sHsps appear to be key in determining their chaperone function as well as the multimerization, either as homo-polymers or heteromers.

CRYAB AND SHSPS THROUGH EVOLUTION: *THE LONG AND WINDING ROAD*

Cardiac myocytes are unique with regards to structure, function and replacement potential. Similar to prokaryotes and yeast, survival of individual cardiac myocytes is critical to maintaining cardiac architecture and function. Thus, it is likely that many mechanisms that are essential for monad survival may also be specifically relevant to cardiac myocyte homeostasis, but not necessarily for homeostasis in other replicating cell types. Given the importance of proteostasis in cardiac myocytes (as discussed above), looking for phylogenetic survival and proteostatic pathways in lower organisms could be key in understanding the role of human cardiac proteostasis in homeostasis. Of the multitude of proteins that participate in the proteostatic pathways, αB-crystallin/CRYAB//HspB5 is unique in being very heavily expressed in the cardiac myocytes (3–5%) of total cardiac protein (Bennardini et al., 1992). At baseline, αB-crystallin functions as a chaperone as a ∼24–40 mer, with a soccer ball shaped 0.5–1 mDa complex (Aquilina et al., 2003). Stress-induced activation of p38 MAPK (Ito et al., 2001) results in phosphorylation of CryAB at S59 (Simon et al., 2007), thus changing it from a 24 to 32-mer to a 6-mer and is associated with increased partitioning to the insoluble fraction. This phenomenon is observed in the myocardium during ischemia-reperfusion (Golenhofen et al., 1998), oxidative stress (Prasad et al., 2013), hyperglycemia (Reddy et al., 2014), high fat diet (Prasad et al., 2013), hemodynamic stress with transverse aortic constriction (Pereira et al., 2014), and chronic heart failure (Dohke et al., 2006; Marunouchi et al., 2013; Fung et al., 2017); and appears to portend a poorer prognosis in human studies (Clements et al., 2007, 2011). From a functional standpoint as a chaperone, 30–40-mer multimeric αB-crystallin chaperone binds the N2B subunit of titin (Bullard et al., 2004), thus preventing unfolding and colocalizes with the Z-line, along with desmin (Ma X. et al., 2019). This association is disrupted by the R120G mutation, associated with Z-line disruption, as seen in heart failure models (Zhu et al., 2009). While the αB-crystallin/HspB2 double knockout (due to overlapping exons), has increased stress induced cardiomyopathy with ischemia-reperfusion injury (Morrison et al., 2004) and myocardial pressure overload (Kumarapeli et al., 2008), the phenotype is not seen with a functional HspB2 knockout (Ishiwata et al., 2012), reinforcing αB-crystallin's importance. As aging is often associated with protein aggregates and increased αB-crystallin S59 phosphorylation, it is interesting that the αB-crystallin/HspB2 null is protected against ischemia in aging mice (Benjamin et al., 2007). Therefore, understanding and extrapolating the properties and phenomena associated with primordial homologs of this unique cardiac enriched protein hold considerable promise for development of targeted therapeutics for myocardial pathology.

An interesting example of a bacterial crystallin homolog is Hsp16.3 in Mycobacterium tuberculosis. Functioning as a chaperone, this protein is able to facilitate the survival of the bacterium by promoting the dormant state during stress (Jee et al., 2018). Similarly, the chaperone sHsp16 in *Trypanosoma cruzi* functions by allowing the organism to resist oxidative and heat stress (Perez-Morales et al., 2009). However, the earliest example of sHsp is MjHsp16.5 in the archaean, *Methanococcus jannaschii* (Feil et al., 2001). Analysis of the ACD shows considerable homology with the MTB Hsp16.3, Ohhsp16.9 (rice), Hsp16.2 (*C. elegans*); as well as murine HspB6 and bovine CRYAB/HspB5 (Kim et al., 1998). The most impressive demonstration of the significance of sHsp homologs appears to be in *C. elegans* where the lifespan prolongation in the ultra-long-lived insulin resistant *daf-2* mutant was dependent on protein aggregates containing the CryAB homolog Hsp16.1 (Walther et al., 2015). Furthermore, recent work indicates that a non-canonical sHsp (Hsp-17) functions as an "aggregase" and loss of function mutants have shorter lifespan (Iburg et al., 2020). Similarly, the yeast analog Hsp42, harboring a prion-like domain in the N-terminus, is endowed with both chaperone and aggregase functions (Grousl et al., 2018). As in *C. elegans*, this aggregase function appears to be critical for proteostasis in heat stress (Grousl et al., 2018). In yeast, there are subcellular deposition sites called the "insoluble protein deposit (IPOD)", where, upon exposure to environmental stress, damaged or misfolded proteins are targeted for degradation or refolding helped by molecular chaperones (Rothe et al., 2018). Soluble protein aggregates are targeted to JUNQ/INQ (juxtanuclear or intranuclear aggregates), or to the CytoQ (cytoplasmic accumulation); whereas amyloid aggregates accumulate in IPOD site (Rothe et al., 2018). In *Drosophila*, sHSPs have diverse

functions. Hsp23, Hsp26, and Hsp27 could be involved in embryo morphogenesis by their ability to bind actin and microtubule (Goldstein and Gunawardena, 2000; Gong et al., 2004; Fisher et al., 2008; Hughes et al., 2008). Hsp26 has been shown to interact with myosin 10A, the *Drosophila* myosin XV homolog, a protein involved in regulating filopodial dynamics during dorsal closure (Liu et al., 2008). Hsp22 is the sHsp preferentially expressed during aging and its level of expression is partially predictive of longevity in individual flies (King and Tower, 1999; Yang and Tower, 2009). *Drosophila* host defense against pathogenic bacteria, fungi and viruses involves Toll, Imd, JNK, JAK-STAT, and p38 MAPK pathways (Eleftherianos and Castillo, 2012; Kingsolver et al., 2013); and these pathways activate Hsf and requires the proper expression of Hsp26, Hsp27, Hsp60D, and Hsp70Bc to mediate host defense (Chen et al., 2010). These observations point to the evolutionary conserved nature of sHsp biology as well as the remarkable ability of organisms to harness their potential to sustain critical life-sustaining processes, which culminate in mechanisms that maintain cellular homeostasis in highly specialized and long-lived cell types such as the cardiac myocytes.

TARGETING HEAT SHOCK PROTEINS FOR CARDIOPROTECTION: *LET'S COME TOGETHER TO A BETTER PLACE*

Understanding and exploring sHsps as a therapeutic target has been at the forefront of protein quality-centric efforts to prevent and treat pathology. Studies have demonstrated protective effects of exogenous sHsps on cardiac myocytes under various stresses, *in vitro*: (1) with expression of multiple heat shock proteins in ischemia (reviewed in Martin et al., 1997); (2) with activation of HspB1 in preventing aggregate formation with R120G αB-crystallin mutant expression (Zhang et al., 2010); and (3) with αB-Crystallin expression that prevents adrenergic stimulation-induced hypertrophic growth (Kumarapeli et al., 2008). Transgenic overexpression of αB-crystallin was effective in restoring mitochondrial quality and rescuing cardiac myocytes death in mice with genetic ablation of desmin (Diokmetzidou et al., 2016), a mouse model for desminopathies that result from loss of function of desmin due to genetic mutations. Cardiac myocyte targeted overexpression of αB-crystallin was also sufficient in attenuating development of dilated cardiomyopathy in a mouse model of H222P mutation in Lamin A/C gene, by restoring desmin localization (Galata et al., 2018). Transgenic αB-crystallin overexpression in cardiac myocytes protects against development of pathologic hypertrophy by attenuating NFAT activation after pressure overload (Kumarapeli et al., 2008); and αB-crystallin interacts with focal adhesion kinase and protects its proteolysis by calpains under stretch, protecting cardiac myocytes from apoptosis under pressure overload stress (Pereira et al., 2014). αB-crystallin was also shown to be a part of the cardiac sodium channel complex by interacting with Nv1.5, the pore-forming submit, with effects on increased sodium channel density and current (Huang et al., 2016); pointing to the potential for harnessing this biology toward treatment of arrhythmias induced by sodium channel dysfunction. Substantial evidence has also accumulated indicating a beneficial role for BAG3 gain of function in protecting against various stress stimuli. *In vitro* studies have demonstrated the efficacy of exogenous BAG3 in protecting against hypoxia-induced cell death, (Zhang et al., 2016), improving mitochondrial quality in hypoxia-reoxygenation injury (Cheung et al., 2019), in suppressing αB-crystallin R120G mutant-induced protein aggregation and cell death (Hishiya et al., 2011) and in nuclear protein quality control under proteotoxic stress (Gupta et al., 2019). Analogously, we have demonstrated that TFEB-induced upregulation of HspB8, a BAG3 partner, was essential for chaperoning desmin back to its physiologic localization state in a mouse model of R120G αB-crystallin induced cardiomyopathy (Ma X. et al., 2019). Our findings with shRNA mediated knockdown on HspB8 demonstrated that the benefits of enhancing the autophagy-lysosome-pathway on R120G-induced cardiomyopathy were lost with loss-of-function of HspB8. HspB8 (Hsp22) also plays a critical role in cardiac homeostasis as mice with germline ablation of HspB8 develop worse cardiomyopathy and increased mortality as compared with wild-type controls in response to pressure overload (Qiu et al., 2011). Interestingly, transgenic expression of BAG3 in cardiac myocytes reduced small heat shock protein levels specifically leading to a reduction in αB-crystallin and HspB1 accompanied by development of cardiomyopathy (Inomata et al., 2018), pointing to the critical stoichiometric balance with these protein families in cardiac physiology.

Targeted activation of the large heat-shock chaperone family members has also been explored as a potentially useful target for cardioprotection. Transgenic expression of Hsp70 or its interacting protein CHIP (Carboxyl terminus of Hsp70-interacting protein (CHIP), a ubiquitin ligase) was protective against doxorubicin-induced cardiomyopathy (Naka et al., 2014; Wang et al., 2016). Furthermore, an aggregate of studies suggest that activation of Hsp70 signaling in protective against cardiac ischemia-reperfusion injury (Song et al., 2019). However, a note of caution is relevant given a role for Hsp70 described in promoting cardiac hypertrophy in response to pressure overload, which is typically pathologic and results in decompensation (Kee et al., 2008). Also, treatment with a Hsp90 inhibitor attenuated activation of Ras/Mek/Erk mitogen activated protein kinase (MAPK) signaling pathway to attenuate cardiac hypertrophy in the remote non-infarcted myocardium in the post-myocardial infarction left ventricle (Tamura et al., 2019).

Intriguingly, recent studies point to the exciting prospect of employing oxysterols to alter the aggregation properties of cHsps such as the R120 mutant of αB-crystallin (Makley et al., 2015; Molnar et al., 2019), and cataract-causing Y118D mutant in αA-crystallin (Zhao et al., 2015) which were highly effective in restoring protein solubility in the lens to attenuate established cataracts. Understanding how heat shock proteins are regulated via post-translational mechanisms (Gomez-Pastor et al., 2018) will be essential to develop novel therapeutics (such as oxysterols) to therapeutically target them for prevention and treatment of cardiac pathologies.

CONCLUSION

Cardiac myocytes are characterized by the roles of semi-crystalline protein assembly (the sarcomere) as well as by the various roles of the cardiac-enriched sarcostatic oligomeric complexes of heat shock proteins, i.e., the "crystallins." These crystalline proteins mirror their function in the ocular lens, to turn large insoluble proteins into a dynamic robust and durable machine with uninterrupted function through the lifetime of an organism. While prior work indicated that akin to neurodegeneration, the appearance of protein aggregation was purely a pathogenic phenomenon, recent studies indicate that a more nuanced approach is necessary. An enhanced understanding of the evolutionarily preserved small heat shock proteins (that share the same oligomeric properties from *Archaea* to man), as well as the potential protective roles of amyloid and aggregates in lower species associated with these sHsps is essential in developing new sarcomere-preserving strategies. It is our hope that development of such sarcomere-targeted approaches will foster development of the next generation of therapies for heart failure.

AUTHOR CONTRIBUTIONS

All authors participated in drafting the manuscript and approved it prior to submission.

FUNDING

This study was supported by grants from the National Institutes of Health (HL107594 and HL143431) and the Department of Veterans Affairs (I01BX004235) to AD. KM was supported by a Seed Grant from the St. Louis VA Medical Center.

REFERENCES

Aquilina, J. A., Benesch, J. L., Bateman, O. A., Slingsby, C., and Robinson, C. V. (2003). Polydispersity of a mammalian chaperone: mass spectrometry reveals the population of oligomers in alphaB-crystallin. *Proc. Natl. Acad. Sci. U.S.A.* 100, 10611–10616. doi: 10.1073/pnas.1932958100

Aragam, K. G., Chaffin, M., Levinson, R. T., McDermott, G., Choi, S. H., Shoemaker, M. B., et al. (2018). Phenotypic refinement of heart failure in a national biobank facilitates genetic discovery. *Circulation* 139, 489–501 doi: 10.1161/circulationaha.118.035774

Avellaneda, M. J., Franke, K. B., Sunderlikova, V., Bukau, B., Mogk, A., and Tans, S. J. (2020). , Processive extrusion of polypeptide loops by a Hsp100 disaggregase. *Nature* 578, 317–320. doi: 10.1038/s41586-020-1964-y

Baker, J. D., Shelton, L. B., Zheng, D., Favretto, F., Nordhues, B. A., Darling, A., et al. (2017). Human cyclophilin 40 unravels neurotoxic amyloids. *PLoS Biol.* 15:e2001336. doi: 10.1371/journal.pbio.2001336

Bard, J. A. M., Goodall, E. A., Greene, E. R., Jonsson, E., Dong, K. C., and Martin, A. (2018). Structure and Function of the 26S proteasome. *Annu. Rev. Biochem.* 87, 697–724.

Benjamin, I. J., Guo, Y., Srinivasan, S., Boudina, S., Taylor, R. P., Rajasekaran, N. S., et al. (2007). CRYAB and HSPB2 deficiency alters cardiac metabolism and paradoxically confers protection against myocardial ischemia in aging mice. *Ame. J. Physiol. Heart Circ. Physiol.* 293, H3201–H3209.

Bennardini, F., Wrzosek, A., and Chiesi, M. (1992). Alpha B-crystallin in cardiac tissue. Association with actin and desmin filaments. *Circ. Res.* 71, 288–294. doi: 10.1161/01.res.71.2.288

Bhuiyan, M. S., Pattison, J. S., Osinska, H., James, J., Gulick, J., McLendon, P. M., et al. (2013). Enhanced autophagy ameliorates cardiac proteinopathy. *J Clini. Investig.* 123, 5284–5297. doi: 10.1172/jci70877

Bova, M. P., Yaron, O., Huang, Q., Ding, L., Haley, D. A., Stewart, P. L., et al. (1999). Mutation R120G in alphaB-crystallin, which is linked to a desmin-related myopathy, results in an irregular structure and defective chaperone-like function. *Proc. Natl. Acad. Sci. U.S.A.* 96, 6137–6142. doi: 10.1073/pnas.96.11.6137

Brady, J. P., Garland, D. L., Green, D. E., Tamm, E. R., Giblin, F. J., and Wawrousek, E. F. (2001). AlphaB-crystallin in lens development and muscle integrity: a gene knockout approach. *Invest. Ophthalmol. Vis. Sci.* 42, 2924–2934.

Brody, M. J., Vanhoutte, D., Bakshi, C. V., Liu, R., Correll, R. N., Sargent, M. A., et al. (2019). Disruption of valosin-containing protein activity causes cardiomyopathy and reveals pleiotropic functions in cardiac homeostasis. *J. Biol. Chem.* 294, 8918–8929. doi: 10.1074/jbc.ra119.007585

Bukach, O. V., Seit-Nebi, A. S., Marston, S. B., and Gusev, N. B. (2004). Some properties of human small heat shock protein Hsp20 (HspB6). *Eur. J. Biochem.* 271, 291–302. doi: 10.1046/j.1432-1033.2003.03928.x

Bullard, B., Ferguson, C., Minajeva, A., Leake, M. C., Gautel, M., Labeit, D., et al. (2004). Association of the chaperone alphaB-crystallin with titin in heart muscle. *J. Biol. Chem.* 279, 7917–7924. doi: 10.1074/jbc.m307473200

Cabet, E., Batonnet-Pichon, S., Delort, F., Gausseres, B., Vicart, P., and Lilienbaum, A. (2015). Antioxidant treatment and induction of autophagy cooperate to reduce desmin aggregation in a cellular model of desminopathy. *PLoS One* 10:e0137009. doi: 10.1371/journal.pone.0137009

Chen, J., Xie, C., Tian, L., Hong, L., Wu, X., and Han, J. (2010). Participation of the p38 pathway in *Drosophila* host defense against pathogenic bacteria and fungi. *Proc. Natl. Acad. Sci. U.S.A.* 107, 20774–20779. doi: 10.1073/pnas.1009223107

Chen, Q., Liu, J. B., Horak, K. M., Zheng, H., Kumarapeli, A. R., Li, J., et al. (2005). Intrasarcoplasmic amyloidosis impairs proteolytic function of proteasomes in cardiomyocytes by compromising substrate uptake. *Circ. Res.* 97, 1018–1026. doi: 10.1161/01.res.0000189262.92896.0b

Cheung, J. Y., Gordon, J., Wang, J., Song, J., Zhang, X. Q., Prado, F. J., et al. (2019). Mitochondrial dysfunction in human immunodeficiency virus-1 transgenic mouse cardiac myocytes. *J. Cell Physiol.* 234, 4432–4444. doi: 10.1002/jcp.27232

Clark, K. A., McElhinny, A. S., Beckerle, M. C., and Gregorio, C. C. (2002). Striated muscle cytoarchitecture: an intricate web of form and function. *Annu. Rev. Cell Dev. Biol.* 18, 637–706. doi: 10.1146/annurev.cellbio.18.012502.105840

Clements, R. T., Feng, J., Cordeiro, B., Bianchi, C., and Sellke, F. W. (2011). p38 MAPK-dependent small HSP27 and alphaB-crystallin phosphorylation in regulation of myocardial function following cardioplegic arrest. *Am. J. Physiol. Heart Circ. Physiol.* 300, H1669–H1677. doi: 10.1152/ajpheart.00272.2010

Clements, R. T., Sodha, N. R., Feng, J., Mieno, S., Boodhwani, M., Ramlawi, B., et al. (2007). Phosphorylation and translocation of heat shock protein 27 and alphaB-crystallin in human myocardium after cardioplegia and cardiopulmonary bypass. *J. Thorac. Cardiovasc. Surg.* 134, 1461–1470.

Coats, C. J., Heywood, W. E., Virasami, A., Ashrafi, N., Syrris, P., Dos Remedios, C., et al. (2018). Proteomic analysis of the myocardium in hypertrophic obstructive cardiomyopathy. *Circ. Genom. Precis. Med.* 11:e001974.

Cox, D., Raeburn, C., Sui, X., and Hatters, D. M. (2018). Protein aggregation in cell biology: an aggregomics perspective of health and disease. *Semin. Cell Dev. Biol.* 99, 40–54. doi: 10.1016/j.semcdb.2018.05.003

da, K., Silva, Lopes, Pietas, A., Radke, M. H., and Gotthardt, M. (2011). Titin visualization in real time reveals an unexpected level of mobility within and between sarcomeres. *J. Cell Biol.* 193, 785–798. doi: 10.1083/jcb.201010099

D'Agostino, M., Scerra, G., Cannata Serio, M., Caporaso, M. G., Bonatti, S., and Renna, M. (2019). Unconventional secretion of alpha-Crystallin B requires the Autophagic pathway and is controlled by phosphorylation of its serine 59 residue. *Sci. Rep.* 9:16892.

Dahl-Halvarsson, M., Olive, M., Pokrzywa, M., Ejeskar, K., Palmer, R. H., Uv, A. E., et al. (2018). *Drosophila* model of myosin myopathy rescued by overexpression of a TRIM-protein family member. *Proc. Natl. Acad. Sci. U.S.A.* 115, E6566–E6575.

Dalakas, M. C., Park, K. Y., Semino-Mora, C., Lee, H. S., Sivakumar, K., and Goldfarb, L. G. (2000). Desmin myopathy, a skeletal myopathy with cardiomyopathy caused by mutations in the desmin gene. *N. Engl. J. Med.* 342, 770–780. doi: 10.1056/nejm200003163421104

Del Monte, F., and Agnetti, G. (2014). Protein post-translational modifications and misfolding: new concepts in heart failure. *Proteomics Clin. Appl.* 8, 534–542. doi: 10.1002/prca.201400037

Demuro, A., Smith, M., and Parker, I. (2011). Single-channel Ca(2+) imaging implicates Abeta1-42 amyloid pores in Alzheimer's disease pathology. *J. Cell Biol.* 195, 515–524. doi: 10.1083/jcb.201104133

DeSantis, M. E., Leung, E. H., Sweeny, E. A., Jackrel, M. E., Cushman-Nick, M., Neuhaus-Follini, A., et al. (2012). Operational plasticity enables hsp104 to disaggregate diverse amyloid and nonamyloid clients. *Cell* 151, 778–793. doi: 10.1016/j.cell.2012.09.038

Dikic, I., and Elazar, Z. (2018). Mechanism and medical implications of mammalian autophagy. *Nat. Rev Mol. Cell Biol.* 19, 349–364. doi: 10.1038/s41580-018-0003-4

Diokmetzidou, A., Soumaka, E., Kloukina, I., Tsikitis, M., Makridakis, M., Varela, A., et al. (2016). Desmin and alphaB-crystallin interplay in the maintenance of mitochondrial homeostasis and cardiomyocyte survival. *J. Cell Sci.* 129, 3705–3720. doi: 10.1242/jcs.192203

Dohke, T., Wada, A., Isono, T., Fujii, M., Yamamoto, T., Tsutamoto, T., et al. (2006). Proteomic analysis reveals significant alternations of cardiac small heat shock protein expression in congestive heart failure. *J. Card. Fail.* 12, 77–84. doi: 10.1016/j.cardfail.2005.07.006

Dominguez, F., Cuenca, S., Bilinska, Z., Toro, R., Villard, E., Barriales-Villa, R., et al. (2018). Dilated cardiomyopathy Due to BLC2-associated athanogene 3 (BAG3) mutations. *J. Am. Coll. Cardiol.* 72, 2471–2481.

Eleftherianos, I., and Castillo, J. C. (2012). Molecular mechanisms of aging and immune system regulation in *Drosophila*. *Int. J. Mol. Sci.* 13, 9826–9844. doi: 10.3390/ijms13089826

Esslinger, U., Garnier, S., Korniat, A., Proust, C., Karakigas, G., Muller-Nurasyid, M., et al. (2017). Exome-wide association study reveals novel susceptibility genes to sporadic dilated cardiomyopathy. *PLoS One* 12:e0172995. doi: 10.1371/journal.pone.0172995

Fang, X., Bogomolovas, J., Trexler, C., and Chen, J. (2019). The BAG3-dependent and -independent roles of cardiac small heat shock proteins. *JCI Insight* 4:e126464.

Fang, X., Bogomolovas, J., Wu, T., Zhang, W., Liu, C., Veevers, J., et al. (2017). Loss-of-function mutations in co-chaperone BAG3 destabilize small HSPs and cause cardiomyopathy. *J. Clin. Investig.* 127, 3189–3200. doi: 10.1172/jci94310

Feil, I. K., Malfois, M., Hendle, J., van Der Zandt, H., and Svergun, D. I. (2001). A novel quaternary structure of the dimeric alpha-crystallin domain with chaperone-like activity. *J. Biol. Chem.* 276, 12024–12029. doi: 10.1074/jbc.m010856200

Feng, H. Z., Hossain, M. M., Huang, X. P., and Jin, J. P. (2009). Myofilament incorporation determines the stoichiometry of troponin I in transgenic expression and the rescue of a null mutation. *Arch. Biochem. Biophys.* 487, 36–41. doi: 10.1016/j.abb.2009.05.001

Fichna, J. P., Potulska-Chromik, A., Miszta, P., Redowicz, M. J., Kaminska, A. M., Zekanowski, C., et al. (2017). A novel dominant D109A CRYAB mutation in a family with myofibrillar myopathy affects alphaB-crystallin structure. *BBA Clin.* 7, 1–7. doi: 10.1016/j.bbacli.2016.11.004

Fisher, K. H., Deane, C. M., and Wakefield, J. G. (2008). The functional domain grouping of microtubule associated proteins. *Commun. Integr. Biol.* 1, 47–50. doi: 10.4161/cib.1.1.6795

Fung, G., Wong, J., Berhe, F., Mohamud, Y., Xue, Y. C., and Luo, H. (2017). Phosphorylation and degradation of alphaB-crystallin during enterovirus infection facilitates viral replication and induces viral pathogenesis. *Oncotarget* 8, 74767–74780. doi: 10.18632/oncotarget.20366

Galata, Z., Kloukina, I., Kostavasili, I., Varela, A., Davos, C. H., Makridakis, M., et al. (2018). Amelioration of desmin network defects by alphaB-crystallin overexpression confers cardioprotection in a mouse model of dilated cardiomyopathy caused by LMNA gene mutation. *J. Mol. Cell. Cardiol.* 125, 73–86. doi: 10.1016/j.yjmcc.2018.10.017

Galves, M., Rathi, R., Prag, G., and Ashkenazi, A. (2019). Ubiquitin signaling and degradation of aggregate-prone proteins. *Trends Biochem. Sci.* 44, 872–884. doi: 10.1016/j.tibs.2019.04.007

Gates, S. N., Yokom, A. L., Lin, J., Jackrel, M. E., Rizo, A. N., Kendsersky, N. M., et al. (2017). Ratchet-like polypeptide translocation mechanism of the AAA+ disaggregase Hsp104. *Science* 357, 273–279. doi: 10.1126/science.aan1052

Glazier, A. A., Hafeez, N., Mellacheruvu, D., Basrur, V., Nesvizhskii, A. I., Lee, L. M., et al. (2018). HSC70 is a chaperone for wild-type and mutant cardiac myosin binding protein C. *JCI Insight* 3:e99319.

Godar, R. J., Ma, X., Liu, H., Murphy, J. T., Weinheimer, C. J., Kovacs, A., et al. (2015). Repetitive stimulation of autophagy-lysosome machinery by intermittent fasting preconditions the myocardium to ischemia-reperfusion injury. *Autophagy* 11, 1537–1560. doi: 10.1080/15548627.2015.1063768

Goldfarb, L. G., and Dalakas, M. C. (2009). Tragedy in a heartbeat: malfunctioning desmin causes skeletal and cardiac muscle disease. *J. Clin. Invest* 119, 1806–1813. doi: 10.1172/jci38027

Goldstein, L. S., and Gunawardena, S. (2000). Flying through the *Drosophila* cytoskeletal genome. *J. Cell Biol.* 150, F63–F68.

Golenhofen, N., Ness, W., Koob, R., Htun, P., Schaper, W., and Drenckhahn, D. (1998). Ischemia-induced phosphorylation and translocation of stress protein alpha B-crystallin to Z lines of myocardium. *Am. J. Physiol.* 274, H1457–H1464. doi: 10.1152/ajpheart.1998.274.5.H1457

Gomez-Pastor, R., Burchfiel, E. T., and Thiele, D. J. (2018). Regulation of heat shock transcription factors and their roles in physiology and disease. *Nat. Rev. Mol. Cell Biol.* 19, 4–19. doi: 10.1038/nrm.2017.73

Gong, L., Puri, M., Unlu, M., Young, M., Robertson, K., Viswanathan, S., et al. (2004). *Drosophila* ventral furrow morphogenesis: a proteomic analysis. *Development* 131, 643–656. doi: 10.1242/dev.00955

Grousl, T., Ungelenk, S., Miller, S., Ho, C. T., Khokhrina, M., Mayer, M. P., et al. (2018). A prion-like domain in Hsp42 drives chaperone-facilitated aggregation of misfolded proteins. *J. Cell Biol.* 217, 1269–1285. doi: 10.1083/jcb.201708116

Gupta, M. K., Gordon, J., Glauser, G. M., Myers, V. D., Feldman, A. M., Cheung, J. Y., et al. (2019). Lamin B is a target for selective nuclear PQC by BAG3: implication for nuclear envelopathies. *Cell Death Dis.* 10:23. doi: 10.1038/s41419-018-1255-9

Gupta, M. K., Gulick, J., Liu, R., Wang, X., Molkentin, J. D., and Robbins, J. (2014). Sumo E2 enzyme UBC9 is required for efficient protein quality control in cardiomyocytes. *Circ. Res.* 115, 721–729. doi: 10.1161/circresaha.115.304760

Gupta, M. K., McLendon, P. M., Gulick, J., James, J., Khalili, K., and Robbins, J. (2016). UBC9-mediated sumoylation favorably impacts cardiac function in compromised hearts. *Circ. Res.* 118, 1894–1905. doi: 10.1161/circresaha.115.308268

Haslbeck, M., Weinkauf, S., and Buchner, J. (2019). Small heat shock proteins: simplicity meets complexity. *J. Biol. Chem.* 294, 2121–2132. doi: 10.1074/jbc.rev118.002809

Heffler, J., Shah, P. P., Robison, P., Phyo, S., Veliz, K., Uchida, K., et al. (2020). Intermediate filaments and microtubules maintains nuclear architecture in the cardiomyocyte. *Circ. Res.* 126, e10–e26.

Henderson, C. A., Gomez, C. G., Novak, S. M., Mi-Mi, L., and Gregorio, C. C. (2017). Overview of the muscle cytoskeleton. *Compr. Physiol.* 7, 891–944. doi: 10.1002/cphy.c160033

Henning, R. H., and Brundel, B. (2017). Proteostasis in cardiac health and disease. *Nat. Rev. Cardiol.* 14, 637–653. doi: 10.1038/nrcardio.2017.89

Herman, D. S., Lam, L., Taylor, M. R., Wang, L., Teekakirikul, P., Christodoulou, D., et al. (2012). Truncations of titin causing dilated cardiomyopathy. *N. Engl. J. Med.* 366, 619–628.

Herrmann, J., Wohlert, C., Saguner, A. M., Flores, A., Nesbitt, L. L., Chade, A., et al. (2013). Primary proteasome inhibition results in cardiac dysfunction. *Eur. J. Heart Fail.* 15, 614–623. doi: 10.1093/eurjhf/hft034

Hipp, M. S., Park, S. H., and Hartl, F. U. (2014). Proteostasis impairment in protein-misfolding and -aggregation diseases. *Trends Cell Biol.* 24, 506–514. doi: 10.1016/j.tcb.2014.05.003

Hishiya, A., Kitazawa, T., and Takayama, S. (2010). BAG3 and Hsc70 interact with actin capping protein CapZ to maintain myofibrillar integrity under mechanical stress. *Circ. Res.* 107, 1220–1231. doi: 10.1161/circresaha.110.225649

Hishiya, A., Salman, M. N., Carra, S., Kampinga, H. H., and Takayama, S. (2011). BAG3 directly interacts with mutated alphaB-crystallin to suppress its aggregation and toxicity. *PLoS One* 6:e16828. doi: 10.1371/journal.pone.0016828

Hoorntje, E. T., Bollen, I. A., Barge-Schaapveld, D. Q., van Tienen, F. H., Te Meerman, G. J., Jansweijer, J. A., et al. (2017). Lamin A/C-related cardiac

disease: late onset with a variable and mild phenotype in a large cohort of patients with the lamin A/C p.(Arg331Gln) founder mutation. *Circ. Cardiovasc. Genet.* 10:e001631.

Horwitz, J. (1992). Alpha-crystallin can function as a molecular chaperone. *Proc. Natl. Acad. Sci. U.S.A.* 89, 10449–10453. doi: 10.1073/pnas.89.21.10449

Horwitz, J. (2000). The function of alpha-crystallin in vision. *Semin. Cell Dev. Biol.* 11, 53–60. doi: 10.1006/scdb.1999.0351

Hu, C., Tian, Y., Xu, H., Pan, B., Terpstra, E. M., Wu, P., et al. (2018). Inadequate ubiquitination-proteasome coupling contributes to myocardial ischemia-reperfusion injury. *J. Clini. Investig.* 128, 5294–5306. doi: 10.1172/jci98287

Huang, Y., Wang, Z., Liu, Y., Xiong, H., Zhao, Y., Wu, L., et al. (2016). Alphab-crystallin interacts with nav1.5 and regulates ubiquitination and internalization of cell surface nav1.5. *J. Biol. Chem.* 291, 11030–11041. doi: 10.1074/jbc.M115.695080

Hughes, J. R., Meireles, A. M., Fisher, K. H., Garcia, A., Antrobus, P. R., Wainman, A., et al. (2008). A microtubule interactome: complexes with roles in cell cycle and mitosis. *PLoS Biol.* 6:e98. doi: 10.1371/journal.pbio.0060098

Hussein, R. M., Benjamin, I. J., and Kampinga, H. H. (2015). Rescue of alphaB crystallin (HSPB5) mutants associated protein aggregation by Co-expression of HSPB5 partners. *PLoS One* 10:e0126761. doi: 10.1371/journal.pone.0126761

Iburg, M., Puchkov, D., Rosas-Brugada, I. U., Bergemann, L., Rieprecht, U., and Kirstein, J. (2020). The non-canonical small heat shock protein HSP-17 from *C. elegans* is a selective protein aggregase. *J. Biol. Chem.* 295:jbc.RA119.011185.

Inagaki, N., Hayashi, T., Arimura, T., Koga, Y., Takahashi, M., Shibata, H., et al. (2006). Alpha B-crystallin mutation in dilated cardiomyopathy. *Biochem. Biophys. Res. Commun.* 342, 379–386.

Inomata, Y., Nagasaka, S., Miyate, K., Goto, Y., Hino, C., Toukairin, C., et al. (2018). Bcl-2-associated athanogene 3 (BAG3) is an enhancer of small heat shock protein turnover via activation of autophagy in the heart. *Biochem. Biophys. Res. Commun.* 496, 1141–1147. doi: 10.1016/j.bbrc.2018.01.158

Ishiwata, T., Orosz, A., Wang, X., Mustafi, S. B., Pratt, G. W., Christians, E. S., et al. (2012). HSPB2 is dispensable for the cardiac hypertrophic response but reduces mitochondrial energetics following pressure overload in mice. *PLoS One* 7:e42118. doi: 10.1371/journal.pone.0042118

Ito, H., Kamei, K., Iwamoto, I., Inaguma, Y., Nohara, D., and Kato, K. (2001). Phosphorylation-induced change of the oligomerization state of alpha B-crystallin. *J. Biol. Chem.* 276, 5346–5352. doi: 10.1074/jbc.m009004200

Jackrel, M. E., DeSantis, M. E., Martinez, B. A., Castellano, L. M., Stewart, R. M., Caldwell, K. A., et al. (2014). Potentiated Hsp104 variants antagonize diverse proteotoxic misfolding events. *Cell* 156, 170–182. doi: 10.1016/j.cell.2013.11.047

Janowska, M. K., Baughman, H. E. R., Woods, C. N., and Klevit, R. E. (2019). Mechanisms of small heat shock proteins. *Cold Spring Harb. Perspect. Biol.* 11:a034025.

Javaheri, A., Bajpai, G., Picataggi, A., Mani, S., Foroughi, L., Evie, H., et al. (2019). TFEB activation in macrophages attenuates postmyocardial infarction ventricular dysfunction independently of ATG5-mediated autophagy. *JCI Insight* 4:e127312.

Jee, B., Singh, Y., Yadav, R., and Lang, F. (2018). Small heat shock protein16.3 of mycobacterium tuberculosis: after two decades of functional characterization. *Cell Physiol. Biochem.* 49, 368–380. doi: 10.1159/000492887

Johnston, J. A., Ward, C. L., and Kopito, R. R. (1998). Aggresomes: a cellular response to misfolded proteins. *J. Cell Biol.* 143, 1883–1898. doi: 10.1083/jcb.143.7.1883

Judge, L. M., Perez-Bermejo, J. A., Truong, A., Ribeiro, A. J., Yoo, J. C., Jensen, C. L., et al. (2017). A BAG3 chaperone complex maintains cardiomyocyte function during proteotoxic stress. *JCI Insight* 2:e94623.

Kedar, V., McDonough, H., Arya, R., Li, H. H., Rockman, H. A., and Patterson, C. (2004). Muscle-specific RING finger 1 is a bona fide ubiquitin ligase that degrades cardiac troponin I. *Proc. Natl. Acad. Sci. U.S.A.* 101, 18135–18140. doi: 10.1073/pnas.0404341102

Kedia, N., Arhzaouy, K., Pittman, S. K., Sun, Y., Batchelor, M., Weihl, C. C., et al. (2019). Desmin forms toxic, seeding-competent amyloid aggregates that persist in muscle fibers. *Proc. Natl.Acade. Sci. U.S.A.* 116, 16835–16840. doi: 10.1073/pnas.1908263116

Kee, H. J., Eom, G. H., Joung, H., Shin, S., Kim, J. R., Cho, Y. K., et al. (2008). Activation of histone deacetylase 2 by inducible heat shock protein 70 in cardiac hypertrophy. *Circ. Res.* 103, 1259–1269. doi: 10.1161/01.res.0000338570.27156.84

Kim, K. K., Kim, R., and Kim, S. H. (1998). Crystal structure of a small heat-shock protein. *Nature* 394, 595–599. doi: 10.1038/29106

Kimura, H., Eguchi, S., Sasaki, J., Kuba, K., Nakanishi, H., Takasuga, S., et al. (2017). Vps34 regulates myofibril proteostasis to prevent hypertrophic cardiomyopathy. *JCI Insight* 2:e89462.

King, V., and Tower, J. (1999). Aging-specific expression of *Drosophila* hsp22. *Dev. Biol.* 207, 107–118. doi: 10.1006/dbio.1998.9147

Kingsolver, M. B., Huang, Z., and Hardy, R. W. (2013). Insect antiviral innate immunity: pathways, effectors, and connections. *J. Mol. Biol.* 425, 4921–4936. doi: 10.1016/j.jmb.2013.10.006

Komatsu, M., Waguri, S., Koike, M., Sou, Y. S., Ueno, T., Hara, T., et al. (2007). Homeostatic levels of p62 control cytoplasmic inclusion body formation in autophagy-deficient mice. *Cell* 131, 1149–1163. doi: 10.1016/j.cell.2007.10.035

Kotter, S., Unger, A., Hamdani, N., Lang, P., Vorgerd, M., Nagel-Steger, L., et al. (2014). Human myocytes are protected from titin aggregation-induced stiffening by small heat shock proteins. *J. Cell Biol.* 204, 187–202. doi: 10.1083/jcb.201306077

Kucukoglu, O., Guldiken, N., Chen, Y., Usachov, V., El-Heliebi, A., Haybaeck, J., et al. (2014). High-fat diet triggers mallory-denk body formation through misfolding and crosslinking of excess keratin 8. *Hepatology* 60, 169–178. doi: 10.1002/hep.27068

Kumarapeli, A. R., Su, H., Huang, W., Tang, M., Zheng, H., Horak, K. M., et al. (2008). Alpha B-crystallin suppresses pressure overload cardiac hypertrophy. *Circ. Res.* 103, 1473–1482. doi: 10.1161/CIRCRESAHA.108.180117

Kwon, Y. T., and Ciechanover, A. (2017). The ubiquitin code in the ubiquitin-proteasome system and autophagy. *Trends Biochem. Sci.* 42, 873–886. doi: 10.1016/j.tibs.2017.09.002

Lewis, Y. E., Moskovitz, A., Mutlak, M., Heineke, J., Caspi, L. H., and Kehat, I. (2018). Localization of transcripts, translation, and degradation for spatiotemporal sarcomere maintenance. *J. Mol. Cell. Cardiol.* 116, 16–28. doi: 10.1016/j.yjmcc.2018.01.012

Li, J., Horak, K. M., Su, H., Sanbe, A., Robbins, J., and Wang, X. (2011). Enhancement of proteasomal function protects against cardiac proteinopathy and ischemia/reperfusion injury in mice. *J. Clin. Investig.* 121, 3689–3700. doi: 10.1172/jci45709

Li, Y., Xue, Y., Xu, X., Wang, G., Liu, Y., Wu, H., et al. (2019). A mitochondrial FUNDC1/HSC70 interaction organizes the proteostatic stress response at the risk of cell morbidity. *EMBO J.* 38:e98786.

Liu, J., Chen, Q., Huang, W., Horak, K. M., Zheng, H., Mestril, R., et al. (2006a). Impairment of the ubiquitin-proteasome system in desminopathy mouse hearts. *FASEB J.* 20, 362–364. doi: 10.1096/fj.05-4869fje

Liu, J., Tang, M., Mestril, R., and Wang, X. (2006b). Aberrant protein aggregation is essential for a mutant desmin to impair the proteolytic function of the ubiquitin-proteasome system in cardiomyocytes. *J. Mol. Cell. Cardiol.* 40, 451–454. doi: 10.1016/j.yjmcc.2005.12.011

Liu, R., Woolner, S., Johndrow, J. E., Metzger, D., Flores, A., and Parkhurst, S. M. (2008). Sisyphus, the *Drosophila* myosin XV homolog, traffics within filopodia transporting key sensory and adhesion cargos. *Development* 135, 53–63. doi: 10.1242/dev.011437

Ma, K., Luo, D., Tian, T., Li, N., He, X., Rao, C., et al. (2019). A novel homozygous initiation codon variant associated with infantile alpha-Bcrystallinopathy in a Chinese family. *Mol. Genet. Genomic Med.* 7, e825.

Ma, X., Liu, H., Foyil, S. R., Godar, R. J., Weinheimer, C. J., and Diwan, A. (2012a). Autophagy is impaired in cardiac ischemia-reperfusion injury. *Autophagy* 8, 1394–1396. doi: 10.4161/auto.21036

Ma, X., Liu, H., Foyil, S. R., Godar, R. J., Weinheimer, C. J., Hill, J. A., et al. (2012b). Impaired autophagosome clearance contributes to cardiomyocyte death in ischemia/reperfusion injury. *Circulation* 125, 3170–3181. doi: 10.1161/circulationaha.111.041814

Ma, X., Liu, H., Murphy, J. T., Foyil, S. R., Godar, R. J., Abuirqeba, H., et al. (2015). Regulation of the transcription factor EB-PGC1alpha axis by beclin-1 controls mitochondrial quality and cardiomyocyte death under stress. *Mol. Cell. Biol.* 35, 956–976. doi: 10.1128/mcb.01091-14

Ma, X., Mani, K., Liu, H., Kovacs, A., Murphy, J. T., Foroughi, L., et al. (2019). Transcription factor EB activation rescues advanced alphaB-Crystallin

mutation-induced cardiomyopathy by normalizing desmin localization. *J. Am. Heart Assoc.* 8:e010866.

Macario, A. J., Dugan, C. B., and Conway de Macario, E. (1991). A dnaK homolog in the archaebacterium Methanosarcina mazei S6. *Gene* 108, 133–137. doi: 10.1016/0378-1119(91)90498-z

Maejima, Y., Kyoi, S., Zhai, P., Liu, T., Li, H., Ivessa, A., et al. (2013). Mst1 inhibits autophagy by promoting the interaction between Beclin1 and Bcl-2. *Nat. Med.* 19, 1478–1488. doi: 10.1038/nm.3322

Makley, L. N., McMenimen, K. A., DeVree, B. T., Goldman, J. W., McGlasson, B. N., Rajagopal, P., et al. (2015). Pharmacological chaperone for alpha-crystallin partially restores transparency in cataract models. *Science* 350, 674–677. doi: 10.1126/science.aac9145

Maloyan, A., Sanbe, A., Osinska, H., Westfall, M., Robinson, D., Imahashi, K., et al. (2005). Mitochondrial dysfunction and apoptosis underlie the pathogenic process in alpha-B-crystallin desmin-related cardiomyopathy. *Circulation* 112, 3451–3461. doi: 10.1161/circulationaha.105.572552

Mani, K., Javaheri, A., and Diwan, A. (2018). Lysosomes mediate benefits of intermittent fasting in cardiometabolic disease: the janitor is the undercover boss. *Compr. Physiol.* 8, 1639–1667. doi: 10.1002/cphy.c180005

Martin, A. F. (1981). Turnover of cardiac troponin subunits. Kinetic evidence for a precursor pool of troponin-I. *J. Biol. Chem.* 256, 964–968.

Martin, J. L., Mestril, R., Hilal-Dandan, R., Brunton, L. L., and Dillmann, W. H. (1997). Small heat shock proteins and protection against ischemic injury in cardiac myocytes. *Circulation* 96, 4343–4348. doi: 10.1161/01.cir.96.12.4343

Marunouchi, T., Abe, Y., Murata, M., Inomata, S., Sanbe, A., Takagi, N., et al. (2013). Changes in small heat shock proteins HSPB1, HSPB5 and HSPB8 in mitochondria of the failing heart following myocardial infarction in rats. *Biol. Pharm. Bull.* 36, 529–539. doi: 10.1248/bpb.b12-00796

McDermott-Roe, C., Lv, W., Maximova, T., Wada, S., Bukowy, J., Marquez, M., et al. (2019). Investigation of a dilated cardiomyopathy-associated variant in BAG3 using genome-edited iPSC-derived cardiomyocytes. *JCI Insight* 4:e128799.

McKenna, W. J., Maron, B. J., and Thiene, G. (2017). Classification, epidemiology, and global burden of cardiomyopathies. *Circ. Res.* 121, 722–730. doi: 10.1161/circresaha.117.309711

McLendon, P. M., Ferguson, B. S., Osinska, H., Bhuiyan, M. S., James, J., McKinsey, T. A., et al. (2014). Tubulin hyperacetylation is adaptive in cardiac proteotoxicity by promoting autophagy. *Proc. Natl. Acad. Scie. U.S.A.* 111, E5178–E5186.

McMillan, D. R., Xiao, X., Shao, L., Graves, K., and Benjamin, I. J. (1998). Targeted disruption of heat shock transcription factor 1 abolishes thermotolerance and protection against heat-inducible apoptosis. *J. Biol. Chem.* 273, 7523–7528. doi: 10.1074/jbc.273.13.7523

McNally, E. M., and Mestroni, L. (2017). Dilated cardiomyopathy: genetic determinants and mechanisms. *Circ. Res.* 121, 731–748. doi: 10.1161/circresaha.116.309396

Meister-Broekema, M., Freilich, R., Jagadeesan, C., Rauch, J. N., Bengoechea, R., Motley, W. W., et al. (2018). Myopathy associated BAG3 mutations lead to protein aggregation by stalling Hsp70 networks. *Nat. Commun.* 9:5342.

Mercer, E. J., Lin, Y. F., Cohen-Gould, L., and Evans, T. (2018). Hspb7 is a cardioprotective chaperone facilitating sarcomeric proteostasis. *Dev. Biol.* 435, 41–55. doi: 10.1016/j.ydbio.2018.01.005

Meriin, A. B., Narayanan, A., Meng, L., Alexandrov, I., Varelas, X., and Cisse, M. Y. II (2018). Sherman, Hsp70-Bag3 complex is a hub for proteotoxicity-induced signaling that controls protein aggregation. *Proc. Natl. Acad. Sci. U.S.A.* 115, E7043–E7052.

Milner, D. J., Mavroidis, M., Weisleder, N., and Capetanaki, Y. (2000). Desmin cytoskeleton linked to muscle mitochondrial distribution and respiratory function. *J. Cell Biol.* 150, 1283–1298. doi: 10.1083/jcb.150.6.1283

Milner, D. J., Taffet, G. E., Wang, X., Pham, T., Tamura, T., Hartley, C., et al. (1999). The absence of desmin leads to cardiomyocyte hypertrophy and cardiac dilation with compromised systolic function. *J. Mol. Cell. Cardiol.* 31, 2063–2076. doi: 10.1006/jmcc.1999.1037

Mitrea, D. M., and Kriwacki, R. W. (2016). Phase separation in biology; functional organization of a higher order. *Cell Commun. Signal.* 14:1.

Mogk, A., and Bukau, B. (2017). Role of sHsps in organizing cytosolic protein aggregation and disaggregation. *Cell Stress Chaperones* 22, 493–502. doi: 10.1007/s12192-017-0762-4

Mogk, A., Bukau, B., and Kampinga, H. H. (2018). Cellular handling of protein aggregates by disaggregation machines. *Mol. Cell* 69, 214–226. doi: 10.1016/j.molcel.2018.01.004

Molnar, K. S., Dunyak, B. M., Su, B., Izrayelit, Y., McGlasson-Naumann, B., Hamilton, P. D., et al. (2019). Mechanism of action of VP1-001 in cryAB(R120G)-associated and age-related cataracts. *Invest Ophthalmol. Vis. Sci.* 60, 3320–3331.

Moran Luengo, T., Mayer, M. P., and Rudiger, S. G. D. (2019). The Hsp70-Hsp90 chaperone cascade in protein folding. *Trends Cell Biol.* 29, 164–177. doi: 10.1016/j.tcb.2018.10.004

Morrison, L. E., Whittaker, R. J., Klepper, R. E., Wawrousek, E. F., and Glembotski, C. C. (2004). Roles for alphaB-crystallin and HSPB2 in protecting the myocardium from ischemia-reperfusion-induced damage in a KO mouse model. *Am. J. Physiol. Heart Circ. Physiol.* 286, H847–H855.

Mukai, R., Zablocki, D., and Sadoshima, J. (2019). intermittent fasting reverses an advanced form of cardiomyopathy. *J. Am. Heart Assoc.* 8:e011863.

Murshid, A., Prince, T. L., Lang, B., and Calderwood, S. K. (2018). Role of heat shock factors in stress-induced transcription. *Methods Mol. Biol.* 1709, 23–34. doi: 10.1007/978-1-4939-7477-1_2

Myers, V. D., Gerhard, G. S., McNamara, D. M., Tomar, D., Madesh, M., Kaniper, S., et al. (2018). Association of variants in BAG3 with cardiomyopathy outcomes in african american individuals. *JAMA Cardiol.* 3, 929–938.

Naka, K. K., Vezyraki, P., Kalaitzakis, A., Zerikiotis, S., Michalis, L., and Angelidis, C. (2014). Hsp70 regulates the doxorubicin-mediated heart failure in Hsp70-transgenic mice. *Cell Stress Chaperones* 19, 853–864. doi: 10.1007/s12192-014-0509-4

Nakano, S. J., Walker, J. S., Walker, L. A., Li, X., Du, Y., Miyamoto, S. D., et al. (2019). Increased myocyte calcium sensitivity in end-stage pediatric dilated cardiomyopathy. *Am. J. Physiol. Heart Circ. Physiol.* 317, H1221–H1230.

Pan, B., Lewno, M. T., Wu, P., and Wang, X. (2019). Highly dynamic changes in the activity and regulation of macroautophagy in hearts subjected to increased proteotoxic stress. *Front. Physiol.* 10:758. doi: 10.3389/fphys.2019.00758

Pan, B., Li, J., Parajuli, N., Tian, Z., Wu, P., Lewno, M. T., et al. (2020). The Calcineurin-TFEB-p62 pathway mediates the activation of cardiac macroautophagy by proteasomal malfunction. *Circ. Res.* doi: 10.1161/CIRCRESAHA.119.316007 [Epub ahead of print].

Pan, B., Zhang, H., Cui, T., and Wang, X. (2017). TFEB activation protects against cardiac proteotoxicity via increasing autophagic flux. *J. Mol. Cell. Cardiol.* 113, 51–62. doi: 10.1016/j.yjmcc.2017.10.003

Pan, J. A., Sun, Y., Jiang, Y. P., Bott, A. J., Jaber, N., Dou, Z., et al. (2016). TRIM21 ubiquitylates SQSTM1/p62 and suppresses protein sequestration to regulate redox homeostasis. *Mol. Cell* 62, 149–151. doi: 10.1016/j.molcel.2016.03.015

Pattison, J. S., Osinska, H., and Robbins, J. (2011). Atg7 induces basal autophagy and rescues autophagic deficiency in CryABR120G cardiomyocytes. *Circ. Res.* 109, 151–160. doi: 10.1161/circresaha.110.237339

Pattison, J. S., Sanbe, A., Maloyan, A., Osinska, H., Klevitsky, R., and Robbins, J. (2008). Cardiomyocyte expression of a polyglutamine preamyloid oligomer causes heart failure. *Circulation* 117, 2743–2751. doi: 10.1161/circulationaha.107.750232

Pereira, M. B., Santos, A. M., Goncalves, D. C., Cardoso, A. C., Consonni, S. R., Gozzo, F. C., et al. (2014). alphaB-crystallin interacts with and prevents stress-activated proteolysis of focal adhesion kinase by calpain in cardiomyocytes. *Nat. Commun.* 5:5159. doi: 10.1038/ncomms6159

Perez-Morales, D., Ostoa-Saloma, P., and Espinoza, B. (2009). Trypanosoma cruzi SHSP16: characterization of an alpha-crystallin small heat shock protein. *Exp. Parasitol.* 123, 182–189. doi: 10.1016/j.exppara.2009.06.019

Platt, F. M., Boland, B., and van der Spoel, A. C. (2012). The cell biology of disease: lysosomal storage disorders: the cellular impact of lysosomal dysfunction. *J. Cell Biol.* 199, 723–734. doi: 10.1083/jcb.201208152

Poelmann, R. E., and Gittenberger-de Groot, A. C. (2019). Development and evolution of the metazoan heart. *Dev. Dyn.* 248, 634–656. doi: 10.1002/dvdy.45

Pohl, C., and Dikic, I. (2019). Cellular quality control by the ubiquitin-proteasome system and autophagy. *Science* 366, 818–822. doi: 10.1126/science.aax3769

Prasad, V., Lorenz, J. N., Miller, M. L., Vairamani, K., Nieman, M. L., Wang, Y., et al. (2013). Loss of NHE1 activity leads to reduced oxidative stress in heart and mitigates high-fat diet-induced myocardial stress. *J. Mol. Cell. Cardiol.* 65, 33–42. doi: 10.1016/j.yjmcc.2013.09.013

Predmore, J. M., Wang, P., Davis, F., Bartolone, S., Westfall, M. V., Dyke, D. B., et al. (2010). Ubiquitin proteasome dysfunction in human hypertrophic

and dilated cardiomyopathies. *Circulation* 121, 997–1004. doi: 10.1161/circulationaha.109.904557

Qiu, H., Lizano, P., Laure, L., Sui, X., Rashed, E., Park, J. Y., et al. (2011). H11 kinase/heat shock protein 22 deletion impairs both nuclear and mitochondrial functions of STAT3 and accelerates the transition into heart failure on cardiac overload. *Circulation* 124, 406–415. doi: 10.1161/CIRCULATIONAHA.110.013847

Rainer, P. P., Dong, P., Sorge, M., Fert-Bober, J., Holewinski, R. J., Wang, Y., et al. (2018). Desmin phosphorylation triggers preamyloid oligomers formation and myocyte dysfunction in acquired heart failure. *Circ. Res.* 122, e75–e83.

Rajasekaran, N. S., Connell, P., Christians, E. S., Yan, L. J., Taylor, R. P., Orosz, A., et al. (2007). Human alpha B-crystallin mutation causes oxido-reductive stress and protein aggregation cardiomyopathy in mice. *Cell* 130, 427–439. doi: 10.1016/j.cell.2007.06.044

Ranek, M. J., Stachowski, M. J., Kirk, J. A., and Willis, M. S. (2018). The role of heat shock proteins and co-chaperones in heart failure. *Philos. Trans. R. Soc. Lond. B Biol. Sci.* 373:20160530. doi: 10.1098/rstb.2016.0530

Ranek, M. J., Terpstra, E. J., Li, J., Kass, D. A., and Wang, X. (2013). Protein kinase g positively regulates proteasome-mediated degradation of misfolded proteins. *Circulation* 128, 365–376. doi: 10.1161/circulationaha.113.001971

Rauch, J. N., Tse, E., Freilich, R., Mok, S. A., Makley, L. N., Southworth, D. R., et al. (2017). BAG3 is a modular, scaffolding protein that physically links heat shock protein 70 (hsp70) to the small heat shock proteins. *J. Mol. Biol.* 429, 128–141. doi: 10.1016/j.jmb.2016.11.013

Reddy, V. S., Ch, U. Kumar, Raghu, G., and Reddy, G. B. (2014). , Expression and induction of small heat shock proteins in rat heart under chronic hyperglycemic conditions. *Arch. Biochem. Biophys.* 558, 1–9. doi: 10.1016/j.abb.2014.06.008

Rothe, S., Prakash, A., and Tyedmers, J. (2018). The insoluble protein deposit (IPOD) in yeast. *Front. Mol. Neurosci.* 11:237. doi: 10.3389/fnmol.2018.00237

Ruan, L., Zhou, C., Jin, E., Kucharavy, A., Zhang, Y., Wen, Z., et al. (2017). Cytosolic proteostasis through importing of misfolded proteins into mitochondria. *Nature* 543, 443–446. doi: 10.1038/nature21695

Rudolph, F., Huttemeister, J., da Silva Lopes, K., Juttner, R., Yu, L., Bergmann, N., et al. (2019). , Resolving titin's lifecycle and the spatial organization of protein turnover in mouse cardiomyocytes. *Proc. Natl. Acad. Sci. U.S.A.* 116, 25126–25136. doi: 10.1073/pnas.1904385116

Saad, S., Cereghetti, G., Feng, Y., Picotti, P., Peter, M., and Dechant, R. (2017). Reversible protein aggregation is a protective mechanism to ensure cell cycle restart after stress. *Nat. Cell Biol.* 19, 1202–1213. doi: 10.1038/ncb3600

Sacconi, S., Feasson, L., Antoine, J. C., Pecheux, C., Bernard, R., Cobo, A. M., et al. (2012). A novel CRYAB mutation resulting in multisystemic disease. *Neuromuscul. Disord.* 22, 66–72. doi: 10.1016/j.nmd.2011.07.004

Sanbe, A., Osinska, H., Saffitz, J. E., Glabe, C. G., Kayed, R., Maloyan, A., et al. (2004). Desmin-related cardiomyopathy in transgenic mice: a cardiac amyloidosis. *Proc. Natl. Acad. Sci. U.S.A.* 101, 10132–10136. doi: 10.1073/pnas.0401900101

Schanzer, A., Rupp, S., Graf, S., Zengeler, D., Jux, C., Akinturk, H., et al. (2018). Dysregulated autophagy in restrictive cardiomyopathy due to Pro209Leu mutation in BAG3. *Mol. Genet. Metab.* 123, 388–399. doi: 10.1016/j.ymgme.2018.01.001

Schessl, J., Zou, Y., McGrath, M. J., Cowling, B. S., Maiti, B., Chin, S. S., et al. (2008). Proteomic identification of FHL1 as the protein mutated in human reducing body myopathy. *J. Clin. Investig.* 118, 904–912.

Schlossarek, S., Englmann, D. R., Sultan, K. R., Sauer, M., Eschenhagen, T., and Carrier, L. (2012). Defective proteolytic systems in Mybpc3-targeted mice with cardiac hypertrophy. *Basic Res. Cardiol.* 107:235.

Schreiber, S. S., Evans, C. D., Oratz, M., and Rothschild, M. A. (1981). Protein synthesis and degradation in cardiac stress. *Circ. Res.* 48, 601–611. doi: 10.1161/01.res.48.5.601

Sciarretta, S., Maejima, Y., Zablocki, D., and Sadoshima, J. (2018a). The role of autophagy in the heart. *Annu. Rev. Physiol.* 80, 1–26.

Sciarretta, S., Yee, D., Nagarajan, N., Bianchi, F., Saito, T., Valenti, V., et al. (2018b). Trehalose-induced activation of autophagy improves cardiac remodeling after myocardial infarction. *J. Am. Coll. Cardiol.* 71, 1999–2010. doi: 10.1016/j.jacc.2018.02.066

Scott, G., Ramlackhansingh, A. F., Edison, P., Hellyer, P., Cole, J., Veronese, M., et al. (2016). Amyloid pathology and axonal injury after brain trauma. *Neurology* 86, 821–828. doi: 10.1212/wnl.0000000000002413

Settembre, C., Di, M. C., Polito, V. A., Garcia, A. M., Vetrini, F., Erdin, S., et al. (2011). TFEB links autophagy to lysosomal biogenesis. *Science* 332, 1429–1433. doi: 10.1126/science.1204592

Shah, S., Henry, A., Roselli, C., Lin, H., Sveinbjornsson, G., Fatemifar, G., et al. (2020). Genome-wide association and mendelian randomisation analysis provide insights into the pathogenesis of heart failure. *Nat. Commun.* 11:163.

Sharma, S., Conover, G. M., Elliott, J. L., Der Perng, M., Herrmann, H., and Quinlan, R. A. (2017). alphaB-crystallin is a sensor for assembly intermediates and for the subunit topology of desmin intermediate filaments. *Cell Stress Chaperones* 22, 613–626. doi: 10.1007/s12192-017-0788-7

Shatov, V. M., Weeks, S. D., Strelkov, S. V., and Gusev, N. B. (2018). The role of the arginine in the conserved N-Terminal Domain RLFDQxFG motif of human small heat shock proteins HspB1, HspB4, HspB5, HspB6, and HspB8. *Int. J. Mol. Sci.* 19:2112. doi: 10.3390/ijms19072112

Shorter, J. (2017). Designer protein disaggregases to counter neurodegenerative disease. *Curr. Opin. Genet. Dev.* 44, 1–8. doi: 10.1016/j.gde.2017.01.008

Simon, S., Fontaine, J. M., Martin, J. L., Sun, X., Hoppe, A. D., Welsh, M. J., et al. (2007). Myopathy-associated alphaB-crystallin mutants: abnormal phosphorylation, intracellular location, and interactions with other small heat shock proteins. *J. Biol. Chem.* 282, 34276–34287. doi: 10.1074/jbc.m703267200

Song, Y. J., Zhong, C. B., and Wang, X. B. (2019). Heat shock protein 70: a promising therapeutic target for myocardial ischemia-reperfusion injury. *J. Cell Physiol.* 234, 1190–1207. doi: 10.1002/jcp.27110

Su, H., Li, J., Zhang, H., Ma, W., Wei, N., Liu, J., et al. (2015). COP9 signalosome controls the degradation of cytosolic misfolded proteins and protects against cardiac proteotoxicity. *Circ. Res.* 117, 956–966. doi: 10.1161/circresaha.115.306783

Sun, D., Wu, R., Li, P., and Yu, L. (2020). Phase separation in regulation of aggrephagy. *J. Mol. Biol.* 432, 160–169. doi: 10.1016/j.jmb.2019.06.026

Szikora, S., Gajdos, T., Novak, T., Farkas, D., Foldi, I., Lenart, P., et al. (2020). Nanoscopy reveals the layered organization of the sarcomeric H-zone and I-band complexes. *J. Cell Biol.* 219:e2019.

Taguchi, Y. V., Gorenberg, E. L., Nagy, M., Thrasher, D., Fenton, W. A., Volpicelli-Daley, L., et al. (2019). Hsp110 mitigates alpha-synuclein pathology in vivo. *Proc. Natl. Acad. Sci. U.S.A.* 116, 24310–24316. doi: 10.1073/pnas.1903268116

Tamura, S., Marunouchi, T., and Tanonaka, K. (2019). Heat-shock protein 90 modulates cardiac ventricular hypertrophy via activation of MAPK pathway. *J. Mol. Cell. Cardiol.* 127, 134–142. doi: 10.1016/j.yjmcc.2018.12.010

Tan, S., and Wong, E. (2017). Kinetics of protein aggregates disposal by aggrephagy. *Methods Enzymol.* 588, 245–281. doi: 10.1016/bs.mie.2016.09.084

Tannous, P., Zhu, H., Nemchenko, A., Berry, J. M., Johnstone, J. L., Shelton, J. M., et al. (2008). Intracellular protein aggregation is a proximal trigger of cardiomyocyte autophagy. *Circulation* 117, 3070–3078. doi: 10.1161/circulationaha.107.763870

Tharp, C. A., Haywood, M. E., Sbaizero, O., Taylor, M. R. G., and Mestroni, L. (2019). The giant protein titin's role in cardiomyopathy: genetic, transcriptional, and post-translational modifications of TTN and their contribution to cardiac disease. *Front. Physiol.* 10:1436. doi: 10.3389/fphys.2019.01436

Torrente, M. P., and Shorter, J. (2013). The metazoan protein disaggregase and amyloid depolymerase system: Hsp110, Hsp70, Hsp40, and small heat shock proteins. *Prion* 7, 457–463. doi: 10.4161/pri.27531

Tsikitis, M., Galata, Z., Mavroidis, M., Psarras, S., and Capetanaki, Y. (2018). Intermediate filaments in cardiomyopathy. *Biophys. Rev.* 10, 1007–1031. doi: 10.1007/s12551-018-0443-2

Tskhovrebova, L., and Trinick, J. (2003). Titin: properties and family relationships. *Nat. Rev. Mol. Cell Biolo.* 4, 679–689. doi: 10.1038/nrm1198

Ulbricht, A., Eppler, F. J., Tapia, V. E., van der Ven, P. F., Hampe, N., Hersch, N., et al. (2013). Cellular mechanotransduction relies on tension-induced and chaperone-assisted autophagy. *Curr. Biol.* 23, 430–435. doi: 10.1016/j.cub.2013.01.064

Ungelenk, S., Moayed, F., Ho, C. T., Grousl, T., Scharf, A., Mashaghi, A., et al. (2016). Small heat shock proteins sequester misfolding proteins in near-native conformation for cellular protection and efficient refolding. *Nat. Commun.* 7:13673.

Uversky, V. N. (2017). Intrinsically disordered proteins in overcrowded milieu: membrane-less organelles, phase separation, and intrinsic disorder. *Curr. Opin. Struct. Biol.* 44, 18–30. doi: 10.1016/j.sbi.2016.10.015

van der Velden, J., and Stienen, G. J. M. (2019). Cardiac disorders and pathophysiology of sarcomeric proteins. *Physiol. Rev.* 99, 381–426. doi: 10.1152/physrev.00040.2017

Vicart, P., Caron, A., Guicheney, P., Li, Z., Prevost, M. C., Faure, A., et al. (1998). A missense mutation in the alphaB-crystallin chaperone gene causes a desmin-related myopathy. *Nat. Genet.* 20, 92–95. doi: 10.1038/1765

Virani, S. S., Alonso, A., Benjamin, E. J., Bittencourt, M. S., Callaway, C. W., Carson, A. P., et al. (2020). Heart disease and stroke statistics-2020 update: a report from the american heart association. *Circulation* 141, e139–e596.

Vonk, W. I. M., Rainbolt, T. K., Dolan, P. T., Webb, A. E., Brunet, A., and Frydman, J. (2020). Differentiation drives widespread rewiring of the neural stem cell chaperone network. *Mol. Cell* 78, 329–345e9.

Walther, D. M., Kasturi, P., Zheng, M., Pinkert, S., Vecchi, G., Ciryam, P., et al. (2015). Widespread proteome remodeling and aggregation in aging *C. elegans*. *Cell* 161, 919–932. doi: 10.1016/j.cell.2015.03.032

Wang, J., Choi, J. M., Holehouse, A. S., Lee, H. O., Zhang, X., Jahnel, M., et al. (2018). A molecular grammar governing the driving forces for phase separation of prion-like RNA binding proteins. *Cell* 174, 688.e16–699e16.

Wang, L., Zhang, T. P., Zhang, Y., Bi, H. L., Guan, X. M., Wang, H. X., et al. (2016). Protection against doxorubicin-induced myocardial dysfunction in mice by cardiac-specific expression of carboxyl terminus of hsp70-interacting protein. *Sci. Rep.* 6:28399.

Wang, X., Li, J., Zheng, H., Su, H., and Powell, S. R. (2011). Proteasome functional insufficiency in cardiac pathogenesis. *Am. J. Physiol. Heart Circ. Physiol.* 301, H2207–H2219.

Wang, X., Osinska, H., Klevitsky, R., Gerdes, A. M., Nieman, M., Lorenz, J., et al. (2001). Expression of R120G-alphaB-crystallin causes aberrant desmin and alphaB-crystallin aggregation and cardiomyopathy in mice. *Circ. Res.* 89, 84–91. doi: 10.1161/hh1301.092688

Williams, A. B., Decourten-Myers, G. M., Fischer, J. E., Luo, G., Sun, X., and Hasselgren, P. O. (1999). Sepsis stimulates release of myofilaments in skeletal muscle by a calcium-dependent mechanism. *FASEB J.* 13, 1435–1443. doi: 10.1096/fasebj.13.11.1435

Wojtowicz, I., Jablonska, J., Zmojdzian, M., Taghli-Lamallem, O., Renaud, Y., Junion, G., et al. (2015). *Drosophila* small heat shock protein CryAB ensures structural integrity of developing muscles, and proper muscle and heart performance. *Development* 142, 994–1005. doi: 10.1242/dev.115352

Yang, J., and Tower, J. (2009). Expression of hsp22 and hsp70 transgenes is partially predictive of *Drosophila* survival under normal and stress conditions. *J. Gerontol A Biol. Sci. Med. Sci.* 64, 828–838. doi: 10.1093/gerona/glp054

Yokom, A. L., Gates, S. N., Jackrel, M. E., Mack, K. L., Su, M., Shorter, J., et al. (2016). Spiral architecture of the Hsp104 disaggregase reveals the basis for polypeptide translocation. *Nat. Struct. Mol. Biol.* 23, 830–837. doi: 10.1038/nsmb.3277

Zhang, H., Pan, B., Wu, P., Parajuli, N., Rekhter, M. D., Goldberg, A. L., et al. (2019). PDE1 inhibition facilitates proteasomal degradation of misfolded proteins and protects against cardiac proteinopathy. *Sci. Adv.* 5:eaaw5870. doi: 10.1126/sciadv.aaw5870

Zhang, H., Rajasekaran, N. S., Orosz, A., Xiao, X., Rechsteiner, M., and Benjamin, I. J. (2010). Selective degradation of aggregate-prone CryAB mutants by HSPB1 is mediated by ubiquitin-proteasome pathways. *J. Mol. Cell. Cardiol.* 49, 918–930. doi: 10.1016/j.yjmcc.2010.09.004

Zhang, J., He, Z., Xiao, W., Na, Q., Wu, T., Su, K., et al. (2016). Overexpression of BAG3 attenuates hypoxia-induced cardiomyocyte apoptosis by inducing autophagy. *Cell Physiol. Biochem.* 39, 491–500. doi: 10.1159/000445641

Zhao, L., Chen, X. J., Zhu, J., Xi, Y. B., Yang, X., Hu, L. D., et al. (2015). Lanosterol reverses protein aggregation in cataracts. *Nature* 523, 607–611. doi: 10.1038/nature14650

Zheng, Q., Su, H., Ranek, M. J., and Wang, X. (2011). Autophagy and p62 in cardiac proteinopathy. *Circ. Res.* 109, 296–308. doi: 10.1161/circresaha.111.244707

Zhu, Y., Bogomolovas, J., Labeit, S., and Granzier, H. (2009). Single molecule force spectroscopy of the cardiac titin N2B element: effects of the molecular chaperone alphaB-crystallin with disease-causing mutations. *J. Biol. Chem.* 284, 13914–13923. doi: 10.1074/jbc.M809743200 doi: 10.1074/jbc.m809743200

Conflict of Interest: The authors declare that the research was conducted in the absence of any commercial or financial relationships that could be construed as a potential conflict of interest.

frontiers in Physiology

ORIGINAL RESEARCH
published: 09 June 2020
doi: 10.3389/fphys.2020.00625

Deficiency of the Immunoproteasome LMP10 Subunit Attenuates Angiotensin II-Induced Cardiac Hypertrophic Remodeling via Autophagic Degradation of gp130 and IGF1R

Wen Yan[1†], Zhi-Chao Dong[2†], Jing-Jing Wang[3], Yun-Long Zhang[1], Hong-Xia Wang[4], Bo Zhang[2] and Hui-Hua Li[1*]*

[1] Department of Emergency Medicine, Beijing Key Laboratory of Cardiopulmonary Cerebral Resuscitation, Beijing Chaoyang Hospital, Capital Medical University, Beijing, China, [2] Department of Cardiology, Institute of Cardiovascular Diseases, First Affiliated Hospital of Dalian Medical University, Dalian, China, [3] Department of Laboratory Animal Sciences, School of Basic Medical Sciences, Capital Medical University, Beijing, China, [4] Department of Physiology and Physiopathology, School of Basic Medical Sciences, Capital Medical University, Beijing, China

OPEN ACCESS

Edited by:
Peter J. Reiser,
The Ohio State University,
United States

Reviewed by:
Huabo Su,
Augusta University Medical College of Georgia, United States
Sebastiano Sciarretta,
Sapienza University of Rome, Italy

***Correspondence:**
Bo Zhang
dalianzhangbo@yahoo.com
Hui-Hua Li
hhli1935@aliyun.com

[†] These authors have contributed equally to this work

Specialty section:
This article was submitted to Striated Muscle Physiology, a section of the journal Frontiers in Physiology

Received: 07 February 2020
Accepted: 18 May 2020
Published: 09 June 2020

Citation:
Yan W, Dong Z-C, Wang J-J, Zhang Y-L, Wang H-X, Zhang B and Li H-H (2020) Deficiency of the Immunoproteasome LMP10 Subunit Attenuates Angiotensin II-Induced Cardiac Hypertrophic Remodeling via Autophagic Degradation of gp130 and IGF1R. Front. Physiol. 11:625. doi: 10.3389/fphys.2020.00625

Background/Aim: Hypertensive cardiac hypertrophy is the leading cause of cardiac remodeling and heart failure. We recently demonstrated that the immunoproteasome, an inducible form of the constitutive proteasome, plays a critical role in regulating cardiovascular diseases. However, the role of the immunoproteasome LMP10 (β2i) catalytic subunit in the regulation of angiotensin II (Ang II)-induced cardiac hypertrophic remodeling remains unclear.

Methods: Wild-type (WT) and LMP10 knockout (KO) mice were infused with Ang II 1,000 ng/kg/min for 2 weeks. Blood pressure was measured using a tail-cuff system. Cardiac function and hypertrophic remodeling were examined by echocardiography and histological staining. The expression levels of genes and proteins were examined with quantitative real-time PCR and immunoblotting analysis, respectively.

Results: LMP10 mRNA and protein expression was significantly increased in Ang II-stimulated hearts and primary cardiomyocytes. Moreover, Ang II infusion for 2 weeks increased systolic blood pressure, abnormal cardiac function, hypertrophy, fibrosis, and inflammation in WT mice, which were significantly reversed in KO mice. Moreover, a marked reduction in the protein levels of insulin growth factor-1 receptor (IGF1R), glycoprotein 130 (gp130), and phosphorylated AKT, mTOR, STAT3, and ERK1/2 and an increase in the LC3II/I ratio were also observed in LMP10 KO mice compared with WT mice after Ang II infusion. *In vitro* culture experiments confirmed that LMP10 knockdown activated autophagy and increased IGF1R and gp130 degradation, leading to the inhibition of cardiomyocyte hypertrophy. However, inhibiting autophagy with chloroquine reversed this effect.

Conclusion: The results of this study indicate that LMP10 KO attenuates Ang II-induced cardiac hypertrophic remodeling via the autophagy-dependent degradation of IGF1R and gp130, and suggests that LMP10 may be a novel therapeutic target for hypertrophic heart diseases.

Keywords: cardiac hypertrophy, immunoproteasome subunit, LMP10, ATG7, autophagy, gp130, IGF1R

INTRODUCTION

Sustained cardiac hypertrophy is associated with a significant increase in the risk for heart failure and sudden death (Frey and Olson, 2003). Cardiomyocyte hypertrophy is the cellular response to a variety of extrinsic and intrinsic stimuli. The pathological changes of hypertrophy are characterized by myocyte growth, fibrosis, enhanced protein synthesis, and fetal gene expression (Frey and Olson, 2003). Neurohormonal stimuli such as angiotensin II (Ang II) play important roles in the pathogenesis of cardiac remodeling in a variety of diseases (Wang et al., 2016; Wang L. et al., 2018). Increasing evidence has demonstrated that Ang II can activate G protein-coupled receptors, receptor tyrosine/serine/threonine kinases, and cytokine/growth factor receptors, thereby stimulating intracellular signal transduction pathways that play an important role in the initiation, regulation, and adaptation of cardiac hypertrophy (Frey and Olson, 2003). Among these receptors, insulin growth factor-1 receptor (IGF1R) and glycoprotein 130 (gp130) modulate cell proliferation and differentiation through the constitutive activation of the PI3K/AKT, MAPK/ERK, and JAK/STAT3 pathways. Interestingly, IGF1R and gp130 are activated in hypertrophic hearts and contribute to the initiation of cardiac hypertrophy and heart failure as a response to pathological hypertrophic stress (Toyozaki et al., 1993; Hirota et al., 1995, 1999; Pan et al., 1998; Yasukawa et al., 2001; Matsui et al., 2002, 2003). Thus, strategies that modulate the expression and activation of IGF1R and gp130 may be promising approaches for the treatment of hypertrophic heart diseases.

The two major intracellular protein degradation pathways, the ubiquitin-proteasome system (UPS) and the autophagy-lysosomal system, play critical roles in the development of various diseases such as cancer and neurodegenerative and cardiovascular diseases (Powell and Divald, 2010; Xie, 2010; Li Z. et al., 2015). The UPS represents the major pathway for the selective degradation of short-lived and abnormal proteins (Powell and Divald, 2010; Xie, 2010). In contrast, autophagy primarily degrades long-lived proteins, such as receptors, and maintains amino acid pools in the setting of chronic starvation (Korolchuk et al., 2010). The 26S proteasome is the key component of the UPS and comprises two subcomplexes, the 20S proteasome and two 19S regulatory particles. The β1, β2, and β5 subunits of the proteasome perform caspase-like, trypsin-like, and chymotrypsin-like proteolysis, respectively (Angeles et al., 2012; Ferrington and Gregerson, 2012). Interestingly, under cytokine stimulation, such as interferon-γ, three additional catalytic β subunits, namely β1i (LMP2), β2i (LMP10 and MECL1), and β5i (LMP7) are induced and preferentially incorporated during proteasome assembly to form the immunoproteasome (Angeles et al., 2012; Ferrington and Gregerson, 2012). It is now clear that dysregulation of the immunoproteasome is associated with many human diseases, including cancer and autoimmune, neurodegenerative, cancer, and cardiovascular diseases (Angeles et al., 2012; Ferrington and Gregerson, 2012). Our recent data and other reports showed that the physiological low level and activity of immunoproteasome β subunits that are expressed in cardiac tissues are highly upregulated in response to hypertrophic stimuli such as Ang II, deoxycorticosterone acetate (DOCA)-salt, and pressure overload (Ferrington and Gregerson, 2012). In contrast, blockage of proteasome activity using an inhibitor represses cardiac hypertrophy (Li N. et al., 2015). Recently, we demonstrated that the upregulation of LMP7 contributes to the development of several cardiovascular diseases, including pressure overload-induced cardiac hypertrophy, Ang II-induced atrial fibrillation, abdominal aortic aneurysm, and retinopathy (Li F. D. et al., 2019; Li J. et al., 2019; Xie et al., 2019). Moreover, LMP10 plays a critical role in DOCA-salt-induced myocardial fibrosis (Yan et al., 2017); however, the role of LMP10 in the development of Ang II-induced cardiac hypertrophic remodeling remains unclear.

In this study, we discovered that LMP10 expression was significantly upregulated in Ang II-stimulated cardiomyocytes and hypertrophic hearts. Knockout (KO) of LMP10 markedly attenuated cardiac hypertrophic remodeling and improved adverse contractile function in mice. Mechanistically, LMP10 deficiency activated autophagy, which promoted the degradation of IGF1R and gp130, thereby inhibiting cardiac hypertrophy. Thus, our data suggest that LMP10 plays a critical role in modulating cardiac hypertrophic remodeling, and targeting LMP10 may be a new therapeutic approach for the treatment of hypertrophic diseases.

MATERIALS AND METHODS

Animal Models

Wild-type (WT) C57BL/6 and LMP10 KO mice were initially obtained from Jackson Laboratory (Bar Harbor, ME, United States). Male mice (8–10 weeks old) were infused with saline or Ang II (Sigma-Aldrich, St. Louis, MO, United States) at a dose of 1,000 ng/kg/min using osmotic mini-pumps (Alzet, Cupertino, CA, United States) as described in our previous work (Wang L. et al., 2018). Blood pressure was measured in conscious mice by using a tail-cuff system (BP2010A; Softron, Tokyo, Japan) after Ang II infusion (Wang et al., 2016; Zhang et al., 2019). All animals were kept in a pathogen-free facility at Capital Medical University. All procedures were approved by

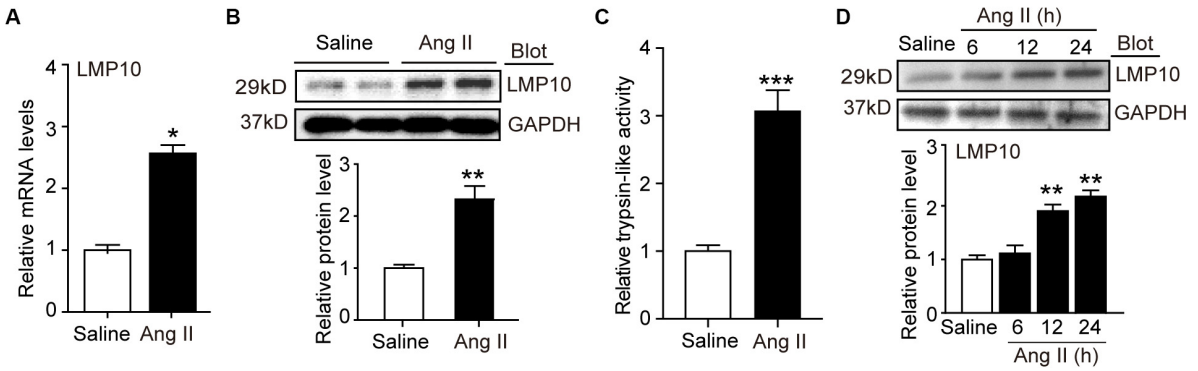

FIGURE 1 | LMP10 was upregulated in Ang II-treated hearts and cardiomyocytes. **(A)** Wild-type (WT) mice were infused with angiotensin II (Ang II) at dose of 1,000 ng/kg/min for 2 weeks. qPCR analysis of LMP10 mRNA expression in Ang II-infused mouse hearts (n = 6). **(B)** Immunoblotting analyses of LMP10 protein levels in the hearts after Ang II infusion (upper). Quantification of the relative protein level (lower; n = 4). **(C)** Measurement of proteasome trypsin-like activity in Ang II-infused mouse hearts (n = 6). **(D)** Immunoblotting analyses of LMP10 protein levels in neonatal rat cardiomyocytes (NRCMs) exposed to Ang II (100 nM) at different time points (upper; h: hour). Quantification of the relative protein level (lower; n = 3 independent experiments). Data are presented as mean ± SEM, and n represents number of samples per group. $^{*}P < 0.05$; $^{**}P < 0.01$ versus saline; $^{***}P < 0.001$ versus saline.

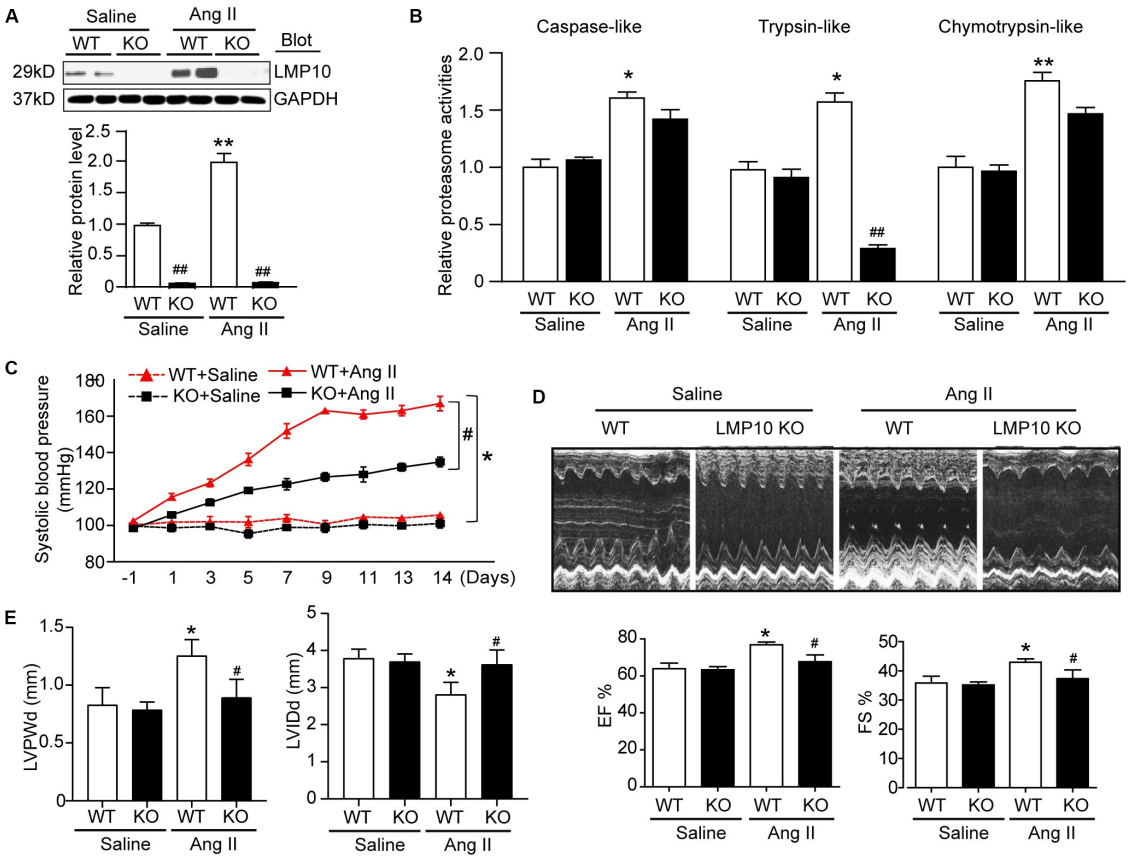

FIGURE 2 | Knockdown of LMP10 ameliorates cardiac function in mice after Ang II infusion. Wild-type (WT) or LMP10 knockout (KO) mice were infused with angiotensin II (Ang II) at dose of 1,000 ng/kg/min for 2 weeks. **(A)** Immunoblotting analyses of LMP10 protein levels in the hearts (upper). Quantification of the relative protein level (lower; n = 6). **(B)** Measurement of proteasome caspase-like, trypsin-like, and chymotrypsin-like activities in the hearts (n = 6). **(C)** Representative M-mode echocardiography of left ventricular chamber. **(D)** Assessment of left ventricular ejection fraction (EF%) and fractional shortening (FS%) (n = 8). **(E)** Measurement of left ventricular inner diameter at end-diastole (LVIDd) and left ventricular posterior wall thickness at end-diastole (LVPWd) (n = 8). Data are presented as mean ± SEM, and n represents number of animals per group. $^{*}P < 0.05$, $^{**}P < 0.01$ versus saline; $^{\#}P < 0.05$, $^{\#\#}P < 0.01$ versus WT + Ang II.

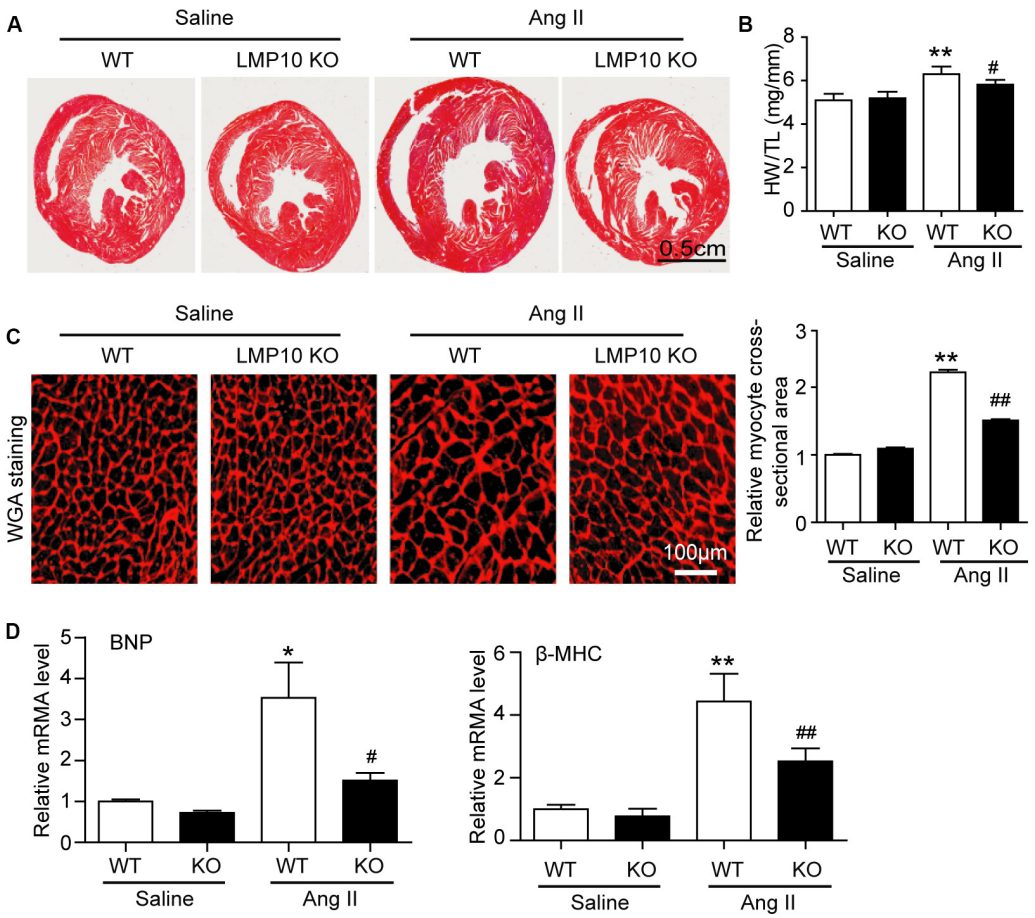

FIGURE 3 | Deficiency of LMP10 attenuates Ang II-induced cardiac hypertrophy in mice. **(A)** Wild-type (WT) or LMP10 knockout (KO) mice were infused with angiotensin II (Ang II) at dose of 1,000 ng/kg/min for 2 weeks. Representative images of Hematoxylin and eosin (H&E) staining of the heart sections (lower). Scale bar 0.5 cm. **(B)** The ratios of heart weight to body weight (HW/BW) and heart weight to tibia length (HW/TL) (n = 6 per group). **(C)** TRITC-WGA staining of cardiac myocytes (left). Scale bar 100 μm. Quantification of the relative myocyte cross-sectional area (150–200 cells counted per heart, right) (n = 6 per group). **(D)** qPCR analyses of BNP and β-MHC mRNA levels in the hearts. Results are normalized to the GAPDH level (n = 6 per group). Data are presented as mean ± SEM, and n represents number of animals per group. $^{*}P < 0.05$, $^{**}P < 0.01$ versus saline; $^{\#}P < 0.05$, $^{\#\#}P < 0.01$ versus WT + Ang II.

the Institutional Animal Care and Use Committee of Capital Medical University and performed in accordance with the National Institutes of Health Guide for the Care and Use of Laboratory Animals.

Cell Culture and Transfection

Neonatal rat cardiomyocytes (NRCMs) were obtained from 1–3-day-old Sprague-Dawley rats as described previously (Li et al., 2004; Chen et al., 2019). NRCMs were transfected with small interfering RNA (siRNA) against LMP10 (siRNA-LMP10) or scramble control (siRNA-control) for 24 h. To induce a hypertrophic response, NRCMs were treated with Ang II (100 nM) for 24 h, as described previously (Xie et al., 2019).

Echocardiographic Assessment

All animals were lightly anesthetized with 1.5% isoflurane. Cardiac left ventricular (LV) structure and function were measured by M-mode echocardiography by using a 30-MHz probe (Vevo 2100 System; VisualSonics, Toronto, ON, Canada). LV inner diameter (LVID) and LV posterior wall thickness (LVPW) were measured at systole and diastole. LV ejection fraction (EF%) and LV fractional shortening (FS%) were calculated as follows: 100 × [(LVEDV − LVESV)/LVEDV] (%) and 100 × [(LVDd − LVDs)/LVDd] (%), respectively (Wang L. et al., 2018; Xie et al., 2019).

Histopathological Examinations

Heart samples were fixed in a 4% formalin solution overnight, embedded in paraffin, and cut into 5-μm sections. Hematoxylin and eosin (H&E), wheat germ agglutinin (WGA) and Masson's trichrome staining were performed as described previously (Wang L. et al., 2018; Xie et al., 2019). Images were taken at ×100 or ×200 magnification of 15–20 random fields from each heart sample. Myocyte size, fibrotic areas, and Mac-2-positive cells were analyzed by Image Pro Plus 3.0 (Nikon, Tokyo, Japan).

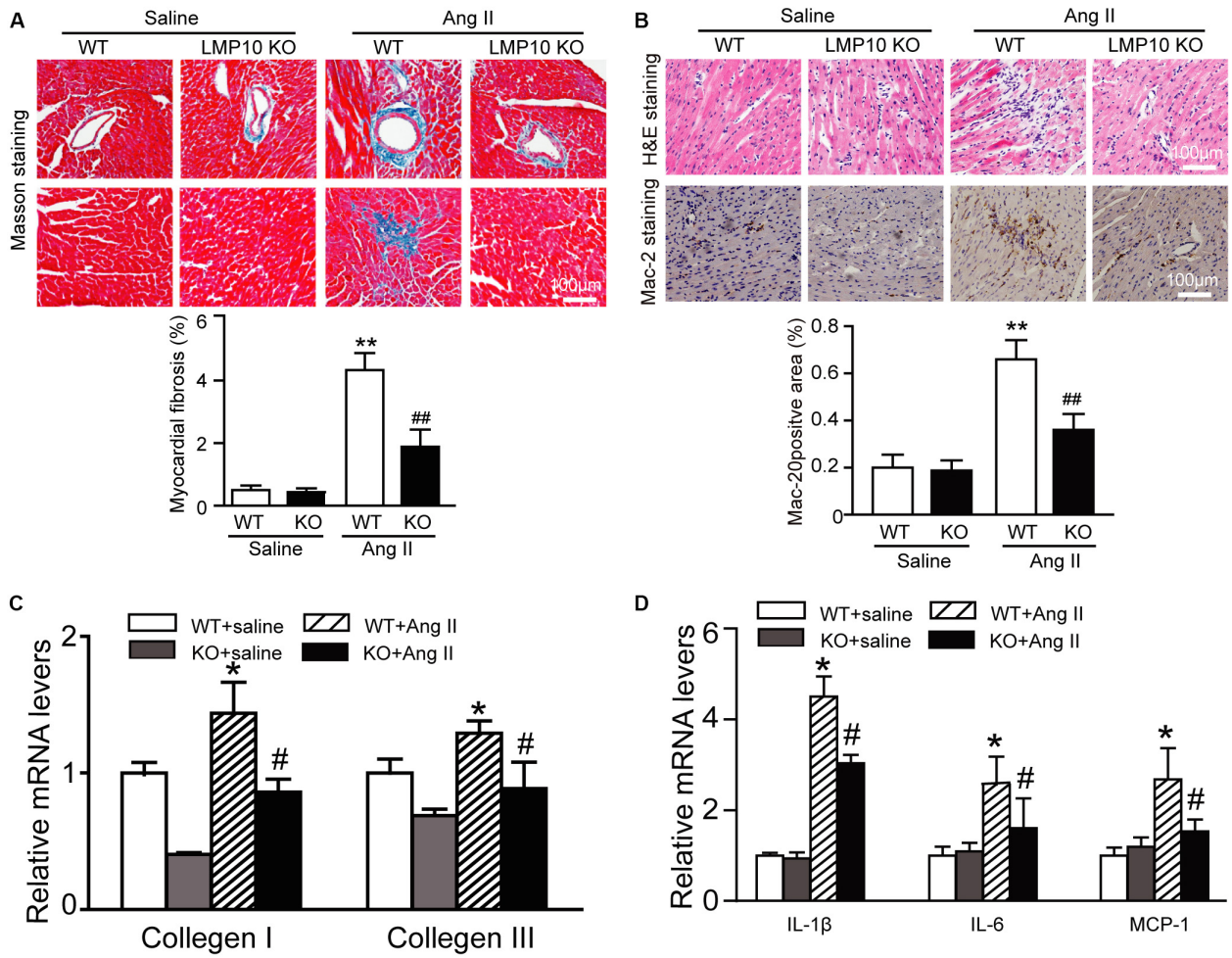

FIGURE 4 | Deficiency of LMP10 attenuates Ang II-induced cardiac hypertrophy in mice. **(A)** Wild-type (WT) or LMP10 knockout (KO) mice were infused with angiotensin II (Ang II) at dose of 1,000 ng/kg/min for 2 weeks. Masson's Trichrome staining of cardiac perivascular and interstitial fibrosis detected by (upper). Scale bar 100 μm. Quantification of the relative fibrosis area (lower, $n = 6$). **(B)** Hematoxylin and eosin (H&E) staining of the heart sections (upper). Immunochemical staining of heart sections with anti-Mac-2 antibody (middle). Scale bar 100 μm. Quantification of Mac-2-positive area (lower) ($n = 6$ per group). **(C)** qPCR analyses of collagen I and collagen III mRNA levels ($n = 6$). **(D)** qPCR analyses of IL-1β, IL-6 and MCP-1 mRNA levels ($n = 6$). The data are normalized to the GAPDH level. Data are presented as mean (SEM, and n represents number of animals per group. $^{*}P < 0.05$, $^{**}P < 0.01$ versus saline; $^{\#}P < 0.05$, $^{\#\#}P < 0.01$ versus WT + Ang II.

Immunostaining

Neonatal rat cardiomyocytes were transfected with siRNA-control or siRNA-LMP10 for 24 h and stimulated with Ang II (100 nM) for an additional 24 h. Double immunostaining was performed with an anti-α-actinin, anti-LC3B, anti-IGF1R, or anti-gp130 antibody, and nuclei were stained with DAPI (blue). Cardiomyocyte surface area was measured in 150 cells in each experiment as described previously (Wang L. et al., 2018; Xie et al., 2019).

Immunogold Electron Microscopy

Neonatal rat cardiomyocytes were fixed in 0.1% glutaraldehyde (Polysciences, Inc., Warrington, PA, United States) and 4% paraformaldehyde in 0.1 mol/L cacodylic acid for 30 min. The samples were probed with a mouse monoclonal antibody against IGF1R or gp130 (1:200 dilution) and viewed on an HT-7700 transmission electron microscope (Hitachi, Tokyo, Japan) as described previously (Swanlund et al., 2010).

Immunoblotting Analysis

Heart tissues or NRCMs were lysed with RIPA lysis buffer (Solarbio, Beijing, China). Proteins (50–60 μg) were separated by sodium dodecyl sulfate-polyacrylamide gel electrophoresis, transferred to polyvinylidene difluoride membranes, and incubated with primary antibodies against AKT, phosphorylated (p)-AKT, mTOR, p-mTOR, STAT3, p-STAT3, ERK1/2, p-ERK1/2, calcineurin A, PTEN, and GAPDH (Cell Signaling Technologies, Boston, MA, United States), MKP-1 (Santa Cruz Biotechnology, Inc., Dallas, TX, United States), and LMP10 (Abcam, Cambridge, United Kingdom) as indicated in each experiment, and then with horseradish peroxidase-conjugated secondary antibodies (1:2,500) as described previously (Wang L. et al., 2018; Xie et al.,

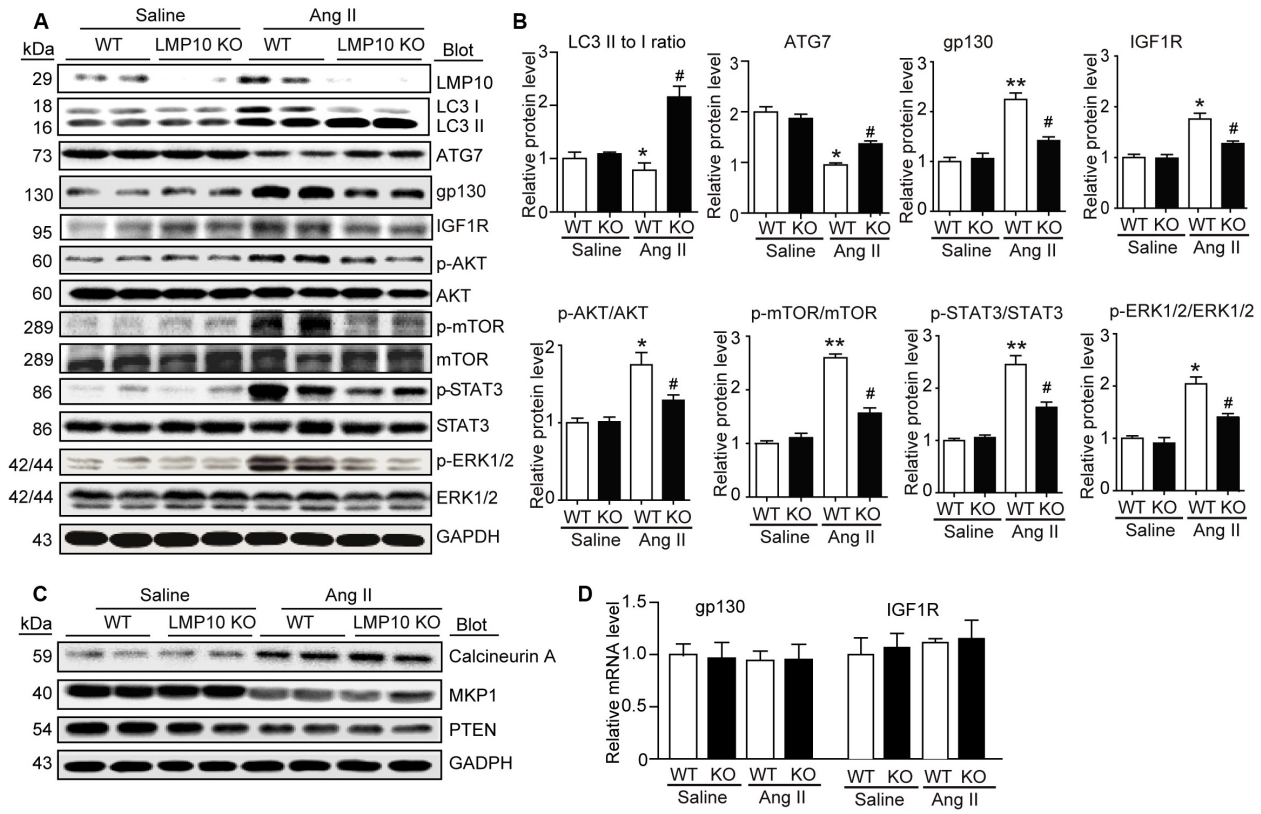

FIGURE 5 | Deficiency of LMP10 reduces protein levels of IGF1R and gp130 and activation of the downstream mediators in Ang II-infused hearts. **(A)** Wild-type (WT) or LMP10 knockout (KO) mice were infused with angiotensin II (Ang II) at dose of 1,000 ng/kg/min for 2 weeks. Immunoblotting analyses of LMP10, LC3 II/I, ATG7, IGF1R, gp130, AKT, p-AKT, mTOR, p-mTOR, STAT3, p-STAT3, ERK1/2, and p-ERK1/2 protein levels in the heart tissues (left). **(B)** Quantification of the relative protein level (n = 4, right). **(C)** Immunoblotting analyses of calcineurin A, PTEN, and MKP-1 protein levels in the heart tissues. **(D)** qPCR analyses of IGF1R and gp130 mRNA levels (n = 6). The data are normalized to the GAPDH level. Data are expressed as the mean ± SEM. $^{*}P < 0.05$, $^{**}P < 0.01$ versus saline. $^{\#}P < 0.05$ versus WT + Ang II.

2019). Blot signal intensities were analyzed using a Gel-pro 4.5 Analyzer (Media Cybernetics, Rockville, MD, United States).

Quantitative Real-Time PCR Analysis

Quantitative real-time PCR was conducted using an S1000 Thermal Cycler (Bio-Rad, Hercules, CA, United States). Total RNA was extracted from heart tissue with TRIzol (Invitrogen, Carlsbad, CA, United States) and reverse transcribed. cDNA (1–2 μg) was used for PCR amplification with gene-specific primers for LMP10, B-type natriuretic peptide (BNP), β-myosin heavy chain (β-MHC), interleukin (IL)-1β, IL-6, monocyte chemoattractant protein 1 (MCP-1), collagen I, and collagen III as described previously (Wang L. et al., 2018; Zhang et al., 2019). The amount of detected mRNA was normalized to the amount of endogenous GAPDH control.

Proteasome Activity

Proteins were isolated from heart tissue with HEPES buffer (50 mM, pH 7.5) containing 20 mmol/L KCl, 5 mmol/L $MgCl_2$, and 1 mmol/L DTT. Proteasome trypsin-like activity was measured in heart tissue using the fluorogenic peptide substrate Ac-RLRAMC (40 μmol/L) with excitation at 380 nm and emission at 460 nm as described previously (Chen et al., 2019).

Statistical Analysis

Results are presented as the mean ± SEM. All statistical tests were performed using SPSS version 19.0. If each group satisfied normality and the variance among the groups was equal, differences in means for continuous variables were compared with Student's t-test (two groups) or ANOVA (multiple groups). If these conditions were not met, a non-parametric Mann–Whitney U test was used. P-values < 0.05 were considered significant.

RESULTS

Ang II Upregulates LMP10 Expression in Primary Cardiomyocytes and Mouse Hearts

To investigate the role of LMP10 in the development of cardiac hypertrophy, we examined LMP10 expression in Ang

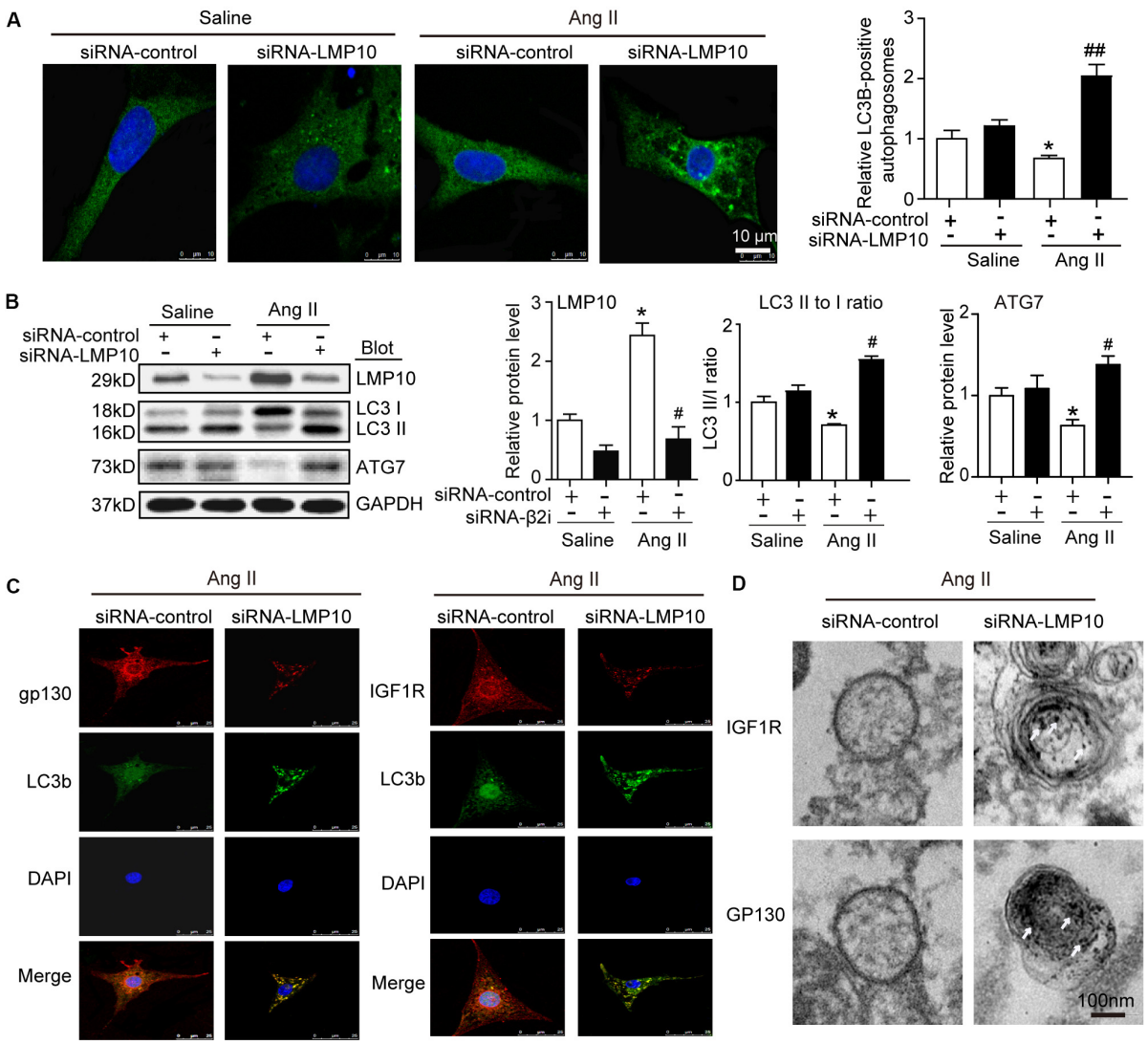

FIGURE 6 | Knockdown of LMP10 increases autophagy and localization of IGF1R and gp130 in autophagosomes in cultured cardiomyocytes. Neonatal rat cardiomyocytes (NRCMs) were transfected with siRNA-LMP10 or siRNA-control for 24 h and then exposed to Ang II (100 nM) for 48 h. **(A)** Immunofluorescence staining of autophagosomes with anti-LC3B (green, left). DAPI staining for nuclei (blue). Quantification of LC3B-positive fluorescent dots (n = 10–12 cells per group, right). **(B)** Immunoblotting analysis of LC3 (upper) and ATG7 (middle). The ratios of LC3-II to LC3-I and quantitation of ATG7 protein level (n = 3 independent experiments). **(C)** Immunofluorescence staining for IGF1R or gp130 (red), and LC3B (green). DAPI staining for nuclei (blue) in NRCMs after Ang II. The data are normalized to the GAPDH level. **(D)** IGF1R and gp130 were respectively labeled using anti-IGF1R or gp130 antibody and the secondary antibody coupled to gold beads. Electron microscopic examination of EGFR and IGF1R in autophagosomes in NRCMs after Ang II. White arrows indicate IGF1R or GP130-positive particles. Data are expressed as the mean ± SEM. $^{*}P < 0.05$ versus saline. $^{\#}P < 0.05$, $^{\#\#}P < 0.01$ versus WT + Ang II.

II-infused hearts. After 3 weeks, quantitative real-time PCR analysis revealed that LMP10 mRNA expression was significantly increased in Ang II-infused hearts compared with control saline-treated hearts (**Figure 1A**). Moreover, immunoblotting confirmed increased LMP10 protein expression in Ang II-infused hearts (**Figure 1B**). Accordingly, the proteasome trypsin-like activity generated by LMP10 was also increased in Ang II-infused heart tissue (**Figure 1C**). In addition, Ang II (100 nM) treatment upregulated the expression of LMP10 protein in NRCMs in a time-dependent manner (**Figure 1C**). Thus, these results suggest that the upregulation of LMP10 in cardiomyocytes may play a role in Ang II-infused cardiac hypertrophy.

LMP10 Knockout Improves Ang II-Induced Contractile Function Abnormality and Cardiac Hypertrophy

To test the functional role of LMP10 in pathological hypertrophic remodeling, WT and LMP10 KO mice were infused with Ang II for 2 weeks. We found that Ang II infusion significantly increased LMP10 protein expression and systolic blood pressure

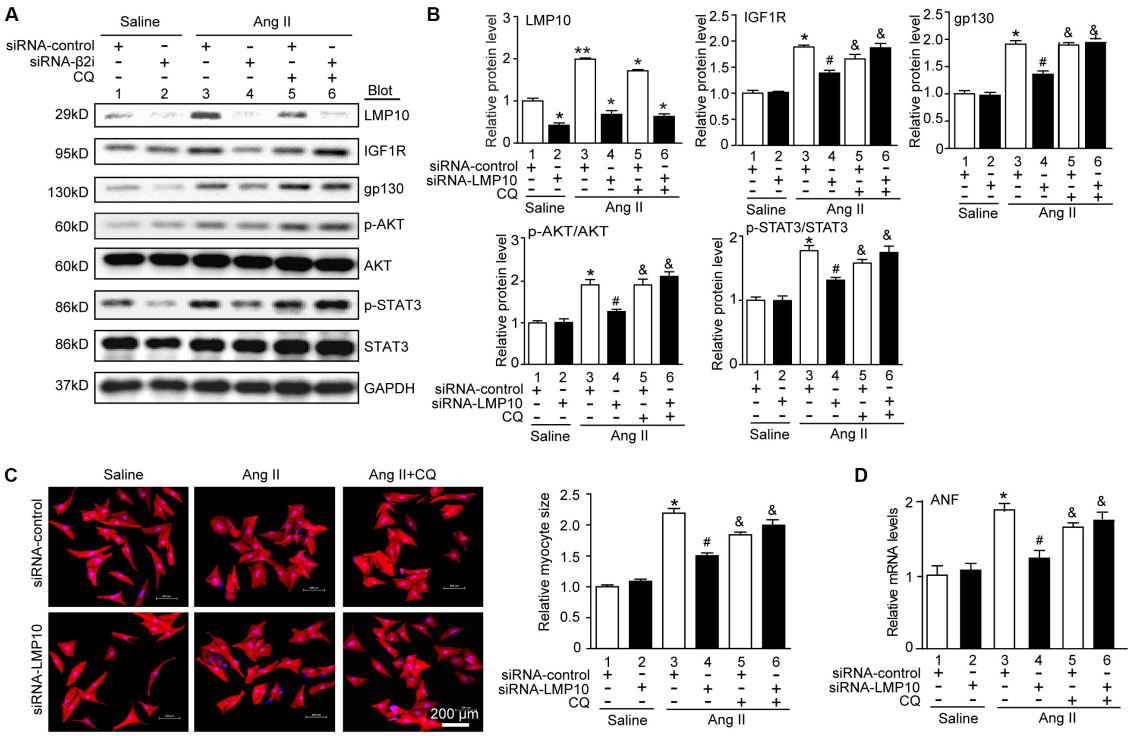

FIGURE 7 | Knockdown of LMP10 inhibits cardiomyocyte hypertrophy through autophagic degradation of IGF1R and gp130 *in vitro*. **(A)** Immunoblotting analysis of protein levels of LMP10, IGF1R, gp130, p-AKT, AKT, p-STAT3, and STAT3 ($n = 3$). The data are normalized to the GAPDH level. **(B)** Quantification of the relative protein level ($n = 4$, right). **(C)** Neonatal rat cardiomyocytes (NRCMs) were transfected with siRNA-LMP10 or siRNA-control for 24 hours and then exposed to Ang II (100 nM) for 48 hours. Double immunostaining (red: α-actinin for cardiomyocytes; blue: DAPI for nuclei) of cardiomyocytes for measurement of cell size. Quantification of cardiomyocyte surface area (right, 150 cells counted per experiment, $n = 3$). Scale bar, 50 μm. **(D)** qPCR analysis of ANF mRNA expression ($n = 3$ independent experiments). Data are presented as means ± SEM. $^{*}P < 0.05$ versus siRNA-control + saline; $^{\#}P < 0.05$ versus siRNA-control + Ang II; $^{\&}P < 0.05$ versus siRNA-control + Ang II.

in WT mice, whereas these increases were markedly attenuated in LMP10 KO mice (**Figures 2A,B**). Echocardiographic assessment reveled that the Ang II infusion-induced increase in cardiac contractile function, as reflected by an increased LV EF% and FS% in WT mice, was also significantly improved in LMP10 KO mice (**Figure 2D**). The Ang II-induced increase of LVPW was markedly reduced in LMP10 KO mice compared with WT control. The Ang II-induced decrease of left ventricular inner diameter at end-diastole (LVIDd) was also reversed in LMP10 KO mice (**Figure 2E**). Moreover, the features of Ang II-induced cardiac hypertrophy, as characterized by an increase in LV wall thickness (**Figure 3A**), heart weight/tibia length (HW/TL) ratios (**Figure 3B**), cross-sectional area of myocytes (**Figure 3C**), and atrial natriuretic peptide (ANP) and β-MHC mRNA expression (**Figure 3D**), were also remarkably attenuated in LMP10 KO mice (**Figures 3A–D**), suggesting that LMP10 exerts a prohypertrophic role *in vivo*.

LMP10 Deficiency Inhibits Ang II-Induced Cardiac Fibrosis and Inflammation in Mice

Myocardial fibrosis is a hallmark of cardiac remodeling; thus, we examined the extent of collagen deposition in the heart. Masson's trichrome staining showed that Ang II infusion caused a significant increase in the myocardial perivascular and interstitial fibrotic areas and collagen I and III expression in WT mice, while this effect was markedly suppressed in Ang II-infused LMP10 KO mice (**Figure 4A**). Since inflammation is an important driver of myocardial fibrosis, we performed H&E and immunohistochemical staining. The Ang II infusion-induced accumulation of interstitial proinflammatory cells and Mac-2-positive macrophages in WT mice was evidently attenuated in Ang II-treated LMP10 KO mice (**Figure 4B**). Accordingly, the mRNA levels of collagen I, collagen III, IL-1β, IL-6, and MCP-1 were also obviously lower in LMP10 KO mice compared with WT mice after Ang II infusion (**Figures 4C,D**). No significant difference in these parameters was observed between the WT and LMP10 KO groups after saline infusion (**Figures 4A–D**).

LMP10 Deficiency Reduces IGF1R and gp130 Protein Levels in Ang II-Infused Hearts

To explore the molecular mechanism by which LMP10 KO attenuates Ang II-induced cardiac hypertrophy, we examined a range of prohypertrophic signaling pathways, including IGF1R, gp130, EGFR, and calcineurin A, and their downstream

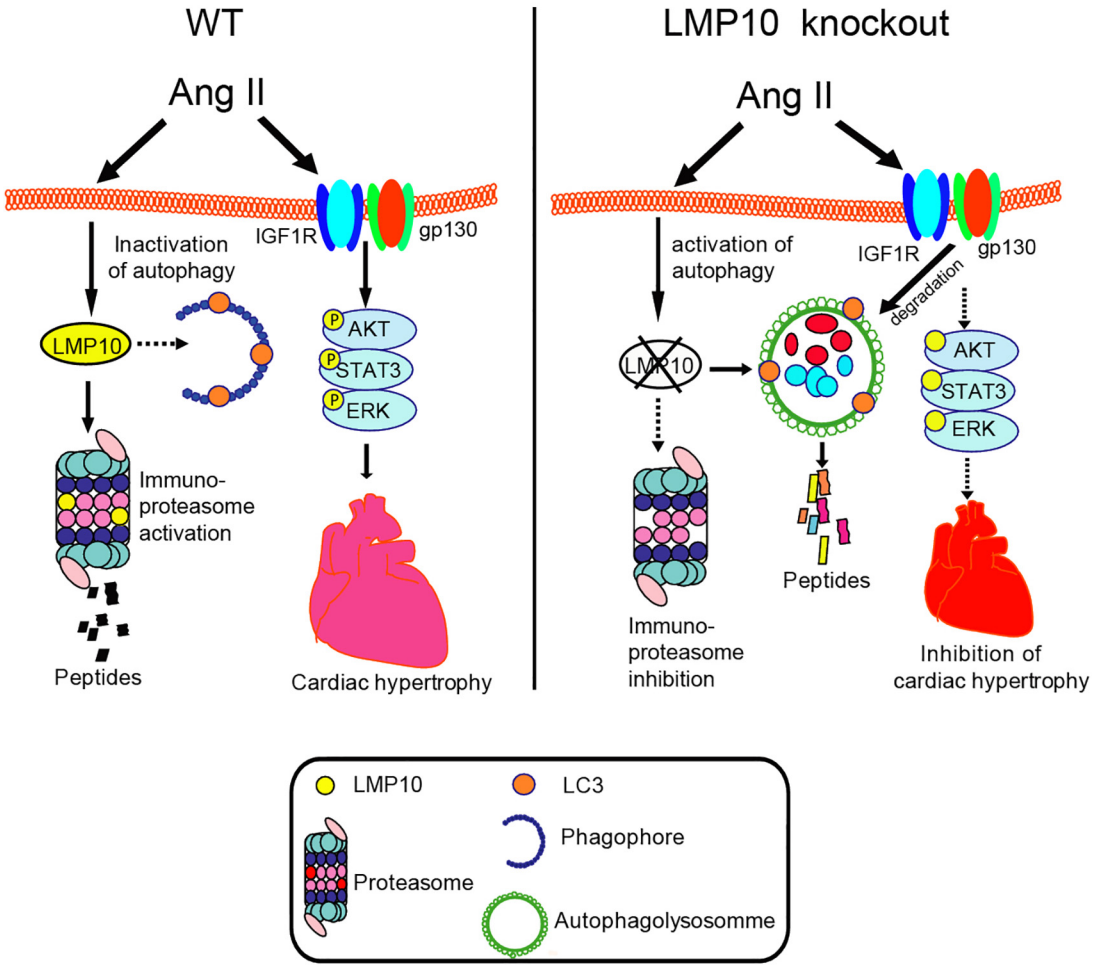

FIGURE 8 | The summarized diagram showing that the proposed mechanisms underlying LMP10 regulate cardiac hypertrophy. Upon Ang II stimulation, upregulation of LMP10 inhibits autophagy activation, which then increases protein levels of IGF1R and gp130 and activation of the downstream mediators leading to cardiac hypertrophy. Conversely, LMP10 KO attenuates these effects.

mediators. Immunoblotting revealed that LMP10 knockdown significantly increased the protein levels of LC3II/I ratio and ATG7 protein levels but reduced the protein levels of IGF1R, gp130, and phosphorylated AKT, mTOR JAK2, STAT3, and ERK1/2 compared with WT controls after Ang II treatment (**Figures 5A,B**). However, there was no significant difference in the protein levels of calcineurin A, MKP-1, and PTEN as well as the mRNA levels of IGF1R and gp130 between both groups after saline treatment (**Figures 5C,D**), suggesting that LMP10 is involved in the degradation of IGF1R and gp130 proteins.

LMP10 Knockdown Activates Autophagy to Increase IGF1R and gp130 Degradation *in vitro*

Increasing evidence suggests a link between the proteasome and autophagy in cancer and other cells (Korolchuk et al., 2010). Therefore, we tested whether LMP10 regulated the activation of autophagy in cardiomyocytes. Immunostaining showed that LMP10 knockdown by siRNA significantly increased the number of LC3-positive autophagosomes (a reliable marker of autophagosomes) in NRCMs after Ang II treatment compared with siRNA-control (**Figure 6A**). Furthermore, immunoblotting indicated that the conversion of LC3 I to LC3 II and protein level of ATG7 (markers for the activation of autophagy) were significantly higher in siRNA-LMP10-transfected NRCMs than in siRNA-control cells (**Figure 6B**).

To further evaluate whether LMP10 is required for the colocalization of IGF1R or gp130 with LC3B in cardiomyocytes, we performed immunofluorescence staining with an anti-IGF1R, anti-gp130, or anti-LC3B antibody. A smaller number of IGF1R- or gp130-positive vesicles colocalized within LC3B-positive autophagosomes in the siRNA-control group, but this colocalization was significantly increased in siRNA-LMP10-transfected NRCMs after Ang II treatment (**Figure 6C**). Electron microscopy further indicated that the number of immunogold-labeled IGF1R- or gp130-positive particles within autophagosomes was higher in

siRNA-LMP10-transfected NRCMs than in siRNA-control cells after Ang II treatment (**Figure 6D**).

LMP10 Knockdown Attenuates Cardiomyocyte Hypertrophy by Increasing IGF1R and gp130 Degradation

To assess whether LMP10 regulates the degradation of IGF1R or gp130 via an autophagy-dependent pathway, NRCMs were transfected with siRNA-control or siRNA-LMP10 in the presence or absence of the autophagy inhibitor chloroquine (CQ). After Ang II treatment, LMP10 knockdown markedly reduced the protein levels of IGF1R, gp130, p-AKT, and p-STAT3 compared with Ang II alone (**Figure 7A**, lane 4 vs 3). This effect was fully reversed by CQ (**Figure 7C**, lane 5 vs lane 4), and by siRNA-LMP10 plus CQ (**Figure 7C**, lane 6 vs lane 5), indicating that that LMP10 regulates IGF1R and gp130 degradation via autophagy. Accordingly, LMP10 knockdown markedly attenuated Ang II-induced cardiomyocyte hypertrophy and ANP expression compared with Ang II stimulation (**Figures 7D,E**, lane 4 vs lane 3), whereas this effect was markedly restored by CQ and the combination of CQ with siRNA-LMP10 (**Figures 7D,E**, lane 5 vs lane 4 and lane 6 vs lane 5, respectively). Overall, these results demonstrate that LMP10 knockdown induces the autophagic degradation of IGF1R and gp130, which in turn inhibits cardiomyocyte hypertrophy.

DISCUSSION

Here, we provided new evidence that LMP10 exerts a prohypertrophic role *in vitro* and *in vivo*. We demonstrated that LMP10 expression was significantly upregulated in Ang II-infused hearts. LMP10 KO inhibited Ang II-induced cardiac hypertrophic remodeling and improved abnormal cardiac function. Mechanistically, the Ang II-induced upregulation of LMP10 inhibited the activation of autophagy, which in turn increased the stability of IGF1R and gp130 and subsequent development of cardiac hypertrophy. Therefore, our results revealed a functional link between LMP10 and autophagy in cardiomyocytes, and thus LMP10 may represent a therapeutic target for treating hypertrophic diseases. These data are summarized in **Figure 8**.

Previous studies have demonstrated that immunoproteasome dysregulation is associated with many human diseases, including cancer and autoimmune, and neurodegenerative diseases (Angeles et al., 2012; Ferrington and Gregerson, 2012). Recently, we reported that the immunoproteasome is involved in the regulation of several cardiovascular diseases. The functional roles of LMP7 in cardiac hypertrophy, atrial fibrillation, abdominal aortic aneurysm, and retinopathy have been investigated extensively (Li F. D. et al., 2019; Li J. et al., 2019; Xie et al., 2019; Wang et al., 2020). Meanwhile, we found that LMP10 (β2i) plays a critical role in DOCA-salt-induced myocardial fibrosis and high-dose Ang II-induced atrial fibrillation and retinopathy (Yan et al., 2017; Li J. et al., 2018; Wang S. et al., 2018). However, the elevation of blood pressure induced by a high dose of Ang II (2,000–3,000 ng/kg/min) in WT mice was not observed in LMP10 KO mice (Li J. et al., 2018; Wang S. et al., 2018). Interestingly, the present study showed that LMP10 KO markedly reduced medium-dose (1,000 ng/kg/min) Ang II-induced hypertension, but suppressed Ang II-induced cardiac hypertrophic remodeling and improved abnormal cardiac function (**Figures 2–4**), suggesting that LMP10 KO exerts a cardioprotective effect, likely through a blood-dependent mechanism. However, the mechanism by which LMP10 affects vascular remodeling and function needs to be determined in the future.

It is well documented that proteasomal inhibition usually increases autophagy, leading to the degradation of receptors in cancer and other cells (Korolchuk et al., 2010; Larrue et al., 2016). Although the exact mechanisms by which the proteasome regulates autophagy remain unknown, several potential mechanisms have been proposed. For example, the unfolded protein response induces ATF4 expression, which upregulates ATG5, ATG7, and LC3 expression or increases IRE1 and JNK1 levels, leading to Bcl-2 phosphorylation and the release of ATG6 (Ding et al., 2007; Milani et al., 2009; Zhu et al., 2010). Recently, we revealed that LMP7 can interact with and promote the degradation of ubiquitinated ATG5, which inhibits autophagy, thereby leading to pressure overload- or Ang II-induced cardiac hypertrophy (Xie et al., 2019). Here, we further showed that LMP10 KO in mice or LMP10 knockdown by siRNA in primary cardiomyocytes significantly increased the LC3II/I ratio, ATG7 protein level, and number of LC3B-positive particles (**Figures 5A**, **6A,B**, respectively), indicating that LMP10 is a negative regulator of autophagy in cardiomyocytes.

Autophagy is a catabolic process essential for maintaining cardiac homeostasis in response to various forms of stresses. Autophagy is initiated by the formation of autophagosomes, which are regulated by ATG7 (E1 enzyme), ATG3 (E2 enzyme), ATG8 (also known as LC3, ubiquitin-like protein), ATG5, and ATG6 (Beclin 1) (Li Z. et al., 2015). Several studies have demonstrated that the dysregulation of autophagy is associated with cardiac hypertrophy (Nakai et al., 2007; Bhuiyan et al., 2013; Eisenberg et al., 2016). Increasing evidence suggests that autophagy exerts a cardioprotective effect through multiple mechanisms, including the degradation and recycling of long-lived proteins, lipid droplets, or damaged organelles, the clearance of reactive oxygen species, and the collaboration between autophagy and the UPS in protein quality control (Li Z. et al., 2015). It is well reported that IGF1R and gp130 mediate three major downstream pathways, JAK/STAT, Ras/MEK/ERK, and PI3K/AKT, which play different roles in myocardial infarction, cardiac hypertrophy, and heart failure (Toyozaki et al., 1993; Hirota et al., 1995; Pan et al., 1998; Hirota et al., 1999; Yasukawa et al., 2001; Matsui et al., 2002, 2003). Previous studies demonstrated that suppressor of cytokine signaling 3 (SOCS3) binds directly to gp130 and inhibits its downstream mediators (Yasukawa et al., 2001). A recent study suggested that

the proteasome inhibitor YSY01A downregulates gp130 and the activation of JAK2 and STAT3 through a lysosome-autophagy pathway in cancer cells (Huang et al., 2017). Moreover, we recently demonstrated that the activation of autophagy by gallic acid induces the degradation of EGFR and gp130, leading to the inhibition of the downstream signaling cascades (Yan et al., 2019). In the present study, we further revealed that LMP10 KO induced autophagy, which promoted the colocalization of IGF1R and gp130 within autophagosomes and their subsequent degradation, leading to the inhibition of downstream mediators (mTOR, AKT STAT3, and ERK1/2) and cardiac hypertrophy (**Figures 6**, **7**), indicating that LMP10 regulates cardiomyocyte hypertrophy via the autophagy-dependent degradation of IGF1R and gp130.

CONCLUSION

Our data revealed a novel non-immune function for LMP10 in cardiac hypertrophy and dysfunction. We identified a regulatory mechanism by which LMP10 inhibited autophagy, leading to a reduction of IGF1R and gp130 degradation in cardiomyocytes. Our findings highlight the functional links between LMP10, autophagy, and receptors in the hypertrophic program of the heart. Further studies are needed to elucidate how LMP10 activates autophagy and how IGF1R and gp130 are degraded by autophagy in cardiomyocytes. Thus, our results suggest that targeting LMP10 may provide an approach for the treatment of hypertrophic diseases.

DATA AVAILABILITY STATEMENT

All datasets generated for this study are included in the article/supplementary material.

ETHICS STATEMENT

All investigations were approved by and performed in accordance with the Animal Care and Use Committee of Capital Medical University, and conformed to the Guide for the Care and Use of Laboratory Animals published by the U.S. NIH.

AUTHOR CONTRIBUTIONS

WY, Z-CD, J-JW, Y-LZ, and H-XW conceived of the experiments, the acquisition of the data and analysis, and interpreted the data. WY and Z-CD participated in the statistical analysis of the primary data. H-HL and BZ drafted the manuscript and provided funding to support the study. H-HL supervised the study. All authors approved the final version of the manuscript.

FUNDING

This study was supported by grants from State Key Program of National Natural Science Foundation of China (81630009 and 81330003 to H-HL).

REFERENCES

Angeles, A., Fung, G., and Luo, H. (2012). Immune and non-immune functions of the immunoproteasome. *Front. Biosci.* 17, 1904–1916. doi: 10.2741/4027

Bhuiyan, M. S., Pattison, J. S., Osinska, H., James, J., Gulick, J., McLendon, P. M., et al. (2013). Enhanced autophagy ameliorates cardiac proteinopathy. *J. Clin. Invest.* 123, 5284–5297. doi: 10.1172/JCI70877

Chen, C., Zou, L. X., Lin, Q. Y., Yan, X., Bi, H. L., Xie, X., et al. (2019). Resveratrol as a new inhibitor of immunoproteasome prevents PTEN degradation and attenuates cardiac hypertrophy after pressure overload. *Redox Biol.* 20, 390–401. doi: 10.1016/j.redox.2018.10.021

Ding, W. X., Ni, H. M., Gao, W., Yoshimori, T., Stolz, D. B., Ron, D., et al. (2007). Linking of autophagy to ubiquitin-proteasome system is important for the regulation of endoplasmic reticulum stress and cell viability. *Am. J. Pathol.* 171, 513–524. doi: 10.2353/ajpath.2007.070188

Eisenberg, T., Abdellatif, M., Schroeder, S., Primessnig, U., Stekovic, S., Pendl, T., et al. (2016). Cardioprotection and lifespan extension by the natural polyamine spermidine. *Nat. Med.* 22, 1428–1438. doi: 10.1038/nm.4222

Ferrington, D. A., and Gregerson, D. S. (2012). Immunoproteasomes: structure, function, and antigen presentation. *Prog. Mol. Biol. Transl. Sci.* 109, 75–112. doi: 10.1016/B978-0-12-397863-9.00003-1

Frey, N., and Olson, E. N. (2003). Cardiac hypertrophy: the good, the bad, and the ugly. *Annu. Rev. Physiol.* 65, 45–79. doi: 10.1146/annurev.physiol.65.092101.142243

Hirota, H., Chen, J., Betz, U. A., Rajewsky, K., Gu, Y., Ross, J., et al. (1999). Loss of a gp130 cardiac muscle cell survival pathway is a critical event in the onset of heart failure during biomechanical stress. *Cell* 97, 189–198. doi: 10.1016/s0092-8674(00)80729-1

Hirota, H., Yoshida, K., Kishimoto, T., and Taga, T. (1995). Continuous activation of gp130, a signal-transducing receptor component for interleukin 6-related cytokines, causes myocardial hypertrophy in mice. *Proc. Natl. Acad. Sci. U.S.A.* 92, 4862–4866. doi: 10.1073/pnas.92.11.4862

Huang, W., Yuan, X., Sun, T., Fan, S., Wang, J., Zhou, Q., et al. (2017). Proteasome inhibitor YSY01A abrogates constitutive STAT3 signaling via down-regulation of Gp130 and JAK2 in human A549 lung cancer cells. *Front. Pharmacol.* 8:476. doi: 10.3389/fphar.2017.00476

Korolchuk, V. I., Menzies, F. M., and Rubinsztein, D. C. (2010). Mechanisms of cross-talk between the ubiquitin-proteasome and autophagy-lysosome systems. *FEBS Lett.* 584, 1393–1398. doi: 10.1016/j.febslet.2009.12.047

Larrue, C., Saland, E., Boutzen, H., Vergez, F., David, M., Joffre, C., et al. (2016). Proteasome inhibitors induce FLT3-ITD degradation through autophagy in AML cells. *Blood* 127, 882–892. doi: 10.1182/blood-2015-05-646497

Li, F. D., Nie, H., Tian, C., Wang, H. X., Sun, B. H., Ren, H. L., et al. (2019). Ablation and inhibition of the immunoproteasome catalytic subunit LMP7 attenuate experimental abdominal aortic aneurysm formation in mice. *J. Immunol.* 202, 1176–1185. doi: 10.4049/jimmunol.1800197

Li, H. H., Kedar, V., Zhang, C., McDonough, H., Arya, R., Wang, D. Z., et al. (2004). Atrogin-1/muscle atrophy F-box inhibits calcineurin-dependent cardiac hypertrophy by participating in an SCF ubiquitin ligase complex. *J. Clin. Invest.* 114, 1058–1071. doi: 10.1172/JCI22220

Li, J., Wang, S., Bai, J., Yang, X. L., Zhang, Y. L., Che, Y. L., et al. (2018). Novel role for the immunoproteasome subunit PSMB10 in angiotensin II-induced atrial fibrillation in mice. *Hypertension* 71, 866–876. doi: 10.1161/HYPERTENSIONAHA.117.10390

Li, J., Wang, S., Zhang, Y. L., Bai, J., Lin, Q. Y., Liu, R. S., et al. (2019). Immunoproteasome subunit beta5i promotes Ang II (Angiotensin II)-induced atrial fibrillation by targeting ATRAP (Ang II type I receptor-associated protein) degradation in mice. *Hypertension* 73, 92–101. doi: 10.1161/HYPERTENSIONAHA.118.11813

Li, N., Wang, H. X., Han, Q. Y., Li, W. J., Zhang, Y. L., Du, J., et al. (2015). Activation of the cardiac proteasome promotes angiotension II-induced hypertrophy by down-regulation of ATRAP. *J. Mol. Cell Cardiol.* 79, 303–314. doi: 10.1016/j.yjmcc.2014.12.007

Li, Z., Wang, J., and Yang, X. (2015). Functions of autophagy in pathological cardiac hypertrophy. *Int. J. Biol. Sci.* 11, 672–678. doi: 10.7150/ijbs.11883

Matsui, T., Li, L., Wu, J. C., Cook, S. A., Nagoshi, T., Picard, M. H., et al. (2002). Phenotypic spectrum caused by transgenic overexpression of activated Akt in the heart. *J. Biol. Chem.* 277, 22896–22901. doi: 10.1074/jbc.M200347200

Matsui, T., Nagoshi, T., and Rosenzweig, A. (2003). Akt and PI 3-kinase signaling in cardiomyocyte hypertrophy and survival. *Cell Cycle* 2, 220–223.

Milani, M., Rzymski, T., Mellor, H. R., Pike, L., Bottini, A., Generali, D., et al. (2009). The role of ATF4 stabilization and autophagy in resistance of breast cancer cells treated with Bortezomib. *Cancer Res.* 69, 4415–4423. doi: 10.1158/0008-5472.CAN-08-2839

Nakai, A., Yamaguchi, O., Takeda, T., Higuchi, Y., Hikoso, S., Taniike, M., et al. (2007). The role of autophagy in cardiomyocytes in the basal state and in response to hemodynamic stress. *Nat. Med.* 13, 619–624. doi: 10.1038/nm1574

Pan, J., Fukuda, K., Kodama, H., Sano, M., Takahashi, T., Makino, S., et al. (1998). Involvement of gp130-mediated signaling in pressure overload-induced activation of the JAK/STAT pathway in rodent heart. *Heart Vessels* 13, 199–208. doi: 10.1007/bf01745045

Powell, S. R., and Divald, A. (2010). The ubiquitin-proteasome system in myocardial ischaemia and preconditioning. *Cardiovasc. Res.* 85, 303–311. doi: 10.1093/cvr/cvp321

Swanlund, J. M., Kregel, K. C., and Oberley, T. D. (2010). Investigating autophagy: quantitative morphometric analysis using electron microscopy. *Autophagy* 6, 270–277. doi: 10.4161/auto.6.2.10439

Toyozaki, T., Hiroe, M., Hasumi, M., Horie, T., Hosoda, S., Tsushima, T., et al. (1993). Insulin-like growth factor I receptors in human cardiac myocytes and their relation to myocardial hypertrophy. *Jpn. Circ. J.* 57, 1120–1127. doi: 10.1253/jcj.57.1120

Wang, L., Zhang, Y. L., Lin, Q. Y., Liu, Y., Guan, X. M., Ma, X. L., et al. (2018). CXCL1-CXCR2 axis mediates angiotensin II-induced cardiac hypertrophy and remodelling through regulation of monocyte infiltration. *Eur. Heart J.* 39, 1818–1831. doi: 10.1093/eurheartj/ehy085

Wang, L., Zhao, X. C., Cui, W., Ma, Y. Q., Ren, H. L., Zhou, X., et al. (2016). Genetic and pharmacologic inhibition of the chemokine receptor CXCR2 prevents experimental hypertension and vascular dysfunction. *Circulation* 134, 1353–1368. doi: 10.1161/CIRCULATIONAHA.115.020754

Wang, S., Li, J., Bai, J., Li, J. M., Che, Y. L., Lin, Q. Y., et al. (2018). The immunoproteasome subunit LMP10 mediates angiotensin II-induced retinopathy in mice. *Redox Biol.* 16, 129–138. doi: 10.1016/j.redox.2018.02.022

Wang, S., Li, J., Wang, T., Bai, J., Zhang, Y. L., Lin, Q. Y., et al. (2020). Ablation of immunoproteasome beta5i subunit suppresses hypertensive retinopathy by blocking ATRAP degradation in mice. *Mol. Ther.* 28, 279–292. doi: 10.1016/j.ymthe.2019.09.025

Xie, X., Bi, H. L., Lai, S., Zhang, Y. L., Li, N., Cao, H. J., et al. (2019). The immunoproteasome catalytic beta5i subunit regulates cardiac hypertrophy by targeting the autophagy protein ATG5 for degradation. *Sci. Adv.* 5:eaau0495. doi: 10.1126/sciadv.aau0495

Xie, Y. (2010). Feedback regulation of proteasome gene expression and its implications in cancer therapy. *Cancer Metastasis Rev.* 29, 687–693. doi: 10.1007/s10555-010-9255-y

Yan, W., Bi, H. L., Liu, L. X., Li, N. N., Liu, Y., Du, J., et al. (2017). Knockout of immunoproteasome subunit beta2i ameliorates cardiac fibrosis and inflammation in DOCA/Salt hypertensive mice. *Biochem. Biophys. Res. Commun.* 490, 84–90. doi: 10.1016/j.bbrc.2017.05.011

Yan, X., Zhang, Y. L., Zhang, L., Zou, L. X., Chen, C., Liu, Y., et al. (2019). Gallic acid suppresses cardiac hypertrophic remodeling and heart failure. *Mol. Nutr. Food Res.* 63:e1800807. doi: 10.1002/mnfr.201800807

Yasukawa, H., Hoshijima, M., Gu, Y., Nakamura, T., Pradervand, S., Hanada, T., et al. (2001). Suppressor of cytokine signaling-3 is a biomechanical stress-inducible gene that suppresses gp130-mediated cardiac myocyte hypertrophy and survival pathways. *J. Clin. Invest.* 108, 1459–1467. doi: 10.1172/JCI13939

Zhang, Y. L., Geng, C., Yang, J., Fang, J., Yan, X., Li, P. B., et al. (2019). Chronic inhibition of chemokine receptor CXCR2 attenuates cardiac remodeling and dysfunction in spontaneously hypertensive rats. *Biochim. Biophys. Acta Mol. Basis Dis.* 1865:165551. doi: 10.1016/j.bbadis.2019.165551

Zhu, K., Dunner, K. Jr., and McConkey, D. J. (2010). Proteasome inhibitors activate autophagy as a cytoprotective response in human prostate cancer cells. *Oncogene* 29, 451–462. doi: 10.1038/onc.2009.343

Conflict of Interest: The authors declare that the research was conducted in the absence of any commercial or financial relationships that could be construed as a potential conflict of interest.

frontiers in Physiology

REVIEW
published: 25 June 2020
doi: 10.3389/fphys.2020.00689

Distal Arthrogryposis and Lethal Congenital Contracture Syndrome – An Overview

*Darshini Desai, Danielle Stiene, Taejeong Song and Sakthivel Sadayappan**

Division of Cardiovascular Health and Disease, Department of Internal Medicine, Heart, Lung and Vascular Institute, College of Medicine, University of Cincinnati, Cincinnati, OH, United States

Distal arthrogryposis (DA) is a skeletal muscle disorder which can be classified under a broader term as Arthrogryposis multiplex contractures. DA is characterized by the presence of joint contractures at various parts of the body, particularly in distal extremities. It is identified as an autosomal dominant and a rare X-linked recessive disorder associated with increased connective tissue formation around joints in such way that immobilizes muscle movement causing deformities. DA is again classified into various types since it manifests as a range of conditions representing different etiologies. Myopathy is one of the most commonly listed etiologies of DA. The mutations in sarcomeric protein-encoding genes lead to decreased sarcomere integrity, which is often associated with this disorder. Also, skeletal disorders are often associated with cardiac disorders. Some studies mention the presence of cardiomyopathy in patients with skeletal dysfunction. Therefore, it is hypothesized that the congenitally mutated protein that causes DA can also lead to cardiomyopathy. In this review, we will summarize the different forms of DA and their clinical features, along with gene mutations responsible for causing DA in its different forms. We will also examine reports that list mutations also known to cause heart disorders in the presence of DA.

Keywords: distal arthrogryposis, LCCS4, striated muscle, *MYBPC1*, *MYBPC2*, titin

OPEN ACCESS

Edited by:
Xuejun Wang,
University of South Dakota,
United States

Reviewed by:
Charles K. Thodeti,
Northeast Ohio Medical University,
United States
Lina Shehadeh,
University of Miami, United States

****Correspondence:***
Sakthivel Sadayappan
sadayasl@ucmail.uc.edu

Specialty section:
This article was submitted to Striated Muscle Physiology, a section of the journal Frontiers in Physiology

Received: *29 April 2020*
Accepted: *27 May 2020*
Published: *25 June 2020*

Citation:
Desai D, Stiene D, Song T and Sadayappan S (2020) Distal Arthrogryposis and Lethal Congenital Contracture Syndrome – An Overview. Front. Physiol. 11:689. doi: 10.3389/fphys.2020.00689

INTRODUCTION

Arthrogryposis is a common disorder characterized by the development of non-progressive contractures affecting the muscles congenitally. It is coined as arthrogryposis multiplex contractures – multiplex because it affects multiple parts of the body (Sucuoglu et al., 2015). Multiple congenital joint contractures are classified into amyoplasia, distal arthrogryposis (DA), and syndromic. Distal Arthrogryposis, as the name suggests, affects the distal parts of the limbs, and it can occur in the absence of any primary neurological disorder, or, indeed, any type of muscular disorder (Bamshad et al., 2009). Most symptoms involve contractures affecting two or more areas of the body with least involvement of the proximal joints. It is highly lucid, meaning that symptoms often vary among individuals of the same family presenting with the same disorder. DA is associated with syndromes like Freeman-Sheldon syndrome (FSS), Gordon

Abbreviations: DA, distal arthrogryposis; FSS, Freeman Sheldon syndrome; *LCCS*, lethal congenital contracture syndrome; *MYBPC1*, slow skeletal myosin binding protein-C gene; *MYBPC2*, fast skeletal myosin binding protein-C gene; *PIEZO2*, piezo-type mechanosensitive ion channel component 2 gene; *TPM2*, β-tropomyosin gene; *TTN*, titin gene.

syndrome, Sheldon-Hall syndrome, multiple pterygium syndrome and trismus-pseudocamptodactyly syndrome. As the syndrome is associated with a multiplicity of other conditions, causation varies from type to type. However, the most common etiology is reduced fetal movement which leads to the formation of congenital contractures. These are very severe since decreased fetal movement causes extra connective tissue formation around joints (Gordon, 1998). Previous reports suggest that fetus movement is compromised by the lack of space in the uterus, which then causes impaired vascular supply to the fetus. Other major etiologies associated with DA include neurological abnormalities, muscle abnormalities, and abnormalities in the formation of connective tissues. Sometimes maternal diseases can also contribute to the development of this syndrome (Hall, 1997). The overall objectives of this review article are to provide an extensive overview of DA and its clinical, genetic and molecular aspects, and determine opportunities to expand research studies to cure DAs.

CLINICAL FEATURES OF DISTAL ARTHROGRYPOSIS

To date, more than ten different types of Distal Arthrogryposis have been identified. They are classified as Distal Arthrogryposis Type 1 (DA1), Distal Arthrogryposis Type 2A (DA2A) and 2B (DA2B), and Distal Arthrogryposis Types 3–10 (DA3–10) (Bamshad et al., 2009). Each type is further classified according to its clinical features and pathology.

Distal Arthrogryposis Type 1 sometimes overlaps with a disorder called FSS owing to the similarity of respective clinical features (Gurnett et al., 2010; Alvarado et al., 2011; Beck et al., 2013; Wang et al., 2016; Jin et al., 2017; Poling et al., 2017). The prevalence of DA is estimated to be ∼1 in every 3,000 people worldwide (Hall et al., 1982; Bamshad et al., 1996; Beals, 2005), and it is more common than other types. It is characterized by the presence of camptodactyly, meaning that patients have bent fingers and toes (**Figure 1**). Patients also suffer from a type of hand deformity such that all fingers are angled outward toward the fifth finger, termed as ulnar deviation, and they have fingers that overlap. Intelligence is not said to be compromised in patients with this syndrome, nor do neurological reports show any abnormalities (Bamshad et al., 1996). Other clinical features include the presence of clubfoot, which is an inward- and downward-turning foot (**Figure 1**). These patients have a triangular face with prominent nasolabial folds, downward-slanting palpebral fissures, and other calcaneovalgus deformities (Krakowiak et al., 1997).

Distal Arthrogryposis Type 2 is further classified into two groups termed as DA2A (FSS) and DA2B (Sheldon-Hall syndrome). DA2B is an intermediary phenotype between DA1 and FSS. DA2B is also referred to as a variant of FSS (Krakowiak et al., 1998). Clinical features are likely similar to those of DA1, including ulnar deviation, overriding fingers at birth and camptodactyly. Major clinical features for this type are related to lower limbs and consist of talipes equinovarus (clubfoot), calcaneovalgus deformities, vertical talus (flatfoot), and metatarsus varus (Guell et al., 2015; Li et al., 2015; Staff, 2015). Minor features include triangular face, descending-slanting palpebral fissures, joined ear lobules, small mouth, small mandible, arched palate, webbed neck, and shorten height (Krakowiak et al., 1997).

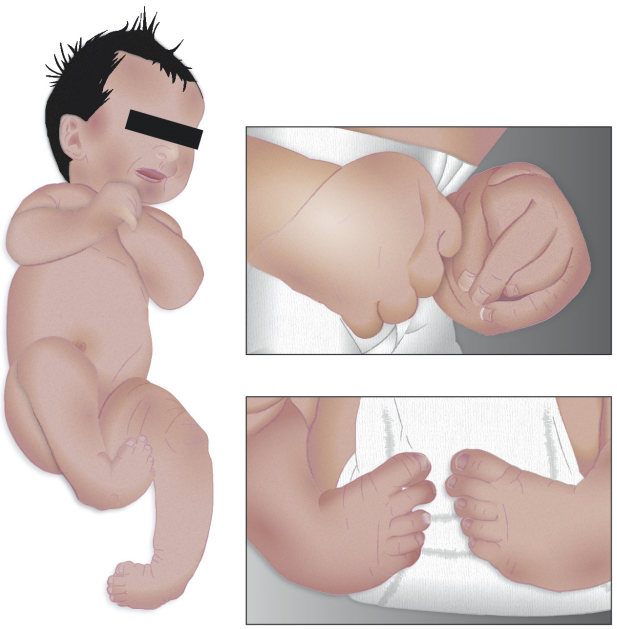

FIGURE 1 | Morphological features of distal arthrogryposis. A child born with distal arthrogryposis, showing characteristic camptodactyly, such as one or more fingers permanently bent. The characteristic clubfoot is also seen, as well as the abnormal finger positions of the hand (Modified from Chen, 2015).

Distal arthrogryposis type 3 (Gordon syndrome) is a rare and inherited disorder that affects movement in the joints of the upper and lower limbs (Hall et al., 1982). Patients are born with stiff joints that function improperly and are difficult to move. They also suffer from camptodactyly and clubfoot. However, this type of DA is distinct from others by the presence of shorten height and cleft palate (Bamshad et al., 2009). The range and severity of these features can vary from patient to patient. Usually, the patient's intelligence is unaffected and mostly normal (Poling et al., 2017). Other clinical features include rigid fingers, bilateral congenital clubfoot, constrained horizontal and vertical eye movements, inflexible back, stiff walk, anteverted slouched shoulders, and pectus excavatum (Schrander-Stumpel et al., 1993).

Distal arthrogryposis 4 (scoliosis) **and 6** (sensorineural hearing loss) are newer and rarer types. They are scarcely studied; therefore, only a very few reports are available. However, they do have unique clinical features, making them distinct from other types of DA. Specifically, DA4 is characterized by the presence of curvature of the spine, which is a critical feature (Bamshad et al., 2009). Scoliosis is often described as a sideway curvature of the spine, which is inherited in an autosomal dominant manner. Other clinical features include camptodactyly and torticollis, i.e., twisted neck, where patients have their neck

tilted to one side (Baraitser, 1982). DA6 is distinguished by the presence of hand anomaly and sensorineural deafness. These clinical features range from moderate to severe, and the disorder is often inherited from males.

Distal arthrogryposis type 5 (ophthalmoplegia) is another type of DA characterized by the presence of ptosis/oculomotor dysfunction. This is not always true as affected individuals have also been known to show some non-ocular features. They also show contractures of the distal joints, limited ocular movements, peculiar facial highlights with deep−set eyes, and shortening of the first and fifth toes. Sometimes patients also have restrictive lung failure which is recognized as a syndromic component of DA5 in adults (Okubo et al., 2015).

Distal arthrogryposis type 7 (trismus-pseudocamptodactyly) involves in failure to open the mouth fully (trismus) which complicates dental alignment and care, feeding at post-natal stage, and intubation for anesthesia. It also shows the presence of pseudocamptodactyly in which the wrist causes flexion contracture of distal and proximal interphalangeal joints causing occupational and social disability (Veugelers et al., 2004; Minzer-Conzetti et al., 2008).

Distal arthrogryposis type 8 (autosomal dominant multiple pterygium syndrome, DA8) clinical features include contractures of proximal and distal joints, pterygia involving the neck, axillae, elbows, and knees. Researchers performed exome sequencing in three families with similar clinical features like DA8 and identified a heterozygous mutation in the *MYH3* gene (Chong et al., 2015). Mutations in these families were highly conserved residues and hence predicted to play a major role in developing the DA8-like phenotype. Many other studies also confirmed that mutations in the *MYH3* contribute to the development of DA8. Altogether, DA8 is termed as an autosomal dominant type of DA attributed to mutation in the *MYH3* gene (Zieba et al., 2017; Cameron-Christie et al., 2018; Scala et al., 2018).

Distal arthrogryposis type 9 (congenital contractural arachnodactyly, DA9) is also called congenital contractural arachnodactyly (CCA) and Beals syndrome named after the researcher who first studied it (Beals and Hecht, 1971). It is noted by several researchers that CCA is caused by heterozygous mutation in the fibrillin-2 gene (FBN2) (Wang et al., 1996; Park et al., 1998). CCA is an uncommon autosomal dominant disorder described by contractures, abnormally long fingers, scoliosis, and scrunched ears (Hecht and Beals, 1972). The clinical features of DA9 overlap with Marfan syndrome which is attributed to mutations in fibrillin-1, *FBN1*. In a comparison between Marfan syndrome and DA9, one researcher reported that the abnormally shaped auricular helices were the trademark of CCA and, hence, absent in individuals with Marfan syndrome (Godfrey et al., 1995). Both syndromes are said to have clinically different structural and functional characteristics. For instance, one study suggests that structural defects, such as complete closure of the lumen of the duodenum, esophageal atresia, and intestinal malrotation, are evidently seen in CCA. In contrast, Marfan syndrome has more functional defects like valvular insufficiency and aortic root dilatation (Wang et al., 1996). This is mainly attributed to mutations in the proteins found in these syndromes. For example, Fibrillin-2 mediates the assembly of elastic fibers at prenatal stages, whereas fibrillin-1 provides the stiffness to the microfibrils (Zhang et al., 1994, 1995).

Distal arthrogryposis type 10 (congenital plantar syndrome, DA10) is a rare genetic disease characterized by plantar flexion contractures, presenting with toe-walking in infancy and variably associated with milder contractures of the hip, elbow, wrist, and finger joints (Levine, 1973). No ocular or neurological abnormalities are associated with DA10 (Hall et al., 1967), similar to other DAs, but this type is still poorly studied. However, in a study conducted on a Utah family of five generations, multiple individuals showed plantar flexion contractures in an autosomal dominant, and the author termed it as DA10. Onset was typically in early childhood and manifested as toe walking. Contractures of joints often involved the elbows, but nerve and bone morphology appeared to be normal. However, family members with wrist contractures could still function normally (Stevenson et al., 2006).

CURRENT TREATMENTS FOR DISTAL ARTHROGRYPOSIS

The primary goal for the treatment of the patients with DA is to improve their quality and quantity of life toward independent living. This requires help in improving the motor function of any affected joints, strengthening any functional muscles, and correcting any fixed deformities that affect daily activities (Kowalczyk and Felus, 2016). A variety of treatment tools are used, the first being rehabilitation, which includes physiotherapy, manipulation of contractures, and occupational therapy. More targeted and individually designed treatments like orchestrated orthotic management is done to prevent any repeated deformities. However, the most preferred option for treatment is surgical correction of musculoskeletal deformities. For upper limbs like the shoulder joint, a subcapital derotation osteotomy of the humerus is performed, usually in severe internal rotation contractures (Zlotolow and Kozin, 2012). The presence of extended contracture of the elbow joint makes routine activities very difficult. The treatment for such patients includes capsulotomy which helps improve passive elbow flexion, active flexion by triceps, or both (Axt et al., 1997). Patients with contractures related to knee joints are very common and those with severe knee dislocations usually require surgical treatment that has to be done in the early stages. Surgical procedures to correct such deformities vary, depending on the severity of the contractures and age of the patients. A few examples are as follows: soft-tissue release, femoral shortening-extension surgery, correction with Ilizarov, which is an external fixation to lengthen or reshape limb bones, and femoral anterior epiphysiodesis, which involves surgical intervention to stop bone growth around the knee. Many clinicians prefer surgical options like percutaneous quadriceps tenotomy, in which the tendon is cut to correct the deformity, open quadricepsplasty to improve knee flexion, and femoral shortening osteotomy (Lampasi et al., 2012). The Ponseti method of manipulation has been successfully performed on pediatric patients to correct clubfoot, and this procedure is followed by Achilles tenotomy.

More major surgeries can then be avoided in these patients, and the above method has also proven to be a good initial treatment in children with DA (Kowalczyk and Felus, 2016).

GENE MUTATIONS LINKED TO DISTAL ARTHROGRYPOSIS

Distal arthrogryposis type 1 is said to involve at least two genes, namely *TPM2 (β-tropomyosin)* and *MYBPC1 (Slow skeletal myosin binding protein-C)*. These genes are expressed in muscle cells, and their interaction with sarcomeric proteins helps in regulating muscle contraction (**Figure 2**). We still do not know how these two gene mutations can lead to the formation of joint contractures characteristic of DA type 1. However, some researchers suggest that the contractures result from a lack of movement in the fetus which, in turn, leads to improper muscle tissue formation. Nevertheless, researchers are still searching for genetic changes that can cause this condition (Sung et al., 2003). Another mutation linked to DA2B involves the *TNNI2* gene which plays a role in affecting the C'-terminal domain of troponin I (TnI) and alters troponin-tropomyosin (Tc-Tm) complex (Sung et al., 2003). To assess the effects of human DA mutations, *MYBPC1* mRNAs, resembling W236R and Y856H mutations, were administrated into zebrafish embryos, after which mild bent body curvatures and decreased motor activity were observed. Another skeletal myosin binding protein-C paralog, *MYBPC2* (fast skeletal myosin binding protein-C), is also involved in developing a severe form of DA (Bayram et al., 2016). Gene set enrichment analysis (GSEA) in over 400 different DA cases showed the association of *MYBPC2* mutation with DA (Hall and Kiefer, 2016). In a patient with unclassified DA, compound heterozygous mutations of *MYBPC2* were found with homozygous GPR126 mutation (19C > T, Arg7X) known to cause postnatal death (Langenhan et al., 2013). *MYBPC2* mutations (T236I and S255T) in patients are highly conserved in vertebrates and localized in the protein's N-terminal region, the binding site of myosin S2 which is crucial for the regulation of thick and thin filaments (Bayram et al., 2016). Recently, two new heterozygous *MYBPC2* variants (V307A and A1065V) were also reported in a patient with DA (Pehlivan et al., 2019). In the zebrafish model, *MYBPC2* protein knockdown by morpholino

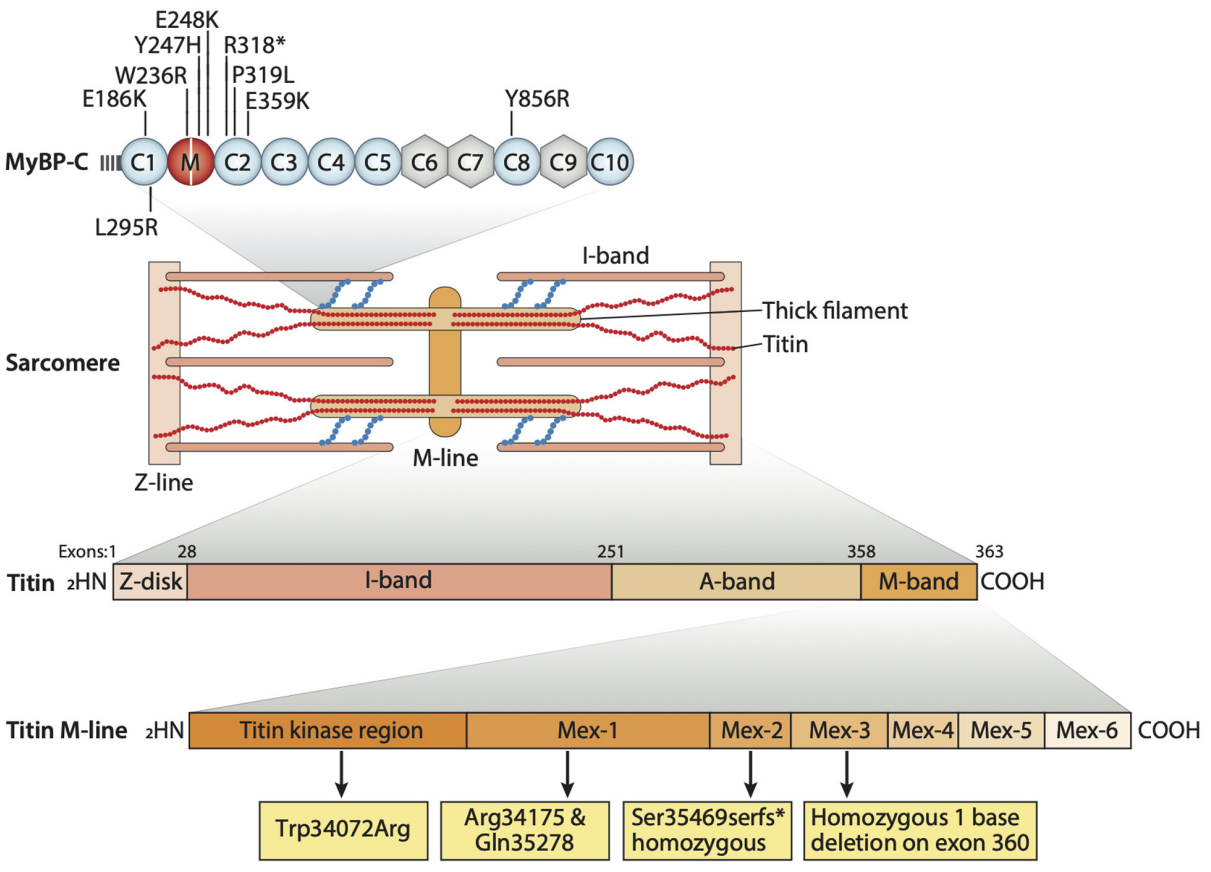

FIGURE 2 | Sarcomere structure containing sarcomeric proteins responsible for proper function. Various regions of titin consisting of Z-disk, I-band, A-band, and M-band. M-line region of titin consists of the titin kinase region (Tk region). In the top panel, known mutations in *MYBPC1* gene are listed. Patients with TK mutation (Trp34072Arg) presented dilated cardiomyopathy and DA phenotype. Mutations in Mex-1 Arg34175 and Gln35278* show DCM and joint contractures. Mutations in Mex-2 Ser35469serfs* show DCM and moderate to severe joint contractures. Homozygous 1 base deletion on exon 360 also presents with skeletal muscle disorder and fetal cardiomyopathy.

antisense nucleotides (>50%) reduced sarcomere length and muscle strength with significantly increasing expressions of atrophic gene (Li et al., 2016). According to the studies, these sarcomeric gene mutations might be causing or exacerbating DA by either altering sarcomere integrity or by changing the muscle contractility through their interaction with other sarcomeric proteins (Ha et al., 2013). DA3 is reported to be caused by mutations in the piezo-type mechanosensitive ion channel component 2 (*PIEZO2)* gene, which are also likely to be involved in causing DA type 5 and Marden-Walker syndrome. This gene is known to encode a mechanosensitive ion channel, negatively affecting joints, ocular muscles, lung function, and bone development (McMillin et al., 2014). Titin is another sarcomeric protein and one considered to be the largest protein known in the body (**Figure 2**). It plays an integral role in changing the integrity of sarcomeric structure and its stability. It spans the half-sarcomere from Z-disk to M-band. It is also known to take part in the development of cardiac and skeletal muscle, and it is encoded by the 363-exon titin gene called *TTN*. Many studies have reported on the mutations in titin found in patients with skeletal disorders. Various mutations in the M line region of *TTN* can be linked to congenital myopathy and cardiac disorders (**Figure 2**). Also, mutations affecting the serine/threonine kinase region of titin, a very conserved and important region for gene expression and cell signaling in heart development, have been reported in patients suffering from DA and cardiac hypertrophy (Carmignac et al., 2007; Chauveau et al., 2014). Overall, the genetic and molecular aspects of DA remain to be studied systematically.

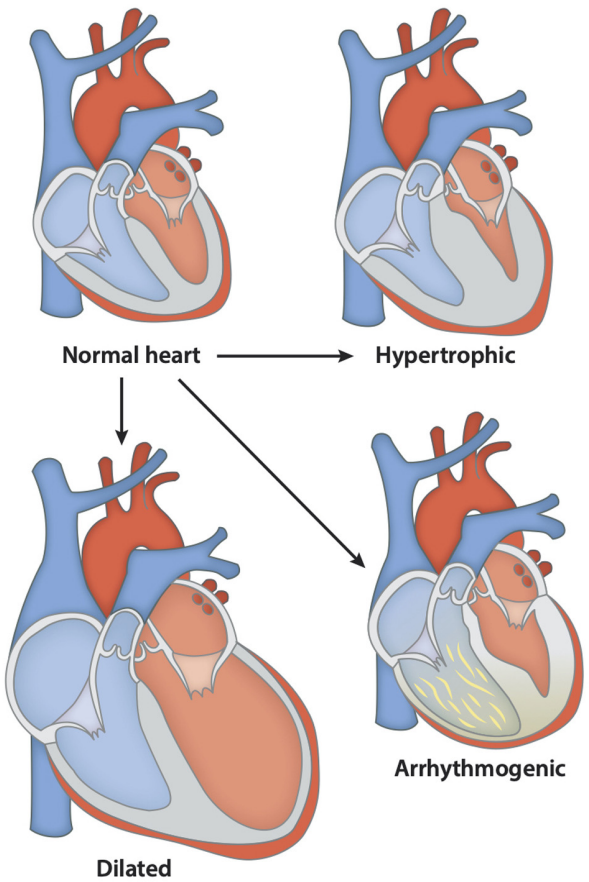

FIGURE 3 | Various forms of cardiomyopathies associated with the development of DAs. The different forms of cardiomyopathy caused by different mutations shown in **Table 1**. These lead to morphological changes in the heart and dysfunction. In the above figure, mutations can lead to hypertrophic heart where the ventricular wall thickens, and the ventricular chamber gets smaller, leading to cardiac dysfunction. In contrast, the dilated heart shows thinner ventricular walls and bigger ventricular chamber, leading to reduced cardiac function. Arrhythmogenic heart is characterized by the presence of fat or fibrous tissue causing abnormal heart rhythms and, in severe cases, sudden cardiac arrest.

DA AND HEART DISEASE

As mentioned above, the mutations in titin are reported to play a role in causing skeletal and cardiac disorders. A study performed in 2007 discovered two homozygous deletions in M-line *TTN* gene (Mex1 and Mex3 exons) resulting in truncation of the protein's C-terminal. The pathophysiological effects of these mutations helped gain insight into the role and importance of M line stability in titin. Titin is known to take part in organizing the sarcomeric proteins during myofibrillogenesis. The resultant truncated form of titin, owing to mutations, gets incorporated into the sarcomere and can cause disease. This clue led the authors to speculate that any critical disruptions in the C-terminal of titin could, theoretically, lead to decreased M line stability and sarcomere disarrangements, thus increasing the mechanical load on heart muscles. Such constant mechanical stress on heart muscle could then be considered as a probable mechanism contributing to the phenotype related to myopathy and heart disease (Carmignac et al., 2007).

Another study done in 2014 further explored these *TTN* mutations believed to play a role in the etiology of skeletal disorders and cardiomyopathies (**Figure 3**). The study consisted of 31 patients who showed the presence of congenital core myopathy and primary heart disease. Subjects with genes typically related to myopathy and cardiac disease, such as *FHL1, LMNA, LAMP2, MYBPC3, ACTA1, MYL2, MYL3, PRKAG2, MYH7, TNNT2, TPM1, DES*, and *RYR1*, were excluded from the study. Sanger sequencing of the *TTN* M-line-encoding exons from Mex1 to Mex6 was performed (**Figure 2**). Results showed two patients homozygous for a two base-pair deletion in Mex2 (pSer35469Serfs*11) presumed to produce a truncated titin protein at its C-terminal. Another patient also showed two heterozygous nonsense mutations in Mex1, p.Arg34175* and p.Gln35278. Using immunohistochemistry, a truncated titin was shown to be incorporated in a normal-looking sarcomere. Interestingly, two other patients were found to have mutations in Mex1, p.Asn34020Thrfs*9 and p.Trp34072Arg, constituting a paternally inherited mutation critically affecting titin's TK domain by causing deletions of its many C-terminal amino acids (**Figure 2**). The presence of a paternal mutation was suspected to be a recessive inheritance, causing a second mutation in these patients, and the authors concluded that this

TABLE 1 | Genes and mutations associated with both skeletal and cardiac disorders.

Gene	Mutations	Cardiac disorder	Skeletal muscle disorder	References	Organism
Mybpc1	Humanized W236R and Y856H	Cardiac enlargement, low heart rate	Mild bent body curvatures and decreased motor activity	Ha et al., 2013	Zebrafish
TTN	pSer35469Serfs*11 homozygous	Dilated cardiomyopathy	Elbow and ankle joint contractures	Chauveau et al., 2014	Human
TTN	p.Arg34175* p.Gln35278	Dilated cardiomyopathy	Severe elbow and ankle joint contractures, scoliosis, neonatal hypotonia	Chauveau et al., 2014	Human
TTN	p.Asn34020Thrfs*9	Arrhythmia and dilated cardiomyopathy	Ankle joint contractures, scoliosis	Chauveau et al., 2014	Human
TTN	p.Trp34072Arg	Terminal heart failure and dilated cardiomyopathy	Distal arthrogryposis with knee, hip, digit and elbow contractures, neonatal hypotonia, dislocated hips	Chauveau et al., 2014	Human

This table summarizes the different specific gene mutations and their cardiac disorder phenotypes. These mutations are also linked to skeletal muscle disorders, as these proteins are found in different muscle types throughout the body.

was responsible for the disease phenotype. As reproduced in **Table 1**, we can see how the authors link these mutations to different pathophysiologies seen in these patients. They also proposed a diagnostic screen to look for any mutations in six M-line-encoding *TTN* exons in patients who showed early-onset myopathies and cardiomyopathy (Chauveau et al., 2014).

Studies have suggested the involvement of *MYBPC1* in causing DA type1 and 2 (Li et al., 2015). *MYBPC1*, which is primarily found in slow-twitch skeletal muscles in humans, was also found to be present in zebrafish heart. This study on a zebrafish model of DA with human W236R and Y856H *MYBPC1* mutation showed cardiac edema, low pulse and cardiac hypertrophy (Ha et al., 2013). This study indicates the possible role of *MYBPC1* mutation in causing cardiac disorder, along with skeletal disorder.

LETHAL CONGENITAL CONTRACTURE SYNDROME AND ITS FEATURES

Lethal congenital contracture syndrome (LCCS) is a rare severe and lethal class of arthrogryposis multiplex contracture syndrome. LCCS is an autosomal recessive syndrome, in comparison to Distal Arthrogryposis, which is autosomal dominant. Akinesia of the limbs and degeneration of motoneurons are main characteristics of LCCS. These clinical manifestations are accompanied by malformed joints and limbs. Eleven subtypes of LCCS have been known and described. LCCS1 is, as mentioned before, an autosomal recessive and neonatally lethal form of LCCS. It is characterized by the presence of congenital non-progressive joint contractures involving the upper and lower limbs and, sometimes, vertebral column. This leads to flexion or extension limitations, very evidently seen at birth (Makela-Bengs et al., 1998). Subtype 1 can be identified as early as week 13 of pregnancy *via* sonogram, as the fetus shows total akinesia with malformed limbs (Nousiainen et al., 2008). Other clinical symptoms of LCCS are incomplete lung development and fluid collection in the body. If born, neonates can die quickly from respiratory distress, other neurological deficits, and from akinesia. LCCS1 is caused by homozygous or compound mutation in GLE1 (GLE-like protein), which is required for export of mRNAs in eukaryotic cells (Nousiainen et al., 2008). LCCS2 is different from other subtypes owing to the presence of craniofacial/ocular deformities, lack of hydrops, multiple pterygia, distended urinary bladder, and other urinary abnormalities. Duration of pregnancy appears to be normal, but the prenatal diagnosis is possible as early as the 15th week of gestation (Landau et al., 2003). Researchers found a homozygous mutation in the ERBB3 (erb-b2 receptor tyrosine kinase 3) gene in affected members of a large cognate and in an isolated case (Narkis et al., 2004).

Lethal congenital contracture syndrome type 3 is also an autosomal recessive LCCS differing from LCCS2 by the lack of distended bladder. Affected individuals showed multiple joint contractures, and muscle atrophy. Individuals die within few minutes post-birth owing to respiratory failure. The phenotype can also be well distinguished from LCCS1 by the absence of body fluid accumulation, fractures, and facial anomalies. LCCS3 is caused by a homozygous missense mutation in the PIP5K1C gene, encoding a member of the type I phosphatidylinositol-4-phosphate 5-kinase family of enzymes. The mutation can affect a very conserved residue on the enzyme and abolishes its kinase activity (Narkis et al., 2004). LCCS4, specifically, is caused by a mutation in *MYBPC1*. This gene encodes *MYBPC1* found in slow and fast-twitch skeletal muscle. This is a nonsense mutation, causing truncation and non-functioning of the MYBPC1 protein. The mutation occurs in the C2 domain of MYBPC1 and causes malformation of the skeletal muscles. This homozygous mutation causes a similar, yet more severe, phenotype than the mutation that causes DA (Markus et al., 2012).

Lethal congenital contracture syndrome type 5 is also a lethal congenital neuromuscular syndrome known to be caused by homozygous mutations in the DNM2 gene, encoding for protein dynamin-2. A study reported that LCCS5 exhibited fetal movements, polyhydramnios, and decreased birth weight. However, at birth, all affected individuals showed severe hypotonia with respiratory insufficiency, lack of reflexes, retinal hemorrhages, joint contractures, and thin ribs and bones. Death associated with this syndrome is reported to occur at 5 days, 19 days, and 4 months after birth. Parents of these infants showed decreased reflexes on examination, and

maternal skeletal muscle biopsy showed fiber size changes and centralized nuclei, suggesting a mild form of centronuclear myopathy (Koutsopoulos et al., 2013). LCCS6, found in 3 to 4 infants, showed reduced fetal movements, and antenatal ultrasound presented polyhydramnios, absent stomach, and other multiple contracture deformities. However, they did not exhibit any major renal or central nervous system malformations. The severity of polyhydramnios required patients to undergo reductive amniocentesis. The hip joints were affected and showed adducted lower limbs, symmetric deformity of the knees, flexion of hands, and foot dorsiflexion. Genetic mapping of LCCS6 patients showed that it is caused by homozygous mutation in the ZBTB42 gene (Patel et al., 2014).

Lethal congenital contracture syndrome type 7 is said to be an axoglial form of DA characterized by congenital distal joint contractures, excess of amniotic fluid, reduced fetal movements, and loss of motor function leading to death early in the prenatal period. Genetic mapping and whole-exome sequencing identified a homozygous frameshift mutation in the CNTNAP1 gene in affected individuals (Laquerriere et al., 2014). A study reported distinct clinical features associated with LCCS7, such as severe hypotonia with severe contractures and muscle wasting. Muscle biopsy of LCCS7 patients shows neurogenic muscular atrophy with reduced conduction velocities of motor nerves in the upper limbs and no responses in the lower limbs, indicating that sensory responses are absent. Brain imaging in some patients shows cerebral and cerebellar atrophy, no white matter, and smaller basal ganglia and hippocampi (Lakhani et al., 2017). LCCS8 is also an axoglial form of congenital arthrogryposis multiplex where affected patients show the presence of hypotonia, respiratory distress, facial diplegia, areflexia, and swallowing defect. Death occurs within 3 months of life owing to severe motor paralysis. It is different from LCCS7 by the absence of variability in motor nerve conduction velocity. Patients' nerve immunohistochemistry showed Schwann cells with no myelin, and transmission electron microscopic analysis of nerve also showed no myelinated axons. LCCS8 is associated with genetic homozygous mutation in the ADCY6 gene, encoding for proteins which belong to the adenylyl cyclase family necessary for cyclic AMP production (Laquerriere et al., 2014).

Lethal congenital contracture syndrome type 9 is associated with homozygous mutation in the GPR126 gene, encoding for the G protein-coupled receptor family proteins. Clinical features show abnormal distance between the inner eye corners, upper limb DA with ulnar deviation of hands, bent fingers, sparse dermal ridges, ankylosis of the knee joint, and foot abnormality (**Figure 1**). Facial features include triangular face, pixie ears, depressed nasal root and bridge, thin upper lip, and micrognathia. Histologic examination of patients' muscle biopsies shows variability in muscle-fiber diameter with small atrophic and large hypertrophic fibers. Analysis of peripheral nerves also showed an absence of myelin basic protein, indicating the defective myelination of the peripheral axons during prenatal (Ravenscroft et al., 2015). LCCS10 is caused by homozygous mutation in the NEK9 gene, encoding the never in mitosis gene a (NIM-A) family of serine/threonine protein kinases. It is associated with the presence of decreased fetal movement, multiple contractures, shortened upper and lower limbs, short broad ribs, narrow chest, incomplete lung development and protruding abdomen (Casey et al., 2016). LCCS11 is caused by mutations in the GLDN gene, a protein gliomedin necessary for the interaction between Schwann cell microvilli and axons. The pregnancies were characterized by marked polyhydramnios and fetal akinesia on prenatal ultrasound at about 27–32 weeks of gestation; however, earlier ultrasounds appeared to be normal. Clinical features also include flexion of the upper limb and extension contractures of lower limbs, as well as flexion of the wrists and fingers. Affected individuals always show pulmonary hypoplasia, sometimes retrognathia, camptodactyly, and bilateral clubfoot. Transmission electron microscopy conducted on the sciatic nerve from one of the affected fetuses demonstrated a reduced number of myelinated fibers (Maluenda et al., 2016).

SUMMARY

Common birth defects like congenital contractures severely complicate daily activity and cause an economic burden to the patient's family. Arthrogryposis is one of those disorders in which patients show signs of congenital contractures in many parts of the body. DA affects the distal parts of the body, making normal life virtually impossible. Some genetic mutations reported to cause the disease were also speculated to play a role in cardiomyopathy. Genes encoding titin, for example, showed mutations responsible for developing a cardiac and skeletal disorder phenotype. Further studies are required to identify the linkage between these two disorders. Depending on the identification of suitable targets, it may be possible to treat both cardiac and skeletal muscle diseases with some form of combinatorial regimen in the future.

AUTHOR CONTRIBUTIONS

DD, DS, TS, and SS wrote the review manuscript. All authors approved the final version of the manuscript.

FUNDING

SS has received support from the National Institutes of Health grants (R01 HL130356, R56 HL139680, R01 AR067279, R01 HL105826, and R01 HL143490); American Heart Association 2019 Institutional Undergraduate Student (19UFEL34380251), and transformation (19TPA34830084) awards; and the PLN Foundation (PLN crazy idea). DS (20PRE35120272) and TS (19POST34380448) were supported with American Heart Association Fellowship training grants.

REFERENCES

Alvarado, D. M., Buchan, J. G., Gurnett, C. A., and Dobbs, M. B. (2011). Exome sequencing identifies an MYH3 mutation in a family with distal arthrogryposis type 1. *J. Bone Joint Surg. Am.* 93, 1045–1050. doi: 10.2106/jbjs.j.02004

Axt, M. W., Niethard, F. U., Doderlein, L., and Weber, M. (1997). Principles of treatment of the upper extremity in arthrogryposis multiplex congenita type I. *J. Pediatr. Orthop. B* 6, 179–185. doi: 10.1097/01202412-199707000-00005

Bamshad, M., Jorde, L. B., and Carey, J. C. (1996). A revised and extended classification of the distal arthrogryposes. *Am. J. Med. Genet.* 65, 277–281. doi: 10.1002/(sici)1096-8628(19961111)65:4<277::aid-ajmg6>3.0.co;2-m

Bamshad, M., Van Heest, A. E., and Pleasure, D. (2009). Arthrogryposis: a review and update. *J. Bone Joint Surg. Am.* 91(Suppl. 4), 40–46. doi: 10.2106/jbjs.i.00281

Baraitser, M. (1982). A new camptodactyly syndrome. *J. Med. Genet.* 19, 40–43.

Bayram, Y., Karaca, E., Coban Akdemir, Z., Yilmaz, E. O., Tayfun, G. A., Aydin, H., et al. (2016). Molecular etiology of arthrogryposis in multiple families of mostly Turkish origin. *J. Clin. Invest.* 126, 762–778. doi: 10.1172/jci84457

Beals, R. K. (2005). The distal arthrogryposes: a new classification of peripheral contractures. *Clin. Orthop. Relat. Res.* 435, 203–210. doi: 10.1097/01.blo.0000157540.75191.1d

Beals, R. K., and Hecht, F. (1971). Congenital contractural arachnodactyly. A heritable disorder of connective tissue. *J. Bone Joint Surg. Am.* 53, 987–993. doi: 10.2106/00004623-197153050-00013

Beck, A. E., McMillin, M. J., Gildersleeve, H. I., Kezele, P. R., Shively, K. M., Carey, J. C., et al. (2013). Spectrum of mutations that cause distal arthrogryposis types 1 and 2B. *Am. J. Med. Genet. A* 161A, 550–555. doi: 10.1002/ajmg.a.35809

Cameron-Christie, S. R., Wells, C. F., Simon, M., Wessels, M., Tang, C. Z. N., Wei, W., et al. (2018). Recessive spondylocarpotarsal synostosis syndrome due to compound heterozygosity for variants in MYH3. *Am. J. Hum. Genet.* 102, 1115–1125. doi: 10.1016/j.ajhg.2018.04.008

Carmignac, V., Salih, M. A., Quijano-Roy, S., Marchand, S., Al Rayess, M. M., Mukhtar, M. M., et al. (2007). C-terminal titin deletions cause a novel early-onset myopathy with fatal cardiomyopathy. *Ann. Neurol.* 61, 340–351. doi: 10.1002/ana.21089

Casey, J. P., Brennan, K., Scheidel, N., McGettigan, P., Lavin, P. T., Carter, S., et al. (2016). Recessive NEK9 mutation causes a lethal skeletal dysplasia with evidence of cell cycle and ciliary defects. *Hum. Mol. Genet.* 25, 1824–1835. doi: 10.1093/hmg/ddw054

Chauveau, C., Bonnemann, C. G., Julien, C., Kho, A. L., Marks, H., Talim, B., et al. (2014). Recessive TTN truncating mutations define novel forms of core myopathy with heart disease. *Hum. Mol. Genet.* 23, 980–991. doi: 10.1093/hmg/ddt494

Chen, H. (ed.). (2015). *Atlas of Genetic Diagnosis and Counseling*, New York: Springer Science Business Media. doi: 10.1007/978-1-4614-6430-3_16-2

Chong, J. X., Burrage, L. C., Beck, A. E., Marvin, C. T., McMillin, M. J., Shively, K. M., et al. (2015). Autosomal-dominant multiple pterygium syndrome is caused by mutations in MYH3. *Am. J. Hum. Genet.* 96, 841–849.

Godfrey, M., Raghunath, M., Cisler, J., Bevins, C. L., DePaepe, A., Di Rocco, M., et al. (1995). Abnormal morphology of fibrillin microfibrils in fibroblast cultures from patients with neonatal Marfan syndrome. *Am. J. Pathol.* 146, 1414–1421.

Gordon, N. (1998). Arthrogryposis multiplex congenita. *Brain Dev.* 20, 507–511.

Guell, J. L., Verdaguer, P., Elies, D., Gris, O., and Manero, F. (2015). Corneal impairment in a patient with type 2 distal arthrogryposis. *Eye Contact Lens* 41, e5–e8. doi: 10.1097/icl.0b013e3182a2f881

Gurnett, C. A., Desruisseau, D. M., McCall, K., Choi, R., Meyer, Z. I., Talerico, M., et al. (2010). Myosin binding protein C1: a novel gene for autosomal dominant distal arthrogryposis type 1. *Hum. Mol. Genet.* 19, 1165–1173. doi: 10.1093/hmg/ddp587

Ha, K., Buchan, J. G., Alvarado, D. M., McCall, K., Vydyanath, A., Luther, P. K., et al. (2013). MYBPC1 mutations impair skeletal muscle function in zebrafish models of arthrogryposis. *Hum. Mol. Genet.* 22, 4967–4977. doi: 10.1093/hmg/ddt344

Hall, J. E., Salter, R. B., and Bhalla, S. K. (1967). Congenital short tendo calcaneus. *J. Bone Joint Surg. Br.* 49, 695–697. doi: 10.1302/0301-620x.49b4.695

Hall, J. G. (1997). Arthrogryposis multiplex congenita: etiology, genetics, classification, diagnostic approach, and general aspects. *J. Pediatr. Orthop. B* 6, 159–166. doi: 10.1097/01202412-199707000-00002

Hall, J. G., and Kiefer, J. (2016). Arthrogryposis as a syndrome: gene ontology analysis. *Mol. Syndromol.* 7, 101–109. doi: 10.1159/000446617

Hall, J. G., Reed, S. D., and Greene, G. (1982). The distal arthrogryposes: delineation of new entities–review and nosologic discussion. *Am. J. Med. Genet.* 11, 185–239. doi: 10.1002/ajmg.1320110208

Hecht, F., and Beals, R. K. (1972). "New" syndrome of congenital contractural arachnodactyly originally described by Marfan in 1896. *Pediatrics* 49, 574–579.

Jin, J. Y., Wu, P. F., Fan, L. L., Yu, F., Li, J. J., Fan, X. F., et al. (2017). A mutation of beta-tropomyosin gene in a Chinese family with distal arthrogryposis type I. *Int. J. Clin. Exp. Pathol.* 10, 11137–11142.

Koutsopoulos, O. S., Kretz, C., Weller, C. M., Roux, A., Mojzisova, H., Bohm, J., et al. (2013). Dynamin 2 homozygous mutation in humans with a lethal congenital syndrome. *Eur. J. Hum. Genet.* 21, 637–642. doi: 10.1038/ejhg.2012.226

Kowalczyk, B., and Felus, J. (2016). Arthrogryposis: an update on clinical aspects, etiology, and treatment strategies. *Arch. Med. Sci.* 12, 10–24. doi: 10.5114/aoms.2016.57578

Krakowiak, P. A., Bohnsack, J. F., Carey, J. C., and Bamshad, M. (1998). Clinical analysis of a variant of Freeman-Sheldon syndrome (DA2B). *Am. J. Med. Genet.* 76, 93–98. doi: 10.1002/(sici)1096-8628(19980226)76:1<93::aid-ajmg17>3.0.co;2-k

Krakowiak, P. A., O'Quinn, J. R., Bohnsack, J. F., Watkins, W. S., Carey, J. C., Jorde, L. B., et al. (1997). A variant of Freeman-Sheldon syndrome maps to 11p15.5-pter. *Am. J. Hum. Genet.* 60, 426–432.

Lakhani, S., Doan, R., Almureikhi, M., Partlow, J. N., Al Saffar, M., Elsaid, M., et al. (2017). Identification of a novel CNTNAP1 mutation causing arthrogryposis multiplex congenita with cerebral and cerebellar atrophy. *Eur. J. Med. Genet.* 60, 245–249. doi: 10.1016/j.ejmg.2017.02.006

Lampasi, M., Antonioli, D., and Donzelli, O. (2012). Management of knee deformities in children with arthrogryposis. *Musculoskelet Surg.* 96, 161–169. doi: 10.1007/s12306-012-0218-z

Landau, D., Mishori-Dery, A., Hershkovitz, R., Narkis, G., Elbedour, K., and Carmi, R. (2003). A new autosomal recessive congenital contractural syndrome in an Israeli Bedouin kindred. *Am. J. Med. Genet. A* 117A, 37–40. doi: 10.1002/ajmg.a.10894

Langenhan, T., Aust, G., and Hamann, J. (2013). Sticky signaling–adhesion class G protein-coupled receptors take the stage. *Sci. Signal.* 6:re3. doi: 10.1126/scisignal.2003825

Laquerriere, A., Maluenda, J., Camus, A., Fontenas, L., Dieterich, K., Nolent, F., et al. (2014). Mutations in CNTNAP1 and ADCY6 are responsible for severe arthrogryposis multiplex congenita with axoglial defects. *Hum. Mol. Genet.* 23, 2279–2289.

Levine, M. S. (1973). Congenital short tendo calcaneus: report of a family. *Am. J. Dis. Child.* 125, 858–859.

Li, M., Andersson-Lendahl, M., Sejersen, T., and Arner, A. (2016). Knockdown of fast skeletal myosin-binding protein C in zebrafish results in a severe skeletal myopathy. *J. Gen. Physiol.* 147, 309–322. doi: 10.1085/jgp.201511452

Li, X., Zhong, B., Han, W., Zhao, N., Liu, W., Sui, Y., et al. (2015). Two novel mutations in myosin binding protein C slow causing distal arthrogryposis type 2 in two large Han Chinese families may suggest important functional role of immunoglobulin domain C2. *PLoS One* 10:e0117158. doi: 10.1371/journal.pone.0117158

Makela-Bengs, P., Jarvinen, N., Vuopala, K., Suomalainen, A., Ignatius, J., Sipila, M., et al. (1998). Assignment of the disease locus for lethal congenital contracture syndrome to a restricted region of chromosome 9q34, by genome scan using five affected individuals. *Am. J. Hum. Genet.* 63, 506–516. doi: 10.1086/301968

Maluenda, J., Manso, C., Quevarec, L., Vivanti, A., Marguet, F., Gonzales, M., et al. (2016). Mutations in GLDN, encoding gliomedin, a critical component of the nodes of ranvier, are responsible for lethal arthrogryposis. *Am. J. Hum. Genet.* 99, 928–933. doi: 10.1016/j.ajhg.2016.07.021

Markus, B., Narkis, G., Landau, D., Birk, R. Z., Cohen, I., and Birk, O. S. (2012). Autosomal recessive lethal congenital contractural syndrome type 4 (LCCS4) caused by a mutation in MYBPC1. *Hum. Mutat.* 33, 1435–1438. doi: 10.1002/humu.22122

McMillin, M. J., Beck, A. E., Chong, J. X., Shively, K. M., Buckingham, K. J., Gildersleeve, H. I., et al. (2014). Mutations in PIEZO2 cause Gordon syndrome,

Marden-Walker syndrome, and distal arthrogryposis type 5. *Am. J. Hum. Genet.* 94, 734–744. doi: 10.1016/j.ajhg.2014.03.015

Minzer-Conzetti, K., Wu, E., Vargervik, K., and Slavotinek, A. (2008). Phenotypic variation in trismus-pseudocamptodactyly syndrome caused by a recurrent MYH8 mutation. *Clin. Dysmorphol.* 17, 1–4. doi: 10.1097/mcd.0b013e3282efdad8

Narkis, G., Landau, D., Manor, E., Elbedour, K., Tzemach, A., Fishelson, M., et al. (2004). Homozygosity mapping of lethal congenital contractural syndrome type 2 (LCCS2) to a 6 cM interval on chromosome 12q13. *Am. J. Med. Genet. A* 130A, 272–276. doi: 10.1002/ajmg.a.30266

Nousiainen, H. O., Kestila, M., Pakkasjarvi, N., Honkala, H., Kuure, S., Tallila, J., et al. (2008). Mutations in mRNA export mediator GLE1 result in a fetal motoneuron disease. *Nat. Genet.* 40, 155–157. doi: 10.1038/ng.2007.65

Okubo, M., Fujita, A., Saito, Y., Komaki, H., Ishiyama, A., Takeshita, E., et al. (2015). A family of distal arthrogryposis type 5 due to a novel PIEZO2 mutation. *Am. J. Med. Genet. A* 167A, 1100–1106.

Park, E.-S., Putnam, E. A., Chitayat, D., Child, A., and Milewicz, D. M. (1998). Clustering of FBN2 mutations in patients with congenital contractural arachnodactyly indicates an important role of the domains encoded by exons 24 through 34 during human development. *Am. J. Med. Genet.* 78, 350–355. doi: 10.1002/(sici)1096-8628(19980724)78:4<350::aid-ajmg9>3.0.co;2-p

Patel, N., Smith, L. L., Faqeih, E., Mohamed, J., Gupta, V. A., and Alkuraya, F. S. (2014). ZBTB42 mutation defines a novel lethal congenital contracture syndrome (LCCS6). *Hum. Mol. Genet.* 23, 6584–6593. doi: 10.1093/hmg/ddu384

Pehlivan, D., Bayram, Y., Gunes, N., Coban Akdemir, Z., Shukla, A., Bierhals, T., et al. (2019). The genomics of arthrogryposis, a complex trait: candidate genes and further evidence for oligogenic inheritance. *Am. J. Hum. Genet.* 105, 132–150. doi: 10.1016/j.ajhg.2019.05.015

Poling, M. I., Morales Corado, J. A., and Chamberlain, R. L. (2017). Findings, phenotypes, and outcomes in Freeman-Sheldon and Sheldon-Hall syndromes and distal arthrogryposis types 1 and 3: protocol for systematic review and patient-level data meta-analysis. *Syst. Rev.* 6:46.

Ravenscroft, G., Nolent, F., Rajagopalan, S., Meireles, A. M., Paavola, K. J., Gaillard, D., et al. (2015). Mutations of GPR126 are responsible for severe arthrogryposis multiplex congenita. *Am. J. Hum. Genet.* 96, 955–961.

Scala, M., Accogli, A., De Grandis, E., Allegri, A., Bagowski, C. P., Shoukier, M., et al. (2018). A novel pathogenic MYH3 mutation in a child with Sheldon-Hall syndrome and vertebral fusions. *Am. J. Med. Genet. A* 176, 663–667. doi: 10.1002/ajmg.a.38593

Schrander-Stumpel, C. T., Howeler, C. J., Reekers, A. D., De Smet, N. M., Hall, J. G., and Fryns, J. P. (1993). Arthrogryposis, ophthalmoplegia, and retinopathy: confirmation of a new type of arthrogryposis. *J. Med. Genet.* 30, 78–80. doi: 10.1136/jmg.30.1.78

Staff, P. O. (2015). Correction: two novel mutations in myosin binding protein C slow causing distal arthrogryposis type 2 in two large Han Chinese families may suggest important functional role of immunoglobulin domain C2. *PLoS One* 10:e0125310. doi: 10.1371/journal.pone.0125310

Stevenson, D. A., Swoboda, K. J., Sanders, R. K., and Bamshad, M. (2006). A new distal arthrogryposis syndrome characterized by plantar flexion contractures. *Am. J. Med. Genet. A* 140, 2797–2801. doi: 10.1002/ajmg.a.31528

Sucuoglu, H., Ornek, N. I., and Caglar, C. (2015). Arthrogryposis multiplex congenita: multiple congenital joint contractures. *Case Rep. Med.* 2015:379730.

Sung, S. S., Brassington, A. M., Grannatt, K., Rutherford, A., Whitby, F. G., Krakowiak, P. A., et al. (2003). Mutations in genes encoding fast-twitch contractile proteins cause distal arthrogryposis syndromes. *Am. J. Hum. Genet.* 72, 681–690. doi: 10.1086/368294

Veugelers, M., Bressan, M., McDermott, D. A., Weremowicz, S., Morton, C. C., Mabry, C. C., et al. (2004). Mutation of perinatal myosin heavy chain associated with a Carney complex variant. *N. Engl. J. Med.* 351, 460–469. doi: 10.1056/nejmoa040584

Wang, B., Zheng, Z., Wang, Z., Zhang, X., Yang, H., Cai, H., et al. (2016). A novel missense mutation of TNNI2 in a Chinese family cause distal arthrogryposis type 1. *Am. J. Med. Genet. A* 170A, 135–141. doi: 10.1002/ajmg.a.37391

Wang, M., Clericuzio, C. L., and Godfrey, M. (1996). Familial occurrence of typical and severe lethal congenital contractural arachnodactyly caused by missplicing of exon 34 of fibrillin-2. *Am. J. Hum. Genet.* 59, 1027–1034.

Zhang, H., Apfelroth, S. D., Hu, W., Davis, E. C., Sanguineti, C., Bonadio, J., et al. (1994). Structure and expression of fibrillin-2, a novel microfibrillar component preferentially located in elastic matrices. *J. Cell Biol.* 124, 855–863. doi: 10.1083/jcb.124.5.855

Zhang, H., Hu, W., and Ramirez, F. (1995). Developmental expression of fibrillin genes suggests heterogeneity of extracellular microfibrils. *J. Cell Biol.* 129, 1165–1176. doi: 10.1083/jcb.129.4.1165

Zieba, J., Zhang, W., Chong, J. X., Forlenza, K. N., Martin, J. H., Heard, K., et al. (2017). A postnatal role for embryonic myosin revealed by MYH3 mutations that alter TGFbeta signaling and cause autosomal dominant spondylocarpotarsal synostosis. *Sci. Rep.* 7:41803.

Zlotolow, D. A., and Kozin, S. H. (2012). Posterior elbow release and humeral osteotomy for patients with arthrogryposis. *J. Handb. Surg. Am.* 37, 1078–1082. doi: 10.1016/j.jhsa.2012.02.032

Conflict of Interest: SS provided consulting and collaborative research studies to the Leducq Foundation (CURE-PLAN), Red Saree Inc., Greater Cincinnati Tamil Sangam, AstraZeneca, MyoKardia, Merck and Amgen, but such work is unrelated to the content of this manuscript.

The remaining authors declare that the research was conducted in the absence of any commercial or financial relationships that could be construed as a potential conflict of interest.

frontiers in Physiology

MINI REVIEW
published: 09 July 2020
doi: 10.3389/fphys.2020.00722

The Dark Side of Nrf2 in the Heart

*Huimei Zang[1], Roy Oomen Mathew[2] and Taixing Cui[1]**

[1] Department of Cell Biology and Anatomy, University of South Carolina School of Medicine, Columbia, SC, United States,
[2] Division of Nephrology, Department of Medicine, Columbia VA Healthcare System, Columbia, SC, United States

Nuclear factor-erythroid factor 2-related factor 2 (Nrf2) is a critical transcription factor that regulates the expression of over 1000 genes in the cell under normal and stressed conditions. These transcripts can be categorized into different groups with distinct functions, including antioxidative defense, detoxification, inflammatory responses, transcription factors, proteasomal and autophagic degradation, and metabolism. Nevertheless, Nrf2 has been historically considered as a crucial regulator of antioxidant defense to protect against various insult-induced organ damage and has evolved as a promising drug target for the treatment of human diseases, such as heart failure. However, burgeoning evidence has revealed a detrimental role of Nrf2 in cardiac pathological remodeling and dysfunction toward heart failure. In this mini-review, we outline recent advances in structural features of Nrf2 and regulation of Nrf2 activity and discuss the emerging dark side of Nrf2 in the heart as well as the potential mechanisms of Nrf2-mediated myocardial damage and dysfunction.

Keywords: Nrf2, oxidative stress, reductive stress, autophagy, heart failure

OPEN ACCESS

Edited by:
Xuejun Wang,
University of South Dakota,
United States

Reviewed by:
Jiliang Zhou,
Georgia Health Sciences University,
United States
Rajasekaran
Namakkal-Soorappan,
University of Alabama at Birmingham,
United States

****Correspondence:***
Taixing Cui
taixing.cui@uscmed.sc.edu

Specialty section:
This article was submitted to Striated Muscle Physiology, a section of the journal Frontiers in Physiology

Received: *29 March 2020*
Accepted: *02 June 2020*
Published: *09 July 2020*

Citation:
Zang H, Mathew RO and Cui T (2020) The Dark Side of Nrf2 in the Heart. Front. Physiol. 11:722. doi: 10.3389/fphys.2020.00722

INTRODUCTION

Heart failure is defined as "a complex clinical syndrome that can result from any structural or functional cardiac disorder that impairs the ability of the ventricle to fill with or eject blood" (Hunt et al., 2005; Yancy et al., 2013). Recent studies have revealed that heart failure affects 1 in 5 Americans, and the prevalence and incidence of heart failure are still increasing (Yancy et al., 2013; Virani et al., 2020). Heart failure is usually the last stage of different cardiovascular diseases, such as hypertension that causes sustained pressure overload to the heart; coronary arterial diseases, leading to myocardial infarction or ischemia reperfusion–related cardiac injury; valvular disease, resulting in volume overload to the heart; and congenital heart disease. Despite the differential etiologies, the progression of heart failure goes through a common path; i.e., cardiac remodeling, which has been considered as epigenetic and genomic alterations as well as molecular and cellular responses, resulting in clinically manifested changes in geometry and function of the heart after cardiac pressure or volume overload and/or injury (Swynghedauw, 1999; Cohn et al., 2000; Heusch et al., 2014). Cardiac remodeling may be initially adaptive against various harmful insults but, when sustained, turns out to be maladaptive, or pathological, progressing to structural and functional changes that lead to heart failure. Cardiac maladaptive remodeling is usually characterized by myocardial hypertrophy, fibrosis, and cell death, which may be resulted from a complex interaction between cardiac myocytes and non-myocytes. The molecular mechanism of cardiac maladaptive remodeling that leads to heart failure in diverse pathological settings is poorly understood. The treatment of heart failure remains at a level of controlling symptoms and reducing risk factors without a cure.

Oxidative stress, a state that occurs when the oxidative force, e.g., production of reactive oxygen species (ROS) exceeds the antioxidant capacity, is a common mechanism of various cardiac pathologies leading to heart failure (Tsutsui et al., 2011; Ahmed and Tang, 2012). However, several large clinical trials using antioxidant supplements, such as non-selective ROS scavenger vitamin C, vitamin E, and allopurinol, have found that non-specific scavenging of ROS does not help to prevent cardiovascular disease; instead, it may even be harmful (Li et al., 2009a; Ahmed and Tang, 2012). These studies suggest that effective therapeutic approaches for the treatment of cardiovascular disease may not be achieved without specific targeting the source of oxidative stress or the intrinsic antioxidant system. In this regard, nuclear factor-erythroid factor 2-related factor 2 (Nrf2), which has been historically considered as a master transcription factor of antioxidant defense, has evolved as an attracting therapeutic target for cardiovascular disease (Li et al., 2009a; Chen and Maltagliati, 2018; Ge et al., 2019). Despite the fact that Nrf2 appears to be a critical regulator of cellular defense against various pathological insults in the heart, burgeoning evidence has demonstrated a detrimental role of Nrf2 in cardiac disease progression (Cui et al., 2016). In this mini-review, we update recent advances in structural features and activity regulation of vertebrate Nrf2 and then have a close look on the dual effects of Nrf2 in the heart and discuss the potential molecular mechanisms underlying Nrf2-mediated dichotomy in the heart.

Nrf2 SIGNALING

Nrf2-related factor 2 is a member of the Cap "n" Collar (CNC) family of basic leucine zipper (bZip) transcription factors that include nuclear factor-erythroid factor 2 (NF-E2), Nrf1-3, and broad-complex, tramtrack, and bric-a-brac (BTB) and CNC homolog 1 (Bach 1) and Bach 2. The differences between these transcription factors have been broadly reviewed (Li et al., 2009a; Maher and Yamamoto, 2010). Concisely, NF-E2 and Nrf1-3 act as transcriptional activators, whereas Bach 1 and 2 serve as transcriptional repressors. The expression of Nrf proteins is ubiquitous in the body. Nrf1 plays a role in controlling the basal gene expression level of some cytoprotective enzymes but does not regulate their inducible expression. Although marginal, Nrf3 is capable of regulating the gene expression of phase 2 enzymes. In contrast, Nrf2 binds to a *cis*-acting enhancer with a core nucleotide sequence of 5′-RTGACNNNGC-3′, that is also known as the antioxidant response element (ARE), or the electrophile response element (EpRE), to control the basal and inducible expression of over 1000 genes that can be clustered into several groups with distinct functions, including antioxidative defense, detoxification, inflammatory responses, transcription factors, proteasomal and autophagic degradation, and metabolism (Hayes and Dinkova-Kostova, 2014; Cui et al., 2016; Kopacz et al., 2020). Thus, Nrf2 is multifunctional with cellular functions ranging from antioxidative defense to protein quality control to metabolism regulation.

Structural features of vertebrate Nrf2 have been revised and updated in detail (Hayes and Dinkova-Kostova, 2014; Silva-Islas and Maldonado, 2018; Kopacz et al., 2020). Briefly, Nrf2 has 7 Nrf2-erythroid-derived CNC homology (ECH; Neh) domains (Neh1-7), which are critical for its activity or its repression (**Figure 1A**). The amino-terminal Neh2 via the DLG and ETGE motifs binds the double glycine repeat (DGR) domain of Kelch-like ECH associating protein 1 (Keap1), a negative regulator of Nrf2. A nuclear localization signal (NLS) sequence is localized in this domain. The Neh6 is another degron region, a portion of a protein important for its degradation, which via the DSGIS and DSAPGS motifs, recruits the dimeric β–transducin repeat-containing protein (β-TrCP), a substrate adaptor for the S-phase kinase 1 (Skp1)-Cullin 1 (Cul1)-Ring box protein 1 (Rbx1) core E3 ligase (i.e., $SCF^{\beta-TrCP}$). The Neh6 is important for Nrf2 degradation in stressed cells independent of Keap1. The carboxyl-terminal Neh3 is necessary for transcriptional activation of Nrf2 by recruiting coactivator, chromo-ATPase/helicase DNA-binding protein (CDH) 6. The Neh3 contains a second NLS sequence. The Neh1 adjacent to the Neh3 contains a bZip structure, which is critical for DNA binding and dimerization with other transcription factors. A nuclear export signal (NES) sequence is localized in the Neh1. The Neh4 and Neh5 are two independent transactivation domains that interact with cAMP response element-binding protein (CREB)-binding protein (CBP) and/or receptor-associated coactivator 3 (RAC3). The Neh7 mediates repression of Nrf2 by physical interaction with retinoid X receptor alpha (RXRα).

Nrf2-related factor 2 is a short-lived protein with a half-life less than 20 min in the cell (Li et al., 2009a; Chen and Maltagliati, 2018). The expression and activity of Nrf2 are tightly regulated at multiple levels, which have been recently reviewed (Hayes and Dinkova-Kostova, 2014; Chen and Maltagliati, 2018; Silva-Islas and Maldonado, 2018; Kopacz et al., 2020). Generally, the transcription of Nrf2 is activated by itself and other transcription factors, including the aryl hydrocarbon receptor (AhR), peroxisome proliferator-activated receptor (PPAR)α or PPARγ, nuclear factor (NF)-κB (NF-κB), specificity protein 1 (Sp-1), p53, myocyte-specific enhancer factor 2 D (MEF2D), c-Jun, c-Myc, and breast cancer 1 (BRCA1). Epigenetic regulations, such as methylation of the Nrf2 promoter in CpG islands or H3 histone and acetylation of H4 histone, are also involved in Nrf2 transcriptional control. Moreover, Nrf2 synthesis can be downregulated by several miRNAs, including miR27a, miR-28, miR-34a, miR-93, miR-129-5p, miR-142-5p, miR-144, miR-153, miR-155, miR-200c, miR-340-5p, miR-350a, miR-507, and miR-634 at the posttranscriptional level. Nevertheless, the protein stability and transcriptional activity of Nrf2 are mainly regulated by Keap1. Keap1 contains two major domains, BTB and DGR or Kelch, and three additional domains, the N-terminal region (NTR), the intervening region (IVR), and CTR (**Figure 1A**). The BTB is critical for Keap1 homodimerization and interaction with Cul3-Rbx1-E3 ligase complex while the Kelch binds to the DLG and ETGE motifs in Neh2 of Nrf2. Keap1 contains many cysteine residues sensing oxidative and/or electrophilic molecules in both BTB and IVR. Normally, Keap1 constantly targets Nrf2 for degradation.

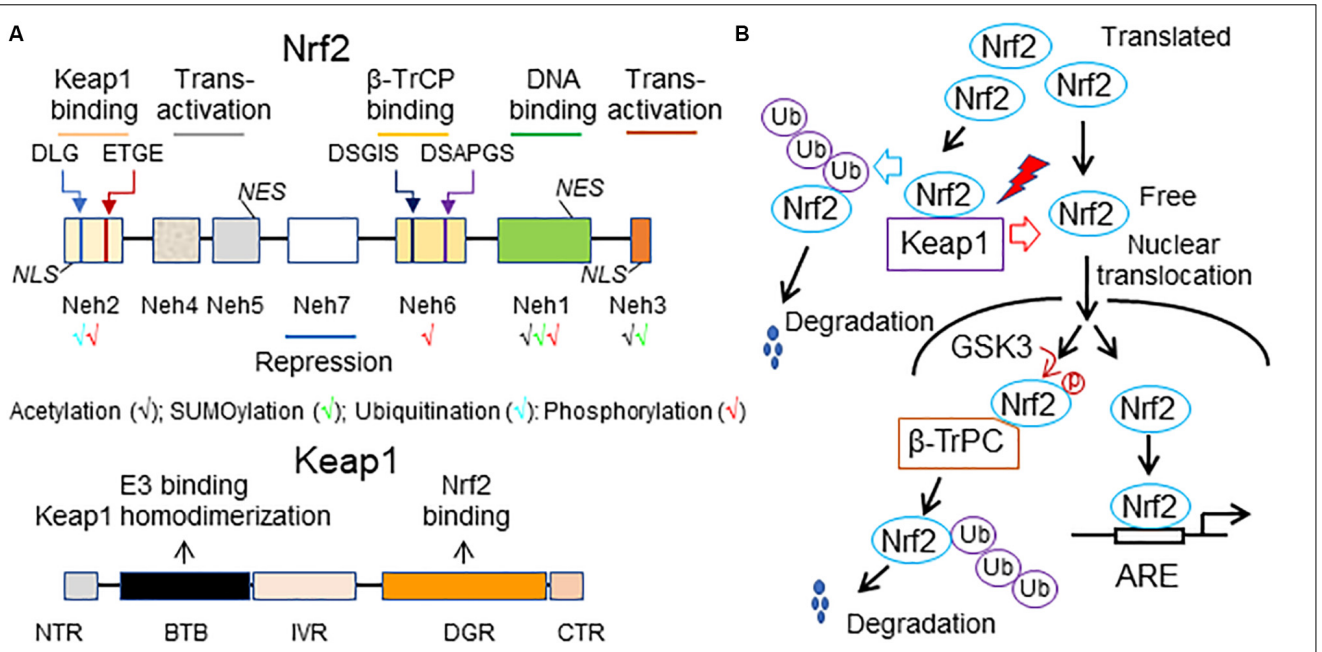

FIGURE 1 | A working model of Nrf2 signaling. **(A)** Structural features of Nrf2 and Keap1. The high-affinity ETGE and low-affinity DLG motifs in the Neh2 domain of Nrf2 are bound by the Kelch domain of Keap1 for Nrf2 ubiquitination and degradation. Neh, Nrf2-erythroid-derived CNC homology (ECH) domain; NES, nuclear export signal; β-TrCP, the dimeric β–transducin repeat-containing protein; NLS, nuclear localization signal; BTB, broad-complex, tramtrack and bric-a-brac domain; DGR or Kelch, double glycine repeat domain; NTR, the N-terminal region; IVR, intervening region; CTR, the carboxyl terminal region. **(B)** A scheme of Nrf2 activity regulation. Under homeostatic conditions, translated Nrf2 binds to Keap1, leading to ubiquitination of Nrf2 and subsequent proteasomal degradation of the ubiquitinated Nrf2. As a result, there is only a small amount of free Nrf2 translocating into the nucleus and activating the basal expression of Nrf2 target genes. Under stressed conditions, various stressors (red lighting symbol) interrupt the interaction of Keap1 with Nrf2, thus resulting in decreases in proteasomal degradation of Nrf2 and increases in *de novo* Nrf2 free of Keap1 binding. Accordingly, the nuclear translocation of Nrf2 and subsequent Nrf2-driven transcription are increased, thereby intensifying Nrf2-mediated defense against the stress-induced imbalance of redox status and damage in the cell. An alternative mechanism of proteasomal degradation of Nrf2 independent of Keap1 is mediated by glycogen synthase kinase 3 (GSK3) and β-TrCP. Under normal conditions, GSK3 is maintained in an inactive state due to its inhibition by AKT-mediated phosphorylation at its N-terminal pseudosubstrate domain. However, once AKT is inactivated, GSK3 phosphorylates Nrf2 at the Neh6 domain. This phosphorylation recruits β-TrCP and initiates β-TrCP-mediated proteasomal degradation of Nrf2. Ub, ubiquitin.

The current diagram of Keap1 and Nrf2 interaction for Nrf2 degradation is the "hinge and latch" model: The ETGE motif of Nrf2 acts as the "hinge" while the DIG motif of Nrf2 functions as the "latch." Nrf2 sequentially binds to first one of the Keap1 homodimers via the ETGE motif to form an "open" conformation, prior to the DLG motif being captured by the other Keap1 to form a "closed" conformation that enables Nrf2 ubiquitination by Clu3-Rbx1-E3 ligase for proteasomal degradation and subsequently release of free Keap1. The free or regenerated Keap1 bind to newly synthesized Nrf2 to start another cycle of the Nrf2 degradation. Only a small and steady amount of Nrf2 that is not sequestered by Keap1 for degradation translocate into the nucleus, contributing to the basal expression of ARE-driven genes (**Figure 1B**). Under stressed conditions, the stressors that are usually oxidative or electrophilic molecules react with the cysteine residues of Keap1 to cause conformational changes in Keap1, leading to downregulation of Keap1-mediated ubiquitination and degradation of Nrf2. However, such modulation of Keap1 does not result in release of Nrf2; instead, it stabilizes the Keap1-Nrf2 interaction that blocks Nrf2 ubiquitination, thereby saturating the cellular pool of the Keap1-E3 complex. As a result, *de novo* Nrf2 free of Keap1 binding that translocates into the nucleus is increased, thereby enhancing the transcription of Nrf2-driven genes. However, there is an alternative mechanism for proteasomal degradation of Nrf2 independent of Keap1, which is mediated by glycogen synthase kinase 3 (GSK3) and β-TrCP (**Figure 1B**). Under normal conditions, GSK3 is maintained in an inactive state due to its inhibition by AKT-mediated phosphorylation at its N-terminal pseudosubstrate domain. However, once AKT is inactive, GSK3 phosphorylates Nrf2 at the Neh6. This phosphorylation recruits β-TrCP and initiates β-TrCP-mediated proteasomal degradation of Nrf2. Usually, Keap1-mediated proteasomal degradation of Nrf2 occurs in the cytosol, whereas GSK3-mediated proteasomal degradation of Nrf2 happens in the nucleus. The relative importance of Keap1 and GSK3-β-TrCP in controlling the magnitude and duration of Nrf2 activation remains poorly understood.

It should be noted that not only GSK3, but also other kinases, such as AMP-activated protein kinase (AMPK) and mechanistic target of rapamycin complex 1 (mTORC1), directly or indirectly regulate Nrf2 stability and activity (Hayes and Dinkova-Kostova, 2014; Silva-Islas and Maldonado, 2018). In addition, ubiquitination of Nrf2 at the Neh2 can suppress Nrf2 activity, whereas acetylation of Nrf2 at the Neh1 and Neh3 may activate Nrf2 activity. SUMOylation of Nrf2 at the Neh1 and

Neh3 may result in either Nrf2 activation or Nrf2 repression (Hayes and Dinkova-Kostova, 2014; Silva-Islas and Maldonado, 2018). Moreover, not only oxidative and electrophilic reactions, but also other types of posttranslational modifications of Keap1, such as ubiquitination and phosphorylation, appear to be critical for regulating Nrf2 activity, which has been comprehensively discussed in a recent review (Kopacz et al., 2020). However, the pathophysiological relevance of these findings in the heart remains to be investigated.

Nrf2-MEDIATED CARDIAC PROTECTION

Zhu et al. (2008) demonstrated for the first time an Nrf2-dependent cytoprotection against oxidative and electrophilic stress in cardiomyocytes using neonatal mouse ventricular myocytes of Nrf2 knockout (KO) mice. He et al. subsequently documented that KO of Nrf2 enhances ROS production and exaggerates cell death in cultured adult cardiomyocytes in a setting of high glucose-induced oxidative stress (He et al., 2009). While Sussan et al. (2009) found that global KO of Nrf2 enhances cigarette smoke–induced cardiac dysfunction in mice, we further demonstrated that the loss of Nrf2 function accelerates the transition from cardiac compensatory adaptation to heart failure in a setting of pressure overload (Li et al., 2009b). As we demonstrated that pharmacological activation of Nrf2 suppresses oxidative stress-dependent death in cardiac myocytes (Ichikawa et al., 2009; Li et al., 2010), Zhang et al. (2010) documented that Nrf2-deficient cardiomyocytes are more susceptible to 4-hydroxy-2-nonenal (4-HNE) challenge, and the cardiac protection of 4-HNE pre-conditioning is dependent on Nrf2-operated antioxidant defense. Ashrafian et al. (2012) also showed that fumarate-induced suppression of ischemia-reperfusion myocardial injury is wiped out in global Nrf2 KO mice, and Katsumata et al. revealed that Nrf2 is also essential for prostaglandin D2 (PGD_2)-mediated cardiac protection against ischemia-reperfusion injury in mice (Katsumata et al., 2014). We further demonstrated that conventionally cardiomyocyte-restricted (CR) transgenic overexpression of Nrf2 protects against myocardial oxidative stress, cell death, fibrosis, hypertrophy, and dysfunction in a setting of sustained pressure overload induced by 4 weeks of transverse aortic arch constriction (TAC) in mice (Wang et al., 2014). Moreover, He et al. reported that global KO of Nrf2 could exaggerate cardiac oxidative stress, fibrosis, and apoptosis; contractility of cardiomyocytes; and death within 2 weeks after onset of type 1 diabetes induced by a single i.p. injection of 150 mg/kg streptozotocin (STZ) in mice (He and Ma, 2012), and Gu et al. (2017) showed similar phenotypes in Nrf2 KO mice associated with type 2 diabetes, that is induced by 7 months of a high fat diet (HFD) containing 60% kcal fat with a single i.p. injection of 100 mg/kg STZ at 3 months. Collectively, these findings clearly demonstrate a cardioprotective role of Nrf2 in various pathological settings. Other studies regarding Nrf2-mediated cardiac protection and potential underlying mechanisms have been recently reviewed (Cui et al., 2016; Chen and Maltagliati, 2018; da Costa et al., 2019; Ge et al., 2019). Mechanistically, Nrf2 may activate antioxidant defense, regulate metabolism, and control autophagy and proteasome function, thereby contributing to cardiac protection.

Nrf2-MEDIATED CARDIAC DAMAGE

A Nrf2-mediated myocardial injury was first observed by Kannan et al. (2013) in aging cardiomyocyte-restricted human mutant CryAB transgenic (CR-hCryAB Tg) mice. Of note, CR-hCryAB overexpression-induced death and cardiac dysfunction associated with aging were dramatically rescued by global KO of Nrf2. At the molecular level, the persistent activation of Nrf2-driven antioxidant gene expression toward a reductive stress has been proposed as a contributing mechanism to CR-hCryAB Tg-induced cardiomyopathy (Kannan et al., 2013). While Allwood et al. found that CR transgenic overexpression of Ho1, an established downstream gene of Nrf2 in the heart (Li et al., 2009b), results in spontaneous development of heart failure at age of 1 year and exacerbates pressure overload-induced cardiomyopathy in mice (Allwood et al., 2014), we demonstrated that pathophysiological consequences of Nrf2 activation are linked to the functional integrity of autophagy in pressure overloaded mouse hearts (Qin et al., 2016). We have established that pressure overload via TAC initially results in an adaptive cardiac hypertrophy with preserved cardiac function (weeks 1–2) followed by maladaptive cardiac remodeling and dysfunction (weeks 2–4), which eventually causes heart failure in wild-type mice (Li et al., 2009b). Using this TAC model, we found that TAC-induced myocardial necrosis and death rate are increased in Nrf2 KO mice in a C57BL/6J genetic background within first 2 weeks (Qin et al., 2016). These results underscore a critical role of Nrf2 in mediating cardiac protection during the initial stage of pressure overload-induced cardiac adaptation. However, we found unexpectedly that Nrf2 KO attenuates cardiac hypertrophy and ameliorates progression of cardiac dysfunction by 8 weeks after TAC (Qin et al., 2016). These results reveal a mediator role of Nrf2 in pressure overload–induced cardiac maladaptive remodeling and dysfunction. A time course study of autophagy functional states in wild-type C57BL/6J mice showed that myocardial autophagy flux is intact at 2 weeks, suppressed at 4 weeks, and blocked at 8 weeks in the hearts after TAC (Qin et al., 2016). Since Nrf2 KO diminishes cardiac adaptation and leads to cardiac dysfunction at 2 weeks after TAC (Li et al., 2009b), when cardiac autophagy flux remains normal, it is most likely that Nrf2 activation is cardioprotective in pressure overloaded hearts when myocardial autophagy function is intact. Given that the Nrf2-mediated cardiac pathological hypertrophy and dysfunction are associated with impaired autophagy in the heart, it is conceivable that Nrf2 activation is detrimental to autophagy-impaired hearts. Indeed, genetic inhibition of autophagy, such as CR-Atg5 KO, in combination with pharmacological kinase inhibitors, demonstrated that cardiac autophagy inhibition activates Fyn-operating Nrf2 nuclear export for degradation, thus enhancing Nrf2-driven transcription of angiotensinogen in cardiomyocytes, thereby leading to pathological activation of renin-angiotensin system in pressure overloaded hearts. These

results are seemly contradictory to our findings that Nrf2 activation enhances autophagosome formation and autophagic degradation of protein aggregates, thereby protecting against 4-week TAC-induced cardiac maladaptive remodeling and dysfunction in FVB/N mice (Wang et al., 2014). However, it should be noted that Nrf2 does not regulate the expression of any autophagy-related genes, suggesting that Nrf2 may not directly activate autophagy but indirectly facilitates autophagy activation and degradation in cardiomyocytes (Wang et al., 2014). Given that genetic backgrounds have great impact on autophagy regulation in the heart (Moulis and Vindis, 2017), TAC induces myocardial autophagy inhibition at 4 weeks in C57BL/6J mice (Qin et al., 2016), but it may not induce the same phenotype at 4 weeks in FVB/N mice. Although this notion remains to be clarified, previous studies have shown that the basal level of myocardial autophagy is much higher in FVB/N mice (∼1-fold increases in autophagic flux by 6 h of chloroquine at a dose of 50 mg/kg, i.p.) compared to C57BL/6J mice (∼0.5-fold increases in autophagic flux by 6 h of chloroquine at a dose of 50 mg/kg, i.p.; Fernandez et al., 2018; Deng et al., 2020). Thus, a plausible explanation is that CR-Nrf2 Tg overexpression-induced cardiac protection is mostly likely due to an intact state of myocardial autophagy by 4 weeks after TAC in FVB/N mice. Collectively, our findings suggest that autophagy impairment switches on Nrf2-mediated cardiac pathological remodeling and dysfunction. Interestingly, Bhide et al. (2018) documented that in a Drosophila model of laminopathy, laminopathy-associated age-dependent cardiac dysfunction, could be rescued by knockdown of Nrf2, or enhancement of autophagy in the heart. These findings suggest that age-dependent autophagy deficiency may turn on Nrf2-mediated cardiac dysfunction in the Drosophila model of laminopathy. On the other hand, Erkens et al. (2018) reported that global KO of Nrf2 attenuates myocardial ischemia-reperfusion injury and dysfunction most likely due to

TABLE 1 | Nrf2 signaling cascade in mediating cardiac damage and dysfunction.

Study	Nrf2 signaling	Animal model	Pathological setting	Intervention	Phenotype	Proposed mechanism
Kannan et al., 2013	Nrf2	CR-hCryAB Tg and global Nrf2 KO in C57BL/6J mice	Aging	None	CR-hCryAB Tg-induced cardiac accumulation of protein aggregates and reductive stress, cardiomyopathy, and heart failure are rescued by additional global KO of Nrf2	Nrf2-mediated reductive stress in the heart
Allwood et al., 2014	HO-1	CR-Ho1 Tg in FVB mice	Aging, Pressure overload (PO), Excess beta-adrenergic activity (Isoproterenol infusion),	None	CR-Ho1 Tg mice develop spontaneous heart failure at age of 1 year, and exacerbated cardiac dysfunction induced by PO	HO-1-mediated loss of adaptive angiogenesis
Qin et al., 2016	Nrf2	Global Nrf2 KO in C57BL/6J mice	Pressure overload (PO)	None	Sustained PO leads to cardiac autophagy impairment and Nrf2 activation; Nrf2 KO attenuates progression of cardiac pathological remodeling and dysfunction in PO hearts.	Sustained PO leads to cardiac autophagy impairment, which in turn activates Nrf2-driven angiotensinogen expression, thereby contributing to progression of cardiac pathological remodeling and dysfunction
Erkens et al., 2018	Nrf2	Global Nrf2 KO in C57BL/6J mice	30 min myocardial ischemia followed by 24 h of reperfusion *in vivo*	Infusion of NOS inhibitor S-ethylisothiourea hydrobromide (ETU)	Nrf2KO attenuates myocardial ischemia/reperfusion injury and dysfunction	Nrf2KO upregulates cardiac NO
Bhide et al., 2018	Nrf2	CR-LamC-R205W and G489V Tg and CncC (Nrf2) RNAi in Drosophila	Aging, Laminopathy	None	CR-LamC mutant Tg-induced age-dependent cardiac dysfunction is rescued by knockdown of Nrf2	Autophagy impairment; Nrf2 persistent activation leading to disruption of redox homeostasis, defective mitochondria, dysregulation of energy homeostasis and energy sensor

an increase in cardiac nitric oxide (NO) production in mice, revealing a detrimental effect of Nrf2-mediated suppression of NO production to the heart. Taken together, these genetic studies have clearly demonstrated a detrimental role of Nrf2 in the heart and Nrf2-mediated myocardial damage is likely occurring during the disease progression (**Table 1**). Since cardiac function is normal in CR-Nrf2 Tg mice at the age of ∼3 months (Wang et al., 2014), it is highly possible that additional factors are required to turn on the Nrf2-mediated reductive stress causing cardiomyopathy. Although the precise mechanisms activating Nrf2-mediated cardiac damage are unclear, myocardial autophagy inhibition may be one of the critical triggers. However, the downstream signaling of Nrf2-mediated myocardial damage remains to be dissected.

FINAL REMARK

It is evident that Nrf2 could either protect against or exacerbate cardiac damage and dysfunction depending on the pathological nature of disease settings. Our data shows that Nrf2 is crucial for cardiac adaptation when cardiac autophagy is normal while exaggerating cardiac pathological decompensation when myocardial autophagy is impaired in pressure-overloaded hearts (Qin et al., 2016). Notably, autophagy inhibition is a contributory mechanism of protein aggregate-induced cardiomyopathies in aging CR-hCryAB Tg mice (Bhuiyan et al., 2013), sustained pressure overloaded mice (Qin et al., 2016), myocardial ischemia-reperfusion mice (Ma et al., 2012), and aging Drosophila with laminopathy (Bhide et al., 2018). Therefore, it is likely that autophagy inhibition is essential for activating Nrf2-mediated cardiac damage toward heart failure. These results raise a concern regarding the potential activation of Nrf2-mediated cardiac damage in the clinical therapies when treated subjects are compounded with diabetic, hypertensive, and ischemic cardiomyopathies, all of which likely have myocardial autophagy inhibition (Wang and Cui, 2017).

Notably, the clinical phase III trial testing the therapeutic effect of Bardoxolone methyl, a potent Nrf2 activator, on chronic renal disease associated with type 2 diabetes was terminated because of an increased rate of cardiovascular events, including heart failure and deaths (de Zeeuw et al., 2013). The underlying mechanism remains to be determined. Given that autophagy inhibition also occurs in diabetic hearts (Ouyang et al., 2014; Kobayashi and Liang, 2015), it is intriguing whether the "dark" side of Nrf2 activation contributes to the failure of the Bardoxolone methyl clinical trial. Nevertheless, the enthusiasm for activating Nrf2 as a novel approach to treat human disease, at least non-cardiac diseases, remains very high (Al-Sawaf et al., 2015; Robledinos-Anton et al., 2019). Several clinical trials of a few Nrf2 activators for treating other types of disease, including Bardoxolone methyl, Omaveloxolone, dimethyl fumarate, ALKS-8700 (a fumarate acid ester), Oltipraz, Ursodiol, Sulforaphane, Sulforadex, and Curcumin are still actively ongoing (Robledinos-Anton et al., 2019). All these pharmacological Nrf2 activators are electrophilic compounds that could covalently modify cysteine residues in Keap1 by oxidation or alkylation to cause conformational changes in Keap1, leading to inhibition of Keap1-mediated degradation of Nrf2, thus increasing the amount of newly synthesized and free Nrf2 and consequent enhancement of Nrf2-operating transcription (Robledinos-Anton et al., 2019). Thus, these so-called "Nrf2 activators" are actually "Keap1 inhibitors." Recent studies have revealed that Keap1 is not limited to control Nrf2 activity, but also required for S-nitrosation, proteostasis, mitochondria homeostasis, cytoskeleton regulation, and cell cycle progression (Kopacz et al., 2020). However, the impact of these Nrf2 activators or Keap1 inhibitors on the Keap1-mediated actions beyond inactivation of Nrf2 remains largely unknown.

Taken together, further investigation of molecular mechanisms of Nrf2-mediated myocardial damage, such as autophagy-mediated control of Nrf2 signaling in the heart, will lead to a better understanding of Nrf2-medicated dichotomy in the pathogenesis of cardiomyopathies toward heart failure. The off-target effects of Nrf2 activating compounds (Keap1 inhibitors) in the heart, particularly the possibility of interrupting Keap1 functions independent of Nrf2 degradation, have to be characterized. As a result, the outcome will provide novel insight into the development of new effective approaches to target Nrf2 signaling for the treatment of cardiac and non-cardiac diseases.

AUTHOR CONTRIBUTIONS

HZ and RM wrote the draft. TC provided research funds and finalized the manuscript. All authors contributed to the article and approved the submitted version.

FUNDING

This work was supported by the National Institute of Health (R01 HL131667) and American Diabetes Association (1-16-IBS-059).

REFERENCES

Ahmed, Z., and Tang, W. H. (2012). Pharmacologic strategies to target oxidative stress in heart failure. *Curr. Heart Fail Rep.* 9, 14–22. doi: 10.1007/s11897-011-0081-5

Allwood, M. A., Kinobe, R. T., Ballantyne, L., Romanova, N., Melo, L. G., Ward, C. A., et al. (2014). Heme oxygenase-1 overexpression exacerbates heart failure with aging and pressure overload but is protective against isoproterenol-induced cardiomyopathy in mice. *Cardiovasc. Pathol.* 23, 231–237. doi: 10.1016/j.carpath.2014.03.007

Al-Sawaf, O., Clarner, T., Fragoulis, A., Kan, Y. W., Pufe, T., Streetz, K., et al. (2015). Nrf2 in health and disease: current and future clinical implications. *Clin. Sci.* 129, 989–999. doi: 10.1042/cs20150436

Ashrafian, H., Czibik, G., Bellahcene, M., Aksentijevic, D., Smith, A. C., Mitchell, S. J., et al. (2012). Fumarate is cardioprotective via activation of the Nrf2 antioxidant pathway. *Cell Metab.* 15, 361–371.

Bhide, S., Trujillo, A. S., O'Connor, M. T., Young, G. H., Cryderman, D. E., Chandran, S., et al. (2018). Increasing autophagy and blocking Nrf2 suppress laminopathy-induced age-dependent cardiac dysfunction and shortened lifespan. *Aging Cell* 17, e12747. doi: 10.1111/acel.12747

Bhuiyan, M. S., Pattison, J. S., Osinska, H., James, J., Gulick, J., McLendon, P. M., et al. (2013). Enhanced autophagy ameliorates cardiac proteinopathy. *J. Clin. Invest.* 123, 5284–5297. doi: 10.1172/jci70877

Chen, Q. M., and Maltagliati, A. J. (2018). Nrf2 at the heart of oxidative stress and cardiac protection. *Physiol. Genomics* 50, 77–97. doi: 10.1152/physiolgenomics.00041.2017

Cohn, J. N., Ferrari, R., and Sharpe, N. (2000). Cardiac remodeling–concepts and clinical implications: a consensus paper from an international forum on cardiac remodeling. Behalf of an International Forum on Cardiac Remodeling. *J. Am. Coll. Cardiol.* 35, 569–582. doi: 10.1016/s0735-1097(99)00630-0

Cui, T., Lai, Y., Janicki, J. S., and Wang, X. (2016). Nuclear factor erythroid-2 related factor 2 (Nrf2)-mediated protein quality control in cardiomyocytes. *Front. Biosci.* 21:192–202. doi: 10.2741/4384

da Costa, R. M., Rodrigues, D., Pereira, C. A., Silva, J. F., Alves, J. V., Lobato, N. S., et al. (2019). Nrf2 as a potential mediator of cardiovascular risk in metabolic diseases. *Front. Pharmacol.* 10:382. doi: 10.3389/fphar.2019.00382

de Zeeuw, D., Akizawa, T., Audhya, P., Bakris, G. L., Chin, M., Christ-Schmidt, H., et al. (2013). Bardoxolone methyl in type 2 diabetes and stage 4 chronic kidney disease. *N. Engl. J. Med.* 369, 2492–2503.

Deng, S., Essandoh, K., Wang, X., Li, Y., Huang, W., Chen, J., et al. (2020). Tsg101 positively regulates P62-Keap1-Nrf2 pathway to protect hearts against oxidative damage. *Redox Biol.* 32:101453. doi: 10.1016/j.redox.2020.101453

Erkens, R., Suvorava, T., Sutton, T. R., Fernandez, B. O., Mikus-Lelinska, M., Barbarino, F., et al. (2018). Nrf2 deficiency unmasks the significance of nitric oxide synthase activity for cardioprotection. *Oxid. Med. Cell Longev.* 2018:8309698.

Fernandez, A. F., Sebti, S., Wei, Y., Zou, Z., Shi, M., McMillan, K. L., et al. (2018). Disruption of the beclin 1-BCL2 autophagy regulatory complex promotes longevity in mice. *Nature* 558, 136–140. doi: 10.1038/s41586-018-0162-7

Ge, Z. D., Lian, Q., Mao, X., and Xia, Z. (2019). Current status and challenges of NRF2 as a potential therapeutic target for diabetic cardiomyopathy. *Int. Heart J.* 60, 512–520. doi: 10.1536/ihj.18-476

Gu, J., Cheng, Y., Wu, H., Kong, L., Wang, S., Xu, Z., et al. (2017). Metallothionein is downstream of Nrf2 and partially mediates sulforaphane prevention of diabetic cardiomyopathy. *Diabetes* 66, 529–542. doi: 10.2337/db15-1274

Hayes, J. D., and Dinkova-Kostova, A. T. (2014). The Nrf2 regulatory network provides an interface between redox and intermediary metabolism. *Trends Biochem. Sci.* 39, 199–218. doi: 10.1016/j.tibs.2014.02.002

He, X., Kan, H., Cai, L., and Ma, Q. (2009). Nrf2 is critical in defense against high glucose-induced oxidative damage in cardiomyocytes. *J. Mol. Cell Cardiol.* 46, 47–58. doi: 10.1016/j.yjmcc.2008.10.007

He, X., and Ma, Q. (2012). Disruption of Nrf2 synergizes with high glucose to cause heightened myocardial oxidative stress and severe Cardiomyopathy in diabetic mice. *J. Diabetes Metab.* 7:002.

Heusch, G., Libby, P., Gersh, B., Yellon, D., Bohm, M., Lopaschuk, G., et al. (2014). Cardiovascular remodelling in coronary artery disease and heart failure. *Lancet* 383, 1933–1943. doi: 10.1016/s0140-6736(14)60107-0

Hunt, S. A., Abraham, W. T., Chin, M. H., Feldman, A. M., Francis, G. S., Ganiats, T. G., et al. (2005). ACC/AHA 2005 Guideline Update for the Diagnosis and Management of Chronic Heart Failure in the Adult: a report of the American College of Cardiology/American Heart Association Task Force on Practice Guidelines (Writing Committee to Update the 2001 Guidelines for the Evaluation and Management of Heart Failure): developed in collaboration with the American College of Chest Physicians and the International Society for Heart and Lung Transplantation: endorsed by the Heart Rhythm Society. *Circulation* 112, e154–e235.

Ichikawa, T., Li, J., Meyer, C. J., Janicki, J. S., Hannink, M., and Cui, T. (2009). Dihydro-CDDO-trifluoroethyl amide (dh404), a novel Nrf2 activator, suppresses oxidative stress in cardiomyocytes. *PLoS One* 4:e8391. doi: 10.1371/journal.pone.0008391

Kannan, S., Muthusamy, V. R., Whitehead, K. J., Wang, L., Gomes, A. V., Litwin, S. E., et al. (2013). Nrf2 deficiency prevents reductive stress-induced hypertrophic cardiomyopathy. *Cardiovasc. Res.* 100, 63–73. doi: 10.1093/cvr/cvt150

Katsumata, Y., Shinmura, K., Sugiura, Y., Tohyama, S., Matsuhashi, T., Ito, H., et al. (2014). Endogenous prostaglandin D2 and its metabolites protect the heart against ischemia-reperfusion injury by activating Nrf2. *Hypertension* 63, 80–87. doi: 10.1161/hypertensionaha.113.01639

Kobayashi, S., and Liang, Q. (2015). Autophagy and mitophagy in diabetic cardiomyopathy. *Biochim. Biophys. Acta* 1852, 252–261. doi: 10.1016/j.bbadis.2014.05.020

Kopacz, A., Kloska, D., Forman, H. J., Jozkowicz, A., and Grochot-Przeczek, A. (2020). Beyond repression of Nrf2: an update on Keap1. *Free Radic. Biol. Med.* doi: 10.1016/j.freeradbiomed.2020.03.023 [Online ahead of print].

Li, J., Ichikawa, T., Janicki, J. S., and Cui, T. (2009a). Targeting the Nrf2 pathway against cardiovascular disease. *Expert Opin. Ther. Targets* 13, 785–794. doi: 10.1517/14728220903025762

Li, J., Ichikawa, T., Villacorta, L., Janicki, J. S., Brower, G. L., Yamamoto, M., et al. (2009b). Nrf2 protects against maladaptive cardiac responses to hemodynamic stress. *Arterioscler. Thromb. Vasc. Biol.* 29, 1843–1850. doi: 10.1161/atvbaha.109.189480

Li, J., Ichikawa, T., Jin, Y., Hofseth, L. J., Nagarkatti, P., Nagarkatti, M., et al. (2010). An essential role of Nrf2 in American ginseng-mediated anti-oxidative actions in cardiomyocytes. *J. Ethnopharmacol.* 130, 222–230. doi: 10.1016/j.jep.2010.03.040

Ma, X., Liu, H., Foyil, S. R., Godar, R. J., Weinheimer, C. J., Hill, J. A., et al. (2012). Impaired autophagosome clearance contributes to cardiomyocyte death in ischemia/reperfusion injury. *Circulation* 125, 3170–3181. doi: 10.1161/circulationaha.111.041814

Maher, J., and Yamamoto, M. (2010). The rise of antioxidant signaling–the evolution and hormetic actions of Nrf2. *Toxicol. Appl. Pharmacol.* 244, 4–15. doi: 10.1016/j.taap.2010.01.011

Moulis, M., and Vindis, C. (2017). Methods for measuring autophagy in mice. *Cells* 6:E14.

Ouyang, C., You, J., and Xie, Z. (2014). The interplay between autophagy and apoptosis in the diabetic heart. *J. Mol. Cell Cardiol.* 71, 71–80. doi: 10.1016/j.yjmcc.2013.10.014

Qin, Q., Qu, C., Niu, T., Zang, H., Qi, L., Lyu, L., et al. (2016). Nrf2-mediated cardiac maladaptive remodeling and dysfunction in a setting of autophagy insufficiency. *Hypertension* 67, 107–117. doi: 10.1161/hypertensionaha.115.06062

Robledinos-Anton, N., Fernandez-Gines, R., Manda, G., and Cuadrado, A. (2019). Activators and inhibitors of NRF2: a review of their potential for clinical development. *Oxid. Med. Cell Longev.* 2019:9372182.

Silva-Islas, C. A., and Maldonado, P. D. (2018). Canonical and non-canonical mechanisms of Nrf2 activation. *Pharmacol. Res.* 134, 92–99. doi: 10.1016/j.phrs.2018.06.013

Sussan, T. E., Rangasamy, T., Blake, D. J., Malhotra, D., El-Haddad, H., Bedja, D., et al. (2009). Targeting Nrf2 with the triterpenoid CDDO-imidazolide attenuates cigarette smoke-induced emphysema and cardiac dysfunction in mice. *Proc. Natl. Acad. Sci. U.S.A.* 106, 250–255. doi: 10.1073/pnas.0804333106

Swynghedauw, B. (1999). Molecular mechanisms of myocardial remodeling. *Physiol. Rev.* 79, 215–262. doi: 10.1152/physrev.1999.79.1.215

Tsutsui, H., Kinugawa, S., and Matsushima, S. (2011). Oxidative stress and heart failure. *Am. J. Physiol. Heart Circ. Physiol.* 301, H2181–H2190.

Virani, S. S., Alonso, A., Benjamin, E. J., Bittencourt, M. S., Callaway, C. W., Carson, A. P., et al. (2020). Heart disease and stroke statistics-2020 update: a report from the american heart association. *Circulation* 141, e139–e596.

Wang, W., Li, S., Wang, H., Li, B., Shao, L., Lai, Y., et al. (2014). Nrf2 enhances myocardial clearance of toxic ubiquitinated proteins. *J. Mol. Cell Cardiol.* 72, 305–315. doi: 10.1016/j.yjmcc.2014.04.006

Wang, X., and Cui, T. (2017). Autophagy modulation: a potential therapeutic approach in cardiac hypertrophy. *Am. J. Physiol. Heart Circ. Physiol.* 313, H304–H319.

Yancy, C. W., Jessup, M., Bozkurt, B., Butler, J., Casey, D. E. Jr., Drazner, M. H., et al. (2013). 2013 ACCF/AHA guideline for the management of heart failure: executive summary: a report of the American College of Cardiology

Foundation/American Heart Association Task Force on practice guidelines. *Circulation* 128, 1810–1852.

Zhang, Y., Sano, M., Shinmura, K., Tamaki, K., Katsumata, Y., Matsuhashi, T., et al. (2010). 4-hydroxy-2-nonenal protects against cardiac ischemia-reperfusion injury via the Nrf2-dependent pathway. *J. Mol. Cell Cardiol.* 49, 576–586. doi: 10.1016/j.yjmcc.2010.05.011

Zhu, H., Jia, Z., Misra, B. R., Zhang, L., Cao, Z., Yamamoto, M., et al. (2008). Nuclear factor E2-related factor 2-dependent myocardiac cytoprotection against oxidative and electrophilic stress. *Cardiovasc. Toxicol.* 8, 71–85. doi: 10.1007/s12012-008-9016-0

Conflict of Interest: The authors declare that the research was conducted in the absence of any commercial or financial relationships that could be construed as a potential conflict of interest.

frontiers in Physiology

MINI REVIEW
published: 28 July 2020
doi: 10.3389/fphys.2020.00858

Targeting Protein Kinase G to Treat Cardiac Proteotoxicity

*Christian U. Oeing[1,2,3], Sumita Mishra[1], Brittany L. Dunkerly-Eyring[1] and Mark J. Ranek[1]**

[1] Division of Cardiology, Department of Medicine, The Johns Hopkins Medical Institutions, Baltimore, MD, United States, [2] Department of Cardiology, Charité – University Medicine Berlin, Campus Virchow Klinikum (CVK), Berlin, Germany, [3] DZHK (German Centre for Cardiovascular Research), Partner Site Berlin, Berlin, Germany

Impaired or insufficient protein kinase G (PKG) signaling and protein quality control (PQC) are hallmarks of most forms of cardiac disease, including heart failure. Their dysregulation has been shown to contribute to and exacerbate cardiac hypertrophy and remodeling, reduced cell survival and disease pathogenesis. Enhancement of PKG signaling and PQC are associated with improved cardiac function and survival in many pre-clinical models of heart disease. While many clinically used pharmacological approaches exist to stimulate PKG, there are no FDA-approved therapies to safely enhance cardiomyocyte PQC. The latter is predominantly due to our lack of knowledge and identification of proteins regulating cardiomyocyte PQC. Recently, multiple studies have demonstrated that PKG regulates PQC in the heart, both during physiological and pathological states. These studies tested already FDA-approved pharmacological therapies to activate PKG, which enhanced cardiomyocyte PQC and alleviated cardiac disease. This review examines the roles of PKG and PQC during disease pathogenesis and summarizes the experimental and clinical data supporting the utility of stimulating PKG to target cardiac proteotoxicity.

Keywords: proteostasis, PKG, proteotoxicity, proteasome, autophagy, heart failure

OPEN ACCESS

Edited by:
Julian Stelzer, Case Western Reserve University, United States

Reviewed by:
Robert Morris Blanton, Tufts Medical Center, United States
John Jeshurun Michael, Cornell University, United States

***Correspondence:**
Mark J. Ranek
mranek1@jh.edu;
mranek1@jhmi.edu

Specialty section:
This article was submitted to Striated Muscle Physiology, a section of the journal Frontiers in Physiology

Received: *15 February 2020*
Accepted: *26 June 2020*
Published: *28 July 2020*

Citation:
Oeing CU, Mishra S, Dunkerly-Eyring BL and Ranek MJ (2020) Targeting Protein Kinase G to Treat Cardiac Proteotoxicity. Front. Physiol. 11:858. doi: 10.3389/fphys.2020.00858

INTRODUCTION

Protein kinase G (PKG) elicits cardioprotection during various forms of cardiac stress by transducing a vast array of beneficial processes (Dunkerly-Eyring and Kass, 2019; Pinilla-Vera et al., 2019). PKG stimulates left ventricular relaxation and counters pathological hypertrophy and remodeling (Dunkerly-Eyring and Kass, 2019). Insufficient PKG signaling has been implicated in the pathogenesis of cardiac disease toward heart failure, giving considerable interest to strategies to enhance PKG signaling (Kokkonen and Kass, 2017; Dunkerly-Eyring and Kass, 2019). New pharmacological approaches to stimulate PKG are being evaluated as therapy for heart failure and other forms of cardiac disease in clinical trials (Pinilla-Vera et al., 2019). However, a better understanding of the substrates targeted by PKG for cardioprotection is needed. Recently the activation of PKG was demonstrated to regulate protein homeostasis (proteostasis), to attenuate disease pathogenesis (Dunkerly-Eyring and Kass, 2019). The protein targets, underlying mechanisms, and therapeutic strategies to facilitate PKG regulation of proteostasis are only beginning to be identified.

Cardiomyocyte proteostasis is maintained by elaborate protein quality control (PQC) systems. These systems help fold polypeptide chains into properly functioning proteins, refold proteins that become misfolded or damaged during stress, and then remove terminally misfolded and/or

aggregated proteins by degradation (Wang and Robbins, 2006; Wang et al., 2008). Cardiomyocyte PQC is maintained by three separate but interlinking systems: molecular chaperones (protein folding/refolding), the ubiquitin proteasome system (UPS) (proteasome mediated degradation of soluble proteins), and autophagy (lysosomal degradation of protein aggregates and organelles) (Wang et al., 2008). Similar to PKG signaling, cardiomyocyte PQC is also perturbed/insufficient during cardiac disease pathogenesis. This results in the intracellular accumulation of proteins targeted for degradation, aggregation of proteins, and subsequent declined cardiac function; a class of disorders termed cardiac proteotoxicity (Wang and Robbins, 2006; Willis and Patterson, 2013). The proteins and macromolecular structures that are responsible for maintaining cardiomyocyte PQC are known; however, only recently have we begun to understand the proteins and/or posttranslational modifications that regulate PQC. Pharmacological strategies to safely enhance PQC are beginning to be explored. This review focuses on one protein, PKG, which has shown promise as a cardiac PQC-enhancing therapy. We will detail the studies that demonstrate a role for PKG regulating PQC during physiological and pathological states, examine the therapeutic potential of targeting PKG, and discuss potential future directions.

PROTEOTOXICITY IN HEART FAILURE

The ubiquitin-proteasome system (UPS) removes damaged and/or misfolded proteins that are first tagged by ubiquitination for degradation by the proteasome (Wang et al., 2008). Ubiquitination is mediated by multiprotein ubiquitin-activating enzymes (E1), ubiquitin-conjugating enzymes (E2), and ubiquitin ligases (E3). Ubiquitinated proteins are then translocated to the core proteasome for degradation (Amerik and Hochstrasser, 2004; Reyes-Turcu et al., 2009; Metzger et al., 2012). The mammalian proteasome is a multi-subunit protease complex composed of the 20S catalytic core particle and two 19S regulatory cap particles. The 19S regulatory subunits recognize the polyubiquitin chain and unfold the protein for subsequent degradation by the 20S catalytic core (Nussbaum et al., 1998; Lasker et al., 2012).

All forms of cardiac disease, including heart failure, present with an accumulation of ubiquitinated proteins, demonstrating the vital role the UPS has during pathogenesis (Drews et al., 2010; Su and Wang, 2010; Willis et al., 2010; Wang et al., 2011; Powell et al., 2012; Day, 2013). Indeed, dysfunctional UPS has been reported in human end-stage heart failure, ischemic heart disease, and cardiac hypertrophy (Hein et al., 2003; Weekes et al., 2003; Drews et al., 2010; Powell and Divald, 2010; Predmore et al., 2010). Weekes et al. first reported increased levels of ubiquitinated proteins in myocardial samples obtained from patients with familial dilated cardiomyopathies, which has been supported by others (Weekes et al., 2003; Chen et al., 2005; Liu et al., 2006a,b). Left ventricular unloading in humans with chronic heart failure leads to improved proteasome activity (Wohlschlaeger et al., 2010). Similar results were reported by Predmore et al. (2010), who demonstrated markedly reduced proteolytic activities in failing human hearts that was restored after LV unloading. The mechanism by which ventricular unloading stimulates proteasome activity remains unknown; however, there are multiple potential explanations: (1) LV unloading decreases intracellular ROS, thus oxidized proteins for proteasomal degradation along with less oxidation of the proteasome itself; (2) a separate post-translational modification(s) of the UPS by yet to be identified kinase(s) (Predmore et al., 2010). Proteasome inhibition in pre-clinical models is associated with exacerbated or accelerated pathogenesis of cardiac disease. Mice treated with bortezomib (proteasome inhibitor) worsened transaortic constriction (TAC)-induced cardiac hypertrophy, resulting in early heart failure and death in mice (Tang et al., 2010). These findings were supported by a study using a genetic cardiomyocyte restricted-proteasome inhibited mouse model (beta5^{T60A}) following TAC surgery (Ranek et al., 2015). Similarly, models of myocardial ischemia demonstrated that pretreatment of isolated rat hearts with a proteasome inhibitor dose-dependently decreased post-ischemic cardiac function (Powell et al., 2005). Tian et al. (2012) reported mice that express a threonine 60 to alanine mutation on the proteasome subunit beta 5 (beta5^{T60A}) to reduce the proteolytic activity of the proteasome had worsened myocardial ischemia-reperfusion injury. Impaired or insufficient proteasome activity has been associated with myocarditis (Szalay et al., 2006) and diabetic cardiomyopathy (Li and Wang, 2011). Genetic overexpression of key proteasome subunits enhances proteasome-mediated protein degradation and protects the heart against oxidative stress, proteotoxicity, and myocardial ischemia (Li et al., 2011a,b). Together, these studies demonstrate the prominent role the UPS has in degrading proteins to maintain proteostasis during cardiac disease.

The other primary mediator of cardiomyocyte proteostasis is autophagy, which is comprised of macroautophagy, microautophagy, chaperone-mediated autophagy, and organelle-specific autophagy (e.g., mitophagy) (Ghosh and Pattison, 2018). Macroautophagy involves the formation of an autophagosome which surrounds the cargo for degradation by the lysosome. Microautophagy is the direct engulfment of cellular debris by the lysosome. Chaperone-mediated autophagy degrades proteins containing a KFERQ pentapeptide motif that are translocated into the lysosome via a heat shock cognate 70 (Hsc70) chaperone complex (Dice, 1990). Autophagy is required for the development, differentiation, and function of cardiomyocytes (Nakai et al., 2007; Zhang et al., 2012; Ikeda et al., 2015) and has an important role in cardioprotection (Gustafsson and Gottlieb, 2008; Sciarretta et al., 2014).

Dysregulated autophagic flux is associated with and has been implicated in the pathogenesis of many forms of cardiac disease. Formation of autophagosomes in dilated cardiomyopathy patients has a positive correlation with better prognosis, indicating the protective role of autophagy in heart failure (Saito et al., 2016). Many pre-clinical models have associated reduced autophagy with heart failure and cardiac functional decline (Eisenberg et al., 2016; Shirakabe et al., 2016; Ghosh

and Pattison, 2018). Mice with mutations in *MYBPC3* (cardiac myosin-binding protein C) and in *MYH7* (β-myosin heavy) forms of hypertrophic cardiomyopathy (HCM) present with an accumulation of autophagic vacuoles, suggesting impaired autophagic flux (Schlossarek et al., 2012; Song et al., 2014; Carrier et al., 2015; Singh et al., 2017). Further, deletion of Atg5 (autophagy related gene 5), a key protein involved in the extension of the phagophore membrane during autophagic vesicle formation, causes cardiac hypertrophy and left ventricular dysfunction (Nakai et al., 2007; Pattison et al., 2011). In a cardiac proteinopathy model ($CryAB^{R120G}$), cardiac-specific overexpression of Atg7 increased autophagic activity and improved cardiac function (Bhuiyan et al., 2013). Obese mice see the downregulation of several autophagic genes, including Atg7 (Sciarretta et al., 2012). The exact mechanism for the downregulation of Atg7 was not revealed in these studies; however, it is known that proteinopathy and obesity are characterized by increased mammalian (mechanistic) target of rapamycin complex 1 (mTORC1) activity, which suppresses Atg7 expression (Sciarretta et al., 2018). Interestingly the increased expression of Atg7 in the heart prevents the heart from hypertrophying in response to high-fat diet-induced obesity (Tong et al., 2018). Autophagic flux was reduced in both type 1 and 2 diabetic mouse models and in aged mice (Epstein et al., 1989; Lee et al., 1996; Xie et al., 2011; Kanamori et al., 2015; Munasinghe et al., 2016; Nakamura and Sadoshima, 2018).

Collectively, these studies demonstrate the pivotal role that proteostasis, specifically the UPS and autophagy, has during cardiac pathogenesis (**Figure 1**). To translate these findings to the clinic to directly target cardiac proteotoxicity, a better understanding of the mechanisms regulating PQC and identification of druggable targets is needed. This review describes exciting investigations into a potential target that has the ability to enhance cardiomyocyte PQC and has many therapeutic strategies available.

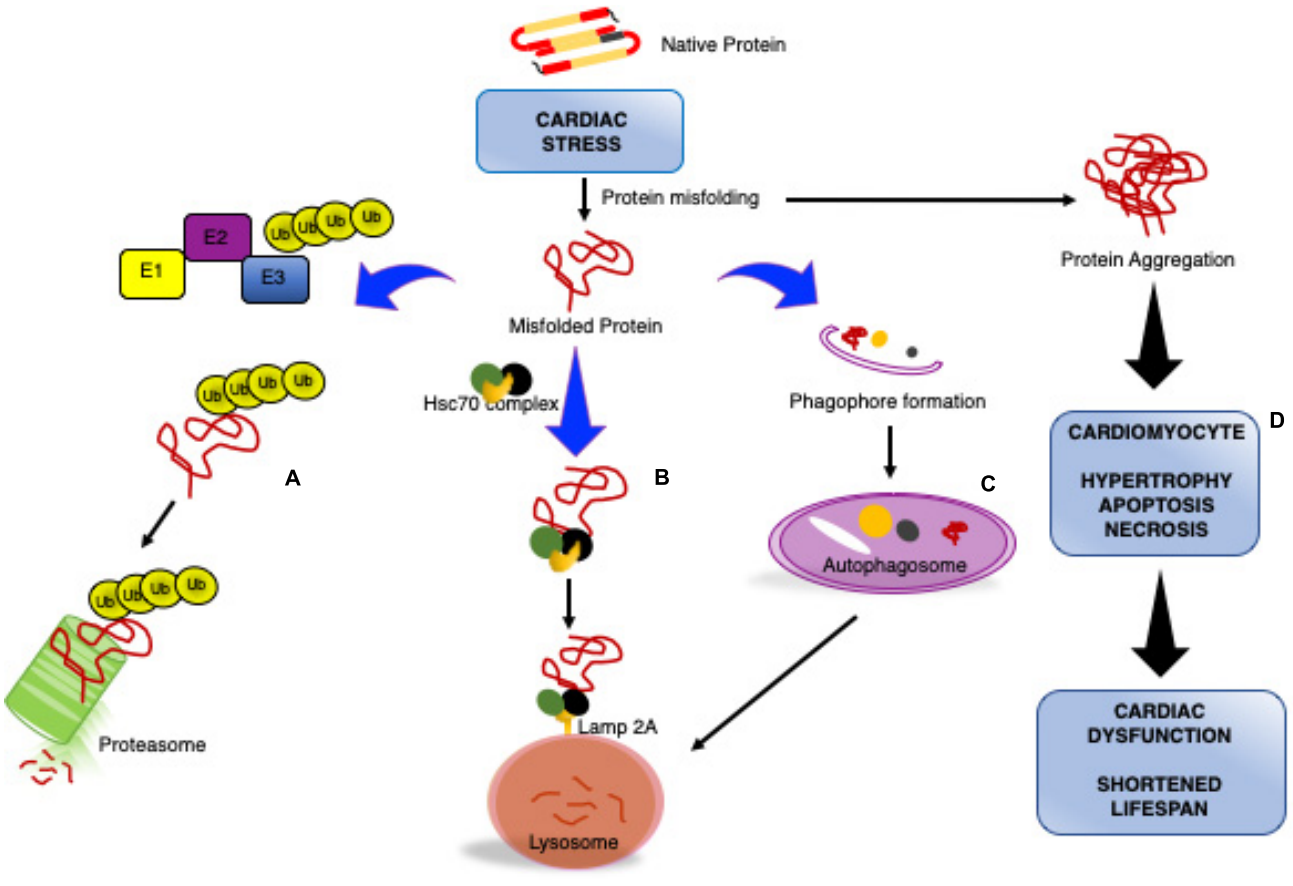

FIGURE 1 | Impaired cardiomyocyte proteostasis results in cardiac dysfunction. Cardiac pathologic stress increases production/formation of misfolded proteins that if not removed form large, insoluble protein aggregates. Cardiomyocytes utilize various processes to maintain proteostasis: misfolded proteins will be catalyzed by the ubiquitin proteasome system (UPS) through ubiquitination via a series of enzymatic reactions involving an ubiquitin activating enzyme (E1), ubiquitin conjugating enzyme (E2), and ubiquitin ligase (E3) for degradation by the proteasome **(A)**. Chaperone-mediated autophagy is a process by which the heat shock cognate 70 (HSC70) complex recognizes and binds select protein targets for internalization and degradation to the lysosome through the lysosome-associated membrane protein 2A (LAMP2A) receptor **(B)**. Macroautophagy is the bulk removal of proteins, protein aggregates, and organelles by first forming an autophagosome to surround the cargo followed by merging with the lysosome for degradation **(C)**. The insufficiency or overwhelming of the protein degradation systems during cardiac stress results in an accumulation of aggregated proteins, culminating in reduced cardiac function and lifespan **(D)**.

The Role of PKG in Proteotoxicity

Protein kinase G is stimulated by cyclic guanosine monophosphate (cGMP). cGMP is generated downstream of nitric oxide (NO) or natriuretic peptide (NP) activation of guanylate cyclase (GC-1, formerly soluble—sGC) and GC-2 (formerly particulate—pGC), respectively (Dunkerly-Eyring and Kass, 2019). Phosphodiesterases (PDEs) selective for cGMP (PDEs 5 and 9 in the heart) negatively regulate PKG activity. PDE regulation of PKG activity is known to be highly compartmentalized within the cardiomyocyte, adding a level of regulation (Kokkonen and Kass, 2017; Dunkerly-Eyring and Kass, 2019). Indeed, PDE5A primarily regulates NO-generated cGMP, which tends to be dispersed throughout the cytosol of the cardiomyocyte, whereas PDE9A regulates the cGMP pool that is localized at the membrane (Kokkonen and Kass, 2017). PDE1, a dual cAMP and cGMP esterase, regulates PKA and PKG activity in an isoform-specific manner in the heart (Hashimoto et al., 2018; Kokkonen-Simon et al., 2018; Dunkerly-Eyring and Kass, 2019).

Multiple strategies of PKG activation have proven to be cardioprotective in response to various pathological stimuli: inhibition of PDE5 or PDE9 reduced cardiac hypertrophy and improved function following left ventricular pressure overload (PO) induced by TAC (Takimoto et al., 2005; Nagayama et al., 2009; Lee et al., 2015). Stimulating PKG directly reduced infarct size and myocardial fibrosis/remodeling following myocardial infarction and ischemia-reperfusion injury (Das et al., 2006; Salloum et al., 2008; Krieg et al., 2009). Neurohormonal stimulation of G-protein-coupled (Gq and Gi) receptor signaling is suppressed by PKG phosphorylation of and/or binding to the regulator of G protein signaling (RGS) proteins, RGS2 and RGS4 (Takimoto et al., 2009). PKG phosphorylates and inhibits the transient receptor potential cation channels type 6 (TRPC6) to block calcineurin/NFAT signaling (Kinoshita et al., 2010; Koitabashi et al., 2010; Nishida et al., 2010) and RhoA to decrease Rho-kinase (Sawada et al., 2001). PKG also regulates mechanosensing via phosphorylation of the sarcomeric proteins: myosin-binding protein C, phospholamban, TnI, and titin (Raeymaekers et al., 1988; Kruger et al., 2009; Thoonen et al., 2015; Rainer and Kass, 2016). Collectively, these studies demonstrate the ability of PKG to correct pathological imbalances, but evidence that PKG stimulation could restore proteostasis during cardiac disease is more recent and forthcoming.

With PKG acting as a brake on many pathological processes, the attention turned to a potential regulation of cardiomyocyte proteostasis. Over the last decade, multiple studies have indicated that PKG activation enhances PQC as a primary mechanism of action to protect the myocardium. Pioneering studies from the Wang lab discovered PKG positively regulates proteasome activity by phosphorylating key proteasome subunits, Rpt6 of the 19S cap and Beta5 of the 20S proteolytic core (Ranek et al., 2013). Intriguingly, activation of PKG pharmacologically (PDE5 inhibitor, sildenafil) or genetically (expression of a constitutively active PKG) in a proteinopathy model ($CryAB^{R120G}$) reduced the accumulation of ubiquitinated proteins and cleared the degradation of misfolded, but not normal, proteins (Ranek et al., 2013). Enhanced PQC with PKG stimulation was associated with reduced cytotoxicity (*in vitro*) and improved cardiac function (*in vivo*) (Ranek et al., 2013). Similarly, VerPlank et al. (2020) reported stimulation PKG with both a PDE5 inhibitor or GC-1 activator enhanced proteasome proteolytic activity, the degradation of short lived-and long lived proteins, and determined a direct relationship between PKG and purified proteasomes. Stimulation of PKG via activation of the muscarinic 2 receptor also increased proteasome activity (Ranek et al., 2014), suggesting both the plasma membrane localized and cytosolic localized pools of PKG can enhance proteasome activity. Inhibition of PKG or antagonizing muscarinic 2 receptors decreased the proteasome peptidase activities in both the absence or presence of ATP (Ranek et al., 2013, 2014), suggesting that PKG basally regulates proteasome peptidase activities. These data were supported by and expanded on by a recent study using a PDE1 inhibitor, IC86430 (Zhang et al., 2019). Here the authors utilized $CryAB^{R120G}$ proteinopathy mice, which develop a heart failure with a preserved ejection fraction (HFpEF)-like phenotype, and show increased expression of the PDE1A isoform. Inhibition of PDE1 in these mice and cultured cardiomyocytes attenuated proteotoxic stress, increased proteasome activity, and extended mouse lifespan in a PKA and PKG-dependent manner (Zhang et al., 2019). Collectively these findings demonstrate that PKG regulates proteasome activities, proteasome-mediated degradation of misfolded proteins, and that pharmacological approaches can be utilized to elicit these responses.

Recently, it was reported that PKG can also enhance macroautophagy to enhance cardiomyocyte PQC to attenuate cardiac hypertrophy. Tuberous sclerosis complex 2 (TSC2, tuberin), an upstream negative regulator of mTORC1, is phosphorylated by various kinases that can either inhibit (Akt and ERK) or stimulate (AMPK and GSK-3β) its activity. The Kass lab recently reported a new signaling paradigm whereby PKG phosphorylates TSC2 at serine 1365 (1364 in humans) (Ranek et al., 2019). Interestingly, this regulation is itself dependent on the redox state of PKG with reduced phosphorylation of TSC2 detected with oxidation of PKG at cysteine 42 (Oeing et al., 2020). Unlike other TSC2 phosphorylation sites, the phosphorylation of 1365 did not affect basal mTORC1 activity. However, a potent inhibition of mTORC1 hyperactivity was observed once mouse hearts were subjected to hemodynamic (left ventricular pressure overload), or cardiomyocytes to hormonal, stress (endothelin-1). PQC was enhanced as evidenced by upregulation of autophagic flux, clearance of ubiquitinated proteins, and decreased protein aggregation (Ranek et al., 2019). TSC2 S1365 phospho-mimetic decreased, whereas phospho-null exacerbated cardiomyocyte cell size and cytotoxicity following endothelin-1 treatment. Phospho-mimetic mice had attenuated cardiac hypertrophy, improved function, and extended lifespan in response to pressure overload, with opposing findings yielded in phospho-null mice (Ranek et al., 2019). This phosphosite on TSC2 is unique in that there only appears to be mTORC1 regulation in the presence of a pathological co-stimulus, thereby not altering the physiological homeostatic role of mTORC1 (Manning, 2019). Considering the issues with chronic, broad mTORC1 inhibition, utilizing a

pharmacological approach with a PKG stimulator represents a unique advantage.

THERAPEUTIC STRATEGIES TO TARGET PROTEOTOXICITY VIA PKG

Currently, there are no approved therapeutic strategies to enhance PQC. However, interest has increased as more and more studies implicate exacerbated disease pathogenesis with proteotoxicity, and the evidence in pre-clinical models that PQC enhancement strategies elicit cardioprotection. PKG is an attractive therapeutic target for multiple reasons: (1) PKG modulators have been used in clinic for decades, (2) PKG activators/stimulators boast an excellent safety profile and are well tolerated, and (3) there are many proteins available to interrogate the PKG pathway (Kokkonen-Simon et al., 2018; Dunkerly-Eyring and Kass, 2019; Pinilla-Vera et al., 2019). The first PKG activators were used in the 1800 s in the form of inhaled organic nitrates to treat angina pectoris (Kots et al., 2009; Daiber and Munzel, 2015). It would be roughly 100 years before it was discovered that these work by releasing NO and enhancing cGMP levels (Schlossmann and Schinner, 2012). Therapeutic strategies available to activate the PKG pathway either aim to promote cGMP synthesis (e.g., GC-1 stimulators and activators) or to inhibit cGMP degradation (e.g., PDE5 inhibitors), or both. The GC-1 stimulator, Riociguat, is approved for the treatment of pulmonary arterial hypertension (PAH) as well as inoperable chronic thromboembolic pulmonary hypertension. GC-1 stimulators are being tested in heart failure, diabetic nephropathy, systemic sclerosis, as well as sickle cell disease and central nervous system disease (Xiao et al., 2019). The GC-1 stimulator, vericiguat, was tested in clinical trials for both heart failure with a reduced ejection fraction (HFrEF) [SOCRATES-REDUCED NCT01951625 (Gheorghiade et al., 2015) and VICTORIA NCT02861534 (Armstrong et al., 2018)] and in HFpEF (SOCRATES-PRESERVE NCT01951638) (Filippatos et al., 2017; Pieske et al., 2017). Sacubitril/valsartan (entresto) that combines a neprilysin inhibitor with an angiotensin receptor blocker is increasingly popular as a heart failure therapy, as demonstrated in the PARADIGM-HF (NCT01035255) trial (McMurray et al., 2014; Fala, 2015). The ability of neprilysin inhibitors to increase the levels of natriuretic peptides make PKG a potential target of sacubitril/valsartan (Yan et al., 2003; Riddell and Vader, 2017). Indeed, a 2019 study determined that sacubitril/valsartan decreased cardiac fibrosis in a mouse cardiac hypertrophy model and protected cardiac fibroblasts from myofibroblast transition via PKG-dependent inhibition of RhoA activation (Burke et al., 2019).

These trials did not specifically implicate impairment in proteostasis; however, existing data from human heart tissue suggest that proteostasis is impaired in a disease specific manner. Understanding the PQC systems that are perturbed in different diseases will allow for selective therapeutic targeting. Polyubiquitinated proteins are increased in failing hearts in early as well as late stage disease, suggesting that accumulation of polyubiquitinated proteins occurs before the development of decompensated heart failure (Day, 2013). A histological study from human failing hearts due to idiopathic dilated cardiomyopathy (DCM) noted colocalization of ubiquitin with monodansylcadaverine, a specific marker for autophagic vacuoles, suggesting a link between ubiquitin conjugate accumulation and autophagy (Kostin et al., 2003). Patients with ischemic cardiomyopathy (ICM) and DCM show differential UPS activity patterns. Human ICM heart tissue exhibits reduced trypsin-like proteasomal activity compared to DCM, while both chymotrypsin- and caspase-like proteasomal activities were reduced in DCM and ICM hearts compared to non-failing controls (Spanig et al., 2019). HCM is also characterized by a reduction in chymotrypsin- and caspase-like activities compared to control hearts (Predmore et al., 2010). Failing human hearts exhibit reduced proteasome activity compared to donor controls, which is thought to be related to reduced docking of the 19S proteasome to the 20S proteasome and decreased phosphorylation of Rpt6 (Day, 2013), a potential target of PKG (Ranek et al., 2013). Right ventricular heart disease has not been focused on in clinical trials regarding proteostasis despite emerging data of its important role (Rajagopalan et al., 2013; Drews, 2014; Drews and Taegtmeyer, 2014). Hence, new insights into the regulation of proteostasis via PKG signaling in these diseases might help select the correct patient cohort for successful therapy.

Although the PKG pathway has long been a focus to treat cardiac disease, only recently has the stimulation of PKG been suggested as a new therapeutic strategy to treat cardiac proteinopathies (**Figure 2**). HFpEF is a lethal syndrome for which there are no evidence-based therapies, characterized by an imbalance in NO levels and low myocardial cGMP and PKG activity (Rainer and Kass, 2016; Schiattarella et al., 2019). A novel murine HFpEF model required metabolic stress accompanied by L-NAME, an NO synthase inhibitor, hence PKG inhibitor, to present some HFpEF symptoms (Schiattarella et al., 2019). These findings suggest that decreased PKG activity facilitates the development and pathogenesis of HFpEF. PDE5 inhibition reduced ER stress in isoproterenol-treated rats and pressure-overloaded mice (Rainer and Kass, 2016) and could successfully treat a desmin-related proteinopathy of the murine heart (Ranek et al., 2013). Xuejun Wang's group reported that inhibiting PDE1, which hydrolyzes both cAMP and cGMP, increases 26S proteasome activity in a $CryAB^{R120G}$-based proteinopathy of the murine heart (Zhang et al., 2019). Treatment with PDE1 inhibitor IC86430 increased proteasome phosphorylation, reduced misfolded CryAB protein in the murine heart, attenuated HFpEF-like phenotype, and ultimately improved survival (Zhang et al., 2019). These studies further support the notion that activating PKG could be beneficial in HFpEF therapy, at least in part by enhancing PQC. Inhibitors of mTORC1 potently increase autophagic flux, attenuate cardiac hypertrophy, and enhance function; however, chronic use leads to cardiac dilation and failure along with immunosuppression and metabolic disturbances (Benjamin et al., 2011; Zeng et al., 2013). These deleterious side effects can be avoided by

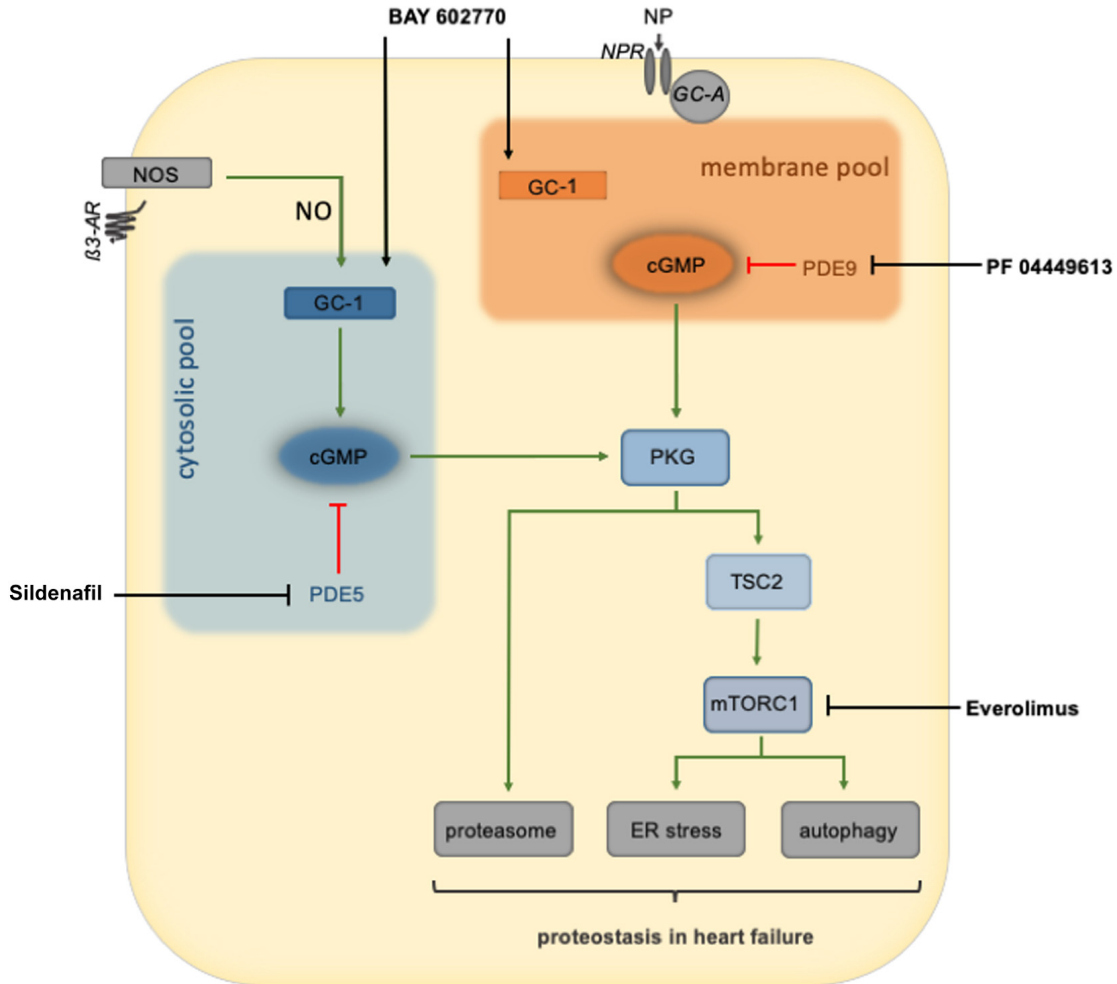

FIGURE 2 | An overview of PKG regulation of cardiomyocyte protein quality control and therapeutic interventions to stimulate PKG activity. PKG is thought to be divided into two primary pools: the membrane and cytosolic pools. Natriuretic peptides binding to the natriuretic peptide receptor activate guanylate cyclase to produce cGMP and ultimately stimulate the membrane pool of PKG. Nitric oxide, produced by nitric oxide synthase, activates guanylate cyclase-1 to produce cGMP, culminating in the activation of the cytosolic PKG pool. Once activated, PKG can increase the activity of the proteasome or phosphorylation of TSC2 to inhibit mTORC1 and enhance autophagic flux. PKG stimulation of the proteasome or autophagy restores cardiomyocyte proteostasis during cardiac stress. AR, adrenoreceptor; GC-1, soluble guanylate cyclase 1; GC-A, guanylyl cyclase-A (*receptor*); GMP, cyclic guanylyl monophosphate; ER, endoplasmatic reticulum; mTORC1, mammalian target of rapamycin complex 1; NOS, nitric oxide synthase; NP, natriuretic peptide; NPR, NP receptor; PDE, phosphodiesterase; PKG, protein kinase G; PQC, protein quality control; TSC2, tuberin/tuberous sclerosis complex 2.

stimulating PKG to inhibit mTORC1, hence might present a better tool than mTOR inhibitors (Manning, 2019; Ranek et al., 2019). Collectively these studies demonstrate that (1) PKG is vital to maintain proteostasis basally, (2) many therapeutic targets (NO, NPs, PDEs) are available to stimulate PKG, and (3) PKG activators/stimulators could be the first therapy that enhances PQC, is cardioprotective, and does so without deleterious side effects.

CONCLUSION

Our knowledge of the protein kinases that regulate cardiomyocyte PQC has vastly expanded. The discovery of new targets to pursue, pharmacological strategies to test, and increased understanding of the regulatory mechanisms are pivotal to translating successful experimental studies into efficacious clinical therapies. Several crucial hurdles remain. The first being the safety of a therapy, as agents may increase PQC but as a compensatory mechanism for damage induced by the therapy. Second issue is having druggable targets for therapeutic interventions. The third hurdle is to match the appropriate disease state to the PQC deficiency to the microdomain in which the kinase and PQC system reside. PKG activators/stimulators are safe and well tolerated and many are already in clinical use. Further research to gain a precise understanding of the microdomains these compounds work in and PQC machinery they associate with will identify the conditions and patient

subsets that will likely benefit from specific PKG modulation. The final hurdle is the need for a blood biomarker capable of detecting impaired proteostasis in the heart, which to the best of our knowledge has not been verified. This would be essential to detect patients that might benefit from strategies to improve cardiomyocyte PQC and to monitor potential success of the therapy.

DISCLOSURE STATEMENT

BD-E and MR are co-inventors on a patent application (PCT: 448070145WO1) that was filed in July 2018 (provisional filed in June 2017). The patent relates to the use of TSC2(S1365/S1364) modifications for immunological applications.

AUTHOR CONTRIBUTIONS

MR conceived and designed the framework for the review and supervised the writing. CO wrote the manuscript with assistance from SM and BD-E. All authors provided critical feedback while writing the manuscript.

FUNDING

This study was supported by the NIH – National Heart, Lung, and Blood Institute grant F31-HL143905 (BD-E), the Deutsche Forschungsgemeinschaft (German Research Foundation) OE 688/1-1 (CO), the BIH Charité Clinician Scientist Program (CO), Amyloidosis Foundation Donald C. Brockman Memorial Research Grant (MR), and an American Heart Association Career Development Award 18CDA34110140 (MR).

REFERENCES

Amerik, A. Y., and Hochstrasser, M. (2004). Mechanism and function of deubiquitinating enzymes. *Biochim. Biophys. Acta* 1695, 189–207. doi: 10.1016/j.bbamcr.2004.10.003

Armstrong, P. W., Roessig, L., Patel, M. J., Anstrom, K. J., Butler, J., Voors, A. A., et al. (2018). A multicenter, randomized, double-blind, placebo-controlled trial of the efficacy and safety of the oral soluble guanylate cyclase stimulator: the VICTORIA trial. *JACC Heart Fail.* 6, 96–104. doi: 10.1016/j.jchf.2017.08.013

Benjamin, D., Colombi, M., Moroni, C., and Hall, M. N. (2011). Rapamycin passes the torch: a new generation of mTOR inhibitors. *Nat. Rev. Drug Discov.* 10, 868–880. doi: 10.1038/nrd3531

Bhuiyan, M. S., Pattison, J. S., Osinska, H., James, J., Gulick, J., McLendon, P. M., et al. (2013). Enhanced autophagy ameliorates cardiac proteinopathy. *J. Clin. Invest.* 123, 5284–5297. doi: 10.1172/jci70877

Burke, R. M., Lighthouse, J. K., Mickelsen, D. M., and Small, E. M. (2019). Sacubitril/valsartan decreases cardiac fibrosis in left ventricle pressure overload by restoring PKG signaling in cardiac fibroblasts. *Circ. Heart Fail.* 12: e005565.

Carrier, L., Mearini, G., Stathopoulou, K., and Cuello, F. (2015). Cardiac myosin-binding protein C (MYBPC3) in cardiac pathophysiology. *Gene* 573, 188–197. doi: 10.1016/j.gene.2015.09.008

Chen, Q., Liu, J. B., Horak, K. M., Zheng, H., Kumarapeli, A. R., Li, J., et al. (2005). Intrasarcoplasmic amyloidosis impairs proteolytic function of proteasomes in cardiomyocytes by compromising substrate uptake. *Circ. Res.* 97, 1018–1026. doi: 10.1161/01.res.0000189262.92896.0b

Daiber, A., and Munzel, T. (2015). Organic nitrate therapy, nitrate tolerance, and nitrate-induced endothelial dysfunction: emphasis on redox biology and oxidative stress. *Antioxid. Redox Signal.* 23, 899–942. doi: 10.1089/ars.2015.6376

Das, A., Smolenski, A., Lohmann, S. M., and Kukreja, R. C. (2006). Cyclic GMP-dependent protein kinase Ialpha attenuates necrosis and apoptosis following ischemia/reoxygenation in adult cardiomyocyte. *J. Biol. Chem.* 281, 38644–38652. doi: 10.1074/jbc.m606142200

Day, S. M. (2013). The ubiquitin proteasome system in human cardiomyopathies and heart failure. *Am. J. Physiol. Heart Circ. Physiol.* 304, H1283–H1293.

Dice, J. F. (1990). Peptide sequences that target cytosolic proteins for lysosomal proteolysis. *Trends Biochem. Sci.* 15, 305–309. doi: 10.1016/0968-0004(90)90019-8

Drews, O. (2014). The left and right ventricle in the grip of protein degradation: similarities and unique patterns in regulation. *J. Mol. Cell. Cardiol.* 72, 52–55. doi: 10.1016/j.yjmcc.2014.02.016

Drews, O., and Taegtmeyer, H. (2014). Targeting the ubiquitin-proteasome system in heart disease: the basis for new therapeutic strategies. *Antioxid. Redox Signal.* 21, 2322–2343. doi: 10.1089/ars.2013.5823

Drews, O., Tsukamoto, O., Liem, D., Streicher, J., Wang, Y., and Ping, P. (2010). Differential regulation of proteasome function in isoproterenol-induced cardiac hypertrophy. *Circ. Res.* 107, 1094–1101. doi: 10.1161/circresaha.110.222364

Dunkerly-Eyring, B., and Kass, D. A. (2019). Myocardial phosphodiesterases and their role in cGMP regulation. *J. Cardiovasc. Pharmacol.* 75, 483–493. doi: 10.1097/fjc.0000000000000773

Eisenberg, T., Abdellatif, M., Schroeder, S., Primessnig, U., Stekovic, S., Pendl, T., et al. (2016). Cardioprotection and lifespan extension by the natural polyamine spermidine. *Nat. Med.* 22, 1428–1438.

Epstein, P. N., Overbeek, P. A., and Means, A. R. (1989). Calmodulin-induced early-onset diabetes in transgenic mice. *Cell* 58, 1067–1073. doi: 10.1016/0092-8674(89)90505-9

Fala, L. (2015). Entresto (Sacubitril/Valsartan): first-in-class angiotensin receptor neprilysin inhibitor FDA approved for patients with heart failure. *Am. Health Drug Benefits* 8, 330–334.

Filippatos, G., Maggioni, A. P., Lam, C. S. P., Pieske-Kraigher, E., Butler, J., Spertus, J., et al. (2017). Patient-reported outcomes in the SOluble guanylate Cyclase stimulatoR in heArT failurE patientS with PRESERVED ejection fraction (SOCRATES-PRESERVED) study. *Eur. J. Heart Fail.* 19, 782–791. doi: 10.1002/ejhf.800

Gheorghiade, M., Greene, S. J., Butler, J., Filippatos, G., Lam, C. S., Maggioni, A. P., et al. (2015). Effect of vericiguat, a soluble Guanylate Cyclase stimulator, on natriuretic peptide levels in patients with worsening chronic heart failure and reduced ejection fraction: the socrates-reduced randomized trial. *JAMA* 314, 2251–2262.

Ghosh, R., and Pattison, J. S. (2018). Macroautophagy and chaperone-mediated autophagy in heart failure: the known and the unknown. *Oxid. Med. Cell Longev.* 2018:8602041.

Gustafsson, A. B., and Gottlieb, R. A. (2008). Recycle or die: the role of autophagy in cardioprotection. *J. Mol. Cell. Cardiol.* 44, 654–661. doi: 10.1016/j.yjmcc.2008.01.010

Hashimoto, T., Kim, G. E., Tunin, R. S., Adesiyun, T., Hsu, S., Nakagawa, R., et al. (2018). Acute enhancement of cardiac function by phosphodiesterase type 1 inhibition. *Circulation* 138, 1974–1987. doi: 10.1161/circulationaha.117.030490

Hein, S., Arnon, E., Kostin, S., Schonburg, M., Elsasser, A., Polyakova, V., et al. (2003). Progression from compensated hypertrophy to failure in the pressure-overloaded human heart: structural deterioration and compensatory mechanisms. *Circulation* 107, 984–991. doi: 10.1161/01.cir.0000051865.66123.b7

Ikeda, Y., Shirakabe, A., Maejima, Y., Zhai, P., Sciarretta, S., Toli, J., et al. (2015). Endogenous Drp1 mediates mitochondrial autophagy and protects the heart

against energy stress. *Circ. Res.* 116, 264–278. doi: 10.1161/circresaha.116.303356

Kanamori, H., Takemura, G., Goto, K., Tsujimoto, A., Mikami, A., Ogino, A., et al. (2015). Autophagic adaptations in diabetic cardiomyopathy differ between type 1 and type 2 diabetes. *Autophagy* 11, 1146–1160. doi: 10.1080/15548627.2015.1051295

Kinoshita, H., Kuwahara, K., Nishida, M., Jian, Z., Rong, X., Kiyonaka, S., et al. (2010). Inhibition of TRPC6 channel activity contributes to the antihypertrophic effects of natriuretic peptides-guanylyl cyclase-A signaling in the heart. *Circ. Res.* 106, 1849–1860. doi: 10.1161/circresaha.109.208314

Koitabashi, N., Aiba, T., Hesketh, G. G., Rowell, J., Zhang, M., Takimoto, E., et al. (2010). Cyclic GMP/PKG-dependent inhibition of TRPC6 channel activity and expression negatively regulates cardiomyocyte NFAT activation Novel mechanism of cardiac stress modulation by PDE5 inhibition. *J. Mol. Cell. Cardiol.* 48, 713–724. doi: 10.1016/j.yjmcc.2009.11.015

Kokkonen, K., and Kass, D. A. (2017). Nanodomain regulation of cardiac cyclic nucleotide signaling by phosphodiesterases. *Annu. Rev. Pharmacol. Toxicol.* 57, 455–479. doi: 10.1146/annurev-pharmtox-010716-104756

Kokkonen-Simon, K. M., Saberi, A., Nakamura, T., Ranek, M. J., Zhu, G., Bedja, D., et al. (2018). Marked disparity of microRNA modulation by cGMP-selective PDE5 versus PDE9 inhibitors in heart disease. *JCI Insight* 3:e121739.

Kostin, S., Pool, L., Elsasser, A., Hein, S., Drexler, H. C., Arnon, E., et al. (2003). Myocytes die by multiple mechanisms in failing human hearts. *Circ. Res.* 92, 715–724. doi: 10.1161/01.res.0000067471.95890.5c

Kots, A. Y., Martin, E., Sharina, I. G., and Murad, F. (2009). A short history of cGMP, guanylyl cyclases, and cGMP-dependent protein kinases. *Handb. Exp. Pharmacol.* 191, 1–14. doi: 10.1007/978-3-540-68964-5_1

Krieg, T., Liu, Y., Rutz, T., Methner, C., Yang, X. M., Dost, T., et al. (2009). BAY 58-2667, a nitric oxide-independent guanylyl cyclase activator, pharmacologically post-conditions rabbit and rat hearts. *Eur. Heart J.* 30, 1607–1613. doi: 10.1093/eurheartj/ehp143

Kruger, M., Kotter, S., Grutzner, A., Lang, P., Andresen, C., Redfield, M. M., et al. (2009). Protein kinase G modulates human myocardial passive stiffness by phosphorylation of the titin springs. *Circ. Res.* 104, 87–94. doi: 10.1161/circresaha.108.184408

Lasker, K., Forster, F., Bohn, S., Walzthoeni, T., Villa, E., Unverdorben, P., et al. (2012). Molecular architecture of the 26S proteasome holocomplex determined by an integrative approach. *Proc. Natl. Acad. Sci. U.S.A.* 109, 1380–1387. doi: 10.1073/pnas.1120559109

Lee, D. I., Zhu, G., Sasaki, T., Cho, G. S., Hamdani, N., Holewinski, R., et al. (2015). Phosphodiesterase 9A controls nitric-oxide-independent cGMP and hypertrophic heart disease. *Nature* 519, 472–476. doi: 10.1038/nature14332

Lee, G. H., Proenca, R., Montez, J. M., Carroll, K. M., Darvishzadeh, J. G., Lee, J. I., et al. (1996). Abnormal splicing of the leptin receptor in diabetic mice. *Nature* 379, 632–635. doi: 10.1038/379632a0

Li, J., Horak, K. M., Su, H., Sanbe, A., Robbins, J., and Wang, X. (2011a). Enhancement of proteasomal function protects against cardiac proteinopathy and ischemia/reperfusion injury in mice. *J. Clin. Invest.* 121, 3689–3700. doi: 10.1172/jci45709

Li, J., Powell, S. R., and Wang, X. (2011b). Enhancement of proteasome function by PA28α overexpression protects against oxidative stress. *FASEB J.* 25, 883–893. doi: 10.1096/fj.10-160895

Li, Y. F., and Wang, X. (2011). The role of the proteasome in heart disease. *Biochim. Biophys. Acta* 1809, 141–149. doi: 10.1016/j.bbagrm.2010.09.001

Liu, J., Chen, Q., Huang, W., Horak, K. M., Zheng, H., Mestril, R., et al. (2006a). Impairment of the ubiquitin-proteasome system in desminopathy mouse hearts. *FASEB J.* 20, 362–364. doi: 10.1096/fj.05-4869fje

Liu, J., Tang, M., Mestril, R., and Wang, X. (2006b). Aberrant protein aggregation is essential for a mutant desmin to impair the proteolytic function of the ubiquitin-proteasome system in cardiomyocytes. *J. Mol. Cell. Cardiol.* 40, 451–454. doi: 10.1016/j.yjmcc.2005.12.011

Manning, B. D. (2019). Signalling protein protects the heart muscle from pressure-related stress. *Nature* 566, 187–188. doi: 10.1038/d41586-019-00245-3

McMurray, J. J., Packer, M., Desai, A. S., Gong, J., Lefkowitz, M. P., Rizkala, A. R., et al. (2014). Angiotensin-neprilysin inhibition versus enalapril in heart failure. *N. Engl. J. Med.* 371, 993–1004.

Metzger, M. B., Hristova, V. A., and Weissman, A. M. (2012). HECT and RING finger families of E3 ubiquitin ligases at a glance. *J. Cell. Sci.* 125, 531–537. doi: 10.1242/jcs.091777

Munasinghe, P. E., Riu, F., Dixit, P., Edamatsu, M., Saxena, P., Hamer, N. S., et al. (2016). Type-2 diabetes increases autophagy in the human heart through promotion of Beclin-1 mediated pathway. *Int. J. Cardiol.* 202, 13–20. doi: 10.1016/j.ijcard.2015.08.111

Nagayama, T., Hsu, S., Zhang, M., Koitabashi, N., Bedja, D., Gabrielson, K. L., et al. (2009). Sildenafil stops progressive chamber, cellular, and molecular remodeling and improves calcium handling and function in hearts with pre-existing advanced hypertrophy caused by pressure overload. *J. Am. Coll. Cardiol.* 53, 207–215. doi: 10.1016/j.jacc.2008.08.069

Nakai, A., Yamaguchi, O., Takeda, T., Higuchi, Y., Hikoso, S., Taniike, M., et al. (2007). The role of autophagy in cardiomyocytes in the basal state and in response to hemodynamic stress. *Nat. Med.* 13, 619–624. doi: 10.1038/nm1574

Nakamura, M., and Sadoshima, J. (2018). Mechanisms of physiological and pathological cardiac hypertrophy. *Nat. Rev. Cardiol.* 15, 387–407. doi: 10.1038/s41569-018-0007-y

Nishida, M., Watanabe, K., Sato, Y., Nakaya, M., Kitajima, N., Ide, T., et al. (2010). Phosphorylation of TRPC6 channels at Thr69 is required for anti-hypertrophic effects of phosphodiesterase 5 inhibition. *J. Biol. Chem.* 285, 13244–13253. doi: 10.1074/jbc.m109.074104

Nussbaum, A. K., Dick, T. P., Keilholz, W., Schirle, M., Stevanovic, S., Dietz, K., et al. (1998). Cleavage motifs of the yeast 20S proteasome beta subunits deduced from digests of enolase 1. *Proc. Natl. Acad. Sci. U.S.A.* 95, 12504–12509. doi: 10.1073/pnas.95.21.12504

Oeing, C. U., Nakamura, T., Pan, S., Mishra, S., Dunkerly-Eyring, B., Kokkonen-Simon, K. M., et al. (2020). PKG1alpha cysteine-42 redox state controls mTORC1 activation in pathological cardiac hypertrophy. *Circ. Res.* doi: 10.1161/CIRCRESAHA.119.315714 [Epub ahead of print].

Pattison, J. S., Osinska, H., and Robbins, J. (2011). Atg7 induces basal autophagy and rescues autophagic deficiency in CryABR120G cardiomyocytes. *Circ. Res.* 109, 151–160. doi: 10.1161/circresaha.110.237339

Pieske, B., Maggioni, A. P., Lam, C. S. P., Pieske-Kraigher, E., Filippatos, G., Butler, J., et al. (2017). Vericiguat in patients with worsening chronic heart failure and preserved ejection fraction: results of the SOluble guanylate Cyclase stimulatoR in heArT failurE patientS with PRESERVED EF (SOCRATES-PRESERVED) study. *Eur. Heart J.* 38, 1119–1127. doi: 10.1093/eurheartj/ehw593

Pinilla-Vera, M., Hahn, V. S., and Kass, D. A. (2019). Leveraging signaling pathways to treat heart failure with reduced ejection fraction. *Circ. Res.* 124, 1618–1632. doi: 10.1161/circresaha.119.313682

Powell, S. R., and Divald, A. (2010). The ubiquitin-proteasome system in myocardial ischaemia and preconditioning. *Cardiovasc. Res.* 85, 303–311. doi: 10.1093/cvr/cvp321

Powell, S. R., Herrmann, J., Lerman, A., Patterson, C., and Wang, X. (2012). The ubiquitin-proteasome system and cardiovascular disease. *Prog. Mol. Biol. Transl. Sci.* 109, 295–346.

Powell, S. R., Wang, P., Katzeff, H., Shringarpure, R., Teoh, C., Khaliulin, I., et al. (2005). Oxidized and ubiquitinated proteins may predict recovery of postischemic cardiac function: essential role of the proteasome. *Antioxid. Redox Signal.* 7, 538–546. doi: 10.1089/ars.2005.7.538

Predmore, J. M., Wang, P., Davis, F., Bartolone, S., Westfall, M. V., Dyke, D. B., et al. (2010). Ubiquitin proteasome dysfunction in human hypertrophic and dilated cardiomyopathies. *Circulation* 121, 997–1004. doi: 10.1161/circulationaha.109.904557

Raeymaekers, L., Hofmann, F., and Casteels, R. (1988). Cyclic GMP-dependent protein kinase phosphorylates phospholamban in isolated sarcoplasmic reticulum from cardiac and smooth muscle. *Biochem. J.* 252, 269–273. doi: 10.1042/bj2520269

Rainer, P. P., and Kass, D. A. (2016). Old dog, new tricks: novel cardiac targets and stress regulation by protein kinase G. *Cardiovasc. Res.* 111, 154–162. doi: 10.1093/cvr/cvw107

Rajagopalan, V., Zhao, M., Reddy, S., Fajardo, G., Wang, X., Dewey, S., et al. (2013). Altered ubiquitin-proteasome signaling in right ventricular hypertrophy and failure. *Am. J. Physiol. Heart Circ. Physiol.* 305, H551–H562.

Ranek, M. J., Kokkonen-Simon, K. M., Chen, A., Dunkerly-Eyring, B. L., Vera, M. P., Oeing, C. U., et al. (2019). PKG1-modified TSC2 regulates mTORC1

activity to counter adverse cardiac stress. *Nature* 566, 264–269. doi: 10.1038/s41586-019-0895-y

Ranek, M. J., Kost, C. K. Jr., Hu, C., Martin, D. S., and Wang, X. (2014). Muscarinic 2 receptors modulate cardiac proteasome function in a protein kinase G-dependent manner. *J. Mol. Cell. Cardiol.* 69, 43–51. doi: 10.1016/j.yjmcc.2014.01.017

Ranek, M. J., Terpstra, E. J., Li, J., Kass, D. A., and Wang, X. (2013). Protein kinase g positively regulates proteasome-mediated degradation of misfolded proteins. *Circulation* 128, 365–376. doi: 10.1161/circulationaha.113.001971

Ranek, M. J., Zheng, H., Huang, W., Kumarapeli, A. R., Li, J., Liu, J., et al. (2015). Genetically induced moderate inhibition of 20S proteasomes in cardiomyocytes facilitates heart failure in mice during systolic overload. *J. Mol. Cell. Cardiol.* 85, 273–281. doi: 10.1016/j.yjmcc.2015.06.014

Reyes-Turcu, F. E., Ventii, K. H., and Wilkinson, K. D. (2009). Regulation and cellular roles of ubiquitin-specific deubiquitinating enzymes. *Annu. Rev. Biochem.* 78, 363–397. doi: 10.1146/annurev.biochem.78.082307.091526

Riddell, E., and Vader, J. M. (2017). Potential expanded indications for neprilysin inhibitors. *Curr. Heart Fail. Rep.* 14, 134–145. doi: 10.1007/s11897-017-0327-y

Saito, T., Asai, K., Sato, S., Hayashi, M., Adachi, A., Sasaki, Y., et al. (2016). Autophagic vacuoles in cardiomyocytes of dilated cardiomyopathy with initially decompensated heart failure predict improved prognosis. *Autophagy* 12, 579–587. doi: 10.1080/15548627.2016.1145326

Salloum, F. N., Abbate, A., Das, A., Houser, J. E., Mudrick, C. A., Qureshi, I. Z., et al. (2008). Sildenafil (Viagra) attenuates ischemic cardiomyopathy and improves left ventricular function in mice. *Am. J. Physiol. Heart Circ. Physiol.* 294, H1398–H1406.

Sawada, N., Itoh, H., Yamashita, J., Doi, K., Inoue, M., Masatsugu, K., et al. (2001). cGMP-dependent protein kinase phosphorylates and inactivates RhoA. *Biochem. Biophys. Res. Commun.* 280, 798–805. doi: 10.1006/bbrc.2000.4194

Schiattarella, G. G., Altamirano, F., Tong, D., French, K. M., Villalobos, E., Kim, S. Y., et al. (2019). Nitrosative stress drives heart failure with preserved ejection fraction. *Nature* 568, 351–356.

Schlossarek, S., Englmann, D. R., Sultan, K. R., Sauer, M., Eschenhagen, T., and Carrier, L. (2012). Defective proteolytic systems in Mybpc3-targeted mice with cardiac hypertrophy. *Basic Res. Cardiol.* 107:235.

Schlossmann, J., and Schinner, E. (2012). cGMP becomes a drug target. *Naunyn Schmiedebergs Arch. Pharmacol.* 385, 243–252. doi: 10.1007/s00210-012-0730-6

Sciarretta, S., Forte, M., Frati, G., and Sadoshima, J. (2018). New insights into the role of mTOR signaling in the cardiovascular system. *Circ. Res.* 122, 489–505. doi: 10.1161/circresaha.117.311147

Sciarretta, S., Volpe, M., and Sadoshima, J. (2012). Is reactivation of autophagy a possible therapeutic solution for obesity and metabolic syndrome? *Autophagy* 8, 1252–1254. doi: 10.4161/auto.20670

Sciarretta, S., Yee, D., Shenoy, V., Nagarajan, N., and Sadoshima, J. (2014). The importance of autophagy in cardioprotection. *High Blood Press. Cardiovasc. Prev.* 21, 21–28. doi: 10.1007/s40292-013-0029-9

Shirakabe, A., Ikeda, Y., Sciarretta, S., Zablocki, D. K., and Sadoshima, J. (2016). Aging and autophagy in the heart. *Circ. Res.* 118, 1563–1576.

Singh, S. R., Zech, A. T. L., Geertz, B., Reischmann-Dusener, S., Osinska, H., Prondzynski, M., et al. (2017). Activation of autophagy ameliorates cardiomyopathy in Mybpc3-targeted Knockin mice. *Circ. Heart Fail.* 10:e004140.

Song, L., Su, M., Wang, S., Zou, Y., Wang, X., Wang, Y., et al. (2014). MiR-451 is decreased in hypertrophic cardiomyopathy and regulates autophagy by targeting TSC1. *J. Cell. Mol. Med.* 18, 2266–2274. doi: 10.1111/jcmm.12380

Spanig, S., Kellermann, K., Dieterlen, M. T., Noack, T., Lehmann, S., Borger, M. A., et al. (2019). The ubiquitin proteasome system in ischemic and dilated cardiomyopathy. *Int. J. Mol. Sci.* 20:6354. doi: 10.3390/ijms20246354

Su, H., and Wang, X. (2010). The ubiquitin-proteasome system in cardiac proteinopathy: a quality control perspective. *Cardiovasc. Res.* 85, 253–262. doi: 10.1093/cvr/cvp287

Szalay, G., Meiners, S., Voigt, A., Lauber, J., Spieth, C., Speer, N., et al. (2006). Ongoing coxsackievirus myocarditis is associated with increased formation and activity of myocardial immunoproteasomes. *Am. J. Pathol.* 168, 1542–1552. doi: 10.2353/ajpath.2006.050865

Takimoto, E., Champion, H. C., Li, M., Belardi, D., Ren, S., Rodriguez, E. R., et al. (2005). Chronic inhibition of cyclic GMP phosphodiesterase 5A prevents and reverses cardiac hypertrophy. *Nat. Med.* 11, 214–222. doi: 10.1038/nm1175

Takimoto, E., Koitabashi, N., Hsu, S., Ketner, E. A., Zhang, M., Nagayama, T., et al. (2009). Regulator of G protein signaling 2 mediates cardiac compensation to pressure overload and antihypertrophic effects of PDE5 inhibition in mice. *J. Clin. Invest.* 119, 408–420.

Tang, M., Li, J., Huang, W., Su, H., Liang, Q., Tian, Z., et al. (2010). Proteasome functional insufficiency activates the calcineurin-NFAT pathway in cardiomyocytes and promotes maladaptive remodelling of stressed mouse hearts. *Cardiovasc. Res.* 88, 424–433. doi: 10.1093/cvr/cvq217

Thoonen, R., Giovanni, S., Govindan, S., Lee, D. I., Wang, G. R., Calamaras, T. D., et al. (2015). Molecular screen identifies cardiac myosin-binding protein-C as a protein kinase G-Ialpha substrate. *Circ. Heart Fail.* 8, 1115–1122. doi: 10.1161/circheartfailure.115.002308

Tian, Z., Zheng, H., Li, J., Li, Y., Su, H., and Wang, X. (2012). Genetically induced moderate inhibition of the proteasome in cardiomyocytes exacerbates myocardial ischemia-reperfusion injury in mice. *Circ. Res.* 111, 532–542. doi: 10.1161/circresaha.112.270983

Tong, M., Saito, T., Zhai, P., Oka, S., and Sadoshima, J. (2018). Atg7-dependent autophagy is essential for cardiac function with high fat diet. *FASEB J.* 32, 35.1–35.1.

VerPlank, J. J. S., Tyrkalska, S. D., Fleming, A., Rubinsztein, D. C., and Goldberg, A. L. (2020). cGMP via PKG activates 26S proteasomes and enhances degradation of proteins, including ones that cause neurodegenerative diseases. *Proc. Natl. Acad. Sci. U.S.A.* 117, 14220–14230. doi: 10.1073/pnas.2003277117

Wang, X., Li, J., Zheng, H., Su, H., and Powell, S. R. (2011). Proteasome functional insufficiency in cardiac pathogenesis. *Am. J. Physiol. Heart Circ. Physiol.* 301, H2207–H2219.

Wang, X., and Robbins, J. (2006). Heart failure and protein quality control. *Circ. Res.* 99, 1315–1328. doi: 10.1161/01.res.0000252342.61447.a2

Wang, X., Su, H., and Ranek, M. J. (2008). Protein quality control and degradation in cardiomyocytes. *J. Mol. Cell. Cardiol.* 45, 11–27. doi: 10.1016/j.yjmcc.2008.03.025

Weekes, J., Morrison, K., Mullen, A., Wait, R., Barton, P., and Dunn, M. J. (2003). Hyperubiquitination of proteins in dilated cardiomyopathy. *Proteomics* 3, 208–216. doi: 10.1002/pmic.200390029

Willis, M. S., and Patterson, C. (2013). Proteotoxicity and cardiac dysfunction–Alzheimer's disease of the heart? *N. Engl. J. Med.* 368, 455–464. doi: 10.1056/nejmra1106180

Willis, M. S., Townley-Tilson, W. H., Kang, E. Y., Homeister, J. W., and Patterson, C. (2010). Sent to destroy: the ubiquitin proteasome system regulates cell signaling and protein quality control in cardiovascular development and disease. *Circ. Res.* 106, 463–478. doi: 10.1161/circresaha.109.208801

Wohlschlaeger, J., Sixt, S. U., Stoeppler, T., Schmitz, K. J., Levkau, B., Tsagakis, K., et al. (2010). Ventricular unloading is associated with increased 20s proteasome protein expression in the myocardium. *J. Heart Lung Transplant* 29, 125–132. doi: 10.1016/j.healun.2009.07.022

Xiao, S., Li, Q., Hu, L., Yu, Z., Yang, J., Chang, Q., et al. (2019). Soluble guanylate cyclase stimulators and activators: where are we and where to go? *Mini Rev. Med. Chem.* 19, 1544–1557. doi: 10.2174/1389557519666190730110600

Xie, Z., Lau, K., Eby, B., Lozano, P., He, C., Pennington, B., et al. (2011). Improvement of cardiac functions by chronic metformin treatment is associated with enhanced cardiac autophagy in diabetic OVE26 mice. *Diabetes* 60, 1770–1778. doi: 10.2337/db10-0351

Yan, C., Kim, D., Aizawa, T., and Berk, B. C. (2003). Functional interplay between angiotensin II and nitric oxide: cyclic GMP as a key mediator.

Arterioscler Thromb Vasc. Biol. 23, 26–36. doi: 10.1161/01.atv.0000046231.17365.9d

Zeng, H., Yang, K., Cloer, C., Neale, G., Vogel, P., and Chi, H. (2013). mTORC1 couples immune signals and metabolic programming to establish T(reg)-cell function. *Nature* 499, 485–490. doi: 10.1038/nature12297

Zhang, H., Pan, B., Wu, P., Parajuli, N., Rekhter, M. D., Goldberg, A. L., et al. (2019). PDE1 inhibition facilitates proteasomal degradation of misfolded proteins and protects against cardiac proteinopathy. *Sci. Adv.* 5:eaaw5870. doi: 10.1126/sciadv.aaw5870

Zhang, J., Liu, J., Huang, Y., Chang, J. Y., Liu, L., McKeehan, W. L., et al. (2012). FRS2alpha-mediated FGF signals suppress premature differentiation of cardiac stem cells through regulating autophagy activity. *Circ. Res.* 110, e29–e39.

Conflict of Interest: MR is a co-founder and shareholder of Meta-T Cellular, a start-up company that aims to develop applications of this intellectual property for immune therapy.

The remaining authors declare that the research was conducted in the absence of any commercial or financial relationships that could be construed as a potential conflict of interest.

frontiers in Physiology

REVIEW
published: 27 August 2020
doi: 10.3389/fphys.2020.01054

Molecular Perspectives of Mitochondrial Adaptations and Their Role in Cardiac Proteostasis

*Shafiul Alam[1], Chowdhury S. Abdullah[1], Richa Aishwarya[2], Mahboob Morshed[1] and Md. Shenuarin Bhuiyan[1,2]**

[1] Department of Pathology and Translational Pathobiology, Louisiana State University Health Sciences Center, Shreveport, LA, United States, [2] Department of Molecular and Cellular Physiology, Louisiana State University Health Sciences Center, Shreveport, LA, United States

OPEN ACCESS

Edited by:
P. Bryant Chase, Florida State University, United States

Reviewed by:
Huabo Su, Medical College of Georgia at Augusta University, United States
Junichi Sadoshima, University of Medicine and Dentistry of New Jersey, United States

***Correspondence:**
Md. Shenuarin Bhuiyan
mbhuiy@lsuhsc.edu

Specialty section:
This article was submitted to Striated Muscle Physiology, a section of the journal Frontiers in Physiology

Received: *28 March 2020*
Accepted: *31 July 2020*
Published: *27 August 2020*

Citation:
Alam S, Abdullah CS, Aishwarya R, Morshed M and Bhuiyan MS (2020) Molecular Perspectives of Mitochondrial Adaptations and Their Role in Cardiac Proteostasis. Front. Physiol. 11:1054. doi: 10.3389/fphys.2020.01054

Mitochondria are the key to properly functioning energy generation in the metabolically demanding cardiomyocytes and thus essential to healthy heart contractility on a beat-to-beat basis. Mitochondria being the central organelle for cellular metabolism and signaling in the heart, its dysfunction leads to cardiovascular disease. The healthy mitochondrial functioning critical to maintaining cardiomyocyte viability and contractility is accomplished by adaptive changes in the dynamics, biogenesis, and degradation of the mitochondria to ensure cellular proteostasis. Recent compelling evidence suggests that the classical protein quality control system in cardiomyocytes is also under constant mitochondrial control, either directly or indirectly. Impairment of cytosolic protein quality control may affect the position of the mitochondria in relation to other organelles, as well as mitochondrial morphology and function, and could also activate mitochondrial proteostasis. Despite a growing interest in the mitochondrial quality control system, very little information is available about the molecular function of mitochondria in cardiac proteostasis. In this review, we bring together current understanding of the adaptations and role of the mitochondria in cardiac proteostasis and describe the adaptive/maladaptive changes observed in the mitochondrial network required to maintain proteomic integrity. We also highlight the key mitochondrial signaling pathways activated in response to proteotoxic stress as a cellular mechanism to protect the heart from proteotoxicity. A deeper understanding of the molecular mechanisms of mitochondrial adaptations and their role in cardiac proteostasis will help to develop future therapeutics to protect the heart from cardiovascular diseases.

Keywords: mitochondria, cardiac proteostasis, mitochondrial proteostasis, mitochondrial dysfunction, mitochondrial unfolded protein response, proteotoxicity

INTRODUCTION

Proteins are complex macromolecules with versatile molecular functions implicated in every biological process (Hartl et al., 2011). The precise folding of newly synthesized proteins is essential for proper functioning through numerous posttranslation modifications. Protein quality control (PQC), the mechanism controlling protein homeostasis, includes protein maturation, transportation to the executive site, and degradation of misfolded or overproduced proteins. Protein homeostasis plays a crucial role in the maintenance of overall cellular health, and its alteration results in the activation of either adaptive signaling pathways to avoid pathological consequences or maladaptive pathways that lead to cellular death (Kroemer et al., 2009; Galluzzi et al., 2015). The term "proteotoxicity" refers to the cellular pathogenic features that result from protein misfolding and aggregation, which is regulated by myriad factors that affect protein folding and misfolding. Under conditions of environmental stress or disease, protein folding is disturbed, which leads ultimately to the generation of misfolded intermediates. Protein homeostasis in cardiomyocytes is subject to several layers of surveillance by the PQC system. Early in the process, misfolded proteins are refolded or directed to degradation by the molecular chaperones. If refolding is impossible due to the extent of misfolding and/or the size of the protein, the ubiquitin-proteosome system or autophagy (including mitochondrial autophagy, mitophagy) ensures protein degradation as a secondary defense mechanism. Some pathological conditions result in the PQC system becoming so overwhelmed that misfolded proteins accumulate, resulting in aggregate formation (Fauconnier, 2018). In addition to these classical PQC system processes, mitochondria play an important role in cytosolic proteostasis through the uptake of aggregates by the mitochondrial import system, which degrades them using mitochondrial serine proteases (Ruan et al., 2017).

The heart is a terminally differentiated organ that undergoes adaptive remodeling by changing cardiomyocyte size as well as mitochondrial content to help it cope with pathological stress (Fauconnier, 2018). The extent of changes in the activity or inhibition of the activity of the PQC system causes one of two results for cardiomyocytes: hyperactivity of the PQC system, leading to the excessive degradation of proteins and thus myolysis, or inactivation of the PQC system, leading to cardiac failures such as amyloidogenic cardiomyopathy, idiopathic cardiomyopathy, hypertrophic cardiomyopathy, dilated cardiomyopathy, or atrial fibrillation. The observed mitochondrial dysfunction related to these pathologies includes alteration of mitophagy, aberrant mitochondrial fission/fusion, or altered branched-chain amino acid catabolism (Huang et al., 2011; Nan et al., 2017). Currently, the mechanisms underlying mitochondrial dysfunction that contribute to the initiation or acceleration of cardiac proteostasis remain elusive. This review encompasses current understanding of the molecular insights concerning the adaptive changes in mitochondria in cardiac proteostasis, the maladaptive effect of mitochondrial dysfunction in cardiac proteostasis, and the impact of impaired cardiac proteostasis on mitochondrial function.

CHALLENGES OF PROTEOSTASIS IN THE HEART

Cardiomyocytes are highly contractile cells requiring a large amount of energy to maintain contractility on a beat-to-beat basis. In the heart, mitochondria occupy nearly one-third of the cardiomyocyte volume (Zhou and Tian, 2018). Due to their high contractility and abundance of mitochondria, cardiomyocytes are subject to continuous generation of proteotoxic agents and the cellular stress response. Cardiomyocytes, as terminally differentiated cells, confront several extra obstacles in their efforts to maintain cellular proteostasis compared to most other cells. Firstly, cardiomyocytes contain highly specialized proteins that participate in electrical conduction and contraction. Therefore, these demand specialized PQC surveillance, such as that provided by small heat shock proteins [e.g., αB-crystallin (CryAB)] that favorably bind to the proteins of the sarcomere to preserve healthy cardiomyocyte function (Golenhofen et al.,

Abbreviations: $\Delta\psi$, mitochondrial membrane potential; $\Delta\Psi m$, IMM potential; AAA, ATPases associated with diverse cellular activities; AD, Alzheimer's disease; Akt, protein kinase B; ALS, amyotrophic lateral sclerosis; AMPK, AMP-activated protein kinase; ATF4, activating transcription factor 4; ATF5, activating transcription factor 5; ATFS-1, activating transcription factor associated with stress; Ca^{2+}, calcium; CHOP, C/EBP homologous protein; ClpP, caseinolytic mitochondrial matrix protease proteolytic subunit; COA6, cytochrome c oxidase assembly factor 6 homolog; COX10, cytochrome C oxidase assembly homolog 10; COX15, cytochrome C oxidase assembly homolog 15; COX2, cytochrome C oxidase subunit 2; CryAB, αB-crystallin; $CryAB^{R120G}$, cardiomyocyte-specific overexpression of mutant (R120G) CryAB; D7−Des Tg, desmin transgenic mouse with 7-amino acid deletion R172−E178 in desmin; DRC, desmin-related cardiomyopathy; Drp1, dynamin-related protein 1; ETC, electron transport chain; Fis1, mitochondrial fission 1 protein; FUNDC1, FUN14 domain-containing protein 1; H_2O_2, hydrogen per oxide; HD, Huntington disease; HDAC6, histone deacetylase 6; HF, heart failure; HSC70, heat shock cognate 71-kDa protein; HSP104, heat shock protein 104; HSP60, heat shock protein 60; HSP70, heat shock protein 70; HSP75/TRAP1, heat shock protein 75 kDa; iCa^{2+}, intracellular calcium; IF, intermediate filament; IMF, interfibrillar mitochondria; IMS, mitochondrial intermembrane space; IPS, ischemic preconditioning; IR, ischemic-reperfusion; LC, light chain; LonP1, Lon protease I; MAGIC, mitochondrion as a guardian for cytosol; mCa^{2+}, mitochondrial calcium; MCU, mitochondria calcium uniporter; Mff, mitochondrial fusion factor; Mfn1, Mitofusins 1; Mfn2, Mitofusins 2; MiD49/51, mitochondrial dynamics proteins of 49 and 51 kDa; Miro2, mitochondrial Rho GTPase 2; MitoQ, mitoquinone; mito-TEMPO, triphenylphosphonium chloride; MnSOD, manganese (Mn)-dependent superoxide dismutase; MNTs, membrane nanotubes; MPTP, mitochondrial permeability transition pore; MT, Microtubulin; mtDNA, mitochondrial DNA; mtHsp70, mitochondrial 70-kDa heat shock protein; MURE, mitochondrial unfolded protein response element; NCLX, mitochondrial sodium-calcium exchanger; OMA1, metalloendopeptidase OMA1; OMM, outer mitochondrial membrane; OPA1, optic atrophy protein 1; OXPHOS, oxidative phosphorylation; PD, Parkinson disease; PERK, protein kinase R-like ER kinase; Pim1, Lon protease homolog in mammals; PNM, perinuclear mitochondria; PolG, mitochondrial polymerase gamma; PQC, protein quality control; RNOS, reactive nitrogen and oxygen species; ROS, reactive oxygen species; SCO1, synthesis of cytochrome oxidase1; SCO2, synthesis of cytochrome oxidase2; SDH, succinate dehydrogenase; SSM, subsarcolemmal mitochondria; TAC, transverse aortic constriction; TIM, translocase of inner membrane; TIM44, translocase of inner membrane 44; TOM, translocase of outer membrane; Tom40, translocase of outer membrane 40; UPR, unfolded protein response; UPR^{am}, unfolded protein response activated by the mistargeting of proteins; UPR^{ER}, endoplasmic reticulum (ER)-unfolded protein response; UPR^{mt}, mitochondrial unfolded protein response; UPS^{mt}, mitochondrial unfolded protein response; VDAC, voltage-dependent anionic channel.

2000). Secondly, cardiomyocytes abundantly express heat shock proteins (e.g., heat shock protein 70 (HSP70) that work in both the cytosol and in the mitochondria to maintain mitochondrial proteostasis. In addition, mitochondria in cardiomyocytes have their own PQC system comprising abundant proteases such as Lon Protease I (LonP1), metalloendopeptidase OMA1 (OMA1), and caseinolytic mitochondrial matrix protease proteolytic subunit (ClpP) (Acin-Perez et al., 2018; Smyrnias et al., 2019; Venkatesh et al., 2019). Thirdly, cardiomyocytes are terminally differentiated cells, making them unable to clear protein aggregates during cell division. The protein aggregates accumulate at the microtubule-organizing center in dividing cells during mitosis; one daughter cell receives all of the aggregates through asymmetric distribution, leaving the other one free of aggregates. The daughter cell that contains the asymmetrically distributed aggregates undergoes apoptosis (Rujano et al., 2006). Therefore, cardiomyocytes depend greatly on a balanced PQC system to counteract stress-induced protein misfolding and aggregation (Powers and Balch, 2013; Willis and Patterson, 2013). Fourthly, the huge metabolic demands made by continuously contracting cardiomyocytes are met by oxidative phosphorylation in the mitochondria, which also generates highly reactive and abundant proteotoxic reactive oxygen species (ROS) as a by-product even under healthy conditions (Zhang et al., 2013). A growing number of studies suggest that intricate cross-talk occurs between mitochondrial quality control and cellular proteostasis in cardiomyocytes under pathophysiological conditions.

MITOCHONDRIAL POSITION, DISTRIBUTION, AND COMMUNICATION IN CARDIAC PROTEOSTASIS

Healthy mitochondrial function is affected by proper mitochondrial positioning with respect to other organelles, as well as their communication and distribution. Mitochondria show substantial plasticity in shape and distribution and display dynamic behavior in positioning in growing cells. Mitochondria in cardiac muscle are often confined to specific cytoplasmic regions rather than being randomly distributed (Rappaport et al., 1998; Yaffe, 1999). Numerous studies in both animal models and isolated cell cultures have suggested that proper mitochondrial function relies on the interaction among the cytoskeleton, the mitochondria, and other organelles. In the healthy heart, desmin upholds the proper mitochondrial positioning along the sarcomere and plays a crucial role in maintaining normal mitochondrial function by preserving mitochondrial spatial organization (Bär et al., 2004). Desmin intermediate filaments (IF) in skeletal and cardiac muscle connecting the interfibrillar space between neighboring Z discs establish a connection between mitochondria and the IF cytoskeleton (Tokuyasu et al., 1983). Desmin disorganization can alter mitochondrial positioning, compromise mitochondrial function, and lead to cardiomyocyte dysfunction (Bär et al., 2004). The molecular function of desmin networks in maintaining mitochondrial position along with other organelles in cardiomyocytes was revealed in studies using desmin−null mice. These mice displayed a progressive and generalized myopathy affecting the function and structure of the myocardium. The striated muscles in desmin-null mice showed irregular mitochondrial shape and distribution, with a hallmark aggregation of the sarcolemmal mitochondria attributable to weakened muscles and increased fatigue (Li et al., 1996; Milner et al., 1996).

Clinically relevant mouse models of cardiac proteotoxicity, such as the mutant desmin transgenic mouse with 7-amino acid deletion R172-E178 in desmin (D7-Des Tg) (Goldfarb et al., 1998; Dalakas et al., 2000; Wang et al., 2001; Zheng et al., 2011), display a collapse of the desmin network and an accumulation of desmin aggregates that contributes to the development of cardiomyopathy (Wang et al., 2001). Collapse of the desmin network results in early perturbations in mitochondrial structure. We recently reported that the D7-Des Tg mouse model of desmin-related cardiomyopathy (DRC) demonstrated altered mitochondrial morphology and localization along the sarcomere resulting in mitochondrial dysfunction (Alam et al., 2018). Disorganization and collapse of the desmin network were also observed in another mouse model of DRC developed by cardiomyocyte-specific overexpression of mutant (R120G) CryAB (CryAB^{R120G}). The chaperone protein CryAB is a small heat shock protein responsible for the maintenance of the desmin network. Mutation of CryAB^{R120G} perturbed the desmin network leading to the disruption of the sarcomere structure (Maloyan et al., 2005). These collapses in desmin networks contribute to altered mitochondrial position and distribution, resulting in dysfunctional cardiac proteostasis and the development of cardiomyopathy.

Microtubulin (MT) plays an important role in the maintenance of sarcoplasmic/ER-mitochondrial contact; disruption of this contact is attributed to the alteration of mitochondrial position (Friedman et al., 2010, 2011; Lewis et al., 2016; Phillips and Voeltz, 2016). Acetylation of the tubulin leads to the stabilization of MT playing a pivotal role in maintaining ER-mitochondria contact. Increased activity of histone deacetylase 6 (HDAC6) induced depolymerization, which perturbed the contact site (Friedman et al., 2010). Indeed, increased activity of HDAC6 leading to mitochondrial-ER contract site disruption has been reported in atrial fibrillation (AF) (Zhang et al., 2014). Muscle mitochondria are confined to a specific subcellular domain within sarcomeres (Stromer and Bendayan, 1988, 1990; Ogata and Yamasaki, 1997), suggesting immobilization of the mitochondria through stable linkages within the cytoskeleton. However, several studies have suggested that mitochondria may also undergo translocation in muscles. Active transport of mitochondria along MT occurs in the axon of neurons through the involvement of kinesin (Leopold et al., 1992; Jellali et al., 1994; Nangaku et al., 1994; Elluru et al., 1995). Some studies have also provided evidence of conventional MT-dependent molecular motor kinesis in the heart and involvement of the kinesin associated with cardiac mitochondria in the dynamic interaction between the organelle and the MT (Lindén et al., 2001). However, the association between kinesin and the mitochondria is absent in the desmin-null mouse heart tissue, suggesting a possible role for intermediate filament (IF)

organization in kinesin-mediated interactions between MT and mitochondria (Lindén et al., 2001). Interestingly, new evidence has suggested that membrane nanotubes (MNT) mediated the transportation of cardiac mitochondria between cardiomyocytes and fibroblasts. MNT are identified as long, thin, membrane-based distant connections (Shen et al., 2018) requiring MT and motor protein kinesin for the movement of mitochondria. MNT are also known to be involved in the intercellular transfer of calcium (Ca^{2+}) to the mitochondria (He et al., 2011). For the maintenance of proper cardiac function, intimate communication between cardiomyocytes and cardiac fibroblasts is very important (Baudino et al., 2008; Porter and Turner, 2009). Although *in vitro* coculture of neonatal rat cardiomyocytes and fibroblasts has suggested the involvement of the MNT-like structure, there is no direct evidence of mitochondrial transport through the MTN *in vivo* in the adult heart, where the mitochondria are confined within a rigid structure. Despite considerable debate regarding mitochondrial transport in the heart, we can speculate that the disorganization of the desmin network in cardiac proteotoxicity perturbs the transport of mitochondria between cardiomyocytes and fibroblasts, affecting normal cardiomyocyte function.

Recent studies have also suggested that mitochondrial intercommunication through the nano-tunnel is necessary to maintain cellular proteostasis. For the maintenance of mitochondrial function, exchanges of mitochondrial matrix contents between mitochondria are essential. Cardiac mitochondrial matrix exchanges can occur either through direct contact with adjacent mitochondria, called mitochondrial kissing, or by extrusion of a tubular protrusion, called a nano-tunnel, for communication with distant mitochondria. Mitochondrial kissing, the result of physical contact between two adjacent mitochondria, allows transient and incomplete mixing without affecting the mitochondrial membrane potential. Use of a nano-tunnel, a dynamic thin tubular protrusion bridging mitochondria at a relatively long distance, allows the continuous and complete mixing of mitochondrial content without affecting the intermediate mitochondria (Huang et al., 2013). It has been well established that mitochondrial Rho GTPase 2 (Miro2) in the neuronal system plays an important role in the transport of mitochondria to the site of energy demands (Nguyen et al., 2014). Although mitochondrial transportation is believed to be difficult in cardiomyocytes due to their rigid sarcomeric structure, the abundance of Miro2 in cardiomyocytes suggests their possible direct function in mitochondrial intercommunication (Cao et al., 2019). This possibility is supported by a study showing that adenovirus-mediated expression of Miro2 in cardiomyocytes increased the inter-mitochondrial communication through both adjacent mitochondrial kissing and nano-tunneling between distant mitochondria. This finding suggests that in adult cardiomyocytes, Miro2 may be involved in mitochondrial intercommunication through mitochondrial kissing and nano-tunneling, rather than mitochondrial transportation. Interestingly, Miro2 transgenic mice showed increased inter-mitochondrial communication, improved mitochondrial function, and ameliorated cardiac function in a transverse aortic constriction (TAC) model of cardiac injury (Cao et al., 2019). Therefore, these studies suggest that mitochondrial inter-communication plays a critical role in preserving cardiac structure and function.

ELECTRON TRANSPORT CHAIN AND OXIDATIVE STRESS IN CARDIAC PROTEOSTASIS

ROS have been implicated in the pathophysiology of cardiovascular diseases and aging processes (Munzel et al., 2017). Studies have shown the involvement of ROS in several cardiac pathophysiologies, such as hindrance in excitation–contraction coupling (Zhang et al., 2015), induction of arrhythmias (Wagner et al., 2014; Kim et al., 2017), and cardiac hypertrophy (Ago et al., 2008). ROS are formed as by-products of cellular respiration during energy production and metabolism, and also by some specialized enzymes (Burgoyne et al., 2012). Mitochondria are the major source of ROS production, along with their primary functions involved with energy production and metabolism (Munzel et al., 2015). The mitochondrial electron transport chain (ETC) is composed of flavoprotein-containing complexes and super-complexes (Letts et al., 2016). During electron transport and O_2 reduction (respiration), small numbers of electrons can move from complexes I and III to form superoxide ($\cdot O_2^-$), which in turn is converted to the more stable hydrogen peroxide (H_2O_2) by manganese (Mn)-dependent superoxide dismutase (MnSOD) (Balaban et al., 2005). Although ROS intermediate products (e.g., $\cdot O_2^-$) and hydroxyl radicals ($\cdot$OH) have extremely short half-lives (milliseconds to nanoseconds), they are capable of oxidizing and damaging almost all organic molecules (Leichert and Dick, 2015; **Figure 1**). More stable ROS (e.g., H_2O_2) produced during the detoxification of $\cdot O_2^-$ can serve as mediators of intracellular signaling. Maintaining optimal levels of ROS balance through production and detoxification is critical for proper cellular function and survival (Aon et al., 2010). Mitochondrial ETC complexes also possess an iron–sulfur cluster (Chang et al., 2016), important for the function of the oxidation–reduction reactions of mitochondrial electron transport. Multiple iron–sulfur clusters have been reported in both Complex I and Complex II of oxidative phosphorylation. ROS have been shown to affect the stability and function of the iron–sulfur cluster (Jang and Imlay, 2007). In the degenerative disease Friedreich's ataxia, ROS have been shown to damage mitochondrial iron–sulfur clusters, triggering heme deficiency, and leading to further generation of ROS (Napoli et al., 2006). However, a direct link between the altered iron–sulfur cluster and cellular proteostasis remains unknown.

Under normal physiological conditions, the increased levels of ROS are involved in pro-survival signaling (Zorov et al., 2014). The sensitivity of mitochondria to ROS within the heart varies due to the heterogenicity of the spatial mitochondrial distribution. While the majority of the mitochondria are situated between myofibrils (interfibrillar mitochondria, IMF), the rest are located beneath the sarcolemma (subsarcolemmal mitochondria, SSM) and around the nucleus (perinuclear mitochondria, PNM) (Lu X. et al., 2019). Therefore, mitochondria have a varying

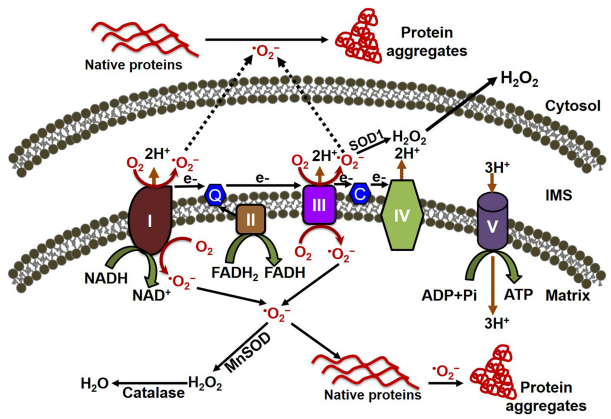

FIGURE 1 | Mitochondrial oxidative stress contributes to both cytosolic and mitochondrial protein aggregation. The electron transport chain (ETC) of the mitochondria, located in the inner mitochondrial membrane is composed of five multi-subunit enzyme complexes (denoted by I, II, III, IV, and V). Electron (e-) flow through the ETC follows the order of electrons donated by coenzymes (NADH and $FADH_2$) as they are accepted and transferred to complex I (NADH ubiquinone reductase) or complex II (succinate dehydrogenase) and then consecutively to complex III (ubiquinol-cytochrome C reductase), complex IV (cytochrome c oxidase), and finally to oxygen (O_2) to produce water (H_2O). The electrochemical gradient established through the electron transfer along with the ETC couple protons transport across the inner membrane, resulting in ATP generation through complex V (F0F1 ATP synthase). Electron leakage in the ETC, mainly from complex I and III, generates reactive oxygen species such as superoxide anion (O_2^-). The transfer of electrons to O_2 generates O_2^-, which is then converted to hydrogen peroxide (H_2O_2) by the enzymes superoxide dismutase (MnSOD) and catalase in the mitochondria. O_2^- can oxidize either the mitochondrial protein inside the mitochondria, forming the misfolded protein aggregate that affects the mitochondrial function, or the cytosolic protein after being released into the cytosol, leading to the formation of protein aggregate in the cytosol.

capacity for oxidative phosphorylation depending upon their spatial distribution, as demonstrated in data from a study showing IFM with a 50% higher level of substrate oxidation, as well as higher activity of oxidative phosphorylating enzymes, compared to SSM (Shimada et al., 1984). Moreover, data from a recent study have shown that, compared to PNM, IFM exhibited a greater sensitivity to oxidative stress (Lu X. et al., 2019). It is plausible that IFM could generate more ROS, as increased mitochondrial respiration is associated with an increase in ROS production due to increased ETC activity (Zhou and Tian, 2018). The majority of the cardiac mitochondria are IFM to meet the high energy demands of myofibrillar contractility. Taken together, the data from these studies lead to the speculation that, under pathological conditions, cardiac mitochondria are more susceptible to oxidative stress than non-cardiac dividing cells; however, direct evidence from comparative studies is still lacking.

In the heart, MnSOD plays a critical role to counteract ROS. MnSOD is encoded by the nuclear genome but localizes in the mitochondria through the mitochondrial targeting sequence. MnSOD represents 90% of the activity in the cardiomyocytes. The rest of the SOD is primarily copper-zinc (CuZn) SOD (CuZnSOD or SOD1), which resides mainly in the cytosol. Extracellular SODs are encoded by distinct genes but are also CuZn-containing enzymes (Assem et al., 1997). As MnSOD is located in the mitochondria, representing 90% of SOD activity in cardiomyocytes, it plays a vital role by counteracting oxidative stress in the mitochondria. MnSOD dysfunction causes severe oxidative stress in the mitochondria as well as at the cellular level. Oxidative stress can cause posttranslational modification of the protein, which ultimately alters its function. When under oxidative stress, the amino acids of cardiac proteins undergo modification, reversibly or irreversibly; the extent of the modification depends on the severity of the reactive nitrogen and oxygen species (RNOS) exposure (Kumar et al., 2012; Chung et al., 2013; Go and Jones, 2013). Irreversible oxidative stress-induced posttranslational modification can initiate the pathway involved in protein degradation as well as causing deregulation of protein folding and impairing the clearance of misfolded proteins (Gregersen et al., 2005). Highly oxidized aggregates are resistant to the proteolytic system due to their bulky size and can block the proteasome, leading to the inhibition of proteasomal function (Ayyadevara et al., 2015, 2016). Oxidized lipofuscin aggregate has been reported in aging (Kakimoto et al., 2019) and also neurodegenerative proteotoxic disease (Hohn et al., 2011; Kakimoto et al., 2019). The generation of ROS by damaged mitochondria leads to the oxidation of lipofuscin, inhibiting proteasome activity and resulting in aggregate accumulation (Kakimoto et al., 2019). Moreover, studies have shown a positive correlation between intracellular lipofuscin contents and ROS production and mitochondrial damage in primary cardiomyocytes (Terman et al., 2004) and also in HeLa cells (Konig et al., 2017). Moreover, lipofuscin accumulation was also observed in human cardiac samples obtained from sudden cardiac death (Kakimoto et al., 2019), the end stage of human heart failure with dilated cardiomyopathy and ischemic cardiomyopathy (Rayment et al., 1999; Radu et al., 2012; Nozynski et al., 2013). Lipofuscin accumulation in cardiac proteotoxicity indicates that mitochondrial oxidative stress plays a causative role in both disease initiation and progression.

Similarly, oxidative stress has also been implicated in the cardiac proteotoxicity induced by amyloidosis. Particularly, amyloidogenic light chain (LC) proteins from human patients with amyloid cardiomyopathy affect cellular redox, cause increased ROS production, and lead to impaired contractility and relaxation in cardiomyocytes (Brenner et al., 2004). The mechanisms of increased cellular ROS production may be due to the mitochondrial dysfunction induced by proteotoxicity, similar to that observed in neurodegenerative diseases (Miranda et al., 2000; Eckert et al., 2003). Similarly, human primary cardiac fibroblasts exposed to amyloidogenic LC isolated from light chain amyloidosis patients also induced oxidative stress in the mitochondria (Imperlini et al., 2017).

MITOCHONDRIAL GENE MUTATIONS IN CARDIAC PROTEOSTASIS

Several pieces of evidence indicate that mutation in the genes encoding for mitochondrial ETC complex proteins

may affect cellular proteostasis. Mutations in mitochondrial complexes I, II, and IV components are associated with Leigh syndrome, a neurological disorder; they have also been associated with hypertrophic or dilated cardiomyopathy (Berardo et al., 2011). Similarly, a recessive homozygous mutation in succinate dehydrogenase (SDH), a TCA cycle enzyme involved in linking electron transfer from the TCA cycle to mitochondrial complex II, has been shown to lead to the development of prenatal hypertrophic cardiomyopathy with severe complex II deficiency (Alston et al., 2015). Microdeletion of mitochondrial complex III component cytochrome B has also been linked to multisystem disease including left ventricular hypertrophy in humans (Carossa et al., 2014). Mutations in the complex IV components cytochrome C oxidase assembly homolog 10 (COX10) and 15 (COX15) have been shown to have a relationship with hypertrophic cardiomyopathy (Antonicka et al., 2003a,b). COX10 and COX15 are assembly factors of complex IV and play a critical role in the mitochondrial heme biosynthetic pathway by catalyzing the conversion of protoheme (heme B) to heme A (Antonicka et al., 2003a,b). Mutation in the cytochrome oxidase assembly factor 6 homolog (COA6) has been associated with hypertrophic cardiomyopathy with severe complex IV deficiency, and a mild decrease in complex I activity in heart tissue (Calvo et al., 2012; Baertling et al., 2015). COA6 is involved in the stability of the cytochrome C oxidase subunit 2 (COX2); mutation of COA6 results in COX2 deficiency in the heart (Pacheu-Grau et al., 2015, 2018). Mutation during the synthesis of cytochrome oxidase1 (SCO1) and 2 (SCO2) has been reported to lead to the development of hypertrophic cardiomyopathy (Jaksch et al., 2000; Stiburek et al., 2009; Pacheu-Grau et al., 2015). SCO1 and SCO2 are responsible for the transfer of copper to COX1 and COX2 (Herrmann and Funes, 2005; Pacheu-Grau et al., 2015). In general, mutation in these proteins leads to impairment of mitochondrial respiration and ATP production and enhanced ROS production and ultimately causes the cellular stress that impairs bioenergetics. The direct manner by which mutations in mtDNA alter mitochondrial quality control has been reported in a recent study using the mtDNA mutator mouse, which expresses a proofreading-deficient (D257A) version of mitochondrial polymerase gamma (PolG) (Joseph et al., 2013). mtDNA mutations in the PolG mouse altered several mitochondrial quality-control processes, including biogenesis, fusion/fission, and autophagy, contributing to the development of sarcopenia (Joseph et al., 2013). In fact, a wide range of aged tissues from both humans and animals demonstrated increased levels of mtDNA point mutations and deletions linked to a number of pathological conditions (Corral-Debrinski et al., 1992; Wallace, 2001; Wanagat et al., 2002; Khaidakov et al., 2003). Moreover, the loss of muscle mass observed in PolG mice is closely associated with reduced ETC complexes, impaired mitochondrial bioenergetics, and induction of apoptosis (Kujoth et al., 2005). Despite all of these studies linking mtDNA mutations to altered mitochondrial quality control, it remains unknown whether they affect cellular proteostasis, turnover of the whole organelle, or both processes.

MITOCHONDRIAL Ca^{2+} SUSCEPTIBILITY AND CARDIAC PROTEOSTASIS

Cardiomyocytes possess a unique feature: a large and variable intracellular calcium (iCa^{2+}) flux that regulates myocyte contraction on a beat-to-beat basis (Bers, 2008). The Ca^{2+} environment in the heart is dynamic to cope with this variable flux of Ca^{2+}. Moreover, the demands of the heart force the cardiac mitochondria to have an intricate and super-regulated exchange system competent to deal with these variable changes in Ca^{2+} load. Ca^{2+} influx to the mitochondrial matrix occurs via the mitochondria calcium uniporter (MCU). This influx is counteracted by efflux, which occurs through the mitochondrial sodium–calcium exchanger (NCLX) (Luongo et al., 2017). The mitochondrial membrane potential ($\Delta\psi$ = approximately –180 mV) generated by the proton gradient across the electron transport chain drives the MCU to take up Ca^{2+} (Kirichok et al., 2004). Mitochondria, the main site of the oxidative metabolism that generates ATP, are tightly controlled by the intra-mitochondrial Ca^{2+} concentration, which is closely aligned with the cellular metabolic demand (Berg et al., 2002). Several studies have demonstrated a correlation between an increased mitochondrial Ca^{2+} (mCa^{2+}) load and an increase in oxidative phosphorylation and ATP production (Unitt et al., 1989; Brandes and Bers, 2002). Therefore, Ca^{2+} appears to modulate mitochondrial metabolism via various mechanisms, including the regulation of Ca^{2+}-dependent dehydrogenases and modulation of ETC complexes (Glancy and Balaban, 2012). Despite the critical role played by Ca^{2+} in meeting the energy demands of cardiomyocytes, numerous studies have also demonstrated the detrimental effects of mCa^{2+} overload on the cardiomyocyte through activation of apoptosis and necrosis (Rasola and Bernardi, 2011). Ca^{2+} is also implicated as the major priming agent in the opening of the mitochondrial permeability transition pore (MPTP), resulting in the collapse of $\Delta\psi$ and dampening of ATP production, which activates apoptotic and necrotic cell death (Foo et al., 2005).

Recently, using the DRC mouse model, we demonstrated that mitochondrial MPTP opening is critical to the development of mitochondrial dysfunction in the heart (Alam et al., 2018). Mitochondrial swelling induced by Ca^{2+} challenge revealed that the mitochondria in D7-Des Tg mouse heart tissue were already swollen before any experimental Ca^{2+} challenges. Mitochondria from the D7-Des Tg heart also showed a significantly lower mitochondrial calcium retention capacity compared with control, indicating that the MPTP in mitochondria isolated from D7-Des Tg heart tissue were much more susceptible to Ca^{2+} loading. Mitochondrial MPTP opening caused by the increased localization of Bax to the outer membrane of the mitochondria was also evident in D7-Des Tg heart tissue. Similarly, $CryAB^{R120G}$ Tg mouse models of DRC also showed a similar susceptibility to mitochondrial swelling induced by Ca^{2}, which led to mitochondrial rupture and subsequent apoptosis (Maloyan et al., 2005). It can be speculated that protein aggregates may directly interact with mitochondria, affecting

the components of either the Ca^{2+} entry pathway or the mitochondrial permeability transition pore. Indeed, studies in neurodegenerative diseases have shown that misfolded protein aggregates directly associate with mitochondrial membrane proteins resulting in mitochondrial dysfunction. Exposure of isolated mitochondria from the brain to β-amyloid resulted in the dissipation of mitochondrial membrane potential, which is a common feature of mitochondrial Ca^{2+} overload (Casley et al., 2002). Moreover, β-amyloid can also trigger MPTP opening, a result of activation of mitochondrial swelling (Cardoso et al., 2001).

Consistent with the effects observed in neurodegenerative diseases, protein aggregates in $CryAB^{R120G}$ Tg heart tissue interact with mitochondrial protein, affecting the entry of Ca^{2+} into the mitochondria and influencing MPTP opening (Maloyan et al., 2005). Evidence for a possible interaction of the aggregate protein with the mitochondria was provided by a study showing aggregate protein accumulation in a mitochondrial fraction isolated from $CryAB^{R120G}$ Tg heart and $CryAB^{R120G}$ immunoprecipitation with mitochondrial protein voltage-dependent anionic channel (VDAC) (Maloyan et al., 2005). Observations of the interaction of aggregate protein $CryAB^{R120G}$ with VDAC provides a deeper insight into mitochondrial susceptibility to Ca^{2+} overload, oxidative stress, and reduced ATP synthesis in cardiac proteotoxicity. VDAC are highly abundant proteins in the outer mitochondrial membrane (OMM). The conformational state of the VDAC depends on the voltage, with different selectivity and permeability for small ions (Rostovtseva and Colombini, 1996; Hodge and Colombini, 1997). VDAC is considered the critical channel for the exchange of metabolites and small ions between the cytosol and the mitochondrial intermembrane space (IMS) (Camara et al., 2010, 2011). Interaction of protein aggregates with the VDAC impairs VDAC activity, altering the entry of Ca^{2+} into the mitochondria (**Figure 2**). Interestingly, in the mouse model of DRC in which protein aggregation alters the organization of the cytoskeleton (provided by desmin and tubulin, for example) and the interaction of the aggregates with VDAC, cardiac proteotoxicity alters mitochondrial Ca^{2+} loading, leading to MPTP opening and apoptotic cell death. Studies also suggest that tubulin-mediated regulation of VDAC function limits mitochondrial metabolism and alters the IMM potential ($\Delta\Psi m$), as well (Rostovtseva et al., 2008; Rostovtseva and Bezrukov, 2012). Cardiac LC amyloidosis also altered mitochondrial function in cardiac fibroblasts exposed to patient-derived pre-amyloidogenic LC (Imperlini et al., 2017) through the interaction of the amyloidogenic LC with the mitochondrial protein VDAC1 and optic atrophy protein 1 (OPA1) (Lavatelli et al., 2015).

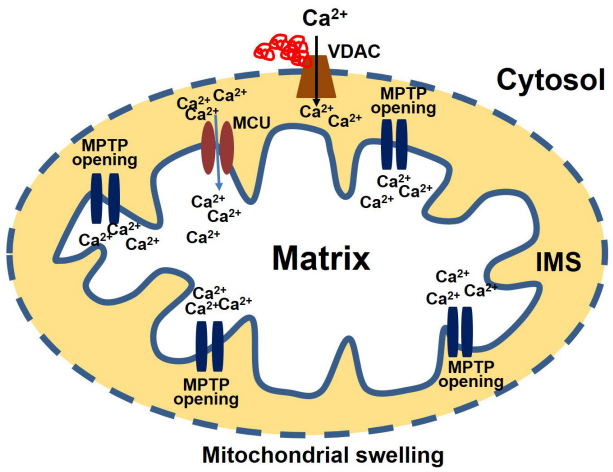

FIGURE 2 | Protein aggregate interacts with VDAC leading to an increase in Ca^{2+} susceptibility. Aggregate proteins may interact with the VDAC, affecting the entry of Ca^{2+} into the mitochondria. Ca^{2+} enters the matrix via the mitochondrial calcium uniporter (MCU). After entering the matrix, Ca^{2+} binds to the mitochondrial permeability transition pore (MPTP) and triggers it to open. Excessive mitochondrial Ca^{2+} causes the MPTP to remain open for a long time. As a result, the mitochondria undergo swelling and rupture, releasing apoptosis-inducing factors into the cytosol.

MITOCHONDRIAL PROTEOSTASIS IN CARDIAC PROTEINOPATHY

Mitochondrial chaperones and proteases maintain proteostasis through the mitochondrial unfolded protein response (UPR^{mt}) regulated by mitochondrial-to-nuclear communication. UPR^{mt} is a conserved transcriptional response activated by multiple forms of mitochondrial dysfunction during which the molecular chaperones function to refold the damaged proteins and misfolded proteins are degraded by proteases. Mitochondria contain approximately 1100 proteins, of which only 13 are encoded by their own genome; the rest are encoded by the nuclear genome. Nuclear encoded mitochondrial proteins are transported to the mitochondria through the mitochondrial outer and inner membrane transport machinery, which is generally termed as TOM (translocase of outer membrane) and TIM (translocase of inner membrane). For efficient transport, the transporting polypeptide needs to be in an unfolded condition; immediately after entry into the mitochondria, the unfolded polypeptide needs to be refolded. The canonical cytoplasmic proteostasis systems, including those of heat-shock proteins and proteasomes, are incapable of eliciting actions inside the mitochondria, as the mitochondria are double membrane-bound organelles (**Figure 3**). Moreover, as mentioned above, the mitochondrial complexes are made up of both mitochondrial genome-encoded and nuclear-encoded protein. Maintaining the balance of proteins from these two sources is a prerequisite for the proper function of the complex, as imbalance can promote protein aggregation (Voos, 2013; Moehle et al., 2019). In addition, mitochondrial proteins are constantly subjected to mitochondrial oxidative stress due to the production of the ETC by ROS. Oxidative stress may lead to the oxidation of mitochondrial proteins, such as carbonylation by reactive aldehyde and the reduction of cysteine. This results in structural changes to the protein, leading ultimately to the accumulation of non-functional toxic proteins (Hoshino et al., 2014). Altogether, the inability of the canonical cytoplasmic proteostasis system to function inside the mitochondria, the requirement for the intricate balance

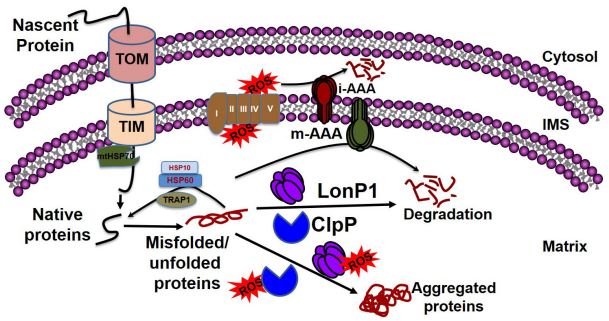

FIGURE 3 | Mitochondrial quality control by chaperones and proteases. Mitochondrial proteins enter into the mitochondria through the TOM and TIM complexes with the help of HSP70, which disaggregates the protein. Following a cascade of the chaperone proteins TRAP1, HSP10, and HSP60, the protein develops its native conformation. ROS generated from the leakage of electrons from the electron transport chain can affect mitochondrial protein conformation. The inner membrane-embedded protease i-AAA degrades the misfolded proteins in the intermembrane space, while m-AAA acts on misfolded proteins in the matrix. Misfolded proteins can be refolded to their native forms by the chaperone proteins, including TRAP1, HSP60, and HSP10. The soluble proteases LonP1 and ClpP clear the aggregates in the matrix. If excessive ROS generation compromises the function of LonP1 and ClpP, the protein cannot be refolded, resulting in aggregate formation in the mitochondria leading to mitochondrial dysfunction.

between nuclear and mitochondrial encoded proteins, and the vulnerability of the mitochondrial protein to oxidative stress requires the specialized mitochondrial proteostasis system as described below.

Mitochondrial Chaperone

Accumulating evidence has implicated the disturbance of mitochondrial proteostasis in the cellular toxicities associated with neurodegenerative diseases. Only recently have researchers begun to pay more attention to understanding how the molecular mechanisms of mitochondrial proteostasis contribute to the development of cardiac proteotoxicity. Among the mitochondrial chaperones, heat shock protein 60 (HSP60) has been well studied due to its molecular function in the transportation and refolding of proteins from the cytoplasm into the mitochondrial matrix. The molecular function of HSP60 in mitochondrial protein transport is mediated by catalyzing the folding of proteins destined for the matrix and maintaining the protein in an unfolded state for transport across the inner membrane of the mitochondria (Koll et al., 1992). Studies carried out using animal models of HF have shown that the cellular distribution of HSP60 changes as a cardiac pathology evident progresses (Lin et al., 2007). In the rat coronary ligation model of cardiac injury, the cellular distribution of HSP60 was altered; increased expression was observed in the mitochondria along with a concomitant decrease in the cytosol (Lin et al., 2007). Elevated expression of HSP60 has also been reported in human hearts with dilated and ischemic cardiomyopathy (Knowlton et al., 1998). Similar to HSP60, another chaperonin heat shock protein 10 (HSP10) also participates in various aspects of HSP60 and is an essential component of the mitochondrial protein folding apparatus (Jia et al., 2011). HSP10 potential function involved in the folding and assembly of the proteins imported into the matrix compartment (Hohfeld and Hartl, 1994). Moreover, HSP60 and HSP10 have been reported to function together as a complex in the mitochondria (**Figure 3**) and their simultaneous overexpression confers protection against simulated ischemia (Lau et al., 1997) and ischemic injury in cardiomyocytes (Lin et al., 2001; Hollander et al., 2003). HSP 60 and HSP 10 have also shown promise as cardioprotection against doxorubicin-induced cardiomyopathy (Shan et al., 2003).

Similarly, another mitochondrial 70-kDa heat shock protein (mtHsp70, also known as Mortalin) has been reported to be involved in cardiac protein homeostasis (Shepherd et al., 2018). MtHsp70 resides in the mitochondrial matrix and is a core subunit of the presequence translocase-associated motor (PAM) complex (**Figure 3**). MtHsp70 has been reported to attach to the importing protein by anchoring to the translocase of the inner membrane 44 (TIM44). TIM44 helps the translocation by trapping and pulling the anchored protein through the inner mitochondrial membrane. In conjunction with the translocation of the protein, mtHsp70 also provides the proper folding of the translocating protein (Baseler et al., 2012). Proteomic analysis revealed the relevance of mtHsp70 to neurodegenerative diseases such as Parkinson's disease (PD) (Jin et al., 2006). Decreased expression of mtHsp70 leads to compromised mitochondrial function, affecting mitochondrial protein import with concomitant decreased antioxidant defense and resulting in an increase in protein misfolding (Baseler et al., 2012). *In vitro* overexpression of mtHSP70 by adenoviral infection protects against simulated ischemia–reperfusion (IR) injury by enhancing antioxidant protein import and reducing ROS generation (Williamson et al., 2008). Moreover, it has been suggested that mtHsp70 restores mitochondrial function by decreasing changes to the mitochondrial protein structure through the inhibition of ROS generation as a result of increased import of nuclear-encoded mitochondrial antioxidant protein. Indeed, Hsp70 provides protection against myocardial injury in transgenic Hsp70 mice, presumably by refolding the misfolded protein caused by excessive ROS production (Marber et al., 1995).

Another chaperone protein localized to the mitochondria is a 75 kDa heat shock protein (HSP75 or TRAP1) known to function as a negative regulator of mitochondrial respiration owing to its ability to modulate the balance between oxidative phosphorylation and aerobic glycolysis (Yoshida et al., 2013). Studies have suggested that the impact of TRAP1 on mitochondrial respiration may be mediated by modulation of mitochondrial c-SRC and inhibition of succinate dehydrogenase (Sciacovelli et al., 2013). Mutation in TRAP1 is associated with decreased oxidative phosphorylation (OXPHOS) activity and loss of membrane potential in PD (Fitzgerald et al., 2017). Studies have demonstrated that a physiological function for TRAP1 in the heart as TRAP1 expression in the heart has been shown to decrease during natural aging (Ayyadevara et al., 2016). Overexpression of TRAP1 has been shown to protect against pressure overload-induced cardiac hypertrophy (Zhang et al., 2011). In addition, TRAP1 expression has been reported to

be induced by various stresses such as oxidative injury (Hua et al., 2007; Pridgeon et al., 2007; Landriscina et al., 2010). Overexpression of TRAP1 elicits protection against cardiac hypertrophy by improving mitochondrial function, presumably by maintaining mitochondrial proteostasis. Studies have also shown that TRAP1 protects the cardiomyocyte from hypoxic injury by regulating mitochondrial permeability transition pores (Xiang et al., 2010).

Mitochondrial Protease

In parallel with the mitochondrial chaperones, mitochondrial proteases play a pivotal role in the maintenance of mitochondrial proteostasis (**Figure 3**). Mitochondria contain four compartmentally based proteases: mitochondrial matrix-localized LonP1 and ClpP, and mitochondrial inner membrane ATP-dependent AAA family proteases (ATPases associated with diverse cellular activities) including i-AAA and m-AAA. Although both i-AAA and m-AAA are embedded in the inner mitochondrial membrane and contain ATPase and protease domains, their protease functions are spatially different; i-AAA is oriented in the direction of the intermembrane space, whereas m-AAA is oriented in the direction of the matrix. Due to spatial relationships, the inner membrane proteases are important for the surveillance of the OXPHOS machinery, which are constantly susceptible to oxidative damage due to their continuous production of ROS. Among these four proteases, LonP1 has been more studied for its role in the heart. LonP1 is associated with cardioprotection by ischemic preconditioning (IPS) through inhibiting ROS generation and consequent reduction in protein misfolding. Overexpression of Lonp1, as shown in LonP1 Tg mouse hearts, elicited cardioprotection by reducing the infarct size in IR injury (Venkatesh et al., 2019). Induction of LonP1 expression in cardiomyocytes has been reported in response to cellular and cardiac disturbances. Increased expression of LonP1 and ClpP1 has been reported in the hearts of Friedreich's ataxia mice associated with the loss of mitochondrial iron–sulfur proteins during the progression of the disease (Guillon et al., 2009). In addition to unfolded or oxidized protein, LonP1 has been reported to degrade the phosphorylated proteins as indicated by degradation of phosphorylated cytochrome c oxidase under hypoxic conditions (Sepuri et al., 2017). Phosphorylation may alter the three dimensional structure of cytochrome C oxidase, affecting its function and leading ultimately to its degradation by LonP1 (Sepuri et al., 2017). Recently, it has been shown that LonP1 deficiency leads to the activation of both the endoplasmic reticulum (ER)-unfolded protein response (UPR^{ER}) and the mitochondrial unfolded protein response (UPR^{mt}) (Lu B. et al., 2019), resulting in a metabolic shift toward glycolysis, glycogenesis, and amino acid metabolism from the mitochondrial oxidative phosphorylation to relieve mitochondrial stress. However, the molecular mechanisms of LonP1 mediated induction of UPR^{ER}, as well as UPR^{mt} and molecular signaling between UPR^{ER} and UPR^{mt}, remains unknown. It is possible that UPR^{ER} acts before UPR^{mt} as a first defense to protect the mitochondria against mitochondrial stress (Lu B. et al., 2019). Moreover, UPR^{ER} induction by LonP1 deficiency could be a feedback response mechanism, as suggested by the fact that overexpression of LonP1 requires the activity of protein kinase R-like ER kinase (PERK) regulated transcription factor activating transcription factor 4 (ATF4) (Onat et al., 2019). Future studies may provide insight in this regard (Lu B. et al., 2019). Apart from the LonP1-mediated signaling during cardiac stress, it has also been suggested that oxidative modification of LonP1, such as carbonylation, tyrosine nitrosylation, and cysteine reduction, can inhibit the proteolytic activity of LonP1 in pressure overloaded mice hearts (Hoshino et al., 2014).

Communication Between Mitochondria and the Nucleus in UPR^{mt}

Most proteins involved in mitochondrial biogenesis are controlled by nuclear transcription requiring tight communication between the two organelles. Under cellular conditions requiring high mitochondrial function, coordinated transcriptional activation of both nuclear and mitochondrial genes results in an increase in mitochondrial mass (Kotiadis et al., 2014). In *C. elegans*, communication between the mitochondria and the nucleus is mediated by the activating transcription factor associated with stress (ATFS-1), which has both mitochondrial and nuclear-targeted sequences (**Figure 4**). ATFS-1 is routed to the mitochondria under basal conditions when mitochondrial membrane potential is high and protein import is optimal where it is degraded by mitochondrial protease. The mitochondrial target sequence of ATFS-1 has a low net charge, and cannot enter into the mitochondria with low mitochondrial membrane potential. Under this scenario, ATFS-1 is routed to the nucleus to initiate the transcription of an array of genes to mitigate mitochondrial stress (Nargund et al., 2012; Rolland et al., 2019). In mammalian mitochondria, activating transcription factor 5 (ATF5, an ortholog of ATFS1) has been reported to regulate the mitochondrial unfolded protein response (UPS^{mt}) (Smyrnias et al., 2019). Studies have also shown that UPR upregulates

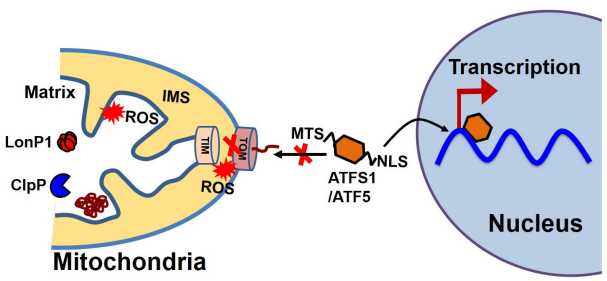

FIGURE 4 | Mitochondrial and nuclear communication during UPR^{mt}. Mitochondrial and nuclear communication is mediated through the transcription factor ATFS1 in *C. elegans* and ATF5 in mammals. ATFS1/ATF5 contains both a mitochondrial target sequence (MTS) and a nuclear localization signal (NLS). Under basal conditions, the mitochondrial transport system functions optimally. ATFS1/ATF5 preferentially enters the mitochondria and is degraded by mitochondrial proteases, including LonP1 and ClpP. Under stress conditions, mitochondrial entry systems are compromised due to excessive ROS generation by the mitochondria, making conditions favorable for ATFS1/ATF5 to enter the nucleus and trigger the array of gene transcription for UPR^{mt}.

C/EBP homologous protein (CHOP), which dimerizes with members of the CAAT/enhancer binding protein (C/EBP) family, regulating the expression of mitochondrial stress genes containing a mitochondrial unfolded protein response element (MURE) (Ryan and Hoogenraad, 2007). Another pathway of mitochondrial proteostasis regulation is mediated through a process called unfolded protein response activated by the mistargeting of proteins (UPR^{am}) in yeast cells (Wang and Chen, 2015; Wrobel et al., 2015). This pathway links the defects in mitochondrial biogenesis with proteasome activity, which buffers the consequences of a physiological slowdown in mitochondrial protein import. A mitochondrial targeting sequence (MTS) is necessary for the import of most mitochondrial protein, which requires a physiological mitochondrial membrane potential. Under conditions of decreased mitochondrial membrane potential, a massive accumulation of mitochondria precursors in the cytosol occurs, which activates the proteasome and attenuates the cytosolic synthesis of proteins (Wang and Chen, 2015; Wrobel et al., 2015).

Mitochondrial Contribution to the Degradation of Cytosolic Protein Aggregates

Cytosolic soluble misfolded proteins are usually degraded by the classical PQC system, including chaperones, UPS systems, and autophagy. In addition to the classical pathway, a recent study revealed another PQC pathway that involves the import of aggregate proteins into the mitochondria through mitochondrial import machinery via presumed disaggregation of the aggregate by heat shock protein 104 (HSP104). After the entry of the cytosolic aggregate into the mitochondria, the aggregates are degraded by the mitochondrial protease Pim1 (Lon protease homolog in mammals) (Ruan et al., 2017). This PQC system, which degrades the cytosolic protein imported into the mitochondria, has been given the acronym MAGIC (mitochondrion as a guardian for cytosol) (**Figure 5**). However, the molecular mechanism responsible for the MAGIC proteostasis pathway is not well understood and remains elusive. Extensive research is still needed to explore whether a protein without a mitochondrial targeting sequence can enter into the mitochondria, the consequence of the import of a misfolded protein on mitochondrial function, and the molecular fate of the misfolded protein in overburdened mitochondria. A recent study in an AD mouse model indicated that induction of UPR^{mt} could decrease protein aggregation, which seems to indicate that misfolded proteins from the cytosol can enter the mitochondria and ultimately become degraded (Sorrentino et al., 2017). In another study, it was shown that the downregulation of Tom40 is associated with cytosolic protein aggregation and disrupted neuronal integrity (Liu et al., 2018). Similarly, a study in human cells revealed that mitochondrial outer membrane protein FUN14 domain-containing protein 1 (FUNDC1) interacts with a 71-kDa heat shock cognate protein (HSC70) and promotes the entry of misfolded cytosolic protein into the mitochondria, followed by digestion of the translocated misfolded protein by the mitochondrial protease LonP1 (Li et al., 2019). Although it is too early to assume that the MAGIC pathway also plays a role in the heart, one could speculate that the MAGIC mechanism may also play a part in cardiac pathological stress, based on some reported evidence. Several studies have shown that decreased levels of HSP70 and mitochondrial dysfunction are positively correlated with postoperative atrial fibrillation (Mandal et al., 2005; Montaigne et al., 2013; Fauconnier, 2018). Moreover, chronic pressure overload has been associated with activation of UPR^{mt}, and increased levels of mitochondrial chaperone HSP60, proteases ClpP and LonP1, and mitochondrial-nuclear communication marker ATF5 (Smyrnias et al., 2019). These studies provide some clues about the entry of misfolded cytosolic proteins into the mitochondria, followed by degradation of the aggregates by the mitochondrial protease system, indicating that the MAGIC pathway could be functionally involved in the pathological stress conditions of the heart by clearing misfolded cytosolic proteins.

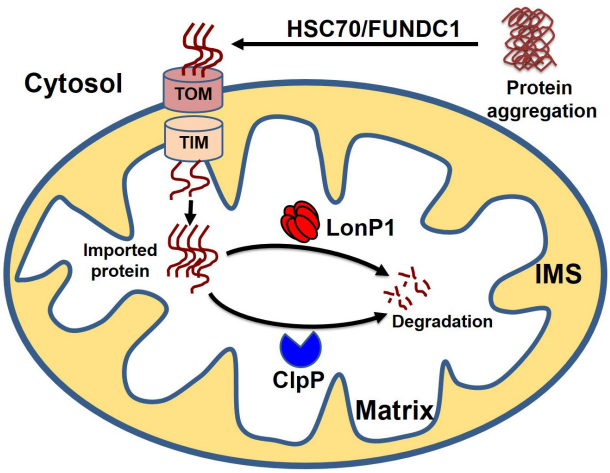

FIGURE 5 | Cytosolic protein clearance by mitochondrial guidance. In addition to classical mitochondrial proteostasis, the cytosolic aggregate can be cleared by the MAGIC (mitochondria as guidance in the cytosol) pathway. Presumably, the cytosolic aggregates are disaggregated by HSC70 or FUNDC1, followed by the entry of disaggregated protein into the mitochondria. Finally, cytosolic protein transported to the mitochondria undergoes degradation by mitochondrial protease LonP1 and ClpP.

MITOCHONDRIAL DYNAMICS IN CARDIAC PROTEOSTASIS

Mitochondria are highly dynamic organelles constantly undergoing the rapid and opposing processes of fission and fusion to maintain their shape, distribution, and size. Mitochondrial fission is regulated and maintained by dynamin-related protein 1 (Drp1). Drp1 is a cytosolic protein that translocates to the outer membrane of the mitochondria where it interacts with multiple adaptor proteins, including mitochondrial fission 1 protein (Fis1), mitochondrial dynamics proteins of 49 and 51 kDa (MiD49/51), and mitochondrial fusion factor (Mff) to form fission sites where Drp1 gathers to assemble

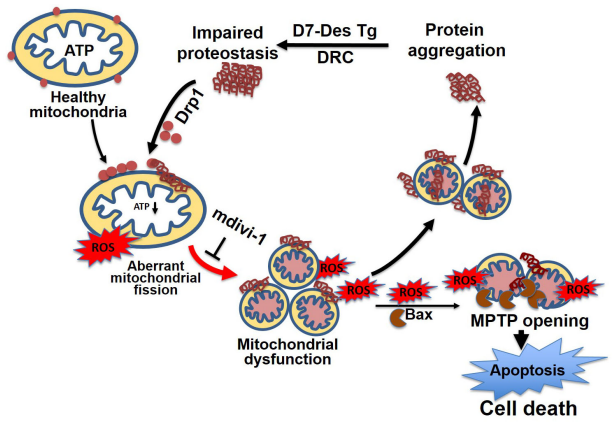

FIGURE 6 | Mitochondrial dynamics in cellular proteostasis. Proteotoxicity associated with DRC leads to the accumulation of cytosolic toxic protein aggregates that activate sequential events leading to cardiomyocyte death. These cytosolic aggregate proteins activate Drp1-dependent aberrant mitochondrial fission, activate Bax-dependent MPTP opening, result in excessive ROS generation, and ultimately lead to a reduction in ATP production. The mitochondrial membrane potential is decreased as a consequence of exacerbated ROS production, which, coupled with other signaling molecules, ultimately increases the mitochondrial membrane permeability, and causes the release of apoptotic contents into the cytosol, activating apoptotic cell death. This results in decreased levels of cellular ATP, aberrant mitochondrial fragmentation, and a release of excessive ROS, which contributes to dysfunctional mitochondrial proteostasis and exacerbates the accumulation of protein aggregates. Inhibition of aberrant mitochondrial fragmentation induced by DRC in cardiomyocytes by treatment with mitochondrial fission inhibitor (mdivi-1) restored mitochondrial function and reduced the cytosolic aggregate load.

the higher-ordered spiral complexes that constrict mitochondria for asymmetric division (Loson et al., 2013; Gao et al., 2017). Mitochondrial fusion is regulated by mitofusin 1 (Mfn1) and mitofusin 2 (Mfn2) mediated fusion of the OMM, and OPA1 mediated fusion of the inner mitochondrial membrane. Physiological fission is essential for maintaining normally functioning mitochondria, but Drp1-mediated excessive fission causes mitochondrial fragmentation, mitochondrial membrane depolarization, and an increase in ROS generation and oxidative stress, all of which lead to the development of mitochondrial dysfunction (Wu et al., 2011). In fact, proteotoxic neurodegenerative diseases such as AD, Huntington disease (HD), amyotrophic lateral sclerosis (ALS), and PD exhibit excessive mitochondrial fission, producing increased levels of ROS and defective mitochondrial function (Reddy, 2014b). Moreover, biochemical experiments in affected neurons have shown that the causative mutant proteins, including β-amyloid, phosphorylated Tau, mutant Htt, mutant LRRK2, and mutant DJ1 proteins, interact with the mitochondria (Reddy, 2014a). Inhibition of excessive Drp1 activity through blocking its interaction with Fis1 showed protective effects in HD (Guo et al., 2013) and PD models (Qi et al., 2013). Studies have also demonstrated that the interactions of misfolded protein aggregates with mitochondria ultimately result in impairment of mitochondrial dynamics, dysfunction, and neuronal damage.

Similar to observations in neurodegenerative diseases, the DRC mice expressing either D7-Des Tg or CryAB^{R120G} Tg showed highly perturbed mitochondrial spatial organization, and myofibrils interspersed with electron-dense aggregates. In association with this, reduced mitochondrial complex I activity was observed (Reimann et al., 2003; Vincent et al., 2016). The desmin knockout mouse is reported to have defects in cardiac mitochondrial morphology, positioning, and respiratory enzyme function, demonstrating a link between mitochondrial dysfunction and desminopathy (Joshi et al., 2014). In fact, expression of DRC causing mutant proteins in cardiomyocytes is associated with aberrant mitochondrial fission and increased expression of mitochondrial fission regulatory proteins. We reported that mutated desmin expression in D7-Des Tg mouse caused a reduction in mitochondrial respiration in both isolated mitochondria and intact cardiomyocytes (Alam et al., 2018) (**Figure 6**). Excessive mitochondrial fission is also attributable to hypertensive cardiac hypertrophy (Hasan et al., 2018) and sepsis-induced cardiomyopathy (Haileselassie et al., 2019). Aberrant mitochondrial fission may involve several possible mechanisms such as excessive production of reactive oxygen species and activation of fission regulatory proteins (Hasan et al., 2018).

Mitochondrial fission, fusion, and mitophagy are closely related processes that combat cellular proteotoxic stress. Mitophagy has been shown to be transiently activated with concomitant translocation of Drp1 to the mitochondria during the early stages of pressure-overload HF as an adaptive stress response. However, mitophagy is downregulated during the chronic phase of HF, in conjunction with a decrease in Drp1-dependent mitochondrial fission accompanied by mitochondrial enlargement. Surprisingly, the stimulation of mitophagy by Tat-Beclin (TB1) partially rescues the cardiac dysfunction, suggesting that mitophagy activation represents a potential therapeutic target in cardiac injury (Shirakabe et al., 2016). In the heart, one of the hallmarks of aging is accumulation of the lipofuscin inclusion body, which is made up of modified protein and lipid aggregate. Mitochondrial ROS have been implicated in the formation of lipofuscin aggregate in cardiomyocytes. The mitochondria in the aging heart are also larger in size as the result of the loss of mitochondrial fission and the consequent failure of mitophagy. Moreover, inhibition of mitochondrial fission has been shown to result in increased lipofuscin formation (Terman and Brunk, 2005). Reduced mitochondrial fission accompanied by loss of mitophagy in the senescent cell has also been reported (König et al., 2017; Rizza et al., 2018). Recently, it has been shown that mice deficient in both protein kinase B (Akt) and AMP-activated protein kinase (AMPK) are predisposed to cardiac aging, presumably due to compromised autophagy and mitophagy (Wang et al., 2019). Both mitochondrial fission and fusion regulatory proteins are decreased in the aged heart; a slight concomitant increase in UPR^{mt} and mitophagy markers has been observed in mice (Song et al., 2017). Complete abolishment of both fission (Drp1) and fusion (Mfn1 and Mfn2) markers in the mouse heart caused elevation of UPR^{mt} along with decreased mitophagy, indicating that complete abolishment of mitochondrial dynamics may not activate mitophagy (Song et al., 2017). In addition

to the mitochondrial dynamics, the accumulation of misfolded protein causes severe damage to the mitochondria leading to the degradation of the mitochondria by mitophagy. It has been shown that protein aggregation in the mitochondrial matrix activates the mitochondrial unfolded response as well as Pink1/Parkin-mediated mitophagy to alleviate the proteotoxicity and the mitophagy selectively facilitated by fission in mammals (Burman et al., 2017). Inhibition of mitochondrial fission results in the accumulation of large-sized mitochondria, leading to defects in mitophagy (Burman et al., 2017).

MITOCHONDRIA-TARGETED THERAPY TO PRESERVE CARDIAC PROTEOSTASIS

Mitochondria-targeted therapy represents a potential strategy for the treatment of proteostasis imbalance in the heart. So far, very few studies have demonstrated any possible mitochondrial-targeted therapy for the treatment of cardiac proteinopathy or proteostasis imbalance. Several studies have provided support for the idea that the mitochondria could be a therapeutic target. Possible mitochondrial therapy could include antioxidants that prevent mitochondrial protein modification due to excessive oxidative stress, agents that help preserve mitochondrial dynamics during stress conditions, and pharmacological agents that stimulate mitochondrial stress and thereby maintain mitochondrial proteostasis. It is evident that mitochondria play a central role in maintaining both cytosolic and their own proteostasis. There is considerable cross-talk between global proteostasis and mitochondrial proteostasis. The oxidative stress experienced by the mitochondria might endanger cytosolic proteostasis, whereas the mitochondrial import of misfolded cytosolic proteins could be a possible mechanism to preserve cytosolic proteostasis.

Antioxidants targeting the mitochondria have the potential to preserve proteostasis against the pressure overload induced heart failure. A pressure overloaded HF model showed the accumulation of misfolded LonP1 due to excessive oxidative stress, and treatment with antioxidant rescued the heart failure (Hoshino et al., 2014). Moreover, in TAC mice, treatment with a mitochondria-targeted superoxide dismutase mimetic, triphenylphosphonium chloride (mito-TEMPO), decreased the level of reduced cysteine in LonP1 and restored the proteolytic activity to degrade fluorescein isothiocyanate-labeled casein (Hoshino et al., 2014). Mito-TEMPO also has been reported to prevent HF by reducing mitochondrial ROS production in both the mitochondrial and cytosolic compartments. Notably, treatment with mito-TEMPO after the onset of cardiac hypertrophy reversed cardiac remodeling, demonstrating the relevance of mitochondrial targeting/ROS scavenging as a therapy following the onset of disease (Dey et al., 2018). Another mitochondrial-targeted antioxidant is MitoQ (mitoquinone), which contains a naturally occurring antioxidant, ubiquinone, conjugated with the lipophilic cation triphenylphosphonium. The lipophilicity and positive charge allow the molecule to cross the cell membrane and enter the mitochondrial matrix to counteract mtROS (Murphy and Smith, 2007; Rossman et al., 2018). It acts by facilitating electron transfer between Complex I/II and Complex III and decreasing lipid peroxidation (Kelso et al., 2001). Recently, MitoQ has been shown to be protective in prolonged TAC-induced HF in mice by reducing H_2O_2 and improving mitochondrial respiration and calcium retention capacity (Ribeiro et al., 2018). Studies carried out both *in vitro* and *in vivo* have provided evidence that MitoQ represents a potential target for use clinically as a mitochondria-targeted therapy (Murphy and Smith, 2007; Smith and Murphy, 2010; Rossman et al., 2018), which has led to its inclusion in several clinical trials (Gane et al., 2010; Smith and Murphy, 2010; Snow et al., 2010). A recent clinical trial (identification no: NCT02597023) has shown that chronic supplementation with MitoQ improves vascular function in healthy older adults. These results suggest targeting mtROS using MitoQ as a potential therapeutic option for reducing age-related cardiovascular disease (CVD) (Rossman et al., 2018). Currently, MitoQ is part of a Phase 4 clinical trial to investigate the role of mitochondrial derived oxidative stress on exercise capacity and arterial hemodynamics in heart failure with preserved ejection fraction (HFpEF) patients with and without chronic kidney disease (NCT03960073, clinicaltrials.gov).

We recently reported that excessive mitochondrial fission contributes to the disease process of DRC in the mouse. Inhibition of mitochondrial fission by mdivi-1 inhibited protein aggregation and rescued mitochondrial function, including the restoration of mitochondrial oxygen consumption (Alam et al., 2018). Mdivi1 is an allosteric inhibitor of GTPase assembly and inhibits GTP hydrolysis (Cassidy-Stone et al., 2008). Mdivi-1 has also been shown to confer cytoprotection in ischemia–reperfusion injury (Ong et al., 2010) (Sharp et al., 2014) and doxorubicin-induced cardiomyopathy (Gharanei et al., 2013) by reducing the production of ROS, attenuating cytosolic calcium overload, restoring mitochondrial membrane potential, and delaying hypercontracture of cardiomyocytes. However, a recent study reported that mdivi-1 functions as a reversible inhibitor of mitochondrial complex I, affecting mitochondrial respiration on COS-7 cells (Bordt et al., 2017). Similarly, mdivi-1 impaired DNA replication and repressed mitochondrial respiration independent of Drp1 in multidrug-resistant tumor cells (Qian et al., 2014). Treatment with mdivi-1 under high glucose-induced energy stress increased complex I activity and mitochondrial density in human neuronal SK cells (Huang et al., 2015). Although extensive studies use mdivi-1 as a mitochondrial fission inhibitor, other studies published in the literature to date have demonstrated context and cell type-dependent off-target effects of mdivi-1 through Drp1 dependent/independent pathways. Another mitochondrial fission inhibitor is P110, a 7-amino acid peptide harboring a homolog sequence between Fis1 and Drp1. This peptide selectively inhibits the interaction between Drp1 and Fis1. Several growing bodies of evidence indicate that P110 mediates mitochondrial fission inhibition and rescues the mitochondrial structure and interconnectivity in proteotoxic neuronal animal models of ALS (Joshi et al., 2018a), and Parkinson disease (Filichia et al., 2016). P110 treatment showed a reduction in Aβ accumulation, energetic failure, and

oxidative stress in the AD mouse model (Joshi et al., 2018b). P110 also has been shown to play a protective role in the heart subjected to the transient coronary artery occlusion (Ong et al., 2010). The mechanism underlying the protective effect of fission inhibition under stress conditions is presumably that it controls ROS generation, thereby protecting the protein against ROS induced modification.

Several studies have suggested that the UPR^{mt} and mitophagy pathways can be effectively induced in various mammalian tissues by supplementation with NAD^+-boosting compounds, including nicotinamide riboside (NR) and olaparib (AZD2281 or AZD) (Mouchiroud et al., 2013; Fang et al., 2016; Gariani et al., 2016; Zhang et al., 2016). Increasing the levels of NAD^+ by supplementation with NR induces the UPR^{mt} in cardiomyocytes and is implicated in the protective effect against chronic pressure overload in the mouse heart (Smyrnias et al., 2019). The beneficial effects of boosting NAD^+ were also observed in agonist-induced pathological hypertrophy, chronic pressure overload, and mitochondrial cardiomyopathy associated with Friedreich's ataxia (Pillai et al., 2010; Lee et al., 2016). A recent clinical study elucidated the pharmacokinetics of NR in healthy volunteers and reported that NR is safe in humans (Airhart et al., 2017). Several current clinical trials are investigating the efficacy of boosting NAD + to improve mitochondrial function in treating cardiomyopathy (NCT03727646, NCT03423342 clinicaltrials.gov) and Friedreich's ataxia (NCT04192136 clinicaltrials.gov).

OUTLOOK AND CONCLUSION

Mitochondria are essential organelles that play numerous critical metabolic roles in cardiomyocytes, and their dysfunction leads to the development of different cardiovascular diseases. Despite extensive studies of the biology of the mitochondria with respect to health and disease, the molecular processes involved in mitochondrial proteostasis remain relatively unstudied in the heart. Most of the proteotoxic diseases, including cardiac proteotoxicity and neurodegenerative diseases, are associated with the accumulation of misfolded protein aggregates, which leads to the progressive development of cellular pathology as organisms age. Importantly, in animal models of proteotoxicity, such as DRC, PD, and AD mouse models, mitochondrial dysfunction develops before the clinical manifestation of the disease. These studies suggest the possible involvement of dysfunctional proteostasis at the early stages of disease, leading to the gradual overwhelming of the mitochondrial PQC, alteration of mitochondrial dynamics (biogenesis as well as function), and eventual alteration of mitophagy, which may explain the gradual development of proteotoxic diseases during aging. Therefore, understanding the molecular signaling regulating mitochondrial proteostasis and its dysfunction under pathological conditions is critical to developing new therapies. Studies suggest that the mitochondria may contribute to clearing the cytosolic aggregate in non-cardiac cells (Ruan et al., 2017; Sorrentino et al., 2017), and there is a possibility that the mitochondria in cardiac cells may also take up cytosolic aggregates (Fauconnier, 2018). In this context, studies with direct molecular evidence showing the participation of cardiac mitochondria in the clearance of cytosolic protein aggregates remain unknown. Therefore, future studies are required to determine whether the cardiac mitochondria function to clear the cytosolic protein aggregates and, if so, to dissect the molecular mechanism. Research over the past few decades has identified multiple mechanisms and potential therapeutic targets, especially mitochondrial-targeted therapy, for the protection of cardiac proteostasis. Moving these targets into therapy requires recognizing the multitude of mitochondrial mechanisms in cardiac proteostasis. Future investigations of the balance among mitochondrial function regulators, including ROS, Ca^{2+}, and the redox state, would minimize the gap. In this review, we have gathered together the current understanding of the molecular signaling and regulatory mechanisms of mitochondrial proteostasis under pathophysiological conditions. However, to develop new therapies, further studies are required to understand the deeper mechanisms of mitochondrial proteostasis in cardiac diseases.

AUTHOR CONTRIBUTIONS

SA and MB conceptualized, designed, and wrote the manuscript. CA, RA, and MM participated in the conceptualization and editing of the manuscript. All co-authors edited and proofread the manuscript and approved the final version.

FUNDING

This work was supported by the National Institutes of Health grants: HL122354 and HL145753 to MB. LSUHSC-S Feist-Weiller Cancer Center IDEA grant to MB. AHA Postdoctoral Fellowship to SA 18POST34080495. LSUHSC-S Malcolm Feist and AHA Postdoctoral Fellowship to CA 20POST35210789. LSUHSC-S Malcolm Feist Pre-doctoral Fellowship to RA.

REFERENCES

Acin-Perez, R., Lechuga-Vieco, A. V., Del Mar Munoz, M., Nieto-Arellano, R., Torroja, C., Sanchez-Cabo, F., et al. (2018). Ablation of the stress protease OMA1 protects against heart failure in mice. *Sci. Transl. Med.* 10:eaan4935. doi: 10.1126/scitranslmed.aan4935

Ago, T., Liu, T., Zhai, P., Chen, W., Li, H., Molkentin, J. D., et al. (2008). A redox-dependent pathway for regulating class II HDACs and cardiac hypertrophy. *Cell* 133, 978–993. doi: 10.1016/j.cell.2008.04.041

Airhart, S. E., Shireman, L. M., Risler, L. J., Anderson, G. D., Nagana Gowda, G. A., Raftery, D., et al. (2017). An open-label, non-randomized study of the pharmacokinetics of the nutritional supplement nicotinamide riboside (NR) and its effects on blood NAD+ levels in healthy volunteers. *PLoS One* 12:e0186459. doi: 10.1371/journal.pone.0186459.

Alam, S., Abdullah, C. S., Aishwarya, R., Miriyala, S., Panchatcharam, M., Peretik, J. M., et al. (2018). Aberrant mitochondrial fission is maladaptive in desmin mutation–induced cardiac proteotoxicity. *J. Am. Heart Assoc.* 7:e009289.

Alston, C. L., Ceccatelli Berti, C., Blakely, E. L., Olahova, M., He, L., McMahon, C. J., et al. (2015). A recessive homozygous p.Asp92Gly SDHD mutation causes prenatal cardiomyopathy and a severe mitochondrial complex II deficiency. *Hum. Genet.* 134, 869–879. doi: 10.1007/s00439-015-1568-z

Antonicka, H., Leary, S. C., Guercin, G. H., Agar, J. N., Horvath, R., Kennaway, N. G., et al. (2003a). Mutations in COX10 result in a defect in mitochondrial heme A biosynthesis and account for multiple, early-onset clinical phenotypes associated with isolated COX deficiency. *Hum. Mol. Genet.* 12, 2693–2702. doi: 10.1093/hmg/ddg284

Antonicka, H., Mattman, A., Carlson, C. G., Glerum, D. M., Hoffbuhr, K. C., Leary, S. C., et al. (2003b). Mutations in COX15 produce a defect in the mitochondrial heme biosynthetic pathway, causing early-onset fatal hypertrophic cardiomyopathy. *Am. J. Hum. Genet.* 72, 101–114. doi: 10.1086/345489

Aon, M. A., Cortassa, S., and O'Rourke, B. (2010). Redox-optimized ROS balance: a unifying hypothesis. *Biochim. Biophys. Acta* 1797, 865–877. doi: 10.1016/j.bbabio.2010.02.016

Assem, M., Teyssier, J. R., Benderitter, M., Terrand, J., Laubriet, A., Javouhey, A., et al. (1997). Pattern of superoxide dismutase enzymatic activity and RNA changes in rat heart ventricles after myocardial infarction. *Am. J. Pathol.* 151, 549–555.

Ayyadevara, S., Balasubramaniam, M., Gao, Y., Yu, L. R., Alla, R., Shmookler Reis, R., et al. (2015). Proteins in aggregates functionally impact multiple neurodegenerative disease models by forming proteasome-blocking complexes. *Aging Cell* 14, 35–48. doi: 10.1111/acel.12296

Ayyadevara, S., Mercanti, F., Wang, X., Mackintosh, S. G., Tackett, A. J., Prayaga, S. V., et al. (2016). Age-and hypertension-associated protein aggregates in mouse heart have similar proteomic profiles. *Hypertension* 67, 1006–1013. doi: 10.1161/hypertensionaha.115.06849

Baertling, F., A M van den Brand M., Hertecant J. L., Al-Shamsi A., van den Heuvel P. L., Distelmaier F. et al. (2015). Mutations in COA6 cause cytochrome c oxidase deficiency and neonatal hypertrophic cardiomyopathy. *Hum. Mutat.* 36, 34–38. doi: 10.1002/humu.22715

Balaban, R. S., Nemoto, S., and Finkel, T. (2005). Mitochondria, oxidants, and aging. *Cell* 120, 483–495. doi: 10.1016/j.cell.2005.02.001

Bär, H., Strelkov, S. V., Sjöberg, G., Aebi, U., and Herrmann, H. (2004). The biology of desmin filaments: how do mutations affect their structure, assembly, and organisation? *J. Struct. Biol.* 148, 137–152. doi: 10.1016/j.jsb.2004.04.003

Baseler, W. A., Croston, T. L., and Hollander, J. M. (2012). "Functional characteristics of mortalin," in *Mortalin Biology: Life, Stress and Death*. eds R Wadhwa, S. Kaul (Berlin: Springer), 55–80. doi: 10.1007/978-94-007-3027-4_4

Baudino, T. A., McFadden, A., Fix, C., Hastings, J., Price, R., Borg, T. K., et al. (2008). Cell patterning: interaction of cardiac myocytes and fibroblasts in three-dimensional culture. *Microsc. Microanal.* 14, 117–125. doi: 10.1017/s1431927608080021

Berardo, A., Musumeci, O., and Toscano, A. (2011). Cardiological manifestations of mitochondrial respiratory chain disorders. *Acta Myol.* 30, 9–15.

Berg, J., Tymoczko, J., Stryer, L., and Gatto, G. (2002). *Biochemistry*. New York, NY: Freeman.

Bers, D. M. (2008). Calcium cycling and signaling in cardiac myocytes. *Annu. Rev. Physiol.* 70, 23–49. doi: 10.1146/annurev.physiol.70.113006.100455

Bordt, E. A., Clerc, P., Roelofs, B. A., Saladino, A. J., Tretter, L., Adam-Vizi, V., et al. (2017). The putative Drp1 inhibitor mdivi-1 Is a reversible mitochondrial complex i inhibitor that modulates reactive oxygen species. *Dev. Cell* 40, 583.e6–594.e6. doi: 10.1016/j.devcel.2017.02.020

Brandes, R., and Bers, D. M. (2002). Simultaneous measurements of mitochondrial NADH and Ca2+ during increased work in intact rat heart trabeculae. *Biophys. J.* 83, 587–604. doi: 10.1016/s0006-3495(02)75194-1

Brenner, D. A., Jain, M., Pimentel, D. R., Wang, B., Connors, L. H., Skinner, M., et al. (2004). Human amyloidogenic light chains directly impair cardiomyocyte function through an increase in cellular oxidant stress. *Circ. Res.* 94, 1008–1010. doi: 10.1161/01.res.0000126569.75419.74

Burgoyne, J. R., Mongue-Din, H., Eaton, P., and Shah, A. M. (2012). Redox signaling in cardiac physiology and pathology. *Circ. Res.* 111, 1091–1106. doi: 10.1161/CIRCRESAHA.111.255216

Burman, J. L., Pickles, S., Wang, C., Sekine, S., Vargas, J. N. S., Zhang, Z., et al. (2017). Mitochondrial fission facilitates the selective mitophagy of protein aggregates. *J. Cell Biol.* 216, 3231–3247. doi: 10.1083/jcb.201612106

Calvo, S. E., Compton, A. G., Hershman, S. G., Lim, S. C., Lieber, D. S., Tucker, E. J., et al. (2012). Molecular diagnosis of infantile mitochondrial disease with targeted next-generation sequencing. *Sci. Transl. Med.* 4:118ra110. doi: 10.1126/scitranslmed.3003310

Camara, A. K., Bienengraeber, M., and Stowe, D. F. (2011). Mitochondrial approaches to protect against cardiac ischemia and reperfusion injury. *Front Physiol.* 2:13. doi: 10.3389/fphys.2011.00013

Camara, A. K., Lesnefsky, E. J., and Stowe, D. F. (2010). Potential therapeutic benefits of strategies directed to mitochondria. *Antioxidants Redox Signal.* 13, 279–347. doi: 10.1089/ars.2009.2788

Cao, Y., Xu, C., Ye, J., He, Q., Zhang, X., Jia, S., et al. (2019). Miro2 regulates inter-mitochondrial communication in the heart and protects against TAC-induced cardiac dysfunction. *Cir. Res.* 125, 728–743. doi: 10.1161/circresaha.119.315432

Cardoso, S. M., Santos, S., Swerdlow, R. H., and Oliveira, C. R. (2001). Functional mitochondria are required for amyloid β-mediated neurotoxicity. *FASEB J.* 15, 1439–1441. doi: 10.1096/fj.00-0561fje

Carossa, V., Ghelli, A., Tropeano, C. V., Valentino, M. L., Iommarini, L., Maresca, A., et al. (2014). A novel in-frame 18-bp microdeletion in MT-CYB causes a multisystem disorder with prominent exercise intolerance. *Hum. Mutat.* 35, 954–958. doi: 10.1002/humu.22596

Casley, C., Canevari, L., Land, J., Clark, J., and Sharpe, M. (2002). β-Amyloid inhibits integrated mitochondrial respiration and key enzyme activities. *J. Neurochem.* 80, 91–100. doi: 10.1046/j.0022-3042.2001.00681.x

Cassidy-Stone, A., Chipuk, J. E., Ingerman, E., Song, C., Yoo, C., Kuwana, T., et al. (2008). Chemical inhibition of the mitochondrial division dynamin reveals its role in Bax/Bak-dependent mitochondrial outer membrane permeabilization. *Dev. Cell* 14, 193–204. doi: 10.1016/j.devcel.2007.11.019

Chang, H. C., Wu, R., Shang, M., Sato, T., Chen, C., Shapiro, J. S., et al. (2016). Reduction in mitochondrial iron alleviates cardiac damage during injury. *EMBO Mol. Med.* 8, 247–267. doi: 10.15252/emmm.201505748

Chung, H. S., Wang, S. B., Venkatraman, V., Murray, C. I., Van Eyk, J. E., et al. (2013). Cysteine oxidative posttranslational modifications: emerging regulation in the cardiovascular system. *Circ. Res.* 112, 382–392. doi: 10.1161/CIRCRESAHA.112.268680

Corral-Debrinski, M., Horton, T., Lott, M. T., Shoffner, J. M., Beal, M. F., Wallace, D. C., et al. (1992). Mitochondrial DNA deletions in human brain: regional variability and increase with advanced age. *Nat. Genet.* 2, 324–329. doi: 10.1038/ng1292-324

Dalakas, M. C., Park, K. -Y., Semino-Mora, C., Lee, H. S., Sivakumar, K., Goldfarb, L. G., et al. (2000). Desmin myopathy, a skeletal myopathy with cardiomyopathy caused by mutations in the desmin gene. *N. Engl. J. Med.* 342, 770–780. doi: 10.1056/nejm200003163421104

Dey, S., DeMazumder, D., Sidor, A., Foster, D. B., and O'Rourke, B. (2018). Mitochondrial ROS drive sudden cardiac death and chronic proteome remodeling in heart failure. *Circ. Res.* 123, 356–371. doi: 10.1161/circresaha.118.312708

Eckert, A., Keil, U., Marques, C. A., Bonert, A., Frey, C., Schussel, K., et al. (2003). Mitochondrial dysfunction, apoptotic cell death, and Alzheimer's disease. *Biochem. Pharmacol.* 66, 1627–1634. doi: 10.1016/s0006-2952(03)00534-3

Elluru, R. G., Bloom, G. S., and Brady, S. T. (1995). Fast axonal transport of kinesin in the rat visual system: functionality of kinesin heavy chain isoforms. *Mol. Biol. Cell* 6, 21–40. doi: 10.1091/mbc.6.1.21

Fang, E. F., Kassahun, H., Croteau, D. L., Scheibye-Knudsen, M., Marosi, K., Lu, H., et al. (2016). NAD+ replenishment improves lifespan and healthspan in ataxia telangiectasia models via mitophagy and DNA repair. *Cell Metab.* 24, 566–581. doi: 10.1016/j.cmet.2016.09.004

Fauconnier, J. (2018). Mitochondria and proteostasis: it'sa kind of MAGIC. *Cardiovasc. Res.* 114, e68-e69.

Filichia, E., Hoffer, B., Qi, X., and Luo, Y. (2016). Inhibition of Drp1 mitochondrial translocation provides neural protection in dopaminergic system in a Parkinson's disease model induced by MPTP. *Sci. Rep.* 6:32656.

Fitzgerald, J. C., Zimprich, A., Carvajal Berrio, D. A., Schindler, K. M., Maurer, B., Schulte, C., et al. (2017). Metformin reverses TRAP1 mutation-associated alterations in mitochondrial function in Parkinson's disease. *Brain* 140, 2444–2459. doi: 10.1093/brain/awx202

Foo, R. S. -Y., Mani, K., and Kitsis, R. N. (2005). Death begets failure in the heart. *J. Clin. Investigat.* 115, 565–571. doi: 10.1172/jci24569

Friedman, J. R., Lackner, L. L., West, M., DiBenedetto, J. R., Nunnari, J., Voeltz, G. K., et al. (2011). ER tubules mark sites of mitochondrial division. *Science* 334, 358–362. doi: 10.1126/science.1207385

Friedman, J. R., Webster, B. M., Mastronarde, D. N., Verhey, K. J., Voeltz, G. K., et al. (2010). ER sliding dynamics and ER–mitochondrial contacts occur on acetylated microtubules. *J. Cell Biol.* 190, 363–375. doi: 10.1083/jcb.200911024

Galluzzi, L., Bravo-San Pedro, J., Vitale, I., Aaronson, S., Abrams, J., Adam, D., et al. (2015). Essential versus accessory aspects of cell death: recommendations of the NCCD 2015. *Cell Death Differ.* 22, 58–73.

Gane, E. J., Weilert, F., Orr, D. W., Keogh, G. F., Gibson, M., Lockhart, M. M., et al. (2010). The mitochondria-targeted anti-oxidant mitoquinone decreases liver damage in a phase II study of hepatitis C patients. *Liver Int.* 30, 1019–1026. doi: 10.1111/j.1478-3231.2010.02250.x

Gao, J., Wang, L., Liu, J., Xie, F., Su, B, and Wang, X. (2017). Abnormalities of mitochondrial dynamics in neurodegenerative diseases. *Antioxidants* 6:25. doi: 10.3390/antiox6020025

Gariani, K., Menzies, K. J., Ryu, D., Wegner, C. J., Wang, X., Ropelle, E. R., et al. (2016). Eliciting the mitochondrial unfolded protein response by nicotinamide adenine dinucleotide repletion reverses fatty liver disease in mice. *Hepatology* 63, 1190–1204. doi: 10.1002/hep.28245

Gharanei, M., Hussain, A., Janneh, O., and Maddock, H. (2013). Attenuation of doxorubicin-induced cardiotoxicity by mdivi-1: a mitochondrial division/mitophagy inhibitor. *PLoS One* 8:e77713. doi: 10.1371/journal.pone.0077713

Glancy, B., and Balaban, R. S. (2012). Role of mitochondrial Ca2+ in the regulation of cellular energetics. *Biochemistry* 51, 2959–2973. doi: 10.1021/bi2018909

Go, Y. M., and Jones, D. P. (2013). The redox proteome. *J. Biol. Chem.* 288, 26512–26520. doi: 10.1074/jbc.R113.464131

Goldfarb, L. G., Park, K. -Y., Cervenáková, L., Gorokhova, S., Lee, H. -S., Vasconcelos, O., et al. (1998). Missense mutations in desmin associated with familial cardiac and skeletal myopathy. *Nat. Genet.* 19, 402–403. doi: 10.1038/1300

Golenhofen, N., Der Perng, M., Quinlan, R. A., and Drenckhahn, D. (2000). Comparison of the small heat shock proteins αB-crystallin, MKBP, HSP25, HSP20, and cvHSP in heart and skeletal muscle. *Histochem. Cell Biol.* 122, 415–425. doi: 10.1007/s00418-004-0711-z

Gregersen, N., Bolund, L., and Bross, P. (2005). Protein misfolding, aggregation, and degradation in disease. *Mol. Biotechnol.* 31, 141–150. doi: 10.1385/MB:31:2:141

Guillon, B., Bulteau, A. L., Wattenhofer-Donzé, M., Schmucker, S., Friguet, B., Puccio, H., et al. (2009). Frataxin deficiency causes upregulation of mitochondrial Lon and ClpP proteases and severe loss of mitochondrial Fe–S proteins. *FEBS J.* 276, 1036–1047. doi: 10.1111/j.1742-4658.2008.06847.x

Guo, X., Disatnik, M. H., Monbureau, M., Shamloo, M., Mochly-Rosen, D., Qi, X., et al. (2013). Inhibition of mitochondrial fragmentation diminishes Huntington's disease-associated neurodegeneration. *J. Clin. Invest.* 123, 5371–5388. doi: 10.1172/JCI70911

Haileselassie, B., Mukherjee, R., Joshi, A. U., Napier, B. A., Massis, L. M., Ostberg, N. P., et al. (2019). Drp1/Fis1 interaction mediates mitochondrial dysfunction in septic cardiomyopathy. *J. Mol. Cell Cardiol.* 130, 160–169. doi: 10.1016/j.yjmcc.2019.04.006

Hartl, F. U., Bracher, A., and Hayer-Hartl, M. (2011). Molecular chaperones in protein folding and proteostasis. *Nature* 475, 324–332. doi: 10.1038/nature10317

Hasan, P., Saotome, M., Ikoma, T., Iguchi, K., Kawasaki, H., Iwashita, T., et al. (2018). Mitochondrial fission protein, dynamin-related protein 1, contributes to the promotion of hypertensive cardiac hypertrophy and fibrosis in Dahl-salt sensitive rats. *J. Mol. Cell Cardiol.* 121, 103–106. doi: 10.1016/j.yjmcc.2018.07.004

He, K., Shi, X., Zhang, X., Dang, S., Ma, X., Liu, F., et al. (2011). Long-distance intercellular connectivity between cardiomyocytes and cardiofibroblasts mediated by membrane nanotubes. *Cardiovasc. Res.* 92, 39–47. doi: 10.1093/cvr/cvr189

Herrmann, J. M., and Funes, S. (2005). Biogenesis of cytochrome oxidase-sophisticated assembly lines in the mitochondrial inner membrane. *Gene* 354, 43–52. doi: 10.1016/j.gene.2005.03.017

Hodge, T., and Colombini, M. (1997). Regulation of metabolite flux through voltage-gating of VDAC channels. *J. Membr. Biol.* 157, 271–279. doi: 10.1007/s002329900235

Hohfeld, J., and Hartl, F. U. (1994). Role of the chaperonin cofactor Hsp10 in protein folding and sorting in yeast mitochondria. *J. Cell Biol.* 126, 305–315. doi: 10.1083/jcb.126.2.305

Hohn, A., Jung, T., Grimm, S., Catalgol, B., Weber, D., Grune, T., et al. (2011). Lipofuscin inhibits the proteasome by binding to surface motifs. *Free Radic. Biol. Med.* 50, 585–591. doi: 10.1016/j.freeradbiomed.2010.12.011

Hollander, J. M., Lin, K. M., Scott, B. T., and Dillmann, W. H. (2003). Overexpression of PHGPx and HSP60/10 protects against ischemia/reoxygenation injury. *Free Radic. Biol. Med.* 35, 742–751. doi: 10.1016/s0891-5849(03)00400-3

Hoshino, A., Okawa, Y., Ariyoshi, M., Kaimoto, S., Uchihashi, M., Fukai, K., et al. (2014). Oxidative post-translational modifications develop LONP1 dysfunction in pressure overload heart failure. *Circ.* 7, 500–509. doi: 10.1161/circheartfailure.113.001062

Hua, G., Zhang, Q., and Fan, Z. (2007). Heat shock protein 75 (TRAP1) antagonizes reactive oxygen species generation and protects cells from granzyme M-mediated apoptosis. *J. Biol. Chem.* 282, 20553–20560. doi: 10.1074/jbc.m703196200

Huang, S., Wang, Y., Gan, X., Fang, D., Zhong, C., Wu, L., et al. (2015). Drp1-mediated mitochondrial abnormalities link to synaptic injury in diabetes model. *Diabetes* 64, 1728–1742. doi: 10.2337/db14-0758

Huang, X., Sun, L., Ji, S., Zhao, T., Zhang, W., Xu, J., et al. (2013). Kissing and nanotunneling mediate intermitochondrial communication in the heart. *Proc. Natl. Acad. Sci. U.S.A.* 110, 2846–2851. doi: 10.1073/pnas.1300741110

Huang, Y., Zhou, M., Sun, H., and Wang, Y. (2011). Branched-chain amino acid metabolism in heart disease: an epiphenomenon or a real culprit? *Cardiovasc. Res.* 90, 220–223. doi: 10.1093/cvr/cvr070

Imperlini, E., Gnecchi, M., Rognoni, P., Sabido, E., Ciuffreda, M. C., Palladini, G., et al. (2017). Proteotoxicity in cardiac amyloidosis: amyloidogenic light chains affect the levels of intracellular proteins in human heart cells. *Sci. Rep.* 7:15661. doi: 10.1038/s41598-017-15424-3

Jaksch, M., Ogilvie, I., Yao, J., Kortenhaus, G., Bresser, H. G., Gerbitz, K. D., et al. (2000). Mutations in SCO2 are associated with a distinct form of hypertrophic cardiomyopathy and cytochrome c oxidase deficiency. *Hum. Mol. Genet.* 9, 795–801. doi: 10.1093/hmg/9.5.795

Jang, S., and Imlay, J. A. (2007). Micromolar intracellular hydrogen peroxide disrupts metabolism by damaging iron-sulfur enzymes. *J. Biol. Chem.* 282, 929–937. doi: 10.1074/jbc.M607646200

Jellali, A., Metz-Boutigue, M. H., Surgucheva, I., Jancsik, V., Schwartz, C., Filliol, D., et al. (1994). Structural and biochemical properties of kinesin heavy chain associated with rat brain mitochondria. *Cell Motil. Cytoskeleton* 28, 79–93. doi: 10.1002/cm.970280108

Jia, H., Halilou, A. I., Hu, L., Cai, W., Liu, J., and Huang, B. (2011). Heat shock protein 10 (Hsp10) in immune-related diseases: one coin, two sides. *Int. J. Biochem. Mol. Biol.* 2, 47–57.

Jin, J., Hulette, C., Wang, Y., Zhang, T., Pan, C., Wadhwa, R., et al. (2006). Proteomic identification of a stress protein, mortalin/mthsp70/GRP75: relevance to Parkinson disease. *Mol. Cell. Proteomics* 5, 1193–1204. doi: 10.1074/mcp.m500382-mcp200

Joseph, A. M., Adhihetty, P. J., Wawrzyniak, N. R., Wohlgemuth, S. E., Picca, A., Kujoth, G. C., et al. (2013). Dysregulation of mitochondrial quality control processes contribute to sarcopenia in a mouse model of premature aging. *PLoS One* 8:e69327. doi: 10.1371/journal.pone.0069327

Joshi, A. U., Saw, N. L., Shamloo, M., and Mochly-Rosen, D. (2018a). Drp1/Fis1 interaction mediates mitochondrial dysfunction, bioenergetic failure and cognitive decline in Alzheimer's disease. *Oncotarget* 9, 6128–6143. doi: 10.18632/oncotarget.23640

Joshi, A. U., Saw, N. L., Vogel, H., Cunnigham, A. D., Shamloo, M., Mochly-Rosen, D., et al. (2018b). Inhibition of Drp1/Fis1 interaction slows progression of amyotrophic lateral sclerosis. *EMBO Mol. Med.* 10:e8166.

Joshi, P. R., Hauburger, A., Kley, R., Claeys, K. G., Schneider, I., Kress, W., et al. (2014). Mitochondrial abnormalities in myofibrillar myopathies. *Clin. Neuropathol.* 33, 134–142. doi: 10.5414/NP300693

Kakimoto, Y., Okada, C., Kawabe, N., Sasaki, A., Tsukamoto, H., Nagao, R., et al. (2019). Myocardial lipofuscin accumulation in ageing and sudden cardiac death. *Sci. Rep.* 9:3304. doi: 10.1038/s41598-019-40250-0

Kelso, G. F., Porteous, C. M., Coulter, C. V., Hughes, G., Porteous, W. K., Ledgerwood, E. C., et al. (2001). Selective targeting of a redox-active ubiquinone to mitochondria within cells: antioxidant and antiapoptotic properties. *J. Biol. Chem.* 276, 4588–4596. doi: 10.1074/jbc.M009093200

Khaidakov, M., Heflich, R. H., Manjanatha, M. G., Myers, M. B., and Aidoo, A. (2003). Accumulation of point mutations in mitochondrial DNA of aging mice. *Mutat. Res.* 526, 1–7. doi: 10.1016/s0027-5107(03)00010-1

Kim, T. Y., Terentyeva, R., Roder, K. H., Li, W., Liu, M., Greener, I., et al. (2017). SK channel enhancers attenuate Ca2+-dependent arrhythmia in hypertrophic hearts by regulating mito-ROS-dependent oxidation and activity of RyR. *Cardiovasc. Res.* 113, 343–353. doi: 10.1093/cvr/cvx005

Kirichok, Y., Krapivinsky, G., and Clapham, D. E. (2004). The mitochondrial calcium uniporter is a highly selective ion channel. *Nature* 427, 360–364. doi: 10.1038/nature02246

Knowlton, A. A., Kapadia, S., Torre-Amione, G., Durand, J. -B., Bies, R., Young, J., et al. (1998). Differential expression of heat shock proteins in normal and failing human hearts. *J. Mol. Cell. Cardiol.* 30, 811–818. doi: 10.1006/jmcc.1998.0646

Koll, H., Guiard, B., Rassow, J., Ostermann, J., Horwich, A. L., Neupert, W., et al. (1992). Antifolding activity of hsp60 couples protein import into the mitochondrial matrix with export to the intermembrane space. *Cell* 68, 1163–1175. doi: 10.1016/0092-8674(92)90086-r

König, J., Ott, C., Hugo, M., Jung, T., Bulteau, A. -L., Grune, T., et al. (2017). Mitochondrial contribution to lipofuscin formation. *Redox Biol.* 11, 673–681.

Konig, J., Ott, C„ Hugo, M„ Jung, T., Bulteau, A. L„ Grune, T., et al. (2017). Mitochondrial contribution to lipofuscin formation. *Redox Biol.* 11, 673–681. doi: 10.1016/j.redox.2017.01.017

Kotiadis, V. N., Duchen, M. R., and Osellame, L. D. (2014). Mitochondrial quality control and communications with the nucleus are important in maintaining mitochondrial function and cell health. *Biochim. Biophys. Acta* 1840, 1254–1265. doi: 10.1016/j.bbagen.2013.10.041

Kroemer, G., Galluzzi, L., Vandenabeele, P., Abrams, J., Alnemri, E. S., Baehrecke, E. H., et al. (2009). Classification of cell death: recommendations of the Nomenclature committee on cell death 2009. *Cell Death Differ.* 16, 3–11. doi: 10.1038/cdd.2008.150

Kujoth, G. C., Hiona, A., Pugh, T. D., Someya, S., Panzer, K., Wohlgemuth, S. E., et al. (2005). Mitochondrial DNA mutations, oxidative stress, and apoptosis in mammalian aging. *Science* 309, 481–484. doi: 10.1126/science.1112125

Kumar, V., Calamaras, T. D, Haeussler, D., Colucci, W. S., Cohen, R. A., McComb, M. E., et al. (2012). Cardiovascular redox and ox stress proteomics. *Antioxid Redox Signal.* 17, 1528–1559. doi: 10.1089/ars.2012.4706

Landriscina, M., Laudiero, G., Maddalena, F., Amoroso, M. R., Piscazzi, A., Cozzolino, F., et al. (2010). Mitochondrial chaperone Trap1 and the calcium binding protein Sorcin interact and protect cells against apoptosis induced by antiblastic agents. *Cancer Res.* 70, 6577–6586. doi: 10.1158/0008-5472.can-10-1256

Lau, S., Patnaik, N., Sayen, M. R., and Mestril, R. (1997). Simultaneous overexpression of two stress proteins in rat cardiomyocytes and myogenic cells confers protection against ischemia-induced injury. *Circulation* 96, 2287–2294. doi: 10.1161/01.cir.96.7.2287

Lavatelli, F., Imperlini, E., Orrù, S., Rognoni, P., Sarnataro, D., Palladini, G., et al. (2015). Novel mitochondrial protein interactors of immunoglobulin light chains causing heart amyloidosis. *FASEB J.* 29, 4614–4628. doi: 10.1096/fj.15-272179

Lee, C. F., Chavez, J. D., Garcia-Menendez, L., Choi, Y., Roe, N. D., Chiao, Y. A., et al. (2016). Normalization of NAD+ redox balance as a therapy for heart failure. *Circulation* 134, 883–894. doi: 10.1161/circulationaha.116.022495

Leichert, L. I., and Dick, T. P. (2015). Incidence and physiological relevance of protein thiol switches. *Biol. Chem.* 396, 389–399. doi: 10.1515/hsz-2014-0314

Leopold, P..L., McDowall, A..W., Pfister, K. K., Bloom, G. S., and Brady, S. T. (1992). Association of kinesin with characterized membrane-bounded organelles. *Cell Motil. cytoskeleton* 23, 19–33. doi: 10.1002/cm.970230104

Letts, J. A., Fiedorczuk, K., and Sazanov, L. A. (2016). The architecture of respiratory supercomplexes. *Nature* 537, 644–648. doi: 10.1038/nature19774

Lewis, S. C., Uchiyama, L. F., and Nunnari, J. (2016). ER-mitochondria contacts couple mtDNA synthesis with mitochondrial division in human cells. *Science* 353:aaf5549. doi: 10.1126/science.aaf5549

Li, Y., Xue, Y., Xu, X., Wang, G., Liu, Y., Wu, H., et al. (2019). A mitochondrial FUNDC1/HSC70 interaction organizes the proteostatic stress response at the risk of cell morbidity. *EMBO J.* 38:e98786

Li, Z., Colucci-Guyon, E., Pinçon-Raymond, M., Mericskay, M., Pournin, S., Paulin, D., et al. (1996). Cardiovascular lesions and skeletal myopathy in mice lacking desmin. *Dev. Biol.* 175, 362–366. doi: 10.1006/dbio.1996.0122

Lin, K. M., Lin, B., Lian, I. Y., Mestril, R., Scheffler, I. E., Dillmann, W. H., et al. (2001). Combined and individual mitochondrial HSP60 and HSP10 expression in cardiac myocytes protects mitochondrial function and prevents apoptotic cell deaths induced by simulated ischemia-reoxygenation. *Circulation* 103, 1787–1792. doi: 10.1161/01.cir.103.13.1787

Lin, L., Kim, S. -C., Wang, Y., Gupta, S., Davis, B., Simon, S. I., et al. (2007). HSP60 in heart failure: abnormal distribution and role in cardiac myocyte apoptosis. *Am. J. Physiol. Heart Circ. Physiol.* 293, H2238–H2247.

Lindén, M., Li, Z., Paulin, D., Gotow, T., and Leterrier, J. -F. (2001). Effects of desmin gene knockout on mice heart mitochondria. *J. Bioenerg. Biomembr.* 33, 333–341.

Liu, W., Duan, X., Fang, X., Shang, W., and Tong, C. (2018). Mitochondrial protein import regulates cytosolic protein homeostasis and neuronal integrity. *Autophagy* 14, 1293–1309. doi: 10.1080/15548627.2018.1474991

Loson, O. C., Song, Z., Chen, H.., and Chan, D. C. (2013). Fis1, Mff, MiD49, and MiD51 mediate Drp1 recruitment in mitochondrial fission. *Mol. Biol. Cell* 24, 659–667. doi: 10.1091/mbc.E12-10-0721

Lu, B., Shangguan, F., Huang, D., Gong, S., Shi, Y., Song, Z., et al. (2019). LonP1 orchestrates UPRmt and UPRER and mitochondrial dynamics to regulate heart function. *bioRxiv* [Preprint]. doi: 10.1101/564492

Lu, X., Thai, P. N., Lu, S., Pu, J., and Bers, D. M. (2019). Intrafibrillar and perinuclear mitochondrial heterogeneity in adult cardiac myocytes. *J. Mol. Cell Cardiol.* 136, 72–84. doi: 10.1016/j.yjmcc.2019.08.013

Luongo, T. S., Lambert, J. P., Gross, P., Nwokedi, M., Lombardi, A. A., Shanmughapriya, S., et al. (2017). The mitochondrial Na^+/Ca^{2+} exchanger is essential for Ca^{2+} homeostasis and viability. *Nature* 545, 93–97. doi: 10.1038/nature22082

Maloyan, A., Sanbe, A., Osinska, H., Westfall, M., Robinson, D., Imahashi, K., et al. (2005). Mitochondrial dysfunction and apoptosis underlie the pathogenic process in alpha-B-crystallin desmin-related cardiomyopathy. *Circulation* 112, 3451–3461. doi: 10.1161/CIRCULATIONAHA.105.572552

Mandal, K., Torsney, E., Poloniecki, J., Camm, A. J., Xu, Q., Jahangiri, M., et al. (2005). Association of high intracellular, but not serum, heat shock protein 70 with postoperative atrial fibrillation. *Ann. Thorac. Surg.* 79, 865–871, discussion 871. doi: 10.1016/j.athoracsur.2004.08.018

Marber, M. S., Mestril, R., Chi, S. -H., Sayen, M. R., Yellon, D. M., Dillmann, W. H., et al. (1995). Overexpression of the rat inducible 70-kD heat stress protein in a transgenic mouse increases the resistance of the heart to ischemic injury. *J. Clin. Invest.* 95, 1446–1456. doi: 10.1172/jci117815

Milner, D. J., Weitzer, G., Tran, D., Bradley, A., and Capetanaki, Y. (1996). Disruption of muscle architecture and myocardial degeneration in mice lacking desmin. *J. Cell Biol.* 134, 1255–1270. doi: 10.1083/jcb.134.5.1255

Miranda, S., Opazo, C., Larrondo, L. F., Munoz, F. J., Ruiz, F., Leighton, F., et al. (2000). The role of oxidative stress in the toxicity induced by amyloid beta-peptide in Alzheimer's disease. *Prog. Neurobiol.* 62, 633–648. doi: 10.1016/s0301-0082(00)00015-0

Moehle, E. A., Shen, K., and Dillin, A. (2019). Mitochondrial proteostasis in the context of cellular and organismal health and aging. *J. Biol. Chem.* 294, 5396–5407. doi: 10.1074/jbc.tm117.000893

Montaigne, D., Marechal, X., Lefebvre, P., Modine, T., Fayad, G., Dehondt, H., et al. (2013). Mitochondrial dysfunction as an arrhythmogenic substrate: a translational proof-of-concept study in patients with metabolic syndrome in whom post-operative atrial fibrillation develops. *J. Am. Coll Cardiol.* 62, 1466–1473. doi: 10.1016/j.jacc.2013.03.061

Mouchiroud, L., Houtkooper, R. H., Moullan, N., Katsyuba, E., Ryu, D., Cantó, C., et al. (2013). The NAD+/sirtuin pathway modulates longevity through activation of mitochondrial UPR and FOXO signaling. *Cell* 154, 430–441. doi: 10.1016/j.cell.2013.06.016

Munzel, T., Camici, G. G., Maack, C., Bonetti, N. R., Fuster, V., Kovacic, J..C. et al. (2017). Impact of oxidative stress on the heart and vasculature: part 2 of a 3-part series. *J. Am. Coll Cardiol.* 70, 212–229. doi: 10.1016/j.jacc.2017.05.035

Munzel, T., Gori, T., Keaney, J. F. Jr., Maack, C., and Daiber, A. (2015). Pathophysiological role of oxidative stress in systolic and diastolic heart failure and its therapeutic implications. *Eur. Heart. J.* 36, 2555–2564. doi: 10.1093/eurheartj/ehv305

Murphy, M. P., and Smith, R. A. (2007). Targeting antioxidants to mitochondria by conjugation to lipophilic cations. *Annu. Rev. Pharmacol. Toxicol.* 47, 629–656. doi: 10.1146/annurev.pharmtox.47.120505.105110

Nan, J., Zhu, W., Rahman, M., Liu, M., Li, D., Su, S., et al. (2017). Molecular regulation of mitochondrial dynamics in cardiac disease. *Biochim. Biophys. Acta Mol. Cell Res.* 1864, 1260–1273. doi: 10.1016/j.bbamcr.2017.03.006

Nangaku, M., Sato-Yoshitake, R., Okada, Y., Noda, Y., Takemura, R., Yamazaki, H., et al. (1994). KIF1B, a novel microtubule plus end-directed monomeric motor protein for transport of mitochondria. *Cell* 79, 1209–1220. doi: 10.1016/0092-8674(94)90012-4

Napoli, E., Taroni, F., and Cortopassi, G. A. (2006). Frataxin, iron-sulfur clusters, heme, ROS, and aging. *Antioxid Redox Signal.* 8, 506–516. doi: 10.1089/ars.2006.8.506

Nargund, A. M., Pellegrino, M. W., Fiorese, C. J., Baker, B. M., and Haynes, C. M. (2012). Mitochondrial import efficiency of ATFS-1 regulates mitochondrial UPR activation. *Science* 337, 587–590. doi: 10.1126/science.1223560

Nguyen, T. T., Oh, S. S., Weaver, D., Lewandowska, A., Maxfield, D., Schuler, M. -H., et al. (2014). Loss of Miro1-directed mitochondrial movement results in a novel murine model for neuron disease. *Proc. Natl. Acad. Sci. U.S.A.* 111, E3631–E3640.

Nozynski, J., Zakliczynski, M., Konecka-Mrowka, D., Zakliczynska, H., Pijet, M., Zembala-Nozynska, E., et al. (2013). Advanced glycation end products and lipofuscin deposits share the same location in cardiocytes of the failing heart. *Exp. Gerontol.* 48, 223–228. doi: 10.1016/j.exger.2012.09.002

Ogata, T., and Yamasaki, Y. (1997). Ultra-high-resolution scanning electron microscopy of mitochondria and sarcoplasmic reticulum arrangement in human red, white, and intermediate muscle fibers. *Anat. Record* 248, 214–223. doi: 10.1002/(sici)1097-0185(199706)248:2<214::aid-ar8>3.0.co;2-s

Onat, U. I., Yildirim, A. D., Tufanli, Ö., Çimen, I., Kocatürk, B., Veli, Z., et al. (2019). Intercepting the lipid-induced integrated stress response reduces atherosclerosis. *J. Am. Coll. Cardiol.* 73, 1149–1169. doi: 10.1016/j.jacc.2018.12.055

Ong, S. B., Subrayan, S., Lim, S. Y., Yellon, D. M., Davidson, S. M., Hausenloy, D. J. et al. (2010). Inhibiting mitochondrial fission protects the heart against ischemia/reperfusion injury. *Circulation* 121, 2012–2022. doi: 10.1161/CIRCULATIONAHA.109.906610

Pacheu-Grau, D., Bareth, B., Dudek, J., Juris, L., Vogtle, F. N., Wissel, M., et al. (2015). Cooperation between COA6 and SCO2 in COX2 maturation during cytochrome c oxidase assembly links two mitochondrial cardiomyopathies. *Cell Metab.* 21, 823–833. doi: 10.1016/j.cmet.2015.04.012

Pacheu-Grau, D., Rucktaschel, R., and Deckers, M. (2018). Mitochondrial dysfunction and its role in tissue-specific cellular stress. *Cell Stress* 2, 184–199. doi: 10.15698/cst2018.07.147

Phillips, M. J., and Voeltz, G. K. (2016). Structure and function of ER membrane contact sites with other organelles. *Nat. Rev. Mol. Cell Biol.* 17, 69–82. doi: 10.1038/nrm.2015.8

Pillai, V. B., Sundaresan, N. R., Kim, G., Gupta, M., Rajamohan, S. B., Pillai, J. B., et al. (2010). Exogenous NAD blocks cardiac hypertrophic response via activation of the SIRT3-LKB1-AMP-activated kinase pathway. *J. Biol. Chem.* 285, 3133–3144. doi: 10.1074/jbc.m109.077271

Porter, K. E., and Turner, N. A. (2009). Cardiac fibroblasts: at the heart of myocardial remodeling. *Pharmacol. Ther.* 123, 255–278. doi: 10.1016/j.pharmthera.2009.05.002

Powers, E. T., and Balch, W. E. (2013). Diversity in the origins of proteostasis networks—a driver for protein function in evolution. *Nat. Rev. Mol. Cell Biol.* 14, 237–248. doi: 10.1038/nrm3542

Pridgeon, J. W., Olzmann, J. A., Chin, L. -S., and Li, L. (2007). PINK1 protects against oxidative stress by phosphorylating mitochondrial chaperone TRAP1. *PLoS Biol.* 5:e172. doi: 10.1371/journal.pbio.0050172

Qi, X., Qvit, N., Su, Y. C., and Mochly-Rosen, D. (2013). A novel Drp1 inhibitor diminishes aberrant mitochondrial fission and neurotoxicity. *J. Cell Sci.* 126(Pt. 3), 789–802. doi: 10.1242/jcs.114439

Qian, W., Wang, J., Roginskaya, V., McDermott, L. A., Edwards, R. P., Stolz, D. B., et al. (2014). Novel combination of mitochondrial division inhibitor 1 (mdivi-1) and platinum agents produces synergistic pro-apoptotic effect in drug resistant tumor cells. *Oncotarget* 5, 4180–4194. doi: 10.18632/oncotarget.1944

Radu, R. I., Bold, A., Pop, O. T., Malaescu, D. G., Gheorghisor, I., Mogoanta, L. et al. (2012). Histological and immunohistochemical changes of the myocardium in dilated cardiomyopathy. *Rom. J. Morphol. Embryol.* 53, 269–275.

Rappaport, L., Oliviero, P., and Samuel, J. (1998). "Cytoskeleton and mitochondrial morphology and function," in *Bioenergetics of the Cell: Quantitative Aspects*. Eds V. A. Saks, R. Ventura-Clapier, X. Leverve, A. Rossi, and M. Rigoulet (Berlin: Springer), 101–105. doi: 10.1007/978-1-4615-5653-4_8

Rasola, A., and Bernardi, P. (2011). Mitochondrial permeability transition in Ca2+-dependent apoptosis and necrosis. *Cell Calcium* 50, 222–233. doi: 10.1016/j.ceca.2011.04.007

Rayment, N. B., Haven, A. J., Madden, B., Murday, A., Trickey, R., Shipley, M., et al. (1999). Myocyte loss in chronic heart failure. *J. Pathol.* 188, 213–219. doi: 10.1002/(SICI)1096-9896(199906)188:2<213::AID-PATH348<3.0.CO;2-5

Reddy, P. H. (2014a). Increased mitochondrial fission and neuronal dysfunction in Huntington's disease: implications for molecular inhibitors of excessive mitochondrial fission. *Drug Discov. Today* 19, 951–955. doi: 10.1016/j.drudis.2014.03.020

Reddy, P. H. (2014b). Misfolded proteins, mitochondrial dysfunction, and neurodegenerative diseases. *Biochim. Biophys. Acta* 1842:1167. doi: 10.1016/j.bbadis.2014.03.012

Reimann, J., Kunz, W. S., Vielhaber, S., Kappes-Horn, K., and Schroder, R. (2003). Mitochondrial dysfunction in myofibrillar myopathy. *Neuropathol. Appl. Neurobiol.* 29, 45–51. doi: 10.1046/j.1365-2990.2003.00428.x

Ribeiro, R. F. Jr., Dabkowski, E. R., Shekar, K. C., KA, O. C., Hecker, P. A., Murphy, M. P., et al. (2018). MitoQ improves mitochondrial dysfunction in heart failure induced by pressure overload. *Free Radic. Biol. Med.* 117, 18–29. doi: 10.1016/j.freeradbiomed.2018.01.012

Rizza, S., Cardaci, S., Montagna, C., Di Giacomo, G., De Zio, D., Bordi, M., et al. (2018). S-nitrosylation drives cell senescence and aging in mammals by controlling mitochondrial dynamics and mitophagy. *Proc. Natl. Acad. Sci. U.S.A.* 115, E3388–E3397. doi: 10.1073/pnas.1722452115

Rolland, S. G., Schneid, S., Schwarz, M., Rackles, E., Fischer, C., Haeussler, S., et al. (2019). Compromised mitochondrial protein import acts as a signal for UPRmt. *Cell Rep.* 28, 1659.e5–1669.e5.

Rossman, M. J., Santos-Parker, J. R., Steward, C. A. C., Bispham, N. Z., Cuevas, L. M., Rosenberg, H. L., et al. (2018). Chronic supplementation with a mitochondrial antioxidant (MitoQ) improves vascular function in healthy older adults. *Hypertension* 71, 1056–1063. doi: 10.1161/HYPERTENSIONAHA.117.10787

Rostovtseva, T., and Colombini, M. (1996). ATP flux is controlled by a voltage-gated channel from the mitochondrial outer membrane. *J. Biol. Chem.* 271, 28006–28008. doi: 10.1074/jbc.271.45.28006

Rostovtseva, T. K., and Bezrukov, S. M. (2012). VDAC inhibition by tubulin and its physiological implications. *Biochim. Biophys. Acta Biomembr.* 1818, 1526–1535. doi: 10.1016/j.bbamem.2011.11.004

Rostovtseva, T. K., Sheldon, K. L., Hassanzadeh, E., Monge, C., Saks, V., Bezrukov, S. M., et al. (2008). Tubulin binding blocks mitochondrial voltage-dependent anion channel and regulates respiration. *Proc. Natl. Acad. Sci. U.S.A.* 105, 18746–18751. doi: 10.1073/pnas.0806303105

Ruan, L., Zhou, C., Jin, E., Kucharavy, A., Zhang, Y., Wen, Z., et al. (2017). Cytosolic proteostasis through importing of misfolded proteins into mitochondria. *Nature* 543, 443–446. doi: 10.1038/nature21695

Rujano, M. A., Bosveld, F., Salomons, F. A., Dijk, F., Van Waarde, M. A., Van Der Want, J. J., et al. (2006). Polarised asymmetric inheritance of accumulated protein damage in higher eukaryotes. *PLoS Biol.* 4:e417. doi: 10.1371/journal.pbio.0040417

Ryan, M. T., and Hoogenraad, N. J. (2007). Mitochondrial-nuclear communications. *Annu. Rev. Biochem.* 76, 701–722. doi: 10.1146/annurev.biochem.76.052305.091720

Sciacovelli, M., Guzzo, G., Morello, V., Frezza, C., Zheng, L., Nannini, N., et al. (2013). The mitochondrial chaperone TRAP1 promotes neoplastic growth by inhibiting succinate dehydrogenase. *Cell Metab.* 17, 988–999. doi: 10.1016/j.cmet.2013.04.019

Sepuri, N. B., Angireddy, R., Srinivasan, S., Guha, M., Spear, J., Lu, B., et al. (2017). Mitochondrial LON protease-dependent degradation of cytochrome c oxidase subunits under hypoxia and myocardial ischemia. *Biochim. Biophys. Acta Bioenerget.* 1858, 519–528. doi: 10.1016/j.bbabio.2017.04.003

Shan, Y. -X., Liu, T. -J., Su, H. -F., Samsamshariat, A., Mestril, R., Wang, P. H., et al. (2003). Hsp10 and Hsp60 modulate Bcl-2 family and mitochondria apoptosis signaling induced by doxorubicin in cardiac muscle cells. *J. Mol. Cell. Cardiol.* 35, 1135–1143. doi: 10.1016/s0022-2828(03)00229-3

Sharp, W. W., Fang, Y. H., Han, M., Zhang, H. J., Hong, Z., Banathy, A., et al. (2014). Dynamin-related protein 1 (Drp1)-mediated diastolic dysfunction in myocardial ischemia-reperfusion injury: therapeutic benefits of Drp1 inhibition to reduce mitochondrial fission. *FASEB J.* 28, 316–326. doi: 10.1096/fj.12-226225

Shen, J., Zhang, J.-H., Xiao, H., Wu, J. -M., He, K. -M., Lv, Z. -Z., et al. (2018). Mitochondria are transported along microtubules in membrane nanotubes to rescue distressed cardiomyocytes from apoptosis. *Cell Death Dis.* 9:81.

Shepherd, D. L., Hathaway, Q. A., Nichols, C. E., Durr, A. J., Pinti, M. V., Hughes, K. M., et al. (2018). Mitochondrial proteome disruption in the diabetic heart through targeted epigenetic regulation at the mitochondrial heat shock protein 70 (mtHsp70) nuclear locus. *J. Mol. Cell. Cardiol.* 119, 104–115. doi: 10.1016/j.yjmcc.2018.04.016

Shimada, T., Horita, K., Murakami, M., and Ogura, R. (1984). Morphological studies of different mitochondrial populations in monkey myocardial cells. *Cell Tissue Res.* 238, 577–582. doi: 10.1007/BF00219874

Shirakabe, A., Zhai, P., Ikeda, Y., Saito, T., Maejima, Y., Hsu, C. -P., et al. (2016). Drp1-dependent mitochondrial autophagy plays a protective role against pressure overload–induced mitochondrial dysfunction and heart failure. *Circulation* 133, 1249–1263. doi: 10.1161/circulationaha.115.020502

Smith, R. A., and Murphy, M. P. (2010). Animal and human studies with the mitochondria-targeted antioxidant MitoQ. *Ann. N. Y. Acad. Sci.* 1201, 96–103. doi: 10.1111/j.1749-6632.2010.05627.x

Smyrnias, I., Gray, S. P., Okonko, D. O., Sawyer, G., Zoccarato, A., Catibog, N., et al. (2019). Cardioprotective effect of the mitochondrial unfolded protein response during chronic pressure overload. *J. Am. Coll.Cardiol.* 73, 1795–1806. doi: 10.1016/j.jacc.2018.12.087

Snow, B. J., Rolfe, F. L., Lockhart, M. M., Frampton, C. M., O'Sullivan, J. D., Fung, V., et al. (2010). A double-blind, placebo-controlled study to assess the mitochondria-targeted antioxidant MitoQ as a disease-modifying therapy in Parkinson's disease. *Mov. Disord.* 25, 1670–1674. doi: 10.1002/mds.23148

Song, M., Franco, A., Fleischer, J. A., Zhang, L., Dorn, G. W. II. (2017). Abrogating mitochondrial dynamics in mouse hearts accelerates mitochondrial senescence. *Cell Metab.* 26, 872–883 e875. doi: 10.1016/j.cmet.2017.09.023

Sorrentino, V., Romani, M., Mouchiroud, L., Beck, J. S.., Zhang, H., D'amico, D., et al. (2017). Enhancing mitochondrial proteostasis reduces amyloid-β proteotoxicity. *Nature* 552, 187–193. doi: 10.1038/nature25143

Stiburek, L., Vesela, K., Hansikova, H., Hulkova, H., and Zeman, J. (2009). Loss of function of Sco1 and its interaction with cytochrome c oxidase. *Am. J. Physiol. Cell Physiol.* 296, C1218–C1226. doi: 10.1152/ajpcell.00564.2008

Stromer, M. H., and Bendayan, M. (1988). Arrangement of desmin intermediate filaments in smooth muscle cells as shown by high-resolution immunocytochemistry. *Cell Motil. Cytoskeleton* 11, 117–125. doi: 10.1002/cm.970110205

Stromer, M. H., and Bendayan, M. (1990). Immunocytochemical identification of cytoskeletal linkages to smooth muscle cell nuclei and mitochondria. *Cell Motil. Cytoskeleton* 17, 11–18. doi: 10.1002/cm.970170104

Terman, A., and Brunk, U. T. (2005). The aging myocardium: roles of mitochondrial damage and lysosomal degradation. *HeartLung Circ.* 14, 107–114. doi: 10.1016/j.hlc.2004.12.023

Terman, A., Dalen, H., Eaton, J. W, Neuzil, J., and Brunk, U. T. (2004). Aging of cardiac myocytes in culture: oxidative stress, lipofuscin accumulation, and mitochondrial turnover. *Ann. N. Y. Acad. Sci.* 1019, 70–77. doi: 10.1196/annals.1297.015

Tokuyasu, K., Dutton, A. H., and Singer, S. (1983). Immunoelectron microscopic studies of desmin (skeletin) localization and intermediate filament organization in chicken skeletal muscle. *J. Cell Biol.* 96, 1727–1735. doi: 10.1083/jcb.96.6.1727

Unitt, J. F., McCORMACK, J. G., Reid, D., MacLachlan, L., and England, P. (1989). Direct evidence for a role of intramitochondrial Ca2+ in the regulation of oxidative phosphorylation in the stimulated rat heart. Studies using31P nmr and ruthenium red. *Biochem. J.* 262, 293–301. doi: 10.1042/bj2620293

Venkatesh, S., Li, M., Saito, T., Tong, M., Rashed, E., Mareedu, S., et al. (2019). Mitochondrial LonP1 protects cardiomyocytes from ischemia/reperfusion injury in vivo. *J. Mol. Cell Cardiol.* 128, 38–50. doi: 10.1016/j.yjmcc.2018.12.017

Vincent, A. E., Grady, J. P., Rocha, M. C., Alston, C. L., Rygiel, K. A., Barresi, R., et al. (2016). Mitochondrial dysfunction in myofibrillar myopathy. *Neuromuscul. Disord.* 26, 691–701. doi: 10.1016/j.nmd.2016.08.004

Voos, W. (2013). Chaperone–protease networks in mitochondrial protein homeostasis. *Biochim. Biophys. Acta Mol. Cell Res.* 1833, 388–399. doi: 10.1016/j.bbamcr.2012.06.005

Wagner, S., Dantz, C., Flebbe, H., Azizian, A., Sag, C. M., Engels, S., et al. (2014). NADPH oxidase 2 mediates angiotensin II-dependent cellular arrhythmias via PKA and CaMKII. *J. Mol. Cell Cardiol.* 75, 206–215. doi: 10.1016/j.yjmcc.2014.07.011

Wallace, D. C. (2001). Mouse models for mitochondrial disease. *Am. J. Med. Genet.* 106, 71–93. doi: 10.1002/ajmg.1393

Wanagat, J., Wolff, M. R., and Aiken, J. M. (2002). Age-associated changes in function, structure and mitochondrial genetic and enzymatic abnormalities in the Fischer 344 x Brown Norway F(1) hybrid rat heart. *J. Mol. Cell Cardiol.* 34, 17–28. doi: 10.1006/jmcc.2001.1483

Wang, S., Kandadi, M. R., and Ren, J. (2019). Double knockout of Akt2 and AMPK predisposes cardiac aging without affecting lifespan: role of autophagy and mitophagy. *Biochim. Biophys. Acta Mol. Basis Dis.* 1865, 1865–1875. doi: 10.1016/j.bbadis.2018.08.011

Wang, X., and Chen, X. J. (2015). A cytosolic network suppressing mitochondria-mediated proteostatic stress and cell death. *Nature* 524, 481–484. doi: 10.1038/nature14859

Wang, X., Osinska, H., Dorn, G. W., Nieman, M., Lorenz, J. N., Gerdes, A. M., et al. (2001). Mouse model of desmin-related cardiomyopathy. *Circulation* 103, 2402–2407. doi: 10.1161/01.cir.103.19.2402

Williamson, C. L., Dabkowski, E. R., Dillmann, W. H., and Hollander, J. M. (2008). Mitochondria protection from hypoxia/reoxygenation injury with mitochondria heat shock protein 70 overexpression. *Am. J. Physiol. Heart Circ. Physiol.* 294, H249–H256.

Willis, M. S., and Patterson, C. (2013). Proteotoxicity and cardiac dysfunction—Alzheimer's disease of the heart? *N. Engl. J. Med.* 368, 455–464. doi: 10.1056/nejmra1106180

Wrobel, L., Topf, U., Bragoszewski, P., Wiese, S., Sztolsztener, M. E., Oeljeklaus, S., et al. (2015). Mistargeted mitochondrial proteins activate a proteostatic response in the cytosol. *Nature* 524, 485–488. doi: 10.1038/nature14951

Wu, S., Zhou, F., Zhang, Z., and Xing, D. (2011). Mitochondrial oxidative stress causes mitochondrial fragmentation via differential modulation of mitochondrial fission-fusion proteins. *FEBS J.* 278, 941–954. doi: 10.1111/j.1742-4658.2011.08010.x

Xiang, F., Huang, Y. S., Shi, X. H., and Zhang, Q. (2010). Mitochondrial chaperone tumour necrosis factor receptor-associated protein 1 protects cardiomyocytes from hypoxic injury by regulating mitochondrial permeability transition pore opening. *FEBS J.* 277, 1929–1938. doi: 10.1111/j.1742-4658.2010.07615.x

Yaffe, M. P. (1999). The machinery of mitochondrial inheritance and behavior. *Science* 283, 1493–1497. doi: 10.1126/science.283.5407.1493

Yoshida, S., Tsutsumi, S., Muhlebach, G., Sourbier, C., Lee, M. J., Lee, S., et al. (2013). Molecular chaperone TRAP1 regulates a metabolic switch between mitochondrial respiration and aerobic glycolysis. *Proc. Natl. Acad. Sci. U.S.A.* 110, E1604–1612. doi: 10.1073/pnas.1220659110

Zhang, D., Wu, C. -T., Qi, X., Meijering, R. A., Hoogstra-Berends, F., Tadevosyan, A., et al. (2014). Activation of histone deacetylase-6 induces contractile dysfunction through derailment of α-tubulin proteostasis in experimental and human atrial fibrillation. *Circulation* 129, 346–358. doi: 10.1161/circulationaha.113.005300

Zhang, H., Gomez, A. M., Wang, X., Yan, Y., Zheng, M., and Cheng, H. (2013). ROS regulation of microdomain Ca2+ signalling at the dyads. *Cardiovasc. Res.* 98, 248–258. doi: 10.1093/cvr/cvt050

Zhang, H., Ryu, D., Wu, Y., Gariani, K., Wang, X., Luan, P., et al. (2016). NAD+ repletion improves mitochondrial and stem cell function and enhances life span in mice. *Science* 352, 1436–1443. doi: 10.1126/science.aaf2693

Zhang, M., Prosser, B. L., Bamboye, M. A., Gondim, A. N. S., Santos, C. X., Martin, D., et al. (2015). Contractile function during angiotensin-II activation: increased Nox2 activity modulates cardiac calcium handling via phospholamban phosphorylation. *J Am Coll Cardiol.* 66, 261–272. doi: 10.1016/j.jacc.2015.05.020

Zhang, Y., Jiang, D. S., Yan, L., Cheng, K. J., Bian, Z. Y., and Lin, G. S. (2011). HSP75 protects against cardiac hypertrophy and fibrosis. *J. Cell. Biochem.* 112, 1787–1794. doi: 10.1002/jcb.23091

Zheng, Q., Su, H., Ranek, M. J., and Wang, X. (2011). Autophagy and p62 in cardiac proteinopathy. *Circ. Res.* 109, 296–308. doi: 10.1161/circresaha.111.244707

Zhou, B., and Tian, R. (2018). Mitochondrial dysfunction in pathophysiology of heart failure. *J. Clin. Invest.* 128, 3716–3726. doi: 10.1172/JCI120849

Zorov, D. B., Juhaszova, M., and Sollott, S. J. (2014). Mitochondrial reactive oxygen species (ROS) and ROS-induced ROS release. *Physiol. Rev.* 94, 909–950. doi: 10.1152/physrev.00026.2013

Conflict of Interest: The authors declare that the research was conducted in the absence of any commercial or financial relationships that could be construed as a potential conflict of interest.

The reviewer JS declared a past co-authorship with one of the authors with several of the authors MB, SA, and RA to the handling Editor.

frontiers in Physiology

ORIGINAL RESEARCH
published: 16 October 2020
doi: 10.3389/fphys.2020.570441

Shikonin Ameliorates LPS-Induced Cardiac Dysfunction by SIRT1-Dependent Inhibition of NLRP3 Inflammasome

Tao Guo[1,2], Zhong-Biao Jiang[3], Zhong-Yi Tong[4], Yang Zhou[1], Xiang-Ping Chai[1] and Xian-Zhong Xiao[2]**

[1] Department of Emergency Medicine, Second Xiangya Hospital, Emergency Medicine and Difficult Diseases Institute, Central South University, Changsha, China, [2] Department of Pathophysiology, Sepsis Translational Medicine Key Laboratory of Hunan Province, Xiangya School of Medicine, Central South University, Changsha, China, [3] Department of Radiology, The Second Xiangya Hospital, Central South University, Changsha, China, [4] Department of Pathology, The Second Xiangya Hospital, Central South University, Changsha, China

OPEN ACCESS

Edited by:
Xuejun Wang,
University of South Dakota, United States

Reviewed by:
Michinari Nakamura,
Rutgers University, Newark, United States
Wuqiang Zhu,
Mayo Clinic Arizona, United States
Taixing Cui,
University of South Carolina, United States

***Correspondence:**
Xiang-Ping Chai
chaixiangping@csu.edu.cn
Xian-Zhong Xiao
xiaoxianzhong@csu.edu.cn

Specialty section:
This article was submitted to Clinical and Translational Physiology, a section of the journal Frontiers in Physiology

Received: *08 June 2020*
Accepted: *16 September 2020*
Published: *16 October 2020*

Citation:
Guo T, Jiang Z-B, Tong Z-Y, Zhou Y, Chai X-P and Xiao X-Z (2020) Shikonin Ameliorates LPS-Induced Cardiac Dysfunction by SIRT1-Dependent Inhibition of NLRP3 Inflammasome. Front. Physiol. 11:570441. doi: 10.3389/fphys.2020.570441

Shikonin (SHI) is an anti-inflammatory agent extracted from natural herbs. It is still unknown whether SHI ameliorates lipopolysaccharide (LPS)-induced cardiac dysfunction. This study aims to explore the protective effects of SHI on LPS-induced myocardial injury and its mechanism. The LPS-induced cardiac dysfunction mouse model was employed to investigate the protective effects of SHI. In the present study, we found that SHI treatment improved the survival rate and cardiac function and remarkably ameliorated the release of inflammatory cytokines and macrophage infiltration in heart tissue of LPS-treated mice. SHI also reduced lactate dehydrogenase (LDH) and cardiac troponin (cTn) release, cell inflammation, and apoptosis in LPS plus adenosine triphosphate (ATP)-treated H9c2 cells. In addition, SHI significantly upregulated silent information regulator 1 (SIRT1) expression and suppressed the upregulation of NOD-like receptor protein 3 (NLRP3), cleaved caspase-1, and caspase-1 activity in heart tissues induced by LPS. Meanwhile, we got the same results in LPS plus ATP-treated H9c2 cells *in vitro*. Further, SIRT1 inhibitor or siRNA partially blocked SHI-mediated upregulation of SIRT1 expression and downregulation of NLRP3, cleaved caspase-1, and caspase-1 activity in heart tissues induced by LPS. Therefore, we conclude that SHI ameliorates LPS-induced cardiac dysfunction by inhibiting SIRT1-dependent activation of NLRP3 inflammasomes and might be a promising therapeutic strategy for the treatment of LPS-induced cardiac dysfunction.

Keywords: shikonin, lipopolysaccharide, SIRT1, NLRP3, cardiac dysfunction

INTRODUCTION

Cardiac dysfunction is a common complication of severe sepsis, which represents one of the leading causes of death in intensive care units (Court et al., 2002; Narvaez et al., 2018). Uncontrolled immune and inflammatory responses were involved in the main mechanisms of sepsis-induced cardiac dysfunction (SICD) (Kakihana et al., 2016; Liu et al., 2017). Unfortunately, even largely

supportive therapies of SICD, like the clinical presence of antibiotics and restoration of systemic perfusion and blood pressure, were widely applied in the clinics, but the mortality of SICD was still high. The main reason is that the pathophysiological mechanisms of SICD are very complex. Therefore, further elucidation of the mechanisms is crucial for finding a new therapy for SICD.

The bacterial endotoxin lipopolysaccharide (LPS) was considered as the main culprit responsible for SICD (Bai et al., 2016). LPS stimulation resulted in the central inflammatory response and triggered rapid inflammasome activation, which included NOD-like receptor protein 3 (NLRP3), caspase-1, and apoptosis-associated speck-like protein (ASC). In these processes, inflammasome sensors recruited ASC to generate a caspase-1-activating platform and promote the maturation of pro-inflammatory cytokines, interleukin-1β (IL-1β) and IL-18 (Abderrazak et al., 2015; Karki and Kanneganti, 2019). Recently, many studies have confirmed that NLRP3 inflammasome was activated in sepsis-induced multiple organ injury. Furthermore, suppression of NLRP3 inflammasome activation ameliorated SICD (Kalbitz et al., 2016; Yang et al., 2018). Moreover, it has been reported that silent information regulator 1 (SIRT1), an NAD+-dependent deacetylase that regulates various protein functions, plays a negative role in regulating the activation of NLRP3 inflammasome (Fu et al., 2013; Peng et al., 2018). In addition, growing evidences demonstrated that SIRT1 played a protective role in SICD (Han et al., 2017; Smith et al., 2019). Therefore, activation of SIRT1-dependent pathways has become a promising therapeutic strategy for the treatment of SICD.

Shikonin (SHI) has antioxidant activity and anti-inflammatory properties, which is an active component extracted from Chinese herb radix arnebiae. It was reported that SHI could prevent multiple diseases, such as acute lung injury, lethal endotoxic shock, and cerebral ischemia/reperfusion injury (Wang et al., 2010; Andujar et al., 2013; Yang et al., 2014; Zhang Y. et al., 2018). Recent studies also demonstrated that SHI protected against cardiovascular diseases. For example, SHI ameliorated sympathetic remodeling in chronic heart failure (Liu and Liu, 2019). Additionally, SHI inhibited the activation of NLRP3 inflammasome in macrophages (Jin et al., 2015; Zorman et al., 2016). However, it is still unknown whether SHI could ameliorate LPS-induced cardiac dysfunction *via* an SIRT1-dependent NLRP3 inflammasome pathway. Hence, our study aims to assess the role of SHI in LPS-induced cardiac dysfunction and explore its underlying mechanisms.

MATERIALS AND METHODS

Establishment of Lipopolysaccharide-Induced Cardiac Dysfunction Mouse Model

All animal-related experimental procedures were approved by the Animal Studies Ethics Committee of Central South University (Hunan, China). C57BL/6J male mice aged 6–8 weeks (20–24 g) were purchased from the Laboratory Animal Center of Central South University. LPS-induced cardiac dysfunction model was established in experimental mice by intraperitoneal injection of a dose 15 mg/kg of LPS (from *Escherichia coli* 0111:B4, Sigma Aldrich, St. Louis, MO, United States), which was dissolved in vehicle solution. The same volume of vehicle solution was given to the control group (Niu et al., 2011). Repetitive administration of SHI (#S7576, Sigma Aldrich, St. Louis, MO, United States) was given in each group at 0.5, 12, and 24 h after LPS challenge according to a previous study (Yang et al., 2014). The survival rates of mice were recorded every 6 h until 72 h after LPS challenge.

Mice were randomly divided into three groups as follows (n = 6 per group): (1) control group; (2) LPS group; (3) SHI+LPS group. The mice of the control group were injected intraperitoneally with vehicle solution. The LPS group established the model of SICD according to the method mentioned before. LPS+SHI group was injected intraperitoneally with SHI (8 mg/kg), which was dissolved in vehicle [10% dimethyl sulfoxide (DMSO), 20% cremophor:ethanol (3:1), and 70% phosphate-buffered saline] at 0.5 h before and 12 h after LPS challenge. Serum and heart tissues were collected after LPS challenge for 18 h and stored at −20°C for subsequent experiments.

Echocardiography

Cardiac function was evaluated by echocardiography at 18 h after LPS challenge as previously described (Niu et al., 2011). Briefly, mice were lightly anesthetized and maintained on 0.5∼2.0% isoflurane, then they were placed and fixed in a recumbent position. Echocardiographic images were acquired by using Vevo 2000 imaging system (Toronto, Canada) equipped with a 30-mHz linear transducer (MS 400). Parameters of cardiac function were evaluated on the M-mode images, which were obtained from the parasternal short-axis view at the papillary muscle level. Left ventricle internal diameters at end-diastole and end-systole were determined. The ejection fraction (EF) and fractional shortening (FS) were analyzed to evaluate cardiac function. All data were blindly recorded by an independent investigator.

Cell Culture and Lipopolysaccharide Induction

H9c2 cardiomyoblasts were bought from American Type Culture Collection and maintained in Dulbecco's modified Eagle medium (DMEM) supplemented with 10% fetal bovine serum (FBS) and antibiotics (100 U/ml penicillin, 100 μg/ml streptomycin). Cells were grown on 12-well culture dishes until achieving 80∼90% confluence. The cells were divided into six groups as follows: control group, LPS+ATP group, LPS+ATP+EX527 group, SHI group, SHI+LPS+ATP group, and SHI+LPS+ATP+EX527 group. To examine the effects of SHI on inflammasome activation, cells were preincubated with SHI (5 mM) for 4 h at first, followed by priming with LPS (200 ng/ml) for another 4 h. After the replenishment of fresh medium, then pretreated with or without SIRT1 inhibitor EX527 (1 mM, Selleck Chemicals, Item No S1541) for 1 h immediately before stimulation with ATP. Finally, cells were stimulated with ATP (3 mM) for 1 h.

Cells and supernatants were collected and stored at −80°C for further analysis.

Cell Transfection

H9c2 cells were plated in six-well plates until 60–80% confluent. siRNA-negative control (NC) or siRNA-SIRT1 (50 nM) was diluted in Lipofectamine 2000 (Invitrogen, Carlsbad, CA, United States) and transfected into cells according to the manufacturer's protocol. The sequences of SIRT1 siRNA were as follows: 5′-AGAUAUCAAUACAAUUGAAdTdT-3′ (F) and 5′-UUCAAUUGUAUUGAUAUCUdTdT-3′ (R). After 4 h, the medium was replaced with fresh DMEM containing 10% FBS, and cells were incubated for 48 h. Then, SHI was added to the fresh culture medium of cells for 4 h, and protein expression was measured by Western blot analysis.

3-(4,5-Dimethylthiazol-2-yl)-2,5-Diphenyl-Tetrazolium Bromide Assay

To assess cell viability, H9c2 cells were seeded into 96-well plates (Corning, NY, United States) and cultured at 37°C in the presence of 5% CO_2 under a humidified atmosphere. At the indicated treatments, 20 μl 3-(4,5-dimethylthiazol-2-yl)-2,5-diphenyl-tetrazolium bromide (MTT) (5 mg/ml) was added into each well. After 4 h of incubation, cells were washed three times with NaCl/Pi (pH 7.4). The insoluble formazan product was dissolved in DMSO (150 μl/well). The absorbance was measured using a microplate reader at 570 nm with a 630-nm reference. The attendance of formazan formed in control cells was considered as 100% viability.

Measurement of Creatine Kinase-MB, Lactate Dehydrogenase, Cardiac Troponin, Inflammatory Cytokines, and the Activity of Silent Information Regulator 1 and Caspase-1

The serum was collected and centrifuged at 3,000 rpm for 5 min. The levels of creatine kinase (CK) and CK-MB in serum were determined by Beckman LX-20 Fully Automated Biochemistry Analyzer (Beckman, California, United States) according to the manufacturer's instructions. IL-1β ELISA kits (Cusabio Biotech Co., Ltd., Hubei, China; Item No. 011614MO) and IL-18 ELISA kits (Cusabio Biotech Co., Ltd., Hubei, China; Item No. E04609m) were used to determine IL-1β and IL-18 levels in serum and cell supernatants following manufacturer's instructions. SIRT1 activity assay kit (Abcam, Cambridge, MA, United States; Item No. 156065) and caspase-1 activity assay kit (Beyotime, Nan Jing, China, Item No. C1101) were used to determine SIRT1 and caspase-1 activity in myocardial tissue or cell extracts.

Hematoxylin and Eosin Staining

Mice were sacrificed, and heart tissues were dissected. Tissues from middle left ventricular were sectioned into 5-μm slices and stained with H&E staining solution according to the standard techniques. Histopathological changes were assessed by a light microscope at 200× magnification (Nikon, Tokyo, Japan). The cardiomyocyte cross-sectional areas were determined by testing the circumferential length of the cardiomyocyte using ImageJ software as described previously (Chen et al., 2018).

Flow Cytometry Analysis

Cell apoptosis was assessed with Annexin V-FITC/PI Apoptosis Detection Kit (BD Biosciences, San Jose, CA, United States) and measured by flow cytometry. After stimulation, H9c2 cells were washed with cold PBS and stained with Annexin V-FITC and propidium iodide (PI) for 15 min at room temperature in the dark. Data were acquired by BD FACS flow cytometer (BD Bioscience, San Diego, CA, United States) and analyzed with Flow Jo analytical software (Version X; Tree Star, Ashland, OR, United States).

Immunohistochemistry

The hearts were fixed in 10% formalin and embedded in paraffin. Embedded tissues were cut into 4-μm sections and incubated with macrophage marker F4/80 (1:50 dilution; CI-A3-1, Novus Biologicals, Centennial, CO, United States), followed by incubation with biotin-conjugated secondary antibodies and then treated with avidin peroxidase. The reaction was developed using the 3,3′-diaminobenzidine (DAB) substrate kit. Then, the sections were counterstained with hematoxylin and finally photographed under an optical microscope (Olympus, Tokyo, Japan) at 200× magnification. A semiquantitative evaluation of F4/80 was performed using a method described in the literature (Hu et al., 2013) as follows: the proportion of positive cells was divided into five grades (percentage scores): ≤10% = 0, 11–25% = 1, 26–50% = 2, 51–75% = 3, and >75% = 4. The intensity of staining was divided into four grades (intensity scores): no staining = 0, light brown = 1, brown = 2, and dark brown = 3. Staining positivity was determined by the formula as follows: Overall scores = Percentage score × Intensity score. All measurements were carried out in a double-blind manner by two independent researchers.

Quantitative Real-Time Polymerase Chain Reaction

Total RNA was extracted from heart tissue and H9c2 cells by using TRIzol (Invitrogen, Carlsbad, CA, United States). The isolated RNA was used as a template to synthesize cDNA by using PrimeScript™ RT Master Mix (Takara, Tokyo, Japan). Real-time PCR was carried out by using the One-step SYBR®. PrimeScript™ RT-PCR Kit is a Biosystems 7500 instrument. The amplification conditions were 95°C for 30 s, 95°C for 5 s, and 60°C for 34 s for cycles. The specific primers were as follows: SIRT1, 5′-CCGTGGCAAACTGGTACTTT-3′ and 5′-GACGCCAACATAGACCACCT-3′; β-actin, 5′-AAGTGTGACGTTGACATCCG-3′ and 5′-TCTGCATCCTGTCAGCAATG-3′. Gene expression was normalized to β-actin expression using the software provided with the system.

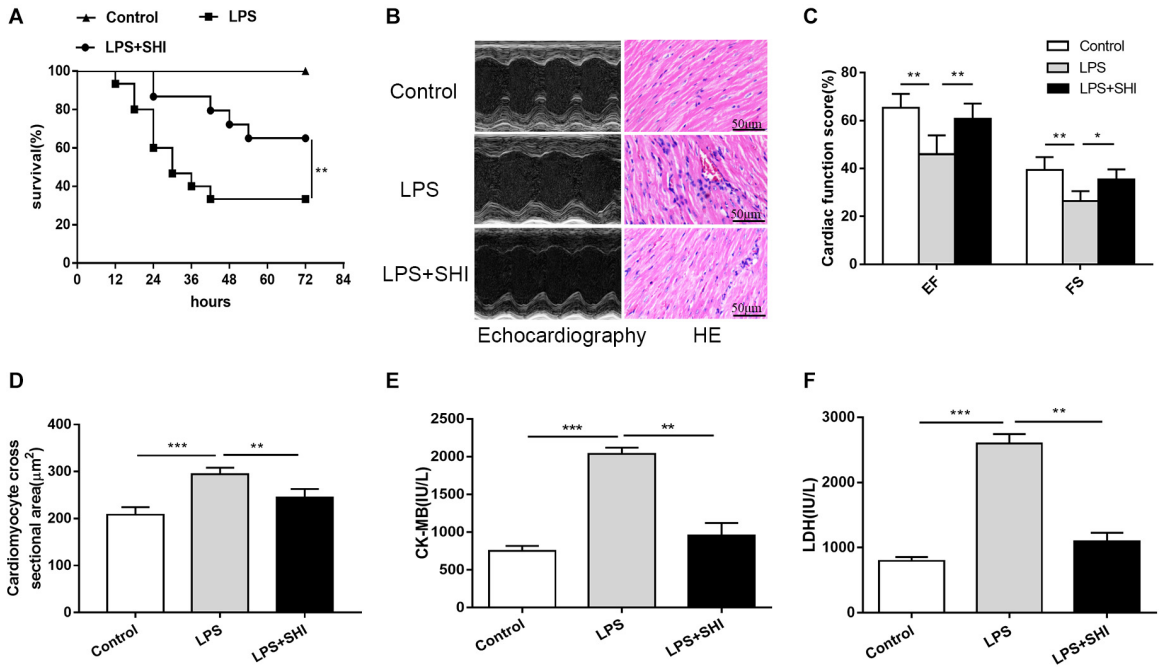

FIGURE 1 | Shikonin (SHI) improves survival and ameliorates cardiac dysfunction in lipopolysaccharide (LPS)-treated mice. **(A)** Effect of SHI on survival rate following LPS challenge in mice (n = 15/group). **(B)** Effect of SHI on cardiac dysfunction and histomorphology after LPS treatment. **(C)** Cardiac function parameters, ejection fraction (EF) and fractional shortening (FS) were measured by echocardiography at 18 h after LPS treatment. **(D)** Cardiomyocyte cross-sectional areas were assessed in different groups. The levels of serum creatine kinase (CK)-MB **(E)** and lactate dehydrogenase (LDH) **(F)** were measured in different groups. All data were represented as mean ± SD (n = 6). $^{*}P < 0.05$, $^{**}P < 0.01$, $^{***}P < 0.001$.

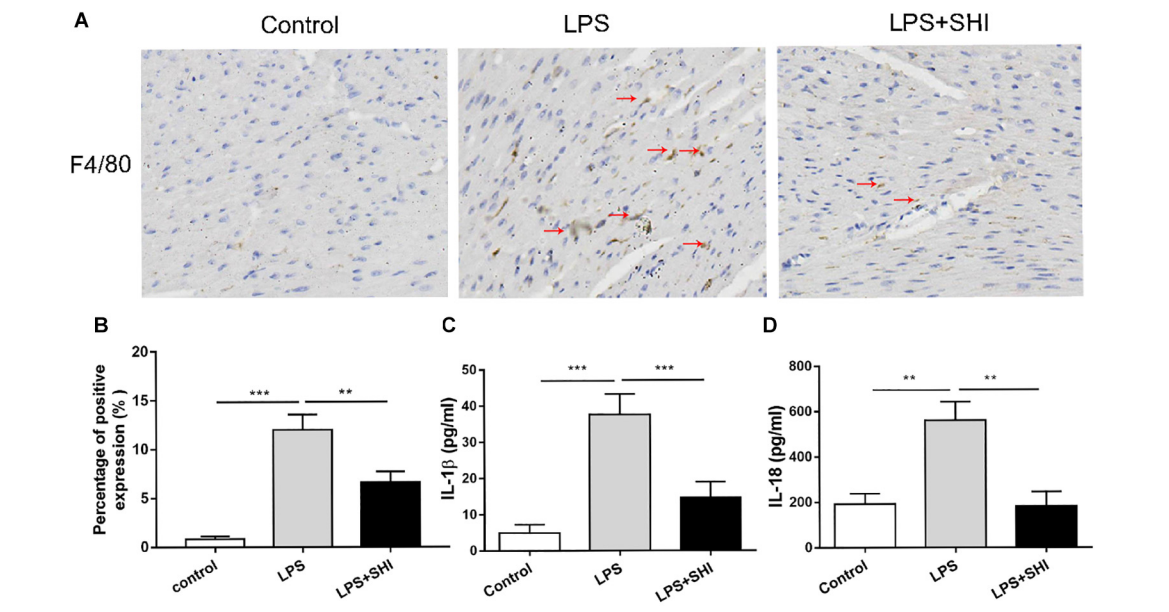

FIGURE 2 | Shikonin (SHI) reduces inflammatory cytokine release and macrophage infiltration in heart tissue of lipopolysaccharide (LPS)-treated mice. **(A)** Immunohistochemistry assay was applied to detect macrophage infiltration (the arrow points to the macrophages). **(B)** Shows the quantification. Serum levels of interleukin (IL)-1β **(C)** and IL-18 **(D)** were determined with ELISA kits at 18 h after LPS treatment. All data were represented as mean ± SD (n = 6). $^{*}P < 0.05$, $^{**}P < 0.01$, $^{***}P < 0.001$.

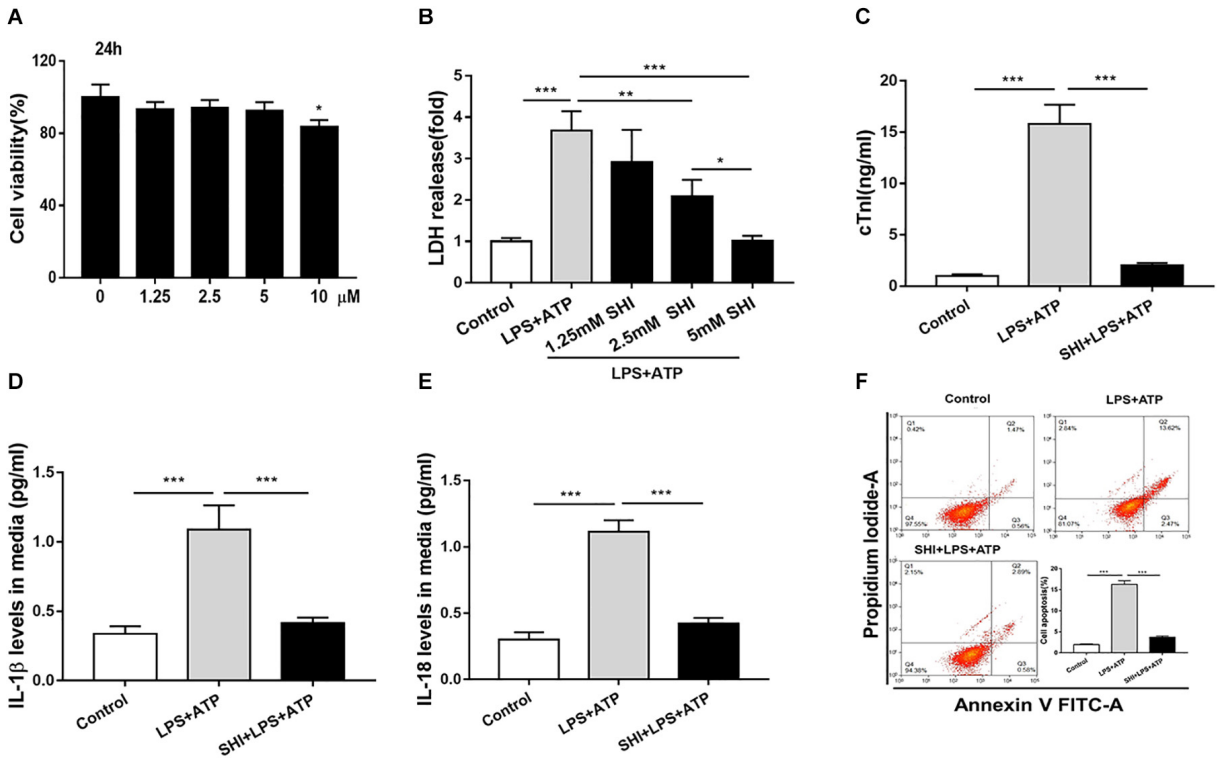

FIGURE 3 | Shikonin (SHI) alleviates lactate dehydrogenase (LDH) releases, cell inflammation, and apoptosis in LPS + ATP-treated H9c2 cells. **(A)** 3-(4,5-Dimethylthiazol-2-yl)-2,5-diphenyl-tetrazolium bromide (MTT) assay was applied to examine cell viability in H9c2 cells that were treated with different concentrations of SHI for 24 h. **(B)** The effect of SHI on LDH release. **(C)** The effect of SHI on cardiac troponin (cTn) levels. The effect of SHI on interleukin (IL)-1β **(D)** and IL-18 **(E)** levels. **(F)** Cell apoptosis was assessed by flow cytometry. All data were represented as mean ± SD. All experiments were repeated at least three times. $^{*}P < 0.05$, $^{**}P < 0.01$. $^{***}P < 0.001$.

Western Blotting Analysis

The expressions of NLRP3, caspase-1, and SIRT1 in heart tissue and H9c2 cells at the protein level were determined by Western blotting analysis as previously described (Wang et al., 2017). Briefly, cardiac tissues and cells were minced and lysed in ice-cold radioimmunoprecipitation assay (RIPA) lysis buffer. Protein concentrations were determined by using the bicinchoninic acid (BCA) method. Equal amounts of proteins were subjected to sodium dodecyl sulfate polyacrylamide gel electrophoresis (SDS-PAGE) and then transferred to polyvinylidene fluoride (PVDF) membranes. The membranes were blocked with 5% milk for 2 h and then incubated with antibodies against SIRT1 (1:1,000 dilution, CST, Danvers, MA, United States; Item No. 8469S), NLRP3 (1:1,000 dilution, CST; Item No. 15101S), caspase-1 (1:1,000 dilution, CST; Item No. 3866S), and glyceraldehyde 3-phosphate dehydrogenase (GAPDH) (1:5,000 dilution, CST; Item No. 5174S) overnight. The membranes were washed three times, followed by incubation with fluorescence-conjugated secondary antibody at room temperature for 1 h. The immunoreactive bands were visualized by enhanced chemiluminescence (ECL) substrate (Bio-Rad, Hercules, CA, United States), and quantification was performed using ImageJ software (NIH, Bethesda, MD, United States).

Statistical Analysis

SPSS 25.0 software was used for statistical analysis. All the values were expressed as means ± SD. A log-rank test was used to analyze survival curves. Comparisons between two groups were performed with a two-tailed Student's *t*-test (parametric). Comparisons between multiple groups were analyzed using a one-way analysis of variance, followed by Tukey's multiple comparison test. $P < 0.05$ was considered statistically significant.

RESULTS

Shikonin Improves Survival and Ameliorates Cardiac Dysfunction in Lipopolysaccharide-Treated Mice

It is still unknown whether SHI presents any protective efficacy on cardiac dysfunction induced by LPS. We firstly established a cardiac dysfunction mouse model induced by LPS and treated the mice with or without SHI. As shown in **Figure 1A**, the survival rate of mice in the LPS group significantly decreased to 26% compared to the control group. In contrast, treatment with 8 mg/kg SHI significantly improved the survival rate to 66%.

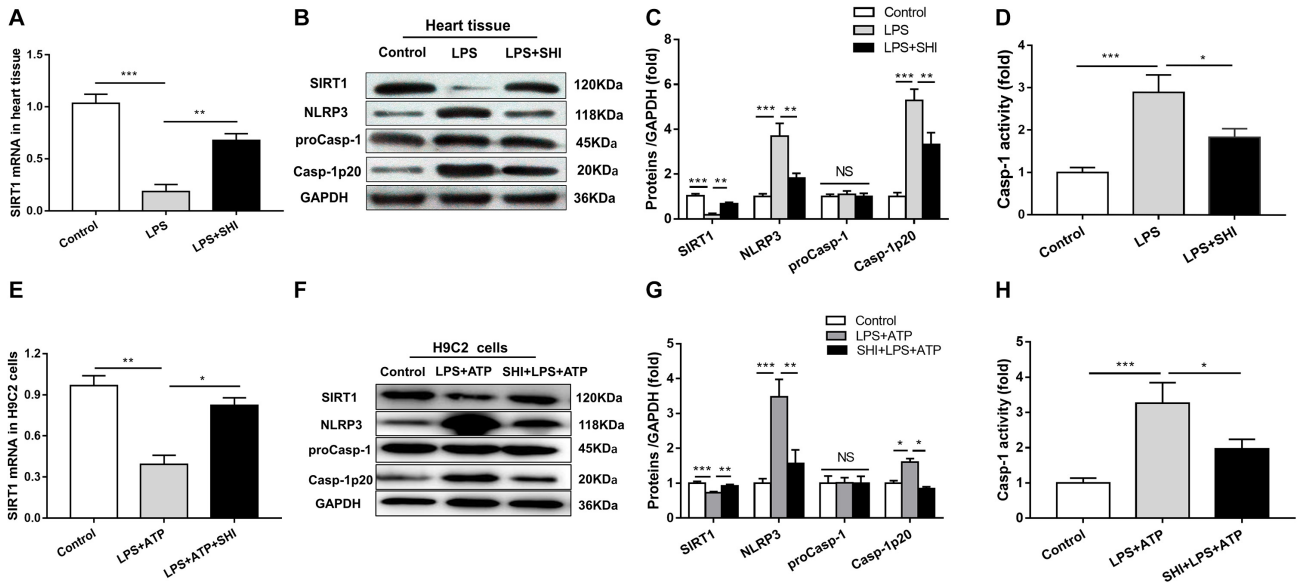

FIGURE 4 | Shikonin (SHI) upregulates the expression of silent information regulator 1 (SIRT1) and inhibits activation of NOD-like receptor protein 3 (NLRP3) inflammasome *in vivo* and *in vitro*. **(A,E)** SIRT1 mRNA was measured by RT-PCR in heart tissue and H9c2 cells. **(B,F)** Expressions of SIRT1, NLRP3, pro-caspase-1, and cleaved caspase-1 were measured by Western blotting analysis in heart tissue and H9c2 cells. **(C,G)** The ratio of SIRT1, NLRP3, pro-caspase-1, cleaved caspase-1 to glyceraldehyde 3-phosphate dehydrogenase (GAPDH) was expressed as protein levels in heart tissue and H9c2 cells. **(D,H)** Caspase-1 activity was detected by a commercial kit in heart tissue and H9c2 cells. All data were represented as mean ± SD. All experiments were repeated at least three times. $^{*}P < 0.05$, $^{**}P < 0.01$, $^{***}P < 0.001$.

Echocardiography evaluation also revealed that EF and FS were significantly reduced by LPS, while SHI treatment reversed the decreased effects on EF and FS induced by LPS (**Figures 1B,C**). Moreover, LPS markedly induced cardiac injury as evidenced by increasing serum levels of CK and LDH (**Figures 1E,F**). In contrast, SHI treatment attenuated the concentration of CK and LDH (**Figures 1E,F**). In addition, H&E staining of heart tissues showed that LPS increased the inflammatory cell infiltration, myocardial degeneration, and cardiomyocyte cross-sectional areas in heart tissues (**Figures 1B,D**). Conversely, SHI treatment significantly alleviated these pathological abnormalities of heart in LPS-challenged mice (**Figures 1B,D**). Thus, these data confirmed a protective effect of SHI against LPS-induced myocardial damage.

Shikonin Reduces Inflammatory Cytokine Release and Macrophage Infiltration in the Heart Tissue of Lipopolysaccharide-Treated Mice

Uncontrolled inflammatory responses were involved in SICD (Kakihana et al., 2016). To assess inflammatory response in SHI-treated mice, we measured the IL-1β and IL-18 in serum and macrophage infiltration in heart tissue. The results showed that macrophage infiltration in heart tissue (**Figures 2A,B**) and the levels of IL-1β and IL-18 in serum were significantly upregulated by LPS, while these effects were reversed by SHI (**Figures 2C,D**). These results confirmed that SHI could ameliorate inflammatory response of heart tissue in LPS-treated mice.

Shikonin Alleviates Lactate Dehydrogenase Releases, Cell Inflammation, and Apoptosis in Lipopolysaccharide + ATP-Treated H9c2 Cells

To investigate the protective role of SHI in LPS + ATP-treated H9c2 cells, cell viability, inflammatory cytokines, and cell apoptosis were determined. We found that SHI at doses of 1.25, 2.5, and 5 mM had no effect on cell viability of H9c2 cells compared to vehicle-treated cells, but at a dose of 10 mM decreased cell viability (**Figure 3A**), and SHI significantly reduced the LDH level in the supernatant of LPS + ATP-treated H9c2 cells at doses of 1.25, 2.5, and 5 mM, respectively, compared to PBS-treated cells (**Figure 3B**). The highest decrease in the levels of LDH was found to occur at a dose of 5 mM of SHI. Thus, we choose 5 mM of SHI as an optimal treatment concentration for the subsequent *in vitro* experiments. Besides, SHI reduced the cTn level in supernatants of LPS + ATP-treated H9c2 cells (**Figure 3C**). Additionally, ATP promoted the release of IL-1β and IL-18 and aggravated cell apoptosis in LPS-primed H9c2 cells, while SHI significantly reversed these effects induced by ATP in LPS-primed H9c2 cells (**Figures 3D–F**). Together, these results showed that SHI played a protective role in LPS + ATP-treated H9c2 cells.

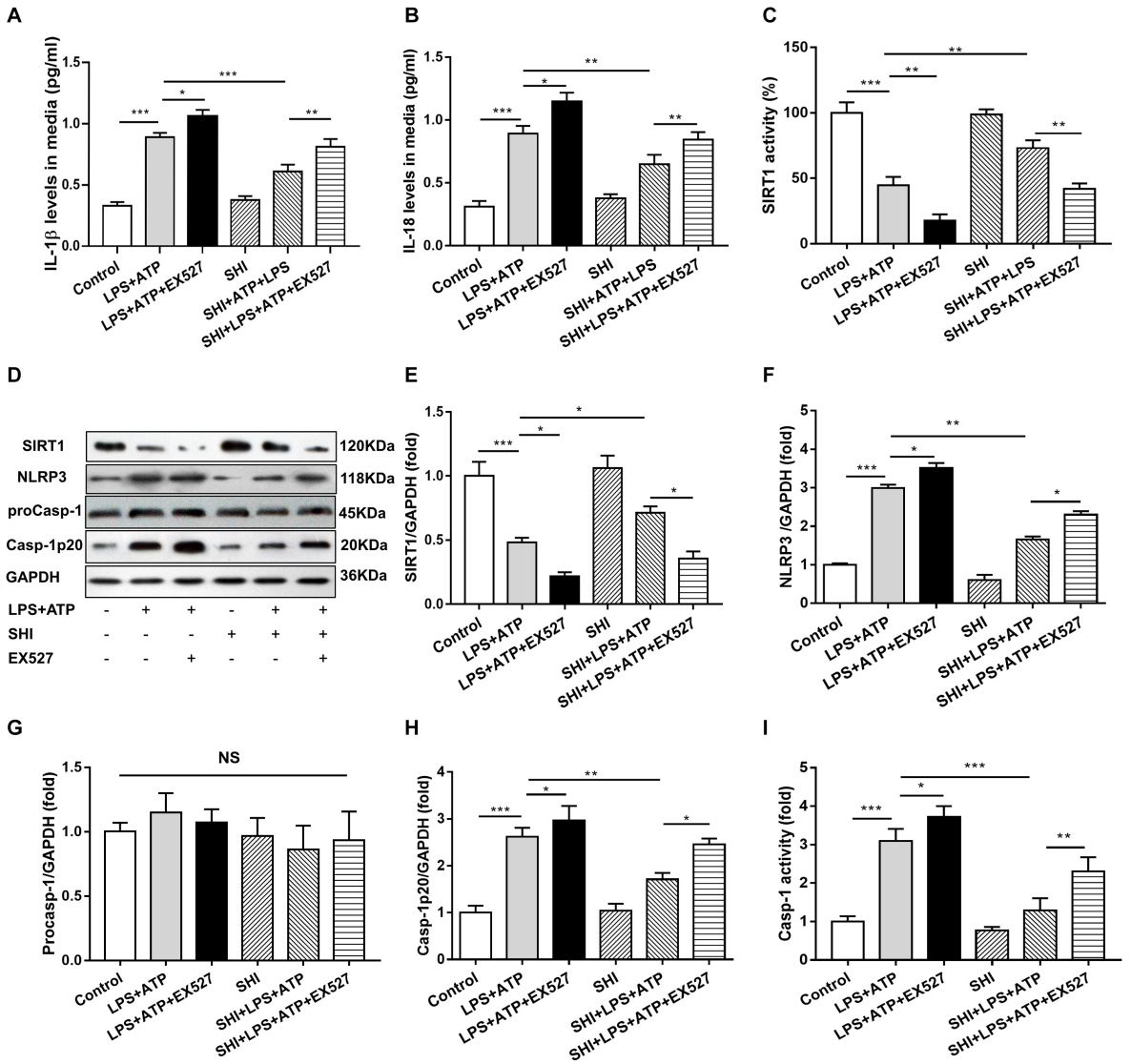

FIGURE 5 | Silent information regulator 1 (SIRT1) inhibitor prevents the inhibitory effect of shikonin (SHI) on inflammation in lipopolysaccharide (LPS) + ATP-treated H9c2 cells.The levels of interleukin (IL)-18 **(A)** and IL-1β **(B)** in the supernatant of LPS + ATP-treated H9c2 cells were determined by ELISA. **(C)** SIRT1 activity in H9c2 cells was measured by a commercial kit. **(D)** Expressions of SIRT1, NOD-like receptor protein 3 (NLRP3), pro-caspase-1, and cleaved caspase-1 protein in H9c2 cells were measured by Western blotting analysis. The ratio of SIRT1 **(E)**, NLRP3 **(F)**, pro-caspase-1 **(G)**, or cleaved caspase-1 **(H)** to glyceraldehyde 3-phosphate dehydrogenase (GAPDH) was expressed at protein levels in H9c2 cells. **(I)** Caspase-1 activity was detected by a commercial kit in H9c2 cells. All data were represented as mean ± SD. All experiments were repeated at least three times. $^{*}P < 0.05$, $^{**}P < 0.01$, $^{***}P < 0.001$.

Shikonin Upregulates the Expression of Silent Information Regulator 1 and Inhibits the Activation of NOD-Like Receptor Protein 3 Inflammasome *In vivo* and *In vitro*

To investigate the mechanism of SHI's protective effect on cardiac injury induced by LPS, the mRNA expression of SIRT1 was assessed by RT-PCR (**Figures 1A,E**), the protein expressions of SIRT1, NLRP3, pro-caspase-1, and cleaved caspase-1 in the heart tissues and H9c2 cells were determined by Western blotting analysis (**Figures 4B,F**), and caspase-1 activity was measured by a commercial kit. We found that the mRNA and protein expressions of SIRT1 in heart tissues were significantly decreased by LPS, while SHI significantly upregulated mRNA and protein levels of SIRT1 in heart tissues of the LPS group (**Figure 4A**). Meanwhile, the protein expressions of NLRP3 and cleaved caspase-1 and caspase-1 activity in heart tissues were significantly upregulated by LPS, while SHI treatment significantly suppressed the upregulation of NLRP3, cleaved caspase-1 (**Figures 4B,C**), and caspase-1 activity (**Figure 4D**) induced by LPS. In addition, we got the same results in H9c2 cells *in vitro*. ATP downregulated the mRNA and protein expressions of SIRT1 in LPS-primed H9c2 cells, while SHI upregulated the mRNA and protein

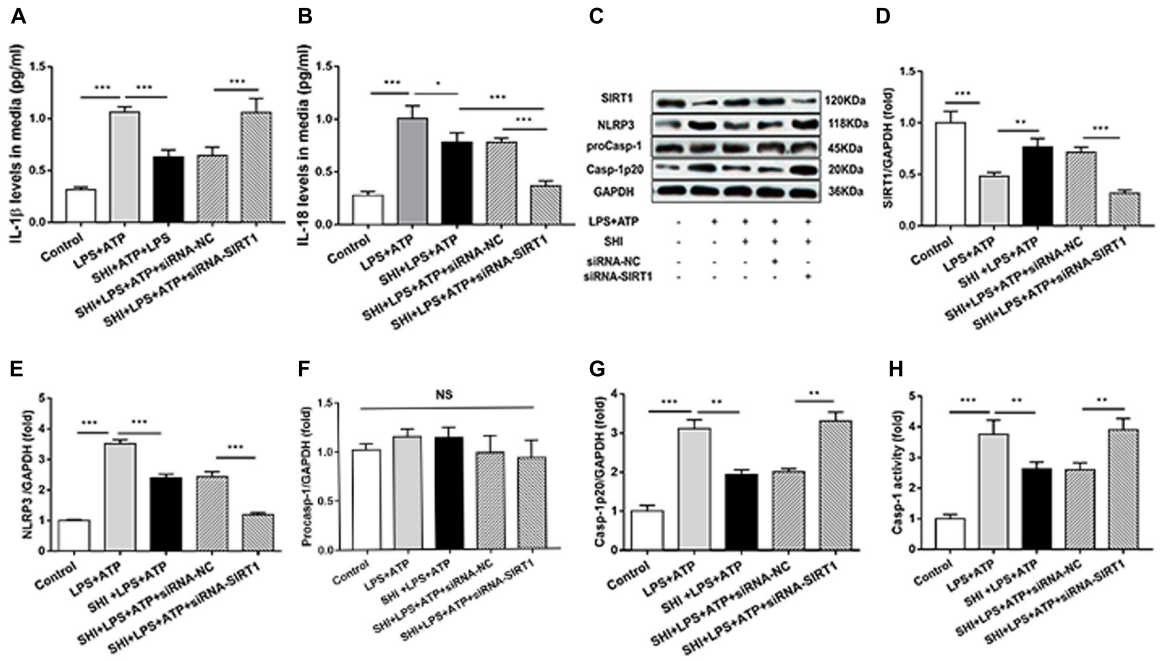

FIGURE 6 | Silent information regulator 1 (SIRT1) knockdown suppresses shikonin (SHI)-mediated anti-inflammatory activity. The levels of interleukin (IL)-18 **(A)** and IL-1β **(B)** in the supernatant of lipopolysaccharide (LPS) + ATP-treated H9c2 cells were determined by ELISA. **(C)** Expressions of SIRT1, NOD-like receptor protein 3 (NLRP3), pro-caspase-1, and cleaved caspase-1 protein in H9c2 cells were measured by Western blotting analysis. The ratio of SIRT1 **(D)**, NLRP3 **(E)**, pro-caspase-1 **(F)**, or cleaved caspase-1 **(G)** to glyceraldehyde 3-phosphate dehydrogenase (GAPDH) was expressed at protein levels in H9c2 cells. Caspase-1 activity **(H)** was detected by a commercial kit in H9c2 cells. All data were represented as mean ± SD. All experiments were repeated at least three times. $^{*}P < 0.05$, $^{**}P < 0.01$, $^{***}P < 0.001$.

levels of SIRT1 in LPS-primed H9c2 cells stimulated with ATP (**Figure 4E**). The protein expressions of NLRP3 and cleaved caspase-1 and caspase-1 activity were enhanced by ATP in LPS-primed H9c2 cells, while SHI treatment significantly decreased the upregulation of NLRP3, cleaved caspase-1 (**Figures 4F,G**), and caspase-1 activity (**Figure 4H**) induced by LPS-primed H9c2 cells. These findings indicated that SHI upregulated SIRT1 expression and inhibited the activation of NLRP3 inflammasome *in vivo* and *in vitro*.

Silent Information Regulator 1 Inhibitor Prevents the Inhibitory Effect of Shikonin on Inflammation in Lipopolysaccharide + ATP-Treated H9c2 Cells

To further confirm whether SHI inhibits the release of inflammatory cytokines through SIRT1 pathway in LPS + ATP-treated H9c2 cells, SHI and SIRT1 inhibitor (EX527) were used. Results indicated that both of the protein expression and activity of SIRT1 were decreased in LPS-primed H9c2 cells stimulated with ATP, while SHI restored the reduction in protein expression and activity of SIRT1. The protein expressions of NLRP3 and cleaved caspase-1 and caspase-1 activity were upregulated in LPS + ATP-treated H9c2 cells. In contrast, SHI inhibited the protein levels of NLRP3 and cleaved caspase-1 (**Figures 5C–H**) and caspase-1 activity (**Figure 5I**) in LPS + ATP-treated H9c2 cells. Moreover, EX527 prevented such inhibitory effects of SHI on the activation of NLRP3 inflammasome. In addition, the production of IL-1β and IL-18 in cell supernatants was increased in LPS + ATP-treated H9c2 cells compared to the control group, which was attenuated by SHI. Nevertheless, EX527 could block SHI-mediated inhibitory effects of pro-inflammatory cytokine release (**Figures 5A,B**). These data indicated that the SIRT1 inhibitor prevented the inhibitory effects of SHI on activation of NLRP3 inflammasome inflammatory factor release in LPS + ATP-treated H9c2 cells.

Silent Information Regulator 1 Knockdown Suppresses Shikonin-Mediated Anti-inflammatory Activity

To provide solid evidence that SIRT1 participates in the anti-inflammatory effects of SHI in H9c2 cells, siRNA-SIRT1 were used to knock down SIRT1 in the present study. The result showed that the expression of SIRT1 was decreased to 44% by siRNA transfection, which indicates that siRNA-SIRT1 transfection was effective (**Figures 6C,D**). The protein levels of NLRP3 and cleaved caspase-1 (**Figures 6E–G**) and caspase-1 activity (**Figure 6H**) were upregulated by ATP in LPS-primed H9c2 cells, while these effects were reversed by treatment with SHI. Moreover, siRNA-SIRT1 suppresses SHI-mediated production of IL-1β and IL-18 and NLRP3 inflammasome activation (**Figures 6A–G**). The IL-1β and IL-18 secretions in cell

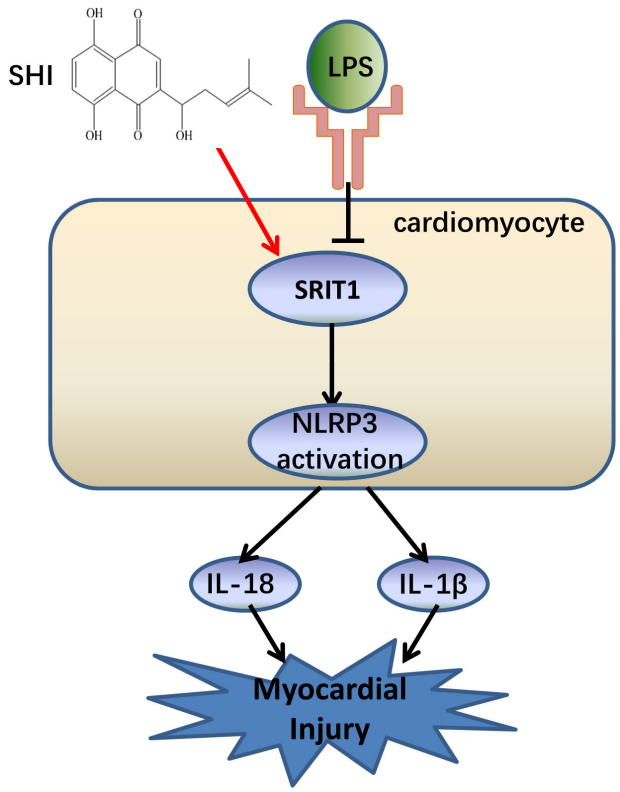

FIGURE 7 | The summary flow diagram.

supernatants were increased by ATP in LPS-primed H9c2 cells compared to the control group, which was reduced by treatment with SHI. Furthermore, siRNA-SIRT1 partially abolished SHI-mediated reduction of IL-1β and IL-18 secretion (**Figures 6A,B**). These results indicated that knockdown of SIRT1 by siRNA could suppress SHI-mediated anti-inflammatory activity in LPS + ATP-challenged H9c2 cells.

DISCUSSION

In the present study, we confirmed that NLRP3 inflammasome activation significantly contributed to the pathogenesis of LPS-induced cardiac dysfunction, which was consistent with a previous study (Yang et al., 2019). Meanwhile, the study was the first time to demonstrate that SHI has a protective effect on LPS-induced cardiac dysfunction. Furthermore, SHI significantly reduced cell inflammation by inhibiting the activation of NLRP3 inflammasome *in vivo* and *in vitro*. Mechanistically, SHI ameliorated LPS-induced cardiac dysfunction by inhibiting the activation of NLRP3 inflammasome that was partly mediated by SIRT1 in mice (**Figure 7**).

SHI has various biological functions, and it is well known due to its effective anti-inflammatory activity. Many studies have shown that SHI is beneficial for many diseases, such as cerebral ischemia- or reperfusion-induced brain injury and sepsis (Wang et al., 2010; Yang et al., 2014). Importantly, Yang et al. (2017) reported that SHI ameliorated isoproterenol-induced myocardial injury. Moreover, some reports recently confirmed that SHI could block high-mobility group box protein 1 (HMGB1) release in activated macrophages. However, the relationship between SHI and LPS-induced cardiac dysfunction has not been studied. Thus, we established a LPS-induced cardiac dysfunction mouse model and found that SHI could reverse cardiac function, restore the destruction of myocardial architecture, reduce serum cardiac enzymes and inflammation response, and elevate survival rate. In addition, we found that SHI could alleviate LDH releases, pro-inflammatory cytokine release (IL-1β and IL-18), and cell apoptosis in LPS-treated H9c2 cells. Some evidences confirmed that IL-18 could induce tumor necrosis factor (TNF)-α, IL-1β, IL-6, and nitric oxide (NO) production, which resulted in cardiac myocyte apoptosis (Keira et al., 2002). Additionally, IL-18 induces proapoptotic Fas, Fas-L, and TNFR1 expression in endothelial cells (Marino and Cardier, 2003). Thus, SHI suppression of ATP-induced cell apoptosis in LPS-primed H9c2 cells is an indirect effect by inhibiting pro-inflammatory cytokine production. Therefore, these results indicated that SHI could play a protective role in LPS-induced cardiac injury.

The activation of the NLRP3 inflammasome requires two steps: priming and activation. The priming step is that pattern recognition receptors (signal 1) such as Toll-like receptors activate nuclear factor-κB (NF-κB) pathways, leading to the formation of the NLRP3–ASC–caspase-1 complex (Swanson et al., 2019). Then, stimulation of damage-associated molecular patterns (signal 2, such as ATP and nigericin) provokes the activation of the NLRP3 inflammasome, mediating the maturation and secretion of IL-1β and IL18 (Mangan et al., 2018; Swanson et al., 2019). Cumulative evidences showed that the activation of NLRP3 inflammasome played a key role in sepsis-induced myocardial injury (Zhang et al., 2015; Wu et al., 2018). Yang et al. (2018) also found that the expression levels of NLRP3 and caspase-1 were increased in myocardial tissue treated with cecal ligation and puncture. Consistent with these results, we also found that the expressions of NLRP3 and cleaved caspase-1 at the protein level in heart tissues and caspase-1 activity were increased by LPS. Additionally, we found that SHI significantly reduced the production of IL-1β and IL-18 and macrophage infiltration of heart tissue in LPS-treated mice, which may be related to the activation of NLRP3 inflammasome. Additionally, we also found that SHI significantly reduced the increased production of IL-1β and IL-18 in cell culture supernatants and also inhibited the activation of NLRP3 inflammasome and enhanced caspase-1 activity by ATP in LPS-primed H9c2 cells. Thus, these data indicated that the protective effect of SHI on the cardiac injury was due to inhibiting the activation of NLRP3 inflammasome and inflammatory cytokine release.

SIRT1, a 3-hydroxy-3-methylglutaryl coenzyme A (HMG-CoA) reductase, is a key regulator in various intracellular processes. A recent study reported that mRNA and protein expression of SIRT1 was increased in septic cardiomyopathy, and treatment with EX527 (a selective SIRT1 inhibitor) could improve cardiac function such as increased global longitudinal strain and longitudinal strain rate (Smith et al., 2019). Notably, SIRT1 has been considered to be involved in the inflammatory

response of macrophages cells (Jia et al., 2018). In the present study, we observed that SHI increased SIRT1 protein levels in heart tissue and H9c2 cells, which may be accountable for its upregulation of SIRT1 mRNA levels. However, some evidences reported that SHI inhibited mRNA and protein expressions of SIRT1 in HepG2 cells with overexpression of SIRT1 (Jin et al., 2015). These differences may be contributed to different regulatory effects of SHI on SIRT1 in different cell models. We further examined whether SIRT1 was involved in the inhibitory effects of SHI in NLRP3 inflammasome activation in H9c2 cells. Here, we found that LPS-induced reduction of SIRT1 activity and protein levels as well as the activation of NLRP3 inflammasome were prevented by SHI. Intriguingly, EX-527 not only inhibited SIRT1 activity but also downregulated SIRT1 at the protein levels. These results were consistent with recent reports (Smith et al., 2019). However, it was previously reported that EX527 only inhibited SIRT1 catalytic activity (Napper et al., 2005; Solomon et al., 2006). The reason may be that after EX527 binds to the active area of SIRT1, it blocks the inhibition of downstream inflammatory factors. These inflammatory cytokines could decrease the protein expression of SIRT1 through positive feedback. In addition, EX527 abolished the inhibitory effects of SHI on the activation of NLRP3 inflammasome, SIRT1 knockdown suppresses SHI-mediated anti-inflammatory activity. The probable mechanisms of SIRT1-induced inhibition of the activation of NLRP3 inflammasome were that SIRT1 deacetylated and blocked some transcriptional factors, such as Kruppel-like factor 4 (KLF4) and NF-κB, and then further decreased the expression of NLRP3 inflammasome-associated protein (Franceschelli et al., 2016; Zhang X. et al., 2018).

CONCLUSION

In summary, our findings provided the first evidence that SHI exerted a protective role against LPS-induced cardiac dysfunction. The protective effect of SHI was attributed to the inhibition of NLRP3 inflammasome activation mediated by SIRT1 *in vivo* and *in vitro*. Consequently, our data demonstrated that SHI is a promising therapeutic target for SICD.

DATA AVAILABILITY STATEMENT

All datasets presented in this study are included in the article/Supplementary Material.

ETHICS STATEMENT

All animal-related experimental procedures were approved by Animal Studies Ethics Committee of Central South University (Hunan, China). Written informed consent was obtained from the owners for the participation of their animals in this study.

AUTHOR CONTRIBUTIONS

TG, Z-BJ, X-PC, and X-ZX conceived and designed the experiments. TG, Z-BJ, and Z-YT executed the experiments and analyzed the samples. TG, Z-BJ, and Z-YT analyzed the data. TG wrote the first version of the manuscript. All authors interpreted the data, critically revised the manuscript, and approved the final version of the manuscript.

FUNDING

This study was partially supported by the Science and Technology Project of Changsha (kq1701092) and the National Science Foundation of China (No. 81501708). All of the funding bodies funded the study design, collection, analysis, interpretation of data, and writing of the manuscript.

REFERENCES

Abderrazak, A., Syrovets, T., Couchie, D., El Hadri, K., Friguet, B., Simmet, T., et al. (2015). NLRP3 inflammasome: from a danger signal sensor to a regulatory node of oxidative stress and inflammatory diseases. *Redox. Biol.* 4, 296–307. doi: 10.1016/j.redox.2015.01.008

Andujar, I., Rios, J. L., Giner, R. M., and Recio, M. C. (2013). Pharmacological properties of shikonin - a review of literature since 2002. *Planta. Med.* 79, 1685–1697. doi: 10.1055/s-0033-1350934

Bai, T., Hu, X., Zheng, Y., Wang, S., Kong, J., and Cai, L. (2016). Resveratrol protects against lipopolysaccharide-induced cardiac dysfunction by enhancing SERCA2a activity through promoting the phospholamban oligomerization. *Am. J. Physiol. Heart Circ. Physiol.* 311, H1051–H1062.

Chen, Y., Luo, H. Q., Sun, L. L., Xu, M. T., Yu, J., Liu, L. L., et al. (2018). Dihydromyricetin Attenuates Myocardial Hypertrophy Induced by Transverse Aortic Constriction via Oxidative Stress Inhibition and SIRT3 Pathway Enhancement. *Int. J. Mol. Sci.* 19:2592. doi: 10.3390/ijms19092592

Court, O., Kumar, A., Parrillo, J. E., and Kumar, A. (2002). Clinical review: Myocardial depression in sepsis and septic shock. *Crit. Care* 6, 500–508.

Franceschelli, S., Pesce, M., Ferrone, A., Patruno, A., Pasqualone, L., Carlucci, G., et al. (2016). A Novel Biological Role of alpha-Mangostin in Modulating Inflammatory Response Through the Activation of SIRT-1 Signaling Pathway. *J. Cell. Physiol.* 231, 2439–2451. doi: 10.1002/jcp.25348

Fu, Y., Wang, Y., Du, L., Xu, C., Cao, J., Fan, T., et al. (2013). Resveratrol inhibits ionising irradiation-induced inflammation in MSCs by activating SIRT1 and limiting NLRP-3 inflammasome activation. *Int. J. Mol. Sci.* 14, 14105–14118. doi: 10.3390/ijms140714105

Han, D., Li, X., Li, S., Su, T., Fan, L., Fan, W. S., et al. (2017). Reduced silent information regulator 1 signaling exacerbates sepsis-induced myocardial injury and mitigates the protective effect of a liver X receptor agonist. *Free Radic. Biol. Med.* 113, 291–303. doi: 10.1016/j.freeradbiomed.2017.10.005

Hu, J., Wang, N., and Wang, Y. J. (2013). XRCC3 and RAD51 expression are associated with clinical factors in breast cancer. *PLoS One* 8:e72104. doi: 10.1371/journal.pone.0072104

Jia, Y., Li, Z., Cai, W., Xiao, D., Han, S., Han, F., et al. (2018). SIRT1 regulates inflammation response of macrophages in sepsis mediated by long noncoding RNA. *Biochim. Biophys. Acta Mol. Basis Dis.* 1864, 784–792. doi: 10.1016/j.bbadis.2017.12.029

Jin, Y. D., Ren, Y., Wu, M. W., Chen, P., and Lu, J. (2015). Effect of shikonin on multidrug resistance in HepG2: The role of SIRT1. *Pharm. Biol.* 53, 1016–1021. doi: 10.3109/13880209.2014.952836

Kakihana, Y., Ito, T., Nakahara, M., Yamaguchi, K., and Yasuda, T. (2016). Sepsis-induced myocardial dysfunction: pathophysiology and management. *J. Inten. Care* 4:22.

Kalbitz, M., Fattahi, F., Grailer, J. J., Jajou, L., Malan, E. A., Zetoune, F. S., et al. (2016). Complement-induced activation of the cardiac NLRP3 inflammasome in sepsis. *FASEB J.* 30, 3997–4006. doi: 10.1096/fj.201600728r

Karki, R., and Kanneganti, T. D. (2019). Diverging inflammasome signals in tumorigenesis and potential targeting. *Nat. Rev. Cancer* 19, 197–214. doi: 10.1038/s41568-019-0123-y

Keira, N., Tatsumi, T., Matoba, S., Shiraishi, J., Yamanaka, S., Akashi, K., et al. (2002). Lethal effect of cytokine-induced nitric oxide and peroxynitrite on cultured rat cardiac myocytes. *J. Mol. Cell Cardiol.* 34, 583–596. doi: 10.1006/jmcc.2002.1539

Liu, W. L., and Liu, Q. (2019). Shikonin attenuates sympathetic remodeling in chronic heart failure mice via regulating miR-124. *Biochem. Biophys. Res. Commun.* 520, 359–365. doi: 10.1016/j.bbrc.2019.10.038

Liu, Y. C., Yu, M. M., Shou, S. T., and Chai, Y. F. (2017). Sepsis-Induced Cardiomyopathy: Mechanisms and Treatments. *Front. Immunol.* 8:1021.

Mangan, M. S. J., Olhava, E. J., Roush, W. R., Seidel, H. M., Glick, G. D., and Latz, E. (2018). Targeting the NLRP3 inflammasome in inflammatory diseases. *Nat. Rev. Drug. Discov.* 17:688.

Marino, E., and Cardier, J. E. (2003). Differential effect of IL-18 on endothelial cell apoptosis mediated by TNF-alpha and Fas (CD95). *Cytokine* 22, 142–148. doi: 10.1016/s1043-4666(03)00150-9

Napper, A. D., Hixon, J., Mcdonagh, T., Keavey, K., Pons, J. F., Barker, J., et al. (2005). Discovery of indoles as potent and selective inhibitors of the deacetylase SIRT1. *J. Med. Chem.* 48, 8045–8054.

Narvaez, I., Canabal, A., Martin, C., Sanchez, M., Moron, A., Alcala, J., et al. (2018). Incidence and evolution of sepsis-induced cardiomyopathy in a cohort of patients with sepsis and septic shock. *Med. Intensiva.* 42, 283–291. doi: 10.1016/j.medine.2018.04.002

Niu, J., Wang, K., Graham, S., Azfer, A., and Kolattukudy, P. E. (2011). MCP-1-induced protein attenuates endotoxin-induced myocardial dysfunction by suppressing cardiac NF-small ka. *CyrillicB activation via inhibition of Ismall ka, CyrillicB kinase activation. J. Mol. Cell Cardiol.* 51, 177–186. doi: 10.1016/j.yjmcc.2011.04.018

Peng, Z., Zhang, W., Qiao, J., and He, B. (2018). Melatonin attenuates airway inflammation via SIRT1 dependent inhibition of NLRP3 inflammasome and IL-1beta in rats with COPD. *Int. Immunopharmacol.* 62, 23–28. doi: 10.1016/j.intimp.2018.06.033

Smith, L. M., Yoza, B. K., Hoth, J. J., Mccall, C. E., and Vachharajani, V. (2019). SIRT1 Mediates Septic Cardiomyopathy in a Murine Model of Polymicrobial Sepsis. *Shock* 54, 96–101. doi: 10.1097/shk.0000000000001429

Solomon, J. M., Pasupuleti, R., Xu, L., Mcdonagh, T., Curtis, R., Distefano, P. S., et al. (2006). Inhibition of SIRT1 catalytic activity increases p53 acetylation but does not alter cell survival following DNA damage. *Mol. Cell Biol.* 26, 28–38. doi: 10.1128/mcb.26.1.28-38.2006

Swanson, K. V., Deng, M., and Ting, J. P. (2019). The NLRP3 inflammasome: molecular activation and regulation to therapeutics. *Nat. Rev. Immunol.* 19, 477–489. doi: 10.1038/s41577-019-0165-0

Wang, Y., Yan, X., Mi, S., Li, Z., Wang, Y., Zhu, H., et al. (2017). Naoxintong attenuates Ischaemia/reperfusion Injury through inhibiting NLRP3 inflammasome activation. *J. Cell Mol. Med.* 21, 4–12. doi: 10.1111/jcmm.12915

Wang, Z., Liu, T., Gan, L., Wang, T., Yuan, X., Zhang, B., et al. (2010). Shikonin protects mouse brain against cerebral ischemia/reperfusion injury through its antioxidant activity. *Eur. J. Pharmacol.* 643, 211–217. doi: 10.1016/j.ejphar.2010.06.027

Wu, D., Shi, L., Li, P., Ni, X., Zhang, J., Zhu, Q., et al. (2018). Intermedin1-53 Protects Cardiac Fibroblasts by Inhibiting NLRP3 Inflammasome Activation During Sepsis. *Inflammation* 41, 505–514. doi: 10.1007/s10753-017-0706-2

Yang, C., Xia, W., Liu, X., Lin, J., and Wu, A. (2019). Role of TXNIP/NLRP3 in sepsis-induced myocardial dysfunction. *Int. J. Mol. Med.* 44, 417–426.

Yang, J., Wang, Z., and Chen, D. L. (2017). Shikonin ameliorates isoproterenol (ISO)-induced myocardial damage through suppressing fibrosis, inflammation, apoptosis and ER stress. *Biomed. Pharmacother.* 93, 1343–1357. doi: 10.1016/j.biopha.2017.06.086

Yang, L., Xie, M., Yang, M., Yu, Y., Zhu, S., Hou, W., et al. (2014). PKM2 regulates the Warburg effect and promotes HMGB1 release in sepsis. *Nat. Commun.* 5:4436.

Yang, L., Zhang, H., and Chen, P. (2018). Sulfur dioxide attenuates sepsis-induced cardiac dysfunction via inhibition of NLRP3 inflammasome activation in rats. *Nitric. Oxide.* 81, 11–20. doi: 10.1016/j.niox.2018.09.005

Zhang, B., Liu, Y., Sui, Y. B., Cai, H. Q., Liu, W. X., Zhu, M., et al. (2015). Cortistatin Inhibits NLRP3 Inflammasome Activation of Cardiac Fibroblasts During Sepsis. *J. Card Fail.* 21, 426–433. doi: 10.1016/j.cardfail.2015.01.002

Zhang, X., Chen, J., Sun, L., and Xu, Y. (2018). SIRT1 deacetylates KLF4 to activate Claudin-5 transcription in ovarian cancer cells. *J. Cell Biochem.* 119, 2418–2426. doi: 10.1002/jcb.26404

Zhang, Y., Xu, T., Pan, Z., Ge, X., Sun, C., Lu, C., et al. (2018). Shikonin inhibits myeloid differentiation protein 2 to prevent LPS-induced acute lung injury. *Br. J. Pharmacol.* 175, 840–854. doi: 10.1111/bph.14129

Zorman, J., Susjan, P., and Hafner-Bratkovic, I. (2016). Shikonin Suppresses NLRP3 and AIM2 Inflammasomes by Direct Inhibition of Caspase-1. *PLoS One* 11:e0159826. doi: 10.1371/journal.pone.0159826

Conflict of Interest: The authors declare that the research was conducted in the absence of any commercial or financial relationships that could be construed as a potential conflict of interest.

frontiers in Physiology

ORIGINAL RESEARCH
published: 16 November 2020
doi: 10.3389/fphys.2020.608473

A Novel Homozygous Intronic Variant in TNNT2 Associates With Feline Cardiomyopathy

James W. McNamara[1†], Maggie Schuckman[2], Richard C. Becker[1] and Sakthivel Sadayappan[1]*

[1] Division of Cardiovascular Health and Disease, Department of Internal Medicine, Heart, Lung and Vascular Institute, University of Cincinnati, Cincinnati, OH, United States, [2] Department of Cardiology, MedVet Cincinnati, Fairfax, OH, United States

Background: Hypertrophic cardiomyopathy (HCM) is a genetic disease of the heart and the most common cause of sudden cardiac death in the young. HCM is considered a disease of the sarcomere owing to the large number of mutations in genes encoding sarcomeric proteins. The riddle lies in discovering how these mutations lead to disease. As a result, treatments to prevent and/or treat HCM are limited to invasive surgical myectomies or ablations. The A31P variant of cardiac myosin binding protein-C, encoded by *MYBPC3*, was found to be more prevalent in a cohort of Maine Coon cats with HCM. However, other mutations in *MYBPC3* and *MYH7* have also been associated with HCM in cats of other breeds. In this study, we expand the spectrum of genes associated with HCM in cats.

Results: Next Generation Whole Genome sequencing was performed using DNA isolated from peripheral blood of a Maine Coon with cardiomyopathy that tested negative for the *MYBPC3* A31P variant. Through risk stratification of variants, we identified a novel, homozygous intronic variant in cardiac troponin T (*TNNT2*). *In silico* analysis of the variant suggested that it may affect normal splicing of exon 3 of *TNNT2*. Both parents tested heterozygous for the mutation, but were unaffected by the disease. Echocardiography analyses revealed that the proband had shown early onset congestive heart failure, which is managed with a treatment regime including ACE and aldosterone inhibitors.

Conclusion: In summary, we are the first to demonstrate the association between *TNNT2* mutations and HCM in felines, suggesting that this gene should be included in the testing panel of genes when performing genetic testing for HCM in cats.

Keywords: Hypertrophic Cardiomyopathy, Maine Coon, MYBPC3, TNNT2, sarcomere

OPEN ACCESS

Edited by:
Xuejun Wang,
University of South Dakota, United States

Reviewed by:
Michelle S. Parvatiyar,
Florida State University, United States
Rongxue Wu,
The University of Chicago, United States

****Correspondence:***
Sakthivel Sadayappan
sadayasl@ucmail.uc.edu

†Present address:
James W. McNamara, Murdoch Children's Research Institute, The Royal Children's Hospital, Parkville, VIC, Australia

Specialty section:
This article was submitted to Striated Muscle Physiology, a section of the journal Frontiers in Physiology

Received: *20 September 2020*
Accepted: *26 October 2020*
Published: *16 November 2020*

Citation:
McNamara JW, Schuckman M, Becker RC and Sadayappan S (2020) A Novel Homozygous Intronic Variant in TNNT2 Associates With Feline Cardiomyopathy. Front. Physiol. 11:608473. doi: 10.3389/fphys.2020.608473

INTRODUCTION

Hypertrophic cardiomyopathy (HCM) is the most common form of genetic heart disease, affecting at least 1 in 500 humans (Ho, 2011). Defined by an unexplained abnormal thickening of the ventricular walls and possible outflow tract obstruction, no cure is currently available for HCM. HCM is primarily caused by mutations in genes that encode sarcomeric proteins. In particular,

mutations in *MYH7* and *MYBPC3*, encoding beta-cardiac myosin heavy chain and cardiac myosin binding protein-C, respectively, are the most commonly mutated genes (Viswanathan et al., 2017), although other sarcomeric genes, including *TNNI3, TNNT2,* and *MYL2,* have also been implicated in humans (Brouwer et al., 2011). How mutations in these sarcomeric genes result in the development of HCM remains poorly understood.

In cats, cardiomyopathy is the main cause of cardiovascular disease, with HCM presenting as the most common form, suggesting that cats may be an excellent non-rodent animal model of HCM (Ferasin et al., 2003). A variant in *MYBPC3*, A31P, was previously linked to the development of HCM in Maine Coon cats (Meurs et al., 2005). This variant occurs within the C0 domain of cardiac myosin binding protein-C (cMyBP-C), and it is expected to cause disease *via* structural defects in this domain important for regulation of actomyosin regulation (Van Dijk et al., 2016). Another variant in *MYBPC3*, A74T, has also been described across multiple cat breeds. However, in-depth follow-up studies demonstrated that this polymorphism is unrelated to cardiomyopathy (Wess et al., 2010; Longeri et al., 2013). A third variant in *MYBPC3*, R820W, has been associated with HCM, most specifically in the Ragdoll (Meurs et al., 2007). More recently, the first variant in *MYH7*, E1883K, has been associated with HCM in a Domestic Shorthair cat, expanding the spectrum of genes associated with feline cardiomyopathy (Schipper et al., 2019). A full list of mutations associated with feline cardiomyopathy is shown in **Table 1**.

In the present study, a male Maine Coon cat with cardiomyopathy and early congestive heart failure was studied. After initially screening negative for the aforementioned A31P mutation, we performed WGS to identify potential mutations and, thus, pinpoint the genetic cause of this cat's cardiomyopathy through study of the diseased cat's family tree. This study expands upon recent Next Generation Sequencing performed in cats (Genova et al., 2018; Ontiveros et al., 2018). As a result, we have identified a novel autosomal recessive mutation in the sarcomeric cardiac troponin T (*TNNT2)* gene that appeared to be associated with feline cardiomyopathy. This is the first known record of such mutation in felines, suggesting that *TNNT2* should be included as a candidate gene in the genetic screenings.

MATERIALS AND METHODS

Phenotyping, Blood Collection and DNA Extraction

All procedures followed the protocol approved by the Institutional Animal Care and Use Committee of the University of Cincinnati and complied with the Guide for the Use and Care of Laboratory Animals published by the National Institutes of Health. The proband's owner established contact to determine if the animal's disease could be linked to a genetic mutation. To establish a full research study, a Material Transfer Agreement was initiated between the proband's owner and the University of Cincinnati. Researchers had no contact with any animals beyond receipt of blood samples. All studies involving contact with animals were performed by board certified veterinarians. Diagnosis and treatment of the proband, regular checkups and echocardiography were performed by a board certified veterinary cardiologist using standard echocardiographic techniques and references from a population of healthy Maine Coon cats (Thomas et al., 1993; Drourr et al., 2005). Peripheral blood was collected by a certified veterinarian or veterinarian nurse at each animal's local hospital following a routine check-up. Blood collected locally was transported back to the laboratory on wet ice. Blood that was collected at veterinary clinics farther from the lab was shipped on cold blocks overnight. Upon receipt at the laboratory, all blood samples were aliquoted into 200 μl samples and stored at −80°C until use. DNA was extracted from a single 200 μl aliquot using the Qiagen QIAamp DNA Mini and Blood DNA isolation kit, following the manufacturer's protocol. Concentration and purity of DNA was analyzed by NanoDrop. For samples sent for WGS, DNA integrity and concentration were also determined using the Agilent 2100 Bioanalyzer and Qubit Fluorometer, respectively.

TABLE 1 | The current list of known mutations associated with feline cardiomyopathy.

Gene	Mutation	Breed	References
MYBPC3	A31P	Maine Coon	Meurs et al. (2005)
MYBPC3	R820W	Ragdoll	Meurs et al. (2007)
MYH7	E1883K	Domestic Shorthair	Schipper et al. (2019)

Whole Genome Sequencing and Analysis

DNA extracted from the whole blood of the proband was submitted to Novogene Co., Ltd., for WGS. DNA quality and quantity were confirmed by Agarose gel electrophoresis and Qubit Fluorometer. A total amount of 1.5 μg high-quality genomic DNA was randomly sheared into short fragments of approximately 350 bp and used for library construction using the NEBNext® DNA Library Prep Kit. Briefly, following end repairing, dA-tailing, and ligation with NEBNext adapter, the fragments were PCR-enriched by P5 and indexed P7 oligos. The concentration of the DNA library was quantified using the Qubit 2.0 fluorometer and diluted to 1 ng/μl. Following dilution, the insert size of the library was assessed with the Agilent 2100 bioanalyzer, and quantitative real-time PCR (qPCR) was performed to detect the effective concentration of the prepared library. Following enrichment and indexing, pair-end sequencing of the qualified library was performed on an Illumina HiSeq X Ten with a read length of PE150bp at each end.

Bioinformatics Analysis

The original sequencing data acquired by high-throughput sequencing platforms (e.g., Illumina HiSeq^{TM}/NovaSeq^{TM}) and recorded in image files were first transformed to sequence reads by base calling with the CASAVA software. Information on sequences and corresponding sequencing quality was stored in a FASTQ file. Following quality control of raw sequencing data for clean data filtration, each clean read was mapped to the reference genome (Felis_Catus_9.0, Ensembl release 93) using the BWA software (Li and Durbin, 2009), and the mapping

rate and coverage were counted according to the alignment results. Duplicates were removed by SAMTOOLS (Li et al., 2009). Single nucleotide polymorphism (SNP) and InDel variants were detected using the GATK software (Depristo et al., 2011). These SNPs were annotated using ANNOVAR as previously described (Wang et al., 2010).

Sanger Sequencing

To test, or confirm, the presence of a genetic variant in parents of the proband, PCR was performed using a high-fidelity *Taq* polymerase to specifically amplify the sequence around the variant. The PCR product was purified and sent for Sanger sequencing using Cincinnati Children's Hospital DNA Sequencing and Genotyping Core Facility.

RESULTS

The proband was a privately-owned male pure-bred Maine Coon. At 8 months of age, he presented with left ventricular, right atrial, and borderline left atrial dilatation and borderline septal hypertrophy, with preserved-to-elevated systolic function (**Figures 1A,B** and **Table 2**), when compared to reference echocardiography values for the Maine Coon (Drourr et al., 2005). Diastolic function could not be quantified as a result of fusion of E and A waves. Progressive enlargement of all four chambers of the heart was noted at 14 months of age, while borderline septal hypertrophy and preserved systolic function was still noted. This was diagnosed as a primary unclassified cardiomyopathy with possible early congestive heart failure. Furosemide, Benazepril, Spironolactone, and Clopidogrel treatments were then initiated by the veterinarian. This combination appeared to stabilize the progression of the heart disease at 18 months (**Table 2**).

TABLE 2 | Echocardiography parameters from serial measurements performed by a board-certified veterinary cardiologist.

Parameter	Proband				References
Age (month)	10	14	18	24	>12
IVSd (mm)	6	5.9	5.88	5.94	3.9–4.1
LVIDd (mm)	19.3	19.9	21.8	21.7	18.1–18.9
LVPWd (mm)	5.1	5.5	5.27	5.55	4.2–4.4
IVSs (mm)	9.6	9.2	N/A	N/A	7.2–7.8
LVIDs (mm)	9	9.6	7.79	8.11	8.5–9.3
LVPWs (mm)	9.6	9.4	N/A	N/A	7.8–8.2
%FS	60.6	59.5	64.2	62.6	50.35–53.35
LA (mm)	17.6	19.8	18.9	19.7	13.4–14.0
LA/Ao	1.33	1.58	1.53	1.44	1.20–1.26
Treatments		Furosemide, Benazepril, Clopidogrel	Spironolactone, Furosemide, Benazepril, Clopidogrel	Spironolactone, Furosemide, Benazepril, Clopidogrel	

Significant dilatation of all cardiac chambers was noted with normal to elevated systolic function. Treatments administered are listed. IVS, interventricular septal thickness; LVID, left ventricular internal diameter; LVPW, left ventricular posterior wall thickness; FS, fractional shortening; LA, left atrial dimension; LA/Ao Left atrium-to-aortic root ratio; d, diastole; s, systole. N/A represents data not available.

DNA was isolated from whole peripheral blood from the proband. PCR was performed to produce a 251 amplicon around the A31P variant in *MYBPC3* previously associated with HCM in Maine Coon cats (primer sequences in **Table 3**). Sanger sequencing of the PCR product showed no mutation at codon 31, indicating that the proband did not carry the pathogenic A31P variant in *MYBPC3* (**Figure 1C**).

As the proband was negative for the A31P mutation in *MYBPC3*, we asked if any other variants could be traced to the proband's cardiomyopathy. Accordingly, DNA was freshly isolated for WGS to identify potential variants present in the proband. High-quality DNA with an approximate size of 22944bp

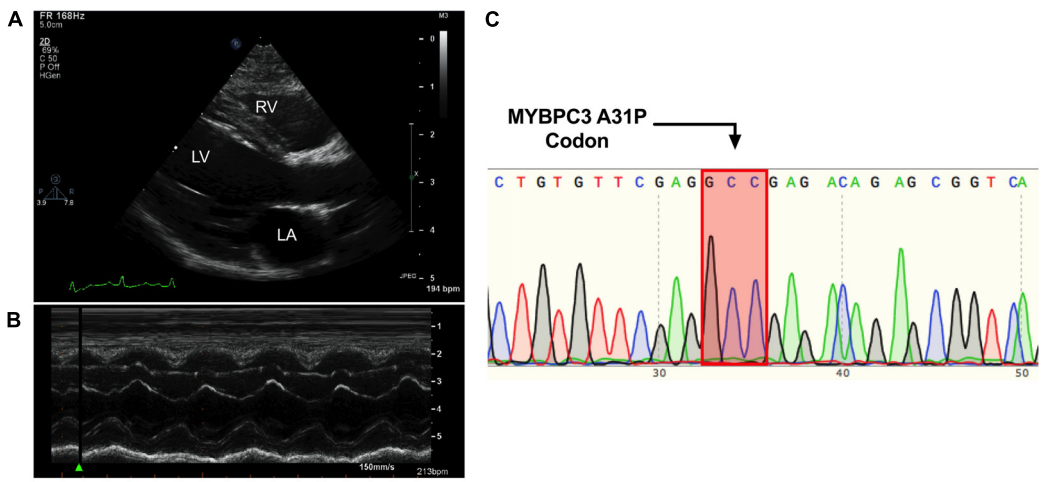

FIGURE 1 | Cardiomyopathy in the absence of the *MYBPC3 A31P* variant. **(A,B)**, Representative echocardiography and outline of cardiovascular disease risk stratification of genetic variants. Representative parasternal long axis B-Mode **(A)** and M-Mode **(B)** images of proband, with left ventricle (LV), left atrium (LA) and right ventricle (RV) labeled. **(C)**, Chromatogram of *MYBPC3* A31P demonstrated that the proband was negative for this variant.

TABLE 3 | List of primer sequences used in this study to test for the presence of variants in *MYBPC3* and *TNNT2 genes*.

Primer name	Primer sequence	Amplicon size (bp)
Cat_A31P_F	AGTCTCAGCCTTCAGCAAGAAGCC	252 bp
Cat_A31P_R	GGTCAAACTTGACCTTGGAGGAGCC	
Cat_TNNT2_F	TGAGTGGATGTGGCTGTGTT	287 bp

was sent for library preparation and sequencing by Novogene. Sequences were aligned against the Felis Catus reference genome (Ensemble release 93). The sequencing resulted in 177419470 raw reads, with an average depth of 17.59 reads per base, an error rate of 0.03, and 94.19% of base reads with a Phred score greater than 30 (**Figures 2A–C**). The detected GC content was 43.06% compared to the reference genome of 41.73%. Together, these data demonstrated sufficiently high quality of sequencing data.

Initial analysis reported more than 20,000 genetic variants identified from the proband, compared to the reference genome. We employed a cardiovascular disease risk stratification step in order to enrich for variants associated with cardiovascular disease. This stratification was with 174 genes covered by the Illumina TruSight Cardio Panel (Pua et al., 2016). This approach reduced the number of variants to 305 (**Figure 2D**). Of these 305 potential variants, only one had been annotated as having "high risk" impact. This particular variant was a single base pair substitution (G to A) within intron 3, corresponding to c.95-108G > A of ENSFCAG00000004613. This variant resulted in the potential inclusion of a *de novo* splice acceptor site (**Figure 3A**). We then used *in silico* analysis to determine the likelihood that this intronic variant indeed acts as a novel splice acceptor site (Wang and Marín, 2006). This *in silico* method correctly identified greater than 96% of canonical splice donors and acceptors within *TNNT2* (**Table 4**). Of note, *in silico* analysis of the c.95-108G > A variant in the proband supported

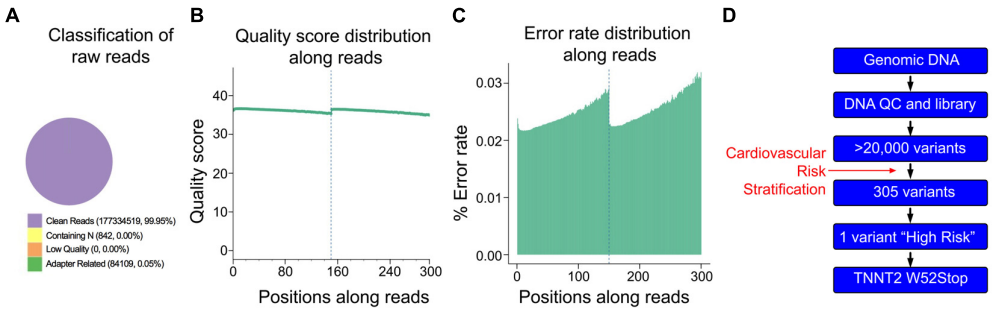

FIGURE 2 | Quality control of Next Generation Sequencing results. **(A)** From 177,419,470 sequencing reads, 99.95% were clean reads, while just 0.05% contained adapter-related contaminations. **(B)** Quantification of sequencing quality distribution along reads demonstrated high-quality scores along entire reads with 94.19% of base reads having a Phred score greater than 30. **(C)** Error rate distribution along reads demonstrated high-fidelity reads with an overall error rate of 0.03%. **(D)** Cardiomyopathy gene stratification strategy using 174 genes from the cardio panel gene list.

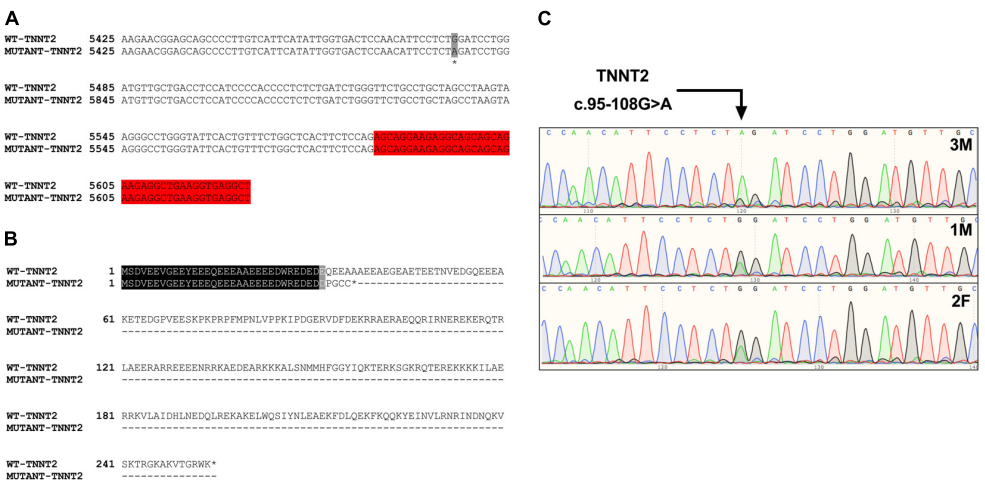

FIGURE 3 | Analysis of the *TNNT2* c.95-108G > A variant. **(A)** Gene sequence alignment of wild-type and mutant *TNNT2*. The variant is highlighted in grey, and the downstream exon is highlighted in red. **(B)** Protein sequence alignment of the wild-type TNNT2 protein and the predicted protein resulting from the *TNNT2* c.95-108G > A variant. **(C)** Sanger sequencing chromatograms demonstrating homozygosity for the *TNNT2* c.95-108G > A variant in the proband and heterozygosity in both parents.

TABLE 4 | *In silico* prediction of exon splicing sites of cat *TNNT2* (ENSFCAG00000004613) gene.

In silico Exon splicing prediction			
Position	**Predicted Splice**	**Score**	**Confidence**
Exon 1 Donor	Constitutive donor	11.931	0.332
Exon 2 Acceptor	Alt. isoform/cryptic acceptor	5.476	0.495
Exon 2 Donor	Constitutive donor	11.4	0.405
Exon 3 **de novo** Acceptor	Constitutive acceptor	4.688	0.396
Exon 3 Acceptor	Alt. isoform/cryptic acceptor	6.649	0.509
Exon 3 Donor	Constitutive donor	13.878	0.871
Exon 4 Acceptor	Constitutive acceptor	5.828	0.568
Exon 4 Donor	Constitutive donor	15.502	0.523
Exon 5 Acceptor	Constitutive acceptor	12.683	0.888
Exon 5 Donor	Constitutive donor	15.343	0.801
Exon 6 Acceptor	Constitutive acceptor	10.572	0.727
Exon 6 Donor	Alt. isoform/cryptic donor	10.982	0.805
Exon 7 Acceptor	Constitutive acceptor	8.308	0.85
Exon 7 Donor	Alt. isoform/cryptic donor	8.771	0.782
Exon 8 Acceptor	Constitutive acceptor	10.214	0.924
Exon 8 Donor	Constitutive donor	13.02	0.872
Exon 9 Acceptor	Not Predicted	N/A	N/A
Exon 9 Donor	Alt. isoform/cryptic donor	11.345	0.347
Exon 10 Acceptor	Constitutive acceptor	8.201	0.438
Exon 10 Donor	Constitutive donor	11.746	0.511
Exon 11 Acceptor	Constitutive acceptor	8.577	0.643
Exon 11 Donor	Alt. isoform/cryptic donor	10.946	0.235
Exon 12 Acceptor	Constitutive acceptor	8.91	0.812
Exon 12 Donor	Constitutive donor	8.271	0.728
Exon 13 Acceptor	Constitutive acceptor	11.353	0.443
Exon 13 Donor	Constitutive donor	12.265	0.581
Exon 14 Acceptor	Constitutive acceptor	10.067	0.841

the hypothesis that this variant alters *TNNT2* splicing. The consequence of this aberrant splicing was investigated at the protein level, which revealed that the variant could cause the loss of 223 carboxyl terminal amino acids and incorporation of only five novel amino acids, rendering the protein non-functional (**Figure 3B**).

Sanger sequencing was performed to validate the WGS annotation of the c.95-108G > A variant in the proband (primer sequence in **Table 3**). Strikingly, this sequencing revealed homozygosity of the c.95-108G > A variant in the proband, further suggesting its disease association (**Figure 3C**). Following this finding, blood samples from both parents of the proband were obtained. Echocardiography did not suggest any cardiac pathology in either of these parents (data not shown). DNA was extracted and PCR performed for Sanger sequencing of the *TNNT2* variant. Strikingly, both parents harbored a single copy of the c.95-108G > A variant (**Figure 3C**). This finding led to investigations into the pedigree of the proband. It was found that the proband was born from consanguineous breeding (**Figure 4**). Taken together, these results implicate a novel intronic mutation which results in the truncation of the sarcomeric protein, cardiac troponin T, as the cause of cardiomyopathy in this Maine Coon cat.

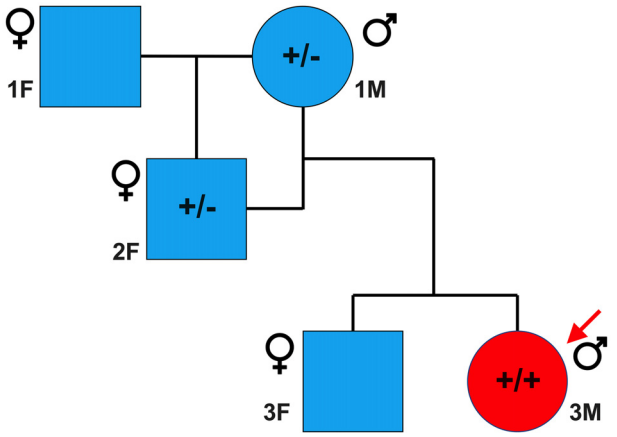

FIGURE 4 | Family pedigree of affected proband. Circles and squares represent males and females, respectively, while blue and red represent unaffected and affected individuals, respectively. A male Maine Coon, heterozygous for the *TNNT2* c.95-108G > A variant, was mated to a female Maine Coon, which resulted in one female offspring. This female offspring, also heterozygous, was then bred with the original male, producing two offspring. The male offspring was the cardiomyopathic proband in this study and was homozygous for the *TNNT2* c.95-108G > A variant. * indicates that samples from these cats were not available at the time of the study.

DISCUSSION

In this study, we identified a novel homozygous intronic variant in *TNNT2* which was associated with a case of feline cardiomyopathy and early heart failure. Mutations in *MYBPC3* and *MYH7* have previously been described. However, to the best of our knowledge, this is the first report of a thin filament mutation associated with feline cardiomyopathy (Meurs et al., 2005; Schipper et al., 2019). Mutations in *TNNT2* have been strongly implicated in the development of HCM and dilated cardiomyopathy (Watkins et al., 1995; Pasquale et al., 2012). In humans, these *TNNT2* mutations are described as phenotypically mild compared to *MYH7* mutations, but with a higher incidence of sudden cardiac death (Watkins et al., 1995). Importantly, mutations in intronic splice sites have been identified as causative of cardiomyopathy in humans (Thierfelder et al., 1994). Taken together, these data support our finding that the *TNNT2* intronic mutation we describe is the most likely cause of this case of feline cardiomyopathy.

The *TNNT2* gene encodes the cardiac-specific sarcomeric protein cardiac troponin-T (cTnT) (Wei and Jin, 2016). Cardiac troponin-C and -I (cTnC and cTnI, respectively), together with cTnT, make up the troponin complex of the heart (Gomes et al., 2002). The troponin complex is associated with the thin filaments, and cTnT is understood to play an important role in anchoring the complex to both actin and tropomyosin (Gomes et al., 2002). When calcium is released from the sarcoplasmic reticulum, it binds to and induces a structural change in cTnC (Vinogradova et al., 2005), ultimately leading to the movement of tropomyosin, allowing the formation of cross-bridges (Boussouf et al., 2007). cTnT has been demonstrated to regulate the calcium

sensitivity of actomyosin ATPase and force (Gomes et al., 2005). Thus, cTnT has a central role in regulating contraction and relaxation of the heart.

Homozygous knockout of the *TNNT2* gene in mice is embryonically lethal (Ahmad et al., 2008; Nishii et al., 2008). As such, it is unlikely that the *de novo* splice acceptor site in the mutant *TNNT2* is fully penetrant. Rather, it is more likely that the aberrant splicing of *TNNT2* is a limited event, resulting in haploinsufficiency of the cTnT protein. This variant results in the significant truncation of the cTnT protein. It is well known that both the middle carboxyl-terminal regions of cTnT are required for its interaction with tropomyosin, cTnI, and cTnC (Wei and Jin, 2016). Therefore, the loss of these regions would likely prevent the incorporation of the truncated protein into the sarcomere. The resultant reduction in cTnT levels would result in an abnormal stoichiometry of thin filament proteins in the sarcomere, which would be sufficient to cause cardiomyopathy. Indeed, haploinsufficiency of cTnT has previously been associated with cardiomyopathy (Bollen et al., 2017). Furthermore, the incorporation of less than 5% of C-terminally truncated cTnT is sufficient to cause cardiomyopathy in mice (Tardiff et al., 1998). Since the proband's symptoms are currently managed *via* treatment, consisting of Furosemide, Spironolactone, Benazepril and Clopidogrel, we cannot confirm the exact level of haploinsufficiency. Unfortunately, DNA from the proband's littermate was not available, but we predict it would be either negative or heterozygous for the *TNNT2* c.95-108G > A variant. While no variants were identified in *MYH6* or *MYH7*, two single nucleotide variants were also identified in *MYBPC3* that were classified as having moderate risk. These variants were a proline substituted to a leucine at position 922 (P922L) and an alanine for a threonine at amino acid 1037 (A1037T), occurring within domains C7 and C8 of cMyBP-C, respectively. However, further investigation of these variants revealed that these amino acids are not evolutionarily conserved, and, furthermore, the substituted amino acids matched those of either human or mouse, effectively ruling out these *MYBPC3* variants as disease-causing.

CONCLUSION

We have identified a novel, homozygous mutation in the sarcomeric gene *TNNT2*, which is associated with cardiomyopathy in a Maine Coon cat. The homozygosity of this mutation resulted from inbreeding. This study is the first to describe a mutation in *TNNT2* that is associated with feline cardiomyopathy, suggesting that this gene should be included in routine genetic testing in felines. Additionally, breeders should be mindful of the dangers associated with close generational consanguineous breeding.

DATA AVAILABILITY STATEMENT

The sequencing data has been deposited into the BioProject database (accession: PRJNA671288).

ETHICS STATEMENT

The animal study was reviewed and approved by Ref: AM07-19-10-03-01 Institutional Animal Care and Use Committee OLAW Assurance D16-00190, AAALAC 00278 University of Cincinnati PO Box 210572, Cincinnati, OH 45267-0572. Written informed consent was obtained from the owner for the participation of their animals in this study.

AUTHOR CONTRIBUTIONS

JM and SS designed the research and wrote the manuscript. JM and MS performed the research. JM, MS, and SS analyzed data. MS and RB edited the manuscript. RB provided project oversight for clinical data. All authors read and approved the final manuscript.

FUNDING

Whole genome sequencing of the proband was funded by a donation from Kathleen and Michael Janson, owners of the proband. JM was supported by an American Heart Association Postdoctoral Fellowship (17POST33630095). SS received funding from the following grants: National Institutes of Health grants R01 AR078001, R01 HL130356, R56 HL139680, R01 AR067279, R01 HL105826, and R01 HL143490; and transformation (19TPA34830084) awards; and MyoKardia, AstraZeneca, Merck, and Amgen.

ACKNOWLEDGMENTS

We would like to thank the staff at Warm Animal, Cincinnati; Big Creek, Cleveland; and Friendship, Washington DC veterinary hospitals for performing the blood draws. We also thank Linda Komar and Joseph Keyerleber for organizing the shipments of the proband's parents' blood. Sanger sequencing was performed by Cincinnati Children's Hospital DNA Sequencing and Genotyping Core. This manuscript has been released as a pre-print at Research Square (McNamara et al., 2020).

REFERENCES

Ahmad, F., Banerjee, S. K., Lage, M. L., Huang, X. N., Smith, S. H., Saba, S., et al. (2008). The role of cardiac troponin T quantity and function in cardiac development and dilated cardiomyopathy. *PLoS One* 3:e2642. doi: 10.1371/journal.pone.0002642

Bollen, I. A. E., Schuldt, M., Harakalova, M., Vink, A., Asselbergs, F. W., Pinto, J. R., et al. (2017). Genotype-specific pathogenic effects in human dilated cardiomyopathy. *J. physiol.* 595, 4677–4693. doi: 10.1113/jp274145

Boussouf, S. E., Maytum, R., Jaquet, K., and Geeves, M. A. (2007). Role of tropomyosin isoforms in the calcium sensitivity of striated muscle thin filaments. *J. Muscle Res. Cell Motil.* 28, 49–58. doi: 10.1007/s10974-007-9103-z

Brouwer, W. P., Van Dijk, S. J., Stienen, G. J., Van Rossum, A. C., Van Der Velden, J., and Germans, T. (2011). The development of familial hypertrophic cardiomyopathy: from mutation to bedside. *Eur. J. Clin. Invest.* 41, 568–578. doi: 10.1111/j.1365-2362.2010.02439.x

Depristo, M. A., Banks, E., Poplin, R., Garimella, K. V., Maguire, J. R., Hartl, C., et al. (2011). A framework for variation discovery and genotyping using next-generation DNA sequencing data. *Nat. Genet.* 43, 491–498.

Drourr, L., Lefbom, B. K., Rosenthal, S. L., and Tyrrell, W. D. Jr. (2005). Measurement of M-mode echocardiographic parameters in healthy adult Maine Coon cats. *J. Am. Vet. Med. Assoc.* 226, 734–737. doi: 10.2460/javma.2005.226.734

Ferasin, L., Sturgess, C. P., Cannon, M. J., Caney, S. M., Gruffydd-Jones, T. J., and Wotton, P. R. (2003). Feline idiopathic cardiomyopathy: a retrospective study of 106 cats (1994-2001). *J. Feline Med. Surg.* 5, 151–159. doi: 10.1016/s1098-612x(02)00133-x

Genova, F., Longeri, M., Lyons, L. A., Bagnato, A., Gandolfi, B., Aberdein, D., et al. (2018). First genome-wide CNV mapping in FELIS CATUS using next generation sequencing data. *BMC Genom.* 19:895. doi: 10.1186/s12864-018-5297-2

Gomes, A. V., Liang, J., and Potter, J. D. (2005). Mutations in human cardiac troponin I that are associated with restrictive cardiomyopathy affect basal ATPase activity and the calcium sensitivity of force development. *J. Biol. Chem.* 280, 30909–30915. doi: 10.1074/jbc.m500287200

Gomes, A. V., Potter, J. D., and Szczesna-Cordary, D. (2002). The role of troponins in muscle contraction. *IUBMB Life* 54, 323–333. doi: 10.1080/15216540216037

Ho, C. Y. (2011). New paradigms in hypertrophic cardiomyopathy: insights from genetics. *Prog. Pediatr. Cardiol.* 31, 93–98. doi: 10.1016/j.ppedcard.2011.02.005

Li, H., and Durbin, R. (2009). Fast and accurate short read alignment with Burrows-Wheeler transform. *Bioinformatics* 25, 1754–1760. doi: 10.1093/bioinformatics/btp324

Li, H., Handsaker, B., Wysoker, A., Fennell, T., Ruan, J., Homer, N., et al. (2009). The Sequence Alignment/Map format and SAMtools. *Bioinformatics* 25, 2078–2079. doi: 10.1093/bioinformatics/btp352

Longeri, M., Ferrari, P., Knafelz, P., Mezzelani, A., Marabotti, A., Milanesi, L., et al. (2013). Myosin-binding protein C DNA variants in domestic cats (A31P, A74T, R820W) and their association with hypertrophic cardiomyopathy. *J. Vet. Intern. Med.* 27, 275–285. doi: 10.1111/jvim.12031

McNamara, J. W., Schuckman, M., Becker, R. C., and Sadayappan, S. (2020). A novel homozygous premature stop mutation in TNNT2 associates with Feline cardiomyopathy. *Res. Sq.* [Preprint]. doi: 10.21203/rs.2.21647/v1

Meurs, K. M., Norgard, M. M., Ederer, M. M., Hendrix, K. P., and Kittleson, M. D. (2007). A substitution mutation in the myosin binding protein C gene in ragdoll hypertrophic cardiomyopathy. *Genomics* 90, 261–264. doi: 10.1016/j.ygeno.2007.04.007

Meurs, K. M., Sanchez, X., David, R. M., Bowles, N. E., Towbin, J. A., Reiser, P. J., et al. (2005). A cardiac myosin binding protein C mutation in the Maine Coon cat with familial hypertrophic cardiomyopathy. *Hum. Mol. Genet.* 14, 3587–3593. doi: 10.1093/hmg/ddi386

Nishii, K., Morimoto, S., Minakami, R., Miyano, Y., Hashizume, K., Ohta, M., et al. (2008). Targeted disruption of the cardiac troponin T gene causes sarcomere disassembly and defects in heartbeat within the early mouse embryo. *Dev. Biol.* 322, 65–73. doi: 10.1016/j.ydbio.2008.07.007

Ontiveros, E. S., Ueda, Y., Harris, S. P., and Stern, J. A. (2018). Precision medicine validation: identifying the MYBPC3 A31P variant with whole-genome sequencing in two Maine Coon cats with hypertrophic cardiomyopathy. *J. Feline Med. Surg.* 21:1098612x18816460.

Pasquale, F., Syrris, P., Kaski, J. P., Mogensen, J., Mckenna, W. J., and Elliott, P. (2012). Long-term outcomes in hypertrophic cardiomyopathy caused by mutations in the cardiac troponin T gene. *Circ. Cardiovasc. Genet.* 5, 10–17. doi: 10.1161/circgenetics.111.959973

Pua, C. J., Bhalshankar, J., Miao, K., Walsh, R., John, S., Lim, S. Q., et al. (2016). Development of a comprehensive sequencing assay for inherited cardiac condition genes. *J. Cardiovasc. Transl. Res.* 9, 3–11. doi: 10.1007/s12265-016-9673-5

Schipper, T., Van Poucke, M., Sonck, L., Smets, P., Ducatelle, R., Broeckx, B. J. G., et al. (2019). A feline orthologue of the human MYH7 c.5647G>A (p.(Glu1883Lys)) variant causes hypertrophic cardiomyopathy in a Domestic Shorthair cat. *Eur. J. Hum. Genet.* 27, 1724–1730. doi: 10.1038/s41431-019-0431-4

Tardiff, J. C., Factor, S. M., Tompkins, B. D., Hewett, T. E., Palmer, B. M., Moore, R. L., et al. (1998). A truncated cardiac troponin T molecule in transgenic mice suggests multiple cellular mechanisms for familial hypertrophic cardiomyopathy. *J. Clin. Invest.* 101, 2800–2811. doi: 10.1172/jci2389

Thierfelder, L., Watkins, H., Macrae, C., Lamas, R., Mckenna, W., Vosberg, H. P., et al. (1994). Alpha-tropomyosin and cardiac troponin T mutations cause familial hypertrophic cardiomyopathy: a disease of the sarcomere. *Cell* 77, 701–712. doi: 10.1016/0092-8674(94)90054-x

Thomas, W. P., Gaber, C. E., Jacobs, G. J., Kaplan, P. M., Lombard, C. W., Moise, N. S., et al. (1993). Recommendations for standards in transthoracic two-dimensional echocardiography in the dog and cat. Echocardiography Committee of the Specialty of Cardiology, American College of Veterinary Internal Medicine. *J. Vet. Intern. Med.* 7, 247–252. doi: 10.1111/j.1939-1676.1993.tb01015.x

Van Dijk, S. J., Bezold Kooiker, K., Mazzalupo, S., Yang, Y., Kostyukova, A. S., Mustacich, D. J., et al. (2016). The A31P missense mutation in cardiac myosin binding protein C alters protein structure but does not cause haploinsufficiency. *Arch. Biochem. Biophys.* 601, 133–140. doi: 10.1016/j.abb.2016.01.006

Vinogradova, M. V., Stone, D. B., Malanina, G. G., Karatzaferi, C., Cooke, R., Mendelson, R. A., et al. (2005). Ca(2+)-regulated structural changes in troponin. *Proc. Natl. Acad. Sci. U.S.A.* 102, 5038–5043. doi: 10.1073/pnas.0408882102

Viswanathan, S. K., Sanders, H. K., Mcnamara, J. W., Jagadeesan, A., Jahangir, A., Tajik, A. J., et al. (2017). Hypertrophic cardiomyopathy clinical phenotype is independent of gene mutation and mutation dosage. *PLoS One* 12:e0187948. doi: 10.1371/journal.pone.0187948

Wang, K., Li, M., and Hakonarson, H. (2010). ANNOVAR: functional annotation of genetic variants from high-throughput sequencing data. *Nucleic Acids Res.* 38:e164. doi: 10.1093/nar/gkq603

Wang, M., and Marín, A. (2006). Characterization and prediction of alternative splice sites. *Gene* 366, 219–227. doi: 10.1016/j.gene.2005.07.015

Watkins, H., Mckenna, W. J., Thierfelder, L., Suk, H. J., Anan, R., O'donoghue, A., et al. (1995). Mutations in the genes for cardiac troponin T and alpha-tropomyosin in hypertrophic cardiomyopathy. *N. Engl. J. Med.* 332, 1058–1064. doi: 10.1056/nejm199504203321603

Wei, B., and Jin, J. P. (2016). TNNT1, TNNT2, and TNNT3: Isoform genes, regulation, and structure-function relationships. *Gene* 582, 1–13. doi: 10.1016/j.gene.2016.01.006

Wess, G., Schinner, C., Weber, K., Kuchenhoff, H., and Hartmann, K. (2010). Association of A31P and A74T polymorphisms in the myosin binding protein C3 gene and hypertrophic cardiomyopathy in Maine Coon and other breed cats. *J. Vet. Intern. Med.* 24, 527–532. doi: 10.1111/j.1939-1676.2010.0514.x

Conflict of Interest: SS provided consulting and collaborative research studies to the Leducq Foundation, Red Saree Inc., Greater Cincinnati Tamil Sangam, MyoKardia, Merck and Amgen, but such work is unrelated to the content of this manuscript. No other disclosures are reported. RB serves on scientific advisory boards for Janssen and Basking Biosciences and DSMB Committees for Ionis Pharmaceuticals, Akcea Therapeutics and Novartis.

The remaining authors declare that the research was conducted in the absence of any commercial or financial relationships that could be construed as a potential conflict of interest.

frontiers in Physiology

MINI REVIEW
published: 30 November 2020
doi: 10.3389/fphys.2020.611275

Modulation of Autophagy by SARS-CoV-2: A Potential Threat for Cardiovascular System

*Puneet Kaur Randhawa[1], Kaylyn Scanlon[1], Jay Rappaport[2] and Manish K. Gupta[1]**

[1]Division of Metabolic and Cardiovascular Sciences, Burnett School of Biomedical Sciences, College of Medicine, University of Central Florida, Orlando, FL, United States, [2]Division of Comparative Pathology, Tulane National Primate Research Center, Covington, LA, United States

Recently, we have witnessed an unprecedented increase in the number of patients suffering from respiratory tract illness caused by severe acute respiratory syndrome coronavirus 2 (SARS-CoV-2). The COVID-19 virus is a single-stranded positive-sense RNA virus with a genome size of ~29.9 kb. It is believed that the viral spike (S) protein attaches to angiotensin converting enzyme 2 cell surface receptors and, eventually, the virus gains access into the host cell with the help of intracellular/extracellular proteases or by the endosomal pathway. Once, the virus enters the host cell, it can either be degraded *via* autophagy or evade autophagic degradation and replicate using the virus encoded RNA dependent RNA polymerase. The virus is highly contagious and can impair the respiratory system of the host causing dyspnea, cough, fever, and tightness in the chest. This disease is also characterized by an abrupt upsurge in the levels of proinflammatory/inflammatory cytokines and chemotactic factors in a process known as cytokine storm. Certain reports have suggested that COVID-19 infection can aggravate cardiovascular complications, in fact, the individuals with underlying co-morbidities are more prone to the disease. In this review, we shall discuss the pathogenesis, clinical manifestations, potential drug candidates, the interaction between virus and autophagy, and the role of coronavirus in exaggerating cardiovascular complications.

Keywords: COVID-19, comorbidities, autophagy, heart failure, cytokine storm

OPEN ACCESS

Edited by:
Xuejun Wang,
University of South Dakota, United States

Reviewed by:
Qiangrong Liang,
New York Institute of Technology, United States
Paras Kumar Mishra,
University of Nebraska Medical Center, United States

****Correspondence:***
Manish K. Gupta
manish.gupta@ucf.edu

Specialty section:
This article was submitted to Striated Muscle Physiology, a section of the journal Frontiers in Physiology

Received: *28 September 2020*
Accepted: *09 November 2020*
Published: *30 November 2020*

Citation:
Randhawa PK, Scanlon K, Rappaport J and Gupta MK (2020) Modulation of Autophagy by SARS-CoV-2: A Potential Threat for Cardiovascular System. Front. Physiol. 11:611275. doi: 10.3389/fphys.2020.611275

COVID-19 OUTBREAK AS A PANDEMIC

Severe acute respiratory syndrome coronavirus 2 (SARS-CoV2), a beta coronavirus, is posing a serious threat to humanity all over the globe. Genomic characterization of COVID-19 revealed that the virus might have evolved from bats as the original animal host of the virus and, eventually, infected human beings (Lake, 2020). The unprecedented rise in the infection rate among individuals across the various nations compelled the WHO to regard the disease as a pandemic. As of September 29, 2020, 235 countries are reporting 31,664,104 confirmed cases and 972,221 confirmed deaths, and these numbers only continue to rise. Within the United States alone, there have been a total of 6,874, 982 cases and 200,274 deaths reported by the Centers for Disease Control and Prevention, to date.

Coronaviruses are one of the major groups of viruses, which belong to the Coronaviridae family and can be further subdivided into four genera *viz*. alpha-coronavirus, beta-coronavirus, gamma-coronavirus, and delta-coronavirus based on their serological and phylogenetic clusterization (Schoeman and Fielding, 2019). Coronaviruses have zoonotic origin but six viruses with low pathogenic potential (alpha-coronaviruses: HCoV-229E and HCoV-NL63 and beta-coronaviruses: SARS, MERS-CoV, HCoV-HKU1, and HCoV-OC43) have been found to infect human hosts as well (Fung and Liu, 2019; Guo et al., 2020c). Coronavirus virions are spherical or pleomorphic in shape and their diameters range from 80 to 125 nm (Neuman et al., 2006; Fung and Liu, 2019).

GENOMIC STRUCTURE AND KEY VIRAL COMPONENTS

Coronaviruses possess the largest known single-stranded positive-sense RNA genome that ranges from 26 to 32 kb in size (Lu et al., 2020). The genome consists of a 5' cap structure accompanied with a 3' poly-A tail, permitting the virus to act as an mRNA for carrying out the translation of replicase polyproteins (Fung and Liu, 2014). Coronavirus particles comprised four main structural proteins including the spike (S), membrane (M), envelope (E), and nucleocapsid (N; **Figure 1**; Schoeman and Fielding, 2019; Lu et al., 2020). The N protein binds with the viral RNA and packages the genome into virions. A homotrimeric spike (S) protein protrudes from the surface of the viral envelope (E), which plays a critical role in viral assembly, release, and maintenance of the viral pathogenicity (Fung and Liu, 2019). The M protein is a viral membrane protein, which is known to help the virus in assembly and budding process (Siu et al., 2008). The genome has multiple open reading frames (ORFs) for encoding the accessory proteins along with two large polypeptide coding genes known as ORF1a and ORF1b, which encode 16 non-structural proteins (nsps) to form the coronavirus replicase complex (**Figure 1**; Chen et al., 2020c).

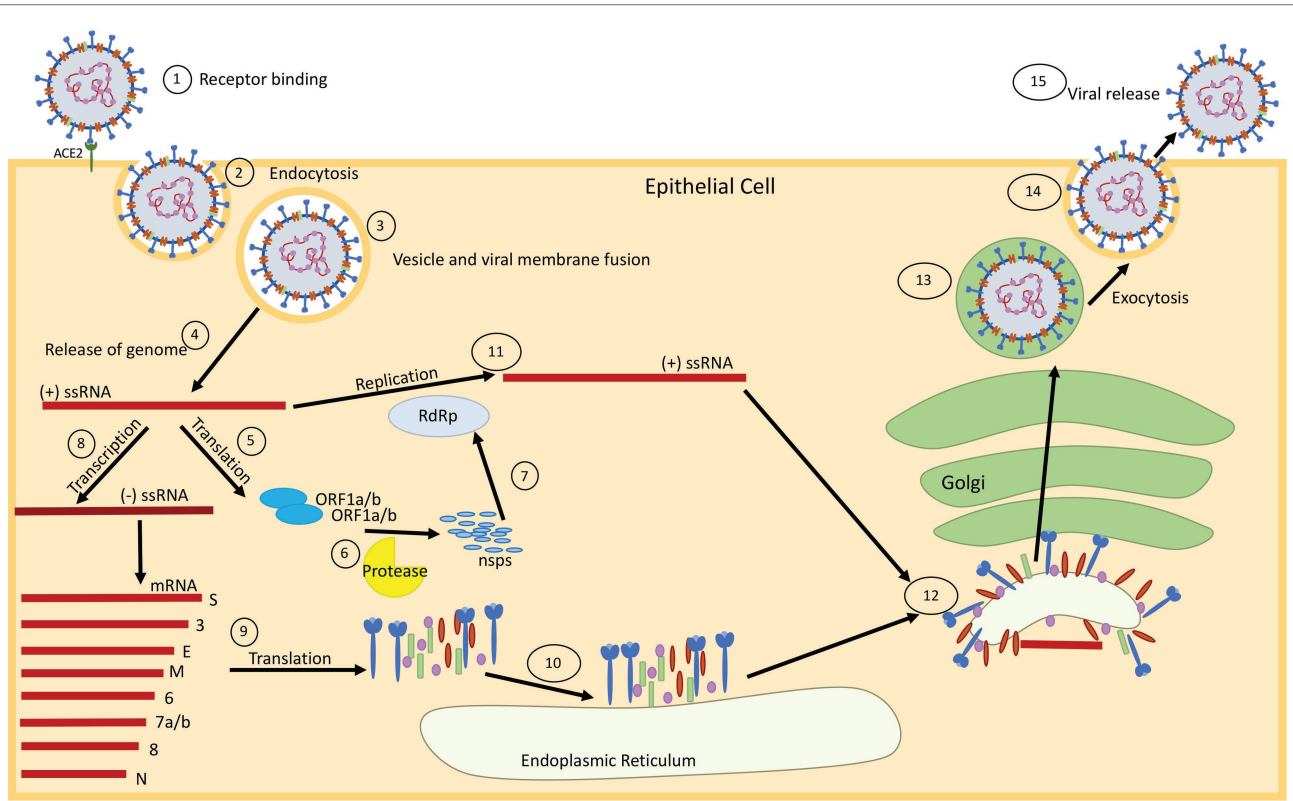

FIGURE 1 | Schematic diagram showing the replication cycle of SARS-CoV-2. (1) SARS-CoV-2 binds to epithelial cells *via* the ACE2 receptor. (2) The virus enters the cell *via* ACE2 mediated endocytosis. (3) The virus membrane and endosome membrane fuse (4) releasing the positive-sense (+) single-stranded RNA (ssRNA) genome into the cytoplasm. (5) The genome is translated to produce ORF1a and ORF1b proteins. (6) These proteins are cleaved into 16 non-structural proteins (nsps) by papain-like protease in a process called proteolysis. (7) The nsps are used to make an RNA-dependent RNA-polymerase (RdRp), which will help with replication of the genome. (8) The original (+) ssRNA genome is also transcribed into negative-sense (–) ssRNA, which is then transcribed into mRNA. (9) The mRNA is translated into the respective structural proteins that (10) gather at the endoplasmic reticulum (ER). (11) The genome is then replicated at full-length, with the help of the RdRp, and assembles with the proteins at the Golgi for packaging. (12) The proteins bud from the ER using the ER membrane (which will become the viral membrane), and migrate to the Golgi apparatus, where the viral package is transported through the Golgi and assembled for (13 and 14) exocytosis. (15) The fully formed virus is then released from the cell surface.

SARS-CoV INDUCES CELLULAR STRESS AND APOPTOSIS

Previous studies have revealed that SARS-CoV has several ORFs including ORF-3a, ORF3b, ORF6, ORF7a, and ORF8 that play critical roles in inducing apoptosis (Law et al., 2005b; Nelson et al., 2005; Yuan et al., 2006; Ye et al., 2008; Shi et al., 2019). ORF3a is exclusively expressed in the ER and Golgi Apparatus and is found to be localized in the nucleolus and the mitochondria. ORF3a is believed to participate in the upregulation of fibrinogen subunits (Aα, Bβ, and γ) and subsequent induction of chromatin condensation, followed by DNA fragmentation in the lung epithelial cells (Law et al., 2005b). ORF3b induces G0/G1 arrest followed by apoptosis after being transfected into the cells. Apparently, ORF6 localizes in the ER and Golgi membrane of infected cells (Chow et al., 2005) and induces apoptosis *via* the caspase-3 dependent pathway and possibly through the phosphorylation of JNK (**Figure 2**; Ye et al., 2008). However, ORF-7a typically localizes in the ER and has the potential to induce apoptosis *via* activating caspases (**Figure 2**; Ye et al., 2008). ORF8b is found to form cellular aggregates and induces cell death through ER stress and robust activation of the NLRP3 inflammasome (Shi et al., 2019). Very recently, the ORF8 gene has been considered as a novel target for identifying COVID-19 disease (Kakhki et al., 2020). Besides this, it has been demonstrated that the E protein of SARS-CoV also elicits an immune response to produce apoptosis of

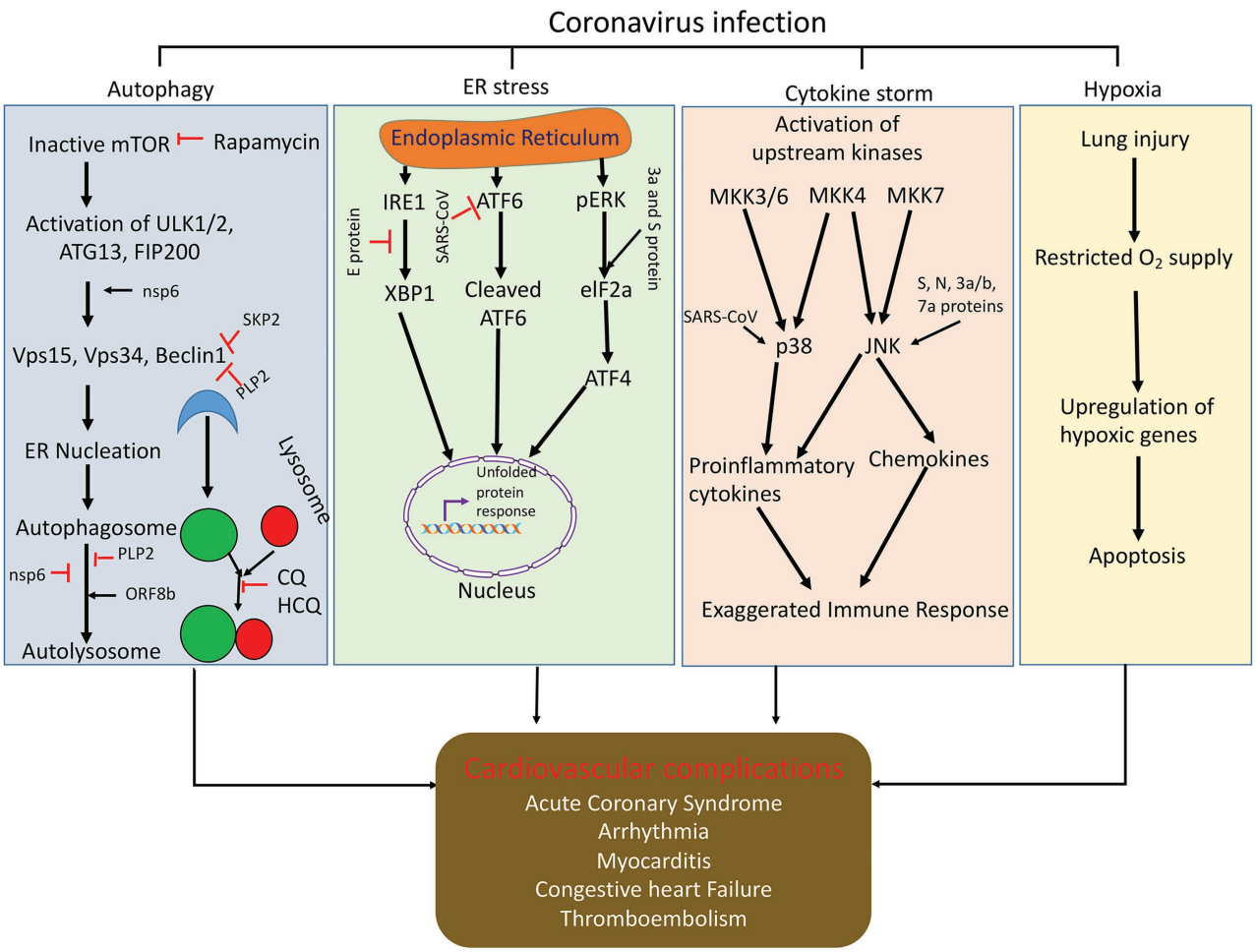

FIGURE 2 | Schematic representation of how coronavirus disrupts signaling pathways (autophagy, ER stress, cytokine storm, and hypoxia) and induces cell death. Autophagy is initiated by the formation of ULK1/2-ATG13-FIP200 complex and then generation of Beclin1 complex and initiation of autophagy vesicle formation. Coronaviral proteins can regulate autophagy through modulating function of autophagy regulatory protein at different stages of autophagy. Viral infection can inhibit ER function and induces ER stress and cell death. Viral protein expresses in ER and upregulates downstream ER stress signaling through modulation the function of ATF6, IRE1 and pERK, and eIF2a. Upstream kinases in the JNK and p38 signaling pathways are activated upon infection with SARS-CoV. This activates the mitogen-activated protein kinase kinases (MKK3/6, MKK4, and MKK7). Mkk3/6 and Mkk4 activate p38. SARS-CoV can also directly activate p38 or the SARS-CoV E protein can activate syntenin, which in tune activates p38. These pathways activate proinflammatory cytokine production. MKK4 and MKK7 can also activate JNK. SARS-CoV s, N, 3a, 3b, and 7a proteins can also directly activate JNK. This pathway activates proinflammatory cytokine production and induction of apoptosis. Also, due to viral infection in the lungs, there is restricted supply of O_2 in the blood, which generate hypoxia and cell death and major organ dysfunction; CQ, chloroquine and HCQ, hydroxychloroquine.

the host cell through T-cell mediated immunity, which can be successfully inhibited by Bcl-xL, an anti-apoptotic protein (Yang et al., 2005). Apart from this, the spike protein of SARS-CoV alone was also observed to induce apoptosis *in vitro* (Chow et al., 2005). The SARS-CoV membrane (M) protein has also been implicated to cause apoptosis *via* disruption of the PDK1-PKB/Akt cell survival signaling pathway (Tsoi et al., 2014). These viruses encode pro-apoptotic or anti-apoptotic proteins such that they can either initiate or delay the progression of apoptosis (Ye et al., 2008). The deferment of apoptosis until the late stages of infection impedes the generation of inflammatory response in the host against the virus and facilitates the dissemination of virus into the whole system (Ye et al., 2008). SARS-CoV protein expression can generate protein aggregates *via* inhibiting the cellular protein quality control thereby increasing endoplasmic reticulum stress (ER stress) such that it causes cell death. Induction of ER stress triggers the activation of inositol-requiring enzyme (IRE1), activating transcription factor ATF6, and protein kinase RNA-like ER kinase (PERK). Activation of these enzymes or proteins either brings about ER homeostasis or apoptosis as an antiviral response. Also, the expression of SARS-CoV proteins can have variant effects on numerous proteins to sequester the host's cell response in order to spread the infection (Fung et al., 2016; **Figure 2**). This gives us a clear indication that targeting the viral machinery, ranging from ORF genes to spike/envelope protein, may aid in hindering the replication of virus and dissemination of infection in the host.

ATTACHMENT AND ENTRY OF COVID-19

Angiotensin converting enzyme 2 (ACE2) is an ectoenzyme expressed in the lungs, heart, kidney, intestine, pancreas, brain, and tongue (Hamming et al., 2004; Guo et al., 2020b), which favors the attachment and entry of the virus into the host cell. In the case of COVID-19 infection, the viral spike (S) protein attaches to the specific cell receptors, for example, ACE2 (found in epithelial cells), which allows the entry of the virus into the cell *via* endocytosis or pore formation (**Figure 1**; Fung and Liu, 2019). After binding the host ACE2 receptor, the enveloped virus can gain access into the host cells with help of intracellular or extracellular proteases (trypsin, thermolysin, and TMPRSS2), which result in pore formation (Matsuyama et al., 2005; Kim et al., 2020). Interestingly, it has also been reported that SARS-CoV-2 can even enter the cell independently of the cell proteases after being preactivated by proprotein convertase furin (Shang et al., 2020) and the entry can be blocked in the presence of a protease inhibitor (Hoffmann et al., 2020). The cleavage of the spike protein *via* a host protease releases the fusion peptide, which subsequently allows entry into the host cell and eventually the replication process in the host commences (Millet and Whittaker, 2015).

CLINICAL SYMPTOMS OF COVID-19

In humans, coronaviruses can cause a number of respiratory diseases ranging from the common cold to SARS (Fung and Liu, 2019; Hui and Zumla, 2019). The majority of COVID-19 cases range from asymptomatic to mild but a subset of cases exhibit severe disease. Comorbid conditions such as hypertention, obesity, cardiovascular, and/or pulmonary disorder are known to increase the risk of infection. In severe cases, the transmission of the virus into an individual typically impairs the respiratory system such that it causes difficulty in breathing, cough, fever, tightness in the chest, and dyspnea (Lake, 2020). A more severe form of the illness can produce acute respiratory distress syndrome (ARDS) and pneumonia-like symptoms (Huang et al., 2020a; Lake, 2020). Also, COVID-19 patients display gastrointestinal symptoms including anorexia, nausea, vomiting, diarrhea, and abdominal pain (Pan et al., 2020; Tian et al., 2020). Some infected patients also show symptoms like anosmia, myalgia, muscle soreness, ocular inflammation, headache, dizziness, and altered mental status (Han et al., 2020a; Heidari et al., 2020; Mao et al., 2020; Sun et al., 2020; Wu et al., 2020). Recent studies suggested that SARS-CoV-2 infection shows COVID-19 like symptoms in macaques, which could be used as a model for development of therapeutics (Blair et al., 2020; Rockx et al., 2020).

CYTOKINE RELEASE SYNDROME

Accumulating evidences have indicated that COVID-19 disease is characterized by an abrupt upsurge in the levels of proinflammatory cytokines, which is known as cytokine storm (Teijaro, 2017; Chen et al., 2020b; Huang et al., 2020a; Ruan et al., 2020a; Zhang et al., 2020). It has been documented that the early infection with SARS CoV-2 is characterized by lymphopenia and is accompanied by the decline in levels of $CD4^+$ and $CD8^+$ T cells. This causes delay in clearance of the virus but later leads to hyper stimulation of macrophages as well as neutrophils (Wang et al., 2020d). Lymphocytes serve as the determinants for maintaining immune homeostasis and innate immune response (Tan et al., 2020). It has been revealed that the ACE2 receptors are expressed in the lymphocytes, residing in the oral mucosal cavity (Xu et al., 2020a). Therefore, it can be postulated that the presence of virus titers in these lymphocytes may induce infection and even cause death of the lymphocytes. This can be one of the possible contributing factors for the acute decline in the number of lymphocytes. Also, the ability of the virus to directly infect the lymphatic organs cannot be undermined. Recently, Tan et al. reported that the percentage of lymphocytes indicate the disease severity and the chances of recovery (Tan et al., 2020). This suggests that the lymphocyte count can be considered as one of the key indicators of disease progression.

Previous *in-vitro* studies involving infection of macrophages with SARS-CoV indicated that the virus induced the expression of chemotactic proteins, but they produced very low levels of interferons, which are considered as decisive elements in activating an immune response against viral infections (Cheung et al., 2005). In corroboration with the above study, SARS-CoV infection in dendritic cells also led to reduced production of interferons but was associated with a modest increase in the formation of proinflammatory cytokines (TNF-α and IL-6,

interleukin-6). However, there was also a remarkable surge in the levels of inflammatory chemokines (macrophage inflammatory protein 1α, regulated on activation normal T cell expressed and secreted, interferon-inducible protein-10, and monocyte chemoattractant protein-1; Law et al., 2005a). This suggests that the viral infection produces a delayed but exaggerated immune response. Studies have also shown that the infection with SARS-CoV can trigger the mitogen-activated protein kinase (MAPK) cascade to induce the release of proinflammatory cytokines through the activation of p38 signaling (**Figure 2**; Fung et al., 2016).

Intruingly, IL-6 plays a crucial role in the modulation of inflammation (Jones and Jenkins, 2018), and it has been demonstrated to monitor the progression of cytokine release syndrome (Zheng et al., 2020). Furthermore, the level of IL-6 in plasma has been correlated with progression of COVID-19 disease. Several therapeutic approaches are now undergoing clinical trials targeting IL-6 to combat COVID-19 infection (Zhang et al., 2020). As the disease progresses, the COVID-19 patients witness a remarkable increase in the levels of cytokines *viz*. IL-2, IL-7, IL-10, granulocyte-colony stimulating factor, interferon-γ inducible protein 10, monocyte chemoattractant protein 1, macrophage inflammatory protein 1-α, tumor necrosis factor-α (Huang et al., 2020a), and IL-6 (Ruan et al., 2020a; Wang et al., 2020d). This uncontrolled production of proinflammatory cytokines increases the vascular permeability causing unrestricted accumulation of fluid and blood cells into the alveoli. This results in dyspnea and respiratory distress (Leiva-Juarez et al., 2018). Ruan et al. also reported that one of the major causes for COVID-19-associated mortality was virus-induced cytokine storm (Ruan et al., 2020a). In fact, Liu et al. reported that the unrestricted cytokine production in the vascular system can produce diffuse microangiopathy with thrombosis, myocarditis, acute coronary syndrome, arrhythmia, and even multi-organ failure (Wang et al., 2020d). Consistent with the human data, in a recent experiment with nonhuman primates, it was also discovered that African green monkeys infected with SARS-Cov-2 show strong cytokine storm signal along with ARDS symptoms (Blair et al., 2020). This suggests that limiting the release of cytokines may restrict the development and progression of inflammation in various organs including the heart.

CARDIOVASCULAR DISORDER IN COVID-19 PATIENTS

It has been reported that the patients with pre-existing cardiovascular disease are at increased risk of developing cardiac dysfunctioning as well as heart failure upon being infected (Driggin et al., 2020; Group et al., 2020). A study from Wuhan, China (where the disease was first identified) reported that out of 44,672 confirmed cases, 10.5% of patients had cardiovascular disorder (CVD) and 6.0% had hypertension. COVID-19 patients with comorbidities also have a higher case-fatality rate as well (Driggin et al., 2020). Moreover, a meta-analysis also revealed that COVID-19 infection may exaggerate myocardial damage in patients with pre-existing cardiovascular diseases (Group et al., 2020). Analysis of autopsy samples from COVID-19 patients suggests that the viral infection may cause cardiomegaly, right ventricular dilation, and generation of scattered myocytes necrosis, which may compromise heart function (Fox et al., 2020). Furthermore, a significant fraction of COVID-19 patients develop arrhythmias, which suggest that COVID-19 patients have compromised heart function (Driggin et al., 2020). Troponin I, a known marker of cardiovascular injury (Collins et al., 2001), was found to be significantly increased in COVID-19 patients, especially with severe disease (Lippi et al., 2020). Also, various authors have reported an upsurge in the level of creatine kinase isoenzyme-MB (CK-MB), myohemoglobin (MYO), lactate dehydrogenase, and N-terminal pro-brain natriuretic peptide after COVID-19 infection (Han et al., 2020b; Wang et al., 2020b; Zeng et al., 2020). In fact, some studies have reported circulatory heart failure in some patients (Ruan et al., 2020b; **Table 1**).

Thus, COVID-19 infection can aggravate cardiovascular complications in patients with cardiovascular perturbations. A study by Hanley et al. suggested that COVID-19 patients

TABLE 1 | Cardiovascular complications caused by SARS-CoV-2 virus.

S. No	Clinical presentation	Total participants (N)	Median age	Markers of injury	References
1	Acute cardiac injury	416	64	• Cardiac Troponin I	Shi et al., 2020
2	Acute cardiac injury	273	58.5	• Creatine kinase isoenzyme-MB (CK-MB) Myohemoglobin (MYO) • Cardiac troponin I • N-terminal pro-brain natriuretic peptide	Han et al., 2020b
3	Coronary heart disease	150	N/A	• N-terminal pro B-type natriuretic peptide • Cardiac troponin-I	Chen et al., 2020a
4	Arrhythmia	138	56	• Lactate dehydrogenase	Wang et al., 2020b
5	Circulatory failure	68	N/A	• Myoglobin, Cardiac troponin	Ruan et al., 2020b
6	Acute cardiac injury	269	60	• Cardiac troponin I	Li et al., 2020
7	Malignant arrhythmia	187	58.5	• Cardiac troponin T • N-terminal pro-brain natriuretic peptide	Guo et al., 2020a
8	Myocarditis and heart failure	1	63	• Myohemoglobin (MYO) • Cardiac troponin I • N-terminal pro-brain natriuretic peptide	Zeng et al., 2020

have signs of active viral infection in the cardiac tissue along with pericarditis and necropsy of endocardial tissue, which may lead to cardiac hypertrophy and functional abnormalities (Hanley et al., 2020). Since ACE2 is implicated in monitoring heart function and hypertension development, the high expression of ACE2 both in heart and lung epithelial tissue can be a cause of increased myocardial injury through increased secretion of ACE2 (Zheng et al., 2020). Though it is known that SARS-CoV-2 can infect epithelial cells, discovering the mechanism of infection causing heart complications is still under investigation.

INTERPLAY BETWEEN AUTOPHAGY AND CORONAVIRUS

The interaction between the virus and the host cell is one of the major predetermining factor influencing autophagy-mediated responses in order to combat viral infection. The implication of autophagy in monitoring the progression of viral infection has been investigated by various scientists (Reggiori et al., 2010; Gassen et al., 2019). Autophagy is a quintessential cellular process that is responsible for degrading the damaged cytosolic proteins, intracellular pathogens, and dysfunctional organelles through a double-membrane organelle referred to as autophagosome (Levine and Kroemer, 2019; Yang and Shen, 2020). The autophagosome, eventually fuses with the lysosome, which results in the formation of the autolysosome, the components of which are then degraded by lysosomal enzymes (Levine and Kroemer, 2019; Yang and Shen, 2020). It is manifested that the cell can modulate the autophagy level to maintain homeostasis and counter infection in the cell. Degradation of virus *via* the autophagy process can provide inbuilt defense against the infection (Cottam et al., 2011). Autophagy can either be non-selective (induced by starvation or other stressor stimuli) or selective, whereby the accumulation of specific adaptor proteins including p62, BCL2 and adenovirus E1B 19-kDa-interacting protein 3 (BNIP3), NIP3-like protein X (NIX), and neighbor of BRCA1 gene1 (NBR1) initiate selective autophagy *via* recognizing ubiquitinated protein organelles or complexes and ultimately form autophagosome for degradation (Chiramel et al., 2013; Nascimbeni et al., 2017). The pattern recognition receptors *viz*. toll like receptors recognize pathogen associated molecular patterns (PAMPs) and trigger autophagy and the synthesis of inflammatory cytokines and interferons to generate an anti-viral response (Choi et al., 2018).

The induction of autophagy is a coordinated maneuver involving active participation class III phosphatidylinositol 3-phosphate (PtdIns 3 P), Unc-51 like autophagy activating kinase (ULK1), and autophagy related (Atg-16L1) protein complex at different stages of autophagosome formation. ULK1 complex comprises ULK1, ATG13, RB1CC1, and ATG101; PtdIns 3 P comprises ATG14, BECN1, PIK3R4, and PIK3C3; and ATG16L1 complex comprises ATG16L1, ATG5, and ATG12 (Bello-Perez et al., 2020). Mammalian target of rapamycin (MTOR) is the prime switch to control the initiation of autophagy as it phosphorylates and inactivates ULK complex under resting conditions (Bello-Perez et al., 2020). However, under starving or stressful conditions MTOR is inactivated and the ULK complex is activated, which in turn activates PtdIns 3 P complex to promote the formation of PtdIns 3 P regions on the periphery of a specific structure. PtdIns 3 P binds to FYVE-domain containing protein Zinc finger FYVE domain-containing protein 1 (ZFYVE1) to give rise to specific structure called omegasome, which is regarded as a matrix for autophagosome biogenesis (Nascimbeni et al., 2017). The non-structural protein (Nsp6) can induce these domains and facilitate recruitment of PtdIns 3 P effector proteins to form an autophagosome (Cottam et al., 2014; Bello-Perez et al., 2020; Carmona-Gutierrez et al., 2020). However, it has been reported that Nsp6 dependent autophagy induction produces significantly small diameter autophagosomes in comparison to the ones induced by starvation or other stressors. This possibly limits the expansion of autophagosomes, restricts their capacity to fuse with numerous lysosomes to generate big autolysosome and in turn increase the number of autophagic vesicles at early stage of autophagy (Cottam et al., 2014). The omegasome gives rise to phagophore (pre-autophagosomal double membrane structure), which upon elongation and sealing forms mature autophagosome. The phagophore elongation depends on PtdIns 3 P-WIPI2 (WD repeat domain phosphoinositide-interacting protein 2) interaction. WIPI2 regulates the assembly of Atg conjugation system and facilitates insertion of cytosolic LC3II into the autophagosomes. The level of autophagy is determined either by the intracellular level of LC3II or the movement of cytosolic LC3I into LC3II positive double membrane vesicles. Conventionally, LC3 was regarded as a marker of autophagosome formation in mammalian cells but any of the Atg8 family member can serve as autophagosome marker (Chiramel et al., 2013; Nascimbeni et al., 2017). Apparently, the viral infection can augment autophagosome abundance either *via* generating immature autophagosomes or mitigating their degradation (Chiramel et al., 2013; Nascimbeni et al., 2017; Carmona-Gutierrez et al., 2020). Thus, owing to the dynamic nature of autophagy, it is necessary to evaluate the autophagic flux to comprehend the actual manner, the viral infection affects autophagy in the cells.

As described earlier, the core autophagic machinery, being an indispensable part of immune system, senses the presence of virus and mounts an anti-viral defense response. However, some viruses subvert the autophagic response and exit the autophagic process without lysis or block autophagic degradation at the final stage (Chiramel et al., 2013; Granato et al., 2014; Jackson, 2014). It has been reported that herpes simplex virus encodes a neurovirulence factor ICP34.5, which can counter regulate the activity of eukaryotic initiation factor-2-α (eIF2α), beclin, and TANK-binding kinase to block autophagosome maturation (Talloczy et al., 2002; Kanai et al., 2012; Choi et al., 2018). In corroboration with the above study, Chaumorcel et al. reported that human cytomegalovirus stimulates autophagy at the early stages of infection (increases autophagic flux) but blocks autophagy at later stages of infection *via* mutual interaction between a virulence factor TRS1 and beclin protein

(Chaumorcel et al., 2012; Choi et al., 2018). Also, Kaposi's sarcoma associated herpes virus encodes a functional homolog of B-cell lymphoma 2 (Bcl-2), which mimics cellular Bcl-2 and exhibits the potential to mitigate autophagy *via* interacting with Beclin protein (Cuconati and White, 2002; Choi et al., 2018). Rubicon operates as a part of a Beclin-1-Vps34 autophagy complex (Kim et al., 2017), and it has been reported that K7 protein of Kaposi's sarcoma associated herpes virus facilitates Beclin-Rubicon interaction and prohibits Vps34 (class III phosphatidylinositol-3 kinase) activity to prevent the fusion of autophagosome with lysosome (Liang et al., 2013). Besides this, Kaposi's sarcoma associated herpes virus Flice-like inhibitory protein (FLIP) homolog can inhibit Atg3 to bind and process LC3 during the course of autophagosome elongation to limit autophagy. Also, during the early course of human immunodeficiency virus infection, there is an increased autophagosome formation and a HIV-1 Gag (structural protein) colocalized with endogenous LC3. However, HIV1 negative factor (Nef; prerequisite for replication of virus) interacts with Beclin to prohibit the maturation of autophagosomes (Kyei et al., 2009).

Apparently, the blockade of autophagy by different types of viruses gives us an indication that viruses can manipulate autophagy for immune evasion. The notion that coronavirus requires the formation of double membrane vesicles to aid replication and transcription of the virus gives us an indication that the virus may usurp the autophagosomal machinery to facilitate the formation of double membrane vesicles (Carmona-Gutierrez et al., 2020). Thus, autophagosomes boost infection by assisting the assembly of viral replicase proteins (Cottam et al., 2011). This is further corroborated by the fact that viral nsp6 protein was found to colocalize with the endogenous LC3, indicating a possible co-relation between autophagy and coronavirus replication (Cottam et al., 2011; Bello-Perez et al., 2020). Also, it has been reported that coronaviruses can hijack the EDEMosome (vesicles for endoplasmic reticulum degradation) formation pathway *via* modulating the degradation of endoplasmic reticulum degradation enhancing alpha-mannosidase like protein 1 (EDEM1) and OS-9 protein such that it causes accumulation of both the endoplasmic reticulum-associated degradation (ERAD) regulatory proteins and trap them into double-membrane vesicles (Reggiori et al., 2010). This indicates that if the virus evades autophagy, it can dynamically manipulate autophagy to promote the replication of the virus inside the host.

Various scientists have revealed that Beclin 1 can serve as a potential target to restrict the multiplication of the virus in the host (Gassen et al., 2019). Beclin 1 fairly regulates the autophagy pathway to restrict the multiplication of the virus inside the host cell (Kang et al., 2011; Gassen et al., 2019). Gassen et al. reported that S-phase kinase-associated protein 2 (SKP2), an E3 ligase, is responsible for carrying out poly-ubiquitination and subsequent proteasomal degradation of Beclin 1 (**Figure 2**). The authors witnessed a significant decline in the levels of Beclin 1 protein and successive fusion of autophagosomes with the lysosomes as MERS-CoV started replicating inside the cell. However, inhibition of SKP2 reduced Beclin 1 ubiquitination, consequent degradation, and also enhanced the autophagic flux. The authors reported that SKP2 inhibition enhanced autophagy and also ameliorated the replication of MERS-CoV (Gassen et al., 2019). Thus, the authors proposed that SKP2-Beclin 1 can serve as a potential target for antiviral drugs to reduce the virus multiplication. SARS-CoV can also sequester the autophagy pathway to inhibit the formation of the autolysosome *via* the nsp6 of SARS-CoV (**Figure 2**). Although nsp6 protein activates autophagy, the autophagy flux becomes dysregulated (as mentioned earlier) to favor viral replication (Fung and Liu, 2019). Another *in vitro* study revealed that the membrane-associated papain-like protease 2 (PLP2) of coronaviruses induces inadequate autophagy and commences replication by increasing the buildup of autophagosomes *via* prevention of the autophagosomal-lysosomal fusion (Chen et al., 2014). On the contrary, Zhao et al. reported that an intact autophagic pathway is not a prerequisite for spreading the viral infection in the host (Zhao et al., 2007).

Based on the ability to modulate the autophagic pathway, various unproven drugs like chloroquine, hydroxychloroquine, azithromycin, or their combinations were administered to the infected patients to combat SARS-CoV-2 infection (Gao et al., 2020). The notion that these drugs could prevent the endocytic pathway, which subsequently prevents the virus replication, gave a compelling indication to incorporate these medications in the drug regimen of the infected masses (Gao et al., 2020). It was found that hydroxychloroquine reduced the mortality rate in critically ill patients suffering from COVID-19 (Meo et al., 2020; Yu et al., 2020), but some studies indicated that these autophagy modulators failed to ameliorate the viral load in the infected individuals (Molina et al., 2020; Singh et al., 2020) and lead to prolongation of QT interval (Chorin et al., 2020; Jankelson et al., 2020). This indicates that further studies need to be envisaged to validate the usage of autophagy modulators in order to deter the progression of infection.

POTENTIAL DRUGS FOR THE TREATMENT OF COVID-19

There are a few anti-viral drugs that are being tested for their potential to attenuate COVID-19 viral infection (Parang et al., 2020; Wang et al., 2020c,d). These include remdesivir, lopinavir, ritonavir, chloroquine, and hydroxychloroquine. Remdesivir is a prodrug (adenosine nucleotide analog) and its metabolite inhibits viral RNA polymerases to elicit anti-viral action. Remdesivir has been recognized as an antiviral drug against a wide range of RNA viruses including bat coronavirus, SARS-CoV, MERS-CoV, and human coronavirus 229E (Sheahan et al., 2017; Parang et al., 2020). Sheahan et al. showed that remdesivir administration significantly abrogated SARS-CoV and MERS-CoV replication in primary human airway epithelial cell cultures (Sheahan et al., 2020). Furthermore, remdesivir administration in mice also decreased lung viral load and improved respiratory function (Sheahan et al., 2020).

Recently, another *in vitro* study has revealed that remdesivir exhibits anti-viral activity against COVID-19 (Wang et al., 2020c). Efficacy of remdesivir in the treatment of COVID-19 infected patients is under clinical trial and has been approved by FDA to use as an emergency drug. Chloroquine has been conventionally used as an anti-malarial and immunomodulator drug but it also exhibits antiviral potential against coronaviruses (Savarino et al., 2006) and provides shielding effect against viral infection by increasing the pH of endosomes to prevent the fusion of virus and endosomes. Apart from this, in the presence of chloroquine, ACE2 receptors are under-glycosylated and have lesser affinity for coronavirus spike protein (Vincent et al., 2005). Mauthe et al. reported that the chloroquine treatment decreases autophagic flux because of the lack of fusion between autophagosome and lysosome (Mauthe et al., 2018). Liu et al. also reported that administration of chloroquine and hydroxyl-choloroquine subverted the transport of COVID-19 virus from early endosomes to endolysosomes which is pre-requisite for the release of viral genome (Wang et al., 2020d). Apart from this, it has also been reported that chloroquine is a potent vasodilator and can mitigate hypoxia-induced pulmonary hypertension possibly resulting in reduced injury in tissues including heart (Wu et al., 2017).

However, recently, there have been reports that the anti-viral drugs more effectively reduce the viral load in comparison to hydroxychloroquine (Geleris et al., 2020; Musarrat et al., 2020; Nutho et al., 2020; Singh et al., 2020). Musarrat et al. reported that nelfinavir possesses the potential to inhibit the spike glycoprotein dependent fusion of the viral envelope and the plasma/endosomal membrane to prevent the spread of infection (Musarrat et al., 2020). Although there have been reports that hydroxychloroquine reduces the mortality rate in critically ill patients suffering from COVID-19 (Yu et al., 2020), a meta-analysis revealed that this drug does not aid in clearing the viral load and significantly increases the fatality among the infected individuals (Singh et al., 2020). There have also been compelling evidences indicating that chloroquine, hydroxychloroquine, and azithromycin prolong the QT-interval, which may lead to precipitation of arrhythmia (Chorin et al., 2020; Jankelson et al., 2020). This suggests that the benefits of using chlorquine do not overweigh the risks upon using this unproven therapy. Recent study by the Group et al. suggested that use of dexamethasone can shorten the hospitalization time of COVID-19 positive patients along with lower rate of mortality at 28 days of post COVID-19 infection. Dexamethasone showed protective effect in patients who are on additional life supportion devices (Group et al., 2020). As drug/vaccine development and evaluation is a lengthy process, more studies need to be envisaged using existing anti-viral or autophagy modulators to elucidate the possible mechanisms involved in the progression of the disease to confront the SARS-CoV-2 pandemic (**Table 2**).

LIMITATIONS

Anti-oxidant/novel compounds, which have the capability to modulate autophagy, can be the potential anti-viral candidates and their role in combating anti-viral infection still needs to be explored. Also, the mechanisms and the virulence factor using which the SARS-CoV-2 escapes autophagy need to be explored exclusively.

TABLE 2 | Potential treatment strategies used against SARS-CoV-2 virus.

Treatment strategy	Category	Mechanism of action	References
Remdesivir	Anti-viral (adenosine nucleotide analog)	Decreases RNA replication by reducing RNA dependent RNA polymerase	Parang et al., 2020; Wang et al., 2020c,d
Lopinavir	Anti-viral (protease inhibitor)	Counter regulates 3CLpro, which cleaves the large replicase polyproteins during viral replication	Lim et al., 2020; Liu et al., 2020
Ritonavir	Anti-viral (protease inhibitor)	Counter regulates 3CLpro, which cleaves the large replicase polyproteins during viral replication	Lim et al., 2020; Ye et al., 2020b
Chloroquine	Antimalarial and Autophagy inhibitor	Abrogates endocytic pathways to prevent replication of the virus	Huang et al., 2020b
Hydroxychloroquine	Antimalarial and Autophagy inhibitor	Abrogates endocytic pathways to prevent replication of the virus	Gautret et al., 2020
Azithromycin	Macrolide antibiotic	Prohibits internalization of the virus into the host cell	Tran et al., 2019
Dexamethasone	Anti-inflammatory and immunosuppressant	Reduces the activation of immune system and subsequent production of inflammatory cytokines	Group et al., 2020; Tomazini et al., 2020
47D11 mAb	Monoclonal antibody	Prohibits angiotensin converting enzyme 2 (ACE2)-virus interaction and inhibit the entry of virus.	Wang et al., 2020a
Tocilizumab	Monoclonal antibody	Reduces the level of inflammatory protein IL-6	Melody et al., 2020; Sciascia et al., 2020; Xu et al., 2020b
Lenzilumab	Monoclonal antibody	Targets colony stimulating factor 2/granulocyte-macrophage colony stimulating factor to reduce the systemic inflammatory response	Melody et al., 2020; Temesgen et al., 2020
Telmisartan	Angiotensin receptor antagonist	Mitigates the binding of circulating Angiotensin II to Angiotensin I receptor to reduce vasoconstriction	Rothlin et al., 2020
Convalescent plasma transfusion	Passive immunotherapy	Neutralizes the virus particles	Ye et al., 2020a

AUTHOR CONTRIBUTIONS

All authors listed have made a substantial, direct and intellectual contribution to the work and approved it for publication.

FUNDING

This work was supported by National Heart, Lung and Blood Institute grants 1R01HL141045-01A1.

REFERENCES

Bello-Perez, M., Sola, I., Novoa, B., Klionsky, D. J., and Falco, A. (2020). Canonical and noncanonical autophagy as potential targets for COVID-19. *Cell* 9:1619. doi: 10.3390/cells9071619

Blair, R. V., Vaccari, M., Doyle-Meyers, L. A., Roy, C. J., Russell-Lodrigue, K., Fahlberg, M., et al. (2020). ARDS and Cytokine Storm in SARS-CoV-2 Infected Caribbean Vervets. bioRxiv [Preprint]. doi: 10.1101/2020.06.18.157933

Carmona-Gutierrez, D., Bauer, M. A., Zimmermann, A., Kainz, K., Hofer, S. J., Kroemer, G., et al. (2020). Digesting the crisis: autophagy and coronaviruses. *Microb. Cell* 7, 119–128. doi: 10.15698/mic2020.05.715

Chaumorcel, M., Lussignol, M., Mouna, L., Cavignac, Y., Fahie, K., Cotte-Laffitte, J., et al. (2012). The human cytomegalovirus protein TRS1 inhibits autophagy via its interaction with Beclin 1. *J. Virol.* 86, 2571–2584. doi: 10.1128/JVI.05746-11

Chen, C., Chen, C., Yan, J. T., Zhou, N., Zhao, J. P., and Wang, D. W. (2020a). Analysis of myocardial injury in patients with COVID-19 and association between concomitant cardiovascular diseases and severity of COVID-19. *Zhonghua Xin Xue Guan Bing Za Zhi* 48, 567–571. doi: 10.3760/cma.j.cn112148-20200225-00123

Chen, Y., Liu, Q., and Guo, D. (2020c). Emerging coronaviruses: genome structure, replication, and pathogenesis. *J. Med. Virol.* 92, 418–423. doi: 10.1002/jmv.25681

Chen, X., Wang, K., Xing, Y., Tu, J., Yang, X., Zhao, Q., et al. (2014). Coronavirus membrane-associated papain-like proteases induce autophagy through interacting with Beclin1 to negatively regulate antiviral innate immunity. *Protein Cell* 5, 912–927. doi: 10.1007/s13238-014-0104-6

Chen, C., Zhang, X. R., Ju, Z. Y., and He, W. F. (2020b). Advances in the research of cytokine storm mechanism induced by corona virus disease 2019 and the corresponding immunotherapies. *Zhonghua Shao Shang Za Zhi* 36:E005. doi: 10.3760/cma.j.cn501120-20200224-00088

Cheung, C. Y., Poon, L. L., Ng, I. H., Luk, W., Sia, S. F., Wu, M. H., et al. (2005). Cytokine responses in severe acute respiratory syndrome coronavirus-infected macrophages in vitro: possible relevance to pathogenesis. *J. Virol.* 79, 7819–7826. doi: 10.1128/JVI.79.12.7819-7826.2005

Chiramel, A. I., Brady, N. R., and Bartenschlager, R. (2013). Divergent roles of autophagy in virus infection. *Cell* 2, 83–104. doi: 10.3390/cells2010083

Choi, Y., Bowman, J. W., and Jung, J. U. (2018). Autophagy during viral infection - a double-edged sword. *Nat. Rev. Microbiol.* 16, 341–354. doi: 10.1038/s41579-018-0003-6

Chorin, E., Wadhwani, L., Magnani, S., Dai, M., Shulman, E., Nadeau-Routhier, C., et al. (2020). QT interval prolongation and torsade de pointes in patients with COVID-19 treated with hydroxychloroquine/azithromycin. *Heart Rhythm* 17, 1425–1433. doi: 10.1016/j.hrthm.2020.05.014

Chow, K. Y., Yeung, Y. S., Hon, C. C., Zeng, F., Law, K. M., and Leung, F. C. (2005). Adenovirus-mediated expression of the C-terminal domain of SARS-CoV spike protein is sufficient to induce apoptosis in vero E6 cells. *FEBS Lett.* 579, 6699–6704. doi: 10.1016/j.febslet.2005.10.065

Collins, J. N., Cole, F. J., Weireter, L. J., Riblet, J. L., and Britt, L. D. (2001). The usefulness of serum troponin levels in evaluating cardiac injury. *Am. Surg.* 67, 821–825.

Cottam, E. M., Maier, H. J., Manifava, M., Vaux, L. C., Chandra-Schoenfelder, P., Gerner, W., et al. (2011). Coronavirus nsp6 proteins generate autophagosomes from the endoplasmic reticulum via an omegasome intermediate. *Autophagy* 7, 1335–1347. doi: 10.4161/auto.7.11.16642

Cottam, E. M., Whelband, M. C., and Wileman, T. (2014). Coronavirus NSP6 restricts autophagosome expansion. *Autophagy* 10, 1426–1441. doi: 10.4161/auto.29309

Cuconati, A., and White, E. (2002). Viral homologs of BCL-2: role of apoptosis in the regulation of virus infection. *Genes Dev.* 16, 2465–2478. doi: 10.1101/gad.1012702

Driggin, E., Madhavan, M. V., Bikdeli, B., Chuich, T., Laracy, J., Bondi-Zoccai, G., et al. (2020). Cardiovascular considerations for patients, health care workers, and health systems during the coronavirus disease 2019 (COVID-19) pandemic. *J. Am. Coll. Cardiol.* 75, 2352–2371. doi: 10.1016/j.jacc.2020.03.031

Fox, S. E., Akmatbekov, A., Harbert, J. L., Li, G., Brown, J. Q., and Vander Heide, R. S. (2020). Pulmonary and Cardiac Pathology in Covid-19: The First Autopsy Series from New Orleans. medRxiv [Preprint]. doi: 10.1101/2020.04.06.20050575

Fung, T. S., Liao, Y., and Liu, D. X. (2016). Regulation of stress responses and translational control by coronavirus. *Viruses* 8:184. doi: 10.3390/v8070184

Fung, T. S., and Liu, D. X. (2014). Coronavirus infection, ER stress, apoptosis and innate immunity. *Front. Microbiol.* 5:296. doi: 10.3389/fmicb.2014.00296

Fung, T. S., and Liu, D. X. (2019). Human coronavirus: host-pathogen interaction. *Annu. Rev. Microbiol.* 73, 529–557. doi: 10.1146/annurev-micro-020518-115759

Gao, J., Tian, Z., and Yang, X. (2020). Breakthrough: Chloroquine phosphate has shown apparent efficacy in treatment of COVID-19 associated pneumonia in clinical studies. *Biosci. Trends* 14, 72–73. doi: 10.5582/bst.2020.01047

Gassen, N. C., Niemeyer, D., Muth, D., Corman, V. M., Martinelli, S., Gassen, A., et al. (2019). SKP2 attenuates autophagy through Beclin1-ubiquitination and its inhibition reduces MERS-coronavirus infection. *Nat. Commun.* 10:5770. doi: 10.1038/s41467-019-13659-4

Gautret, P., Lagier, J. C., Parola, P., Hoang, V. T., Meddeb, L., Mailhe, M., et al. (2020). Hydroxychloroquine and azithromycin as a treatment of COVID-19: results of an open-label non-randomized clinical trial. *Int. J. Antimicrob. Agents* 56:105949. doi: 10.1016/j.ijantimicag.2020.105949

Geleris, J., Sun, Y., Platt, J., Zucker, J., Baldwin, M., Hripcsak, G., et al. (2020). Observational study of Hydroxychloroquine in hospitalized patients with Covid-19. *N. Engl. J. Med.* 382, 2411–2418. doi: 10.1056/NEJMoa2012410

Granato, M., Santarelli, R., Farina, A., Gonnella, R., Lotti, L. V., Faggioni, A., et al. (2014). Epstein-barr virus blocks the autophagic flux and appropriates the autophagic machinery to enhance viral replication. *J. Virol.* 88, 12715–12726. doi: 10.1128/JVI.02199-14

Group, R. C., Horby, P., Lim, W. S., Emberson, J. R., Mafham, M., Bell, J. L., et al. (2020). Dexamethasone in hospitalized patients with Covid-19-preliminary report. *N. Engl. J. Med.* doi: 10.1056/NEJMoa2021436 [Epub ahead of print]

Guo, Y. R., Cao, Q. D., Hong, Z. S., Tan, Y. Y., Chen, S. D., Jin, H. J., et al. (2020c). The origin, transmission and clinical therapies on coronavirus disease 2019 (COVID-19) outbreak - an update on the status. *Mil. Med. Res.* 7:11. doi: 10.1186/s40779-020-00240-0

Guo, T., Fan, Y., Chen, M., Wu, X., Zhang, L., He, T., et al. (2020a). Cardiovascular implications of fatal outcomes of patients with coronavirus disease 2019 (COVID-19). *JAMA Cardiol.* 5, 811–818. doi: 10.1001/jamacardio.2020.1017

Guo, W., Li, M., Dong, Y., Zhou, H., Zhang, Z., Tian, C., et al. (2020b). Diabetes is a risk factor for the progression and prognosis of COVID-19. *Diabetes Metab. Res. Rev.* 36:e3319. doi: 10.1002/dmrr.3319

Hamming, I., Timens, W., Bulthuis, M. L., Lely, A. T., Navis, G., and van Goor, H. (2004). Tissue distribution of ACE2 protein, the functional receptor for SARS coronavirus. A first step in understanding SARS pathogenesis. *J. Pathol.* 203, 631–637. doi: 10.1002/path.1570

Han, C., Duan, C., Zhang, S., Spiegel, B., Shi, H., Wang, W., et al. (2020a). Digestive symptoms in COVID-19 patients with mild disease severity: clinical presentation, stool viral RNA testing, and outcomes. *Am. J. Gastroenterol.* 115, 916–923. doi: 10.14309/ajg.0000000000000664

Han, H., Xie, L., Liu, R., Yang, J., Liu, F., Wu, K., et al. (2020b). Analysis of heart injury laboratory parameters in 273 COVID-19 patients in one hospital in Wuhan, China. *J. Med. Virol.* 92, 819–823. doi: 10.1002/jmv.25809

Hanley, B., Naresh, K. N., Roufosse, C., Nicholson, A. G., Weir, J., Cooke, G. S., et al. (2020). Histopathological findings and viral tropism in UK patients with severe fatal COVID-19: a post-mortem study. *Lancet Microbe.* 1, e245–e253. doi: 10.1016/S2666-5247(20)30115-4

Heidari, F., Karimi, E., Firouzifar, M., Khamushian, P., Ansari, R., Mohammadi Ardehali, M., et al. (2020). Anosmia as a prominent symptom of COVID-19 infection. *Rhinology* 58, 302–303. doi: 10.4193/Rhin20.140

Hoffmann, M., Kleine-Weber, H., Schroeder, S., Kruger, N., Herrler, T., Erichsen, S., et al. (2020). SARS-CoV-2 cell entry depends on ACE2 and TMPRSS2 and is blocked by a clinically proven protease inhibitor. *Cell* 181, 271–280.e8. doi: 10.1016/j.cell.2020.02.052

Huang, M., Tang, T., Pang, P., Li, M., Ma, R., Lu, J., et al. (2020b). Treating COVID-19 with Chloroquine. *J. Mol. Cell Biol.* 12, 322–325. doi: 10.1093/jmcb/mjaa014

Huang, C., Wang, Y., Li, X., Ren, L., Zhao, J., Hu, Y., et al. (2020a). Clinical features of patients infected with 2019 novel coronavirus in Wuhan, China. *Lancet* 395, 497–506. doi: 10.1016/S0140-6736(20)30183-5

Hui, D. S. C., and Zumla, A. (2019). Severe acute respiratory syndrome: historical, epidemiologic, and clinical features. *Infect. Dis. Clin. N. Am.* 33, 869–889. doi: 10.1016/j.idc.2019.07.001

Jackson, W. T. (2014). Dangerous membranes: viruses that subvert Autophagosomes. *EBioMedicine* 1, 97–98. doi: 10.1016/j.ebiom.2014.11.015

Jankelson, L., Karam, G., Becker, M. L., Chinitz, L. A., and Tsai, M. C. (2020). QT prolongation, torsades de pointes, and sudden death with short courses of chloroquine or hydroxychloroquine as used in COVID-19: A systematic review. *Heart Rhythm* 17, 1472–1479. doi: 10.1016/j.hrthm.2020.05.008

Jones, S. A., and Jenkins, B. J. (2018). Recent insights into targeting the IL-6 cytokine family in inflammatory diseases and cancer. *Nat. Rev. Immunol.* 18, 773–789. doi: 10.1038/s41577-018-0066-7

Kakhki, R. K., Kakhki, M. K., and Neshani, A. (2020). COVID-19 target: A specific target for novel coronavirus detection. *Gene Rep.* 20:100740. doi: 10.1016/j.genrep.2020.100740

Kanai, R., Zaupa, C., Sgubin, D., Antoszczyk, S. J., Martuza, R. L., Wakimoto, H., et al. (2012). Effect of gamma34.5 deletions on oncolytic herpes simplex virus activity in brain tumors. *J. Virol.* 86, 4420–4431. doi: 10.1128/JVI.00017-12

Kang, R., Zeh, H. J., Lotze, M. T., and Tang, D. (2011). The Beclin 1 network regulates autophagy and apoptosis. *Cell Death Differ.* 18, 571–580. doi: 10.1038/cdd.2010.191

Kim, J. M., Chung, Y. S., Jo, H. J., Lee, N. J., Kim, M. S., Woo, S. H., et al. (2020). Identification of coronavirus isolated from a patient in Korea with COVID-19. *Osong. Public Health Res. Perspect.* 11, 3–7. doi: 10.24171/j.phrp.2020.11.1.02

Kim, J. H., Kim, T. H., Lee, H. C., Nikapitiya, C., Uddin, M. B., Park, M. E., et al. (2017). Rubicon modulates antiviral type I interferon (IFN) signaling by targeting IFN regulatory factor 3 dimerization. *J. Virol.* 91, e00248–e00317. doi: 10.1128/JVI.00248-17

Kyei, G. B., Dinkins, C., Davis, A. S., Roberts, E., Singh, S. B., Dong, C., et al. (2009). Autophagy pathway intersects with HIV-1 biosynthesis and regulates viral yields in macrophages. *J. Cell Biol.* 186, 255–268. doi: 10.1083/jcb.200903070

Lake, M. A. (2020). What we know so far: COVID-19 current clinical knowledge and research. *Clin. Med.* 20, 124–127. doi: 10.7861/clinmed.2019-coron

Law, H. K., Cheung, C. Y., Ng, H. Y., Sia, S. F., Chan, Y. O., Luk, W., et al. (2005a). Chemokine up-regulation in SARS-coronavirus-infected, monocyte-derived human dendritic cells. *Blood* 106, 2366–2374. doi: 10.1182/blood-2004-10-4166

Law, P. T. W., Wong, C. H., Au, T. C. C., Chuck, C. P., Kong, S. K., Chan, P. K. S., et al. (2005b). The 3a protein of severe acute respiratory syndrome-associated coronavirus induces apoptosis in Vero E6 cells. *J. Gen. Virol.* 86, 1921–1930. doi: 10.1099/vir.0.80813-0

Leiva-Juarez, M. M., Kolls, J. K., and Evans, S. E. (2018). Lung epithelial cells: therapeutically inducible effectors of antimicrobial defense. *Mucosal Immunol.* 11, 21–34. doi: 10.1038/mi.2017.71

Levine, B., and Kroemer, G. (2019). Biological functions of autophagy genes: A disease perspective. *Cell* 176, 11–42. doi: 10.1016/j.cell.2018.09.048

Li, X., Xu, S., Yu, M., Wang, K., Tao, Y., Zhou, Y., et al. (2020). Risk factors for severity and mortality in adult COVID-19 inpatients in Wuhan. *J. Allergy Clin. Immunol.* 146, 110–118. doi: 10.1016/j.jaci.2020.04.006

Liang, Q., Chang, B., Brulois, K. F., Castro, K., Min, C. K., Rodgers, M. A., et al. (2013). Kaposi's sarcoma-associated herpesvirus K7 modulates Rubicon-mediated inhibition of autophagosome maturation. *J. Virol.* 87, 12499–12503. doi: 10.1128/JVI.01898-13

Lim, J., Jeon, S., Shin, H. Y., Kim, M. J., Seong, Y. M., Lee, W. J., et al. (2020). Case of the index patient who caused tertiary transmission of COVID-19 infection in Korea: the application of Lopinavir/ritonavir for the treatment of COVID-19 infected pneumonia monitored by quantitative RT-PCR. *J. Korean Med. Sci.* 35:e79. doi: 10.3346/jkms.2020.35.e79

Lippi, G., Lavie, C. J., and Sanchis-Gomar, F. (2020). Cardiac troponin I in patients with coronavirus disease 2019 (COVID-19): evidence from a meta-analysis. *Prog. Cardiovasc. Dis.* 63, 390–391. doi: 10.1016/j.pcad.2020.03.001

Liu, F., Xu, A., Zhang, Y., Xuan, W., Yan, T., Pan, K., et al. (2020). Patients of COVID-19 may benefit from sustained Lopinavir-combined regimen and the increase of eosinophil may predict the outcome of COVID-19 progression. *Int. J. Infect. Dis.* 95, 183–191. doi: 10.1016/j.ijid.2020.03.013

Lu, R., Zhao, X., Li, J., Niu, P., Yang, B., Wu, H., et al. (2020). Genomic characterisation and epidemiology of 2019 novel coronavirus: implications for virus origins and receptor binding. *Lancet* 395, 565–574. doi: 10.1016/S0140-6736(20)30251-8

Mao, L., Jin, H., Wang, M., Hu, Y., Chen, S., He, Q., et al. (2020). Neurologic manifestations of hospitalized patients with coronavirus disease 2019 in Wuhan, China. *JAMA Neurol.* 77, 683–690. doi: 10.1001/jamaneurol.2020.1127

Matsuyama, S., Ujike, M., Morikawa, S., Tashiro, M., and Taguchi, F. (2005). Protease-mediated enhancement of severe acute respiratory syndrome coronavirus infection. *Proc. Natl. Acad. Sci. U. S. A.* 102, 12543–12547. doi: 10.1073/pnas.0503203102

Mauthe, M., Orhon, I., Rocchi, C., Zhou, X., Luhr, M., Hijlkema, K. J., et al. (2018). Chloroquine inhibits autophagic flux by decreasing autophagosome-lysosome fusion. *Autophagy* 14, 1435–1455. doi: 10.1080/15548627.2018.1474314

Melody, M., Nelson, J., Hastings, J., Propst, J., Smerina, M., Mendez, J., et al. (2020). Case report: use of lenzilumab and tocilizumab for the treatment of coronavirus disease 2019. *Immunotherapy* 12, 1121–1126. doi: 10.2217/imt-2020-0136

Meo, S. A., Klonoff, D. C., and Akram, J. (2020). Efficacy of Chloroquine and hydroxychloroquine in the treatment of COVID-19. *Eur. Rev. Med. Pharmacol. Sci.* 24, 4539–4547. doi: 10.26355/eurrev_202004_21038

Millet, J. K., and Whittaker, G. R. (2015). Host cell proteases: critical determinants of coronavirus tropism and pathogenesis. *Virus Res.* 202, 120–134. doi: 10.1016/j.virusres.2014.11.021

Molina, J. M., Delaugerre, C., Le Goff, J., Mela-Lima, B., Ponscarme, D., Goldwirt, L., et al. (2020). No evidence of rapid antiviral clearance or clinical benefit with the combination of hydroxychloroquine and azithromycin in patients with severe COVID-19 infection. *Med. Mal. Infect.* 50:384. doi: 10.1016/j.medmal.2020.03.006

Musarrat, F., Chouljenko, V., Dahal, A., Nabi, R., Chouljenko, T., Jois, S. D., et al. (2020). The anti-HIV drug nelfinavir mesylate (Viracept) is a potent inhibitor of cell fusion caused by the SARSCoV-2 spike (S) glycoprotein warranting further evaluation as an antiviral against COVID-19 infections. *J. Med. Virol.* doi: 10.1002/jmv.25985 [Epub ahead of print]

Nascimbeni, A. C., Codogno, P., and Morel, E. (2017). Local detection of PtdIns3P at autophagosome biogenesis membrane platforms. *Autophagy* 13, 1602–1612. doi: 10.1080/15548627.2017.1341465

Nelson, C. A., Pekosz, A., Lee, C. A., Diamond, M. S., and Fremont, D. H. (2005). Structure and intracellular targeting of the SARS-coronavirus Orf7a accessory protein. *Structure* 13, 75–85. doi: 10.1016/j.str.2004.10.010

Neuman, B. W., Adair, B. D., Yoshioka, C., Quispe, J. D., Orca, G., Kuhn, P., et al. (2006). Supramolecular architecture of severe acute respiratory syndrome coronavirus revealed by electron cryomicroscopy. *J. Virol.* 80, 7918–7928. doi: 10.1128/JVI.00645-06

Nutho, B., Mahalapbutr, P., Hengphasatporn, K., Pattaranggoon, N. C., Simanon, N., Shigeta, Y., et al. (2020). Why are Lopinavir and ritonavir effective against the newly emerged coronavirus 2019? Atomistic insights into the inhibitory mechanisms. *Biochemistry* 59, 1769–1779. doi: 10.1021/acs.biochem.0c00160

Pan, L., Mu, M., Yang, P., Sun, Y., Wang, R., Yan, J., et al. (2020). Clinical characteristics of COVID-19 patients with digestive symptoms in Hubei, China: A descriptive, cross-sectional, multicenter study. *Am. J. Gastroenterol.* 115, 766–773. doi: 10.14309/ajg.0000000000000620

Parang, K., El-Sayed, N. S., Kazeminy, A. J., and Tiwari, R. K. (2020). Comparative antiviral activity of Remdesivir and anti-HIV nucleoside analogs against human coronavirus 229E (HCoV-229E). *Molecules* 25:2343. doi: 10.3390/molecules25102343

Reggiori, F., Monastyrska, I., Verheije, M. H., Cali, T., Ulasli, M., Bianchi, S., et al. (2010). Coronaviruses hijack the LC3-I-positive EDEMosomes, ER-derived vesicles exporting short-lived ERAD regulators, for replication. *Cell Host Microbe* 7, 500–508. doi: 10.1016/j.chom.2010.05.013

Rockx, B., Kuiken, T., Herfst, S., Bestebroer, T., Lamers, M. M., Oude Munnink, B. B., et al. (2020). Comparative pathogenesis of COVID-19, MERS, and SARS in a nonhuman primate model. *Science* 368, 1012–1015. doi: 10.1126/science.abb7314

Rothlin, R. P., Vetulli, H. M., Duarte, M., and Pelorosso, F. G. (2020). Telmisartan as tentative angiotensin receptor blocker therapeutic for COVID-19. *Drug Dev. Res.* 81, 768–770. doi: 10.1002/ddr.21679

Ruan, Q., Yang, K., Wang, W., Jiang, L., and Song, J. (2020a). Clinical predictors of mortality due to COVID-19 based on an analysis of data of 150 patients from Wuhan, China. *Intensive Care Med.* 46, 846–848. doi: 10.1007/s00134-020-05991-x

Ruan, Q., Yang, K., Wang, W., Jiang, L., and Song, J. (2020b). Correction to: clinical predictors of mortality due to COVID-19 based on an analysis of data of 150 patients from Wuhan, China. *Intensive Care Med.* 46, 1294–1297. doi: 10.1007/s00134-020-06028-z

Savarino, A., Di Trani, L., Donatelli, I., Cauda, R., and Cassone, A. (2006). New insights into the antiviral effects of chloroquine. *Lancet Infect. Dis.* 6, 67–69. doi: 10.1016/S1473-3099(06)70361-9

Schoeman, D., and Fielding, B. C. (2019). Coronavirus envelope protein: current knowledge. *Virol. J.* 16:69. doi: 10.1186/s12985-019-1182-0

Sciascia, S., Apra, F., Baffa, A., Baldovino, S., Boaro, D., Boero, R., et al. (2020). Pilot prospective open, single-arm multicentre study on off-label use of tocilizumab in patients with severe COVID-19. *Clin. Exp. Rheumatol.* 38, 529–532.

Shang, J., Ye, G., Shi, K., Wan, Y., Luo, C., Aihara, H., et al. (2020). Structural basis of receptor recognition by SARS-CoV-2. *Nature* 581, 221–224. doi: 10.1038/s41586-020-2179-y

Sheahan, T. P., Sims, A. C., Graham, R. L., Menachery, V. D., Gralinski, L. E., Case, J. B., et al. (2017). Broad-spectrum antiviral GS-5734 inhibits both epidemic and zoonotic coronaviruses. *Sci. Transl. Med.* 9:eaal3653. doi: 10.1126/scitranslmed.aal3653

Sheahan, T. P., Sims, A. C., Leist, S. R., Schafer, A., Won, J., Brown, A. J., et al. (2020). Comparative therapeutic efficacy of remdesivir and combination lopinavir, ritonavir, and interferon beta against MERS-CoV. *Nat. Commun.* 11:222. doi: 10.1038/s41467-019-13940-6

Shi, C. S., Nabar, N. R., Huang, N. N., and Kehrl, J. H. (2019). SARS-coronavirus open Reading frame-8b triggers intracellular stress pathways and activates NLRP3 inflammasomes. *Cell Death Dis.* 5:101. doi: 10.1038/s41420-019-0181-7

Shi, S., Qin, M., Shen, B., Cai, Y., Liu, T., Yang, F., et al. (2020). Association of Cardiac Injury with Mortality in hospitalized patients with COVID-19 in Wuhan, China. *JAMA Cardiol.* 5, 802–810. doi: 10.1001/jamacardio.2020.0950

Singh, A. K., Singh, A., Singh, R., and Misra, A. (2020). Hydroxychloroquine in patients with COVID-19: A systematic review and meta-analysis. *Diabetes Metab. Syndr.* 14, 589–596. doi: 10.1016/j.dsx.2020.05.017

Siu, Y. L., Teoh, K. T., Lo, J., Chan, C. M., Kien, F., Escriou, N., et al. (2008). The M, E, and N structural proteins of the severe acute respiratory syndrome coronavirus are required for efficient assembly, trafficking, and release of virus-like particles. *J. Virol.* 82, 11318–11330. doi: 10.1128/JVI.01052-08

Sun, P., Qie, S., Liu, Z., Ren, J., Li, K., and Xi, J. (2020). Clinical characteristics of hospitalized patients with SARS-CoV-2 infection: A single arm meta-analysis. *J. Med. Virol.* 92, 612–617. doi: 10.1002/jmv.25735

Talloczy, Z., Jiang, W., Virgin, H. W. T., Leib, D. A., Scheuner, D., Kaufman, R. J., et al. (2002). Regulation of starvation- and virus-induced autophagy by the eIF2alpha kinase signaling pathway. *Proc. Natl. Acad. Sci. U. S. A.* 99, 190–195. doi: 10.1073/pnas.012485299

Tan, L., Wang, Q., Zhang, D., Ding, J., Huang, Q., Tang, Y. Q., et al. (2020). Correction: Lymphopenia predicts disease severity of COVID-19: a descriptive and predictive study. *Signal Transduct. Target. Ther.* 5:61. doi: 10.1038/s41392-020-0159-1

Teijaro, J. R. (2017). Cytokine storms in infectious diseases. *Semin. Immunopathol.* 39, 501–503. doi: 10.1007/s00281-017-0640-2

Temesgen, Z., Assi, M., Vergidis, P., Rizza, S. A., Bauer, P. R., Pickering, B. W., et al. (2020). First Clinical Use of Lenzilumab to Neutralize GM-CSF in Patients with Severe COVID-19 Pneumonia. medRxiv [Preprint]. doi: 10.1101/2020.06.08.20125369

Tian, Y., Rong, L., Nian, W., and He, Y. (2020). Review article: gastrointestinal features in COVID-19 and the possibility of faecal transmission. *Aliment. Pharmacol. Ther.* 51, 843–851. doi: 10.1111/apt.15731

Tomazini, B. M., Maia, I. S., Cavalcanti, A. B., Berwanger, O., Rosa, R. G., Veiga, V. C., et al. (2020). Effect of dexamethasone on days alive and ventilator-free in patients with moderate or severe acute respiratory distress syndrome and COVID-19: the CoDEX randomized clinical trial. *JAMA* 324, 1307–1316. doi: 10.1001/jama.2020.17021

Tran, D. H., Sugamata, R., Hirose, T., Suzuki, S., Noguchi, Y., Sugawara, A., et al. (2019). Azithromycin, a 15-membered macrolide antibiotic, inhibits influenza A(H1N1)pdm09 virus infection by interfering with virus internalization process. *J. Antibiot.* 72, 759–768. doi: 10.1038/s41429-019-0204-x

Tsoi, H., Li, L., Chen, Z. S., Lau, K. F., Tsui, S. K., and Chan, H. Y. (2014). The SARS-coronavirus membrane protein induces apoptosis via interfering with PDK1-PKB/Akt signalling. *Biochem. J.* 464, 439–447. doi: 10.1042/BJ20131461

Vincent, M. J., Bergeron, E., Benjannet, S., Erickson, B. R., Rollin, P. E., Ksiazek, T. G., et al. (2005). Chloroquine is a potent inhibitor of SARS coronavirus infection and spread. *Virol. J.* 2:69. doi: 10.1186/1743-422X-2-69

Wang, M., Cao, R., Zhang, L., Yang, X., Liu, J., Xu, M., et al. (2020c). Remdesivir and chloroquine effectively inhibit the recently emerged novel coronavirus (2019-nCoV) in vitro. *Cell Res.* 30, 269–271. doi: 10.1038/s41422-020-0282-0

Wang, D., Hu, B., Hu, C., Zhu, F., Liu, X., Zhang, J., et al. (2020b). Clinical characteristics of 138 hospitalized patients with 2019 novel coronavirus-infected pneumonia in Wuhan, China. *JAMA* 323, 1061–1069. doi: 10.1001/jama.2020.1585

Wang, C., Li, W., Drabek, D., Okba, N. M. A., van Haperen, R., Osterhaus, A., et al. (2020a). A human monoclonal antibody blocking SARS-CoV-2 infection. *Nat. Commun.* 11:2251. doi: 10.1038/s41467-020-16256-y

Wang, Y., Zhang, D., Du, G., Du, R., Zhao, J., Jin, Y., et al. (2020d). Remdesivir in adults with severe COVID-19: a randomised, double-blind, placebo-controlled, multicentre trial. *Lancet* 395, 1569–1578. doi: 10.1016/S0140-6736(20)31022-9

Wu, P., Duan, F., Luo, C., Liu, Q., Qu, X., Liang, L., et al. (2020). Characteristics of ocular findings of patients with coronavirus disease 2019 (COVID-19) in Hubei Province, China. *JAMA Ophthalmol.* 138, 575–578. doi: 10.1001/jamaophthalmol.2020.1291

Wu, K., Zhang, Q., Wu, X., Lu, W., Tang, H., Liang, Z., et al. (2017). Chloroquine is a potent pulmonary vasodilator that attenuates hypoxia-induced pulmonary hypertension. *Br. J. Pharmacol.* 174, 4155–4172. doi: 10.1111/bph.13990

Xu, X., Han, M., Li, T., Sun, W., Wang, D., Fu, B., et al. (2020b). Effective treatment of severe COVID-19 patients with tocilizumab. *Proc. Natl. Acad. Sci. U. S. A.* 117, 10970–10975. doi: 10.1073/pnas.2005615117

Xu, H., Zhong, L., Deng, J., Peng, J., Dan, H., Zeng, X., et al. (2020a). High expression of ACE2 receptor of 2019-nCoV on the epithelial cells of oral mucosa. *Int. J. Oral Sci.* 12:8. doi: 10.1038/s41368-020-0074-x

Yang, N., and Shen, H. M. (2020). Targeting the Endocytic pathway and autophagy process as a novel therapeutic strategy in COVID-19. *Int. J. Biol. Sci.* 16, 1724–1731. doi: 10.7150/ijbs.45498

Yang, Y., Xiong, Z., Zhang, S., Yan, Y., Nguyen, J., Ng, B., et al. (2005). Bcl-xL inhibits T-cell apoptosis induced by expression of SARS coronavirus E protein in the absence of growth factors. *Biochem. J.* 392, 135–143. doi: 10.1042/BJ20050698

Ye, M., Fu, D., Ren, Y., Wang, F., Wang, D., Zhang, F., et al. (2020a). Treatment with convalescent plasma for COVID-19 patients in Wuhan, China. *J. Med. Virol.* doi: 10.1002/jmv.25882 [Epub ahead of print]

Ye, X. T., Luo, Y. L., Xia, S. C., Sun, Q. F., Ding, J. G., Zhou, Y., et al. (2020b). Clinical efficacy of lopinavir/ritonavir in the treatment of coronavirus disease 2019. *Eur. Rev. Med. Pharmacol. Sci.* 24, 3390–3396. doi: 10.26355/eurrev_202003_20706

Ye, Z., Wong, C. K., Li, P., and Xie, Y. (2008). A SARS-CoV protein, ORF-6, induces caspase-3 mediated, ER stress and JNK-dependent apoptosis. *Biochim. Biophys. Acta* 1780, 1383–1387. doi: 10.1016/j.bbagen.2008.07.009

Yu, B., Li, C., Chen, P., Zhou, N., Wang, L., Li, J., et al. (2020). Low dose of hydroxychloroquine reduces fatality of critically ill patients with COVID-19. *Sci. China Life Sci.* 63, 1515–1521. doi: 10.1007/s11427-020-1732-2

Yuan, X., Shan, Y., Yao, Z., Li, J., Zhao, Z., Chen, J., et al. (2006). Mitochondrial location of severe acute respiratory syndrome coronavirus 3b protein. *Mol. Cell* 21, 186–191.

Zeng, J. H., Liu, Y. X., Yuan, J., Wang, F. X., Wu, W. B., Li, J. X., et al. (2020). First case of COVID-19 complicated with fulminant myocarditis: a case report and insights. *Infection* 48, 773–777. doi: 10.1007/s15010-020-01424-5

Zhang, C., Wu, Z., Li, J. W., Zhao, H., and Wang, G. Q. (2020). The cytokine release syndrome (CRS) of severe COVID-19 and Interleukin-6 receptor (IL-6R) antagonist Tocilizumab may be the key to reduce the mortality. *Int. J. Antimicrob. Agents* 55:105954. doi: 10.1016/j.ijantimicag.2020.105954

Zhao, Z., Thackray, L. B., Miller, B. C., Lynn, T. M., Becker, M. M., Ward, E., et al. (2007). Coronavirus replication does not require the autophagy gene ATG5. *Autophagy* 3, 581–585. doi: 10.4161/auto.4782

Zheng, Y. Y., Ma, Y. T., Zhang, J. Y., and Xie, X. (2020). COVID-19 and the cardiovascular system. *Nat. Rev. Cardiol.* 17, 259–260. doi: 10.1038/s41569-020-0360-5

Conflict of Interest: The authors declare that the research was conducted in the absence of any commercial or financial relationships that could be construed as a potential conflict of interest.

frontiers in Physiology

ORIGINAL RESEARCH
published: 10 December 2020
doi: 10.3389/fphys.2020.604069

Mitochondrial Fission and Mitophagy Coordinately Restrict High Glucose Toxicity in Cardiomyocytes

*Satoru Kobayashi[1], Fengyi Zhao[2], Ziying Zhang[3], Tamayo Kobayashi[1], Yuan Huang[1], Bingyin Shi[2], Weihua Wu[3] and Qiangrong Liang[1]**

[1] Department of Biomedical Sciences, New York Institute of Technology, College of Osteopathic Medicine, Old Westbury, NY, United States, [2] Department of Endocrinology, The First affiliated Hospital of Xi'an Jiaotong University, Xi'an, China, [3] Department of Endocrinology, The First Affiliated Hospital of Harbin Medical University, Harbin, China

Hyperglycemia-induced mitochondrial dysfunction plays a key role in the pathogenesis of diabetic cardiomyopathy. Injured mitochondrial segments are separated by mitochondrial fission and eliminated by autophagic sequestration and subsequent degradation in the lysosome, a process termed mitophagy. However, it remains poorly understood how high glucose affects the activities of, and the relationship between, mitochondrial fission and mitophagy in cardiomyocytes. In this study, we determined the functional roles of mitochondrial fission and mitophagy in hyperglycemia-induced cardiomyocyte injury. High glucose (30 mM, HG) reduced mitochondrial connectivity and particle size and increased mitochondrial number in neonatal rat ventricular cardiomyocytes, suggesting an enhanced mitochondrial fragmentation. SiRNA knockdown of the pro-fission factor dynamin-related protein 1 (DRP1) restored mitochondrial size but did not affect HG toxicity, and Mdivi-1, a DRP1 inhibitor, even increased HG-induced cardiomyocyte injury, as shown by superoxide production, mitochondrial membrane potential and cell death. However, DRP1 overexpression triggered mitochondrial fragmentation and mitigated HG-induced cardiomyocyte injury, suggesting that the increased mitochondrial fission is beneficial, rather than detrimental, to cardiomyocytes cultured under HG conditions. This is in contrast to the prevailing hypothesis that mitochondrial fragmentation mediates or contributes to HG cardiotoxicity. Meanwhile, HG reduced mitophagy flux as determined by the difference in the levels of mitochondria-associated LC3-II or the numbers of mitophagy foci indicated by the novel dual fluorescent reporter mt-Rosella in the absence and presence of the lysosomal inhibitors. The ability of HG to induce mitochondrial fragmentation and inhibit mitophagy was reproduced in adult mouse cardiomyocytes. Overexpression of Parkin, a positive regulator of mitophagy, or treatment with CCCP, a mitochondrial uncoupler, induced mitophagy and attenuated HG-induced cardiomyocyte death, while Parkin knockdown had opposite effects, suggesting an essential role of mitophagy in cardiomyocyte survival under HG conditions. Strikingly, Parkin overexpression increased mitochondrial fragmentation, while DRP1 overexpression accelerated mitophagy flux, demonstrating a reciprocal activation loop that controls mitochondrial fission and

OPEN ACCESS

Edited by:
Xuejun Wang, University of South Dakota, United States

Reviewed by:
Abhinav Diwan, Washington University in St. Louis, United States
Zhao Wang, University of Texas Southwestern Medical Center, United States

***Correspondence:**
Qiangrong Liang
qliang03@nyit.edu

Specialty section:
This article was submitted to Striated Muscle Physiology, a section of the journal Frontiers in Physiology

Received: *08 September 2020*
Accepted: *16 November 2020*
Published: *10 December 2020*

Citation:
Kobayashi S, Zhao F, Zhang Z, Kobayashi T, Huang Y, Shi B, Wu W and Liang Q (2020) Mitochondrial Fission and Mitophagy Coordinately Restrict High Glucose Toxicity in Cardiomyocytes. Front. Physiol. 11:604069. doi: 10.3389/fphys.2020.604069

mitophagy. Thus, strategies that promote the mutual positive interaction between mitochondrial fission and mitophagy while simultaneously maintain their levels within the physiological range would be expected to improve mitochondrial health, alleviating hyperglycemic cardiotoxicity.

Keywords: diabetes, hyperglycemia, cardiomyocytes, mitochondrial fission, mitophagy, Parkin, DRP1, cell death

INTRODUCTION

The hallmark feature of diabetes mellitus is the increased blood glucose or hyperglycemia which is an independent risk factor for heart failure in people with diabetes (Stratton et al., 2000; Iribarren et al., 2001; Poornima et al., 2006; Boudina and Abel, 2007). The cellular and molecular mechanisms responsible for hyperglycemia-induced cardiac damage have been extensively studied and multiple hypotheses have been proposed (Jia et al., 2018). A common theory postulates that mitochondrial dysfunction is the major mechanism underlying the pathophysiology of diabetic heart disease (Sivitz and Yorek, 2010; Schilling, 2015). This is supported by both animal and human studies showing the accumulation of damaged mitochondria in the diabetic hearts (Tomita et al., 1996; Frustaci et al., 2000; Shen et al., 2004, 2005; Boudina and Abel, 2006; Bugger and Abel, 2008; Wang et al., 2015). Injured or otherwise dysfunctional mitochondria produce more reactive oxygen species (ROS) and leak out various pro-death factors such as cytochrome C, apoptosis-inducing factor, and Smac/DIABLO (Frustaci et al., 2000; Cai et al., 2002; Ghosh et al., 2005; Malhotra et al., 2005; Shen et al., 2006). Thus, to repair or eliminate injured mitochondrial would be expected to protect against diabetic heart injury.

Mitochondrial quality is controlled by a number of coordinated mechanisms including mitochondrial biogenesis, fission and mitophagy. Dysfunctional mitochondria can be separated by mitochondrial fission and eliminated by autophagic sequestration and subsequent degradation in the lysosome, a process termed mitophagy. Mitochondrial fission is regulated by a number of factors including dynamin-related protein 1 (DRP1), mitochondrial fission protein 1 (Fis1) and mitochondrial fission factor (MFF) (Loson et al., 2013). Fission events generate fragmented mitochondria which is conducive to the sequestration of injured fragments for subsequent degradation through mitophagy. Interestingly, high glucose is able to induce mitochondrial fragmentation in both H9c2 cells (Yu et al., 2006, 2008, 2011) and neonatal cardiomyocytes (Yu et al., 2008, 2017; Makino et al., 2011; Gawlowski et al., 2012) as shown by increased formation of short and small mitochondria. Inhibition of mitochondrial fission by mitochondrial division inhibitor 1 (Mdivi-1) (Yu et al., 2017) and a dominant negative Drp1-K38A mutant (Yu et al., 2008) or increased expression of mitochondrial fusion protein optic atrophy 1 (Opa1) (Makino et al., 2011) attenuates high glucose-induced ROS production and cell death, suggesting that high glucose-induced mitochondrial fragmentation is detrimental. However, blocking mitochondrial fragmentation by Drp1-K38A also inhibits mitochondrial respiration (Yu et al., 2006). The mitochondrial uncoupler FCCP (p-trifluoromethoxy carbonyl cyanide phenyl hydrazone) can induce mitochondrial fragmentation and at the same time reduce high glucose-triggered cardiomyocyte injury (Yu et al., 2006, 2008), suggesting that mitochondrial fragmentation is actually protective under high glucose conditions. Collectively, these opposing results underscore the need of further studies to clarify the true role of mitochondrial fission in hyperglycemic cardiotoxicity.

A well-defined pathway composed of PTEN-induced kinase 1 (PINK1) and Parkin regulates the initiation of mitophagy. Parkin is an E3 ubiquitin ligase that decorates damaged or otherwise depolarized mitochondria for degradation and recycling in the lysosome. Mitophagy is also regulated by a number of adaptors or receptors that are found in cytosol or on mitochondrial membranes (Liang and Kobayashi, 2016). Mitophagy is generally considered to play protective roles in the heart although excessive mitophagy can be detrimental under certain conditions (Song et al., 2015a; Nah et al., 2017). The protein levels of PINK1 and Parkin are decreased in the hearts of both type 1 and 2 diabetic animals (Xu et al., 2013; Tang et al., 2015; Shao et al., 2020), suggesting that mitophagy may be inhibited in the diabetic hearts. Using a novel dual fluorescent mitophagy reporter termed mt-Rosella, we labeled and traced mitochondrial fragments that are sequestered by the autophagosome and delivered to and degraded in the lysosome (Catanzaro et al., 2019; Kobayashi et al., 2020a). We found that mitophagic flux was indeed reduced in high glucose-treated cardiomyocytes and in the heart of streptozocin (STZ)-induced type 1 diabetic mice (Kobayashi et al., 2020a). Deletion of Parkin exacerbated diabetic cardiac injury in mice treated with STZ (Wang et al., 2019) or fed a high fat diet (Tong et al., 2019), suggesting that restoring Parkin-dependent mitophagy may be cardioprotective in diabetes.

Although mitochondrial fission is believed to segregate damaged mitochondria and facilitate their removal by mitophagy (Twig et al., 2008), the functional significance of mitochondrial fission in hyperglycemic cardiotoxicity remains debatable. It is even more controversial how mitochondrial fission couples with and affects mitophagy activity in the

Abbreviations: Fig, Figure; NG, normal glucose (5.5 mM); HG, High glucose (30 mM); ROS, reactive oxygen species; cCasp3, cleaved Caspase 3; PARP, Poly (ADP-ribose) polymerase; DMEM, Dulbecco's modified Eagle medium; DMSO, dimethyl sulfoxide; GAPDH, glyceraldehyde-3-phosphate dehydrogenase; GFP, green fluorescent protein; LAMP-1, lysosomal-associated membrane protein 1; RFP, red fluorescent protein; PGC-1α, Peroxisome proliferator-activated receptor gamma coactivator 1-alpha; COX IV, Cytochrome c oxidase subunit 4; Mfn1/2, Mitofusin 1/2; Opa1, optic atrophy 1; PINK1, PTEN-induced kinase 1; DRP1, dynamin-related protein 1; PepA, Pepstatin A; PI, Propidium iodide; mdivi-1, mitochondrial division inhibitor 1; CCCP, carbonyl cyanide m-chlorophenylhydrazone; siRNA, short interference RNA; β-gal, β-galactosidase; LC3, microtubule-associated protein Light Chain 3; Supp, supplemental.

diabetic heart (Liang and Kobayashi, 2016). In the present study, we determined the activities of, and the interaction between, mitochondrial fission and mitophagy in high glucose-treated cardiomyocytes. Our results demonstrated that high glucose elicited coordinated changes in the activities of mitochondrial fission and mitophagy, which collectively limit high glucose toxicity.

MATERIALS AND METHODS

Neonatal Rat Ventricular Cardiomyocyte Culture and High Glucose and/or Drug Treatments

We prepared neonatal rat ventricular cardiomyocytes (NRVC) from neonatal Harlan Sprague-Dawley rats and cultured them in Dulbecco's Modified Eagle Medium (DMEM, GIBCO, 11966) as described previously (Kobayashi et al., 2012). These NRVCs were cultured for 12–72 h in glucose-free DMEM (Gibco 11966025, Thermo Fisher Scientific) supplemented with 5.5 or 30 mmol/liter of D-(+)-glucose (Sigma, G7021). For some experiments, NRVCs were treated with lysosomal inhibitors Pepstatin A (PepA) (12.5 μg/mL, RPI, P30110, Mount Prospect, IL, United States) and E64d (5 μg/mL, RPI, E57050, Mount Prospect, IL, United States), mdivi-1 (1 uM, Sigma, M0199) and mitochondrial uncoupler Carbonyl cyanide m-chlorophenylhydrazone (CCCP) (5 nM, Sigma, C2759). The osmolarities of all media were adjusted to 30 mM by mannitol (Sigma, M9647). We added 100 units/ml penicillin and streptomycin (Sigma, P4333) to all media.

Replication-Deficient Adenoviruses

We purchased the human DRP1 and Parkin cDNA clones from OriGene and obtained the mitophagy reporter mt-Rosella from Dr. Devenish (Mijaljica et al., 2011). Rosella is a fusion protein that contains a mitochondrial targeting sequence, a pH-stable red fluorescent protein (RFP) and a pH-sensitive green fluorescent protein (GFP). The replication-deficient adenoviral vectors expressing DRP1, Parkin, or mt-Rosella were generated using the AdEasy Adenoviral Vector System (Stratagene, 240009) as we described previously (Catanzaro et al., 2019). Unless otherwise indicated, we infected NRVCs with adenovirus at a multiplicity of infection (MOI) of 100 plaque forming unit (pfu) for 24 h before drug treatment.

Confocal Microscopy and Mitophagy Analysis

Ad-mt-Rosella-infected NRVC were fixed with 4% paraformaldehyde prepared in PBS for 15 min at room temperature. Dual-fluorescent images of NRVC infected with Ad-mt-Rosella were obtained using Nikon C2 (Nikon) confocal microscope at 60× magnification or LSM900 with Airyscan 2 (Zeiss) confocal microscope at 63× magnification (1.4 numerical aperture). The GFP quenched "red only" mitophagy foci were isolated by subtracting the green channel from the red channel using ImageJ's Image Calculator after splitting two color channels. After the image optimization, ImageJ's particle analysis was performed to obtain the number of mitophagy foci with a size threshold of 5 to 50px^2 in order to exclude background noises and large aggregates or nuclei, which were unlikely to represent mitophagy foci. At least five images (each containing between 5 and 8 cells) were captured and analyzed per treatment. For determining mitophagy flux, experiments were duplicated with addition of lysosomal inhibitors PepA (12.5 μg/mL) and E64d (5 μg/mL). Mitophagy flux was calculated by subtracting the mean of red puncta without inhibitors from the corresponding mean value of red puncta with inhibitors.

Mitochondrial Morphology Analysis

For live cell imaging, cultured NRVCs were stained with 20 nM of MitoTracker Green FM (M7514, Thermo Fisher Scientific, Waltham, MA, United States) for 30 min in CO^2 incubator at 5% of CO^2 and 37°C. The cells infected with adenovirus encoding mt-Rosella reporter were fixed with 4% paraformaldehyde. The live cells were imaged at 100× magnification (1.4 numerical aperture) with Fluoview FV1000 (Olympus) and the fixed cells were imaged by using Nikon C2 (Nikon) confocal microscope at 60× magnification (1.4 numerical aperture), using the linear sequential scan mode (excitation/emission filter, 488/510 nm; 561/592 nm), 1072 × 1072 resolution. The images were processed with Fiji/ImageJ. Raw images were contrast enhanced and then binarized to apply a threshold to highlight mitochondrial structures. After optimization, the relative mitochondrial sizes, numbers and relative mass in each cell were obtained by particle analysis measurements. At least five images (each containing between 5 and 8 cells) were captured and analyzed per treatment.

Mitochondrial Superoxide Measurement (MitoSOX Assay)

Prior to imaging, the cells were incubated with 5 μM MitoSOX (M36008, Invitrogen, Thermo Fisher Scientific, Waltham, MA, United States) for 10 min at 37°C. The cells were examined using a fluorescent microscope to detect and image the fluorescent signals. Three to Five images were obtained from each treatment group. The images were analyzed by ImageJ to quantify the red fluorescence intensity of each treatment.

Mitochondrial Membrane Potential Measurement ($\Delta\Psi$m)

MitoPT JC-1 Assay Kit (924, ImmunoChemistry, Bloomington, MN, United States) was used for assessing mitochondrial membrane potential ($\Delta\Psi$m). The cultured cells were incubated with JC-1 dye for 30 min and then analyzed by Cytation fluorescence plate reader (BioTek), with excitation at 488 nm and emission at 590 nm (aggregates) and at 527 nm (monomeric). The stained images were separately obtained by Fluorescence microscopy (IX71 Olympus) at 10× magnification.

Western Blot Analysis

Cultured NRVCs were processed for Western blot analysis as described previously (Xu et al., 2012, 2013). Briefly, NRVCs were collected in 1 × SDS, boiled for 10 min, loaded to polyacrylamide gel for electrophoresis, and then transferred to polyvinylidene difluoride membranes. The membranes

were incubated with primary and secondary antibodies, and processed for chemiluminescent detection using Lumigen ECL Ultra (TMA-6 Lumigen, Southfield, MI, United States). The images were acquired by using Amersham Imager 600 and quantified with ImageJ. The antibodies against cleaved Caspase 3 (cCasp3) (#9664), β-Actin (#4967), microtubule-associated protein Light Chain 3 (LC3B, #3868), Parkin (#2132), glyceraldehyde-3-phosphate dehydrogenase (GAPDH) (#5147), Voltage Dependent Anion Channel 1 (VDAC1) (#4866), Peroxisome proliferator-activated receptor gamma coactivator 1-alpha (PGC-1α) (#4259) and Cytochrome c oxidase subunit 4 (COX IV) (#4850) were purchased from Cell Signaling Technology (Danvers, MA, United States). The OPA1 antibodies (ab42364) were purchased from Abcam (Cambridge, MA, United States). The antibodies against Mfn1 (sc-166644), Mfn2 (sc-100560), PINK1 (sc-33796), and DRP-1 (sc-271583) as well as the horseradish peroxidase-conjugated secondary antibodies (sc-2004, sc-2005, sc-2020, and sc-2438) were obtained from Santa Cruz Biotechnology.

SiRNA Gene Silencing

We obtained short interference RNAs (siRNAs) targeting DRP1 or Parkin mRNA and a Silencer Negative Control siRNA from Ambion (Austin, TX, United States). The knockdown of DRP1 or Parkin was achieved by transfecting NRVCs with a mixture of three different siRNA oligoes, each at a concentration of 16.67 nM as described previously (Catanzaro et al., 2019; Kobayashi et al., 2020b).

Cell Death Assays

The dead cells were identified by staining the NRVCs with 2 μg/mL of Propidium iodide (PI) for 10 min and examined under a fluorescent microscope. Three to five images of red fluorescence and phase contrast were obtained from each treatment group. The number of PI positive cells were counted and expressed as a percentage of the total cell number examined per treatment. Apoptotic cell death was determined by Western blot analysis of cCasp3 and cleaved PARP, as described above.

Preparation and Culture of Adult Mouse Cardiomyocytes

Adult mouse cardiomyocytes (AMCs) were isolated from 8-week-old transgenic mice that express the mitophagy reporter mt-Rosella in the heart (Kobayashi et al., 2020a) and cultured using the method described by Ackers-Johnson (Ackers-Johnson et al., 2016). Briefly, the heart was removed and perfused with collagenase solution by slow injection of the buffer into the left ventricle with a syringe. The isolated AMCs were cultured in M199 media containing the designated concentrations of glucose for 72 h and then fixed with 2% paraformaldehyde in culture media for 15 min for confocal imaging.

Determination of Mitochondrial DNA (mtDNA) Copy Number

Total DNA was extracted from 1.0×10^6 cultured NRVCs by using the Phenol-Chloroform method. Cells were lysed with Phenol:Chloroform:Isoamyl Alcohol (25:24:1), saturated with 10 mM Tris, pH 8.0, 1 mM EDTA (Sigma P3803). Extracted DNA was dissolved in Nuclease free water and quantified by using the NanoDrop ND-1000 Spectrophotometer (Labtech International Ltd.). Quantitative PCR analysis was performed using the SYBR Green PCR Master Mix (Thermo Fisher Scientific, Applied Biosystems, #4364344) on the Applied Biosystems StepOne Real-Time PCR Systems (Applied Biosystems) with 20 uL of reaction mixture containing 50 ng/uL of DNA and 200 nM of primers. The oligonucleotide primers used for reaction are as follows: COX IV gene for mitochondrial DNA, forward: 5′-CCCCTGCTATAACCCAATACA-3′, backward: 5′-CCAAACCCTGGAAGAATTAAGA-3′; GAPDH for nucleic DNA, forward: 5′- TGTTGCTGTAGCCATATTCATTGT-3′, backward: 5′- CCATTCTTCCACCTTTGATGCT -3′.

Statistical Analysis

Data were expressed as the mean ± SEM. Unpaired Student *t*-test and one-way or two-way analysis of variance (ANOVA) were used to analyze the differences between experimental groups followed by Tukey's Multiple Comparison Test using GraphPad Prism Version 8. $p < 0.05$ was considered statistically significant.

RESULTS

High Glucose Induced Mitochondrial Fragmentation in NRVCs

To characterize the effects of high glucose on mitochondrial morphology in cardiomyocytes, NRVCs were cultured with 5.5 mM [normal glucose (NG)] or 30 mM [high glucose, (HG)] for 3 days and then stained with MitoTracker Green for live imaging. Mitochondria in NG-cultured cells appeared elongated and connected. In contrast, mitochondria in HG-cultured cells were smaller and separated, suggesting that HG induces mitochondrial fragmentation (**Figure 1A**). Indeed, the mean mitochondrial particle size was substantially reduced by HG treatment ($p < 0.01$, $n = 6$). Alternatively, NRVCs were infected with adenovirus encoding the dual fluorescent mt-Rosella reporter which stains mitochondria and tracks their whereabouts in the cell as described below and previously (Catanzaro et al., 2019; Kobayashi et al., 2020a). These cells were fixed with 4% paraformaldehyde and imaged. The merged confocal images showed yellow mitochondria which appeared more fragmented in HG-cultured cells compared with NG as indicated by the reduced mitochondrial size ($p < 0.01$, $n = 8$, **Figure 1B**) and increased the mitochondrial number (**Figure 1C**). These results replicated those from live cells stained with MitoTracker Green, reinforcing the notion that HG is able to induce mitochondrial fragmentation. We also performed a time-course study and found that mitochondrial fragmentation started as early as 12 h after HG treatment and plateaued 72 h later as shown by the reduced mitochondrial size and increased mitochondrial number (**Supplementary Figure 1**). Interestingly, HG had no effects on the total mitochondrial area (**Figure 1D**), suggesting that HG might have not affected mitochondrial degradation. To explore the potential

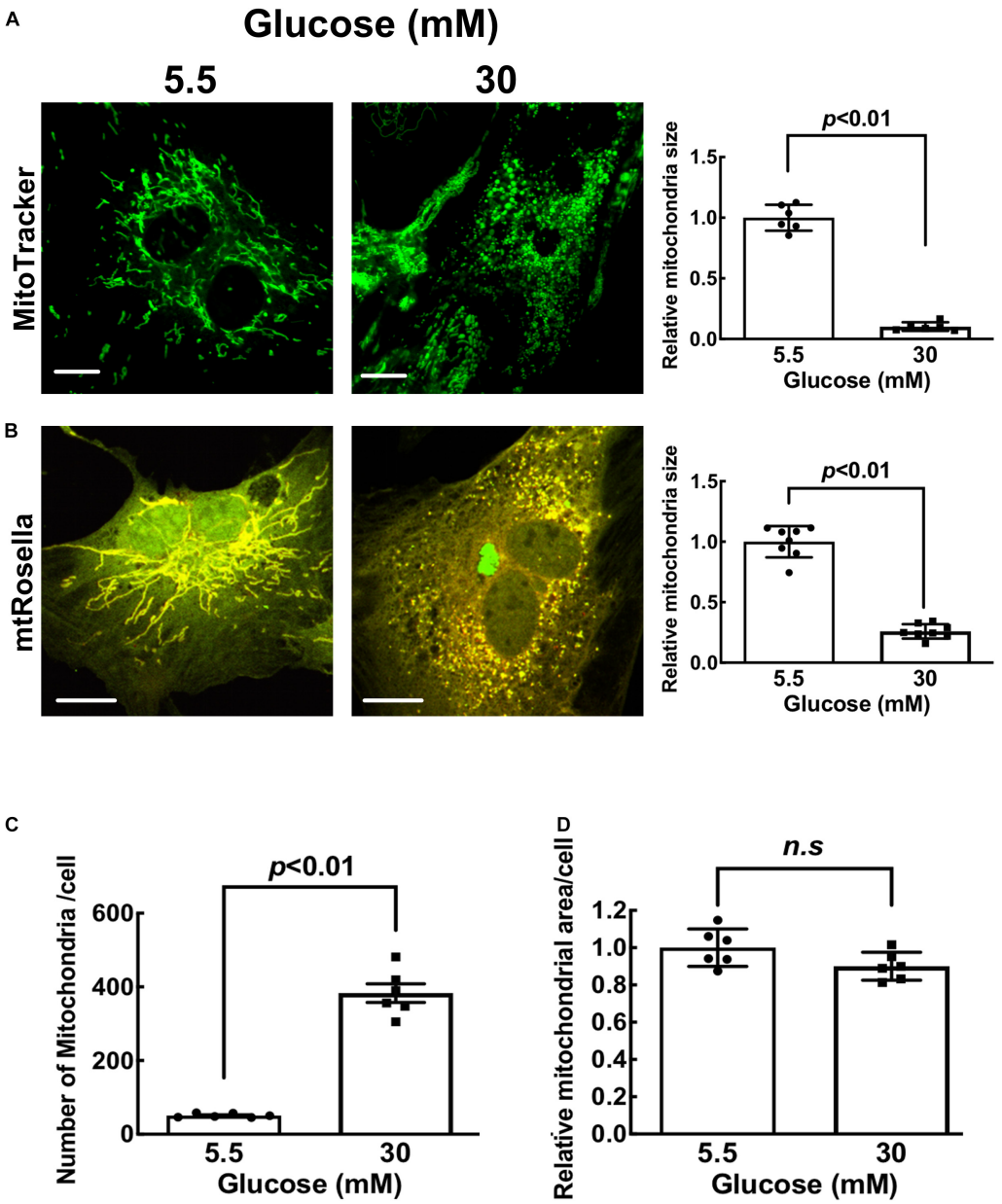

FIGURE 1 | High glucose induces mitochondrial fragmentation in cardiomyocytes. NRVCs were cultured in DMEM with 5.5 or 30 mM glucose for 72 h. Mitochondrial structure was visualized by staining with MitoTracker Green (live cells, panel **A**) or dual fluorescence mt-Rosella mitophagy reporter (fixed cells, panel **B**). The confocal images of MitoTracker and mt-Rosella were analyzed with ImageJ. After image optimization, mitochondrial morphology was analyzed and average particle size **(A,B)**, mitochondrial numbers **(C)** and total areas **(D)** were quantified. At least five images (each containing 5–8 cells) were captured per treatment. The scale bars = 10 μm **(A)** and 20 μm **(B)**. Data are expressed as mean ± SEM and analyzed by using unpaired student *t*-test (*$p < 0.01$ vs. 5.5 mM glucose, $n = 6–8$).

mechanisms responsible for the increased fission, we screened several common regulators of mitochondrial fission and fusion. Although previous studies reported increased levels of Drp1 protein or its phosphorylation by HG (Yu et al., 2017), we did not reproduce these results. Instead, we found that HG treatment decreased the fusion protein mitofusin 1 (Mfn1) in mitochondria fractions (**Supplementary Figure 2A**), suggesting a reduced mitochondrial fusion. Mitochondrial morphology is determined by the balance between mitochondrial fusion and fission. The reduced Mfn1 likely tilted the balance in favor of fission, leading to an increased mitochondrial fragmentation.

Moderate DRP1 Knockdown Did Not Affect High Glucose-Induced Cardiomyocyte Injury

To determine the functional role of fission in high glucose (HG) toxicity in NRVCs, we used synthetic siRNAs to knock down

the protein expression of DRP1, a major factor that promotes mitochondrial fission. Since complete DRP1 knockdown caused cell death, we kept the knockdown at a moderate level (∼50%, **Figure 2B**). As shown in Admt-Rosella-infected NRVCs (**Figure 3A**) and the quantification (**Figure 3B**), moderate DRP1 knockdown increased the mean mitochondrial particle size in NG-cultured NRVCs ($p < 0.01$, $n = 5$), confirming the ability of siDRP1 to reduce baseline mitochondrial fission. SiDRP1 also showed a trend to attenuate HG-induced fragmentation (p = NS, $n = 5$). However, moderate DRP1 knockdown did not impact either the viability of NRVCs under NG conditions or HG-induced cardiomyocyte injury, as shown in **Figure 2** by the number of PI positive cells (**Figure 2A**: $p > 0.05$, $n = 5$), the levels of cCasp3 (**Figure 2B**: cCasp3, $p > 0.05$, $n = 4$), superoxide production (**Figure 2C**: MitoSOX, $p > 0.05$, $n = 3$–4) and mitochondrial membrane potential (**Figure 2D**: $\Delta\Psi$m, JC-1, $p > 0.05$, $n = 3$). More surprisingly, inhibiting DRP1-dependent mitochondrial fission with mdivi-1 exacerbated HG-induced cardiomyocyte death as shown by the increased PI positive cells and cCasp3 (**Supplementary Figures 3A,B**). These results suggested that reducing mitochondrial fragmentation *per se* did not prevent or protect from HG cardiotoxicity; rather, it increased HG cardiotoxicity, in contrast to a previous study showing that inhibition of mitochondrial fission attenuated HG-induced cardiomyocyte death (Yu et al., 2008).

DRP1 Overexpression Triggered Mitochondrial Fission and Protected From HG-Induced Cardiomyocyte Injury

We used adenovirus-mediated gene transfer to determine if DRP1 overexpression could trigger mitochondrial fission in NRVCs. As expected, DRP1 overexpression (AdDRP1) induced mitochondrial fragmentation at NG as shown by the smaller and less connected mitochondria (**Figures 4A,B**, $p < 0.01$, $n = 5$), but it failed to further increase HG-induced mitochondrial fragmentation. In addition, whereas DRP1 overexpression only reduced the production of mitochondrial superoxide (MitoSOX) under NG conditions, it surprisingly mitigated HG-induced cardiomyocyte injury as shown by PI positive cells (**Figure 5A**, $p < 0.01$, $n = 5$), cCasp 3 (**Figure 5B**, $p < 0.01$, $n = 4$), superoxide (**Figure 5C**, $p < 0.01$, $n = 4$) and $\Delta\Psi$m (**Figure 5D**, $p < 0.05$, $n = 3$). These results demonstrated that increasing mitochondrial fragmentation did not contribute to HG cardiotoxicity; instead, it protected against HG-induced cardiomyocyte injury, suggesting that mitochondrial fragmentation was actually an adaptive response that limited HG toxicity, in stark contrast to the study reporting mitochondrial fission as a mediator of HG toxicity (Yu et al., 2008).

High Glucose (HG) Inhibited Mitophagy Flux in NRVCs

To directly visualize and quantify the mitochondrial fragments that are degraded through the mitophagic process, we constructed an adenovirus that encodes mt-Rosella, a novel mitophagy reporter (Catanzaro et al., 2019; Kobayashi et al., 2020a) that is a mitochondria-targeted dual-emission biosensor containing RFP and GFP as a fusion protein (Mijaljica et al., 2011). We infected NRVCs with Ad-mt-Rosella and compared mitophagy events (red fluorescent dots or puncta on the merged confocal images) in cells cultured under HG (30 mM) and NG (5.5 mM) conditions. As shown by the control groups in **Figures 3A,C** (siRNA control), **Figures 4A,C** (Adβgal), **Figures 6A,C** (Adβgal) and **Figures 7A,C** (siRNA control), HG increased the number of red dots compared with NG, suggesting that HG might have enhanced mitophagy. However, treatment with lysosomal degradation inhibitors PepA and E64d resulted in a smaller increase in the number of red dots in cells cultured in HG than in NG, suggesting that HG actually reduced the mitochondria degradation rate in the lysosome. In other words, HG inhibited mitophagy flux, consistent with our previous results (Kobayashi et al., 2020a). Mitophagy flux reflects the number of mitochondria that are delivered to and degraded in the lysosome. It was determined by the difference in the numbers of mitochondria trapped in the lysosome (red puncta on merged confocal images) before and after applying lysosomal degradation inhibitors. The mitophagy flux was denoted by the red number and the red vertical line with arrows at both ends in each of these bar graphs (**Figures 3C**, 4C, 6C, 7C). To further characterize mitophagy flux, we determined the effects of HG on the levels of autophagosomal membrane marker LC3-II that were associated with the mitochondrial fraction with and without PepA and E64d treatment. As shown in **Figure 8**, the LC3-II levels in total cell lysates (**Figure 8A**), cytoplasmic fractions (**Figure 8B**) or mitochondrial fractions (**Figure 8C**) were not significantly different between HG and NG cultures in the absence of PepA and E64d. However, HG caused a considerably less increase in LC3-II levels than NG when PepA and E64d was used to block lysosomal degradation, suggesting that HG inhibited mitophagy flux, consistent with the results from the mt-Rosella mitophagy reporter. Given the reduced mitophagy and the unchanged mitochondrial amount (**Figure 1D**), it's possible that HG might have reduced mitochondrial biogenesis, which could helps maintain a relatively normal mitochondrial mass. Indeed, we found that HG reduced mitochondrial DNA content (**Supplementary Figure 2B**) and had a tendency to decrease the protein levels of PGC-1α (**Supplementary Figure 2A**), a master regulator of mitochondrial biogenesis. These results support the idea that HG inhibited mitochondrial biogenesis which may explain why mitochondrial mass remained normal despite the reduced mitophagy.

DRP1 Overexpression Alleviated the Inhibition of Mitophagy Flux by High Glucose (HG)

Mitochondrial fission and mitophagy are two cellular mechanisms that coordinately control mitochondrial quality. Fission process is essential for mitophagy in that it separates injured mitochondrial segments which in turn are sequestered, delivered to and degraded in the lysosome. We determined if adenovirus-mediated gene transfer of DRP1 could affect mitophagy flux in NRVCs using the mt-Rosella reporter. As

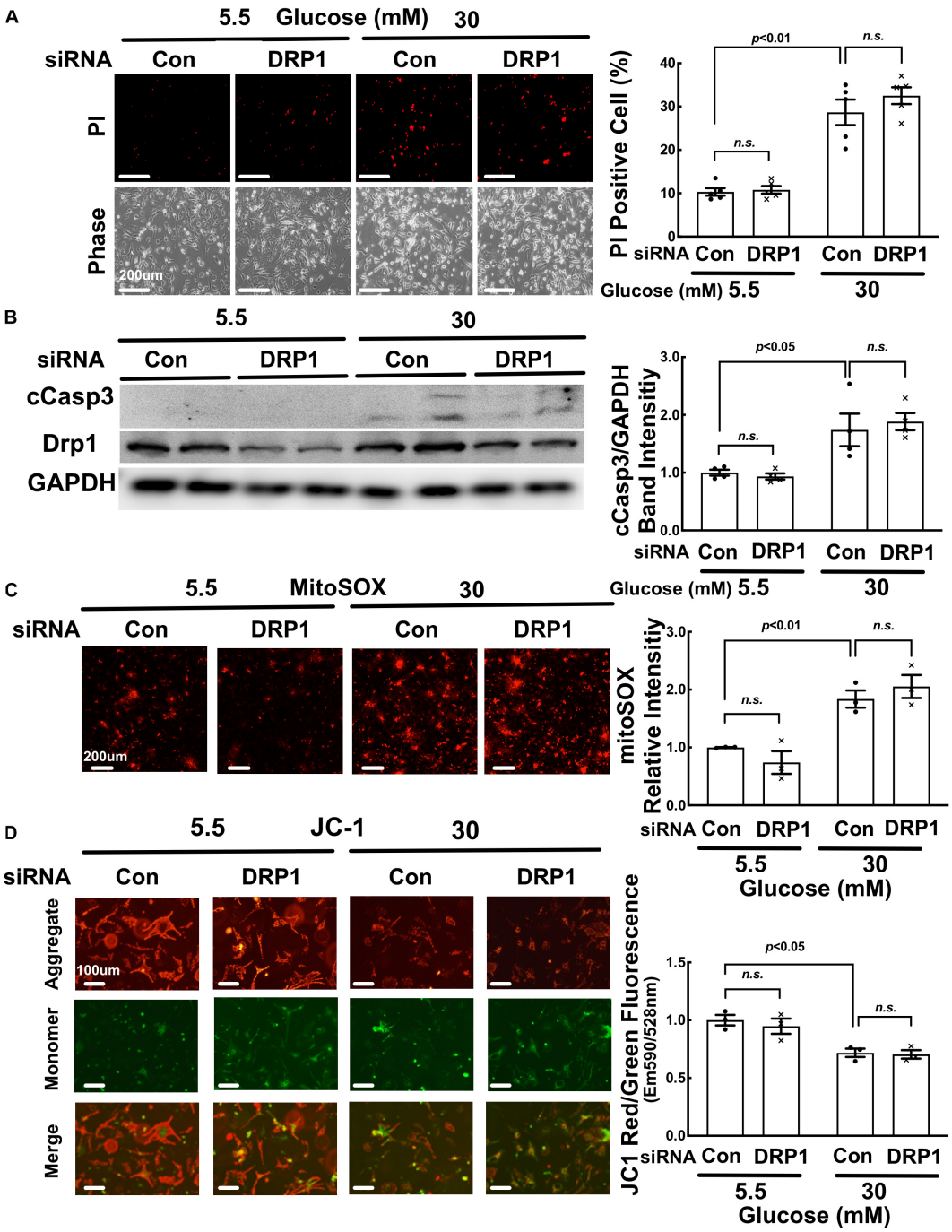

FIGURE 2 | Moderate DRP1 knockdown did not affect high glucose-induced cardiomyocyte injury. NRVCs were transfected with scrambled control or DRP1-targeted synthetic siRNA, cultured with DMEM containing 5.5 or 30 mM glucose for 72 h, and then cardiomyocyte injury was determined by the number of PI positive cells (**A:** $p > 0.05$, $n = 5$), the levels of cCasp3 (**B:** cCasp3, $p > 0.05$, $n = 4$), superoxide production (**C:** MitoSOX, $p > 0.05$, $n = 3$–4) and mitochondrial membrane potential (**D:** $\Delta\Psi$m, JC-1, $p > 0.05$, $n = 3$). Data were expressed as mean ± SEM and analyzed by two-way ANOVA. Scale bars represent **(A)** 200 μm, **(C)** 200 μm, **(D)** 100 μm, respectively.

shown in **Figures 4A,C**, AdDRP1 infection reduced the number of red dots as compared with Adβgal under both NG and HG conditions, suggesting that HG might have attenuated mitophagy. However, treatment with PepA and E64d led to a larger increase in the number of red dots in cells infected with AdDRP1 than those with Adβgal under either NG or HG conditions. The results suggested that DRP1 not only increased mitophagy flux in NRVCs cultured under NG conditions, but

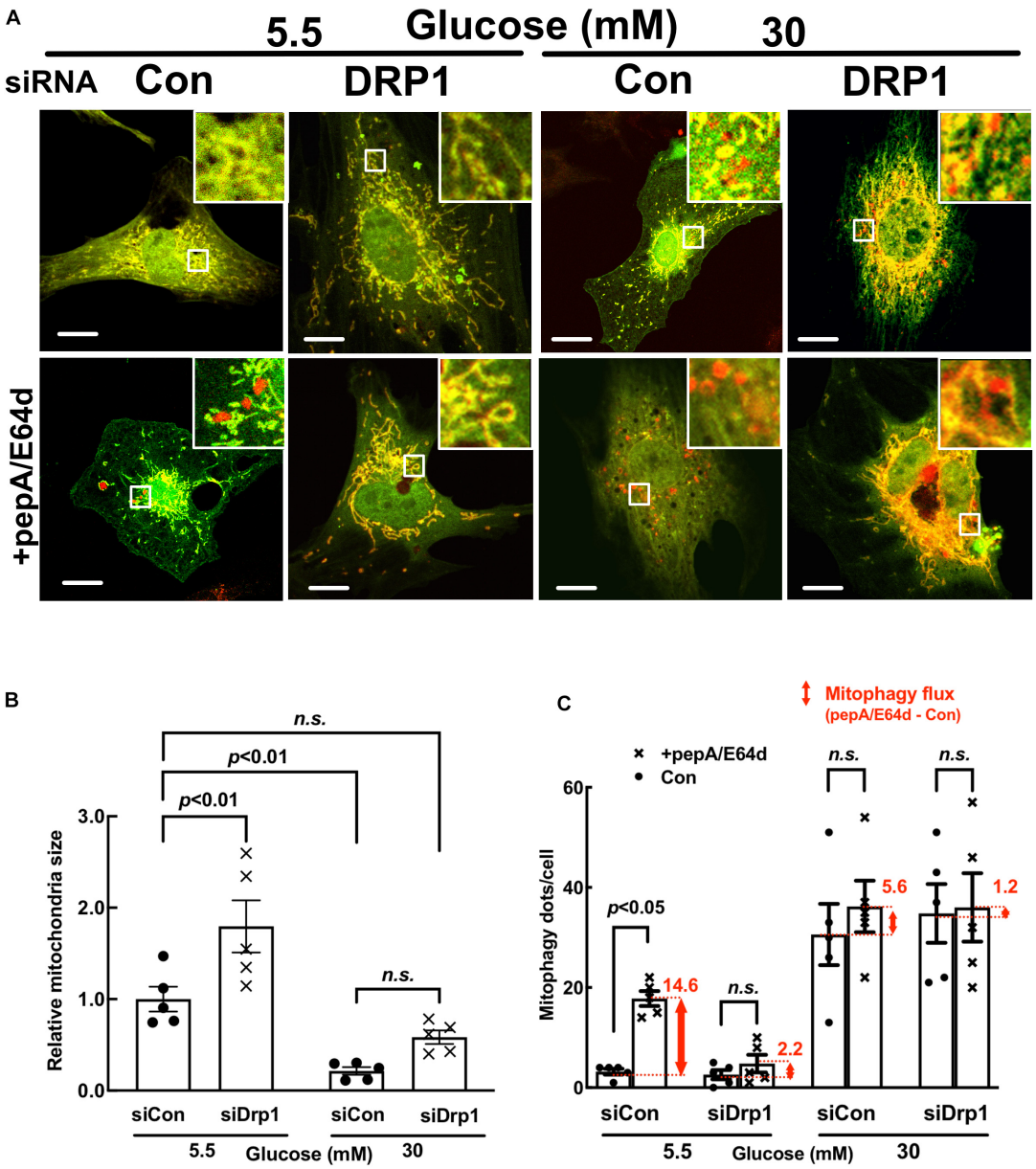

FIGURE 3 | DRP1 knockdown reduced basal mitochondrial fission and mitophagy flux in cardiomyocytes. NRVCs were infected with Admt-Rosella, transfected with scrambled control or DRP1-targeted synthetic siRNA, and then cultured with DMEM containing 5.5 or 30 mM glucose for 72 h. Mitochondrial morphology was observed with confocal microscopy and the merged confocal images **(A)** were analyzed using ImageJ. The relative mitochondrial sizes **(B)** and the number of mitophagy foci (red puncta or dots, **C**) in each cell were obtained by particle analysis measurements. At least five images (each containing between 5 and 8 cells) were captured per treatment. Scale bar = 20 μm. Experiments were repeated with addition of lysosomal inhibitors (PepA and E64D). Mitophagy flux was calculated by subtracting the mean of red puncta without inhibitors from the corresponding mean value of red puncta with inhibitors, which was denoted by the red number and the red vertical line with arrows at both ends in the bar graphs. Data were expressed as mean ± SEM and analyzed by two-way ANOVA ($n = 5$ for each group with p values indicated in the graphs).

also alleviated the inhibition of mitophagy flux by HG. Thus, DRP1 may reduce HG toxicity through its ability to increase mitophagy flux. We also examined the effects of siRNA-mediated DRP1 knockdown on mitophagy. Although siDRP1 substantially slowed mitophagy flux in NRVCs cultured in NG media, its effect on HG-inhibited mitophagy was relatively small (**Figures 3A,C**), probably because mitophagy flux was already depressed by HG. This may explain why DRP1 knockdown did not alter HG toxicity (**Figure 2**).

Parkin Overexpression Accelerated Mitophagy Flux and Reduced HG Toxicity

To determine the role of mitophagy in HG-induced cardiomyocyte injury, we overexpressed or silenced Parkin

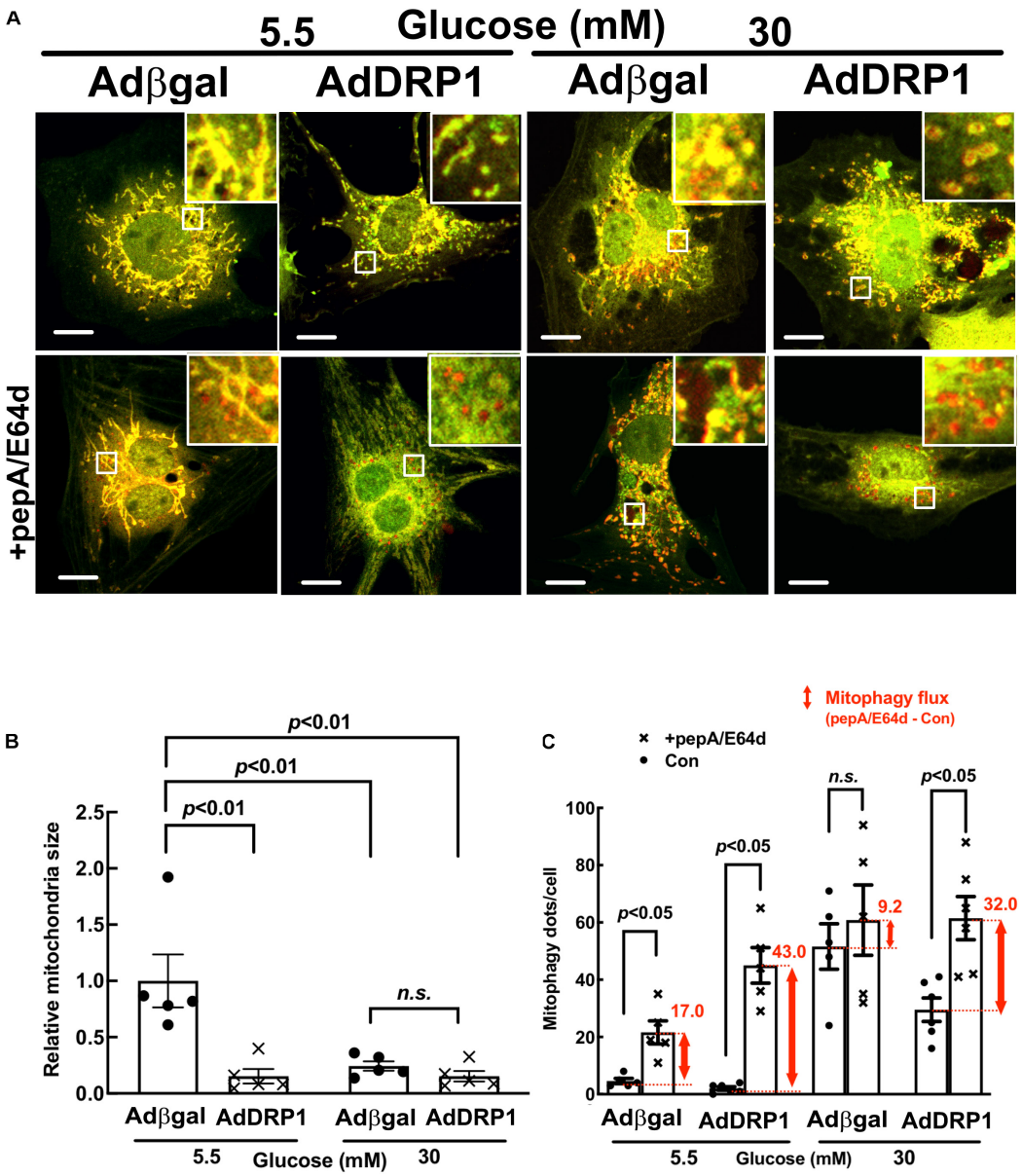

FIGURE 4 | DRP1 overexpression triggered mitochondrial fission, increased basal mitophagy and alleviated the inhibition of mitophagy flux by high glucose (HG). NRVCs were infected with AdDRP1 or Adβgal and cultured with DMEM containing 5.5 or 30 mM glucose for 72 h. Mitochondrial morphology was examined with confocal microscopy and the merged confocal images **(A)** were analyzed using ImageJ. The relative mitochondrial sizes **(B)** and the number of mitophagy foci (red puncta or dots, **C**) in each cell were obtained by particle analysis measurements. At least five images (each containing between 5 and 8 cells) were captured per treatment. Scale bar = 20 μm. Mitophagy flux was measured with and without PepA and E64D, and denoted by the red number and the red vertical line with arrows at both ends in the bar graphs. Data were expressed as mean ± SEM and analyzed by two-way ANOVA ($n = 5$ for each group with p values indicated in the graphs).

in NRVCs using adenovirus or siRNA knockdown, respectively. Parkin is an E3 ubiquitin ligase that ubiquitinates depolarized or otherwise injured mitochondria to trigger their degradation by mitophagy. Compared to Adβgal-infected NRVCs, the AdParkin moderately increased mitophagy flux under NG conditions, as shown by the difference in the numbers of red dots with and without PepA/E64d (**Figures 6A,C**). Parkin overexpression also relieved the inhibition of mitophagy flux by HG. Conversely, Parkin knockdown with siRNA inhibited mitophagy flux in NG-cultured cells. It also dramatically decreased the number of red dots in HG-cultured cells either with or without PepA/E64d, although it did not further reduce mitophagy flux (**Figure 7A,C**). Importantly, increasing mitophagy activity by AdParkin diminished HG-induced cardiomyocyte injury (**Figure 9**), while Parkin knockdown had the opposite effects (**Figure 10**), as measured by the number of PI positive cells and the levels of cCasp3, superoxide and $\Delta\Psi m$. Alternatively, we treated NRVCs with CCCP, a mitochondrial

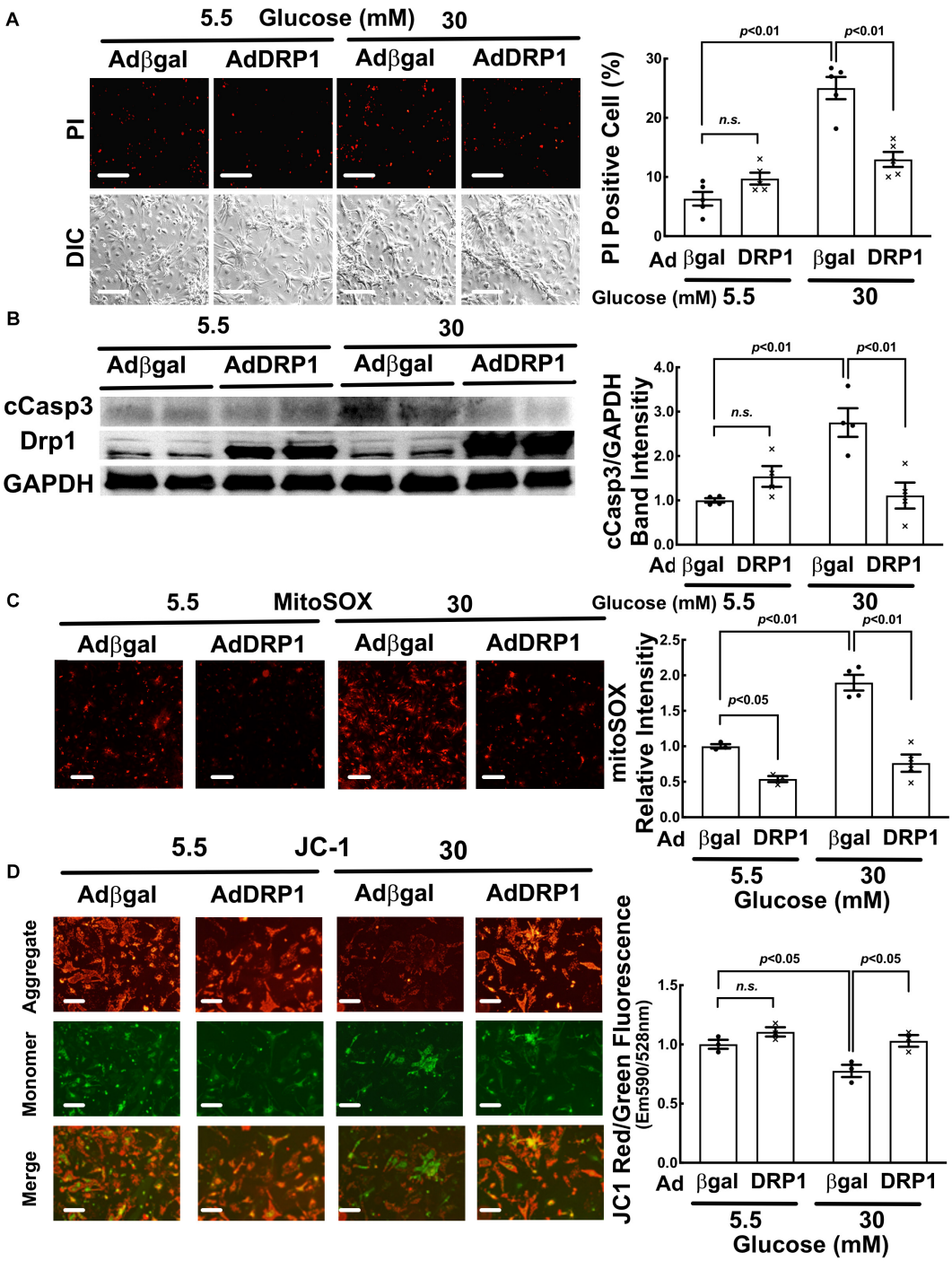

FIGURE 5 | DRP1 overexpression alleviated high glucose-induced cardiomyocytes injury. NRVCs were infected with AdDRP1 or Adβgal and cultured in DMEM containing 5.5 or 30 mM glucose for 72 h, and then cardiomyocyte injury was determined by the number of PI positive cells (**A:** $p < 0.01$, $n = 5$), the levels of cCasp3 (**B:** $p < 0.01$, $n = 4$), MitoSOX (**C:** $p < 0.01$, $n = 3$) and $\Delta\Psi$m (**D:** JC-1, $p < 0.05$, $n = 3$). Data were expressed as mean ± SEM and analyzed by two-way ANOVA. Scale bars represent **(A)** 200 μm, **(C)** 200 μm, **(D)** 100 μm, respectively.

uncoupler that is routinely used to induce mitophagy. We found that a low dose of CCCP (5 nM) protected from HG-induced cardiomyocyte death as shown by the reduced PI positive cells and cCasp3 (**Supplementary Figure 4A,B**). These results strongly suggested that mitophagy is essential for maintaining mitochondrial health and cardiomyocytes survival in response to HG stress. Interestingly, Parkin overexpression also increased mitochondrial fragmentation as shown by the

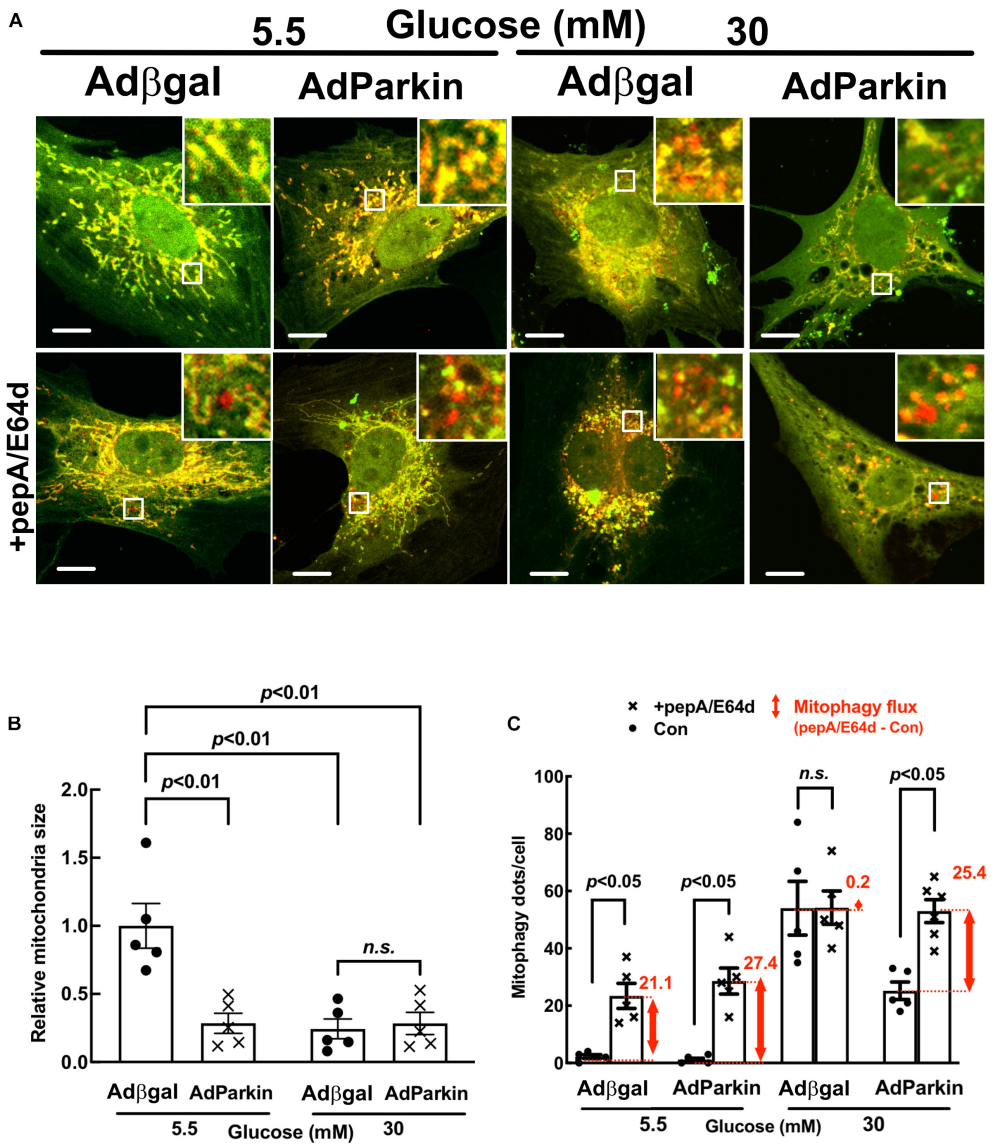

FIGURE 6 | Parkin overexpression increased basal mitophagy and relieved the inhibition of mitophagy flux by high glucose. NRVCs were infected with Admt-Rosella and AdParkin or Adβgal and cultured in DMEM containing 5.5 or 30 mM glucose for 72 h. Mitochondrial morphology was examined with confocal microscopy and the merged confocal images **(A)** were analyzed using ImageJ. The relative mitochondrial sizes **(B)** and the number of mitophagy foci (red puncta or dots, **C**) in each cell were obtained by particle analysis measurements. At least five images (each containing between 5 and 8 cells) were captured per treatment. Scale bar = 20 μm. Mitophagy flux was measured with and without PepA and E64D, and denoted by the red number and the red vertical line with arrows at both ends in the bar graphs. Data were expressed as mean ± SEM and analyzed by two-way ANOVA ($n = 5$ for each group with p values indicated in the graphs).

substantially reduced mitochondrial size (**Figures 6A,B**), despite the inability of Parkin knockdown to affect mitochondrial fission (**Figures 7A,B**), suggesting a positive feedback mechanism linking mitophagy and mitochondrial fission.

High Glucose Induced Mitochondrial Fragmentation but Inhibited Mitophagy in Adult Mouse Cardiomyocytes (AMCs)

Since the mitochondrial morphology and physiology differ between neonate and adult (Eisner et al., 2017), we performed additional experiments using adult mouse cardiomyocytes (AMCs) isolated from the transgenic mice that express the mt-Rosella mitophagy reporter in the heart. As shown in **Figure 11A**, HG treatment reduced the mean mitochondrial particle size by approximately 44% (0.56 ± 0.17 compared to NG, $p < 0.05$, $n = 4$), while increased the mitochondrial number by 1.6 fold (1.60 ± 0.2 compared to NG, $p < 0.05$, $n = 4$), suggesting that HG increased mitochondrial fragmentation. However, HG did not have any effect on the total mitochondrial area in AMC (**Figure 11A**), suggesting that mitochondrial

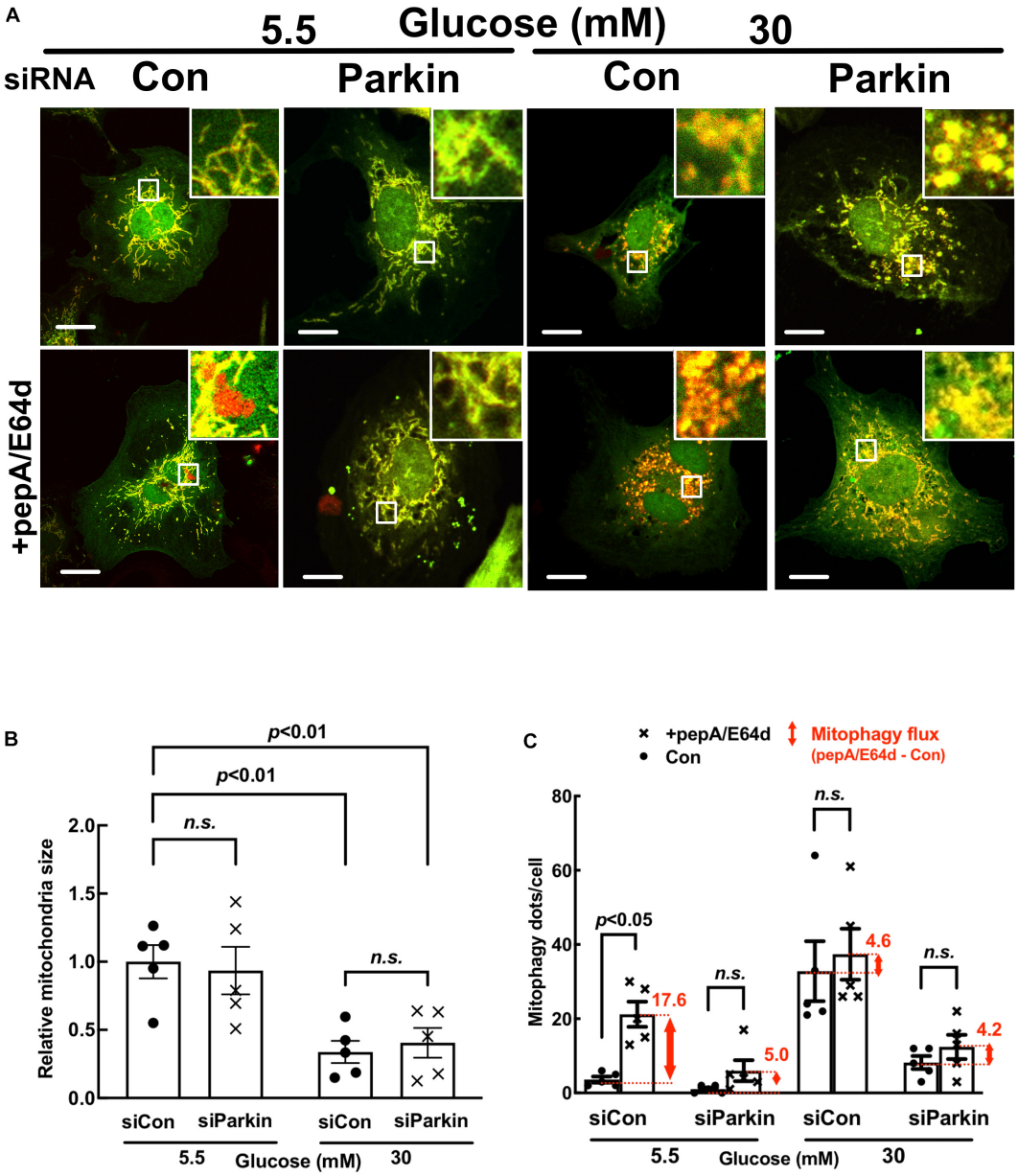

FIGURE 7 | Parkin knockdown inhibited mitophagy flux in cardiomyocytes. NRVCs were infected with Admt-Rosella, transfected with scrambled control or Parkin-targeted synthetic siRNA, and cultured with DMEM containing 5.5 or 30 mM glucose for 72 h. Mitochondrial morphology was examined with confocal microscopy and the merged confocal images **(A)** were analyzed using ImageJ. The relative mitochondrial sizes **(B)** and the number of mitophagy foci **(C)** in each cell were obtained by particle analysis measurements. At least five images (each containing between 5 and 8 cells) were captured per treatment. Scale bar = 20 μm. Experiments were repeated with addition of lysosomal inhibitors (PepA and E64D) for evaluating mitophagy flux which was denoted by the red number and the red vertical line with arrows at both ends in the bar graphs. Data were expressed as mean ± SEM and analyzed by two-way ANOVA ($n = 5$ for each group with p values indicated in the graphs).

degradation might have been decreased. Indeed, HG increased the number of red dots compared with NG, but treatment with PepA/E64d resulted in a much smaller increase in the number of red dots in cells cultured in HG than in NG (**Figure 11B**), indicating that HG inhibited mitophagy flux, consistent with the results obtained from NRVCs.

DISCUSSION

Mitochondrial dysfunction plays a key role in diabetic heart failure. Mitochondrial fission has been observed in the diabetic heart and in cardiomyocytes cultured with high glucose (Liang and Kobayashi, 2016) and has been thought to contribute to glucotoxicity (Yu et al., 2008,

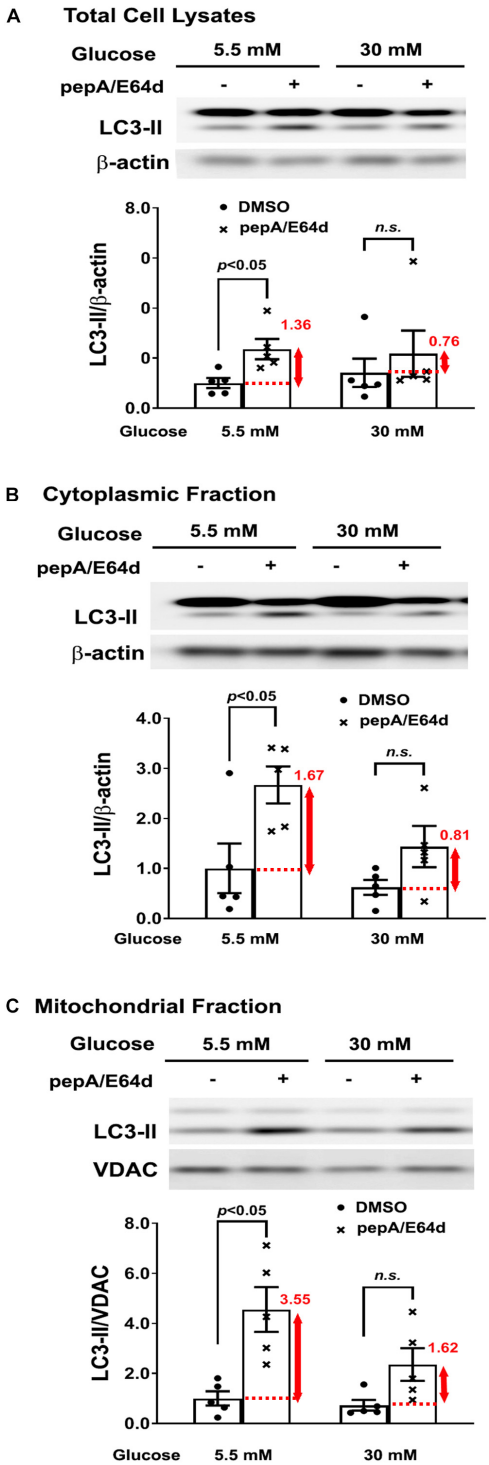

FIGURE 8 | High glucose inhibited mitophagy flux. NRVCs were cultured in DMEM containing 5.5 or 30 mM glucose for 72 h. The LC3-II levels were determined by Western blot analysis in total cell lysates **(A)**, cytoplasmic fractions **(B)** or mitochondrial fractions **(C)** with or without adding PepA and E64d. Mitophagy flux was denoted by the red number and the red vertical line with arrows at both ends in the bar graphs. Data were expressed as mean ± SEM and analyzed by two-way ANOVA ($n = 5$ for each group with p values indicated in the graphs).

2011, 2017; Makino et al., 2011). However, inhibition of mitochondrial fission reduced mitochondrial respiration (Yu et al., 2006). Also, the mitochondrial uncoupler FCCP that can trigger mitochondrial fragmentation abolished HG-induced cardiomyocyte injury (Yu et al., 2006, 2008), suggesting that mitochondrial fragmentation may not necessarily be detrimental. Indeed, our present study showed that DRP1 knockdown did not reduce HG toxicity (**Figure 4**) and Mdivi-1, a chemical inhibitor of mitochondrial fission, even increased HG-induced cardiomyocyte death (**Supplementary Figure 3**). More strikingly, DRP1 overexpression mitigated HG-induced cardiomyocyte injury (**Figure 5**). These results demonstrated that increased mitochondrial fragmentation did not contribute to HG cardiotoxicity; instead, it protected against HG-induced cardiomyocyte injury, strongly supporting the notion that mitochondrial fragmentation was an adaptive response that limited HG toxicity, in sharp contrast to previous studies (Yu et al., 2008, 2011, 2017; Makino et al., 2011).

Our results are surprising but not entirely unexpected given previous studies that demonstrate a dual role for mitochondrial fission in cardiomyocytes. On one hand, suppressing mitochondrial fission diminishes cardiac damage triggered by a number of different stresses or insults such as ischemia/reperfusion (Ong et al., 2010; Disatnik et al., 2013; Sharp et al., 2014), pressure overload (Givvimani et al., 2012) and doxorubicin (Gharanei et al., 2013; Catanzaro et al., 2019), suggesting a detrimental role for mitochondrial fission. On the other hand, a DRP1 loss-of-function mutation (Ashrafian et al., 2010; Cahill et al., 2015) or cardiac specific inactivation of DRP1 (Kageyama et al., 2014; Ikeda et al., 2015; Ishihara et al., 2015; Song et al., 2015a,b) invariably leads to heart failure, underscoring an essential role of mitochondrial fission in maintaining cardiac homeostasis. A protective role of mitochondrial fission has also been shown in cultured cardiomyocytes (Brand et al., 2018). Together, these studies reveal the dichotomous nature of mitochondrial fragmentation that can either protect or damage the heart under different conditions. Then, what determines the ultimate effects of mitochondrial fragmentation on cardiomyocytes? One possibility may have something to do with the functional state of mitophagy. Mitochondrial fission separates injured mitochondrial fragments and channels them into mitophagic process for degradation (Twig et al., 2008). If mitophagy can efficiently eliminate these fragments, the whole process will be cardioprotective. However, if mitophagy is impaired or fission is overwhelming, the fragmented dysfunctional mitochondria will accumulate and cause cardiac injury (Liang and Kobayashi, 2016).

Using a novel dual fluorescent mitophagy reporter known as mt-Rosella, we showed that HG increased mitophagy foci (red dots) in both neonatal and adult cardiomyocytes, suggesting that HG might have enhanced mitophagy. However, treatment with lysosomal degradation inhibitors resulted in a smaller increase in the number of red dots in cells cultured in HG, indicating that HG actually reduced mitophagy flux (**Figures 3A,C**, **4A,C**, **6A,C**, **7A,C**, **11B**). A major positive regulator of mitophagy is Parkin, an E3 ligase that adds ubiquitin tag to the target proteins on the damaged mitochondria, promoting mitophagosome formation.

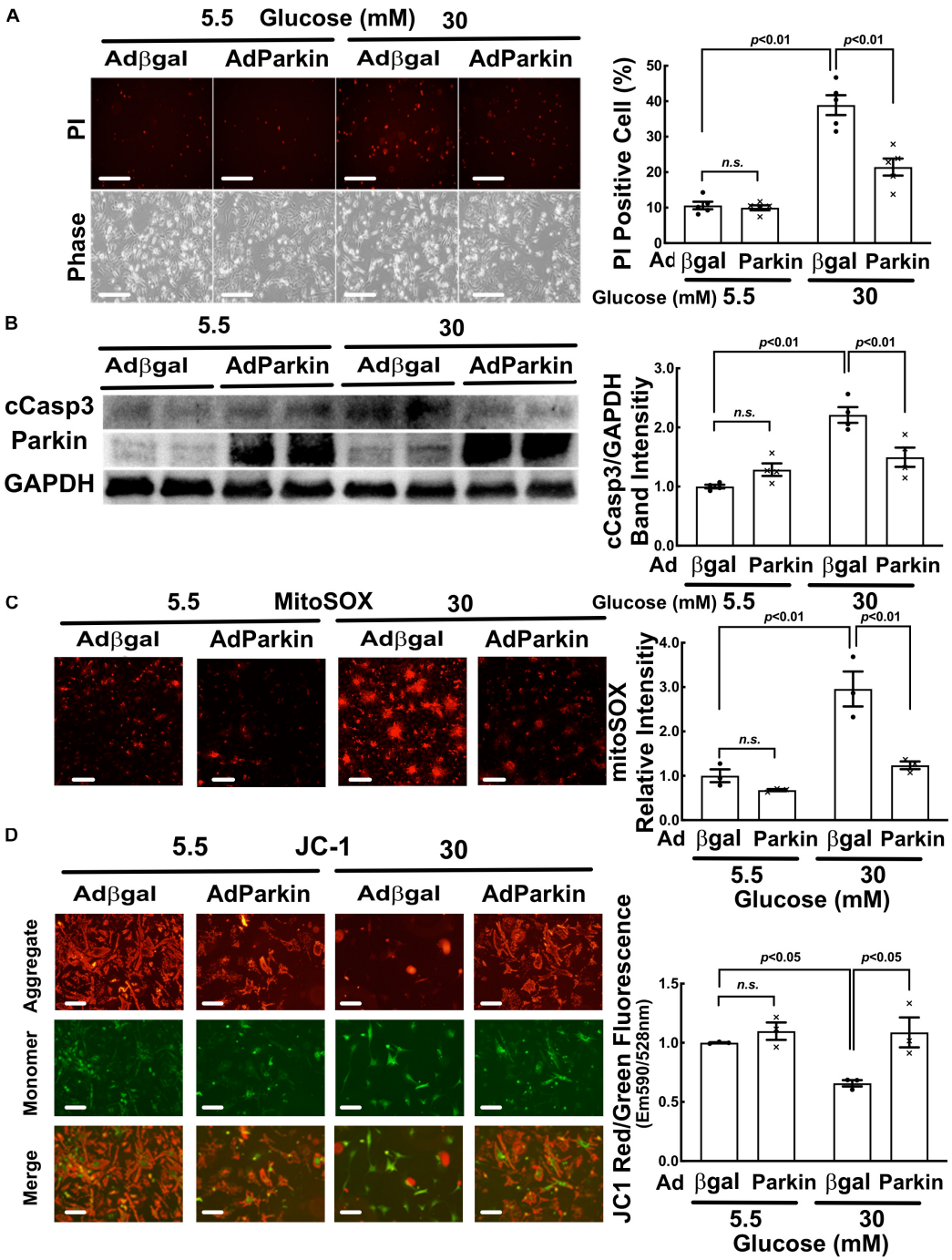

FIGURE 9 | Parkin overexpression diminished high glucose-induced cardiomyocyte injury. NRVCs were infected with AdParkin or Adβgal and cultured in DMEM containing 5.5 or 30 mM glucose for 72 h, and cardiomyocyte injury was determined by the number of PI positive cells (**A:** $p < 0.01$, $n = 5$), the levels of cCasp3 (**B:** $p < 0.01$, $n = 4$), MitoSOX (**C:** $p < 0.01$, $n = 3$) and $\Delta\Psi$m (**D:** JC-1, $p < 0.05$, $n = 3$). Data were expressed as mean ± SEM and analyzed by two-way ANOVA. Scale bars represent **(A)** 200 μm, **(C)** 200 μm, **(D)** 100 μm, respectively.

The expression levels of Parkin did not appear to be altered by HG treatment (**Figures 9B**, **10B** and **Supplementary Figure 2A**), which seemed contradictory to the fact that HG reduced mitophagy flux. However, the Parkin-mediated formation of mitophagosome is only the first step in the entire mitophagy process. If the degradation is insufficient, the mitophagy process cannot be carried out to the completion. Indeed, as we showed recently (Kobayashi et al., 2020b), HG was able to induce lysosomal membrane permeabilization (LMP), which might compromise lysosomal function, impeding mitophagic

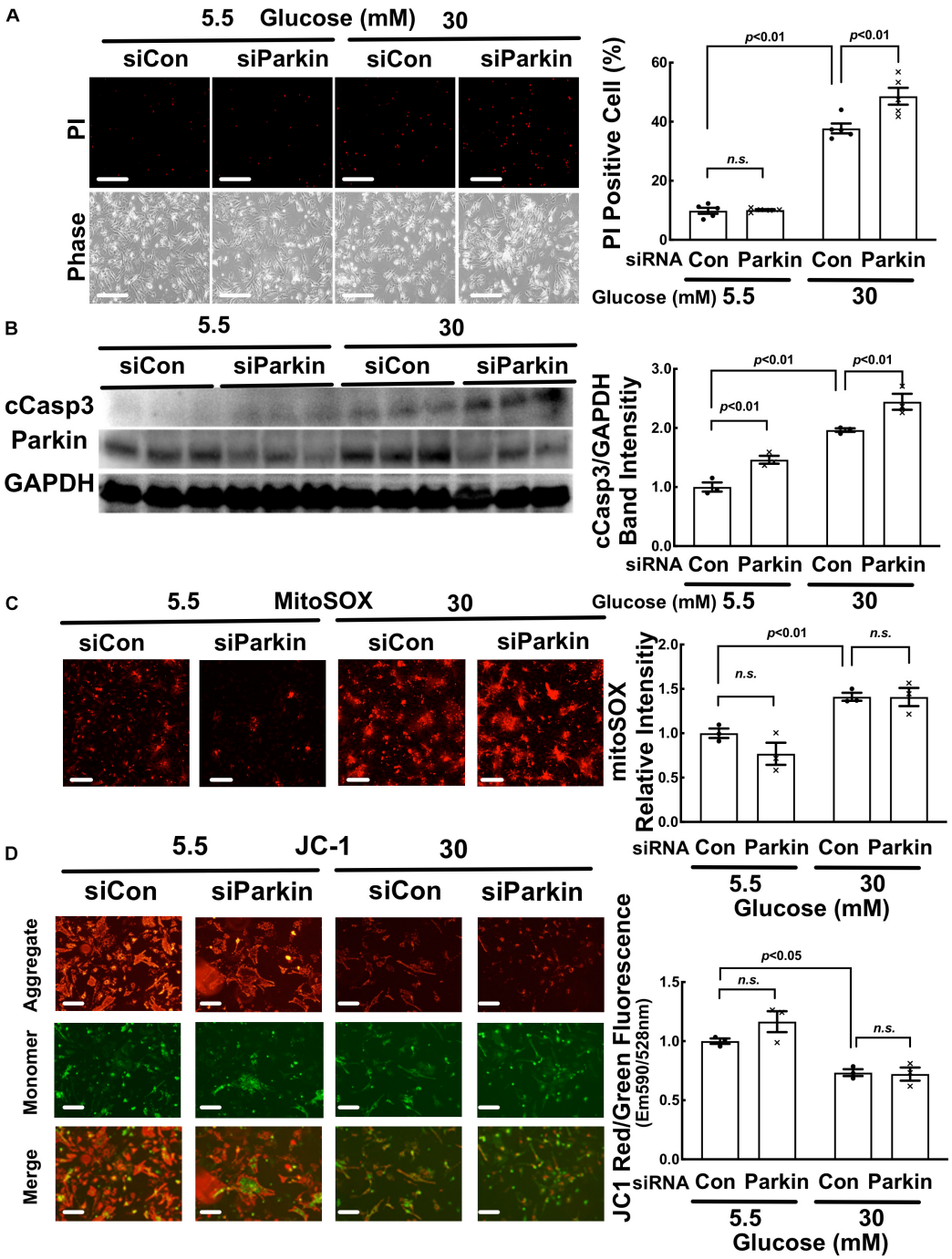

FIGURE 10 | Parkin knockdown exacerbated high glucose-induced cardiomyocyte death. NRVCs were transfected with scrambled control or Parkin-targeted synthetic siRNA, cultured with DMEM containing 5.5 or 30 mM glucose for 72 h, and cardiomyocyte injury was determined by the number of PI positive cells (**A:** $p < 0.01$, $n = 5$), the levels of cCasp3 (**B:** $p < 0.01$, $n = 3$), MitoSOX (**C:** $p < 0.01$, $n = 3$) and $\Delta\Psi$m (**D:** JC-1, $p < 0.05$, $n = 3$). Data were expressed as mean ± SEM and analyzed by two-way ANOVA. Scale bars represent **(A)** 200 μm, **(C)** 200 μm, **(D)** 100 μm, respectively.

degradation. It is thus possible that mitophagy flux may be limited to some degree even if Parkin-mediated mitophagosome formation remains relatively normal under HG conditions. Nevertheless, overexpression of Parkin, a positive regulator of mitophagy, was able to not only accelerate mitophagy (**Figure 6C**) but also attenuate HG-induced cardiomyocyte death (**Figure 9**). These results suggest that enhancing the initiation of mitophagy, i.e., the formation of mitophagosomes, could still be a promising strategy for reducing hyperglycemic cardiotoxicity if the downstream lysosomal function is not severely impaired.

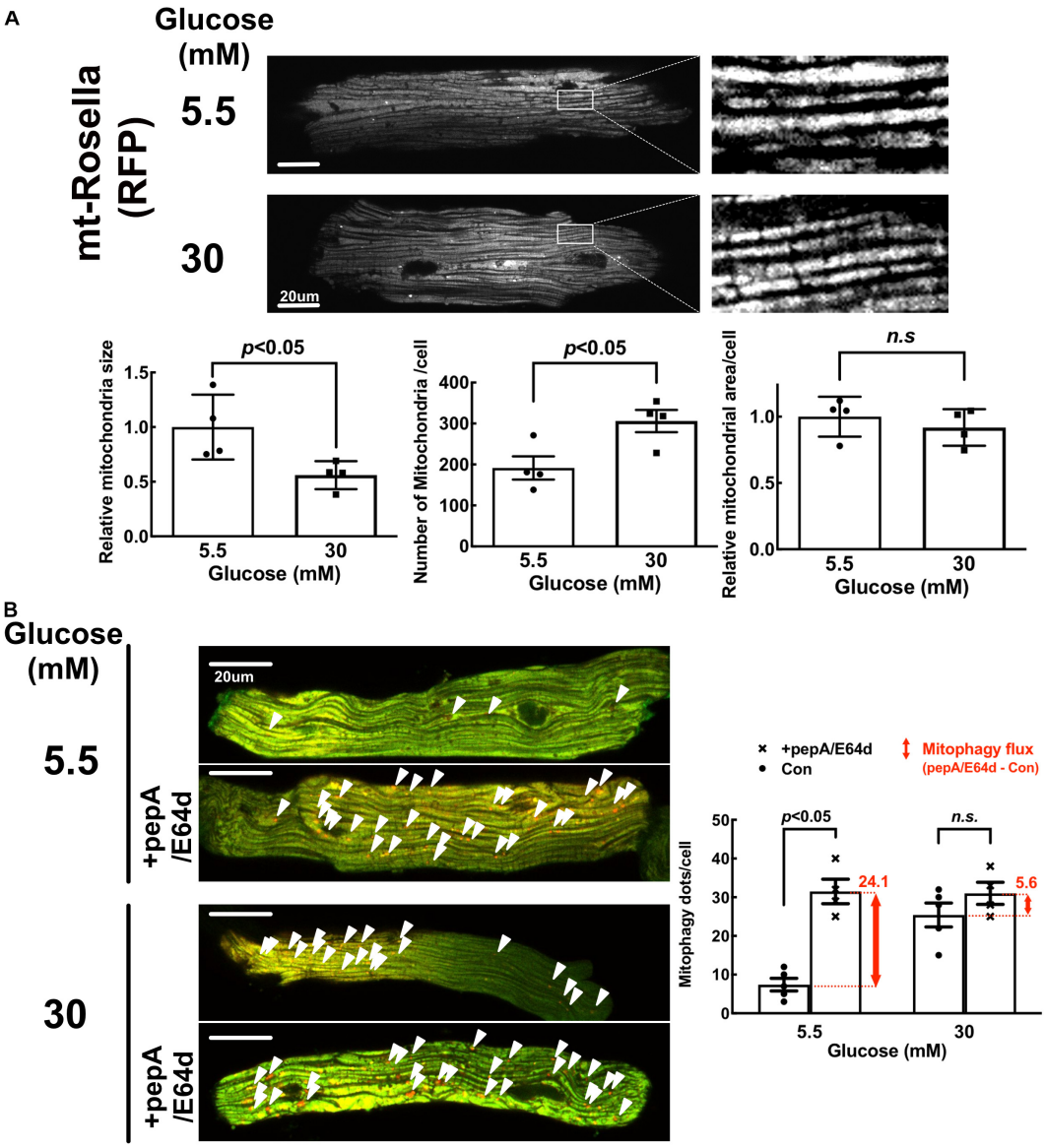

FIGURE 11 | High glucose induced mitochondrial fragmentation but reduced mitophagy flux in adult mouse cardiomyocytes (AMCs). The AMCs were isolated from adult transgenic mouse hearts that express mt-Rosella reporter and cultured with 5.5 or 30 mM glucose for 72 h. **(A)** Red fluorescence images were obtained by confocal microscopy and analyzed with ImageJ. After image optimization, four images were analyzed and the average mitochondrial particle sizes, numbers and areas were calculated. **(B)** The representative images showed mitophagy foci (red puncta indicated by the arrow heads) in AMCs. The number of mitophagy foci was quantified manually. At least four images were captured per treatment. Experiments were repeated with addition of lysosomal inhibitors (PepA and E64D). Mitophagy flux was calculated by subtracting the mean of red puncta without inhibitors from the corresponding mean value of red puncta with inhibitors, which was denoted by the red number and the red vertical line with arrows at both ends in the bar graphs. Data are expressed as mean ± SEM and were analyzed by using unpaired student *t*-test (*$p < 0.01$ vs. 5.5 mM glucose, $n = 5$). Scale bar = 10 μm.

Of note, Parkin overexpression not only enhanced mitophagy but also increased mitochondrial fragmentation (**Figure 6B**), consistent with two previous studies showing that BCL2L13, a mitophagy receptor, was able to concurrently induce mitophagy and mitochondrial fragmentation in HEK293 cells (Dagda et al., 2009; Brand et al., 2018). These results demonstrated a feed-back activation of the fission process by mitophagy which may generate more fragmented mitochondria further stimulating mitophagy as we suggested before (Liang and Kobayashi, 2016). However, other studies showed that Parkin inhibited mitochondrial fragmentation in SH-SY5Y cells (Dagda et al., 2009; Lutz et al., 2009; Wang et al., 2011), exhibiting a feed-back inhibition of fission by mitophagy, in contrast to the above results, which may serve as a brake to prevent excessive mitophagy in this specific context. Nevertheless, it remains to be determined if this

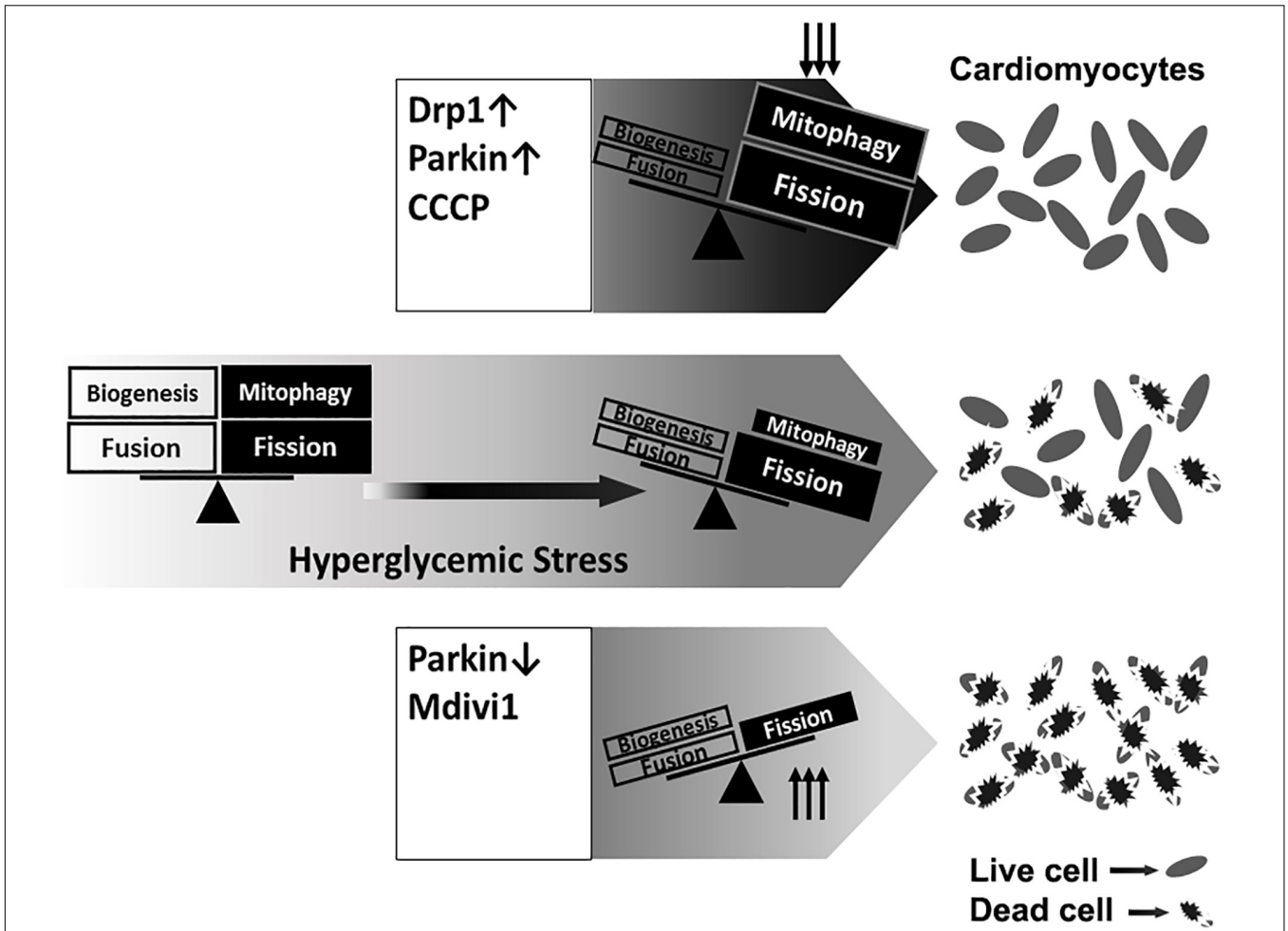

FIGURE 12 | A graphic presentation of the roles of mitochondrial fission and mitophagy in high glucose cardiotoxicity. Mitochondrial quality is controlled by a number of coordinated mechanisms including mitochondrial biogenesis, fission and mitophagy. Injured mitochondrial segments are separated by mitochondrial fission and eliminated by mitophagy. High glucose (hyperglycemic stress) induced mitochondrial fragmentation and inhibited mitophagy, which was associated with increased cardiomyocyte death. Overexpression of DRP1 and Parkin or treatment with the mitochondrial uncoupler CCCP each increased mitophagy and protected from high glucose-induced cardiomyocytes death. Conversely, the fission inhibitor Mdivi-1 and Parkin knockdown exacerbated high glucose-induced cardiomyocyte death. These results suggest that promoting the positive interaction between mitochondrial fission and mitophagy while simultaneously maintain their levels within the physiological range would be expected to improve mitochondrial health, alleviating hyperglycemic cardiotoxicity.

feed-back inhibition mechanism exists in cardiomyocytes under conditions other than HG.

Interestingly but not surprisingly, DRP1 overexpression not only increased mitochondrial fission, but also accelerated mitophagy flux (**Figure 4C**), which may partly account for the protective effects of DRP1-dependent mitochondrial fission. Collectively, these data revealed a reciprocal positive feedback/forward loop that controls mitochondrial fission and mitophagy in cardiomyocytes (**Figure 12**). Apparently, further studies are needed to elucidate the underlying signaling mechanisms that regulate the interaction or cross-talk between mitochondrial fission and mitophagy. This may lead to the identification of new therapeutic strategies to reducing hyperglycemic cardiotoxicity.

In summary, the present study showed that HG-induced mitochondrial fragmentation was an adaptive response that served to limit rather than mediate HG cardiotoxicity as previously thought. We also revealed a positive regulatory loop by which mitochondrial fission and mitophagy activated each other to enhance mitochondrial quality control. Accordingly, strategies that promote the reciprocal positive interaction between mitochondrial fission and mitophagy and simultaneously keep their levels within the physiological range would be expected to improve mitochondrial health, alleviating HG cardiotoxicity.

DATA AVAILABILITY STATEMENT

The original contributions presented in the study are included in the article/**Supplementary Material**, further inquiries can be directed to the corresponding author/s.

ETHICS STATEMENT

The animal study was reviewed and approved by the Institutional Animal Care and Use Committee at NYIT College of Osteopathic Medicine.

AUTHOR CONTRIBUTIONS

SK and QL designed the research, analyzed the data, and wrote the manuscript. SK, FZ, ZZ, TK, and YH performed the research. BS and WW edited the manuscript. All authors contributed to the article and approved the submitted version.

FUNDING

This study was supported by a Scientist Development Grant from American Heart Association (15SDG25080077) to SK and a Career Development Grant (1-09-CD-09) from the American Diabetes Association to QL.

ACKNOWLEDGMENTS

We would like to thank the Center for Biomedical Innovation at New York Institute of Technology (NYIT) for helping obtain the confocal images.

SUPPLEMENTARY MATERIAL

The Supplementary Material for this article can be found online at: https://www.frontiersin.org/articles/10.3389/fphys.2020.604069/full#supplementary-material

REFERENCES

Ackers-Johnson, M., Li, P. Y., Holmes, A. P., O'Brien, S. M., Pavlovic, D., and Foo, R. S. (2016). A simplified, langendorff-free method for concomitant isolation of viable cardiac myocytes and nonmyocytes from the adult mouse heart. *Circ. Res.* 119, 909–920. doi: 10.1161/circresaha.116.309202

Ashrafian, H., Docherty, L., Leo, V., Towlson, C., Neilan, M., Steeples, V., et al. (2010). A mutation in the mitochondrial fission gene Dnm1l leads to cardiomyopathy. *PLoS Genet.* 6:e1001000. doi: 10.1371/journal.pgen.1001000

Boudina, S., and Abel, E. D. (2006). Mitochondrial uncoupling: a key contributor to reduced cardiac efficiency in diabetes. *Physiology* 21, 250–258. doi: 10.1152/physiol.00008.2006

Boudina, S., and Abel, E. D. (2007). Diabetic cardiomyopathy revisited. *Circulation* 115, 3213–3223. doi: 10.1161/circulationaha.106.679597

Brand, C. S., Tan, V. P., Brown, J. H., and Miyamoto, S. (2018). RhoA regulates Drp1 mediated mitochondrial fission through ROCK to protect cardiomyocytes. *Cell. Signal.* 50, 48–57. doi: 10.1016/j.cellsig.2018.06.012

Bugger, H., and Abel, E. D. (2008). Molecular mechanisms for myocardial mitochondrial dysfunction in the metabolic syndrome. *Clin. Sci.* 114, 195–210. doi: 10.1042/cs20070166

Cahill, T. J., Leo, V., Kelly, M., Stockenhuber, A., Kennedy, N. W., Bao, L., et al. (2015). Resistance of dynamin-related Protein 1 oligomers to disassembly impairs mitophagy, resulting in myocardial inflammation and heart failure. *J. Biol. Chem.* 290, 25907–25919. doi: 10.1074/jbc.m115.665695

Cai, L., Li, W., Wang, G., Guo, L., Jiang, Y., and Kang, Y. J. (2002). Hyperglycemia-induced apoptosis in mouse myocardium: mitochondrial cytochrome C-mediated caspase-3 activation pathway. *Diabetes Metab. Res. Rev.* 51, 1938–1948. doi: 10.2337/diabetes.51.6.1938

Catanzaro, M. P., Weiner, A., Kaminaris, A., Li, C., Cai, F., Zhao, F., et al. (2019). Doxorubicin-induced cardiomyocyte death is mediated by unchecked mitochondrial fission and mitophagy. *FASEB J.* 33, 11096–11108. doi: 10.1096/fj.201802663r

Dagda, R. K., Cherra, S. J. III, Kulich, S. M., Tandon, A., Park, D., and Chu, C. T. (2009). Loss of PINK1 function promotes mitophagy through effects on oxidative stress and mitochondrial fission. *J. Biol. Chem.* 284, 13843–13855. doi: 10.1074/jbc.m808515200

Disatnik, M. H., Ferreira, J. C., Campos, J. C., Gomes, K. S., Dourado, P. M., Qi, X., et al. (2013). Acute inhibition of excessive mitochondrial fission after myocardial infarction prevents long-term cardiac dysfunction. *J. Am. Heart Assoc.* 2:e000461.

Eisner, V., Cupo, R. R., Gao, E., Csordas, G., Slovinsky, W. S., Paillard, M., et al. (2017). Mitochondrial fusion dynamics is robust in the heart and depends on calcium oscillations and contractile activity. *Proc. Natl. Acad. Sci. U.S.A.* 114, E859–E868.

Frustaci, A., Kajstura, J., Chimenti, C., Jakoniuk, I., Leri, A., Maseri, A., et al. (2000). Myocardial cell death in human diabetes. *Circ. Res.* 87, 1123–1132. doi: 10.1161/01.res.87.12.1123

Gawlowski, T., Suarez, J., Scott, B., Torres-Gonzalez, M., Wang, H., Schwappacher, R., et al. (2012). Modulation of dynamin-related protein 1 (DRP1) function by increased O-linked-beta-N-acetylglucosamine modification (O-GlcNAc) in cardiac myocytes. *J. Biol. Chem.* 287, 30024–30034. doi: 10.1074/jbc.m112.390682

Gharanei, M., Hussain, A., Janneh, O., and Maddock, H. (2013). Attenuation of doxorubicin-induced cardiotoxicity by mdivi-1: a mitochondrial Division/Mitophagy inhibitor. *PLoS One* 8:e77713. doi: 10.1371/journal.pone.0077713

Ghosh, S., Pulinilkunnil, T., Yuen, G., Kewalramani, G., An, D., Qi, D., et al. (2005). Cardiomyocyte apoptosis induced by short-term diabetes requires mitochondrial GSH depletion. *Am. J. Physiol. Heart Circ. Physiol.* 289, H768–H776.

Givvimani, S., Munjal, C., Tyagi, N., Sen, U., Metreveli, N., and Tyagi, S. C. (2012). Mitochondrial division/mitophagy inhibitor (Mdivi) ameliorates pressure overload induced heart failure. *PLoS One* 7:e32388. doi: 10.1371/journal.pone.0032388

Ikeda, Y., Shirakabe, A., Maejima, Y., Zhai, P., Sciarretta, S., Toli, J., et al. (2015). Endogenous drp1 mediates mitochondrial autophagy and protects the heart against energy stress. *Circ. Res.* 116, 264–278. doi: 10.1161/circresaha.116.303356

Iribarren, C., Karter, A. J., Go, A. S., Ferrara, A., Liu, J. Y., Sidney, S., et al. (2001). Glycemic control and heart failure among adult patients with diabetes. *Circulation* 103, 2668–2673. doi: 10.1161/01.cir.103.22.2668

Ishihara, T., Ban-Ishihara, R., Maeda, M., Matsunaga, Y., Ichimura, A., Kyogoku, S., et al. (2015). Dynamics of mitochondrial DNA nucleoids regulated by mitochondrial fission is essential for maintenance of homogeneously active mitochondria during neonatal heart development. *Mol. Cell. Biol.* 35, 211–223. doi: 10.1128/mcb.01054-14

Jia, G., Whaley-Connell, A., and Sowers, J. R. (2018). Diabetic cardiomyopathy: a hyperglycaemia- and insulin-resistance-induced heart disease. *Diabetologia* 61, 21–28. doi: 10.1007/s00125-017-4390-4

Kageyama, Y., Hoshijima, M., Seo, K., Bedja, D., Sysa-Shah, P., Andrabi, S. A., et al. (2014). Parkin-independent mitophagy requires Drp1 and maintains the integrity of mammalian heart and brain. *EMBO J.* 33, 2798–2813. doi: 10.15252/embj.201488658

Kobayashi, S., Patel, J., Zhao, F., Huang, Y., Kobayashi, T., and Liang, Q. (2020a). Novel dual-fluorescent mitophagy reporter reveals a reduced mitophagy flux

in type 1 diabetic mouse heart. *J. Am. Osteopath. Assoc.* 120, 446–455. doi: 10.7556/jaoa.2020.072

Kobayashi, S., Zhao, F., Kobayashi, T., Hagiwara, M., Kaminaris, A., Li, C., et al. (2020b). Hyperglycemia-induced cardiomyocyte death is mediated by lysosomal membrane injury and aberrant expression of cathepsin D. *Biochem. Biophys. Res. Commun.* 523, 239–245. doi: 10.1016/j.bbrc.2019.12.051

Kobayashi, S., Xu, X., Chen, K., and Liang, Q. (2012). Suppression of autophagy is protective in high glucose-induced cardiomyocyte injury. *Autophagy* 8, 577–592. doi: 10.4161/auto.18980

Liang, Q., and Kobayashi, S. (2016). Mitochondrial quality control in the diabetic heart. *J. Mol. Cell Cardiol.* 95, 57–69. doi: 10.1016/j.yjmcc.2015.12.025

Loson, O. C., Song, Z., Chen, H., and Chan, D. C. (2013). Fis1, Mff, MiD49, and MiD51 mediate Drp1 recruitment in mitochondrial fission. *Mol. Biol. Cell* 24, 659–667. doi: 10.1091/mbc.e12-10-0721

Lutz, A. K., Exner, N., Fett, M. E., Schlehe, J. S., Kloos, K., Lammermann, K., et al. (2009). Loss of parkin or PINK1 function increases Drp1-dependent mitochondrial fragmentation. *J. Biol. Chem.* 284, 22938–22951. doi: 10.1074/jbc.m109.035774

Makino, A., Suarez, J., Gawlowski, T., Han, W., Wang, H., Scott, B. T., et al. (2011). Regulation of mitochondrial morphology and function by O-GlcNAcylation in neonatal cardiac myocytes. *Am. J. Physiol. Regul. Integr. Comp. Physiol.* 300, R1296–R1302.

Malhotra, A., Begley, R., Kang, B. P., Rana, I., Liu, J., Yang, G., et al. (2005). PKC-{varepsilon}-dependent survival signals in diabetic hearts. *Am. J. Physiol. Heart Circ. Physiol.* 289, H1343–H1350.

Mijaljica, D., Prescott, M., and Devenish, R. J. (2011). A fluorescence microscopy assay for monitoring mitophagy in the yeast Saccharomyces cerevisiae. *J. Vis. Exp.* 2011:2779.

Nah, J., Miyamoto, S., and Sadoshima, J. (2017). Mitophagy as a protective mechanism against myocardial stress. *Compr. Physiol.* 7, 1407–1424. doi: 10.1002/cphy.c170005

Ong, S. B., Subrayan, S., Lim, S. Y., Yellon, D. M., Davidson, S. M., and Hausenloy, D. J. (2010). Inhibiting mitochondrial fission protects the heart against ischemia/reperfusion injury. *Circulation* 121, 2012–2022. doi: 10.1161/circulationaha.109.906610

Poornima, I. G., Parikh, P., and Shannon, R. P. (2006). Diabetic cardiomyopathy: the search for a unifying hypothesis. *Circ. Res.* 98, 596–605. doi: 10.1161/01.res.0000207406.94146.c2

Schilling, J. D. (2015). The mitochondria in diabetic heart failure: from pathogenesis to therapeutic promise. *Antioxid. Redox Signal.* 22, 1515–1526. doi: 10.1089/ars.2015.6294

Shao, D., Kolwicz, S. C., Wang, P., Roe, N. D., Villet, O., Nishi, K., et al. (2020). Increasing fatty acid oxidation prevents high fat diet induced cardiomyopathy through regulating parkin mediated mitophagy. *Circulation* 142, 983–997. doi: 10.1161/circulationaha.119.043319

Sharp, W. W., Fang, Y. H., Han, M., Zhang, H. J., Hong, Z., Banathy, A., et al. (2014). Dynamin-related protein 1 (Drp1)-mediated diastolic dysfunction in myocardial ischemia-reperfusion injury: therapeutic benefits of Drp1 inhibition to reduce mitochondrial fission. *FASEB J.* 28, 316–326. doi: 10.1096/fj.12-226225

Shen, X., Ye, G., Metreveli, N. S., and Epstein, P. N. (2005). Cardiomyocyte defects in diabetic models and protection with cardiac-targeted transgenes. *Methods Mol. Med.* 112, 379–388. doi: 10.1385/1-59259-879-x:379

Shen, X., Zheng, S., Metreveli, N. S., and Epstein, P. N. (2006). Protection of cardiac mitochondria by overexpression of MnSOD reduces diabetic cardiomyopathy. *Diabetes Metab. Res. Rev.* 55, 798–805. doi: 10.2337/diabetes.55.03.06.db05-1039

Shen, X., Zheng, S., Thongboonkerd, V., Xu, M., Pierce, W. M. Jr., Klein, J. B., et al. (2004). Cardiac mitochondrial damage and biogenesis in a chronic model of type 1 diabetes. *Am. J. Physiol. Endocrinol. Metab.* 287, E896–E905.

Sivitz, W. I., and Yorek, M. A. (2010). Mitochondrial dysfunction in diabetes: from molecular mechanisms to functional significance and therapeutic opportunities. *Antioxid. Redox Signal.* 12, 537–577. doi: 10.1089/ars.2009.2531

Song, M., Gong, G., Burelle, Y., Gustafsson, A. B., Kitsis, R. N., Matkovich, S. J., et al. (2015a). Interdependence of parkin-mediated mitophagy and mitochondrial fission in adult mouse hearts. *Circ. Res.* 117, 346–351. doi: 10.1161/circresaha.117.306859

Song, M., Mihara, K., Chen, Y., Scorrano, L., and Dorn, G. W. II (2015b). Mitochondrial fission and fusion factors reciprocally orchestrate mitophagic culling in mouse hearts and cultured fibroblasts. *Cell Metab.* 21, 273–285. doi: 10.1016/j.cmet.2014.12.011

Stratton, I. M., Adler, A. I., Neil, H. A., Matthews, D. R., Manley, S. E., Cull, C. A., et al. (2000). Association of glycaemia with macrovascular and microvascular complications of type 2 diabetes (UKPDS 35): prospective observational study. *BMJ* 321, 405–412. doi: 10.1136/bmj.321.7258.405

Tang, Y., Liu, J., and Long, J. (2015). Phosphatase and tensin homolog-induced putative kinase 1 and Parkin in diabetic heart: role of mitophagy. *J. Diabetes Investig* 6, 250–255. doi: 10.1111/jdi.12302

Tomita, M., Mukae, S., Geshi, E., Umetsu, K., Nakatani, M., and Katagiri, T. (1996). Mitochondrial respiratory impairment in streptozotocin-induced diabetic rat heart. *Jpn. Circ. J.* 60, 673–682. doi: 10.1253/jcj.60.673

Tong, M., Saito, T., Zhai, P., Oka, S. I., Mizushima, W., Nakamura, M., et al. (2019). Mitophagy is essential for maintaining cardiac function during high fat diet-induced diabetic cardiomyopathy. *Circ. Res.* 124, 1360–1371. doi: 10.1161/circresaha.118.314607

Twig, G., Elorza, A., Molina, A. J., Mohamed, H., Wikstrom, J. D., Walzer, G., et al. (2008). Fission and selective fusion govern mitochondrial segregation and elimination by autophagy. *EMBO J.* 27, 433–446. doi: 10.1038/sj.emboj.7601963

Wang, H., Song, P., Du, L., Tian, W., Yue, W., Liu, M., et al. (2011). Parkin ubiquitinates Drp1 for proteasome-dependent degradation: implication of dysregulated mitochondrial dynamics in Parkinson disease. *J. Biol. Chem.* 286, 11649–11658. doi: 10.1074/jbc.m110.144238

Wang, S., Zhao, Z., Fan, Y., Zhang, M., Feng, X., Lin, J., et al. (2019). Mst1 inhibits Sirt3 expression and contributes to diabetic cardiomyopathy through inhibiting Parkin-dependent mitophagy. *Biochim. Biophys. Acta Mol. Basis Dis.* 1865, 1905–1914. doi: 10.1016/j.bbadis.2018.04.009

Wang, X., West, J. A., Murray, A. J., and Griffin, J. L. (2015). Comprehensive metabolic profiling of age-related mitochondrial dysfunction in the high-Fat-Fed ob/ob mouse heart. *J. Proteome Res.* 14, 2849–2862. doi: 10.1021/acs.jproteome.5b00128

Xu, X., Chen, K., Kobayashi, S., Timm, D., and Liang, Q. (2012). Resveratrol attenuates doxorubicin-induced cardiomyocyte death via inhibition of p70 S6 kinase 1-mediated autophagy. *J. Pharmacol. Exp. Ther.* 341, 183–195. doi: 10.1124/jpet.111.189589

Xu, X., Kobayashi, S., Chen, K., Timm, D., Volden, P., Huang, Y., et al. (2013). Diminished autophagy limits cardiac injury in mouse models of type 1 diabetes. *J. Biol. Chem.* 288, 18077–18092. doi: 10.1074/jbc.m113.474650

Yu, J., Maimaitili, Y., Xie, P., Wu, J. J., Wang, J., Yang, Y. N., et al. (2017). High glucose concentration abrogates sevoflurane post-conditioning cardioprotection by advancing mitochondrial fission but dynamin-related protein 1 inhibitor restores these effects. *Acta Physiol.* 220, 83–98. doi: 10.1111/apha.12812

Yu, T., Jhun, B. S., and Yoon, Y. (2011). High-glucose stimulation increases reactive oxygen species production through the calcium and mitogen-activated protein kinase-mediated activation of mitochondrial fission. *Antioxid. Redox Signal.* 14, 425–437. doi: 10.1089/ars.2010.3284

Yu, T., Robotham, J. L., and Yoon, Y. (2006). Increased production of reactive oxygen species in hyperglycemic conditions requires dynamic change of mitochondrial morphology. *Proc. Natl. Acad. Sci. U.S.A.* 103, 2653–2658. doi: 10.1073/pnas.0511154103

Yu, T., Sheu, S. S., Robotham, J. L., and Yoon, Y. (2008). Mitochondrial fission mediates high glucose-induced cell death through elevated production of reactive oxygen species. *Cardiovasc. Res.* 79, 341–351. doi: 10.1093/cvr/cvn104

Conflict of Interest: The authors declare that the research was conducted in the absence of any commercial or financial relationships that could be construed as a potential conflict of interest.

frontiers in Physiology

REVIEW
published: 17 December 2020
doi: 10.3389/fphys.2020.612927

Neddylation, an Emerging Mechanism Regulating Cardiac Development and Function

Jie Li[1†], Jianqiu Zou[1†], Rodney Littlejohn[1], Jinbao Liu[2] and Huabo Su[1]*

[1] Vascular Biology Center, Medical College of Georgia, Augusta University, Augusta, GA, United States, [2] Protein Modification and Degradation Lab, School of Basic Medical Sciences, Guangzhou Medical University, Guangzhou, China

Defects in protein quality control have been increasingly recognized as pathogenic factors in the development of heart failure, a persistent devastating disease lacking efficacious therapies. Ubiquitin and ubiquitin-like proteins, a family of post-translational modifying polypeptides, play important roles in controlling protein quality by maintaining the stability and functional diversity of the proteome. NEDD8 (neural precursor cell expressed, developmentally downregulated 8), a small ubiquitin-like protein, was discovered two decades ago but until recently the biological significance of NEDD8 modifications (neddylation) in the heart has not been appreciated. In this review, we summarize the current knowledge of the biology of neddylation, highlighting several mechanisms by which neddylation regulates the function of its downstream targets, and discuss the expanding roles for neddylation in cardiac physiology and disease, with an emphasis on cardiac protein quality control. Finally, we outline challenges linked to the study of neddylation in health and disease.

Keywords: NEDD8 (neural precursor cell expressed developmentally down-regulated 8), Ubiquitin-like protein, Neddylation, cardiomyopathy, Heart Failure

OPEN ACCESS

Edited by:
Hui-Hua Li,
Dalian Medical University, China

Reviewed by:
Md. Shenuarin Bhuiyan,
LSU Health Shreveport, United States
Yi Sun,
Zhejiang University, China

***Correspondence:**
Huabo Su
HSU@augusta.edu

[†] These authors have contributed equally to this work

Specialty section:
This article was submitted to Striated Muscle Physiology, a section of the journal Frontiers in Physiology

Received: *01 October 2020*
Accepted: *20 November 2020*
Published: *17 December 2020*

Citation:
Li J, Zou J, Littlejohn R, Liu J and Su H (2020) Neddylation, an Emerging Mechanism Regulating Cardiac Development and Function. Front. Physiol. 11:612927. doi: 10.3389/fphys.2020.612927

INTRODUCTION

Heart failure is expected to remain the main cardiovascular event responsible for hospitalization throughout the world, including the US (Benjamin et al., 2019). Substantial research efforts in recent decades have identified derangement of cellular protein homeostasis as an important mechanism underlying the initiation and progression of different forms of cardiac disease. These findings have led to heightened interest in protein quality control in cardiomyocytes. In general, protein quality is closely monitored by protein chaperones and degradation machineries. In response to cellular stresses that lead to protein misfolding and damage, chaperones first attempt to restore the tertiary conformation of the protein. The proteasome and (macro) autophagy subsequently serve to degrade proteins that escape the surveillance of chaperones as well as those that are no longer needed by the cell.

Although these key factors have long attracted considerable research attention, an emerging concept posits that diverse post-translational modifications (PTMs) also play pivotal roles in protein quality control and homeostasis. Upon synthesis, nascent proteins can be modified by chemical groups or polypeptides via enzymatic reactions. In eukaryotic cells, more than 300 PTMs have been identified, including acetylation, methylation, phosphorylation, glycosylation, ubiquitination and sumoylation, among many others. PTMs alter the stability, subcellular

distribution, activity and interactome of the modified substrates, and therefore have pleiotropic impacts on the functionality of target proteins. These PTMs represent vital mechanisms that regulate virtually every aspect of cell physiology. Not surprisingly, flaws in these processes can result in many forms of human disease, including heart failure.

The ubiquitin superfamily—the major polypeptide class of protein modifiers—comprises ∼17 members, including ubiquitin (Ub), SUMO proteins, NEDD8, ISG15, FAT10, HUB1, UFM1, URM1, and ATG8 (Li et al., 2018). Ubiquitin-like proteins (UBLs) share varying degrees of similarity in amino acid sequence and tertiary structure with ubiquitin. UBLs are often synthesized as precursor proteins that require proteolytic cleavage and maturation, and employ an E1-E2-E3 enzymatic cascade similar to that of ubiquitination for attachment to protein substrates (Sun, 2003). Despite these broad similarities between Ub and UBLs, individual UBLs are functionally distinct from Ub, and indeed from each other, and have broad biological functions (Gomes, 2018).

Polypeptide PTMs have several unique features compared with chemical modifications. First, addition of one or a chain of polypeptides to proteins can significantly alter the molecular weight and charge of proteins and thereby drastically impact their structure and function. Second, these modifications are catalyzed by a hierarchy of enzymes that are much more complex than those that mediate chemical modifications. In the case of ubiquitination, there are several E1 activating enzymes, a dozen E2 conjugating enzymes and hundreds of E3 ligases (Glickman and Ciechanover, 2002), which coordinately mediate the modification of thousands of protein substrates. Notably, there are approximately 100 deubiquitinases that reverse this modification. Third, proteins can be modified at one or multiple lysine residues by either a single molecule (mono- and multi-mono modification) or a chain of modifiers. Since each individual polypeptide modifier contains multiple lysine residues that can serve as attachment points for chain extension, protein substrates can be modified by homo- and heterotypic polymers, and even branched polymers (Glickman and Ciechanover, 2002), further expanding the diversity of modification patterns. Together, the complexity of the enzymatic cascade and modification linkage types confer multiple points for regulation of protein function and provide countless opportunities for propagating specific signals.

In the heart, ubiquitin, SUMO and ISG15 PTMs have been linked to the pathogenesis of cardiomyopathy (Wang and Robbins, 2006; Kho et al., 2011; Rahnefeld et al., 2014; Willis et al., 2014; Mendler et al., 2016) and have become attractive therapeutic targets in the prevention and treatment of cardiac disease (Henning and Brundel, 2017). In contrast, the significance of other UBLs remains rarely explored in cardiac tissues. Among all UBLs, NEDD8 (neural precursor cell expressed developmentally downregulated 8) shares the highest homology with Ub, exhibiting approximately 60% sequence identity, and like Ub, contains three β-pleated sheet structures centered around one central α helix (Rao-Naik et al., 1998). In the last decade, the conjugation of proteins with NEDD8, hereafter termed neddylation, has emerged as a novel regulatory mechanism for the control of diverse cellular functions. Moreover, recent studies have pointed to the NEDD8 system as a major contributor to tissue homeostasis and as a key player in the progression of different disease states, including developmental defects (Lykke-Andersen et al., 2003; Tomoda et al., 2004; Menon et al., 2007), neointimal hyperplasia (Ai et al., 2018), atherogenesis (Asare et al., 2017), tumorigenesis (Soucy et al., 2010), fatty liver (Zhang X. et al., 2020), obesity (Park et al., 2016), neurodegenerative disorders (Vogl et al., 2015; Zhang L. et al., 2020) and more recently, heart failure (**Figure 1**). In this review, we first provide an overview of the neddylation pathway and outline the mechanisms by which neddylation modulates protein function; we then focus on heart-specific functions of neddylation. In particular, we will examine the involvement of neddylation in cardiac disease; summarize the role of neddylation and deneddylation in regulating cardiac development, contractility and protein quality control; and identify challenges in understanding the significance of neddylation in health and disease.

THE NEDDYLATION ENZYMATIC CASCADE

First cloned from the murine brain in 1993, NEDD8 is ubiquitously expressed, with the highest expression seen in striated muscles (Kumar et al., 1993; Kamitani et al., 1997). NEDD8 is highly evolutionarily conserved, sharing 100% homology among mouse, rat and human orthologs, and 83% homology with *Arabidopsis* paralogs (Kamitani et al., 1997). NEDD8 is initially synthesized as an 81-amino acid precursor protein that subsequently undergoes proteolytic cleavage to expose glycine-76 at the C-terminus. Several isopeptidases,

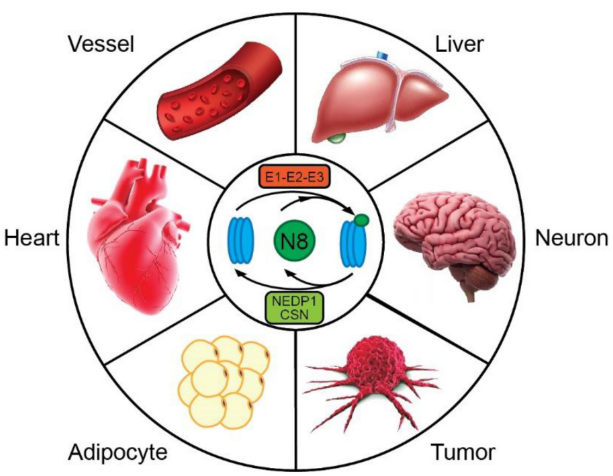

FIGURE 1 | Neddylation has emerged as a powerful mechanism for regulating cellular physiology in a variety of tissues. Dysregulation of neddylation has been linked to vascular diseases, such as neointima formation and atherosclerosis, liver steatosis, cognitive deficits, tumor growth, obesity, and heart failure. Modulation of this pathway may provide opportunities for combating diverse human disorders.

including UCH-L3, USP21 and NEDP1, have been reported to facilitate NEDD8 maturation (Gan-Erdene et al., 2003; Frickel et al., 2007). Deletion of either UCH-L3 in mice or NEDP1 in cells does not abolish neddylation (Kwon et al., 2004; Bailly et al., 2019), suggesting the functional redundancy of enzymes involved in NEDD8 maturation.

Conjugation of NEDD8 to proteins is mediated by NEDD8-specific E1-E2-E3 enzymes in a manner similar to ubiquitination (**Figure 2**). Unlike the highly hierarchical ubiquitination cascade, neddylation is mainly catalyzed by one E1 activating enzyme (NAE), two E2 conjugation enzymes (UBE2M/UBC12 and UBE2F), and a number of E3 ligases. Matured NEDD8 forms a thioester bond with NAE in an ATP-dependent reaction. Once activated, NEDD8 is then transferred between the active cysteine residue of NAE to an E2 conjugating enzyme, either UBE2M or UBE2F. Interaction of the E2 enzyme with an E3 enzyme leads to transfer of the NEDD8 moiety and formation of a covalent isopeptide bond between the C-terminal glycine-76 of NEDD8 and a lysine residue on the substrate protein (Gong and Yeh, 1999; Soucy et al., 2009).

Selective activation of NEDD8, but not other UBLs, is regulated by the NEDD8 E1, NAE. Despite the similarity of NEDD8 and Ub, NAE can distinguish the two protein modifiers at single amino acid resolution by recognizing alanine 72 on NEDD8 (arginine 72 on ubiquitin) (Whitby et al., 1998). NAE is a heterodimer consisting of the regulatory subunit, NAE1, and the catalytic subunit, UBA3, the latter containing an active cysteine residue (C237) essential for the formation of an NAE-NEDD8 thioester. MLN4924 (Pevonedistat), a potent and selective inhibitor of NAE currently in phase I/II/III clinical trials for the treatment of a range of human cancers (https://www.clinicalltrials.gov/), is structurally related to AMP and forms an irreversible covalent NEDD8-MLN4924 adduct. This adduct resembles NEDD8-AMP and blocks the NAE active site, thereby abolishing NEDD8 activation and the NEDD8 pathway. The inhibitory effect of MLN4924 on neddylation is highly specific, and its IC_{50} toward NAE is more than 1000-fold higher than that toward E1s of other UBLs.

Two structurally similar neddylation E2s have been identified in eukaryotic cells: the well-characterized UBC12/UBE2M (Gong and Yeh, 1999) and the less-studied UBE2F (Huang et al., 2009). The two E2s appear to have specificity for different protein substrates, at least with respect to cullin family proteins. For instance, UBC12 pairs with RBX1 to mediate neddylation of CUL1-CUL4, whereas UBC2F interacts with RBX2/SAG to regulate CUL5 neddylation (Kwon et al., 2004). Existing evidence suggests that UBC12 plays a dominant role in neddylation, as overexpression of UBC12 itself is able to induce neddylation, and silencing of UBC12 diminishes neddylation (Gong and Yeh, 1999; Li et al., 2019). Interestingly, a recent study revealed negative regulatory cross-talk between the two E2s such that stress-induced UBC12 acts as a ubiquitin E2 for Parkin that promotes the ubiquitination and degradation of UBE2F (Zhou et al., 2018).

In contrast to the well-defined NEDD8-specific E1 and E2 enzymes, the identities of *bona fide* NEDD8 E3 ligases remain poorly defined. Several research groups have proposed DCN1-5 (defective in cullin neddylation 1-5) as NEDD8 E3 ligases that mediate cullin neddylation, but the exact function of these proteins is controversial. Some groups claim that DCN proteins function independently as NEDD8-specific E3 ligases, whereas others believe that they are simply E3 ligase co-factors (Meyer-Schaller et al., 2009; Huang et al., 2011; Wu et al., 2011). In addition to DCN family proteins, a dozen proteins, including c-Cbl, MDM2, XIAP and SMURF1, have been reported to act as NEDD8 E3 ligases (Xirodimas et al., 2004; Watson et al., 2006; Kim et al., 2008; Broemer et al., 2010; Huang et al., 2011; Embade et al., 2012; Zuo et al., 2013). Interestingly, most of these proteins are also known as Ub E3 ligases. Whether there are specific signals that drive these E3s to promote either neddylation or ubiquitination and whether these E3s work in conjunction with the respective cognate E2 enzymes (either NEDD8 E2 or Ub E2) to determine the fate of the modification remains unclear. Experimental evidence supporting either notion remains scarce.

Like ubiquitination, neddylation is dynamically regulated under normal physiological conditions. Although a number of isopeptidases are capable of deconjugating NEDD8 moieties from protein substrates *in vitro* (Rabut and Peter, 2008; Xirodimas, 2008), only NEDP1 (NEDD8-specific protease 1, also known as SEPN8 and DCN1) and CSN (COP9 signalosome) appear to be NEDD8-specific. CSN is a zinc metalloprotease comprising eight subunits, CSN1-CSN8. CSN primarily removes NEDD8 from cullin family proteins, but also deneddylates other non-cullin proteins (Wei et al., 2008). CSN is indispensable for tissue homeostasis and organismal development, and genetic deletion of any CSN subunit in all tissues and organisms tested causes pathological alterations or lethality (Oron et al., 2002; Lykke-Andersen et al., 2003; Yan et al., 2003; Tomoda et al., 2004; Menon et al., 2007; Zhao et al., 2011). These severe phenotypes are often linked to loss of function of cullin proteins, which are thought to control the stability of approximately 20% of intracellular proteins.

In contrast to CSN, NEDP1, a cysteine protease, appears to be more specific for deconjugation of NEDD8 from non-cullin proteins (Mendoza et al., 2003). Initial studies showed that NEDP1 can remove NEDD8 from both cullins and non-cullin proteins in a cell-free system (Wu et al., 2003). However, deficiency of NEDP1 deficiency in *Arabidopsis*, *Drosophila* or mammalian cells results in substantial accumulation of neddylated proteins without impacting cullin neddylation (Mendoza et al., 2003; Wu et al., 2003; Chan et al., 2008; Vogl et al., 2020), suggesting the specificity of NEDP1 for non-cullin proteins. Interestingly, unlike CSN, NEDP1 is dispensable for the viability of *Drosophila* and *Arabidopsis* (Chan et al., 2008; Mergner et al., 2017), suggesting distinct physiological functions of non-cullin protein neddylation *in vivo*. To date, the physiological function of NEDP-mediated deneddylation in mammals remains unclear.

Similar to the case for ubiquitination and sumoylation, NEDD8 can be conjugated to protein targets in a chain at one or multiple lysine residues. Analyses of neddylated peptides from 609 proteins showed an average of 2.03 neddylation sites per protein, with the majority of NEDD8 substrate having only one or two neddylation sites (Vogl et al., 2020). Proteomics studies

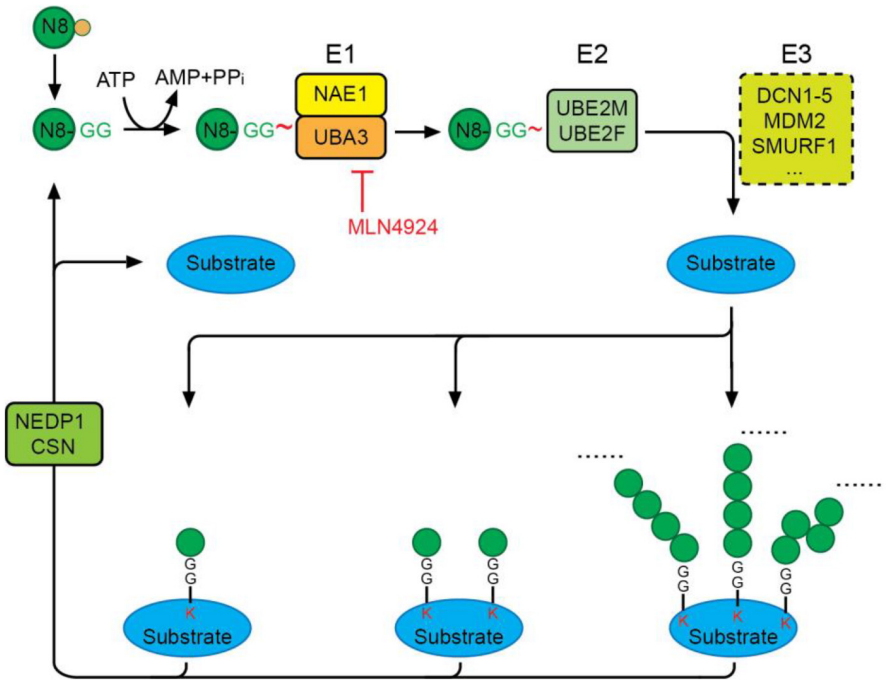

FIGURE 2 | The neddylation cascade. NEDD8 is first synthesized as a precursor that is proteolytically processed to expose its C-terminal glycine. The matured NEDD8 is then activated by forming a thioester linkage with NAE—a heterodimer of UBA3 and NAE1—in an ATP-dependent manner. Activated NEDD8 is then transferred from the active cysteine site of NAE to the active cysteine site of E2 UBE2M or UBE2F. Interaction of E2 with an E3 ligase positions the C-terminal glycine for nucleophilic attack by the lysine residue on the substrate, resulting in covalent linkage of NEDD8 to target proteins via an isopeptide bond. Protein substrates can be modified by mono-, multi-mono, or a chain of NEDD8 via different linkages. The deneddylases, NEDP1 and CSN, catalyze the removal of NEDD8 moieties from substrates. MLN4924 is a specific neddylation inhibitor that acts by preventing NAE-mediated NEDD8 activation.

have provided direct evidence for polyneddylation (Vogl et al., 2020; Leidecker et al., 2012; Singh et al., 2012), reflecting the fact that the NEDD8 chain can be extended on its K6, K11, K22, K27, K48 and K54 residues. Interestingly, NEDP1 appears to be relatively specific for shortening K6-, K11-, K48- and K54-linked NEDD8 chains because loss of NEDP1 results in accumulation of NEDD8 chains with these linkages, whereas other NEDD8 protease may control the lengths of K22- and K27-linked NEDD8 chains (Vogl et al., 2020). Whether polyneddylation with different linkages differentially impacts protein function has thus far remained unknown.

PROTEOME-WIDE IDENTIFICATION OF NEDD8 TARGETS

Given the emerging role of neddylation in health and disease, there is a keen interest in identifying NEDD8 substrates at the proteome-wide level. Cullin family proteins, the first and best characterized NEDD8 targets, serve as scaffolds for cullin-RING E3 Ub ligases (CRLs). Cullin family proteins share a conserved neddylation site (IVRIMK*MR), with neddylation serving to stimulate CRL activity. In addition to cullins, a growing list of proteins have been identified as NEDD8 targets. These include Parkin, PINK1, HIF1α, TGFβRII, MDM2, p53, p73, VHL (Wolf et al., 2020), RPS27L, RPS27 (Xiong et al., 2020) and COFILIN (Vogl et al., 2020), among others [also see reviews (Kandala et al., 2014; Enchev et al., 2015)]. Insights gained from characterizations of these new NEDD8 substrates have expanded our understanding of neddylation in diverse cellular pathways. Nevertheless, proteome-wide identification of NEDD8 substrates has been challenging because of the low abundance of neddylated proteins; the transient and reversible nature of the modification; the inability to discriminate among neddylation, ubiquitination and ISGylation; poor efficiency in enriching neddylated proteins using commercially available NEDD8 antibodies; and concerns about the fidelity of targets identified in cells exogenously overexpressing NEDD8 (Hjerpe et al., 2012; Leidecker et al., 2012). Moreover, the promiscuity of neddylation sites on most identified NEDD8 targets prevents designating a *bona fide* NEDD8 substrate and uncovering the functional significance of neddylation.

Several recent studies have attempted to develop new methods to facilitate unbiased screens of NEDD8 targets. The Sutherland group developed a comprehensive platform for analyzing UBL modifications using *in vivo* biotinylation (Pirone et al., 2017). In this modular multi-cistronic expression platform, the expression of Bio/Avi-tagged NEDD8 and biotin ligase BirA* allows *in vivo* biotinylation of neddylated proteins, and thus efficient enrichment of neddylated proteins, under stringent condition, while the simultaneous introduction of

UBE2M may increase the abundance of neddylated proteins. This approach has been applied to identify several UBL modifications in *Drosophila* cells and transgenic flies. Its effectiveness in identifying NEDD8 targets remains to be demonstrated. Other studies have sought to stabilize the neddylated form of NEDD8 targets utilizing a deconjugation-resistant NEDD8 mutant (L73P) or deletion of NEDP1 (Coleman et al., 2017; Keuss et al., 2019). This strategy has identified UBE2M and NSUN2, among other candidates, as novel NEDD8 substrates in HEK293T and Hela cells. To facilitate the isolation and identification of neddylated peptides, a few groups have taken advantage of a monoclonal antibody that specifically recognizes and captures peptides containing lysine residues modified by diglycine (K-ε-GG) (Xu et al., 2010; Coleman et al., 2017; Vogl et al., 2020), an adduct left at ubiquitin-, NEDD8-, and ISG15-modified sites after trypsin digestion. To discriminate neddylation from the other two modifications, the Sheng group generated NEDD8^{R74K} knock-in HEK293 cells, allowing identification of unique neddylation sites by mass spectrometry after Lys-C digestion and K-ε-GG peptide enrichment. This approach also maintains endogenous NEDD8 levels and thus minimizes potential artifacts resulting from NEDD8 overexpression and non-canonical neddylation mediated by the Ub E1 enzyme, UBE1 (Hjerpe et al., 2012; Leidecker et al., 2012). By screening for differentially expressed neddylated proteins in this NEDD8^{R74K} knock-in cell line upon MLN4924 treatment and NEDP1 deletion, this study identified 607 neddylation sites on 341 proteins. Gene Ontology enrichment analyses revealed that these NEDD8 substrates belong to diverse protein categories, including DNA/RNA-binding proteins, chaperones, ribosomal proteins, chromatin architecture regulators, Ub- and UBL enzymes, and cytoskeletal proteins, indicating a likely crucial function for neddylation in these cellular processes. Notably, analyses of identified neddylated peptides did not reveal a general consensus sequence for NEDD8 modification, a finding that contrasts with the well-known sumoylation motif (Rodriguez et al., 2001). Despite these advancements, there have not yet been efforts to systematically identify NEDD8 targets *in vivo*. However, a 6xHis-FLAG-*Nedd8* knock-in mouse model has been generated and used to validate neddylation of the mitochondrial proteins, ETFA and ETFB (Zhang X. et al., 2020). This unique mouse line could be a valuable tool for profiling the landscape of endogenous NEDD8 proteins in various tissues in a physiologically and pathologically relevant context.

MOLECULAR ACTIONS OF NEDDYLATION

How neddylation precisely regulates protein function is incompletely understood. Similar to other PTMs, neddylation has an impact on the structure and conformation of target proteins, thus altering the assembly/disassembly of protein complexes as well as protein stability, enzymatic activity, subcellular distribution, and/or binding affinity for DNA and proteins. These mechanisms are often intertwined and can act together to regulate protein function.

Regulation of the Assembly of Protein Complexes

The cullin family consists of eight members (cullin 1, 2, 3, 4a, 4b, 5, 7, and 9), which serve as scaffolding units for cullin-RING E3 Ub ligases (CRLs). A typical CRL contains one cullin protein, a Ub E2-interacting RING protein (RBX1 or RBX2), an F-box–interacting adaptor, and a substrate-recognizing F-box protein. Evidence collected from biochemical assays has consistently demonstrated the necessity of reversible cullin neddylation for the assembly and activity of CRLs, as extensively reviewed by others (Keuss et al., 2019). Cryo-electron microscopy analyses of the neddylated CRL1$^{\beta\ TrCP}$-UBE2D complex and the CSN-CRL2 complex further provide insight into structural mechanisms underlying how NEDD8 activation mediates CRL-catalyzed ubiquitination (Faull et al., 2019; Baek et al., 2020). These analyses show that NEDD8 acts as a nexus for conjugating individual cullins and RBX1/RBX2-activated, ubiquitin-charged E2. Local structural alterations of NEDD8 and CRL domains converge to juxtapose the substrate and ubiquitination active site, leading to ubiquitination of the substrate (Xu et al., 2010). Neddylated CRLs can also form complexes with the deconjugating isopeptidase CSN, and this interaction is required for the NEDD8-dependent activation of CSN. CSN-mediated deneddylation of cullins enables binding of CAND1 to the cullin scaffold and prevents binding of substrate-specific adaptor proteins to the CRL complex, thus effectively sequestering E3 ligase from the intracellular environment (Lydeard et al., 2013). Therefore, dynamic cycling of cullin neddylation/deneddylation is central to the assembly and activity of CRLs.

Another piece of evidence comes from neddylation of SHC (Jin et al., 2013), an adaptor protein that bridges the androgen receptor (AR) to the RAS/ERK pathway. It has been proposed that neddylation of SHC at its N-terminal lysine 3 residue facilitates the formation of a ZAP70-SHC-GRB2 complex that is crucial for downstream ERK activation. Consequent inhibition of neddylation prevents ERK activation and suppresses CD4^{+} T-cell function and airway inflammation.

Regulation of Protein Stability

A commonly observed consequence of neddylation is a switch in protein stability, with neddylation either stabilizing or destabilizing the substrate. For instance, PPARγ, a crucial player in the regulation of lipid and glucose metabolism, can be modified at unknown lysine sites, which increases its stability by preventing ubiquitination (Park et al., 2016). Similarly, neddylation of other proteins, including the ribosomal proteins RPS27L and RPS27, mitochondrial proteins ETFA and ETFB, and lipogenic transcription factor SREBP1, also increases their stability (Heo et al., 2020; Xiong et al., 2020; Zhang X. et al., 2020).

In contrast, neddylation of the splicing factor SRSF3, which can be induced by treatment with palmitic acid, promotes SRSF3 degradation by the proteasome (Kumar et al., 2019). Mutation of its neddylation sites prevents SRSF degradation and suppresses

SRSF3-mediated RNA splicing. Similar effects have also been observed for influenza A viral protein PB2, the transcription factor JunB, and TGFβRII (Oved et al., 2006; Li H. et al., 2016; Zhang et al., 2017).

Several scenarios might explain the distinct impact of neddylation on protein stability. First, Ub and NEDD8 share the same modification sites on substrates and thus must compete for these lysine residues. Second, NEDD8 and Ub may target different lysine on a given substrate. In such cases, neddylation of a substrate on one site might serve as a negative or positive signal for ubiquitination at other sites, possibly by altering their conformation and/or accessibility to their cognate Ub ligases. While experimental evidence needed to support these scenarios is currently lacking, the intimate cross-talk between the two modifications confers additional layers of regulation on protein stability and homeostasis.

Regulation of Protein Activity

Neddylation has been shown to control the activity of several E3 Ub ligases. For example, neddylation of Parkin, a Ub ligase that mediates the selective degradation of damaged mitochondria through a process known as mitophagy (Ni et al., 2014), was shown to increase Parkin Ub ligase activity in neuronal and cancer cells, possibly owing to its enhanced association with Ub E2 enzymes and substrates (Choo et al., 2012; Um et al., 2012). Interestingly, PINK1, a protein kinase that positively regulates Parkin activity, was also identified as a NEDD8 target, although the functional consequence of PINK1 neddylation was not determined. In a further example, the HECT ubiquitin ligase SMURF1 is also a target of NEDD8 (Xie et al., 2014). SMURF1 is self-neddylated at multiple lysine residues, and its auto-neddylation requires a C426 active site. Similar to the case for Parkin, neddylation of SMURF1 enhances Ub E2 recruitment and thus SMURF1 Ub ligase activity.

NEDD8 can modify protein kinases and influence their enzymatic activity (Wolf et al., 2020). DNA-dependent protein kinase catalytic subunit (DNA-PKcs) is a core component of nuclear DNA-dependent serine/threonine protein kinase (DNA-PK), the latter of which plays an important role in non-homologous end-joining (NHEJ) repair following DNA damage. Neddylation of DNA-PKcs is mediated by the canonical neddylation enzymes, NAE and UBE2M, as well as the E3 ligase, HUWE1 (Guo et al., 2020). Inhibition of DNA-PKcs neddylation with MLN4924 or by silencing HUWE1 impairs DNA-PKcs autophosphorylation without disturbing its stability, leading to diminished NHEJ efficiency.

Neddylation also regulates the activity of several transcription factors, including p53, p73, E2F1 and HIF1α, among others (Xirodimas et al., 2004; Watson et al., 2006; Ryu et al., 2011; Loftus et al., 2012). Notably, neddylation exerts actions independent of its effects on the stability of these targets. For instance, a recent study identified the AR as a novel NEDD8 target (Yu et al., 2020). Mutation of the AR neddylation sites, K475 and K862, increased AR transcription activity, possibly by enhancing the binding affinity of AR for androgen-response elements on its downstream targets. Deletion of NEDD8 in zebrafish was shown to impair ovarian maturation due to hyperactivation of AR, and loss of one copy of AR rescued the phenotype of NEDD8-null zebrafish (Yu et al., 2020).

Regulation of Subcellular Localization

Several studies have reported that neddylation alters the subcellular distribution of protein targets. Ribosomal proteins are among the most commonly reported neddylation substrates (Xirodimas et al., 2008). For example, neddylation of ribosomal protein L11, mediated by MDM2, prevents L11 translocation from the nucleolus to the nucleoplasm during nucleolar stress (Sundqvist et al., 2009). Nucleolar stress, in turn, induces the rapid and transient recruitment of neddylated L11 to the promoter of p53, thereby enhancing p53 signaling (Mahata et al., 2012). S14, another ribosomal protein, is also modified by NEDD8, and its neddylation is mediated by HDM2 but counteracted by NEDP1 (Zhang et al., 2014). Neddylation appears to cause retention of S14 in the nucleolus and prevent its translocation to the cytoplasm. In addition to ribosomal proteins, the chemokine receptor CXCR5 was reported to be neddylated at lysine 339 in a FANCA-dependent manner (Renaudin et al., 2014). Mutation of this neddylation site diminishes CXCR5 distribution to the cell membrane, suggesting that neddylation is crucial for CXCR5 membrane targeting. In a final example, the E3 ligase RNF111 catalyzes neddylation of the N-terminal lysine of chromatin-localized histone H4. It has been suggested that H4 neddylation may alter chromatin orientation and disrupt internucleosome interactions (Ma et al., 2013), providing access to DNA lesions by DNA damage repair proteins.

ROLE OF NEDDYLATION IN THE HEART

The neddylation pathway has consistently proven critical in maintaining various aspects of cellular, organ and organismal function and development. Perturbations in neddylation or deneddylation pathways using either pharmacological or genetic approaches have been shown to cause developmental defects (Lykke-Andersen et al., 2003; Tomoda et al., 2004; Menon et al., 2007), tumorigenesis (Soucy et al., 2010), metabolic disorders (Park et al., 2016), liver dysfunction (Zhang X. et al., 2020), and neurodegenerative disorders (Vogl et al., 2015; Li L. et al., 2016). The importance of neddylation in health and disease is underscored by its role in regulating cell metabolism, proliferation (Xirodimas et al., 2004; Abida et al., 2007; Guihard et al., 2012), cell death (Knorr et al., 2015), autophagy (Luo et al., 2012), cell signaling (Zuo et al., 2013), protein homeostasis (Petroski and Deshaies, 2005; Lipkowitz and Weissman, 2011), gene transcription (Ryu et al., 2011; Loftus et al., 2012; Aoki et al., 2013), and even mitochondrial turnover (Gong and Yeh, 1999; Kwon et al., 2004; Choo et al., 2012; Um et al., 2012).

NEDD8 is one of the most highly expressed UBL proteins in the heart (Zou et al., 2018) and is highly abundant in skeletal and cardiac muscles compared with other organs (Kamitani et al., 1997). Neddylated proteins with a broad range of molecular weights are readily detected in cardiomyocytes under physiological conditions, suggesting that neddylated proteins are more abundant in these cells than in other cell

types. In this section, we summarize the emerging roles of neddylation in cardiac development and disease and discuss the mechanisms through which neddylation might control pathways that contribute to disease pathogenesis (**Table 1**).

Association of Neddylation With Cardiac Disease

Dysregulation of neddylation has been implicated in cardiomyopathies of various etiologies. This is evidenced by a significant increase in neddylated proteins in failing hearts from patients suffering from dilated and ischemic cardiomyopathy (Li et al., 2015). Similar findings were also obtained in hearts from mouse models recapitulating human desmin-related cardiomyopathy (Li et al., 2015). The aberrant abundance of neddylation is presumably a consequence of activation of neddylation and/or defects in deneddylation, although experimental evidence for the expression of neddylation enzymes is lacking. Thus far, no polymorphisms or mutations in any neddylation enzymes have been linked to cardiac disease, or in fact any other human disease. Given the essential role of neddylation in maintaining organismal viability, it is likely that loss-of-function mutations of neddylation enzymes are developmentally lethal. However, mutations of neddylation targets have been linked to a number of cardiomyopathies. For instance, CUL3 and LZTR1, an adaptor for the CUL3 Ub ligase complex, have been linked to familial hypertension and Noonan syndrome, respectively (Schumacher et al., 2015; Steklov et al., 2018), both of which exhibit cardiac defects. Moreover, homozygous mutations in KLHL24, another substrate-recognizing adaptor protein for CUL3 Ub ligase, have been shown to cause hypertrophic cardiomyopathy in humans (Hedberg-Oldfors et al., 2019). Knockdown of the KLHL24 homolog in zebrafish also results in ventricular failure, providing additional evidence for KLHL24 as a HCM-associated gene (Hedberg-Oldfors et al., 2019). In line with these findings, clinical investigations of the promising anticancer drug MLN4924 have revealed that cardiac failure is a major adverse event (Shah et al., 2016; Swords et al., 2017). Collectively, these lines of evidence implicate neddylation in cardiac disease, calling for an in-depth investigation of its role in the heart.

Neddylation in Cardiac Development and Congenital Heart Disease

Heart development is a complex and tightly regulated series of events requiring precise spatiotemporal regulation of various signaling cascades and cell populations to form a functionally competent pumping organ. As is the case for SUMO modifications (Mendler et al., 2016), PTMs with Ub-like proteins may be an important mechanism underlying cardiac maturation and development.

Existing evidence suggests that highly active and balanced neddylation is critical for perinatal cardiac development. Neddylation is developmentally downregulated in the developing heart: both neddylated proteins and neddylation enzymes are highly expressed in embryonic hearts, but are significantly downregulated at 1 week after birth (Zou et al., 2018), a time when cardiomyocytes exit the cell cycle. αMHC^{Cre}-mediated deletion of the regulatory subunit of the NEDD8 E1 enzyme, NAE1, in mice results in cardiac-specific inhibition of neddylation. Mice lacking NAE1 exhibit cardiomyocyte proliferation arrest as early as embryonic (E) day 14.5 and show pronounced ventricular non-compaction by E16.5, which eventually lead to heart failure and inevitable neonatal lethality (Zou et al., 2018). Moreover, transient inhibition of neddylation by administration of MLN4924 to neonatal rats for 3 days was shown to cause diminished cardiomyocyte proliferation, cardiac hypertrophy and deteriorated cardiac function (Zou et al., 2019), supporting the importance of neddylation in perinatal cardiac growth. Although cardiac function in these animals is restored to a level comparable to their wild-type counterparts in adulthood, they remain more susceptible to isoproterenol-induced heart failure (Zou et al., 2019). This suggests that even transient

TABLE 1 | Roles of neddylation in the heart.

Targeted components	System modified	Phenotypes	Mechanisms	References
Association of neddylation with cardiac disease				
?	Neddylated proteins	Increased in human DCM and ICM	–	Li et al., 2015
?	Neddylated proteins	Increased in mouse DRM	–	Li et al., 2015
Developing heart				
αMHC^{Cre}-NAE1KO	↓neddylation	Perinatal lethality (P2-P3), LVNC	↓CM proliferation, ↓YAP signaling	Zou et al., 2018
MLN4924	↓neddylation	Transient cardiomyopathy	↓CM proliferation	Zou et al., 2019
αMHC^{Cre}-CSN8KO	↓deneddylation	Premature lethality (∼4 weeks), DCM	↓UPS, ↓autophagy, ↑necroptosis	Su et al., 2011b
Post-mitotic heart				
$\alpha MHC^{MerCreMer}$-CSN8KO	↓deneddylation	Lethality in 2 weeks, DCM & HF	↓UPS, ↓autophagy, ↑necroptosis	Su et al., 2013
MLN4924	↓neddylation	Exacerbated ISO-induced HF	?	Zou et al., 2019
Cardiac proteotoxicity				
Global CSN8 hypomorphism	↓deneddylation	Exacerbated DRM	↓UPS, ↑protein aggregates	Wang et al., 2003
NUB1L O/E	↓atypical neddylation	↓CM damage	↑UPS	Li et al., 2015
NUB1L KD	↑atypical neddylation	↑CM damage	↓UPS	Li et al., 2015

DCM, dilated cardiomyopathy; ICM, ischemic cardiomyopathy; DRM, desmin-related cardiomyopathy; KO, knockout; LVNC, left ventricle non-compaction cardiomyopathy; UPS, ubiquitin-proteasome system; HF, heart failure; O/E overexpression; KD, knockdown.

disruption of neddylation in the neonatal stage can lead to permanent deleterious effects on cardiac function in adulthood.

Interestingly, blocking deneddylation in the developing heart can also be catastrophic. Inhibition of CSN deneddylase activity by cardiac-specific deletion of CSN8 was shown to increase total neddylated proteins in the heart. These CSN8-deficient mice developed cardiac hypertrophy by 2 weeks of age, dilated cardiomyopathy with largely reduced contractility at 3 weeks of the age, and ultimately died of heart failure by 4 weeks of age (Su et al., 2011b). These *in vivo* findings indicate that tight control of the degree of neddylation is essential for normal cardiac development.

Myocardial neddylation not only acts through post-translational pathways but also at the transcriptional level to regulate cardiac development. Studies in cancer cells have consistently demonstrated that neddylation directly regulates the stability of a wide range of cell cycle inhibitors (Soucy et al., 2009), an action that may account for the observed arrest of cardiomyocyte proliferation in NAE1-deficient hearts. In the embryonic heart, neddylation also controls the transcription of numerous cell cycle genes through the Hippo-YAP (Yes-associated protein) pathway, which plays a crucial role in heart morphogenesis by enabling cardiomyocyte proliferation and differentiation (Huang et al., 2005; Wackerhage et al., 2014; Zhou et al., 2015; Wang et al., 2018). Inhibition of neddylation in the heart stabilizes the Hippo kinases MST1 and LATS2, which in turn promotes phosphorylation of YAP in the heart, preventing its nuclear translocation and subsequent transactivation of cell cycle genes (Zou et al., 2018). Mechanistically, CUL7 acts as a Ub ligase for MST1 and promotes its degradation in cardiomyocytes (Zou et al., 2018). Thus, neddylation enables cardiac chamber maturation, at least in part, through temporal inactivation of Hippo kinases during development. Consistent with this, transcriptomic analyses of CSN8-deficient hearts have revealed dysregulated expression of a wide array of genes involved in diverse pathways (Abdullah et al., 2017). The role of neddylation in the control of gene expression patterns is also in agreement with studies in flies (Oron et al., 2007; Ullah et al., 2007), which suggest that CSN4 acts as a transcription repressor during embryonic development and controls chromatin remodeling, either directly or indirectly.

The immediate downstream effectors of neddylation in cardiac development could be linked, at least in part, to cullin proteins. In addition to CUL7, mentioned above, CUL3 is also critical for perinatal cardiac development. Mice with a CUL3 deficiency quickly develop heart failure after birth and die within 1 week (Papizan et al., 2018). The underlying mechanisms were purported to be dysregulated cardiac proteome and metabolism, although whether such alterations are primary or secondary to cardiac failure remains unclear. Additionally, the CUL5-Asb2α-Filamin A axis has been implicated in heart morphogenesis (Métais et al., 2018). Asb2α is an adaptor protein of CUL5 Ub ligase that promotes the degradation of the cytoskeleton protein filamin A. Global deletion of Asb2α in mice causes cardiac malformations with defects in valve, atrium and ventricular development before E12.5 and lethality thereafter (Métais et al., 2018), phenotypes that are largely recapitulated in mice with conditional deletion of the same gene in cardiomyocytes. These observations suggest that further efforts to determine the role of cullins in cardiac development are warranted.

Neddylation and Dilated Cardiomyopathy and Heart Failure

Although the biological function of neddylation in developmental processes has been extensively studied and interpreted in the context of cell differentiation and division (Enchev et al., 2015), a number of studies have started to unveil the functional importance of neddylation in post-mitotic organs, including the heart (Su et al., 2011a,b, 2013; Vogl et al., 2015). As noted above, mice lacking CSN8 develop dilated cardiomyopathy and heart failure at the age of 3 to 4 weeks. Since deletion of CSN8 does not cause destabilization of the CSN complex until the first week after birth, when cardiomyocytes have almost completed the last round of proliferation (Su et al., 2011b), the severe cardiac phenotype is not likely attributable to defects in cardiomyocyte proliferation but rather underscores a pivotal role for deneddylation in post-mitotic cardiomyocytes. Indeed, tamoxifen-induced knockout of CSN8 in the adult heart led to the rapid development of heart failure and premature death within 2 weeks after induction (Su et al., 2013). These findings demonstrate the necessity of CSN-mediated deneddylation in the maintenance of cardiac integrity in postnatal and adult hearts. Whether direct modulation of neddylation, for instance, through deletion of the E1 subunits, NAE1 and UBA3, has an impact on adult heart function remains to be explored.

Neddylation appears to be crucial for cardiomyocyte survival in the post-mitotic heart. While inhibition of neddylation has been shown to induce apoptosis in cancer cells (Soucy et al., 2009), this effect seems to be cell-type specific, because neither deletion of NAE1 in embryonic hearts nor knockout of CSN8 in postnatal hearts results in prevalent cardiomyocyte apoptosis. Instead, loss of CSN8 in postnatal and adult hearts induces massive cardiomyocyte necroptosis (Su et al., 2011b, 2013), a form of programed necrotic cell death mediated by the RIPK1-RIPK3 pathway (Del Re et al., 2019). RIPK1, RIPK3, MLKL and protein carbonyls were found to be upregulated in CSN8-deficient heart in association with inhibition of the cleavage/activation of caspase 8 (Xiao et al., 2020). All of these findings are consistent with activation of the RIPK1-RIPK3 pathway. Moreover, both administration of the RIP1K inhibitor necrostatin-1 and deletion of one allele of RIPK3 attenuated cardiomyocyte cell death and increased the lifespan of CSN8-deficient mice (Xiao et al., 2020). The upstream event that triggers necroptosis in CSN8-deficient hearts may be related to dysregulated Ca^{2+} dynamics. Voltage-gated Ca^{2+} channels mediate Ca^{2+} influx into cells and regulate muscle contraction and other intracellular signaling events. Excessive Ca^{2+} influx has been shown to induce necrosis or apoptosis, depending on the energetic status of the cell (Orrenius et al., 2003). Interestingly, a previous

study revealed an interaction between CSN5 and the α1c subunit of the L-type Ca^{2+} channel, and speculated that this interaction inhibits channel activity (Kameda et al., 2006). Thus, a plausible model is that loss of CSN8 triggers Ca^{2+} overload, which in turn activates RIPK1 and RIPK3 leading to necroptosis. Additional experimental evidence is needed to support this hypothesis.

Neddylation and Cardiac Proteotoxicity

Deregulation of protein homeostasis is considered to be a key pathogenic factor in various cardiac diseases (Su and Wang, 2010; Wang and Robbins, 2014). In addition to directly modulating the functionality of protein substrates, neddylation also regulates the proper function of two interconnected proteolytic pathways: the ubiquitin proteasome system (UPS) and autophagy. Direct evidence for this comes from a study that probed the impact of CSN8 hypomorphism on cardiac proteinopathy (Su et al., 2015), a form of cardiomyopathy that manifests as abundant misfolded proteins and protein aggregates in the myocardium (McLendon and Robbins, 2011). Mice with cardiac overexpression of the misfolded proteins, mutant crystallin B ($CryAB^{R120G}$) and mutant desmin (D7-Desmin), exhibit cardiac dysfunction, heart failure and premature lethality (Wang et al., 2003), and thus represent a bona fide mouse model of cardiac proteinopathy. Despite having no impact on cardiac function under basal conditions, CSN8 hypomorphism was shown to aggravate $CryAB^{R120G}$-induced restrictive cardiomyopathy and shorten the lifespan of $CryAB^{R120G}$ mice (Su et al., 2015). The cardiac phenotype was associated with augmented accumulation of protein aggregates, increased neddylated proteins, and reduced total ubiquitinated proteins. These findings collectively suggest a crucial role for CSN-mediated deneddylation in antagonizing proteotoxic stress in cardiomyocytes.

Because the structure of CSN is similar to that of the 19S proteasome lid, and since CSN is capable of controlling CRLs activity, CSN has long been proposed as a UPS regulator (Li and Deng, 2003). In support of this idea, ubiquitinated and oxidized proteins are elevated in CSN8-deficient mouse hearts together with increased protein aggregates (Su et al., 2011b, 2013). Chaperone proteins, such as Hsp25, Hsp90, and α-crystallin B, are also upregulated in these mutant hearts, likely as an adaptive response to the prevalent proteotoxic stress (Su et al., 2011b). Moreover, both CSN8 deficiency and hypomorphism lead to significant accumulation of a UPS functional reporter in mouse hearts (Su et al., 2011b, 2013, 2015), indicating compromised UPS function. Given the well-established role of neddylation in regulating CRL activity, uncoupling of ubiquitination with subsequent degradation by the proteasome may underlie the deficits in UPS function in the CSN8-deficient myocardium.

Neddylation has been shown to impact several steps in autophagy. On the one hand, autophagy initiation appears to be repressed by neddylation, as evidenced by the fact that inhibition of neddylation in cancer cells causes accumulation of DEPTOR, which inhibits mTOR signaling and leads to autophagy induction (Luo et al., 2012). On the other hand, CSN-mediated deneddylation is required for autophagosome maturation (Su et al., 2011a). CSN8 deficiency impairs autophagy flux and results in the accumulation of autophagosomes. Downregulation of RAB7, a critical factor for vesicle trafficking, may account for observed defects in autophagosome fusion with lysosomes.

Neddylation may regulate proteolysis via mechanisms independent of canonical neddylation enzymes. Under various stress conditions, NEDD8 can be incorporated into an existing ubiquitin chain and form mixed Ub- and NEDD8-modified conjugates (Hjerpe et al., 2012; Leidecker et al., 2012). The presence of hybrid Ub/NEDD8 chains has been further confirmed by proteomics studies (Singh et al., 2012; Vogl et al., 2015). Surprisingly, the formation of mixed Ub and NEDD8 chains requires the Ub E1 enzyme UBE1 but not the neddylation E1 enzyme, and therefore is termed atypical neddylation (Hjerpe et al., 2012; Leidecker et al., 2012). The biological consequences of mixed Ub/NEDD8 modifications remain mysterious. It has been proposed that atypical neddylation prevents excessive Ub chain extension and maintains a free Ub pool that otherwise would be toxic to cells (Hjerpe et al., 2012; Leidecker et al., 2012). These hybrid NEDD8/Ub conjugates may also be less efficiently processed by the proteasome and are prone to form protein aggregates in the nucleus (Maghames et al., 2018), which may protect the nuclear UPS from stress-induced dysfunction.

NUB1L (NEDD8 ultimate buster 1 long), a protein that was originally found to decrease neddylated proteins (Kito et al., 2001), has been shown to enhance UPS function in cardiomyocytes (Li et al., 2015). Notably, NUB1L can also bind to atypically neddylated proteins. Ectopic expression of NUB1L in cardiomyocytes reduces mixed Ub- and NEDD8-modified proteins, enhances degradation of a UPS functional reporter and misfolded $CryAB^{R120G}$ protein, and attenuates cellular damage in response to proteotoxic stress, whereas depletion of NUB1L does the opposite (Li et al., 2015). Structurally, NUB1L contains a UBA (Ub-associating domain) domain and a UBL domain and thus belongs to the UBA-UBL protein family. Members of this family often support proteasomal activity by shuttling ubiquitinated proteins to the proteasome for degradation. Indeed, targeting ubiquilin 1, another member of the UBA-UBL family, in mouse hearts has demonstrated the essential role of this protein in coupling cardiac ubiquitination to the proteasome and limiting myocardial ischemia-reperfusion injury (Hu et al., 2018). Future studies are warranted to determine whether NUB1L acts in a similar way to facilitate the removal of mixed Ub- and NEDD8-modified proteins in the myocardium.

FUTURE PERSPECTIVES

Several key findings in the last decade have revealed an important role of the NEDD8 system in cardiac development and function under physiological and pathological conditions. Current evidence suggests that a tight balance between neddylation and deneddylation is essential for the maintenance of normal heart physiology. This regulatory dynamic mainly occurs through regulation of cardiomyocyte proliferation, maturation, survival, and proteolysis and reflects modification of a diverse

cardiac proteome that remains incompletely characterized. Further elucidation of the pathophysiological significance of neddylation in the heart, as well as delineation of the underlying mechanisms, await answers to a number of key questions.

First, does neddylation play any role in early cardiogenic events? Cardiogenesis begins as early as E7.5 in mice and involves the coordination of diverse cardiac resident cells, including atrial and ventricular cardiomyocytes, endothelial cells, smooth muscle cells, pro/epicardial cells, valvular components, and Purkinje cells. NAE1-floxed and UBA3-floxed mouse models are readily available for dissecting the role of neddylation in individual cell lineages and determining their contribution to cardiac development. Also important is the advent of human induced pluripotent stem cell (iPSC) technology, which has generated significant enthusiasm for its potential application in basic cardiac research. By genetically or pharmacologically modulating neddylation in iPSC-derived cardiomyocytes, it may be possible to mechanistically define whether and how neddylation controls cardiomyocyte differentiation and maturation. Findings from such studies may provide new insights into how post-translational mechanisms precisely control cardiogenesis.

Second, neddylation is developmentally downregulated, raising the question of whether it is dispensable for cardiac homeostasis in adulthood. As discussed above, the importance of neddylation in terminally differentiated, post-mitotic/quiescent cells has not yet been established. In the case of neurons, another cell type long purported to lose proliferative capacity soon after birth, inhibition of neddylation results in synaptic spine loss, decreased synaptic activity and cognitive deficits, supporting the conclusion that neddylation likely broadly regulates cellular processes beyond its specific effects on cell division. The cardiotoxicity of the neddylation inhibitor MLN4924 (Shah et al., 2016; Swords et al., 2017) underscores the importance of understanding underlying mechanisms in developing therapeutic options targeting neddylation. Moreover, patients with preexisting cardiovascular disorders, who were excluded from these clinical studies, could be more sensitive to MLN4924-induced cardiotoxicity. Thus, it is also essential that the impact of neddylation on cardiac remodeling be examined in hearts challenged by different pathological insults.

Third, is the neddylation of cullin proteins critical for cardiac development and function? Whether cullin family proteins—the best-characterized NEDD8 targets—are critical regulators of cardiac function has yet to be determined. While *in vivo* studies using animal models deficient for a given cullin have demonstrated the importance of individual cullins in organ and organismal development (Sarikas et al., 2011), the significance of cullin neddylation has not been determined *in vivo*. Generation and characterization of cullin neddylation-deficient mutants will provide proof-of-principal evidence for the functional importance of cullin neddylation.

Fourth, does non-cullin neddylation play any role in the heart? To date, the biological function of neddylation has been interpreted primarily based on its effects on cullin family proteins—important targets of neddylation. Yet there are many other myocardial proteins that are modified by NEDD8. Despite substantial increases in neddylated proteins, including non-cullin proteins, in human and mouse failing hearts (Li et al., 2015), it remains unclear whether the accumulation of non-cullin neddylated proteins is pathogenic or adaptive to the cardiac remodeling process. NEDP1 modulates non-cullin deneddylation (Ehrentraut et al., 2013; Mergner et al., 2015). Thus, targeting the deneddylase NEDP1 could be a feasible strategy for probing the importance of non-cullin neddylation in the heart.

Finally, which proteins are modified by NEDD8 in cardiomyocytes? Thus far, proteomics studies that have profiled the NEDD8 proteome have mainly been conducted using cultured cell lines. However, it is conceivable that the NEDD8 proteome is cell-type specific and varies under different developmental and disease conditions. Thus, it is crucial that physiologically relevant NEDD8 substrates be identified in a cell type- and modification site-specific manner. To this end, inhibition of deneddylation through deletion of either CSN or NEDP1 using a Cre-LoxP strategy may offer an exciting approach for inducing accumulation of neddylated proteins in specific cell types/organs *in vivo*. This could be coupled with enrichment of NEDD8-modified peptides using a K-GG antibody, thereby improving the efficiency and fidelity of the identification. Nevertheless, it is important to bear in mind that the K-GG antibody cannot distinguish peptides generated from Ub-, NEDD8- and ISG15-modified proteins. To address this limitation, researchers have recently developed an antibody (UbiSite) that specifically recognizes the unique ubiquitin remnant on protein substrates after endopeptidase LysC digestion (Akimov et al., 2018). Development of an antibody specific for a unique NEDD8 remnant (K-ε-ILGGSVLHLVLALRGG) following Lys-C digestion could be another option for improving the effectiveness of NEDD8 target identification (Jeram et al., 2010). Thus, identification of the NEDD8 proteome is possible and could provide invaluable new insights into the biological functions of neddylation, an existing and yet unsolved mystery.

AUTHOR CONTRIBUTIONS

JLi, JZ, and RL drafted the manuscript. JLiu and HS revised the manuscript. All authors contributed to the article and approved the submitted version.

FUNDING

This study is in part supported by the US National Institutes of Health grants (R01HL124248 to HS, R01HL146807 to JLi, and F31HL139079 to RL) and the American Heart Association grants (19TPA34880050 to HS and 19CDA34760311 to JZ).

ACKNOWLEDGMENTS

We thank Mr. Juan Ayala and Mr. Travis Anderson for proofreading this manuscript.

REFERENCES

Abdullah, A., Eyster, K. M., Bjordahl, T., Xiao, P., Zeng, E., and Wang, X. (2017). Murine Myocardial Transcriptome Analysis Reveals a Critical Role of COPS8 in the Gene Expression of Cullin-RING Ligase Substrate Receptors and Redox and Vesicle Trafficking Pathways. *Front. Physiol*. 8:594. doi: 10.3389/fphys.2017.00594

Abida, W. M., Nikolaev, A., Zhao, W., Zhang, W., and Gu, W. (2007). FBXO11 promotes the Neddylation of p53 and inhibits its transcriptional activity. *J. Biol. Chem.* 282, 1797–1804. doi: 10.1074/jbc.m609001200

Ai, T. J., Sun, J. Y., Du, L. J., Shi, C., Li, C., Sun, X. N., et al. (2018). Inhibition of neddylation by MLN4924 improves neointimal hyperplasia and promotes apoptosis of vascular smooth muscle cells through p53 and p62. *Cell Death Differ*. 25, 319–329. doi: 10.1038/cdd.2017.160

Akimov, V., Barrio-Hernandez, I., Hansen, S. V. F., Hallenborg, P., Pedersen, A. K., Bekker-Jensen, D. B., et al. (2018). UbiSite approach for comprehensive mapping of lysine and N-terminal ubiquitination sites. *Nat. Struct. Mol. Biol.* 25, 631–640. doi: 10.1038/s41594-018-0084-y

Aoki, I., Higuchi, M., and Gotoh, Y. (2013). NEDDylation controls the target specificity of E2F1 and apoptosis induction. *Oncogene* 32, 3954–3964. doi: 10.1038/onc.2012.428

Asare, Y., Ommer, M., Azombo, F. A., Alampour-Rajabi, S., Sternkopf, M., Sanati, M., et al. (2017). Inhibition of atherogenesis by the COP9 signalosome subunit 5 in vivo. *Proc. Natl. Acad. Sci. U S A*. 114, E2766–E2775.

Baek, K., Krist, D. T., Prabu, J. R., Hill, S., Klugel, M., Neumaier, L. M., et al. (2020). NEDD8 nucleates a multivalent cullin-RING-UBE2D ubiquitin ligation assembly. *Nature* 578, 461–466. doi: 10.1038/s41586-020-2000-y

Bailly, A. P., Perrin, A., Serrano-Macia, M., Maghames, C., Leidecker, O., Trauchessec, H., et al. (2019). The Balance between Mono- and NEDD8-Chains Controlled by NEDP1 upon DNA Damage Is a Regulatory Module of the HSP70 ATPase Activity. *Cell Rep*. 29:e8.

Benjamin, E. J., Muntner, P., Alonso, A., Bittencourt, M. S., Callaway, C. W., Carson, A. P., et al. (2019). Heart Disease and Stroke Statistics-2019 Update: A Report From the American Heart Association. *Circulation* 139, e56–e528.

Broemer, M., Tenev, T., Rigbolt, K. T., Hempel, S., Blagoev, B., Silke, J., et al. (2010). Systematic in vivo RNAi analysis identifies IAPs as NEDD8-E3 ligases. *Mol. Cell* 40, 810–822. doi: 10.1016/j.molcel.2010.11.011

Chan, Y., Yoon, J., Wu, J. T., Kim, H. J., Pan, K. T., Yim, J., et al. (2008). DEN1 deneddylates non-cullin proteins in vivo. *J. Cell Sci.* 121, 3218–3223. doi: 10.1242/jcs.030445

Choo, Y. S., Vogler, G., Wang, D., Kalvakuri, S., Iliuk, A., Tao, W. A., et al. (2012). Regulation of parkin and PINK1 by neddylation. *Hum. Mol. Genet*. 21, 2514–2523. doi: 10.1093/hmg/dds070

Coleman, K. E., Bekes, M., Chapman, J. R., Crist, S. B., Jones, M. J., Ueberheide, B. M., et al. (2017). SENP8 limits aberrant neddylation of NEDD8 pathway components to promote cullin-RING ubiquitin ligase function. *Elife* 6:e24325.

Del Re, D. P., Amgalan, D., Linkermann, A., Liu, Q., and Kitsis, R. N. (2019). Fundamental Mechanisms of Regulated Cell Death and Implications for Heart Disease. *Physiol. Rev*. 99, 1765–1817. doi: 10.1152/physrev.00022.2018

Ehrentraut, S. F., Kominsky, D. J., Glover, L. E., Campbell, E. L., Kelly, C. J., Bowers, B. E., et al. (2013). Central Role for Endothelial Human Deneddylase-1/SENP8 in Fine-Tuning the Vascular Inflammatory Response. *J. Immunol*. 190, 392–400. doi: 10.4049/jimmunol.1202041

Embade, N., Fernandez-Ramos, D., Varela-Rey, M., Beraza, N., Sini, M., Gutierrez, et al. (2012). Murine double minute 2 regulates Hu antigen R stability in human liver and colon cancer through NEDDylation. *Hepatology* 55, 1237–1248. doi: 10.1002/hep.24795

Enchev, R. I., Schulman, B. A., and Peter, M. (2015). Protein neddylation: beyond cullin-RING ligases. *Nat. Rev. Mol. Cell Biol.* 16, 30–44. doi: 10.1038/nrm3919

Faull, S. V., Lau, A. M. C., Martens, C., Ahdash, Z., Hansen, K., Yebenes, H., et al. (2019). Structural basis of Cullin 2 RING E3 ligase regulation by the COP9 signalosome. *Nat. Commun*. 10:3814.

Frickel, E. M., Quesada, V., Muething, L., Gubbels, M. J., Spooner, E., Ploegh, H., et al. (2007). Apicomplexan UCHL3 retains dual specificity for ubiquitin and Nedd8 throughout evolution. *Cell Microbiol.* 9, 1601–1610. doi: 10.1111/j.1462-5822.2007.00896.x

Gan-Erdene, T., Nagamalleswari, K., Yin, L., Wu, K., Pan, Z. Q., and Wilkinson, K. D. (2003). Identification and characterization of DEN1, a deneddylase of the ULP family. *J. Biol. Chem*. 278, 28892–28900. doi: 10.1074/jbc.m302890200

Glickman, M. H., and Ciechanover, A. (2002). The ubiquitin-proteasome proteolytic pathway: destruction for the sake of construction. *Physiol. Rev.* 82, 373–428. doi: 10.1152/physrev.00027.2001

Gomes, A. V. (2018). *Ubiquitin Proteasome System : A Review And Directions For Research*. New York: Nova Medicine & Health.

Gong, L., and Yeh, E. T. (1999). Identification of the activating and conjugating enzymes of the NEDD8 conjugation pathway. *J. Biol. Chem*. 274, 12036–12042. doi: 10.1074/jbc.274.17.12036

Guihard, S., Ramolu, L., Macabre, C., Wasylyk, B., Noel, G., Abecassis, J., et al. (2012). The NEDD8 conjugation pathway regulates p53 transcriptional activity and head and neck cancer cell sensitivity to ionizing radiation. *Int. J. Oncol.* 41, 1531–1540. doi: 10.3892/ijo.2012.1584

Guo, Z., Wang, S., Xie, Y., Han, Y., Hu, S., Guan, H., et al. (2020). HUWE1-dependent DNA-PKcs neddylation modulates its autophosphorylation in DNA damage response. *Cell Death Dis*. 11:400.

Hedberg-Oldfors, C., Abramsson, A., Osborn, D. P. S., Danielsson, O., Fazlinezhad, A., Nilipour, Y., et al. (2019). Cardiomyopathy with lethal arrhythmias associated with inactivation of KLHL24. *Hum. Mol. Genet*. 28, 1919–1929. doi: 10.1093/hmg/ddz032

Henning, R. H., and Brundel, B. (2017). Proteostasis in cardiac health and disease. *Nat. Rev. Cardiol*. 14, 637–653. doi: 10.1038/nrcardio.2017.89

Heo, M. J., Kang, S. H., Kim, Y. S., Lee, J. M., Yu, J., Kim, H. R., et al. (2020). UBC12-mediated SREBP-1 neddylation worsens metastatic tumor prognosis. *Int. J. Cancer* 147, 2550–2563. doi: 10.1002/ijc.33113

Hjerpe, R., Thomas, Y., Chen, J., Zemla, A., Curran, S., Shpiro, N., et al. (2012). Changes in the ratio of free NEDD8 to ubiquitin triggers NEDDylation by ubiquitin enzymes. *Biochem. J.* 441, 927–936. doi: 10.1042/bj20111671

Hu, C., Tian, Y., Xu, H., Pan, B., Terpstra, E. M., Wu, P., et al. (2018). Inadequate ubiquitination-proteasome coupling contributes to myocardial ischemia-reperfusion injury. *J. Clin. Invest*. 128, 5294–5306. doi: 10.1172/jci98287

Huang, D. T., Ayrault, O., Hunt, H. W., Taherbhoy, A. M., Duda, D. M., Scott, D. C., et al. (2009). E2-RING expansion of the NEDD8 cascade confers specificity to cullin modification. *Mol. Cell* 33, 483–495. doi: 10.1016/j.molcel.2009.01.011

Huang, G., Kaufman, A. J., Ramanathan, Y., and Singh, B. (2011). SCCRO (DCUN1D1) promotes nuclear translocation and assembly of the neddylation E3 complex. *J. Biol. Chem*. 286, 10297–10304. doi: 10.1074/jbc.m110.203729

Huang, J., Wu, S., Barrera, J., Matthews, K., and Pan, D. (2005). The Hippo signaling pathway coordinately regulates cell proliferation and apoptosis by inactivating Yorkie, the Drosophila Homolog of YAP. *Cell* 122, 421–434. doi: 10.1016/j.cell.2005.06.007

Jeram, S. M., Srikumar, T., Zhang, X. D., Anne Eisenhauer, H., Rogers, R., Pedrioli, P. G., et al. (2010). An improved SUMmOn-based methodology for the identification of ubiquitin and ubiquitin-like protein conjugation sites identifies novel ubiquitin-like protein chain linkages. *Proteomics* 10, 254–265. doi: 10.1002/pmic.200900648

Jin, H. S., Liao, L., Park, Y., and Liu, Y. C. (2013). Neddylation pathway regulates T-cell function by targeting an adaptor protein Shc and a protein kinase Erk signaling. *Proc. Natl. Acad. Sci. U S A*. 110, 624–629. doi: 10.1073/pnas.1213819110

Kameda, K., Fukao, M., Kobayashi, T., Tsutsuura, M., Nagashima, M., Yamada, Y., et al. (2006). CSN5/Jab1 inhibits cardiac L-type Ca2+ channel activity through protein-protein interactions. *J. Mol. Cell Cardiol*. 40, 562–569. doi: 10.1016/j.yjmcc.2006.01.007

Kamitani, T., Kito, K., Nguyen, H. P., and Yeh, E. T. (1997). Characterization of NEDD8, a developmentally down-regulated ubiquitin-like protein. *J. Biol. Chem.* 272, 28557–28562. doi: 10.1074/jbc.272.45.28557

Kandala, S., Kim, I. M., and Su, H. (2014). Neddylation and deneddylation in cardiac biology. *Am. J. Cardiovasc. Dis.* 4, 140–158.

Keuss, M. J., Hjerpe, R., Hsia, O., Gourlay, R., Burchmore, R., Trost, M., et al. (2019). Unanchored tri-NEDD8 inhibits PARP-1 to protect from oxidative stress-induced cell death. *EMBO J.* 38:e100024.

Kho, C., Lee, A., Jeong, D., Oh, J. G., Chaanine, A. H., Kizana, E., et al. (2011). SUMO1-dependent modulation of SERCA2a in heart failure. *Nature* 477, 601–605. doi: 10.1038/nature10407

Kim, A. Y., Bommelje, C. C., Lee, B. E., Yonekawa, Y., Choi, L., Morris, L. G., et al. (2008). SCCRO (DCUN1D1) is an essential component of the E3 complex for neddylation. *J. Biol. Chem*. 283, 33211–33220. doi: 10.1074/jbc.m804440200

Kito, K., Yeh, E. T., and Kamitani, T. (2001). NUB1, a NEDD8-interacting protein, is induced by interferon and down-regulates the NEDD8 expression. *J. Biol. Chem*. 276, 20603–20609. doi: 10.1074/jbc.m100920200

Knorr, K. L., Schneider, P. A., Meng, X. W., Dai, H., Smith, B. D., Hess, A. D., et al. (2015). MLN4924 induces Noxa upregulation in acute myelogenous leukemia and synergizes with Bcl-2 inhibitors. *Cell Death Differ*. 22, 2133–2142. doi: 10.1038/cdd.2015.74

Kumar, D., Das, M., Sauceda, C., Ellies, L. G., Kuo, K., Parwal, P., et al. (2019). Degradation of splicing factor SRSF3 contributes to progressive liver disease. *J. Clin. Invest*. 129, 4477–4491. doi: 10.1172/jci127374

Kumar, S., Yoshida, Y., and Noda, M. (1993). Cloning of a cDNA which encodes a novel ubiquitin-like protein. *Biochem. Biophys. Res. Commun*. 195, 393–399. doi: 10.1006/bbrc.1993.2056

Kwon, J., Wang, Y. L., Setsuie, R., Sekiguchi, S., Sato, Y., Sakurai, M., et al. (2004). Two closely related ubiquitin C-terminal hydrolase isozymes function as reciprocal modulators of germ cell apoptosis in cryptorchid testis. *Am. J. Pathol*. 165, 1367–1374. doi: 10.1016/s0002-9440(10)63394-9

Leidecker, O., Matic, I., Mahata, B., Pion, E., and Xirodimas, D. P. (2012). The ubiquitin E1 enzyme Ube1 mediates NEDD8 activation under diverse stress conditions. *Cell Cycle* 11, 1142–1150. doi: 10.4161/cc.11.6.19559

Li, H., Zhu, H., Liu, Y., He, F., Xie, P., and Zhang, L. (2016). Itch promotes the neddylation of JunB, and regulates JunB-dependent transcription. *Cell Sign.* 28, 1186–1195. doi: 10.1016/j.cellsig.2016.05.016

Li, J., Johnson, J. A., and Su, H. (2018). Ubiquitin and Ubiquitin-like proteins in cardiac disease and protection. *Curr. Drug Targets* 19, 989–1002. doi: 10.2174/1389450117666151209114608

Li, J., Ma, W., Li, H., Hou, N., Wang, X., Kim, I. M., et al. (2015). NEDD8 Ultimate Buster 1 Long (NUB1L) Protein Suppresses Atypical Neddylation and Promotes the Proteasomal Degradation of Misfolded Proteins. *J. Biol. Chem*. 290, 23850–23862. doi: 10.1074/jbc.m115.664375

Li, L., and Deng, X. W. (2003). The COP9 signalosome: an alternative lid for the 26S proteasome? *Trends Cell Biol*. 13, 507–509. doi: 10.1016/j.tcb.2003.08.002

Li, L., Cao, Y., Wu, H., Ye, X., Zhu, Z., Xing, G., et al. (2016). Enzymatic Activity of the Scaffold Protein Rapsyn for Synapse Formation. *Neuron* 92, 1007–1019. doi: 10.1016/j.neuron.2016.10.023

Li, L., Kang, J., Zhang, W., Cai, L., Wang, S., Liang, Y., et al. (2019). Validation of NEDD8-conjugating enzyme UBC12 as a new therapeutic target in lung cancer. *EBioMedicine* 45, 81–91. doi: 10.1016/j.ebiom.2019.06.005

Lipkowitz, S., and Weissman, A. M. (2011). RINGs of good and evil: RING finger ubiquitin ligases at the crossroads of tumour suppression and oncogenesis. *Nat. Rev. Cancer* 11, 629–643. doi: 10.1038/nrc3120

Loftus, S. J., Liu, G., Carr, S. M., Munro, S., and La Thangue, N. B. (2012). NEDDylation regulates E2F-1-dependent transcription. *EMBO Rep*. 13, 811–818. doi: 10.1038/embor.2012.113

Luo, Z., Pan, Y., Jeong, L. S., Liu, J., and Jia, L. (2012). Inactivation of the Cullin (CUL)-RING E3 ligase by the NEDD8-activating enzyme inhibitor MLN4924 triggers protective autophagy in cancer cells. *Autophagy* 8, 1677–1679. doi: 10.4161/auto.21484

Lydeard, J. R., Schulman, B. A., and Harper, J. W. (2013). Building and remodelling Cullin-RING E3 ubiquitin ligases. *EMBO Rep*. 14, 1050–1061. doi: 10.1038/embor.2013.173

Lykke-Andersen, K., Schaefer, L., Menon, S., Deng, X. W., Miller, J. B., and Wei, N. (2003). Disruption of the COP9 signalosome Csn2 subunit in mice causes deficient cell proliferation, accumulation of p53 and cyclin E, and early embryonic death. *Mol. Cell Biol*. 23, 6790–6797. doi: 10.1128/mcb.23.19.6790-6797.2003

Ma, T., Chen, Y., Zhang, F., Yang, C. Y., Wang, S., and Yu, X. (2013). RNF111-dependent neddylation activates DNA damage-induced ubiquitination. *Mol. Cell* 49, 897–907. doi: 10.1016/j.molcel.2013.01.006

Maghames, C. M., Lobato-Gil, S., Perrin, A., Trauchessec, H., Rodriguez, M. S., Urbach, S., et al. (2018). NEDDylation promotes nuclear protein aggregation and protects the Ubiquitin Proteasome System upon proteotoxic stress. *Nat. Commun*. 9:4376.

Mahata, B., Sundqvist, A., and Xirodimas, D. P. (2012). Recruitment of RPL11 at promoter sites of p53-regulated genes upon nucleolar stress through NEDD8 and in an Mdm2-dependent manner. *Oncogene* 31, 3060–3071. doi: 10.1038/onc.2011.482

McLendon, P. M., and Robbins, J. (2011). Desmin-related cardiomyopathy: an unfolding story. *Am. J. Physiol. Heart Circ. Physiol*. 301, H1220–H1228.

Mendler, L., Braun, T., and Muller, S. (2016). The Ubiquitin-Like SUMO System and Heart Function: From Development to Disease. *Circ. Res*. 118, 132–144. doi: 10.1161/circresaha.115.307730

Mendoza, H. M., Shen, L. N., Botting, C., Lewis, A., Chen, J., Ink, B., et al. (2003). NEDP1, a highly conserved cysteine protease that deNEDDylates Cullins. *J. Biol. Chem*. 278, 25637–25643. doi: 10.1074/jbc.m212948200

Menon, S., Chi, H., Zhang, H., Deng, X. W., Flavell, R. A., and Wei, N. (2007). COP9 signalosome subunit 8 is essential for peripheral T cell homeostasis and antigen receptor-induced entry into the cell cycle from quiescence. *Nat. Immunol*. 8, 1236–1245. doi: 10.1038/ni1514

Mergner, J., Heinzlmeir, S., Kuster, B., and Schwechheimer, C. (2015). DENEDDYLASE1 deconjugates NEDD8 from non-cullin protein substrates in Arabidopsis thaliana. *Plant Cell* 27, 741–753. doi: 10.1105/tpc.114.135996

Mergner, J., Kuster, B., and Schwechheimer, C. (2017). DENEDDYLASE1 Protein Counters Automodification of Neddylating Enzymes to Maintain NEDD8 Protein Homeostasis in Arabidopsis. *J. Biol. Chem*. 292, 3854–3865. doi: 10.1074/jbc.m116.767103

Métais, A., Lamsoul, I., Melet, A., Uttenweiler-Joseph, S., Poincloux, R., Stefanovic, S., et al. (2018). Asb2α-Filamin A Axis Is Essential for Actin Cytoskeleton Remodeling During Heart Development. *Circ. Res*. 122, e34–e48.

Meyer-Schaller, N., Chou, Y. C., Sumara, I., Martin, D. D., Kurz, T., Katheder, N., et al. (2009). The human Dcn1-like protein DCNL3 promotes Cul3 neddylation at membranes. *Proc. Natl. Acad. Sci. U S A*. 106, 12365–12370. doi: 10.1073/pnas.0812528106

Ni, H. M., Williams, J. A., and Ding, W. X. (2014). Mitochondrial dynamics and mitochondrial quality control. *Redox. Biol.* 4C, 6–13. doi: 10.1016/j.redox.2014.11.006

Oron, E., Mannervik, M., Rencus, S., Harari-Steinberg, O., Neuman-Silberberg, S., Segal, D., et al. (2002). COP9 signalosome subunits 4 and 5 regulate multiple pleiotropic pathways in Drosophila melanogaster. *Development* 129, 4399–4409.

Oron, E., Tuller, T., Li, L., Rozovsky, N., Yekutieli, D., Rencus-Lazar, S., et al. (2007). Genomic analysis of COP9 signalosome function in Drosophila melanogaster reveals a role in temporal regulation of gene expression. *Mol. Syst. Biol*. 3:108. doi: 10.1038/msb4100150

Orrenius, S., Zhivotovsky, B., and Nicotera, P. (2003). Regulation of cell death: the calcium-apoptosis link. *Nat. Rev. Mol. Cell Biol*. 4, 552–565. doi: 10.1038/nrm1150

Oved, S., Mosesson, Y., Zwang, Y., Santonico, E., Shtiegman, K., Marmor, M. D., et al. (2006). Conjugation to Nedd8 instigates ubiquitylation and down-regulation of activated receptor tyrosine kinases. *J. Biol. Chem*. 281, 21640–21651. doi: 10.1074/jbc.m513034200

Papizan, J. B., Vidal, A. H., Bezprozvannaya, S., Bassel-Duby, R., and Olson, E. N. (2018). Cullin-3-RING ubiquitin ligase activity is required for striated muscle function in mice. *J. Biol. Chem*. 293, 8802–8811. doi: 10.1074/jbc.ra118.002104

Park, H. S., Ju, U. I., Park, J. W., Song, J. Y., Shin, D. H., Lee, K. H., et al. (2016). PPARgamma neddylation essential for adipogenesis is a potential target for treating obesity. *Cell Death Differ*. 23, 1296–1311. doi: 10.1038/cdd.2016.6

Petroski, M. D., and Deshaies, R. J. (2005). Function and regulation of cullin-RING ubiquitin ligases. *Nat. Rev. Mol. Cell Biol*. 6, 9–20. doi: 10.1038/nrm1547

Pirone, L., Xolalpa, W., Sigurethsson, J. O., Ramirez, J., Perez, C., Gonzalez, M., et al. (2017). A comprehensive platform for the analysis of ubiquitin-like protein modifications using in vivo biotinylation. *Sci. Rep*. 7:40756.

Rabut, G., and Peter, M. (2008). Function and regulation of protein neddylation. 'Protein modifications: beyond the usual suspects' review series. *EMBO Rep*. 9, 969–976. doi: 10.1038/embor.2008.183

Rahnefeld, A., Klingel, K., Schuermann, A., Diny, N. L., Althof, N., Lindner, A., et al. (2014). Ubiquitin-like protein ISG15 (interferon-stimulated gene of 15 kDa) in host defense against heart failure in a mouse model of virus-induced

cardiomyopathy. *Circulation* 130, 1589–1600. doi: 10.1161/circulationaha.114.009847

Rao-Naik, C., delaCruz, W., Laplaza, J. M., Tan, S., Callis, J., and Fisher, A. J. (1998). The rub family of ubiquitin-like proteins. Crystal structure of Arabidopsis rub1 and expression of multiple rubs in Arabidopsis. *J. Biol. Chem.* 273, 34976–34982. doi: 10.1074/jbc.273.52.34976

Renaudin, X., Guervilly, J. H., Aoufouchi, S., and Rosselli, F. (2014). Proteomic analysis reveals a FANCA-modulated neddylation pathway involved in CXCR5 membrane targeting and cell mobility. *J. Cell Sci.* 127, 3546–3554. doi: 10.1242/jcs.150706

Rodriguez, M. S., Dargemont, C., and Hay, R. T. (2001). SUMO-1 conjugation in vivo requires both a consensus modification motif and nuclear targeting. *J. Biol. Chem.* 276, 12654–12659. doi: 10.1074/jbc.m009476200

Ryu, J. H., Li, S. H., Park, H. S., Park, J. W., Lee, B., and Chun, Y. S. (2011). Hypoxia-inducible factor alpha subunit stabilization by NEDD8 conjugation is reactive oxygen species-dependent. *J. Biol. Chem.* 286, 6963–6970. doi: 10.1074/jbc.m110.188706

Sarikas, A., Hartmann, T., and Pan, Z. Q. (2011). The cullin protein family. *Genome Biol.* 12:220. doi: 10.1186/gb-2011-12-4-220

Schumacher, F. R., Siew, K., Zhang, J., Johnson, C., Wood, N., Cleary, S. E., et al. (2015). Characterisation of the Cullin-3 mutation that causes a severe form of familial hypertension and hyperkalaemia. *EMBO Mol. Med.* 7, 1285–1306. doi: 10.15252/emmm.201505444

Shah, J. J., Jakubowiak, A. J., O'Connor, O. A., Orlowski, R. Z., Harvey, R. D., Smith, M. R., et al. (2016). Phase I Study of the Novel Investigational NEDD8-Activating Enzyme Inhibitor Pevonedistat (MLN4924) in Patients with Relapsed/Refractory Multiple Myeloma or Lymphoma. *Clin. Cancer Res.* 22, 34–43. doi: 10.1158/1078-0432.ccr-15-1237

Singh, R. K., Zerath, S., Kleifeld, O., Scheffner, M., Glickman, M. H., and Fushman, D. (2012). Recognition and cleavage of related to ubiquitin 1 (Rub1) and Rub1-ubiquitin chains by components of the ubiquitin-proteasome system. *Mol. Cell Proteom.* 11, 1595–1611. doi: 10.1074/mcp.m112.022467

Soucy, T. A., Dick, L. R., Smith, P. G., Milhollen, M. A., and Brownell, J. E. (2010). The NEDD8 Conjugation Pathway and Its Relevance in Cancer Biology and Therapy. *Genes Cancer* 1, 708–716. doi: 10.1177/1947601910382898

Soucy, T. A., Smith, P. G., Milhollen, M. A., Berger, A. J., Gavin, J. M., and Adhikari, S. (2009). An inhibitor of NEDD8-activating enzyme as a new approach to treat cancer. *Nature* 458, 732–736.

Steklov, M., Pandolfi, S., Baietti, M. F., Batiuk, A., Carai, P., Najm, P., et al. (2018). Mutations in LZTR1 drive human disease by dysregulating RAS ubiquitination. *Science* 362, 1177–1182. doi: 10.1126/science.aap7607

Su, H., and Wang, X. (2010). The ubiquitin-proteasome system in cardiac proteinopathy: a quality control perspective. *Cardiovasc. Res.* 85, 253–262. doi: 10.1093/cvr/cvp287

Su, H., Li, F., Ranek, M. J., Wei, N., and Wang, X. (2011a). COP9 signalosome regulates autophagosome maturation. *Circulation* 124, 2117–2128. doi: 10.1161/circulationaha.111.048934

Su, H., Li, J., Menon, S., Liu, J., Kumarapeli, A. R., Wei, N., et al. (2011b). Perturbation of cullin deneddylation via conditional Csn8 ablation. (impairs)the ubiquitin-proteasome system and causes cardiomyocyte necrosis and dilated cardiomyopathy in mice. *Circ. Res.* 108, 40–50. doi: 10.1161/circresaha.110.230607

Su, H., Li, J., Osinska, H., Li, F., Robbins, J., Liu, J., et al. (2013). The COP9 signalosome is required for autophagy, proteasome-mediated proteolysis, and cardiomyocyte survival in adult mice. *Circ. Heart Fail.* 6, 1049–1057. doi: 10.1161/circheartfailure.113.000338

Su, H., Li, J., Zhang, H., Ma, W., Wei, N., and Liu, J. (2015). COP9 signalosome controls the degradation of cytosolic misfolded proteins and protects against cardiac proteotoxicity. *Circ. Res.* 117, 956–966. doi: 10.1161/circresaha.115.306783

Sun, Y. (2003). Targeting E3 ubiquitin ligases for cancer therapy. *Cancer Biol. Ther.* 2, 623–629.

Sundqvist, A., Liu, G., Mirsaliotis, A., and Xirodimas, D. P. (2009). Regulation of nucleolar signalling to p53 through NEDDylation of L11. *EMBO Rep.* 10, 1132–1139. doi: 10.1038/embor.2009.178

Swords, R. T., Watts, J., Erba, H. P., Altman, J. K., Maris, M., Anwer, F., et al. (2017). Expanded safety analysis of pevonedistat, a first-in-class NEDD8-activating enzyme inhibitor, in patients with acute myeloid leukemia and myelodysplastic syndromes. *Blood Cancer J.* 7:e520. doi: 10.1038/bcj.2017.1

Tomoda, K., Yoneda-Kato, N., Fukumoto, A., Yamanaka, S., and Kato, J. Y. (2004). Multiple functions of Jab1 are required for early embryonic development and growth potential in mice. *J. Biol. Chem.* 279, 43013–43018. doi: 10.1074/jbc.m406559200

Ullah, Z., Buckley, M. S., Arnosti, D. N., and Henry, R. W. (2007). Retinoblastoma protein regulation by the COP9 signalosome. *Mol. Biol. Cell* 18, 1179–1186. doi: 10.1091/mbc.e06-09-0790

Um, J. W., Han, K. A., Im, E., Oh, Y., Lee, K., and Chung, K. C. (2012). Neddylation positively regulates the ubiquitin E3 ligase activity of parkin. *J. Neurosci. Res.* 90, 1030–1042. doi: 10.1002/jnr.22828

Vogl, A. M., Brockmann, M. M., Giusti, S. A., Maccarrone, G., Vercelli, C. A., Bauder, C. A., et al. (2015). Neddylation inhibition impairs spine development, destabilizes synapses and deteriorates cognition. *Nat. Neurosci.* 18, 239–251. doi: 10.1038/nn.3912

Vogl, A. M., Phu, L., Becerra, R., Giusti, S. A., Verschueren, E., Hinkle, T. B., et al. (2020). Global site-specific neddylation profiling reveals that NEDDylated cofilin regulates actin dynamics. *Nat. Struct. Mol. Biol.* 27, 210–220. doi: 10.1038/s41594-019-0370-3

Wackerhage, H., Del, Re, D. P., Judson, R. N., Sudol, M., and Sadoshima, J. (2014). The Hippo signal transduction network in skeletal and cardiac muscle. *Sci. Signal.* 7:re4. doi: 10.1126/scisignal.2005096

Wang, J., Liu, S., Heallen, T., and Martin, J. F. (2018). The Hippo pathway in the heart: pivotal roles in development, disease, and regeneration. *Nat. Rev. Cardiol.* 15, 672–684. doi: 10.1038/s41569-018-0063-3

Wang, X., and Robbins, J. (2006). Heart failure and protein quality control. *Circ. Res.* 99, 1315–1328. doi: 10.1161/01.res.0000252342.61447.a2

Wang, X., and Robbins, J. (2014). Proteasomal and lysosomal protein degradation and heart disease. *J. Mol. Cell Cardiol.* 71, 16–24. doi: 10.1016/j.yjmcc.2013.11.006

Wang, X., Klevitsky, R., Huang, W., Glasford, J., Li, F., and Robbins, J. (2003). AlphaB-crystallin modulates protein aggregation of abnormal desmin. *Circ. Res.* 93, 998–1005. doi: 10.1161/01.res.0000102401.77712.ed

Watson, I. R., Blanch, A., Lin, D. C., Ohh, M., and Irwin, M. S. (2006). Mdm2-mediated NEDD8 modification of TAp73 regulates its transactivation function. *J. Biol. Chem.* 281, 34096–34103. doi: 10.1074/jbc.m603654200

Wei, N., Serino, G., and Deng, X. W. (2008). The COP9 signalosome: more than a protease. *Trends Biochem. Sci.* 33, 592–600. doi: 10.1016/j.tibs.2008.09.004

Whitby, F. G., Xia, G., Pickart, C. M., and Hill, C. P. (1998). Crystal structure of the human ubiquitin-like protein NEDD8 and interactions with ubiquitin pathway enzymes. *J. Biol. Chem.* 273, 34983–34991. doi: 10.1074/jbc.273.52.34983

Willis, M. S., Bevilacqua, A., Pulinilkunnil, T., Kienesberger, P., Tannu, M., and Patterson, C. (2014). The role of ubiquitin ligases in cardiac disease. *J. Mol. Cell Cardiol.* 71, 43–53. doi: 10.1016/j.yjmcc.2013.11.008

Wolf, E. R., Mabry, A. R., Damania, B., and Mayo, L. D. (2020). Mdm2-mediated neddylation of pVHL blocks the induction of antiangiogenic factors. *Oncogene* 39, 5228–5239. doi: 10.1038/s41388-020-1359-4

Wu, K., Yamoah, K., Dolios, G., Gan-Erdene, T., Tan, P., Chen, A., et al. (2003). DEN1 is a dual function protease capable of processing the C terminus of Nedd8 and deconjugating hyper-neddylated CUL1. *J. Biol. Chem.* 278, 28882–28891. doi: 10.1074/jbc.m302888200

Wu, K., Yan, H., Fang, L., Wang, X., Pfleger, C., Jiang, X., et al. (2011). Mono-ubiquitination drives nuclear export of the human DCN1-like protein hDCNL1. *J. Biol. Chem.* 286, 34060–34070. doi: 10.1074/jbc.m111.273045

Xiao, P., Wang, C., Li, J., Su, H., Yang, L., Wu, P., et al. (2020). COP9 Signalosome Suppresses RIPK1-RIPK3-Mediated Cardiomyocyte Necroptosis in Mice. *Circ. Heart Fail.* 13:e006996.

Xie, P., Zhang, M., He, S., Lu, K., Chen, Y., Xing, G., et al. (2014). The covalent modifier Nedd8 is critical for the activation of Smurf1 ubiquitin ligase in tumorigenesis. *Nat. Commun.* 5:3733.

Xiong, X., Cui, D., Bi, Y., Sun, Y., and Zhao, Y. (2020). Neddylation modification of ribosomal protein RPS27L or RPS27 by MDM2 or NEDP1 regulates cancer cell survival. *FASEB J.* 11:32779270.

Xirodimas, D. P. (2008). Novel substrates and functions for the ubiquitin-like molecule NEDD8. *Biochem. Soc. Trans.* 36, 802–806. doi: 10.1042/bst0360802

Xirodimas, D. P., Saville, M. K., Bourdon, J. C., Hay, R. T., and Lane, D. P. (2004). Mdm2-mediated NEDD8 conjugation of p53 inhibits its transcriptional activity. *Cell* 118, 83–97. doi: 10.1016/j.cell.2004.06.016

Xirodimas, D. P., Sundqvist, A., Nakamura, A., Shen, L., Botting, C., and Hay, R. T. (2008). Ribosomal proteins are targets for the NEDD8 pathway. *EMBO Rep*. 9, 280–286. doi: 10.1038/embor.2008.10

Xu, G., Paige, J. S., and Jaffrey, S. R. (2010). Global analysis of lysine ubiquitination by ubiquitin remnant immunoaffinity profiling. *Nat. Biotechnol*. 28, 868–873. doi: 10.1038/nbt.1654

Yan, J., Walz, K., Nakamura, H., Carattini-Rivera, S., Zhao, Q., Vogel, H., et al. (2003). COP9 signalosome subunit 3 is essential for maintenance of cell proliferation in the mouse embryonic epiblast. *Mol. Cell Biol*. 23, 6798–6808. doi: 10.1128/mcb.23.19.6798-6808.2003

Yu, G., Liu, X., Zhang, D., Wang, J., Ouyang, G., and Chen, Z. (2020). Zebrafish Nedd8 facilitates ovarian development and the maintenance of female secondary sexual characteristics via suppression of androgen receptor activity. *Development* 147:dev194886.

Zhang, J., Bai, D., Ma, X., Guan, J., and Zheng, X. (2014). hCINAP is a novel regulator of ribosomal protein-HDM2-p53 pathway by controlling NEDDylation of ribosomal protein S14. *Oncogene* 33, 246–254.

Zhang, L., Jing, H., Li, H., Chen, W., Luo, B., Zhang, H., et al. (2020). Neddylation is critical to cortical development by regulating Wnt/beta-catenin signaling. *Proc. Natl. Acad. Sci. U S A*. 117, 26448–26459.

Zhang, T., Ye, Z., Yang, X., Qin, Y., Hu, Y., Tong, X., et al. (2017). NEDDylation of PB2 Reduces Its Stability and Blocks the Replication of Influenza A Virus. *Sci. Rep*. 7:43691.

Zhang, X., Zhang, Y. L., Qiu, G., Pian, L., Guo, L., Cao, H., et al. (2020). Hepatic neddylation targets, and stabilizes electron transfer flavoproteins to facilitate fatty acid beta-oxidation. *Proc. Natl. Acad. Sci. U S A*. 117, 2473–2483.

Zhao, R., Yeung, S. C., Chen, J., Iwakuma, T., Su, C. H., Chen, B., et al. (2011). Subunit 6 of the COP9 signalosome promotes tumorigenesis in mice through stabilization of MDM2 and is upregulated in human cancers. *J. Clin. Investig*. 121, 851–865.

Zhou, Q., Li, L., Zhao, B., and Guan, K. L. (2015). The hippo pathway in heart development, regeneration, and diseases. *Circ. Res*. 116, 1431–1447.

Zhou, W., Xu, J., Tan, M., Li, H., Li, H., Wei, W., et al. (2018). UBE2M Is a Stress-Inducible Dual E2 for Neddylation and Ubiquitylation that Promotes Targeted Degradation of UBE2F. *Mol. Cell* 70:e6.

Zou, J., Ma, W., Li, J., Littlejohn, R., Zhou, H., Kim, I. M., et al. (2018). Neddylation mediates ventricular chamber maturation through repression of Hippo signaling. *Proc. Natl. Acad. Sci. U S A*. 115, E4101–E4110.

Zou, J., Ma, W., Littlejohn, R., Li, J., Stansfield, B. K., Kim, I. M., et al. (2019). Transient inhibition of neddylation at neonatal stage evokes reversible cardiomyopathy and predisposes the heart to isoproterenol-induced heart failure. *Am. J. Physiol. Heart Circ. Physiol*. 316, H1406–H1416.

Zuo, W., Huang, F., Chiang, Y. J., Li, M., Du, J., Ding, Y., et al. (2013). c-Cbl-mediated neddylation antagonizes ubiquitination and degradation of the TGF-beta type II receptor. *Mol. Cell* 49, 499–510.

Conflict of Interest: The authors declare that the research was conducted in the absence of any commercial or financial relationships that could be construed as a potential conflict of interest.

frontiers in Physiology

SYSTEMATIC REVIEW
published: 27 January 2021
doi: 10.3389/fphys.2020.625974

The Heart of the Alzheimer's: A Mindful View of Heart Disease

Alessandro Evangelisti[1†], *Helen Butler*[2†] *and Federica del Monte*[3*]

[1] Stanford Cardiovascular Institute, Stanford University, Stanford, CA, United States, [2] School of Medicine, Department of Molecular and Cellular Biology and Pathobiology, Medical University of South Carolina, Charleston, SC, United States, [3] Department of Medicine, Medical University of South Carolina, Charleston, SC, United States

Purpose of Review: This review summarizes the current evidence for the involvement of proteotoxicity and protein quality control systems defects in diseases of the central nervous and cardiovascular systems. Specifically, it presents the commonalities between the pathophysiology of protein misfolding diseases in the heart and the brain.

Recent Findings: The involvement of protein homeostasis dysfunction has been for long time investigated and accepted as one of the leading pathophysiological causes of neurodegenerative diseases. In cardiovascular diseases instead the mechanistic focus had been on the primary role of Ca^{2+} dishomeostasis, myofilament dysfunction as well as extracellular fibrosis, whereas no attention was given to misfolding of proteins as a pathogenetic mechanism. Instead, in the recent years, several contributions have shown protein aggregates in failing hearts similar to the ones found in the brain and increasing evidence have highlighted the crucial importance that proteotoxicity exerts via pre-amyloidogenic species in cardiovascular diseases as well as the prominent role of the cellular response to misfolded protein accumulation. As a result, proteotoxicity, unfolding protein response (UPR), and ubiquitin-proteasome system (UPS) have recently been investigated as potential key pathogenic pathways and therapeutic targets for heart disease.

Summary: Overall, the current knowledge summarized in this review describes how the misfolding process in the brain parallels in the heart. Understanding the folding and unfolding mechanisms involved early through studies in the heart will provide new knowledge for neurodegenerative proteinopathies and may prepare the stage for targeted and personalized interventions.

Keywords: Alzheimer's disease, heart failure, proteotoxicity, protein quality control (PQC), amyloid

OPEN ACCESS

Edited by:
Mark J. Ranek,
Johns Hopkins University,
United States

Reviewed by:
Zhao Wang,
University of Texas Southwestern Medical Center, United States
Henrique Girao,
University of Coimbra, Portugal

***Correspondence:**
Federica del Monte
delmonte@musc.edu

[†]*These authors have contributed equally to this work*

Specialty section:
This article was submitted to Clinical and Translational Physiology, a section of the journal Frontiers in Physiology

Received: *04 November 2020*
Accepted: *21 December 2020*
Published: *27 January 2021*

Citation:
Evangelisti A, Butler H and del Monte F (2021) The Heart of the Alzheimer's: A Mindful View of Heart Disease. Front. Physiol. 11:625974. doi: 10.3389/fphys.2020.625974

INTRODUCTION

Heart failure (HF) and Alzheimer's disease (AD) are age-dependent diseases that affect millions of people with rapidly increasing incidence. The lifetime risk of developing HF from 45 to 95 years of age is high (20–45%) and the number of death attributable to HF is also substantially high (Benjamin et al., 2019). Meanwhile, the growth prevalence of AD from 65 to 85 years of age is 3–32% and one in three seniors dies with AD or other dementias(2020). Importantly, HF and AD share risk factors in addition to age, which include epidemiological profiles, genetic predisposition,

redox characteristics, and protein homeostasis (Ames et al., 1993; Willis and Patterson, 2013; Huang et al., 2016; Benjamin et al., 2019). While dementia has been known to co-occur in patients with HF (1977; Cohen and Mather, 2007; De Toledo Ferraz Alves et al., 2010; Cermakova et al., 2015), evidence showed, only recently, that HF may co-occur in patients with AD (Troncone et al., 2016) with an estimate prevalence of about one third of cases (Reitz et al., 2007).

Key pathological hallmark of AD is the accumulation of protein aggregates as plaques, composed mainly of amyloid beta (Aß), and tangles mostly composed of hyperphosphorylated tau protein, featuring a defect in the folding of proteins and/or failure to correct or clear them. While protein homeostasis (proteostasis) has long been known to play a crucial role in the development of numerous neurodegenerative diseases such as AD, Parkinson's, and Huntington's disease, only recently, the importance of proteostasis has been recognized also for numerous diseases of various organs, including the heart. Those are now clustered as "proteinopathies."

Proteostatic failure has been shown in several cardiac pathologies, including hypertrophic, dilated and ischemic cardiomyopathies, atrial fibrillation and cardiac amyloidosis (Gorza and Del Monte, 2005; Predmore et al., 2010; Willis and Patterson, 2013; Del Monte and Agnetti, 2014; Rabbani and Thornalley, 2019).

Thus, in this review we summarize the processes of protein folding and misfolding and present the commonalities between the pathophysiology of protein misfolding diseases in the heart and the central nervous system (CNS) (summarized in the graphic abstract in **Table 1**, **Figure 1**). We will then focus on the direct link between cardiomyopathy and AD and how this finding is changing the current view of cardiac amyloidosis.

AGGREGATES: INDEXES OF MISFOLDING—ORIGIN AND CONSEQUENCES IN THE HEART AND BRAIN

Naturally, each protein undergoes a rigorous folding process to acquire its specific (native) conformation, which ultimately dictates the role and the localization of the protein itself (Hartl, 2011). Although folding of proteins is a necessary step for their function, it represents an energetically unfavorable process requiring a crew of facilitator proteins (participating in the protein quality control—PQC—described below) to timely and correctly achieve protein's native conformation. Failure to fold occurs normally, but is accelerated and amplified under conditions of cellular stress or pathological plights leading to misfold of the proteins from their stable and functional conformations and their precipitation as amyloid aggregates.

Amyloid aggregates are formed from misfolded globular, soluble proteins as a result of a combination of various factors including: a constant increase in the concentration of the precursor proteins with/out an acquired or hereditary mutation, an intrinsic propensity to misfold, or a proteolytic remodeling of a wild-type protein into an amyloidogenic fragment (Merlini, 2017; Picken, 2020). Following these processes, misfolded proteins progressively aggregate as soluble mono to poly-mers, protofibrils and ultimately as mature insoluble fibrils.

As misfolded proteins become hydrophobic, insoluble, and very resistant to degradation during the aggregation process, they also become highly reactive and unstable, leading to cellular stress and death and, ultimately, organ dysfunction (Falk et al., 2016; Merlini, 2017; Picken, 2020). Amply reported within different organ systems, pre-fibrillar species such as the soluble pre-amyloid oligomers (PAO) (Cleary et al., 2005; Demuro et al., 2010; Gianni et al., 2010; Del Monte and Agnetti, 2014 and protofibrils exert a potent toxic effect, known as proteotoxicity, driving, or contributing to the progression of the disease (Liao et al., 2001; Shi et al., 2010; Merlini, 2017; Picken, 2020). PAO and other pre-amyloidogenic species have been found to correlate with disease severity independently of amyloid fibril formation (Balducci et al., 2010; Currais et al., 2016; Chen and Mobley, 2019). For instance, a study by Diociaiuti et al., have shown that globular dimers, trimers and tetramers were the most toxic species, while monomers and larger aggregates such as insoluble amyloid plaques are almost inert in cultured primary hippocampal neurons (Diociaiuti et al., 2014; Mclendon and Robbins, 2015).

The mechanism of proteotoxicity was first identified by Demuro who demonstrated that the application of Aß PAO on neuroblastoma cells rapidly induces intracellular Ca^{2+} release, whereas the increase was not detectable when comparable amounts of monomeric and fibrillar forms were used (Demuro et al., 2005). PAO induced-Ca^{2+} release leading to cytosolic and organelles Ca^{2+} overload would in turn worsen the folding of proteins by inducing ER and oxidative stress, ultimately activating several pathogenic and apoptotic pathways. These findings lead to the introduction of the "Ca^{2+} hypothesis" of AD (Demuro et al., 2005, 2010; Yamasaki-Mann et al., 2010; Demuro and Parker, 2013) appending the "amyloid hypothesis" that wanted the accumulation of misfolded proteins as the primary driver of AD pathogenesis.

Contrary to the brain disease, Ca^{2+} dishomeastasis has been long recognized as key to the pathogenesis of myocardial dysfunction and HF (Gwathmey and Morgan, 1985; Gwathmey et al., 1987; Bers, 2002; Bers et al., 2003). Instead, only in the recent years, protein misfolding has been introduced as a novel pathogenic mechanism of cardiomyopathy. As in the brain, Aß PAO were found in the myocardium of patients diagnosed with idiopathic dilated cardiomyopathy (iDCM) and in the heart of AD patients (Sanbe et al., 2004; Gianni et al., 2010; Troncone et al., 2016). Paralleling the findings in neurons, PAO promote an increase in cytosolic and decrease in sarcoplasmic reticulum (SR) Ca^{2+} in cardiomyocytes, causing cell dysfunction and death (Gianni et al., 2010) adding a new possible cause of Ca^{2+} dishomeastasis in the failing heart. SR is a specialized ER in cardiomyocytes. Among other functions, SR tightly regulates the storage and fine-tuned control of Ca^{2+} spatial distribution and concentrations for the various Ca^{2+}-dependent cellular functions. Those include the cyclic rise and fall of Ca^{2+} that drives cardiomyocytes contractility (Bers, 2002; Glembotski, 2012) as well as the stable SR Ca^{2+} content required for the

TABLE 1 | Summary and references for the major findings described in the review.

Significant feature	Key findings	References
Aβ Aggregates in Heart and Brain	Plaque-like amyloid deposits in patients diagnosed with idiopathic dilated cardiomyopathy (iDCM)	Gianni et al., 2010; Troncone et al., 2016; Tublin et al., 2019
Ca^{2+} Hypothesis	Reduced proteasome activity leads to Ca^{2+} dysregulation which favors protein misfolding	Uddin et al., 2020
	Intracellular Ca^{2+} homeostasis disruption promotes cell dysfunction and death	Demuro et al., 2005, 2010; Gianni et al., 2010; Yamasaki-Mann et al., 2010; Torres et al., 2011; Demuro and Parker, 2013
ER Stress in Heart and Brain	ER stress increases in failing hearts	Okada et al., 2004; Guan et al., 2011; Park et al., 2012; Castillero et al., 2015; Uddin et al., 2018, 2020
	Inhibition of ER stress due to Aβ overload inhibits neurol apoptosis in AD mice	He et al., 2020
	Physical exercise alleviates cognitive impairment in AD mouse by reducing the expression of abnormal ER stress markers	Hong et al., 2020
Enhancing UPR^{ER} and UPR^{mt} to treat neurodegenerative and cardiovascular disease	ATF6 reprograms proteostasis, induces MANF, a protein folding chaperone in the heart, and downregulates the levels of β-site APP cleaving enzyme in AD models.	Blackwood et al., 2019a; Arrieta et al., 2020; Du et al., 2020
	GRP78, an ER Ca^{2+} dependent chaperone, protects against ischemic myocardial injury and restore ER stress in AD models	Vitadello et al., 2003; Pan et al., 2004; Shintani-Ishida et al., 2006
	Overexpression of LonP1, one of the main mitochondrial proteases, can mitigate cardiac injury during ischemic-reperfusion	Venkatesh et al., 2019
	Enhancement of UPR^{mt} in pressure-overloaded mice hearts significantly improves cardiomyocyte survival and and cardiac contractile function	Smyrnias et al., 2019
Targeting UPS to treat neurodegenerative and cardiovascular disease	LMP-2, a proteasome subunit, allows the breakdown of pre-existing sarcomeres, required for cardiac remodeling processes.	Petersen et al., 2020
	Triad3A, a E3 ligase, attenuates cardiac hypertrophy	Lu et al., 2020
	Resveratrol (RES) blocks immunoproteasome subunits (β1i, β2i and β5i) and reduces cardiac hypertrophy	Chen et al., 2019; Xie et al., 2020; Yan et al., 2020
	cAMP/PKA enhances clearance of aggregation-prone proteins in neurodegenerative diseases	Lin et al., 2013; Ranek et al., 2013; Lokireddy et al., 2015; Myeku et al., 2016
	cGMP/PKG positively regulates proteasome-mediated proteolysis degrading mutated CryAB in desmin cardiomyopathy	Liu et al., 2006a,b; Ranek et al., 2013
Enhancing autophagy to treat neurodegenerative and cardiovascular disease	TRAF6/p62 expression may relieve Aβ-mediated inhibition of $p75^{NTR}$ polyubiquitination and restore neuronal cell survival	Babu et al., 2005; Geetha et al., 2012; Chen et al., 2020

proper function of the Ca^{2+} dependent chaperones (GRP78 and 94) and of protein folding. Thus, changes in Ca^{2+} homeostasis and compartmentalization in the SR and Ca^{2+} dysfunction would induce not only the known abnormal cellular contractile function but also misfolding of protein and activation of the cellular response to the unfolded proteins accumulation (UPR) (Torres et al., 2011). Reduced SR Ca^{2+} content, commonly found in failing cardiomyocytes, would induce UPR activation, as demonstrated in AC16 cells treated with SERCA2a inhibitors (Castillero et al., 2015). Those findings highlight the delicate balance required for Ca^{2+} homeostasis in cardiomyocytes and provide a novel mechanism at the origin of the well-known Ca^{2+} dishomeastasis in HF.

In addition to cause intracellular Ca^{2+} dysregulation, *per se* activating the apoptotic pathways, proteotoxicity lead to cellular dysfunction and death through other mechanisms (Ruz et al., 2020). For instance, PAO-induced toxicity can cause disruption of mitochondrial membrane integrity and ultimately lead to metabolic cellular dysfunctions (Mclendon and Robbins, 2015). Moreover, it has been shown that proteotoxicity itself can activate a broad spectrum of pro-inflammatory pathways and lead to cell death independently of amyloid plaque formation (Wright et al., 2013; Currais et al., 2016).

Finally, accumulation of amyloid aggregate can also result from failure of the PQC, i.e., the unfolded protein response (UPR) and the ubiquitin proteasome system (UPS). Those can become overloaded with misfolded proteins or can present with reduced capacity from normal aging or malfunction (Wang et al., 2008; Predmore et al., 2010; Powell et al., 2012; Picken, 2020).

FOLDING OVERSEE: THE PROTEIN QUALITY CONTROL (PQC)

To remedy the natural course of these deleterious processes, the cell has developed molecular defense mechanisms (the PQC), which help preventing or correcting the damage and minimize the level of toxic misfolded proteins (Welch, 2004;

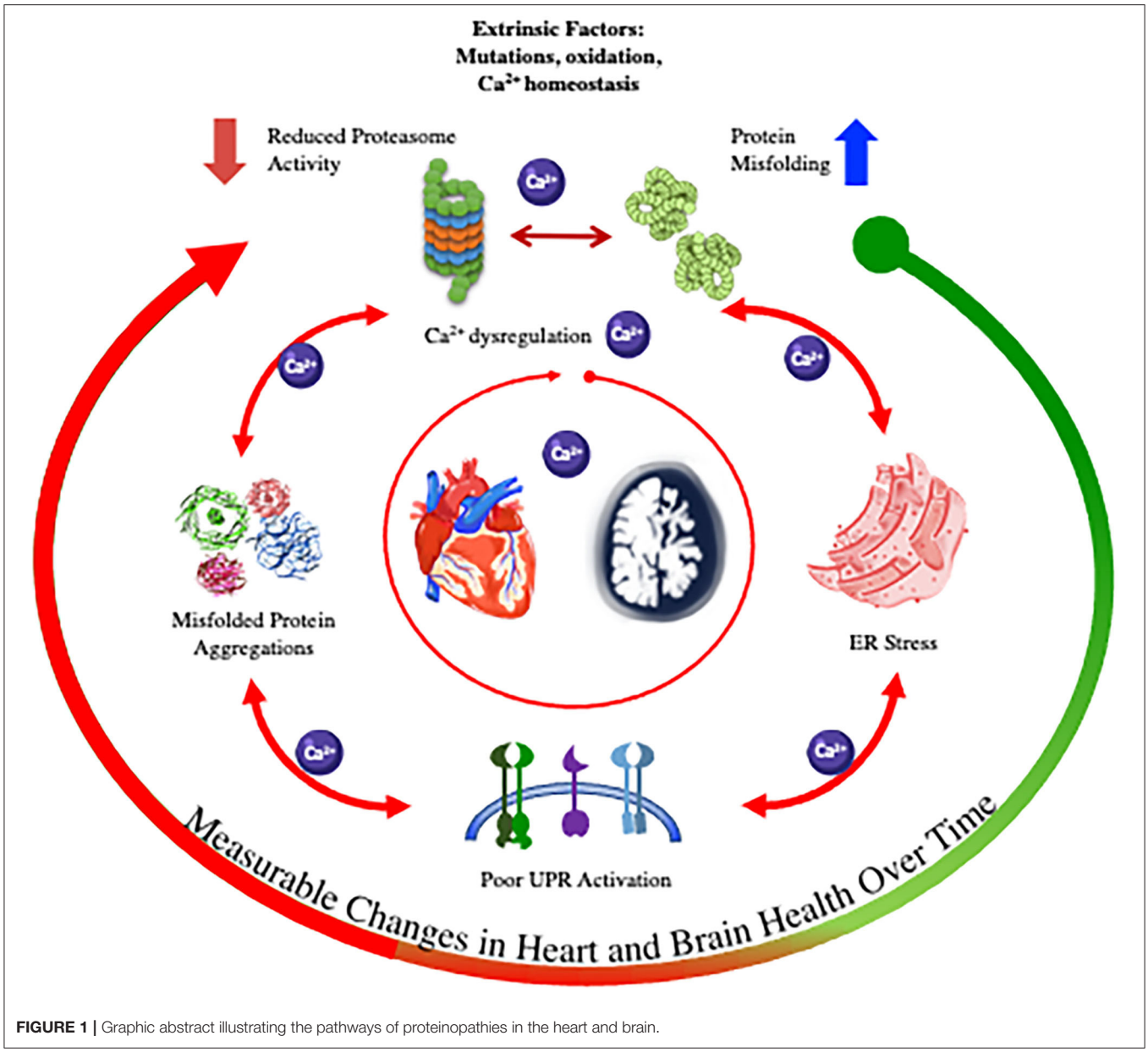

FIGURE 1 | Graphic abstract illustrating the pathways of proteinopathies in the heart and brain.

Glembotski et al., 2019; Wang and Wang, 2020). The PQC efficiently works through the interplay between specialized folding assistant proteins in the different cellular compartments (cytosolic heat shock response—HSR; ER and mitochondrial UPR—UPR^{ER} and UPR^{mt}) and the protein degradation system (Wang et al., 2013).

Due to the limited regenerative capacity of the cells of the central nervous and cardiovascular systems (neurons and cardiomyocytes) (Benfey and Aguayo, 1982; Eschenhagen et al., 2017), the proteolytic control mechanisms and protein turnover are key to their function and survival. In addition, in the heart, proteins of the contractile machinery, sarcomeric proteins, need to be continuously exchanged and remodeled in order to adapt to stressors and uninterrupted shear, making proper protein turnover of sarcomeres essential for cardiac function (Willis et al., 2008). Therefore, not surprisingly, dysfunction of the proteolytic systems and proteotoxicity are pathogenic mechanisms for neurodegenerative diseases and, now, HF (Brenner et al., 2004; Shi et al., 2010; Guan et al., 2014).

While the link between the UPR and degenerative disease of the heart and brain is now established, a conundrum lies in the unclear origin of the misfolding. Do extrinsic factors (e.g., mutations, oxidation, altered Ca^{2+} homeostasis) lead to the accumulation of protein aggregates that results in ER stress and the activation of UPR and ERAD/UPS? Or are these systems primarily dysfunctional (e.g., reduced proteasome activity), which leads to misfolded protein accumulations via Ca^{2+} dysregulation and/or oxidative stress (Uddin et al., 2020).

The Unfolded Protein Response (UPR)

First line of defense, molecular chaperones take part on the PQC pathways by associating with misfolded proteins and assisting in the proper folding or re-folding in the different subcellular compartments.

Heat shock proteins (Hsps) function to help promoting folding of cytosolic proteins and their transportation through membranes (Webster et al., 2019) while the Glucose-Regulated Proteins (GRPs), first described in mammalian cells exposed to glucose deprivation, assist the normal folding and refolding of ER/secretory proteins. Accumulation of misfolded proteins in the ER is sensed by the GRP chaperone proteins that are recruited to assist refolding while releasing the inhibition on three resident ER transmembrane sensors (PERK, IRE-1 and ATF6) (schematically illustrated in **Figure 2**). Those, when activated, lead to a signal cascade that triggers the refolding of proteins in the ER (Scheper et al., 2007; Glembotski, 2008; Arrieta et al., 2018) via the upregulation of the synthesis of chaperone proteins while inhibiting the overall protein synthesis to reduce the ER stress. Part of this response is the proteasome associated ER-associated degradation (ERAD), responsible for degrading terminally misfolded proteins (Plemper and Wolf, 1999). While the ER stress response is the natural reaction to cell threats and is meant to be beneficial to cells, if the ER stress is not resolved, prolonged activation of the UPR will shift to apoptotic cell death mediated by C/EBP homologous protein (CHOP), human caspase-4 and rodent caspase-12 (Wang et al., 1996; Nakagawa et al., 2000; Hitomi et al., 2004) described later. More recently discovered and less studied, the UPR^{mt} recognizes and degrades mitochondrial proteins that failed to fold. Misfolded proteins accumulated in the mitochondrial matrix are recognized by mitochondrial HSP (as HSP60) for refolding or degraded by mitochondrial proteases (as CLPP1) into peptide fragments. Those are exported to the cytosol by the HAF1 transporter enabling the inhibition of the import of the transcription factor ATFS in the mitochondria, shifting to its nuclear translocation for the transcription of protective genes for mitochondrial homeostasis (Rev in Jovaisaite et al., 2014).

UPR in the Brain and Heart

HSR

The first regulators of the cytosolic UPR are the heat-shock proteins Hsps. Hsps like Hsp28, HspB8, and αB-crystallin have been found upregulated in the brain of AD patients and co-localize with Aß plaques (Shinohara et al., 1993; Renkawek et al., 1994; Wilhelmus et al., 2006). Mouse models of AD have been used to investigate the role of Hsps in AD and found that mice, which are deficient in HspB1, are more sensitive to Aß PAO toxicity (Ojha et al., 2011) and crossing Hsp27 overexpressing mice with APPswe/PS1dE9 mice leads to mice that have fewer amyloid plaques and improved cognition (Tóth et al., 2013).

Hsps are also resident in heart tissues and have been shown to have functional roles in cardiovascular disease in humans and mice. Hsp90, Hsp22, and HspB1 have been shown to be cardioprotective from stressors like oxidative stress and ischemic damage (Kupatt et al., 2004; Islam et al., 2020; Wu et al., 2020). On the other hand, mutated αB-crystallin (CryAB(R120G) was the first cytosolic small chaperone linked to cardiomyopathy (Wang et al., 2001) and polymorphisms in HSPB7 have been identified as a risk factor for iDCM through a large SNP panel of patients from Germany and France (Stark et al., 2010). These evidences indicate both a deleterious and protective role of Hsps against amyloid aggregation in both the heart and brain, yet they do not demonstrate causality.

UPR^{ER}

In-vitro, mouse and human studies point to the ER stress response (UPR) as pathogenically involved in the progression of neurodegenerative diseases. Based on finding from cultured neuron, the ER stress response has been shown to be activated by Aß in AD (Yu et al., 1999; Nakagawa et al., 2000; Ferreiro et al., 2006; Seyb et al., 2006), and inhibition of Aß-induced ER stress was found to be effective in inhibiting neuronal apoptosis in some (although not all) transgenic AD mouse models (Lee et al., 2010; He et al., 2020). Impairment of the ER stress has also been shown to be the mechanism by which physical exercise mitigates cognitive impairment accompanied by reduction of the expression of ER stress markers in AD mouse brain (Hong et al., 2020). Either as primary involvement or exhaustion of the system, UPR was found impaired in human AD brains.

In the heart, models of cardiac hypertrophy by transverse aortic constriction (Okada et al., 2004; Uddin et al., 2018) result in increased levels of ER stress markers (i.e., GRP78, p-PERK, p- eIF2α, CHOP, caspase-12), suggesting a role for the UPR in HF progression and implicating ER stress as a mechanism for cardiomyocyte apoptotic cell death (Guan et al., 2011; Park et al., 2012). In human, mRNA levels of ER chaperones and markers of the UPR (GRP78/BiP, eIF2α, and XBP1) are increased in patients with HF (Okada et al., 2004; Castillero et al., 2015) supporting the translational relevance of the mice studies. However, the reversal of the stress markers activation by ventricular unloading may suggest a compensatory rather than causative role of the activation of the UPR in human HF.

As in the brain, UPR was also shown to be effective against the accumulation of PAO in the heart (Maloyan et al., 2007). Whether secondary of causative, chemical chaperones have been tested to alleviate cardiac hypertrophy and neurodegenerative disease in mice, suggesting their potential for relieving ER stress in proteinopathies (Park et al., 2012; Mimori et al., 2019). Additionally, re-chaperone therapy has been tested for neuronopathic lysosomal diseases and cystic fibrosis, a misfolded protein disease of the lungs (Suzuki, 2014). This evidence demonstrates that targeting the UPR may not only benefit the treatment of neurodegenerative diseases, but also degenerative diseases of the heart could substantially be positively adjusted.

Various reports also defined the involvement of the individual players of the UPR^{ER} for the heart and brain diseases. *The molecular chaperone* GRP78 (BiP) is reduced in patients with familial AD due to presenilin-1 (*PSEN*-1) mutations (Katayama et al., 1999; Niwa et al., 1999). The mechanism leading to this reduction was interrogated using cell culture studies of mutant mammalian cells which showed that *PSEN*-1 mutations can decrease GRP78 expression due to disturbed IRE1 function (Katayama et al., 1999; Niwa et al., 1999) while overexpression of

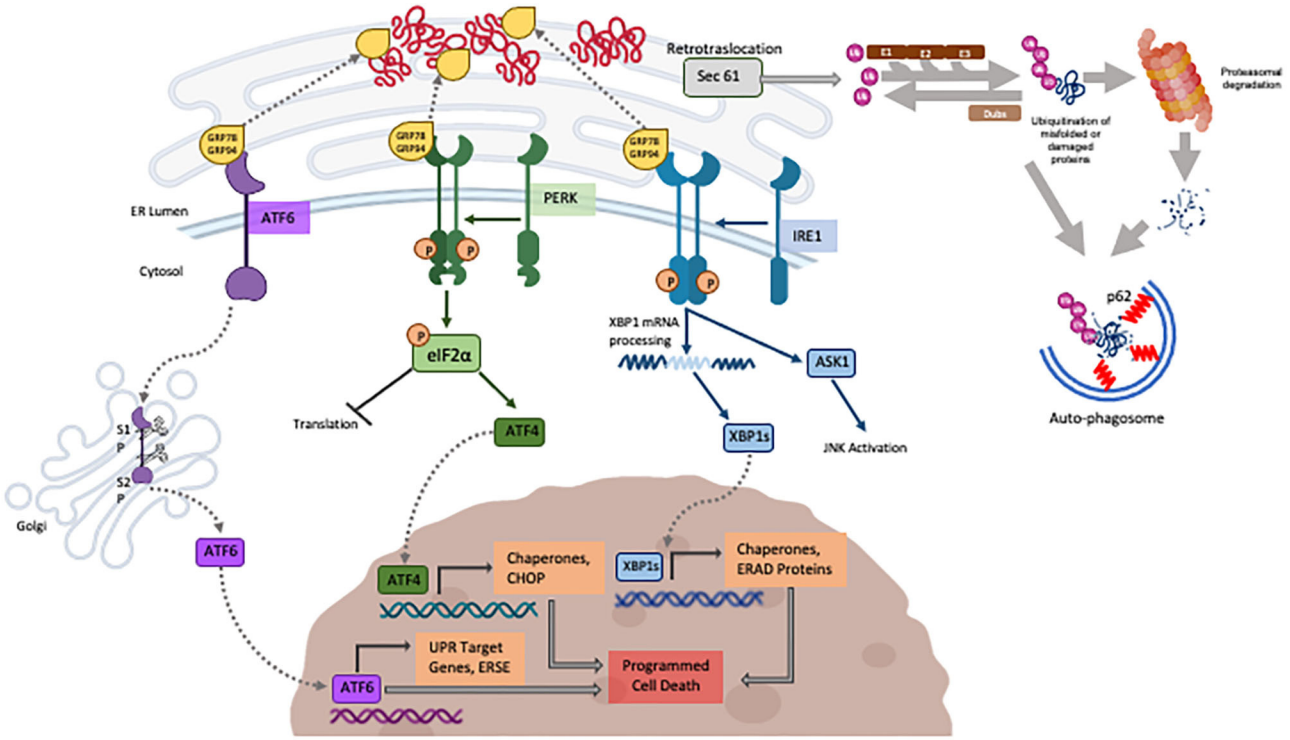

FIGURE 2 | Schematic illustration of the three major known pathways composing the UPR (created with BioRender) the UPS and autophagy described in the review.

GRP78 in *PSEN*-1 mutant cell lines restores ER stress to that of WT cells (Katayama et al., 1999; Niwa et al., 1999). In a follow up study, upregulation of GRP78 was found to be independent of presenilin expression, and the levels of this chaperone were not significantly different in the brains of sporadic AD vs. FAD (Sato et al., 2000). However, later studies found that mutant *PSEN*-1 neurons were more susceptible to cell death via ER stress and showed increased levels of the ER stress induced apoptotic mediator CHOP in *PSEN*-1 mouse models, also suggestive of ER stress (Milhavet et al., 2002; Terro et al., 2002). This suggests that either lack of or variants of *PSEN*-1 have an effect on ER-stress levels of GRP78. On the other hand, this may be due to a secondary activation via protein aggregation rather than presenilin expression or function. Upregulation of GRP78 was found in the neurons of AD patients early in disease progression regardless of presenilin mutation, but this protein did not co-localize with neuro-fibrillary tangles (Hoozemans et al., 2005), suggesting that early activation of the UPR may precede tangle formation or that the GRP78 upregulation occurs in brain cells other than neurons. Thus, while GRP78 may not be pathogenically directly linked to presenilin mutations, it may reflect the response to ER stress and protein aggregation regardless of the initiation event.

Less studied in the heart, GRP78 is upregulated in ischemic preconditioning and contributes to the protection against hypoxic conditions *in-vitro* (Pan et al., 2004) and ischemic myocardial injury *in-vivo* (Shintani-Ishida et al., 2006) while knockout of GRP78 promotes cardiomyocyte loss, HF and death (Wang et al., 2018). Similarly, overexpression of the chaperone GRP94 reduces myocyte degradation due to Ca^{2+} overload or ischemia in cultured skeletal and cardiac muscle cell cultures (Vitadello et al., 2003). Thus, while studies in the heart are limited, the data thus far suggest a cardioprotective role for ER chaperones in the heart.

The *PERK (Protein Kinase R-like ER Kinase)* pathway, one of the three transmembrane ER sensors, is activated in the AD brain (Unterberger et al., 2006). In a study of AD patients, of all ER stress markers tested, p-PERK was the only marker that correlated with disease progression, was increased in AD cases, and was largely associated with tau pathology (Buchanan et al., 2020). Correcting the defect using small-molecule PERK inhibitors showed to have therapeutic effects against neurodegeneration (Rozpedek-Kamińska et al., 2020).

While under unstressed conditions there was no effect on left ventricular mass or function (Misra et al., 2019) nor was there an effect on cardiomyocyte size, stressing the heart by aortic constriction resulted in decreased ejection fraction, increased LV fibrosis, and enhanced cardiomyocyte apoptosis in PERK knockout mice as compared to controls (Liu et al., 2014), suggesting a cardioprotective role for PERK in the heart following injury. As in the brain, PERK was shown to be protective against overload induced HF and lung remodeling in an inducible cardiac specific PERK knockout mouse line (Liu et al., 2014).

ATF6 (Activating Transcription Factor 6), a second transmembrane ER sensor, has been found to downregulate the

levels of β-site APP cleaving enzyme (BACE1), rescuing amyloid pathology in an AD mouse model (Du et al., 2020). Additionally, ATF6 is activated in ischemia/reperfusion injury and has shown to be protective in the brain as in the heart (Blackwood et al., 2019a), while ATF6 deletion in cardiomyocytes abrogates this protection. The mechanism of ATF6 protection in the heart was brought back to transcriptional reprogramming of proteostasis. ATF6 induces mesencephalic astrocyte-derived neurotrophic factor (MANF), which acts as a protein folding chaperone in the heart during periods of reductive stress (Arrieta et al., 2020). Further, RHEB (Ras homolog enriched in brain) was identified as another target of ATF6 in the heart during stressful conditions and acts as an activator of mTORC1 (mammalian target of rapamycin complex 1), which induces protein synthesis. The activation of these pathways during TAC was found to underlie the hypertrophic phenotype in the heart of WT mice, but not in cardiac specific ATF6 knockout mice (Blackwood et al., 2019b) validating the protective/compensatory effect of ATF6 in the heart.

Induction of *IRE1α (Inositol-requiring enzyme)*, a third ER sensing pathway of the UPR, phosphorylates, and activates its downstream regulator XBP-1 (X-box-binding protein) in the AD brain, further supporting the knowledge that also this branch of the UPR may be a defense activated mechanism in AD (Salminen et al., 2009; Lee et al., 2010). XBP1 is an upstream activator of the hexosamine biosynthetic pathway (HBP), the induction of which was found to be protective in the heart. Further, hypoxia has been found to specifically activate XBP1-inducible proteins within cardiac context in an *in-vitro* rat ventricular myocyte cell cultures, but the response was not further activated during reoxygenation (Thuerauf et al., 2006). Those findings support the functional response activation of the UPR in the heart, with the lack, however, of further activation upon reoxygenation possibly indicating the switch off of the response upon resolution of the insult. On the other hand, patients with end stage HF were found to have reduced XBP1 expression (Wang et al., 2014). Whether this represents an exhaustion of the system over a chronic condition or a primary defect leading to chronic myocardial damage is currently unknown. IRE1α also regulates the ASK1 (Apoptosis signal-regulating kinase 1) pathway, which is involved in Aß-induced neuronal cell death as demonstrated by the lack of Aß-induced death in ASK1$^{-/-}$ neurons (Kadowaki et al., 2005). A similar role for ASK1 has been shown in the heart of ASK1$^{-/-}$ mice, which showed reduced cardiomyocyte apoptosis and improved preservation of LV function compared to wildtype (Yamaguchi et al., 2003). Further elucidating the role of ASK1 in the heart, a transgenic mouse model of inducible overexpression of ASK1 found that there was greater injury after ischemia and reperfusion compared to WT (Liu et al., 2009). Thus, induction of IRE1α and its downstream effectors can have either protective or detrimental effects on the heart as shown by the cardioprotective role of XBP1 and the induction of cardiomyocyte death regulated by ASK1.

UPR^{mt}

In addition to the ER's own system of controlling protein homeostasis, UPR^{mt} is lately receiving a lot of attention given the organelle's key role in many metabolic functions, including ATP production and intracellular Ca^{2+} regulation (Duchen, 2004; Bereiter-Hahn et al., 2008; Munch, 2018). Function and quality of mitochondria need to be tightly controlled to ensure proper metabolic supplies and to prevent the production of reactive oxygen species (ROS) (Baker et al., 2011). Thus, mitochondrial dysfunction has been implicated in numerous diseases such as major neurodegenerative diseases, Parkinson's and Alzheimer's diseases and various cardiomyopathies (Duchen, 2004; Mclendon and Robbins, 2015). Stress conditions affecting the folding of proteins would also affect the overall cell viability by impairing mitochondrial function. In such a case, UPR^{mt} is triggered and it is activated in a very short time carrying on an acute response in order to alleviate proteostasis defects and restore cell survival by increasing the expression of mitochondrial proteases and chaperones and promoting biogenesis (Urbina-Varela et al., 2020).

Given its central role for cell metabolism, UPR^{mt} is essential for cell function and for the metabolic support in both brain and heart. On the same line of thoughts as for the other UPRs players, components of the UPR^{mt} are currently been investigated as potential novel therapeutic targets in AD. Activation of UPR^{mt} genes has been showed to be a distinct feature in both familial and sporadic AD compared to healthy individuals (Beck et al., 2016). Recently, a study carried by Sorrentino et al. showed that boosting mitochondrial proteostasis by enhancing the UPR^{mt} and mitophagy ultimately decreased Aβ aggregation, reduced amyloid plaque formation and ameliorated contextual memory in the APP/PSEN1 AD mice (Sorrentino et al., 2017).

Similarly, Venkatesh et al., recently showed that enhancing UPR^{mt} by overexpressing LonP1, one of the main mitochondrial proteases, can mitigate cardiac injury during ischemia-reperfusion by preventing oxidative damage, in part by rebalancing the OXPHOS complex subunit levels (Arrieta et al., 2019; Venkatesh et al., 2019). Additionally, pharmacological enhancement of UPR^{mt} in pressure-overloaded mouse hearts significantly improved mitochondrial respiration, cardiomyocyte survival, and cardiac contractile function (Smyrnias et al., 2019).

Ubiquitin Protease System (UPS)

Failure of the UPR to refold damaged proteins and/or resolve the ER stress result in the activation of the degradation pathways (UPS) aimed at recycling the building blocks for new protein synthesis in a process that begins with substrate polyubiquitination followed by proteasome degradation (Li et al., 2011; Ciechanover and Kwon, 2015; Gilda and Gomes, 2017). Under normal circumstances, the UPS degrades around 90% of proteins and its reach expands to all cellular compartments including nucleus, cytoplasm, ER as well as cell membranes (Schubert et al., 2000; Pagan et al., 2013). In addition to expired or environmentally damaged old proteins, as many as 30% of newly synthesized proteins are also degraded by the proteasome within a few minutes of their synthesis due to inherent difficulties in folding properly (Schubert et al., 2000; Bucciantini et al., 2002; Pagan et al., 2013).

UPS in the Brain and Heart

When the UPR fails, the UPS combats the accumulation of toxic protein aggregates. Therefore, it is not surprising that damage of this system would have severe consequences to the brain and heart structure and function. In both organs, failure of the proteasome activity has been described in degenerative diseases. Within the brain of AD patients, proteasome inhibition is sufficient to cause neuronal death (Keck et al., 2003). In the heart, an imbalance between ubiquitination rates and degradation of ubiquitin labeled substrates is implicated in cardiomyocyte's cell death (Kostin et al., 2003).

As misfolded proteins are central biomarkers in the pathophysiology of numerous neurodegenerative diseases, with aggregates of Aß being central to AD (Willis and Patterson, 2013), several studies have shown that deficiency in Aß clearance may be a major cause of late-onset AD. Moreover, ubiquitin proteins have been observed within the intracellular tangles typical of AD (Mori et al., 1987; Perry et al., 1987). Since then, much attention has been given to the UPS in AD because of both its main role in intracellular proteolytic pathways and its presence within AD protein aggregates (Riederer et al., 2011).

Several hypotheses have been considered to explain the causes of UPS dysfunction; in addition to inherited genetic mutations, which are responsible for familial AD, there is accumulating evidence that oxidative stress signaling may have a crucial early pathogenic role in the late-onset and sporadic AD by irreversibly modifying proteins (Riederer et al., 2011). Various protein modifications such as carbonylation and nitration are generally associated with loss of function leading to either unfolding and degradation of the damaged proteins or to the aggregation and accumulation of the latter as inclusions (Butterfield et al., 2006). Different studies showed that the accumulation of oxidized protein in AD is tightly associated with dysfunction of the 20S proteasome, which is the main player in the proteolytic activity of the UPS (Szweda et al., 2002). Members of the proteasome themselves may be altered due to oxidative stress, which can lead to protein misfolding and may ultimately influence the correct functionality of the proteolytic mechanisms. Some components of the UPS themselves may be subject to oxidation or mutations, consequently influencing misfolded protein accumulation instead of their degradation (Riederer et al., 2011). Defective proteolysis has been manly seen in the hippocampus, para-hippocampal, and middle temporal gyri, and the inferior parietal lobule of AD patients; moreover, proteolytic dysfunction has been hypothesized to cause synaptic dysregulation, which is observed early in AD since protein degradation plays a fundamental role in synaptic plasticity (Wang and Huang, 2012).

In the heart, impaired proteasome activity was first shown in hypertrophic and failing human hearts in absence of changes in proteasome protein expression suggesting that post-translational modifications are responsible for the defective proteasomal degradation capacity (Predmore et al., 2010). Recent studies have focused on the role of the ubiquitin protease system (UPS) in cardiac hypertrophy as a mechanism of cardiac remodeling, a maladaptive and unfavorable outcome that can progress into overt HF (Frey and Olson, 2003), providing a molecular mechanisms for many abnormal signaling pathways in cardiomyopathies. In fact, it has recently been shown that breakdown of pre-existing sarcomeres, required for cardiac remodeling processes is optimized by the induction of the proteasome subunit low molecular weight protein (LMP)-2 (Petersen et al., 2020). Furthermore, a key regulator of normal cardiac growth and activated by exercise and pressure overload as short term adaptive response (Shiojima et al., 2005) AKT leads to cardiac hypertrophy in mice upon sustained induction (Shiojima et al., 2005) and is negatively regulated by PTEN. This signaling pathways has been shown to be modulated by two UPS players, the enzyme that catalyzes the first step in ubiquitin conjugation, UBA1 (Shu et al., 2018) and by TRIM10 (Yang et al., 2020), an E3 ubiquitin ligase that assists in the conjugation of ubiquitin to protein substrate, both degrading PTEN leading to increase AKT and hypertrophy. Additionally, investigations of Triad3A (an E3 ligase) have shown that increased expression of this E3 ligase attenuates cardiac hypertrophy (Lu et al., 2020) through ubiquitination of toll-like receptors 4 and 9 (TLR4 7 TLR9) (Lu et al., 2020). Activation of these TLRs of the innate immune system activates AKT signaling. Notably this enzyme is also implicated in neurodegenerative diseases (Husain et al., 2017). Thus, while the UPS system is implicated in cardiac remodeling and hypertrophy, reduction or activation of AKT signaling can result from divergent manipulations of UPS depending on the pathways invested.

Myocardial hypertrophy is also modulated by the immunoproteasome, an inducible form of the constitutive proteasome. Inhibition or knockout of immunoproteasome subunits (β1i, β2i, and β5i) has been shown to attenuate cardiac hypertrophy (Chen et al., 2019; Xie et al., 2020; Yan et al., 2020) a postulated mechanism underlying the effect of resveratrol (RES) (Chen et al., 2019). RES blocks immunoproteasome activity, thus preventing PTEN degradation and AKT signaling (Xie et al., 2020; Yan et al., 2020).

The role of ubiquitination in cardiac remodeling has also been documented through the inhibition of the de-ubiquitination enzymes (DUBs). Investigations into 19S proteasome deubiquitinates showed that inhibition of these DUBs prevents the breakdown of IκBα and leads to the inactivation of NF-κB, which suppresses cardiac remodeling (Hu et al., 2018). Furthermore, an additional DUB—UCHL1—is known to be dysregulated and is involved both in neurodegenerative disorders and more recently in cardiac hypertrophy (Hu et al., 2018). UCHL1 deubiquitinates epidermal growth factor receptor (Hershberger et al., 2010), preventing its degradation and resulting in the activation of multiple downstream signaling cascades that positively regulate cardiac hypertrophy (Bi et al., 2020).

Much like hypertrophic cardiomyopathy and like in many other diseases in which protein misfolding and aggregation is the major hallmark of their pathophysiology, UPS has been shown to participate to the pathogenesis of restrictive cardiomyopathy. An example is desmin-related myopathy, which affects both skeletal and cardiac muscle ultimately developing desmin-related cardiomyopathy (DRC). Genetic mutations of desmin and of its small chaperone protein, αB-crystallin, can lead to aberrant

aggregation of desmin resulting in cardiomyopathy with poor disease prognosis (Chen et al., 2005). Chen et al. found that the aberrant aggregation of these proteins impairs the UPS system before cardiac hypertrophy occurs leading to heart remodeling (Chen et al., 2005).

On the same line of research, Liu et al. showed that UPS proteolytic function in the heart is severely impaired also when a human mutant desmin is expressed in transgenic mouse hearts (Liu et al., 2006a). Like other groups, they demonstrated that the deficiency likely responsible for the pathophysiology of the disease resides in the 19S regulatory cap, which helps to channel and deliver the substrate into the proteolytic chamber of the 20S core (Chen et al., 2005; Liu et al., 2006a). The results of these studies suggest that malfunctions in the UPS may directly participate in the pathogenesis of the disease, although as a secondary event to the accumulation of misfolded proteins. In fact, in a follow up study, Liu et al. showed that upregulation of members of the heat shock proteins family significantly attenuated the aberrant aggregation of desmin demonstrating that protein aggregation is a major pathogenic pathway in which misfolded proteins cause UPS impairment and malfunction (Liu et al., 2006b).

As protein aggregates are present in dilated cardiomyopathies, a defect in the ubiquitin proteasome system is foreseeable as a consequence of overwhelming of this defense mechanism. Additionally, a primary defect of the UPS has been identified in DCM though mutations in FBXO32, encoding for an E3 ubiquitin ligase (Al-Hassnan et al., 2016), a finding validated in a mouse model where FBXO32 knockout cause DCM (Al-Hassnan et al., 2016).

Additional studies further support the notion that overactivation or dysregulation of ubiquitin mediated protein degradation has a role in the progression of DCM (Li et al., 2017; Murata et al., 2018; Spanig et al., 2019). LIM domain 7 (LMO7) gene, a protein with predicted interaction domains PDZ and LIM, has been long thought to take part in regulation of UPS pathway in cardiac tissues (Li et al., 2017). Recently, it was found that DCM patients display decreased mRNA levels of LMO7 and polymorphisms of the gene have been linked to the susceptibly and prognosis of disease (Li et al., 2017). Protein arginine methyltransferase 1 (PRMT1) is universally expressed, assists in the post-translational modification of proteins, is associated with alternative splicing, and is integral for the function of multiple tissue types (Murata et al., 2018). Deletion of this protein in juvenile mice lead to the formation of cardiac alternative splicing isoforms of four genes, including ASB2, resulting in its truncation and failure to act as the proper component in an E3 ligase complex, leading to development of DCM (Murata et al., 2018). Further support for the role of the UPS in DCM was provided by a study that characterized the UPS activity in human heart tissue from cardiomyopathy patients and found decreased percentage of ubiquitin-positive cells and cells with ubiquitin deposits in end-stage cardiac tissue (Spanig et al., 2019). Additionally, a trend for reduced protein expression of MAFbx (E3-ubiquitin-ligases muscle-atrophy-F-box), a regulator of cardiac remodeling and inhibitor of hypertrophy through ubiquitin degradation of calcineurin, was found in the DCM group (Spanig et al., 2019).

Finally, in a study of 60 human patients with HF, it was found that enhanced expression of ubiquitin in cardiomyocytes is a protective mechanism in early stages of HF, whereas the absence or decreased ubiquitin expression associates with end-stage DCM (Pawlak et al., 2019).

Given the numerous studies that have demonstrated the importance of the UPS in both neurodegenerative and cardiovascular diseases, new ways of targeting the proteasome-ubiquitin machinery have been explored. Among all the post-translation modifications that subunits of the UPS undergo in order to activate the clearance mechanism, and efficiently degrade ubiquitinated proteins, phosphorylation surely plays a central role. This seems to be accomplished by most kinases such as PKA and cGMP-dependent kinase (PKG) (Ranek et al., 2013); therefore, both molecules became ideal therapeutic targets to prime the dysregulated UPS response. A study from Ranek et al. showed that PKG positively regulates proteasome-mediated proteolysis degrading mutated CryAB (Liu et al., 2006a,b; Ranek et al., 2013).

Like in the heart, multiple studies showed that enhancing PKA in different cell lines and mouse models of neurodegenerative diseases, such as tauopathies, Huntington's and Alzheimer's disease, causes an augmented clearance of aggregation-prone proteins in both the soluble and insoluble fractions (Lin et al., 2013; Ranek et al., 2013; Lokireddy et al., 2015; Myeku et al., 2016). In addition to rescue UPS proper function, enhancing cAMP has been shown to improve cognitive and memory functions in Alzheimer's patients (Vitolo et al., 2002). Studies have demonstrated that different phosphodiesters inhibitors can augment cAMP/PKA and cGMP/PKG signaling (Verplank et al., 2019), and therefore strengthen the UPS response in mouse model of AD and cardiac amyloid proteinopathy (Sheng et al., 2017; Verplank et al., 2019).

Autophagy

Autophagy is a highly evolutionary conserved system to degrade retired or damaged proteins and organelles and selectively degrades aggregated proteins. Even though UPS and autophagy are two distinct proteolytic systems, they interact to remove long-lived proteins and unrepairable misfolded ones (Chen et al., 2020). The link between the UPS and autophagy is mediated by p62 (Rusten and Stenmark, 2010), a receptor of autophagy substrate that is activated by phosphorylation upon proteotoxic stress due to UPS inhibition, inducing autophagy (Zheng et al., 2011; Lim et al., 2015; Sha et al., 2018; Pan et al., 2020). Given its central function, changes in p62 have been linked to diseases. Defunct autophagic systems can lead to p62 accumulation, delayed arrival of waste to the proteasome and disturbance of the UPS (Korolchuk et al., 2009).

In the AD brain p62 acts to clear misfolded proteins such as hyperphosphorylated and polyubiquitinated tau through proteasomal degradation (Babu et al., 2005), reinforcing the importance of p62's relationship with AD disease progression. Indeed, decreased expression of p62 aligns with AD progression,

leading to a decline in clearance of polyubiquitinated tau and promotion of tau aggregates (Alonso et al., 1994). Furthermore, cooperation of p62 and TRAF6 inhibits Aβ-mediated neuronal death through p75 ^{NTR} activity (Geetha et al., 2012). Thus, enhancing p62 and TRAF6 expression might relieve tau aggregation and Aβ-mediated neuronal death in the AD brain.

Less studied in the heart, a feedforward loop in the activation of autophagy by proteasome inhibition has been delineated through the PPP3/calcineurin-TFEB-SQSTM1/p62 pathway (Su and Wang, 2020). Studies investigating the role of p62 in protein misfolding diseases of the heart appear limited to desmin cardiomyopathy and atherosclerosis. In a mouse model of desmin cardiomyopathy by DRC-linked mutant desmin or αB-crystallin (CryAB^{R120G}) and in cultured rat neonatal cardiomyocytes expressing the mutant desmin autophagic flux both *in-vivo* and *in-vitro* was augmented together with increased mRNA and protein levels of p62 (Zheng et al., 2011). Those findings provided evidence for p62/autophagy adaptive response to the forced accumulation of misfolded proteins while p62 depletion worsened the misfolded aggregates accumulation and exacerbated cell injury supporting the protective effect of p62/autophagy for proteotoxic stress.

Finally, in the atherosclerotic disease p62-enriched aggregates are recognized as a hallmark of advancing atherosclerotic plaques due to dysfunctional autophagy (Sergin et al., 2016).

THE DIRECT LINK BETWEEN AD AND HF

With still unidentified protein precursor, the discovery of protein aggregates, in the form of both extracellular plaques and intracellular amyloid fibers, in the hearts of patients with primary diagnosis of iDCM (Gianni et al., 2010) helped to link the heart and brain proteinopathies. Subsequent characterization showed that prefibrillar myocardial deposits in iDCM were biochemically analogous to those found in AD (Subramanian et al., 2015), and later, misfolding, aggregation, and deposition of amyloid-beta (Aß) were found in the myocardium of patients with primary diagnosis of AD compromising myocardial function effectively pathogenically linked the disease in both organs (Troncone et al., 2016). Whether the link between HF and AD being of metastatic or systemic etiology is still to be determined, evidence support the possible dual nature of the link. In support of the systemic etiology genetic variants in the presenilin gene (PSEN) were identified not only in familial (Li et al., 2006), but also in sporadic (Gianni et al., 2010) cases of dilated cardiomyopathies, while the abovementioned deposits of Aß in patients with AD may also support the metastatic route of Alzheimer's cardiomyopathy—the traditional route of cardiac involvement in the SAA, AL, and TTR amyloidosis. Either ways, these findings show the heart-brain axis can be framed as an organ system that can be exploited by mechanisms (e.g., protein misfolding) that result in physiological and pathological disease in both organs.

CONCLUSIONS

Emerging data has led to the formation of new hypotheses regarding the relationship between AD and HF and has opened novel research avenues for basic science and clinical research. The common pathogenesis of proteinopathies is supported by the accumulation of misfolded protein aggregates, the involvement of proteotoxicity and defects in protein quality control systems in disease of both the heart and the brain. The focus of future studies should highlight the unclear origin of protein misfolding in degenerative diseases of the cardiovascular and central systems. Increasing understanding of cellular and molecular mechanisms involved in the onset and progression of protein misfolding diseases will overall allow to develop more precise and targeted therapeutic approaches.

DATA AVAILABILITY STATEMENT

The original contributions presented in the study are included in the article/supplementary material, further inquiries can be directed to the corresponding author/s.

AUTHOR CONTRIBUTIONS

AE and HB reviewed the literature and wrote the draft. FdM edited the draft to the final version. All authors contributed to the article and approved the submitted version.

FUNDING

This work was supported by the American Heart Association (17CSA33620007 and 20SRG35540029), The National Institute of Health (R01AG057046), the Medical University of South Carolina Discretionary Funds, The Christie Heart and Brain Program philanthropic donation, The University of Bologna to FdM; Translational Research and Applied Medicine (TRAM) pilot grant at Stanford University to AE; National Institute for General Medical Sciences (NIH) T32GM132055 predoctoral fellowship to HB from the College of Graduate Students of the Medical University of South Carolina.

REFERENCES

(1977). Cardiogenic Dementia. *Lancet* 1, 27–28.

(2020). 2020 Alzheimer's disease facts and figures. Alzheimer's Dement. 16, 391–460. doi: 10.1002/alz.12068

Al-Hassnan, Z. N., Shinwari, Z. M. A., Wakil, S. M., Tulbah, S., Mohammed, S., Rahbeeni, Z., et al. (2016). A substitution mutation in cardiac ubiquitin ligase, FBXO32, is associated with an autosomal recessive form of dilated cardiomyopathy. *BMC Med. Genet.* 17:3. doi: 10.1186/s12881-016-0267-5

Alonso, K., Pontiggia, P., Sabato, A., Calvi, G., Curto, F. C., de Bartolomei, E., et al. (1994). Systemic hyperthermia in the treatment of HIV-related disseminated Kaposi's sarcoma. long-term follow-up of patients treated with low-flow extracorporeal perfusion hyperthermia. *Am. J. Clin. Oncol.* 17, 353–359. doi: 10.1097/00000421-199408000-00015

Ames, B. N., Shigenaga, M. K., and Hagen, T. M. (1993). Oxidants, antioxidants, and the degenerative diseases of aging. *Proc. Natl. Acad. Sci. U.S.A.* 90, 7915–7922. doi: 10.1073/pnas.90.17.7915

Arrieta, A., Blackwood, E. A., and Glembotski, C. C. (2018). ER protein quality control and the unfolded protein response in the heart. *Curr. Top. Microbiol. Immunol.* 414, 193–213. doi: 10.1007/82_2017_54

Arrieta, A., Blackwood, E. A., Stauffer, W. T., and Glembotski, C. C. (2019). Integrating ER and mitochondrial proteostasis in the healthy and diseased heart. *Front. Cardiovasc. Med.* 6:193. doi: 10.3389/fcvm.2019.00193

Arrieta, A., Blackwood, E. A., Stauffer, W. T., Santo Domingo, M., Bilal, A. S., Thuerauf, D. J., et al. (2020). Mesencephalic astrocyte–derived neurotrophic factor is an ER-resident chaperone that protects against reductive stress in the heart. *J. Biol. Chem.* 295, 7566–7583. doi: 10.1074/jbc.RA120.013345

Babu, J. R., Geetha, T., and Wooten, M. W. (2005). Sequestosome 1/p62 shuttles polyubiquitinated tau for proteasomal degradation. *J. Neurochem.* 94, 192–203. doi: 10.1111/j.1471-4159.2005.03181.x

Baker, M. J., Tatsuta, T., and Langer, T. (2011). Quality control of mitochondrial proteostasis. *Cold Spring Harb. Perspect. Biol.* 3:ea007559. doi: 10.1101/cshperspect.a007559

Balducci, C., Beeg, M., Stravalaci, M., Bastone, A., Sclip, A., Biasini, E., et al. (2010). Synthetic amyloid-beta oligomers impair long-term memory independently of cellular prion protein. *Proc. Natl. Acad. Sci. U.S.A.* 107, 2295–2300. doi: 10.1073/pnas.0911829107

Beck, J. S., Mufson, E. J., and Counts, S. E. (2016). Evidence for mitochondrial UPR gene activation in familial and sporadic Alzheimer's disease. *Curr. Alzheimer Res.* 13, 610–614. doi: 10.2174/1567205013666151221145445

Benfey, M., and Aguayo, A. J. (1982). Extensive elongation of axons from rat brain into peripheral nerve grafts. *Nature* 296, 150–152. doi: 10.1038/296150a0

Benjamin, E. J., Muntner, P., Alonso, A., Bittencourt, M. S., Callaway, C. W., Carson, A. P., et al. (2019). Heart disease and stroke statistics-2019 update: a report from the American heart association. *Circulation* 139, e56–e528. doi: 10.1161/CIR.0000000000000659

Bereiter-Hahn, J., Voth, M., Mai, S., and Jendrach, M. (2008). Structural implications of mitochondrial dynamics. *Biotechnol. J.* 3, 765–780. doi: 10.1002/biot.200800024

Bers, D. M., Eisner, D. A., and Valdivia, H. H. (2003). Sarcoplasmic reticulum Ca2+ and heart failure: roles of diastolic leak and Ca2+ transport. *Circ. Res.* 93, 487–490. doi: 10.1161/01.RES.0000091871.54907.6B

Bers, D. M. (2002). Cardiac excitation-contraction coupling. *Nature* 415, 198–205. doi: 10.1038/415198a

Bi, H.-L., Zhang, X.-L., Zhang, Y.-L., Xie, X., Xia, Y.-L., Du, J., et al. (2020). The deubiquitinase UCHL1 regulates cardiac hypertrophy by stabilizing epidermal growth factor receptor. *Sci. Adv.* 6:eaax4826. doi: 10.1126/sciadv.aax4826

Blackwood, E. A., Azizi, K., Thuerauf, D. J., Paxman, R. J., Plate, L., Kelly, J. W., et al. (2019a). Pharmacologic ATF6 activation confers global protection in widespread disease models by reprograming cellular proteostasis. *Nat. Commun.* 10:187. doi: 10.1038/s41467-018-08129-2

Blackwood, E. A., Hofmann, C., Domingo, M. S., Bilal, A. S., Sarakki, A., Stauffer, W., et al. (2019b). ATF6 regulates cardiac hypertrophy by transcriptional induction of the mTORC1 activator, Rheb. *Circ. Res.* 124, 79–93. doi: 10.1161/CIRCRESAHA.118.313854

Brenner, D. A., Jain, M., Pimentel, D. R., Wang, B., Connors, L. H., Skinner, M., et al. (2004). Human amyloidogenic light chains directly impair cardiomyocyte function through an increase in cellular oxidant stress. *Circ. Res.* 94, 1008–1010. doi: 10.1161/01.RES.0000126569.75419.74

Bucciantini, M., Giannoni, E., Chiti, F., Baroni, F., Formigli, L., Zurdo, J., et al. (2002). Inherent toxicity of aggregates implies a common mechanism for protein misfolding diseases. *Nature* 416, 507–511. doi: 10.1038/416507a

Buchanan, H., Mackay, M., Palmer, K., Tothová, K., Katsur, M., Platt, B., et al. (2020). Synaptic loss, ER stress and neuro-inflammation emerge late in the lateral temporal cortex and associate with progressive tau pathology in Alzheimer's disease. *Mol. Neurobiol.* 57, 3258–3272. doi: 10.1007/s12035-020-01950-1

Butterfield, D. A., Perluigi, M., and Sultana, R. (2006). Oxidative stress in Alzheimer's disease brain: new insights from redox proteomics. *Eur. J. Pharmacol.* 545, 39–50. doi: 10.1016/j.ejphar.2006.06.026

Castillero, E., Akashi, H., Pendrak, K., Yerebakan, H., Najjar, M., Wang, C., et al. (2015). Attenuation of the unfolded protein response and endoplasmic reticulum stress after mechanical unloading in dilated cardiomyopathy. *Am. J. Physiol. Heart Circ. Physiol.* 309, H459–H470. doi: 10.1152/ajpheart.00056.2015

Cermakova, P., Eriksdotter, M., Lund, L. H., Winblad, B., Religa, P., and Religa, D. (2015). Heart failure and Alzheimer's disease. *J. Intern. Med.* 277, 406–425. doi: 10.1111/joim.12287

Chen, C., Zou, L.-X., Lin, Q.-Y., Yan, X., Bi, H.-L., Xie, X., et al. (2019). Resveratrol as a new inhibitor of immunoproteasome prevents PTEN degradation and attenuates cardiac hypertrophy after pressure overload. *Redox Biol.* 20, 390–401. doi: 10.1016/j.redox.2018.10.021

Chen, Q., Liu, J. B., Horak, K. M., Zheng, H., Kumarapeli, A. R., Li, J., et al. (2005). Intrasarcoplasmic amyloidosis impairs proteolytic function of proteasomes in cardiomyocytes by compromising substrate uptake. *Circ. Res.* 97, 1018–1026. doi: 10.1161/01.RES.0000189262.92896.0b

Chen, X. Q., and Mobley, W. C. (2019). Alzheimer disease pathogenesis: insights from molecular and cellular biology studies of oligomeric abeta and tau species. *Front. Neurosci.* 13:659. doi: 10.3389/fnins.2019.00659

Chen, Y., Li, Q., Li, Q., Xing, S., Liu, Y., Liu, Y., et al. (2020). p62/SQSTM1, a central but unexploited target: advances in its physiological/pathogenic functions and small molecular modulators. *J. Med. Chem.* 63, 10135–10157. doi: 10.1021/acs.jmedchem.9b02038

Ciechanover, A., and Kwon, Y. T. (2015). Degradation of misfolded proteins in neurodegenerative diseases: therapeutic targets and strategies. *Exp. Mol. Med.* 47:e147. doi: 10.1038/emm.2014.117

Cleary, J. P., Walsh, D. M., Hofmeister, J. J., Shankar, G. M., Kuskowski, M. A., Selkoe, D. J., et al. (2005). Natural oligomers of the amyloid-beta protein specifically disrupt cognitive function. *Nat. Neurosci.* 8, 79–84. doi: 10.1038/nn1372

Cohen, M. B., and Mather, P. J. (2007). A review of the association between congestive heart failure and cognitive impairment. *Am. J. Geriatr. Cardiol.* 16, 171–174. doi: 10.1111/j.1076-7460.2007.06563.x

Currais, A., Quehenberger, O., A, M.A., Daugherty, D., Maher, P., and Schubert, D. (2016). Amyloid proteotoxicity initiates an inflammatory response blocked by cannabinoids. *NPJ Aging Mech. Dis.* 2:16012. doi: 10.1038/npjamd.2016.12

De Toledo Ferraz Alves, T. C., Ferreira, L. K., Wajngarten, M., and Busatto, G. F. (2010). Cardiac disorders as risk factors for Alzheimer's disease. *J. Alzheimers. Dis.* 20, 749–763. doi: 10.3233/JAD-2010-091561

Del Monte, F., and Agnetti, G. (2014). Protein post-translational modifications and misfolding: new concepts in heart failure. *Proteomics Clin. Appl.* 8, 534–542. doi: 10.1002/prca.201400037

Demuro, A., Mina, E., Kayed, R., Milton, S. C., Parker, I., and Glabe, C. G. (2005). Calcium dysregulation and membrane disruption as a ubiquitous neurotoxic mechanism of soluble amyloid oligomers. *J. Biol. Chem.* 280, 17294–17300. doi: 10.1074/jbc.M500997200

Demuro, A., and Parker, I. (2013). Cytotoxicity of intracellular abeta42 amyloid oligomers involves Ca2+ release from the endoplasmic reticulum by stimulated production of inositol trisphosphate. *J. Neurosci.* 33, 3824–3833. doi: 10.1523/JNEUROSCI.4367-12.2013

Demuro, A., Parker, I., and Stutzmann, G. E. (2010). Calcium signaling and amyloid toxicity in Alzheimer disease. *J. Biol. Chem.* 285, 12463–12468. doi: 10.1074/jbc.R109.080895

Diociaiuti, M., Macchia, G., Paradisi, S., Frank, C., Camerini, S., Chistolini, P., et al. (2014). Native metastable prefibrillar oligomers are the most neurotoxic species among amyloid aggregates. *Biochim. Biophys. Acta* 1842, 1622–1629. doi: 10.1016/j.bbadis.2014.06.006

Du, Y., Liu, X., Zhu, X., Liu, Y., Wang, X., and Wu, X. (2020). Activating transcription factor 6 reduces Aβ1–42 and restores memory in Alzheimer's disease model mice. *Int. J. Neurosci.* 130, 1015–1023. doi: 10.1080/00207454.2020.1715977

Duchen, M. R. (2004). Mitochondria in health and disease: perspectives on a new mitochondrial biology. *Mol. Aspects Med.* 25, 365–451. doi: 10.1016/j.mam.2004.03.001

Eschenhagen, T., Bolli, R., Braun, T., Field, L. J., Fleischmann, B. K., Frisén, J., et al. (2017). Cardiomyocyte regeneration. *Circulation* 136, 680–686. doi: 10.1161/CIRCULATIONAHA.117.029343

Falk, R. H., Alexander, K. M., Liao, R., and Dorbala, S. (2016). AL (Light-Chain) cardiac amyloidosis: a review of diagnosis and therapy. *J. Am. Coll. Cardiol.* 68, 1323–1341. doi: 10.1016/j.jacc.2016.06.053

Ferreiro, E., Resende, R., Costa, R., Oliveira, C. R., and Pereira, C. M. F. (2006). An endoplasmic-reticulum-specific apoptotic pathway is involved in prion and amyloid-beta peptides neurotoxicity. *Neurobiol. Dis.* 23, 669–678. doi: 10.1016/j.nbd.2006.05.011

Frey, N., and Olson, E. N. (2003). Cardiac hypertrophy: the good, the bad, and the ugly. *Annu. Rev. Physiol.* 65, 45–79. doi: 10.1146/annurev.physiol.65.092101.142243

Geetha, T., Zheng, C., Unroe, B., Sycheva, M., Kluess, H., and Babu, J. R. (2012). Polyubiquitination of the neurotrophin receptor p75 directs neuronal cell survival. *Biochem. Biophys. Res. Commun.* 421, 286–290. doi: 10.1016/j.bbrc.2012.04.001

Gianni, D., Li, A., Tesco, G., Mckay, K. M., Moore, J., Raygor, K., et al. (2010). Protein aggregates and novel presenilin gene variants in idiopathic dilated cardiomyopathy. *Circulation* 121, 1216–1226. doi: 10.1161/CIRCULATIONAHA.109.879510

Gilda, J. E., and Gomes, A. V. (2017). Proteasome dysfunction in cardiomyopathies. *J. Physiol.* 595, 4051–4071. doi: 10.1113/JP273607

Glembotski, C. C. (2008). The role of the unfolded protein response in the heart. *J. Mol. Cell. Cardiol.* 44, 453–459. doi: 10.1016/j.yjmcc.2007.10.017

Glembotski, C. C. (2012). Roles for the sarco-/endoplasmic reticulum in cardiac myocyte contraction, protein synthesis, and protein quality control. *Physiology* 27, 343–350. doi: 10.1152/physiol.00034.2012

Glembotski, C. C., Rosarda, J. D., and Wiseman, R. L. (2019). Proteostasis and beyond: ATF6 in ischemic disease. *Trends Mol. Med.* 25, 538–550. doi: 10.1016/j.molmed.2019.03.005

Gorza, L., and Del Monte, F. (2005). Protein unfolding in cardiomyopathies. *Heart Fail. Clin.* 1, 237–250. doi: 10.1016/j.hfc.2005.03.009

Guan, H.-S., Shang, Z., Yang, L., Qiao, S.-B., Shangguan, H.-J., and Meng, X.-M. (2011). Endoplasmic reticulum stress caused by left ventricular hypertrophy in rats: effects of telmisartan. *Am. J. Med. Sci.* 342, 318–323. doi: 10.1097/MAJ.0b013e3182112baf

Guan, J., Mishra, S., Qiu, Y., Shi, J., Trudeau, K., Las, G., et al. (2014). Lysosomal dysfunction and impaired autophagy underlie the pathogenesis of amyloidogenic light chain-mediated cardiotoxicity. *EMBO Mol. Med.* 6, 1493–1507. doi: 10.15252/emmm.201404190

Gwathmey, J. K., Copelas, L., Mackinnon, R., Schoen, F. J., Feldman, M. D., Grossman, W., et al. (1987). Abnormal intracellular calcium handling in myocardium from patients with end-stage heart failure. *Circ. Res.* 61, 70–76. doi: 10.1161/01.RES.61.1.70

Gwathmey, J. K., and Morgan, J. P. (1985). Altered calcium handling in experimental pressure-overload hypertrophy in the ferret. *Circ. Res.* 57, 836–843. doi: 10.1161/01.RES.57.6.836

Hartl, F. U. (2011). Chaperone-assisted protein folding: the path to discovery from a personal perspective. *Nat. Med.* 17, 1206–1210. doi: 10.1038/nm.2467

He, Z., Wang, M., Zhao, Q., Li, X., Liu, P., Ren, B., et al. (2020). Bis(ethylmaltolato)oxidovanadium (IV) mitigates neuronal apoptosis resulted from amyloid-beta induced endoplasmic reticulum stress through activating peroxisome proliferator-activated receptor γ. *J. Inorg. Biochem.* 208:111073. doi: 10.1016/j.jinorgbio.2020.111073

Hershberger, R. E., Morales, A., and Siegfried, J. D. (2010). Clinical and genetic issues in dilated cardiomyopathy: a review for genetics professionals. *Genet. Med.* 12, 655–667. doi: 10.1097/GIM.0b013e3181f2481f

Hitomi, J., Katayama, T., Eguchi, Y., Kudo, T., Taniguchi, M., Koyama, Y., et al. (2004). Involvement of caspase-4 in endoplasmic reticulum stress-induced apoptosis and Aβ-induced cell death. *J. Cell Biol.* 165, 347–356. doi: 10.1083/jcb.200310015

Hong, J., Hong, S.-G., Lee, J., Park, J.-Y., Eriksen, J. L., Rooney, B. V., et al. (2020). Exercise training ameliorates cerebrovascular dysfunction in a murine model of Alzheimer's disease: role of the P2Y2 receptor and endoplasmic reticulum stress. *Am. J. Physiol. Heart Circ. Physiol.* 318, H1559–H1569. doi: 10.1152/ajpheart.00129.2020

Hoozemans, J. J. M., Veerhuis, R., Van Haastert, E. S., Rozemuller, J. M., Baas, F., Eikelenboom, P., et al. (2005). The unfolded protein response is activated in Alzheimer's disease. *Acta Neuropathol.* 110, 165–172. doi: 10.1007/s00401-005-1038-0

Hu, M., Zhang, Z., Liu, B., Zhang, S., Chai, R., Chen, X., et al. (2018). Deubiquitinase inhibitor auranofin attenuated cardiac hypertrophy by blocking NF-κB activation. *Cell. Physiol. Biochem.* 45, 2421–2430. doi: 10.1159/000488230

Huang, W. J., Zhang, X., and Chen, W. W. (2016). Role of oxidative stress in Alzheimer's disease (Review). *Biomed. Rep.* 4, 519–522. doi: 10.3892/br.2016.630

Husain, N., Yuan, Q., Yen, Y.-C., Pletnikova, O., Sally, D. Q., Worley, P., et al. (2017). TRIAD3/RNF216 mutations associated with Gordon Holmes syndrome lead to synaptic and cognitive impairments via Arc misregulation. *Aging Cell* 16, 281–292. doi: 10.1111/acel.12551

Islam, M., Diwan, A., and Mani, K. (2020). Come together: protein assemblies, aggregates and the sarcostat at the heart of cardiac myocyte homeostasis. *Front. Physiol.* 11:586. doi: 10.3389/fphys.2020.00586

Jovaisaite, V., Mouchiroud, L., and Auwerx, J. (2014). The mitochondrial unfolded protein response, a conserved stress response pathway with implications in health and disease. *J. Exp. Biol.* 217, 137–143. doi: 10.1242/jeb.090738

Kadowaki, H., Nishitoh, H., Urano, F., Sadamitsu, C., Matsuzawa, A., Takeda, K., et al. (2005). Amyloid beta induces neuronal cell death through ROS-mediated ASK1 activation. *Cell Death Differ.* 12, 19–24. doi: 10.1038/sj.cdd.4401528

Katayama, T., Imaizumi, K., Sato, N., Miyoshi, K., Kudo, T., Hitomi, J., et al. (1999). Presenilin-1 mutations downregulate the signalling pathway of the unfolded-protein response. *Nat. Cell Biol.* 1, 479–485. doi: 10.1038/70265

Keck, S., Nitsch, R., Grune, T., and Ullrich, O. (2003). Proteasome inhibition by paired helical filament-tau in brains of patients with Alzheimer's disease. *J. Neurochem.* 85, 115–122. doi: 10.1046/j.1471-4159.2003.01642.x

Korolchuk, V. I., Mansilla, A., Menzies, F. M., and Rubinsztein, D. C. (2009). Autophagy inhibition compromises degradation of ubiquitin-proteasome pathway substrates. *Mol. Cell* 33, 517–527. doi: 10.1016/j.molcel.2009.01.021

Kostin, S., Pool, L., Elsässer, A., Hein, S., Drexler, H. C. A., Arnon, E., et al. (2003). Myocytes die by multiple mechanisms in failing human hearts. *Circ. Res.* 92, 715–724. doi: 10.1161/01.RES.0000067471.95890.5C

Kupatt, C., Dessy, C., Hinkel, R., Raake, P., Daneau, G., Bouzin, C., et al. (2004). Heat shock protein 90 transfection reduces ischemia-reperfusion-induced myocardial dysfunction via reciprocal endothelial NO synthase serine 1177 phosphorylation and threonine 495 dephosphorylation. *Arterioscler. Thromb. Vasc. Biol.* 24, 1435–1441. doi: 10.1161/01.ATV.0000134300.87476.d1

Lee, J. H., Won, S. M., Suh, J., Son, S. J., Moon, G. J., Park, U.-J., et al. (2010). Induction of the unfolded protein response and cell death pathway in Alzheimer's disease, but not in aged Tg2576 mice. *Exp. Mol. Med.* 42, 386–394. doi: 10.3858/emm.2010.42.5.040

Li, C., Peng, Y., Zhou, B., Bai, W., and Rao, L. (2017). Association of LIM domain 7 gene polymorphisms and plasma levels of LIM domain 7 with dilated cardiomyopathy in a Chinese population. *Appl. Biochem. Biotechnol.* 182, 885–897. doi: 10.1007/s12010-016-2368-1

Li, D., Parks, S. B., Kushner, J. D., Nauman, D., Burgess, D., Ludwigsen, S., et al. (2006). Mutations of presenilin genes in dilated cardiomyopathy and heart failure. *Am. J. Hum. Genet.* 79, 1030–1039. doi: 10.1086/509900

Li, J., Horak, K. M., Su, H., Sanbe, A., Robbins, J., and Wang, X. (2011). Enhancement of proteasomal function protects against cardiac proteinopathy and ischemia/reperfusion injury in mice. *J. Clin. Invest.* 121, 3689–3700. doi: 10.1172/JCI45709

Liao, R., Jain, M., Teller, P., Connors, L. H., Ngoy, S., Skinner, M., et al. (2001). Infusion of light chains from patients with cardiac amyloidosis causes diastolic dysfunction in isolated mouse hearts. *Circulation* 104, 1594–1597. doi: 10.1161/circ.104.14.1594

Lim, J., Lachenmayer, M. L., Wu, S., Liu, W., Kundu, M., Wang, R., et al. (2015). Proteotoxic stress induces phosphorylation of p62/SQSTM1 by ULK1 to regulate selective autophagic clearance of protein aggregates. *PLoS Genet.* 11:e1004987. doi: 10.1371/journal.pgen.1004987

Lin, J. T., Chang, W. C., Chen, H. M., Lai, H. L., Chen, C. Y., Tao, M. H., et al. (2013). Regulation of feedback between protein kinase A and the proteasome system worsens Huntington's disease. *Mol. Cell. Biol.* 33, 1073–1084. doi: 10.1128/MCB.01434-12

Liu, J., Chen, Q., Huang, W., Horak, K. M., Zheng, H., Mestril, R., et al. (2006a). Impairment of the ubiquitin-proteasome system in desminopathy mouse hearts. *FASEB J.* 20, 362–364. doi: 10.1096/fj.05-4869fje

Liu, J., Tang, M., Mestril, R., and Wang, X. (2006b). Aberrant protein aggregation is essential for a mutant desmin to impair the proteolytic function of the

ubiquitin-proteasome system in cardiomyocytes. *J. Mol. Cell. Cardiol.* 40, 451–454. doi: 10.1016/j.yjmcc.2005.12.011

Liu, Q., Sargent, M. A., York, A. J., and Molkentin, J. D. (2009). ASK1 regulates cardiomyocyte death but not hypertrophy in transgenic mice. *Circ. Res.* 105, 1110–1117. doi: 10.1161/CIRCRESAHA.109.200741

Liu, X., Kwak, D., Lu, Z., Xu, X., Fassett, J., Wang, H., et al. (2014). Endoplasmic reticulum stress sensor protein kinase R-like endoplasmic reticulum kinase (PERK) protects against pressure overload-induced heart failure and lung remodeling. *Hypertension* 64, 738–744. doi: 10.1161/HYPERTENSIONAHA.114.03811

Lokireddy, S., Kukushkin, N. V., and Goldberg, A. L. (2015). cAMP-induced phosphorylation of 26S proteasomes on Rpn6/PSMD11 enhances their activity and the degradation of misfolded proteins. *Proc. Natl. Acad. Sci. U.S.A.* 112, E7176–7185. doi: 10.1073/pnas.1522332112

Lu, X., He, Y., Tang, C., Wang, X., Que, L., Zhu, G., et al. (2020). Triad3A attenuates pathological cardiac hypertrophy involving the augmentation of ubiquitination-mediated degradation of TLR4 and TLR9. *Basic Res. Cardiol.* 115:19. doi: 10.1007/s00395-020-0779-1

Maloyan, A., Gulick, J., Glabe, C. G., Kayed, R., and Robbins, J. (2007). Exercise reverses preamyloid oligomer and prolongs survival in alphaB-crystallin-based desmin-related cardiomyopathy. *Proc. Natl. Acad. Sci. U.S.A.* 104, 5995–6000. doi: 10.1073/pnas.0609202104

Mclendon, P. M., and Robbins, J. (2015). Proteotoxicity and cardiac dysfunction. *Circ. Res.* 116, 1863–1882. doi: 10.1161/CIRCRESAHA.116.305372

Merlini, G. (2017). AL amyloidosis: from molecular mechanisms to targeted therapies. *Hematology Am. Soc. Hematol. Educ. Program* 2017, 1–12. doi: 10.1182/asheducation-2017.1.1

Milhavet, O., Martindale, J. L., Camandola, S., Chan, S. L., Gary, D. S., Cheng, A., et al. (2002). Involvement of Gadd153 in the pathogenic action of presenilin-1 mutations. *J. Neurochem.* 83, 673–681. doi: 10.1046/j.1471-4159.2002.01165.x

Mimori, S., Kawada, K., Saito, R., Takahashi, M., Mizoi, K., Okuma, Y., et al. (2019). Indole-3-propionic acid has chemical chaperone activity and suppresses endoplasmic reticulum stress-induced neuronal cell death. *Biochem. Biophys. Res. Commun.* 517, 623–628. doi: 10.1016/j.bbrc.2019.07.074

Misra, P., Blancas-Mejia, L. M., and Ramirez-Alvarado, M. (2019). Mechanistic insights into the early events in the aggregation of immunoglobulin light chains. *Biochemistry* 58, 3155–3168. doi: 10.1021/acs.biochem.9b00311

Mori, H., Kondo, J., and Ihara, Y. (1987). Ubiquitin is a component of paired helical filaments in Alzheimer's disease. *Science* 235, 1641–1644. doi: 10.1126/science.3029875

Munch, C. (2018). The different axes of the mammalian mitochondrial unfolded protein response. *BMC Biol.* 16:81. doi: 10.1186/s12915-018-0548-x

Murata, K., Lu, W., Hashimoto, M., Ono, N., Muratani, M., Nishikata, K., et al. (2018). PRMT1 deficiency in mouse juvenile heart induces dilated cardiomyopathy and reveals cryptic alternative splicing products. *iScience* 8, 200–213. doi: 10.1016/j.isci.2018.09.023

Myeku, N., Clelland, C. L., Emrani, S., Kukushkin, N. V., Yu, W. H., Goldberg, A. L., et al. (2016). Tau-driven 26S proteasome impairment and cognitive dysfunction can be prevented early in disease by activating cAMP-PKA signaling. *Nat. Med.* 22, 46–53. doi: 10.1038/nm.4011

Nakagawa, T., Zhu, H., Morishima, N., Li, E., Xu, J., Yankner, B. A., et al. (2000). Caspase-12 mediates endoplasmic-reticulum-specific apoptosis and cytotoxicity by amyloid-β. *Nature* 403, 98–103. doi: 10.1038/47513

Niwa, M., Sidrauski, C., Kaufman, R. J., and Walter, P. (1999). A role for presenilin-1 in nuclear accumulation of Ire1 fragments and induction of the mammalian unfolded protein response. *Cell* 99, 691–702. doi: 10.1016/S0092-8674(00)81667-0

Ojha, J., Masilamoni, G., Dunlap, D., Udoff, R. A., and Cashikar, A. G. (2011). Sequestration of toxic oligomers by HspB1 as a cytoprotective mechanism. *Mol. Cell. Biol.* 31, 3146–3157. doi: 10.1128/MCB.01187-10

Okada, K.-I., Minamino, T., Tsukamoto, Y., Liao, Y., Tsukamoto, O., Takashima, S., et al. (2004). Prolonged endoplasmic reticulum stress in hypertrophic and failing heart after aortic constriction. *Circulation* 110, 705–712. doi: 10.1161/01.CIR.0000137836.95625.D4

Pagan, J., Seto, T., Pagano, M., and Cittadini, A. (2013). Role of the ubiquitin proteasome system in the heart. *Circ. Res.* 112, 1046–1058. doi: 10.1161/CIRCRESAHA.112.300521

Pan, B., Li, J., Parajuli, N., Tian, Z., Wu, P., Lewno Megan, T., et al. (2020). The calcineurin-TFEB-p62 pathway mediates the activation of cardiac macroautophagy by proteasomal malfunction. *Circ. Res.* 127, 502–518. doi: 10.1161/CIRCRESAHA.119.316007

Pan, Y.-X., Lin, L., Ren, A.-J., Pan, X.-J., Chen, H., Tang, C.-S., et al. (2004). HSP70 and GRP78 induced by endothelin-1 pretreatment enhance tolerance to hypoxia in cultured neonatal rat cardiomyocytes. *J. Cardiovasc. Pharmacol.* 44(Suppl. 1), S117–S120. doi: 10.1097/01.fjc.0000166234.11336.a9

Park, C. S., Cha, H., Kwon, E. J., Sreenivasaiah, P. K., and Kim, D. H. (2012). The chemical chaperone 4-phenylbutyric acid attenuates pressure-overload cardiac hypertrophy by alleviating endoplasmic reticulum stress. *Biochem. Biophys. Res. Commun.* 421, 578–584. doi: 10.1016/j.bbrc.2012.04.048

Pawlak, A., Rejmak-Kozicka, E., Gil, K. E., Ziemba, A., Kaczmarek, L., and Gil, R. J. (2019). Patterns of desmin expression in idiopathic dilated cardiomyopathy are related to the desmin mRNA and ubiquitin expression. *J. Investig. Med.* 67, 11–19. doi: 10.1136/jim-2017-000707

Perry, G., Friedman, R., Shaw, G., and Chau, V. (1987). Ubiquitin is detected in neurofibrillary tangles and senile plaque neurites of Alzheimer disease brains. *Proc. Natl. Acad. Sci. U.S.A.* 84:3033. doi: 10.1073/pnas.84.9.3033

Petersen, A., Kutsche, H. S., Nippert, F., Schreckenberg, R., Schulz, R., and Schlüter, K.-D. (2020). Induction of proteasome subunit low molecular weight protein (LMP)-2 is required to induce active remodeling in adult rat ventricular cardiomyocytes. *Med. Sci.* 8:21. doi: 10.3390/medsci8020021

Picken, M. M. (2020). The pathology of amyloidosis in classification: a review. *Acta Haematol.* 143, 322–334. doi: 10.1159/000506696

Plemper, R. K., and Wolf, D. H. (1999). Endoplasmic reticulum degradation. reverse protein transport and its end in the proteasome. *Mol. Biol. Rep.* 26, 125–130.

Powell, S. R., Herrmann, J., Lerman, A., Patterson, C., and Wang, X. (2012). The ubiquitin-proteasome system and cardiovascular disease. *Prog. Mol. Biol. Transl. Sci.* 109, 295–346. doi: 10.1016/B978-0-12-397863-9.00009-2

Predmore, J. M., Wang, P., Davis, F., Bartolone, S., Westfall, M. V., Dyke, D. B., et al. (2010). Ubiquitin proteasome dysfunction in human hypertrophic and dilated cardiomyopathies. *Circulation* 121, 997–1004. doi: 10.1161/CIRCULATIONAHA.109.904557

Rabbani, N., and Thornalley, P. J. (2019). Hexokinase-2 glycolytic overload in diabetes and ischemia-reperfusion injury. *Trends Endocrinol. Metab.* 30, 419–431. doi: 10.1016/j.tem.2019.04.011

Ranek, M. J., Terpstra, E. J., Li, J., Kass, D. A., and Wang, X. (2013). Protein kinase g positively regulates proteasome-mediated degradation of misfolded proteins. *Circulation* 128, 365–376. doi: 10.1161/CIRCULATIONAHA.113.001971

Reitz, C., Brickman, A. M., Luchsinger, J. A., Wu, W. E., Small, S. A., and Tang, M. X. (2007). Frequency of subclinical heart disease in elderly persons with dementia. *Am. J. Geriatr. Cardiol.* 16, 183–188. doi: 10.1111/j.1076-7460.2007.06511.x

Renkawek, K., Voorter, C. E. M., Bosman, G. J. C. G. M., Van Workum, F. P. A., and De Jong, W. W. (1994). Expression of αB-crystallin in Alzheimer's disease. *Acta Neuropathol* 87, 155–160. doi: 10.1007/BF00296185

Riederer, B. M., Leuba, G., Vernay, A., and Riederer, I. M. (2011). The role of the ubiquitin proteasome system in Alzheimer's disease. *Exp. Biol. Med.* 236, 268–276. doi: 10.1258/ebm.2010.010327

Rozpedek-Kamińska, W., Siwecka, N., Wawrzynkiewicz, A., Wojtczak, R., Pytel, D., Diehl, J. A., et al. (2020). The PERK-dependent molecular mechanisms as a novel therapeutic target for neurodegenerative diseases. *Int. J. Mol. Sci.* 21:2108. doi: 10.3390/ijms21062108

Rusten, T. E., and Stenmark, H. (2010). p62, an autophagy hero or culprit? *Nat. Cell Biol.* 12, 207–209. doi: 10.1038/ncb0310-207

Ruz, C., Alcantud, J. L., Vives Montero, F., Duran, R., and Bandres-Ciga, S. (2020). Proteotoxicity and neurodegenerative diseases. *Int. J. Mol. Sci.* 21:5646. doi: 10.3390/ijms21165646

Salminen, A., Kauppinen, A., Suuronen, T., Kaarniranta, K., and Ojala, J. (2009). ER stress in Alzheimer's disease: a novel neuronal trigger for inflammation and Alzheimer's pathology. *J. Neuroinflammation* 6:41. doi: 10.1186/1742-2094-6-41

Sanbe, A., Osinska, H., Saffitz, J. E., Glabe, C. G., Kayed, R., Maloyan, A., et al. (2004). Desmin-related cardiomyopathy in transgenic mice:

a cardiac amyloidosis. *Proc. Natl. Acad. Sci. U.S.A.* 101, 10132–10136. doi: 10.1073/pnas.0401900101

Sato, N., Urano, F., Yoon Leem, J., Kim, S.-H., Li, M., Donoviel, D., et al. (2000). Upregulation of BiP and CHOP by the unfolded-protein response is independent of presenilin expression. *Nat. Cell Biol.* 2, 863–870. doi: 10.1038/35046500

Scheper, W., Hoozemans, J. J. M., Hoogenraad, C. C., Rozemuller, A. J. M., Eikelenboom, P., and Baas, F. (2007). Rab6 is increased in Alzheimer's disease brain and correlates with endoplasmic reticulum stress. *Neuropathol. Appl. Neurobiol.* 33, 523–532. doi: 10.1111/j.1365-2990.2007.00846.x

Schubert, U., Antón, L. C., Gibbs, J., Norbury, C. C., Yewdell, J. W., and Bennink, J. R. (2000). Rapid degradation of a large fraction of newly synthesized proteins by proteasomes. *Nature* 404, 770–774. doi: 10.1038/35008096

Sergin, I., Bhattacharya, S., Emanuel, R., Esen, E., Stokes, C. J., Evans, T. D., et al. (2016). Inclusion bodies enriched for p62 and polyubiquitinated proteins in macrophages protect against atherosclerosis. *Sci. Signal* 9:ra2. doi: 10.1126/scisignal.aad5614

Seyb, K. I., Ansar, S., Bean, J., and Michaelis, M. L. (2006). β-amyloid and endoplasmic reticulum stress reponses in primary neurons. *J. Mol. Neurosci.* 28, 111–123. doi: 10.1385/JMN:28:2:111

Sha, Z., Schnell, H. M., Ruoff, K., and Goldberg, A. (2018). Rapid induction of p62 and GABARAPL1 upon proteasome inhibition promotes survival before autophagy activation. *J. Cell Biol.* 217, 1757–1776. doi: 10.1083/jcb.201708168

Sheng, M., Lu, H., Liu, P., Li, Y., Ravi, H., Peng, S. L., et al. (2017). Sildenafil improves vascular and metabolic function in patients with Alzheimer's disease. *J. Alzheimers. Dis.* 60, 1351–1364. doi: 10.3233/JAD-161006

Shi, J., Guan, J., Jiang, B., Brenner, D. A., Del Monte, F., Ward, J. E., et al. (2010). Amyloidogenic light chains induce cardiomyocyte contractile dysfunction and apoptosis via a non-canonical p38alpha MAPK pathway. *Proc. Natl. Acad. Sci. U.S.A.* 107, 4188–4193. doi: 10.1073/pnas.0912263107

Shinohara, H., Inaguma, Y., Goto, S., Inagaki, T., and Kato, K. (1993). αB crystallin and HSP28 are enhanced in the cerebral cortex of patients with Alzheimer's disease. *J. Neurol. Sci.* 119, 203–208. doi: 10.1016/0022-510X(93)90135-L

Shintani-Ishida, K., Nakajima, M., Uemura, K., and Yoshida, K.-I. (2006). Ischemic preconditioning protects cardiomyocytes against ischemic injury by inducing GRP78. *Biochem. Biophys. Res. Commun.* 345, 1600–1605. doi: 10.1016/j.bbrc.2006.05.077

Shiojima, I., Sato, K., Izumiya, Y., Schiekofer, S., Ito, M., Liao, R., et al. (2005). Disruption of coordinated cardiac hypertrophy and angiogenesis contributes to the transition to heart failure. *J. Clin. Invest.* 115, 2108–2118. doi: 10.1172/JCI24682

Shu, Q., Lai, S., Wang, X.-M., Zhang, Y.-L., Yang, X.-L., Bi, H.-L., et al. (2018). Administration of ubiquitin-activating enzyme UBA1 inhibitor PYR-41 attenuates angiotensin II-induced cardiac remodeling in mice. *Biochem. Biophys. Res. Commun.* 505, 317–324. doi: 10.1016/j.bbrc.2018.09.100

Smyrnias, I., Gray, S. P., Okonko, D. O., Sawyer, G., Zoccarato, A., Catibog, N., et al. (2019). Cardioprotective effect of the mitochondrial unfolded protein response during chronic pressure overload. *J. Am. Coll. Cardiol.* 73, 1795–1806. doi: 10.1016/j.jacc.2018.12.087

Sorrentino, V., Romani, M., Mouchiroud, L., Beck, J. S., Zhang, H., D'amico, D., et al. (2017). Enhancing mitochondrial proteostasis reduces amyloid-beta proteotoxicity. *Nature* 552, 187–193. doi: 10.1038/nature25143

Spanig, S., Kellermann, K., Dieterlen, M. T., Noack, T., Lehmann, S., Borger, M. A., et al. (2019). The ubiquitin proteasome system in ischemic and dilated cardiomyopathy. *Int. J. Mol. Sci.* 20:6354. doi: 10.3390/ijms20246354

Stark, K., Esslinger, U. B., Reinhard, W., Petrov, G., Winkler, T., Komajda, M., et al. (2010). Genetic association study identifies HSPB7 as a risk gene for idiopathic dilated cardiomyopathy. *PLoS Genet.* 6:e1001167. doi: 10.1371/journal.pgen.1001167

Su, H., and Wang, X. (2020). Proteasome malfunction activates the PPP3/calcineurin-TFEB-SQSTM1/p62 pathway to induce macroautophagy in the heart. *Autophagy* 16, 2114–2116. doi: 10.1080/15548627.2020.1816666

Subramanian, K., Gianni, D., Balla, C., Assenza, G. E., Joshi, M., Semigran, M. J., et al. (2015). Cofilin-2 phosphorylation and sequestration in myocardial aggregates: novel pathogenetic mechanisms for idiopathic dilated cardiomyopathy. *J. Am. Coll. Cardiol.* 65, 1199–1214. doi: 10.1016/j.jacc.2015.01.031

Suzuki, Y. (2014). Emerging novel concept of chaperone therapies for protein misfolding diseases. *Proc. Jpn Acad. Ser. B Phys. Biol. Sci.* 90, 145–162. doi: 10.2183/pjab.90.145

Szweda, P. A., Friguet, B., and Szweda, L. I. (2002). Proteolysis, free radicals, and aging. *Free Radic. Biol. Med.* 33, 29–36. doi: 10.1016/S0891-5849(02)00837-7

Terro, F., Czech, C., Esclaire, F., Elyaman, W., Yardin, C., Baclet, M.-C., et al. (2002). Neurons overexpressing mutant presenilin-1 are more sensitive to apoptosis induced by endoplasmic reticulum-Golgi stress. *J. Neurosci. Res.* 69, 530–539. doi: 10.1002/jnr.10312

Thuerauf, D. J., Marcinko, M., Gude, N., Rubio, M., Sussman, M. A., and Glembotski, C. C. (2006). Activation of the unfolded protein response in infarcted mouse heart and hypoxic cultured cardiac myocytes. *Circ. Res.* 99, 275–282. doi: 10.1161/01.RES.0000233317.70421.03

Torres, M., Encina, G., Soto, C., and Hetz, C. (2011). Abnormal calcium homeostasis and protein folding stress at the ER. *Commun. Integr. Biol.* 4, 258–261. doi: 10.4161/cib.4.3.15019

Tóth, M. E., Szegedi, V., Varga, E., Juhász, G., Horváth, J., Borbély, E., et al. (2013). Overexpression of Hsp27 ameliorates symptoms of Alzheimer's disease in APP/PS1 mice. *Cell Stress Chaperones* 18, 759–771. doi: 10.1007/s12192-013-0428-9

Troncone, L., Luciani, M., Coggins, M., Wilker, E. H., Ho, C. Y., Codispoti, K. E., et al. (2016). Aβ amyloid pathology affects the hearts of patients with alzheimer's disease: mind the heart. *J. Am. Coll. Cardiol.* 68, 2395–2407. doi: 10.1016/j.jacc.2016.08.073

Tublin, J. M., Adelstein, J. M., del Monte, F., Combs, C. K., and Wold, L. E. (2019). Getting to the Heart of Alzheimer Disease. *Circ. Res.* 124, 142–149. doi: 10.1161/CIRCRESAHA.118.313563

Uddin, M. S., Stachowiak, A., Mamun, A. A., Tzvetkov, N. T., Takeda, S., Atanasov, A. G., et al. (2018). Autophagy and Alzheimer's disease: from molecular mechanisms to therapeutic implications. *Front. Aging Neurosci.* 10:4. doi: 10.3389/fnagi.2018.00004

Uddin, M. S., Tewari, D., Sharma, G., Kabir, M. T., Barreto, G. E., Bin-Jumah, M. N., et al. (2020). Molecular mechanisms of ER stress and UPR in the pathogenesis of Alzheimer's disease. *Mol. Neurobiol.* 57, 2902–2919. doi: 10.1007/s12035-020-01929-y

Unterberger, U., Höftberger, R., Gelpi, E., Flicker, H., Budka, H., and Voigtländer, T. (2006). Endoplasmic reticulum stress features are prominent in Alzheimer disease but not in prion diseases *in vivo*. *J. Neuropathol. Exp. Neurol.* 65, 348–357. doi: 10.1097/01.jnen.0000218445.30535.6f

Urbina-Varela, R., Castillo, N., Videla, L. A., and Del Campo, A. (2020). Impact of mitophagy and mitochondrial unfolded protein response as new adaptive mechanisms underlying old pathologies: sarcopenia and non-alcoholic fatty liver disease. *Int. J. Mol. Sci.* 21:7704. doi: 10.3390/ijms21207704

Venkatesh, S., Li, M., Saito, T., Tong, M., Rashed, E., Mareedu, S., et al. (2019). Mitochondrial LonP1 protects cardiomyocytes from ischemia/reperfusion injury *in vivo*. *J. Mol. Cell. Cardiol.* 128, 38–50. doi: 10.1016/j.yjmcc.2018.12.017

Verplank, J. J. S., Lokireddy, S., Zhao, J., and Goldberg, A. L. (2019). 26S Proteasomes are rapidly activated by diverse hormones and physiological states that raise cAMP and cause Rpn6 phosphorylation. *Proc. Natl. Acad. Sci. U.S.A.* 116, 4228–4237. doi: 10.1073/pnas.1809254116

Vitadello, M., Penzo, D., Petronilli, V., Michieli, G., Gomirato, S., Menabò, R., et al. (2003). Overexpression of the stress-protein Grp94 reduces cardiomyocyte necrosis due to calcium overload and simulated ischemia. *FASEB J.* 17, 923–925. doi: 10.1096/fj.02-0644fje

Vitolo, O. V., Sant'angelo, A., Costanzo, V., Battaglia, F., Arancio, O., and Shelanski, M. (2002). Amyloid beta -peptide inhibition of the PKA/CREB pathway and long-term potentiation: reversibility by drugs that enhance cAMP signaling. *Proc. Natl. Acad. Sci. U.S.A.* 99, 13217–13221. doi: 10.1073/pnas.172504199

Wang, C. F., and Huang, Y. S. (2012). Calpain 2 activated through N-methyl-D-aspartic acid receptor signaling cleaves CPEB3 and abrogates CPEB3-repressed translation in neurons. *Mol. Cell. Biol.* 32, 3321–3332. doi: 10.1128/MCB.00296-12

Wang, X., Bi, X., Zhang, G., Deng, Y., Luo, X., Xu, L., et al. (2018). Glucose-regulated protein 78 is essential for cardiac myocyte survival. *Cell Death Differ.* 25, 2181–2194. doi: 10.1038/s41418-018-0109-4

Wang, X., Osinska, H., Klevitsky, R., Gerdes, A. M., Nieman, M., Lorenz, J., et al. (2001). Expression of R120G-alphaB-crystallin causes aberrant desmin and alphaB-crystallin aggregation and cardiomyopathy in mice. *Circ. Res.* 89, 84–91. doi: 10.1161/hh1301.092688

Wang, X., Pattison, J. S., and Su, H. (2013). Posttranslational modification and quality control. *Circ. Res.* 112, 367–381. doi: 10.1161/CIRCRESAHA.112.268706

Wang, X., Su, H., and Ranek, M. J. (2008). Protein quality control and degradation in cardiomyocytes. *J. Mol. Cell. Cardiol.* 45, 11–27. doi: 10.1016/j.yjmcc.2008.03.025

Wang, X., and Wang, H. (2020). Priming the proteasome to protect against proteotoxicity. *Trends Mol. Med.* 26, 639–648. doi: 10.1016/j.molmed.2020.02.007

Wang, X. Z., Lawson, B., Brewer, J. W., Zinszner, H., Sanjay, A., Mi, L. J., et al. (1996). Signals from the stressed endoplasmic reticulum induce C/EBP-homologous protein (CHOP/GADD153). *Mol. Cell. Biol.* 16, 4273–4280. doi: 10.1128/MCB.16.8.4273

Wang, Z. V., Deng, Y., Gao, N., Pedrozo, Z., Li, D. L., Morales, C. R., et al. (2014). Spliced X-box binding protein 1 couples the unfolded protein response to hexosamine biosynthetic pathway. *Cell* 156, 1179–1192. doi: 10.1016/j.cell.2014.01.014

Webster, J. M., Darling, A. L., Uversky, V. N., and Blair, L. J. (2019). Small heat shock proteins, big impact on protein aggregation in neurodegenerative disease. *Front. Pharmacol.* 10, 1047–1047. doi: 10.3389/fphar.2019.01047

Welch, W. J. (2004). Role of quality control pathways in human diseases involving protein misfolding. *Semin. Cell Dev. Biol.* 15, 31–38. doi: 10.1016/j.semcdb.2003.12.011

Wilhelmus, M. M. M., Boelens, W. C., Otte-Höller, I., Kamps, B., Kusters, B., Maat-Schieman, M. L. C., et al. (2006). Small heat shock protein HspB8: its distribution in Alzheimer's disease brains and its inhibition of amyloid-β protein aggregation and cerebrovascular amyloid-β toxicity. *Acta Neuropathol.* 111, 139–149. doi: 10.1007/s00401-005-0030-z

Willis, M. S., and Patterson, C. (2013). Proteotoxicity and cardiac dysfunction–Alzheimer's disease of the heart? *N. Engl. J. Med.* 368, 455–464. doi: 10.1056/NEJMra1106180

Willis, M. S., Schisler, J. C., Portbury, A. L., and Patterson, C. (2008). Build it up–Tear it down: protein quality control in the cardiac sarcomere. *Cardiovasc. Res.* 81, 439–448. doi: 10.1093/cvr/cvn289

Wright, A. L., Zinn, R., Hohensinn, B., Konen, L. M., Beynon, S. B., Tan, R. P., et al. (2013). Neuroinflammation and neuronal loss precede Abeta plaque deposition in the hAPP-J20 mouse model of Alzheimer's disease. *PLoS ONE* 8:e59586. doi: 10.1371/journal.pone.0059586

Wu, W., Lai, L., Xie, M., and Qiu, H. (2020). Insights of heat shock protein 22 in the cardiac protection against ischemic oxidative stress. *Redox Biol.* 34:101555. doi: 10.1016/j.redox.2020.101555

Xie, X., Wang, H.-X., Li, N., Deng, Y.-W., Bi, H.-L., Zhang, Y.-L., et al. (2020). Selective inhibition of the immunoproteasome β5i prevents PTEN degradation and attenuates cardiac hypertrophy. *Front. Pharmacol.* 11:885. doi: 10.3389/fphar.2020.00885

Yamaguchi, O., Higuchi, Y., Hirotani, S., Kashiwase, K., Nakayama, H., Hikoso, S., et al. (2003). Targeted deletion of apoptosis signal-regulating kinase 1 attenuates left ventricular remodeling. *Proc. Natl. Acad. Sci.* 100, 15883–15888. doi: 10.1073/pnas.2136717100

Yamasaki-Mann, M., Demuro, A., and Parker, I. (2010). Modulation of endoplasmic reticulum Ca2+ store filling by cyclic ADP-ribose promotes inositol trisphosphate (IP3)-evoked Ca2+ signals. *J. Biol. Chem.* 285, 25053–25061. doi: 10.1074/jbc.M109.095257

Yan, W., Dong, Z.-C., Wang, J.-J., Zhang, Y.-L., Wang, H.-X., Zhang, B., et al. (2020). Deficiency of the immunoproteasome LMP10 subunit attenuates angiotensin II-induced cardiac hypertrophic remodeling via autophagic degradation of gp130 and IGF1R. *Front. Physiol.* 11:625. doi: 10.3389/fphys.2020.00625

Yang, H., Wang, X.-X., Zhou, C.-Y., Xiao, X., Tian, C., Li, H.-H., et al. (2020). Tripartite motif 10 regulates cardiac hypertrophy by targeting the PTEN/AKT pathway. *J. Cell. Mol. Med.* 24, 6233–6241. doi: 10.1111/jcmm.15257

Yu, Z., Luo, H., Fu, W., and Mattson, M. P. (1999). The endoplasmic reticulum stress-responsive protein GRP78 protects neurons against excitotoxicity and apoptosis: suppression of oxidative stress and stabilization of calcium homeostasis. *Exp. Neurol.* 155, 302–314. doi: 10.1006/exnr.1998.7002

Zheng, Q., Su, H., Ranek, M. J., and Wang, X. (2011). Autophagy and p62 in cardiac proteinopathy. *Circ. Res.* 109, 296–308. doi: 10.1161/CIRCRESAHA.111.244707

Conflict of Interest: The authors declare that the research was conducted in the absence of any commercial or financial relationships that could be construed as a potential conflict of interest.

Advantages of publishing in Frontiers

OPEN ACCESS
Articles are free to read for greatest visibility and readership

FAST PUBLICATION
Around 90 days from submission to decision

HIGH QUALITY PEER-REVIEW
Rigorous, collaborative, and constructive peer-review

TRANSPARENT PEER-REVIEW
Editors and reviewers acknowledged by name on published articles

Frontiers
Avenue du Tribunal-Fédéral 34
1005 Lausanne | Switzerland

Visit us: www.frontiersin.org
Contact us: frontiersin.org/about/contact

REPRODUCIBILITY OF RESEARCH
Support open data and methods to enhance research reproducibility

DIGITAL PUBLISHING
Articles designed for optimal readership across devices

FOLLOW US
@frontiersin

IMPACT METRICS
Advanced article metrics track visibility across digital media

EXTENSIVE PROMOTION
Marketing and promotion of impactful research

LOOP RESEARCH NETWORK
Our network increases your article's readership